frontiers | Research Topics

Advances in molecular biology, pathogenesis, diagnosis, vaccines, and treatment of diseases caused by apicomplexan parasites

Edited by
Mingming Liu, Ningbo xia, William Harold Witola and Kun Li

Published in
Frontiers in Cellular and Infection Microbiology

ISSN 1664-8714
ISBN 978-2-8325-2409-1
DOI 10.3389/978-2-8325-2409-1

About Frontiers

Frontiers is more than just an open access publisher of scholarly articles: it is a pioneering approach to the world of academia, radically improving the way scholarly research is managed. The grand vision of Frontiers is a world where all people have an equal opportunity to seek, share and generate knowledge. Frontiers provides immediate and permanent online open access to all its publications, but this alone is not enough to realize our grand goals.

Frontiers journal series

The Frontiers journal series is a multi-tier and interdisciplinary set of open-access, online journals, promising a paradigm shift from the current review, selection and dissemination processes in academic publishing. All Frontiers journals are driven by researchers for researchers; therefore, they constitute a service to the scholarly community. At the same time, the *Frontiers journal series* operates on a revolutionary invention, the tiered publishing system, initially addressing specific communities of scholars, and gradually climbing up to broader public understanding, thus serving the interests of the lay society, too.

Dedication to quality

Each Frontiers article is a landmark of the highest quality, thanks to genuinely collaborative interactions between authors and review editors, who include some of the world's best academicians. Research must be certified by peers before entering a stream of knowledge that may eventually reach the public - and shape society; therefore, Frontiers only applies the most rigorous and unbiased reviews. Frontiers revolutionizes research publishing by freely delivering the most outstanding research, evaluated with no bias from both the academic and social point of view. By applying the most advanced information technologies, Frontiers is catapulting scholarly publishing into a new generation.

What are Frontiers Research Topics?

Frontiers Research Topics are very popular trademarks of the *Frontiers journals series*: they are collections of at least ten articles, all centered on a particular subject. With their unique mix of varied contributions from Original Research to Review Articles, Frontiers Research Topics unify the most influential researchers, the latest key findings and historical advances in a hot research area.

Find out more on how to host your own Frontiers Research Topic or contribute to one as an author by contacting the Frontiers editorial office: frontiersin.org/about/contact

Advances in molecular biology, pathogenesis, diagnosis, vaccines, and treatment of diseases caused by apicomplexan parasites

Topic editors

Mingming Liu — Hubei University of Arts and Science, China
Ningbo xia — South China Agricultural University, China
William Harold Witola — University of Illinois at Urbana–Champaign, United States
Kun Li — Nanjing Agricultural University, China

Citation

Liu, M., xia, N., Witola, W. H., Li, K., eds. (2023). *Advances in molecular biology, pathogenesis, diagnosis, vaccines, and treatment of diseases caused by apicomplexan parasites*. Lausanne: Frontiers Media SA.
doi: 10.3389/978-2-8325-2409-1

Table of contents

frontiers | Frontiers in Cellular and Infection Microbiology

TYPE Editorial
PUBLISHED 28 April 2023
DOI 10.3389/fcimb.2023.1205563

OPEN ACCESS

EDITED AND REVIEWED BY
Jeroen P. J. Saeij,
University of California, Davis, United States

*CORRESPONDENCE
Mingming Liu
lmm_2010@hotmail.com
Kun Li
lk3005@njau.edu.cn

RECEIVED 14 April 2023
ACCEPTED 18 April 2023
PUBLISHED 28 April 2023

CITATION
Liu M, Xia N, Witola WH and Li K (2023) Editorial: Advances in molecular biology, pathogenesis, diagnosis, vaccines, and treatment of diseases caused by apicomplexan parasites.
Front. Cell. Infect. Microbiol. 13:1205563.
doi: 10.3389/fcimb.2023.1205563

Editorial: Advances in molecular biology, pathogenesis, diagnosis, vaccines, and treatment of diseases caused by apicomplexan parasites

Mingming Liu[1]*, Ningbo Xia[2], William Harold Witola[3] and Kun Li[4,5]*

[1]School of Basic Medicine, Hubei University of Arts and Science, Xiangyang, China, [2]Guangdong Laboratory for Lingnan Modern Agriculture, College of Veterinary Medicine, South China Agricultural University, Guangzhou, China, [3]Department of Pathobiology, College of Veterinary Medicine, University of Illinois Urbana-Champaign, Urbana, IL, United States, [4]Institute of Traditional Chinese Veterinary Medicine, College of Veterinary Medicine, Nanjing Agricultural University, Nanjing, China, [5]MOE Joint International Research Laboratory of Animal Health and Food Safety, College of Veterinary Medicine, Nanjing Agricultural University, Nanjing, China

KEYWORDS

apicomplexan, molecular biology, pathogenesis, diagnosis, vaccines, treatment

Editorial on the Research Topic
Advances in molecular biology, pathogenesis, diagnosis, vaccines, and treatment of diseases caused by apicomplexan parasites

Considering the extensive range of diseases caused by apicomplexan parasites, including babesiosis, cryptosporidiosis, leishmaniasis, malaria, neosporosis, and toxoplasmosis, which significantly contribute to the prevalence of fatal parasitic infections, we anticipate that this research area will provide essential insight to aid in the development of innovative strategies for managing and controlling diseases associated with apicomplexan parasites. Finally, thirteen articles were accepted for publication in our Research Topic "*Advances in Molecular Biology, Pathogenesis, Diagnosis, Vaccines, and Treatment of Diseases Caused by Apicomplexan Parasites.*"

Five articles about recent advances in *Toxoplasma gondii* and *Neospora caninum* research have contributed to this Research Topic. Zhang et al. explored the efficacy of panobinostat (LBH589), a novel histone deacetylase inhibitor, against *T. gondii* for treating ocular toxoplasmosis. *In vitro*, LBH589 inhibits proliferation and activity of *T. gondii* in a dose-dependent manner, with low toxicity in retinal pigment epithelial cells. *In vivo*, LBH589 significantly reduced inflammatory cell infiltration and retinal damage in mice while decreasing mRNA expression levels of inflammatory cytokines. These findings suggest that LBH589 holds promise as a preclinical candidate for controlling and curing ocular toxoplasmosis. Yue et al. determined the seroprevalence of *T. gondii* in captive giant pandas and analyzed associated risk factors. Of 203 serum samples collected from 157 pandas between 2007 and 2022, 35.67% were seropositive for *T. gondii*. Age and transfer history between institutions were identified as risk factors, with age-related seroprevalence

being the main factor. Housing multiple species together may increase cross-infection risk. These findings provide valuable data for creating policies to prevent and control *T. gondii* infections, protecting the health of captive giant pandas and other wildlife. Qi et al. developed serological testing methods using TgSAG1, TgGRA7, and TgBAG1 proteins to detect *T. gondii*-specific immunoglobulin M and immunoglobulin G antibodies in 3,733 animals from the Qinghai Tibetan Plateau. These methods, including rSAG1-ELISA, rGRA7-ELISA, and rBAG1-ELISA, also differentiated between acute and chronic toxoplasmosis infections. The study confirmed that SAG1, GRA7, and BAG1 recombinant antigens can effectively be used to detect specific antibodies and distinguish between acute and chronic *T. gondii* infections, providing significant clinical evidence for toxoplasmosis diagnosis. Zou et al. used high-throughput RNA sequencing to study expression of circRNAs and miRNAs in the liver of mice infected with *T. gondii* during acute and chronic stages. They found 265 and 97 differentially expressed (DE) circRNAs and 171 and 77 DEmiRNAs at acute and chronic stages, respectively. One DEcircRNA showed a significant correlation with two DEmiRNAs in a network associated with liver immunity and disease pathogenesis. These findings help in understanding how circRNA expression in the liver changes after *T. gondii* infection and improve knowledge of hepatic toxoplasmosis in mice. Fereig et al. investigated the prevalence of *T. gondii* and *N. caninum* in camels imported from Sudan for human consumption and found seropositive rates of 25.7% for *T. gondii*, 3.9% for *N. caninum*, and 0.8% for mixed infections in 460 camels. The study also revealed variations in infection rates by region. A systematic review showed an overall global seroprevalence of 28.6% for *T. gondii* and 14.3% for *N. caninum* in camels. These findings provide important information to guide control and prevention strategies for these parasites in camels.

Four articles have been published on this Research Topic, focusing on the current progress in *Babesia* and *Plasmodium*. BmGPI12 which serves as a reliable biomarker for active *B. microti* infection. Chand et al. characterized 18 monoclonal antibodies against BmGPI12, identifying five unique epitopes through serological profiling and competition assays. They found five antibody combinations that specifically detected the secreted form of BmGPI12 in plasma samples from infected mice and humans. This finding may contribute to the development of improved diagnostic tools for human babesiosis. Ji et al. investigated the effectiveness of continuous PI4K-targeting treatment for babesiosis in immunocompromised individuals. *B. microti*-infected SCID mice were treated with MMV390048, a PI4K inhibitor, for 72 days. PCR tests were negative from 64 days. The study also found an atovaquone-resistant *B. microti* strain with a Y272C mutation in the Cytb gene. Significantly, MMV390048 effectively inhibited this resistant strain. The findings suggest that PI4K inhibitors may be a promising therapeutic option for treating human babesiosis. Zhou et al. investigated the mechanisms behind thrombocytopenia and anemia in malaria and babesiosis, demonstrating that infection by *Babesia* and *Plasmodium* species stimulate production of anti-erythrocyte and anti-platelet autoantibodies, with B and T lymphocytes playing a significant role in their production. Membrane-associated cytoskeleton proteins might also influence generation of these autoimmune antibodies. The study suggests that an autoimmune response mediated by autoantibodies contributes to thrombocytopenia and hemolytic anemia and plays a role in regulating the overall autoimmune response in these infections. The malaria vaccine candidate BK-SE36 is based on *P. falciparum* SERA5. Despite promising results in clinical trials, concerns about genetic diversity and allele-specific immunity persist. Arisue et al. found polymorphisms in sera5 to be primarily in repeat regions and identified a consensus sequence with African-specific variations. There was no significant genetic differentiation between parasites in vaccinated and control groups, suggesting that the vaccine does not trigger an allele-specific immune response.

Three articles on *Cryptosporidium* research have also contributed to this Research Topic. Khan and Witola discuss the urgent need for effective anti-*Cryptosporidium* drugs, as the current FDA-approved drug nitazoxanide has limited efficacy in immunodeficient patients, young children, and neonatal livestock. The authors provide an overview of past and present pharmacotherapy in humans and animals for *Cryptosporidium* infections, highlighting progress in the field and discussing various strategies employed for discovering and developing effective treatments for cryptosporidiosis. Dong et al. conducted a study on *Cryptosporidium*-infected and healthy yaks, analyzing 16S rRNA sequencing and short-chain fatty acid (SCFA) concentrations. The results revealed significant differences in the abundance of phyla, genera, enzymes, and pathways between the two groups. Infected yaks also showed notably lower concentrations of various SCFAs. The study suggests that *Cryptosporidium* infection leads to gut dysbiosis and a decrease in SCFA concentrations, offering potential insight for preventing and treating diarrhea in livestock. Li et al. conducted a meta-analysis of 35 articles published before 2021 to determine the global prevalence of *Cryptosporidium* in Equus animals, finding an overall prevalence rate of 7.59%. Higher rates were observed in younger and female animals, with the highest prevalence in scale breeding Equus. *C. muris* was the most common genotype detected, and low altitude, rainy, humid, and tropical climates were associated with higher prevalence rates. To reduce infection, farmers should focus on managing young and female Equus animals, improving water filtration systems, reducing stocking densities, and treating livestock manure.

A study on *Leishmania* was contributed by Khanra et al. They examined three clinical isolates to identify common features in genetically diverse antimony (Sb)-resistant *Leishmania* parasites. The research found that resistant isolates had significantly higher intracellular thiol content and expression of thiol-synthesis genes compared to sensitive isolates. Additionally, resistant isolates had increased expression of Sb-reducing enzymes and Sb transporter genes. This study suggests that diverse Sb-resistant parasites develop a resistant phenotype by enhancing thiol synthesis and Sb transporter gene expression.

In summary, this Research Topic has provided valuable insight into recent advancements in the study of apicomplexan parasites,

each of which warrants further investigation to improve both human and animal health outcomes.

Author contributions

ML organized and wrote the editorial. NX, WW and KL revised it. All authors contributed to the article and approved the submitted version.

Funding

This work was supported by the National Natural Science Foundation of China (32102692), and the Shanxi key lab. for modernization of TCVM (SXKL2022004).

Conflict of interest

The authors declare that the research was conducted in the absence of any commercial or financial relationships that could be construed as a potential conflict of interest.

Publisher's note

frontiers | Frontiers in Cellular and Infection Microbiology

TYPE Original Research
PUBLISHED 12 September 2022
DOI 10.3389/fcimb.2022.1002817

OPEN ACCESS

EDITED BY
Kun Li,
Nanjing Agricultural University, China

REVIEWED BY
Jian Du,
Anhui Medical University, China
Shuai Wang,
Xinxiang Medical University, China
Shannon Moonah,
University of Virginia, United States

*CORRESPONDENCE
Hua Cong
conghua@sdu.edu.cn
Yi Qu
yiqucn@sdu.edu.cn

SPECIALTY SECTION
This article was submitted to Parasite and Host, a section of the journal Frontiers in Cellular and Infection Microbiology

RECEIVED 25 July 2022
ACCEPTED 24 August 2022
PUBLISHED 12 September 2022

CITATION
Zhang Y, Zhang Q, Li H, Cong H and Qu Y (2022) *In vitro* and *in vivo* anti–toxoplasma activities of HDAC inhibitor Panobinostat on experimental acute ocular toxoplasmosis. *Front. Cell. Infect. Microbiol.* 12:1002817. doi: 10.3389/fcimb.2022.1002817

In vitro and *in vivo* anti–*Toxoplasma* activities of HDAC inhibitor Panobinostat on experimental acute ocular toxoplasmosis

Yu Zhang[1], Qingqing Zhang[1], Haiming Li[1], Hua Cong[2]* and Yi Qu[1]*

[1]Department of Geriatrics, Qilu Hospital of Shandong University, Jinan, China, [2]Department of Pathogen Biology, School of Basic Medical Sciences, Cheeloo College of Medicine, Shandong University, Jinan, China

Ocular toxoplasmosis (OT) is retinochoroiditis caused by *Toxoplasma gondii* infection, which poses a huge threat to vision. However, most traditional oral drugs for this disease have multiple side effects and have difficulty crossing the blood-retinal barrier, so the new alternative strategy is required to be developed urgently. Histone deacetylases (HDAC) inhibitors, initially applied to cancer, have attracted considerable attention as potential anti-*Toxoplasma gondii* drugs. Here, the efficacy of a novel HDAC inhibitor, Panobinostat (LBH589), against *T. gondii* has been investigated. *In vitro*, LBH589 inhibited the proliferation and activity of *T. gondii* in a dose-dependent manner with low toxicity to retinal pigment epithelial (RPE) cells. *In vivo*, optical coherence tomography (OCT) examination and histopathological studies showed that the inflammatory cell infiltration and the damage to retinal architecture were drastically reduced in C57BL/6 mice upon treatment with intravitreal injection of LBH589. Furthermore, we have found the mRNA expression levels of inflammatory cytokines were significantly decreased in LBH589–treated group. Collectively, our study demonstrates that LBH589 holds great promise as a preclinical candidate for control and cure of ocular toxoplasmosis.

KEYWORDS

ocular toxoplasmosis, HDAC inhibitor, anti-*Toxoplasma gondii*, therapy, ocular inflammation, intravitreal injection

Introduction

Toxoplasma gondii, a protozoan of the Apicomplexa Phylum, is a highly infectious obligate intracellular parasite (Khosravi et al., 2020). Ocular toxoplasmosis is an inflammatory disease caused by intraocular infection with *T. gondii* (Garweg, 2016). When tachyzoites cross the blood retinal-barrier and access to

the retina, they may infect any nucleated host cells, causing tissue damage and visual impairment (Jones et al., 2017). The typical manifestation of acute disease is usually unilateral necrotizing retinochoroiditis accompanied by severe vitritis (Patel and Vavvas, 2022). In addition, other ocular atypical manifestations and complications include anterior uveitis, cataract, retinal neuritis, scleritis and retinal detachment (Kalogeropoulos et al., 2022). Toxoplasmosis has been proposed to be a leading cause of retinal infection, accounting for 20-60% of the total cases of posterior uveitis worldwide (Fabiani et al., 2022). The incidence rate of OT is about 2% in clinically diagnosed cases of *T. gondii* infection (Kijlstra and Petersen, 2014).

Currently, the clinical treatment of *T. gondii* infection is generally a systematic combination of several oral antimicrobials that target the parasite such as pyrimethamine and sulfadiazine (Feliciano-Alfonso et al., 2021). However, many patients with ocular toxoplasmosis manifest with ocular symptoms alone but systemic symptoms are not obvious. The current problem caused by traditional medication lies in the side effects such as anemia and visceral toxicity; on the other hand, it is difficult for most drugs to cross the blood-retinal barrier to reach effective drug concentration in the eye, leading to the result: the disease cannot be quickly controlled in the acute phase of the disease (Garweg and Pleyer, 2021). To overcome this predicament, there is a recognized necessity to develop new anti-*T. gondii* drugs and treatment strategies.

In recent years, HDAC inhibitors have been developed as an attractive class of targeted agents against cancers in recent years (McClure et al., 2018). However, these compounds have been revealed to induce hyperacetylation in histone and non-histone proteins in tumor cells, causing cell cycle arrest, senescence and apoptosis, and have promising clinical outcomes in hematological neoplasms (Bondarev et al., 2021). Notably, the latest research suggests HDAC inhibitors have been proposed as a potential alternative agent for protozoan infection such as *T. gondii* (Engel et al., 2015; Araujo-Silva et al., 2021). It has been demonstrated that these compounds are resistant to *T. gondii* mainly by controlling the acetylation status of histones, affecting the life cycle of *T. gondii* and leading to the destruction of the microstructure (Mouveaux et al., 2022; Jublot et al., 2022). However, there are relatively few evaluations of the therapeutic effect of HDAC inhibitors on local target organ infections such as OT.

In this study, we have investigated a novel HDAC inhibitor, LBH589, against the infection of *T. gondii*. *In vitro*, RPE cells were selected as host cells to evaluate the inhibitory effect of LBH589 on *T. gondii*. Notably, we have ascertained the LBH589's ability to control this disease by intravitreal injection, using a mouse model of acute OT. We hope that this study could provide new ideas for the treatment of OT.

Materials and methods

Parasites and cell culture

T. gondii tachyzoites of RH and RH-GFP strains were cultured and passaged in human foreskin fibroblast (HFF) cells. Tachyzoites were purified and quantified prior to infecting the cells and mice. Human retinal pigment epithelial cells (ARPE-19, FuHeng Biology, Shanghai, China) were serially cultured in 25 cm culture flasks, and the first 30 passages were used for experiments. All cells above were grown in Dulbecco's modified Eagle's medium (DMEM; Gibco™, USA) supplemented with 10% inactivated fetal bovine serum (FBS; Gibco™, Australia) and 1% penicillin-streptomycin (Solarbio, Beijing, China) at 37°C in sterile atmosphere containing 5% CO_2.

Histone deacetylases inhibitor

LBH589 (Selleck, Shanghai, China) was dissolved in dimethyl sulfoxide (DMSO; Solarbio, Beijing, China), and diluted subsequently in DMEM or phosphate-buffered saline (PBS; Meilunbio, Dalian, China) to different working concentrations for use. To prevent the toxic effects, the final concentration of DMSO should not exceed 0.01% in all experiments.

Cytotoxicity assay

RPE cells (5×10^3 cells/well) were seeded in 96-well plates and grown for 24 h. The medium containing different concentrations of LBH589 (10, 5, 2.5, 1.0, 0.75, 0.5, 0.25 μM) was changed. After the cells were treated with drugs for 48 h, 10 μl Cell Counting Kit-8 reagent (CCK-8; meilunbio, Dalian, China) was added to each well and incubated for 1 h at 37°C in a dark environment. Absorbance was measured at 450 nm by a microplate reader (Tecan, Nanjing, China) and statistical analysis was performed with Graphpad Prism 8 to calculate the 50% cytotoxic concentrations (CC50).

Antiproliferative assay

RPE cells were seeded in 24-well plate until a cell monolayer formed, and RH-GFP tachyzoites were added to each well at a ratio of 10:1 to cells. After 4 h of infection, drug-containing medium (750, 500, 250 nM) was replaced to each well and continued to maintain for 48 h. The proliferation of tachyzoites was observed by randomly selecting fields under the inverted fluorescence microscope (ZEISS, Germany). In order to better

observe the intracellular proliferation of parasite, the cells were infected with RH tachyzoites and treated with the drug (750, 375 nM) for 48 h. Staining according to Wright-Giemsa Stain solution instruction (Solarbio, Beijing, China), random fields of view were selected under light microscope for observation. The image data obtained in the experiment were analyzed with image-J.

Plaque assay

Free RH tachyzoites were purified and pretreated with LBH589 (750, 375 nM) for 8 h, then confluent monolayers of RPE cells in 12-well plate were infected with tachyzoites (500/well) for 10 days. The plate was stained according to the instructions of Crystal Violet Staining Solution (Beyotime, Shanghai, China) and visualized under microscope. Statistical analysis of the number and size of all plaques was performed with image-J.

mRNA expression analysis by using quantitative real-time reverse transcription-polymerase chain reaction (qRT-PCR)

Total RNA was extracted from mouse eyes and cell lines using an RNAfast 200 total RNA rapid extraction kit (Feijie Biotechnology, Shanghai, China). After the quantity and purity were determined by NanoDrop 2000 (Thermo, Shanghai, China), 1 μg of total RNA was used to generate cDNA by miDETECT A Track miRNA qRT-PCR Starter Kit (RiboBio, Guangzhou, China). Quantitative RT-PCR analysis was performed using Blaze Taq™ SYBR Green qPCR Mix 2.0 (GeneCopoeia, Guangzhou, China) to detect the mRNA levels of interleukin (IL)-1β, IL-6, IL-8, granulocyte-macrophage colony-stimulating factor (GM-CSF), and tumor necrosis factor (TNF)-α. Primers used for qRT-PCR are listed in Table 1. The relative mRNA expression of each target gene was normalized to that of the housekeeping gene β-actin and GAPDH, and the result was fold-changed compared to the blank control group (set to 1).

Effect of LBH589 on the *T. gondii* ultrastructure by transmission electron microscopy

The RPE cells were inoculated into a 75 cm culture flask and infected with tachyzoites at a ratio of 10:1 parasites/cells. LBH589 (750 nM) was added and the treatment was continued for additional 48 h. The cells were harvested and preserved in TEM fixative at least 24 h for agarose pre-embedding. After 2 h of post-fixation in 1% OsO_4, the samples were dehydrated in a gradient at room temperature and then osmotically embedded for sectioning. The tissue sections were stained with 2% uranium acetate saturated alcohol solution and images were collected by transmission electron microscope (TEM, Hitachi, Tokyo, Japan).

Animal model of ocular toxoplasmosis

C57BL/6 female mice (PengYue, Jinan, China), 6-8 weeks, were used for the ocular model of *T. gondii* infection. After the pupils of the anesthetized mice were dilated, the eyes were observed under a surgical microscope and a tiny incision was made 1 mm behind the limbus. Free tachyzoites (4000/2 μl) were injected through a Hamilton syringe into the vitreous, making sure that the tip does not damage the lens or retina (Smith et al., 2020). At 12 h after infection, the treatment group was injected with different doses of LBH589 (1, 2, 3 ng/μl) *via* intravitreal injection, and the infection group was injected with an equal volume of PBS. One week post injection, mouse eyes were subjected to follow-up experiments. All experiments involving

TABLE 1 The primer Sequences of genes.

Gene	Sequences (5'-3')	
	Forward primer	Reverse primer
Mus-IL-1β	GTGTCTTTCCCGTGGACCTT	AATGGGAACGTCACACACCA
Mus-IL-6	CTTCTTGGGACTGATGCTGGT	CTCTGTGAAGTCTCCTCTCCG
Mus-TNF-α	AGCCGATGGGTTGTACCTTG	ATAGCAAATCGGCTGACGGT
Mus-GAPDH	TGTCTCCTGCGACTTCAACA	GGTGGTCCAGGGTTTCTTACT
Homo-GM-CSF	AGCCCTGGGAGCATGTGAAT	GCAGCAGTGTCTCTACTCAGG
Homo-IL-1β	CAACAAGTGGTGTTCTCCATGTC	ACACGCAGGACAGGTACAGA
Homo-IL-6	CAATGAGGAGACTTGCCTGGT	GCAGGAACTGGATCAGGACT
Homo-IL-8	CTCTGTGTGAAGGTGCAGTTTT	GTTTTCCTTGGGGTCCAGACA
Homo-β-actin	GAAGAGCTACGAGCTGCCTGA	CAGACAGCACTGTGTTGGCG

mice in this study were approved by Laboratory Animal Ethical and Welfare Committee of Shandong University Cheeloo College of Medicine.

Clinical investigations

One week after the intervention, the retinal structure of the anesthetized mice was assessed by spectral-domain optical coherence tomography (SD-OCT) using the RTVue XR Avanti devices (Optovue Inc, Fremont, CA, USA). The acquired image format was saved in a Tag Image File Format (TIFF) for analysis.

Histopathology

Mouse eyeballs were taken immediately after euthanasia and fixed with eye fixative for 24 h. The tissue was then embedded in paraffin and cut into 4-μm-thick sections for hematoxylin and eosin (HE) staining. Sections were viewed for signs of pathology under a light microscope.

Statistical analysis

Data in all experiments were analyzed and graphed using GraphPad Prism 8.0 unless otherwise stated. Each experiment was repeated independently three times. Data are presented as means ± SD. Student's *t*-test was used to determine the statistical significance of the two-group comparison. Data results with $P < 0.05$ were indicated statistically significant.

Results

Toxicity of LBH589 on RPE cells

To determine a safe drug concentration *in vitro*, we initiated experiments with RPE cells using different concentrations of the drug. The analysis of the results showed that the CC50 of the LBH589 on RPE cells was 8325.33 ± 407.18 nM for 48 h of treatment (Table 2). When the final concentration was less than 750 nM, LBH589 had no significant effect on cells viability (Figure 1).

Antiproliferative effect of LBH589 against tachyzoites *in vitro*

According to the experimental results, tachyzoites exhibited dose-dependent proliferation rate inhibition after LBH589 treatment for 48 h. 50% inhibiting concentration (IC50) of the parasite growth was 424.41 ± 48.07 nM. The drug concentration at 750 nM inhibited the proliferation rate by nearly 90% and showed no obvious toxic effect on cells (Figures 1, 2A). Besides, the LBH589 selectivity index (CC50/IC50) was 19.62, which indicated the cellular safety of LBH589 in inhibiting the proliferation of *T. gondii* (Table 2). The Giemsa staining experiment also found that there were no obvious parasitophorous vacuoles in the cells under the drug concentration of 750 nM (Figure 2B). These data confirmed that strong inhibitory effect of LBH589 on *T. gondii* proliferation.

Antiparasitic activity of LBH589 *in vitro*

To verify whether LBH589 affects parasite viability by plaque assay, we found that the size and number of plaques decreased after *T. gondii* pre-treatment within the safe concentrations of LBH589. As the drug concentration increased, the reduction of parasites was more significant compared to the control group. The number and plaque area of parasites pretreated with LBH589 (750 nM) were reduced by approximately 90% and 92%, respectively (Figure 2C).

Expressions of GM-CSF, IL-1β, IL-6 and IL-8 genes in the *T. gondii*-infected and treated cells

The results revealed that compared with the control, the mRNA expression levels of GM-CSF ($P < 0.01$), IL-1β ($P < 0.01$), IL-6 ($P < 0.01$) and IL-8 ($P < 0.05$) were significantly increased in the *T. gondii*-infected group. When infected cells were treated with LBH589 at a concentration of 750 nM, levels of GM-CSF (30.19-fold, $P < 0.01$), IL-1β (7.64-fold, $P < 0.001$), IL-6 (16.78-fold, $P < 0.01$) and IL-8 (3.68-fold, $P < 0.05$) were decreased compared with the infected group (Figure 3).

TABLE 2 Selective Indexes for RPE cells after treatment with LBH589 for 48 h.

Compound	tachyzoite of RH	RPE cell	SI (Selective Index)
	IC50 (nM)	CC50 (nM)	(CC50/IC50)
LBH589	424.41 ± 48.07	8325.33 ± 407.18	19.62

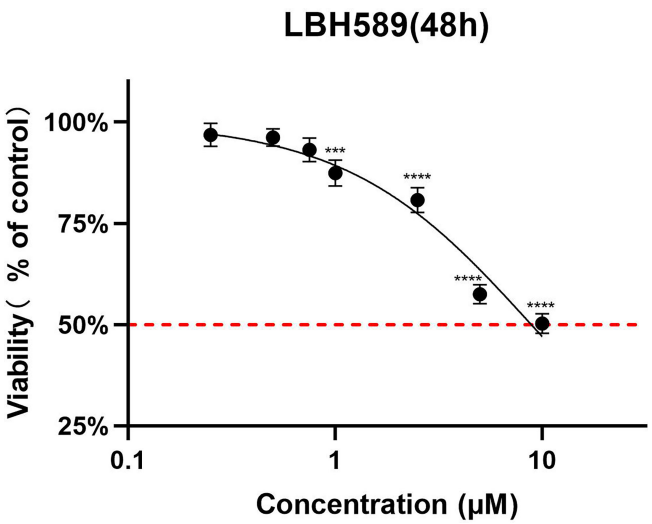

FIGURE 1
Cell toxicity assay of LBH589 on RPE cells for 48h of incubation. To determine a safe drug concentration *in vitro*, RPE cells were treated with different concentrations of drugs. RPE cells treated with DMEM were used as a control. Data are expressed as percent inhibition of cell viability relative to the control. ****$P < 0.001$, ***$P < 0.0001$ in comparison with the control. The experiment was repeated three times, with three wells of each sample.

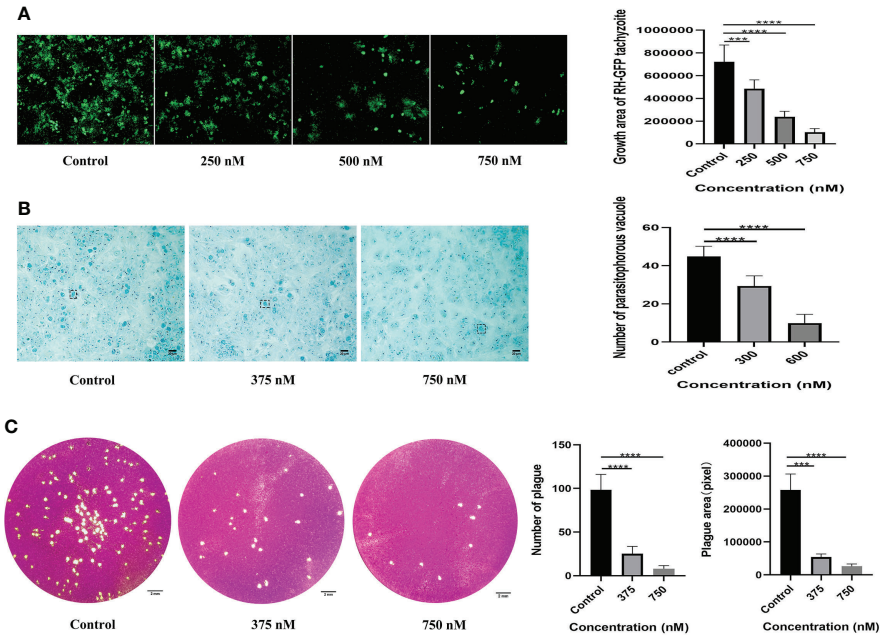

FIGURE 2
Assessing the effect of LBH589 on the proliferation and activity of *T. gondii*. Infected cells cultured with DMEM were used as negative controls. **(A)** The fluorescence area shows the proliferation of *T. gondii* after incubation with different concentrations of drugs for 48 h. **(B)** The number of intracellular parasitophorous vacuole in the treated and infected groups. **(C)** Comparing the overall growth of parasites in the infection group to that of the treatment group *via* plaque assay. ***$P < 0.001$, ****$P < 0.0001$, in comparison with the control. Scale bars: B = 20 μm; C= 2 mm. Each experiment was repeated three times, with three wells of each sample.

Ultrastructural changes in intracellular *T. gondii* tachyzoites

After 24 h incubation with LBH589, the tachyzoites showed disorder of organizational structure. TEM findings showed mitochondrial swelling, vacuole formation, damaged plasmalemma and vacuolar membrane (Figure 4B). LBH589 treatment of the parasites for 48 h caused abundant empty vacuolization in cytoplasm. Besides, the cytoplasmic structure, plasmalemma and vacuolar membranes of tachyzoites had completely disappeared (Figure 4D). However, typical morphology and cytological features of tachyzoite were maintained completely incubated in the absence of LBH589 (Figures 4A, C).

Retinal structure in OCT investigation

We determined whether intravitreal injection of LBH589 affects the intraocular conditions of mice by OCT examination. There were no significant changes on the retinal structure with 1ng of LBH589, but when the dose exceeded 2 ng injected into the eye, it caused varying degrees of vitreous opacity that was not observed in normal mice (Figure 5A). In OCT sets of the infected group, hyper-reflective tiny dots abutting the optic nerve head (papillitis) and floating in vitreous cavity above posterior hyaloid face (vitritis) were clearly observed (Figure 5B). In addition, the hyper-reflectivity foci accompanied by blurring of details in inner retina, disorganizing of retinal layers and serous retinal detachment were common. The degree of vitreous opacity and the size of the lesion of the subretinal fluid were significantly reduced in most animals treated with LBH589. Moreover, the retinal structure was more complete, the damage site was relatively limited and the surrounding structures of the lesion can be clearly distinguished (Figures 5B, C).

Retinal structure in histology analysis

Through histopathological examination, the intravitreal injection of tachyzoites caused a heavy inflammatory infiltrate involving peripapillary retina and the optic nerve head, leading to destruction of normal retinal structure. But the infiltration of inflammatory cells was alleviated and the retinal structure was relatively intact in the treatment group. Besides, there was no obvious abnormality in retinal structure for the intravitreal injection of LBH589 alone compared with the control group (Figure 6).

Expressions of TNF-α, IL-1β and IL-6 genes in the untreated and treated mice

Combined with previous literature reports, we selected several factors that were highly expressed in infected mice (Nagineni et al., 2000; Zhang et al., 2019). Compared with the control, the expression levels of TNF-α ($P < 0.01$), IL-1β ($P < 0.001$) and IL-6 ($P < 0.001$) were significantly increased at 1 week after infection. Compared with the untreated mice, the mRNA expression levels of pro-inflammatory cytokines TNF-α (1.58-fold, $P < 0.05$), IL-1β (1.67-fold, $P < 0.001$) and IL-6 (1.92-fold, $P < 0.001$) were significantly down-regulated in the treated group (Figure 7).

Discussion

Ocular toxoplasmosis, as an infectious disease, often causes damage to the retinal structure during the acute phase, especially for immunocompromised patients. In addition, many patients are healthy adults with only ocular symptoms and no specific general symptoms prior to onset (Ozgonul and Besirli, 2017). The classic clinical treatment is the combined application of

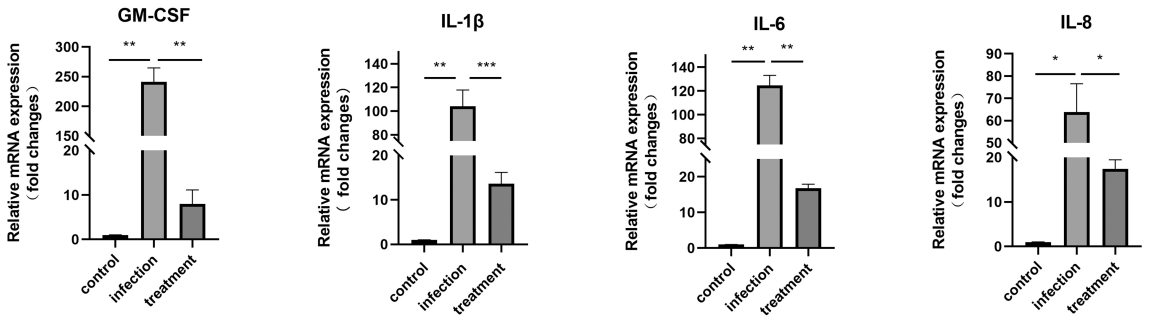

FIGURE 3
mRNA expression of GM-CSF, IL-1β, IL-6 and IL-8 in *T. gondii*-infected RPE cells was verified by qRT-PCR after 48 h of LBH589 treatment. Normal RPE cells served as the control. *$P < 0.05$, **$P < 0.01$, ***$P < 0.001$. Each experiment was repeated independently three times, with three wells of each sample.

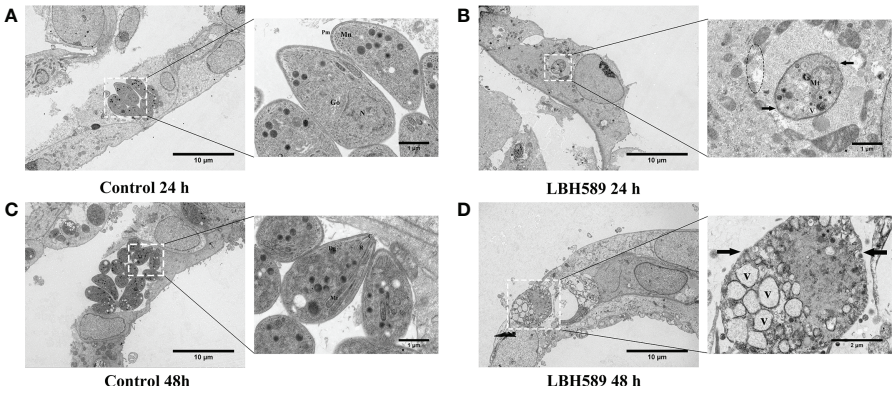

FIGURE 4
Ultrastructural alterations of tachyzoites internalized in RPE cells after LBH589 treatment at 750 nM by TEM. **(A, C)** Untreated parasites in RPE cells (set as the control) present normal morphology at both 24 and 48 h, the inset shows the typical ultrastructure, including the conoid (C), microneme (Mn), rhoptry (R), plasmalemma (Pm), dense granule (Dg), mitochondrion (Mt), golgi apparatus (G), and nucleus (N). **(B)** Exposure to LBH589 for 24 h induced unusual microstructural changes, such as mitochondrial swelling, vacuole (V), disruption of plasmalemma (black arrow) and vacuolar membranes (black circle). **(D)** After 48 h of incubation with LBH589, the parasites lost their biological features and the cytoplasmic structure was almost completely destroyed. Scale bars: A, B, C and D = 10 μm; A, B and C insets = 1 μm, D inset = 2 μm. The experiments were performed in triplicate, in three independent experiments.

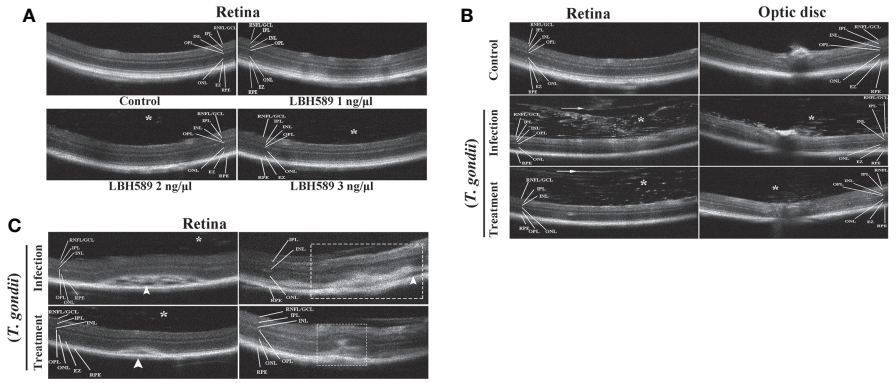

FIGURE 5
Clinical evaluation of vitreous cavity and retina structure after intravitreal injection of LBH589 by OCT. Normal mice were set as controls. **(A)** Scattered hyper-reflected signals (asterisk) are observed in the vitreous from intravitreal LBH589-injected (≥ 2 ng/1 μl) eyes. **(B, C)** Changes in the structure of retina and vitreous cavity of *T. gondii*-infected and LBH589-treated mice. The changes show dense hyper-reflective tiny dots (asterisk), posterior vitreous detachment (white arrow), serous retinal detachment (white arrowhead), blurred full thickness retinal, hyper-reflectivity foci and disorganized of retinal layers (white rectangle). Data are representative of results obtained from six mice in each group.

pyrimethamine and sulfadiazine (P-S). Trimethoprim and sulfamethoxazole (TMP-SMX) can also be used as alternative therapy and other optional drugs include clindamycin, azithromycin and atovaquone (Dunay et al., 2018). The major difficulty is that oral medication needs 4-6 weeks to control the disease, which may cause side effects such as anemia, myelosuppression and drug toxicity (Garweg and Pleyer, 2021). Besides, the existence of the blood-retinal barrier restricts the entry of most drugs into the eye.

During the development of anti-*T. gondii* drugs, HDAC inhibitors have been discovered as a potential drug (Jublot et al., 2022). The previous research has shown that anti-*T. gondii* effect of several HDAC inhibitors such as scriptaid, tubastatin A and suberoylanilide hydroxamic acid in HFF cells (Araujo-Silva et al., 2021). In our study, we have evaluated the anti-*T. gondii* and therapeutic effect of LBH589 on OT for the first time, which was mainly used in cutaneous T-cell lymphoma (CTCL), Hodgkin's lymphoma as well as acute myeloid leukemia

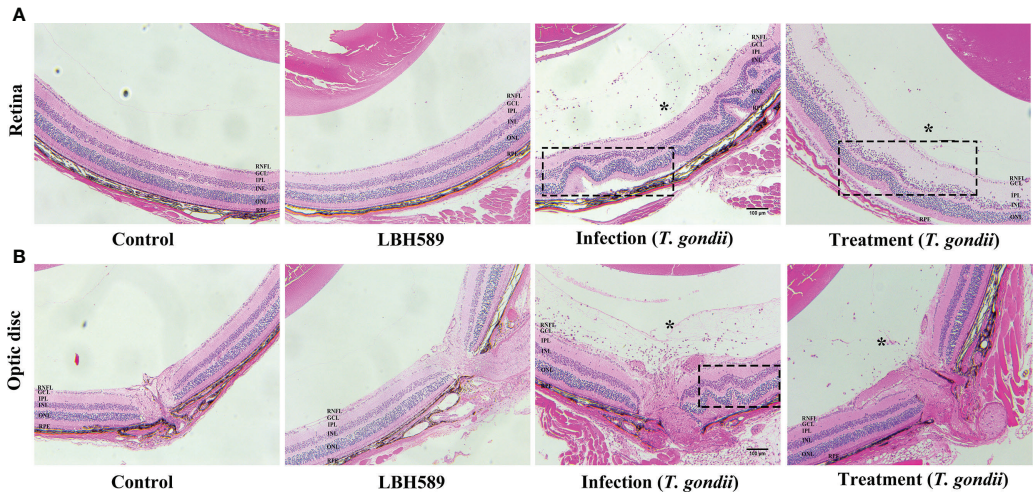

FIGURE 6
Histological changes of mice eyes. Compared with the control, histological retinal **(A)** and optic disc **(B)** changes in the eyes of LBH589-injected, tachyzoites-infected and LBH589-treated mice at 7 dpi such as inflammatory cell infiltrate (asterisk), retinal folding and destruction of retinal architecture (black rectangle). The retinal structure of normal mice injected with LBH589 alone was not significantly abnormal compared with the control. Scale bars: **(A, B)** = 100 μm. Data are representative of results obtained from six mice in each group.

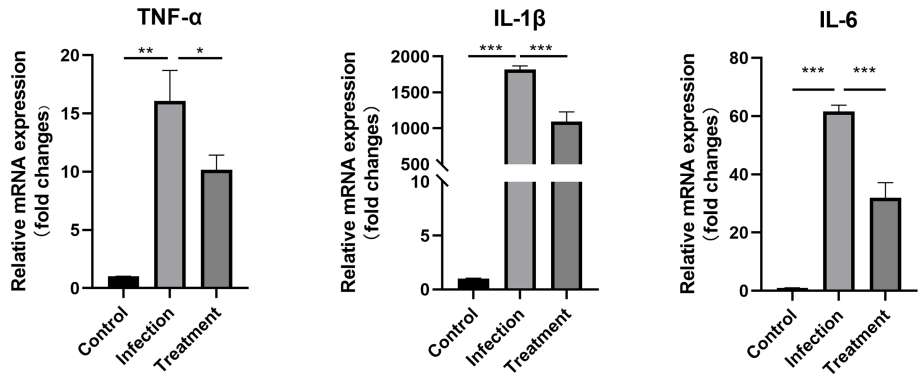

FIGURE 7
The differential mRNA expressions of TNF-α, IL-1β and IL-6 in the eyes of the control, tachyzoites-infected and LBH589-treated mice were measured by qRT-PCR. *$P < 0.05$, **$P < 0.01$, ***$P < 0.001$, the infection group versus the treatment group. The experiments were performed in triplicate, in three independent experiments.

(AML) in preclinical research (Prince et al., 2009; Schroder et al., 2021; Chen et al., 2022). According to the pathogenesis of OT, retinal pigment epithelium has been identified to be the primary target for *T. gondii* infection within the eye (Smith et al., 2021). Unlike previous studies, we therefore selected RPE cells as host cell for subsequent vitro experiments. After 48 h of treatment, LBH589 was shown to inhibit proliferation of tachyzoites in a dose-dependent manner at concentrations ranging from 250 to 750 nM. According to the results of cytotoxicity assay, a selective index of 19.62 was achieved, and we have ensured the low toxicity of LBH589 to RPE cells in this concentration range. In addition, the activity of tachyzoites was significantly weakened after drug pretreatment *via* plaque assay. Therefore, these data preliminarily proved the inhibitory effect of LBH589 on *T. gondii in vitro*.

Five genes of HDAC class I/II (TgHDAC 1-5) have been found in *T. gondii*, which are responsible for the life cycle (Vanagas et al., 2012). In previous studies, it was found that

HDAC inhibitors affect the cell division of *T. gondii* by regulating the acetylation state of histones H3 and H4, which cause damage to cell morphology and microstructure such as acroplasts, mitochondria and nucleus (Mouveaux et al., 2022). Moreover, HDAC inhibitors are capable of causing alterations in cytoskeletal protein such as a decrease in the α-tubulin amount, leading to the formation of masses of damaged parasites (Araujo-Silva et al., 2021). Our transmission electron microscopy also showed a severe damage on parasite pellicle and intracellular organelles such as the presence of nuclear fragmentation, mitochondrion swollen, plasma membrane rupture, a loss of crescent shape and ultimately complete destruction of the structure after treatment. Combined with the results of above experiment, LBH589 may have the ability to cause damage to the cellular structure of parasite by diffusing through the host cell plasma membrane and the parasitophorous vacuole.

In addition, during *T. gondii* infection, RPE cells were proved to enhance the release of proinflammatory cytokines, thereby inducing neutrophils to produce ROS, TNF-α and IL-1β, which further aggravated the tissue damage (Ashander et al., 2019; Zhang et al., 2019; Raouf-Rahmati et al., 2021). Our study has also revealed that after infection of RPE cells with parasites, mRNA expression of GM-CSF, IL-1β, IL-6 and IL-8 showed a statistical increase. 48 h after treatment, infected RPE cells significantly reduced the mRNA expression of four pro-inflammatory factors. The reason for this phenomenon may be that LBH589 inhibits the proliferation of tachyzoites and thus weakens the stimulation of cells.

In the animal model, we induced acute ocular toxoplasmosis by intraocular injection of tachyzoites. It has been reported that the advantage of this method is that it can breach ocular immune privilege and rapidly induces vitritis and retinitis before the onset of systemic disease in mice (Dunay et al., 2018; Smith et al., 2020). In terms of treatment, the general principle of the therapy is to inhibit parasites proliferation, immediately control the inflammatory response, and mitigate tissue damage to protect retina during acute infection (Casoy et al., 2020). Intravitreal injection can limit systemic side effects, increase intraocular drug concentration and enhance the treatment effect in a short time to control the disease, receiving a lot of attention in the research of infectious diseases (Ozgonul and Besirli, 2017). Prospective randomized trial of intravitreal injection of clindamycin has been found to have a better therapeutic effect than oral administration (Baharivand et al., 2013). Therefore, we also selected this method to evaluate the therapeutic effect of LBH589 instead of intraperitoneal injection or oral gavage. In order to minimize the secondary damage to the mouse's eyes and set aside time for *T. gondii* infection, mice were injected with LBH589 into the eyes 12 h after infection with *T. gondii*, and performed clinical evaluation on the 7th day when the ocular symptoms of the mice were most obvious (LaGrow et al., 2017; Lafreniere et al., 2019; Kishimoto et al., 2019; Smith et al., 2020). Here, we first adopted the ophthalmic imaging diagnostic technology, OCT examination, which can directly non-invasive assessment of intraocular lesion in living mice (Cunningham et al., 2022). In the infection group, most of the mice developed severe vitreous, subretinal fluid, posterior vitreous detachment and disorder of retinal structure (Chen et al., 2016; Brandao-de-Resende et al., 2020; Ksiaa et al., 2022), while the symptoms were relatively mild with LBH589 treatment. In addition, we set a drug dose gradient of 1 to 3 ng/μl based on the previous study about pharmacokinetics of LBH589 to avoid the toxicity of drugs to the retina (Van Veggel et al., 2018; Karol et al., 2020; Homan et al., 2021). Though the OCT results found that when the drug concentration was greater than 1 ng, vitreous opacity occurred in the eyes of mice, which was easily confused with the symptoms caused by infection, but the retinal results were not significantly abnormal. At the drug concentration of 1ng, the result showed no obvious difference compared with the control. The reason may be caused by fine drug particles or effect of drug solubility.

However, acute ocular toxoplasma usually causes vitreous opacity or complicated cataract, leading to opacity of the refractive medium, which make it difficult for OCT examination to obtain high-quality images. Subsequently, histopathological studies also showed that the inflammatory cell infiltration and the damage to retinal architecture were drastically reduced upon treatment with LBH589. Retinal structure of uninfected mice injected with LBH589 alone showed no obvious abnormality. Combined with OCT examination and histopathology, we infer that LBH589 can play a certain role in the treatment of ocular toxoplasmosis *in vivo*.

Moreover, one of the reasons for the destruction of tissue structure is the excessive production of inflammatory cytokines (Zhang et al., 2019; Smith et al., 2021). HDAC inhibitors vorinostat, butyrate and tubastatin A showed promising therapeutic potential in the treatment of inflammatory diseases such as rheumatoid arthritis, asthma, contact hypersensitivity and inflammatory bowel diseases, due to their ability to regulate inflammatory cells and cytokines through several G protein–coupled receptors (GPCRs) (Ran and Zhou, 2019; Li et al., 2021; Ni et al., 2021). We found that the mRNA expression levels of TNF-α, IL-1β and IL-6 were significantly increased after 7 days of infection, while the expression of the three inflammatory factors was decreased upon intraocular injection of LBH589. Combined with cell experiments, we infer that LBH589 has a certain anti-inflammatory ability as well as the ability to inhibit the proliferation of *T. gondii*. Though our data can prove that LBH589 has potential therapeutic effect on ocular toxoplasmosis, pharmacokinetics and mechanism of action of the LBH589 in the eye need to be studied further.

In summary, our research demonstrated that LBH589 can effectively inhibit the proliferation and activity of *T. gondii* in RPE cells. And the microstructure of *T. gondii* was significantly damaged, we speculated that LBH589 should have the ability to penetrate host cell plasma membrane and directly damage *T. gondii*. *In vivo*, we established a mouse model of acute OT, and

combined with OCT examination and pathological sections to evaluate the therapeutic effect of intravitreal injection of LBH589. In addition, LBH589 treatment can also reduce mRNA expression levels of inflammatory cytokines. However, pharmacokinetics and the underlying mechanism of LBH589 still warrants further exploration.

Data availability statement

The original contributions presented in the study are included in the article/supplementary material. Further inquiries can be directed to the corresponding authors.

Ethics statement

The animal study was reviewed and approved by Laboratory Animal Ethical and Welfare Committee of Shandong University Cheeloo College of Medicine.

Author contributions

YQ revised the manuscript. HC directed the project. YZ supervised the experiments and wrote the manuscript. QZ and HL conducted the experiments. All authors contributed to the article and approved the submitted version.

Acknowledgments

We thank Dr. Bing Han and Dr. Huaiyu Zhou for providing the *T. gondii* strain and HFF cells and Dr. Chunxue Zhou for the experimental operation guidance.

Conflict of interest

The authors declare that the research was conducted in the absence of any commercial or financial relationships that could be construed as a potential conflict of interest.

Publisher's note

All claims expressed in this article are solely those of the authors and do not necessarily represent those of their affiliated organizations, or those of the publisher, the editors and the reviewers. Any product that may be evaluated in this article, or claim that may be made by its manufacturer, is not guaranteed or endorsed by the publisher.

References

Araujo-Silva, C. A., De Souza, W., Martins-Duarte, E. S., and Vommaro, R. C. (2021). HDAC inhibitors tubastatin a and SAHA affect parasite cell division and are potential anti-toxoplasma gondii chemotherapeutics. *Int. J. Parasitol. Drugs Drug Resist.* 15, 25–35. doi: 10.1016/j.ijpddr.2020.12.003

Ashander, L. M., Lie, S., Ma, Y., Rochet, E., Washington, J. M., Furtado, J. M., et al. (2019). Neutrophil activities in human ocular toxoplasmosis: An *in vitro* study with human cells. *Invest. Ophthalmol. Vis. Sci.* 60, 4652–4660. doi: 10.1167/iovs.19-28306

Baharivand, N., Mahdavifard, A., and Fouladi, R. F. (2013). Intravitreal clindamycin plus dexamethasone versus classic oral therapy in toxoplasmic retinochoroiditis: A prospective randomized clinical trial. *Int. Ophthalmol.* 33, 39–46. doi: 10.1007/s10792-012-9634-1

Bondarev, A. D., Attwood, M. M., Jonsson, J., Chubarev, V. N., Tarasov, V. V., and Schioth, H. B. (2021). Recent developments of HDAC inhibitors: Emerging indications and novel molecules. *Br. J. Clin. Pharmacol.* 87, 4577–4597. doi: 10.1111/bcp.14889

Brandao-de-Resende, C., Balasundaram, M. B., Narain, S., Mahendradas, P., and Vasconcelos-Santos, D. V. (2020). Multimodal imaging in ocular toxoplasmosis. *Ocul. Immunol. Inflammation* 28, 1196–1204. doi: 10.1080/09273948.2020.1737142

Casoy, J., Nascimento, H., Silva, L. M. P., Fernandez-Zamora, Y., Muccioli, C., Dias, J. R. O., et al. (2020). Effectiveness of treatments for ocular toxoplasmosis. *Ocul. Immunol. Inflammation* 28, 249–255. doi: 10.1080/09273948.2019.1569242

Chen, K. C., Jung, J. J., and Engelbert, M. (2016). Single acquisition of the vitreous, retina and choroid with swept-source optical coherence tomography in acute toxoplasmosis. *Retin. cases Brief Rep.* 10, 217–220. doi: 10.1097/ICB.0000000000000230

Chen, E., Liu, N., Zhao, Y., Tang, M., Ou, L., Wu, X., et al. (2022). Panobinostat reverses HepaCAM gene expression and suppresses proliferation by increasing histone acetylation in prostate cancer. *Gene* 808, 145977. doi: 10.1016/j.gene.2021.145977

Cunningham, E. T.Jr., Smit, D. P., and Zierhut, M. (2022). Imaging ocular toxoplasmosis. *Ocul. Immunol. Inflammation* 30, 525–526. doi: 10.1080/09273948.2022.2086395

Dunay, I. R., Gajurel, K., Dhakal, R., Liesenfeld, O., and Montoya, J. G. (2018). Treatment of toxoplasmosis: Historical perspective, animal models, and current clinical practice. *Clin. Microbiol. Rev.* 31(4), e00057-17. doi: 10.1128/CMR.00057-17

Engel, J. A., Jones, A. J., Avery, V. M., Sumanadasa, S. D., Ng, S. S., Fairlie, D. P., et al. (2015). Profiling the anti-protozoal activity of anti-cancer HDAC inhibitors against plasmodium and trypanosoma parasites. *Int. J. Parasitol. Drugs Drug Resist.* 5, 117–126. doi: 10.1016/j.ijpddr.2015.05.004

Fabiani, S., Caroselli, C., Menchini, M., Gabbriellini, G., Falcone, M., and Bruschi, F. (2022). Ocular toxoplasmosis, an overview focusing on clinical aspects. *Acta Trop.* 225, 106180. doi: 10.1016/j.actatropica.2021.106180

Feliciano-Alfonso, J. E., Munoz-Ortiz, J., Marin-Noriega, M. A., Vargas-Villanueva, A., Trivino-Blanco, L., Carvajal-Saiz, N., et al. (2021). Safety and efficacy of different antibiotic regimens in patients with ocular toxoplasmosis: systematic review and meta-analysis. *Syst. Rev.* 10, 206. doi: 10.1186/s13643-021-01758-7

Garweg, J. G. (2016). Ocular toxoplasmosis: An update. *Klin. Monbl. Augenheilkd* 233, 534–539. doi: 10.1055/s-0041-111821

Garweg, J. G., and Pleyer, U. (2021). Treatment strategy in human ocular toxoplasmosis: Why antibiotics have failed. *J. Clin. Med.* 10(5), 1090. doi: 10.3390/jcm10051090

Homan, M. J., Franson, A., Ravi, K., Roberts, H., Pai, M. P., Liu, C., et al. (2021). Panobinostat penetrates the blood-brain barrier and achieves effective brain concentrations in a murine model. *Cancer Chemother. Pharmacol.* 88, 555–562. doi: 10.1007/s00280-021-04313-2

Jones, E. J., Korcsmaros, T., and Carding, S. R. (2017). Mechanisms and pathways of toxoplasma gondii transepithelial migration. *Tissue Barriers* 5, e1273865. doi: 10.1080/21688370.2016.1273865

Jublot, D., Cavailles, P., Kamche, S., Francisco, D., Fontinha, D., Prudencio, M., et al. (2022). A histone deacetylase (HDAC) inhibitor with pleiotropic *In vitro* anti-toxoplasma and anti-plasmodium activities controls acute and chronic toxoplasma infection in mice. *Int. J. Mol. Sci.* 23(6), 3254. doi: 10.3390/ijms23063254

Kalogeropoulos, D., Sakkas, H., Mohammed, B., Vartholomatos, G., Malamos, K., Sreekantam, S., et al. (2022). Ocular toxoplasmosis: A review of the current diagnostic and therapeutic approaches. *Int. Ophthalmol.* 42, 295–321. doi: 10.1007/s10792-021-01994-9

Karol, S. E., Cooper, T. M., Mead, P. E., Crews, K. R., Panetta, J. C., Alexander, T. B., et al. (2020). Safety, pharmacokinetics, and pharmacodynamics of panobinostat in children, adolescents, and young adults with relapsed acute myeloid leukemia. *Cancer* 126, 4800–4805. doi: 10.1002/cncr.33156

Khosravi, M., Mohammad Rahimi, H., Doroud, D., Mirsamadi, E. S., Mirjalali, H., and Zali, M. R. (2020). *In vitro* evaluation of mannosylated paromomycin-loaded solid lipid nanoparticles on acute toxoplasmosis. *Front. Cell Infect. Microbiol.* 10. doi: 10.3389/fcimb.2020.00033

Kijlstra, A., and Petersen, E. (2014). Epidemiology, pathophysiology, and the future of ocular toxoplasmosis. *Ocul. Immunol. Inflammation* 22, 138–147. doi: 10.3109/09273948.2013.823214

Kishimoto, T., Ishida, W., Fukuda, K., Nakajima, I., Suzuki, T., Uchiyama, J., et al. (2019). Therapeutic effects of intravitreously administered bacteriophage in a mouse model of endophthalmitis caused by vancomycin-sensitive or -resistant enterococcus faecalis. *Antimicrob. Agents Chemother.* 63 (11), e01088–19. doi: 10.1128/AAC.01088-19

Ksiaa, I., Khochtali, S., Mefteh, M., Ben Fredj, M., Ben Amor, H., Abroug, N., et al. (2022). Distinguishing swept-source optical coherence tomography findings in active toxoplasmic retinochoroiditis. *Eye (Lond)* 36, 1222–1230. doi: 10.1038/s41433-021-01491-4

Lafreniere, J. D., Toguri, J. T., Gupta, R. R., Samad, A., O'Brien, D. M., Dickinson, J., et al. (2019). Effects of intravitreal bevacizumab in gram-positive and gram-negative models of ocular inflammation. *Clin. Exp. Ophthalmol.* 47, 638–645. doi: 10.1111/ceo.13453

LaGrow, A. L., Coburn, P. S., Miller, F. C., Land, C., Parkunan, S. M., Luk, B. T., et al. (2017). A novel biomimetic nanosponge protects the retina from the enterococcus faecalis cytolysin. *mShere.* 2(6), e00335-17. doi: 10.1128/mSphere.00335-17

Li, G., Lin, J., Zhang, C., Gao, H., Lu, H., Gao, X., et al. (2021). Microbiota metabolite butyrate constrains neutrophil functions and ameliorates mucosal inflammation in inflammatory bowel disease. *Gut Microbes* 13, 1968257. doi: 10.1080/19490976.2021.1968257

McClure, J. J., Li, X., and Chou, C. J. (2018). Advances and challenges of HDAC inhibitors in cancer therapeutics. *Adv. Cancer Res.* 138, 183–211. doi: 10.1016/bs.acr.2018.02.006

Mouveaux, T., Rotili, D., Boissavy, T., Roger, E., Pierrot, C., Mai, A., et al. (2022). A potent HDAC inhibitor blocks toxoplasma gondii tachyzoite growth and profoundly disrupts parasite gene expression. *Int. J. Antimicrob. Agents* 59, 106526. doi: 10.1016/j.ijantimicag.2022.106526

Nagineni, C. N., Detrick, B., and Hooks, J. J. (2000). Toxoplasma gondii infection induces gene expression and secretion of interleukin 1 (IL-1), IL-6, granulocyte-macrophage colony-stimulating factor, and intercellular adhesion molecule 1 by human retinal pigment epithelial cells. *Infect. Immun.* 68, 407–410. doi: 10.1128/IAI.68.1.407-410.2000

Ni, D. X., Wang, Q., Li, Y. M., Cui, Y. M., Shen, T. Z., Li, X. L., et al. (2021). Synthesis of nigranoic acid and manwuweizic acid derivatives as HDAC inhibitors and anti-inflammatory agents. *Bioorg. Chem.* 109, 104728. doi: 10.1016/j.bioorg.2021.104728

Ozgonul, C., and Besirli, C. G. (2017). Recent developments in the diagnosis and treatment of ocular toxoplasmosis. *Ophthalmic. Res.* 57, 1–12. doi: 10.1159/000449169

Patel, N. S., and Vavvas, D. G. (2022). Ocular toxoplasmosis: A review of current literature. *Int. Ophthalmol. Clin.* 62, 231–250. doi: 10.1097/IIO.0000000000000419

Prince, H. M., Bishton, M. J., and Johnstone, R. W. (2009). Panobinostat (LBH589): A potent pan-deacetylase inhibitor with promising activity against hematologic and solid tumors. *Future Oncol.* 5, 601–612. doi: 10.2217/fon.09.36

Ran, J., and Zhou, J. (2019). Targeted inhibition of histone deacetylase 6 in inflammatory diseases. *Thorac. Cancer* 10, 405–412. doi: 10.1111/1759-7714.12974

Raouf-Rahmati, A., Ansar, A. R., Rezaee, S. A., Hosseini, S. M., Garweg, J. G., Ghezeldasht, S. A., et al. (2021). Local and systemic gene expression levels of IL-10, IL-17 and TGF-beta in active ocular toxoplasmosis in humans. *Cytokine* 146, 155643. doi: 10.1016/j.cyto.2021.155643

Schroder, C., Khatri, R., Petry, S. F., and Linn, T. (2021). Class I and II histone deacetylase inhibitor LBH589 promotes endocrine differentiation in bone marrow derived human mesenchymal stem cells and suppresses uncontrolled proliferation. *Exp. Clin. Endocrinol. Diabetes* 129, 357–364. doi: 10.1055/a-1103-1900

Smith, J. R., Ashander, L. M., Arruda, S. L., Cordeiro, C. A., Lie, S., Rochet, E., et al. (2021). Pathogenesis of ocular toxoplasmosis. *Prog. Retin. Eye Res.* 81, 100882. doi: 10.1016/j.preteyeres.2020.100882

Smith, J. R., Ashander, L. M., Ma, Y., Rochet, E., and Furtado, J. M. (2020). Model systems for studying mechanisms of ocular toxoplasmosis. *Methods Mol. Biol.* 2071, 297–321. doi: 10.1007/978-1-4939-9857-9_17

Vanagas, L., Jeffers, V., Bogado, S. S., Dalmasso, M. C., Sullivan, W. J.Jr., and Angel, S. O. (2012). Toxoplasma histone acetylation remodelers as novel drug targets. *Expert Rev. Anti Infect. Ther.* 10, 1189–1201. doi: 10.1586/eri.12.100

Van Veggel, M., Westerman, E., and Hamberg, P. (2018). Clinical pharmacokinetics and pharmacodynamics of panobinostat. *Clin. Pharmacokinet.* 57, 21–29. doi: 10.1007/s40262-017-0565-x

Zhang, Y., He, J., Zheng, H., Huang, S., and Lu, F. (2019). Association of TREM-1, IL-1beta, IL-33/ST2, and TLR expressions with the pathogenesis of ocular toxoplasmosis in mouse models on different genetic backgrounds. *Front. Microbiol.* 10. doi: 10.3389/fmicb.2019.02264

frontiers | Frontiers in Cellular and Infection Microbiology

TYPE Original Research
PUBLISHED 27 October 2022
DOI 10.3389/fcimb.2022.1037586

OPEN ACCESS

EDITED BY
Mingming Liu,
Hubei University of Arts and Science, China

REVIEWED BY
Hongchao Sun,
Zhejiang Academy of Agricultural Sciences, China
Shengyong Feng,
Institute of Zoology, Chinese Academy of Sciences (CAS), China
Yong Yang,
Jilin University, China

*CORRESPONDENCE
Li-Hua Yang
jlylh123@163.com
Xiao-Xuan Zhang
zhangxiaoxuan1988@126.com
Hong-Wei Cao
caohw@yctu.edu.cn

†These authors have contributed equally to this work

SPECIALTY SECTION
This article was submitted to Parasite and Host, a section of the journal Frontiers in Cellular and Infection Microbiology

RECEIVED 06 September 2022
ACCEPTED 07 October 2022
PUBLISHED 27 October 2022

CITATION
Zou Y, Meng J-X, Wei X-Y, Gu X-Y, Chen C, Geng H-L, Yang L-H, Zhang X-X and Cao H-W (2022) CircRNA and miRNA expression analysis in livers of mice with *Toxoplasma gondii* infection. *Front. Cell. Infect. Microbiol.* 12:1037586. doi: 10.3389/fcimb.2022.1037586

CircRNA and miRNA expression analysis in livers of mice with *Toxoplasma gondii* infection

Yang Zou[1,2,3†], Jin-Xin Meng[4†], Xin-Yu Wei[4,5†], Xiao-Yi Gu[1], Chao Chen[6], Hong-Li Geng[4], Li-Hua Yang[2*], Xiao-Xuan Zhang[4*] and Hong-Wei Cao[1*]

[1]School of Pharmacy, Yancheng Teachers University, Yancheng, China, [2]College of Life Sciences, Changchun Sci-Tech University, Changchun, China, [3]State Key Laboratory of Veterinary Etiological Biology, Key Laboratory of Veterinary Parasitology of Gansu Province, Lanzhou Veterinary Research Institute, Chinese Academy of Agricultural Sciences, Lanzhou, China, [4]College of Veterinary Medicine, Qingdao Agricultural University, Qingdao, China, [5]College of Animal Science and Veterinary Medicine, Heilongjiang Bayi Agricultural University, Daqing, China, [6]College of Animal Science and Technology, Jilin Agricultural University, Changchun, China

Toxoplasmosis is an important zoonotic parasitic disease caused by *Toxoplasma gondii* (*T. gondii*). However, the functions of circRNAs and miRNAs in response to *T. gondii* infection in the livers of mice at acute and chronic stages remain unknown. Here, high-throughput RNA sequencing was performed for detecting the expression of circRNAs and miRNAs in livers of mice infected with 20 *T. gondii* cysts at the acute and chronic stages, in order to understand the potential molecular mechanisms underlying hepatic toxoplasmosis. Overall, 265 and 97 differentially expressed (DE) circRNAs were found in livers at the acute and chronic infection stages in comparison with controls, respectively. In addition, 171 and 77 DEmiRNAs were found in livers at the acute and chronic infection stages, respectively. Functional annotation showed that some immunity-related Gene ontology terms, such as "positive regulation of cytokine production", "regulation of T cell activation", and "immune receptor activity", were enriched at the two infection stages. Moreover, the pathways "Valine, leucine, and isoleucine degradation", "Fatty acid metabolism", and "Glycine, serine, and threonine metabolism" were involved in liver disease. Remarkably, DEcircRNA 6:124519352|124575359 was significantly correlated with DEmiRNAs mmu-miR-146a-5p and mmu-miR-150-5p in the network that was associated with liver immunity and pathogenesis of disease. This study revealed that the expression profiling of circRNAs in the livers was changed after *T. gondii* infection, and improved our understanding of the transcriptomic landscape of hepatic toxoplasmosis in mice.

KEYWORDS

***toxoplasma gondii*, non-coding RNAs, high-throughput RNA sequencing, liver, networks**

Introduction

Toxoplasmosis is a widespread zoonotic disease caused by *Toxoplasma gondii* (*T. gondii*) worldwide. *T. gondii* is an intracellular apicomplexan parasite that can infect almost all warm-blooded animals and humans (Tenter et al., 2000). Gamogony and oocyst can form in the epithelium of small intestine after an ingestion of *T. gondii* by definitive feline hosts. Then, the unsporulated oocysts can beare released into the intestinal lumen and excrete with feces, leading to contamination of soil and the environment (Tenter et al., 2000). The people who ingested undercooked food or water containing tissue cysts and sporulated oocysts will be infected by *T. gondii* (Dubey, 2008). The clinical manifestations of toxoplasmosis range from asymptomatic to fatal infection, including abortion, encephalitic illness, and conjunctivitis (Smith et al., 2021). *T. gondii* can attack the host organs, including livers, lymph nodes, eyes, hearts, and central nervous systems (Montoya and Liesenfeld, 2004; Stauffer et al., 2006; Balasundaram, 2010). In livers, *T. gondii* infection can cause several pathological changes, e.g. hepatitis, hepatomegaly, granuloma, and necrosis (Karasawa et al., 1981; Ortego et al., 1990; Hassan et al., 1996; Doğan et al., 2007). However, the molecular mechanisms underlying *T. gondii* infection and liver disease remain poorly understood.

Circular RNAs are one of the novel classes of endogenous noncoding RNAs that are formed by exon-scrambling (Meng et al., 2017). With the development of RNA sequencing (RNA-seq) technology, the abundance, diversity, and dynamic expression patterns of circRNAs in various organisms have been clarified (Conn et al., 2015). CircRNAs can not only antagonize the activity of miRNA through a sponge-like mechanism but also regulate gene expression at the post-transcriptional level (Granados-Riveron and Aquino-Jarquin, 2016). A series of studies showed that circRNAs played roles in the pathological processes of liver disease (Yao et al., 2017; Tang et al., 2020). The circRNAs are used as prognostic biomarkers, owing to remarkably stable characteristics (Lei et al., 2019). In addition, circRNAs are a potential drug target for diseases (Dhamija and Menon, 2018; Zhu et al., 2018). Thus, exploration of circRNA function that connecting with liver disease induced by *T. gondii* infection will provide a novel perspective for hepatic disease treatment and diagnosis.

In the present study, RNA-seq was performed for identifying the expression of circRNAs and miRNAs in the livers of mice after *T. gondii* infection, in order to investigate the relationships between circRNAs and miRNAs in the *T. gondii* infected livers of mice. The simultaneous analyses of the differentially expressed (DE) circRNAs and DE miRNAs were conducted to investigate the relevance of the expression and circRNA-miRNA interactions. Moreover, the potential functional role was predicted. Thus, the correlation networks of circRNAs and miRNAs in the livers of mice after *T. gondii* infection improved our understanding of the transcriptomic landscape of hepatic toxoplasmosis in mice.

Methods

Toxoplasma gondii, mice and infection

T. gondii cysts were collected from the brains of mice that had been infected with *T. gondii* for months. In brief, the mice were sacrificed after anesthetization, and the brains were dissected and collected with a mortar for preparing tissue homogenates. The brain homogenates were rinsed with phosphate-buffered saline (PBS), and then were transferred to a 2 mL EP tube. Then, the *T. gondii* cysts in brain tissues were counted by using a dissection microscope. The 8-10 week-old female BALB/c mice (SPF) were purchased from Spaefer Biotechnology Co., Ltd. (Beijing, China). All mice were housed in cages with an independent ventilation system under a 12-h dark/light cycle, with free food and water ad libitum. The mice (n = 12) were randomly divided into three groups: acute infection group (n = 3); chronic infection group (n = 3); and control group (n=6). In the infection groups, each mouse was infected with 20 *T. gondii* cysts. In the control group, the mice were treated with PBS. A previous study showed the timing of acute and chronic infection stages in mice infected with *T. gondii* (Hu et al., 2018). The mice in each group were sacrificed on day 11 (acute infection group) and 33 (chronic infection group) after infection, respectively. The successful establishment of mouse model was examined based on amplification of *T. gondii* B1 gene as described previously (Hu et al., 2018). At the mentioned time points post infection, the livers of mice in each group were dissected from each mouse. Then, the liver samples were immediately deposited in liquid nitrogen until RNA extraction.

RNA extraction

Approximately 50 mg of liver tissue was subjected to RNA extraction using TRIZOL (Life Technologies, Carlsbad, USA). In brief, the samples were firstly homogenized by liquid nitrogen, and the 1 ml TRIZOL reagent was added to the homogenization to lyse sample. Then, the 0.2 ml of chloroform per was added and shake tubes vigorously by hand for 15 s. The sample was incubated at room temperature for 2 to 3 minutes, and then centrifuged at 11,500 *g* for 15 min at 4°C. The RNA samples remain in the aqueous phase. The aqueous phase was transferred to a new tube, and isopropanol was added to precipitate RNA. The 75% ethanol was used to wash RNA samples; Finally, RNA pellet was redissolved with the water (Chomczynski and Sacchi, 2006). The RNA degradation and contamination were detected with 1% agarose gel test. The RNA Nano 6000 Assay Kit of the Bioanalyzer 2100 system (Agilent Technologies, CA, USA) and Qubit® RNA Assay Kit in Qubit® 2.0 Flurometer (Life Technologies, CA, USA) were used to measure and evaluate the concentration and purity of RNA, respectively. Then, the RNA samples were stored at −80°C for a further analysis.

Library preparation and sequencing

Approximately 5 μg of RNA sample was used for constructing the circRNA library by using NEBNext® Ultra™ Directional RNALibrary Prep Kit for Illumina® (NEB, USA). In brief, the First-strand cDNA was synthesized using M-MuLV Reverse Transcriptase with random hexamer primer. Then, the cDNA fragments were purified by AMPure XP system (Beckman Coulter, Beverly, USA). The cDNA was used for PCR amplification. Agilent Bioanalyzer 2100 system was employed for assessing library quality (Zhou et al., 2017). The sequencing libraries of circRNAs were performed using Illumina Hiseq 4000 platform, and the 150 bp paired-end reads were generated.

The 3 μg of RNA sample and NEBNext® Multiplex Small RNA Library Prep Set for Illumina® (NEB, USA) was used for generating miRNA libraries. Briefly, the first strand of cDNA of miRNA was synthesized through M-MuLV Reverse Transcriptase. Then, the LongAmp Taq 2×Master Mix, index (X) primer, and SR primer were used for PCR amplification. Finally, the library preparations were sequenced on an Illumina Hiseq 2500/2000 platform, and 50 bp single-end reads were generated.

Identification of circRNAs and miRNAs

The raw reads of fastq format were obtained by the Custom Perl and Python scripts. The ploy-N, with 5′ adapter contaminants, without 3′ adapters, and low reads were removed. The GC content, Q20, Q30, and the error rate were performed to assess quality of the clean data. The HISAT2 v2.0.4 and bowtie2 v2.2.8 were used for building and aligning clean data with the *Mus musculus* reference genome, respectively (Langmead and Salzberg, 2012; Pertea et al., 2016). The circRNA identification was performed using find_circ (Memczak et al., 2013) and CIRI2 (Gao et al., 2015). circRNA was predicted by the intersection between the two algorithms. Moreover, the small RNA tags were mapped to obtain known miRNAs using MiRBase 20.0 (Griffiths-Jones, 2016). The novel miRNAs were predicted by using miREvo (Wen et al., 2012) and mirdeep2 (Friedlander et al., 2012). The quantification of circRNA and miRNA expression profiles were normalized by TPM (transcript per million) (Zhou et al., 2010). The differential expression analysis was performed using the DESeq R package (1.8.3) (Anders and Huber, 2010). |Log2 fold change (FC)| ≥ 1.0 and *P*-value < 0.05 were used as thresholds to identify differentially expressed transcripts.

MiRNA target gene prediction and functional analysis

The potential target genes of DE miRNAs were predicted by a combined use of Miranda, PITA, and RNAhybrid softwares. GO enrichment analysis of the potential target genes in the livers of mice infected with *T. gondii* was conducted using the GOseq R package (Young et al., 2010). The KEGG (Kyoto encyclopedia of genes and genome) pathway functional annotation were performed by using KOBAS 3.0 software (Mao et al., 2005). *P*-value < 0.05 was considered as significant enrichment.

Quantitative real-time PCR analysis

The DE circRNAs and DE miRNAs were chosen to verify the RNA-Seq results by using qRT-PCR. The qPCR was performed in a LightCycler480 (Roche, Basel, Switzerland) using a ChamQ SYBR qPCR Master Mix kit (Vazyme, Nanjing, China). The reaction was consisted of 40 cycles, circRNA initial degeneration at 95°C for 30 s, and template degeneration in the PCR cycle at 95°C for 10 s, and finally annealing at 60°C for 30 s. The reactive cycle of miRNA was consisted of 95°C for 30 s, then 40 cycles of 95°C for 5 s and 60°C for 34 s. The amplification was ensured by melting curve analysis in each reaction. The primers of miRNAs and circRNAs were listed in Table 1. L13A and U6 were used as the internal controls of circRNA and miRNA, respectively. The relative expression quantity was calculated using the $2^{-\Delta\Delta Ct}$ method (Livak and Schmittgen, 2001).

TABLE 1 Primers used in lncRNA and mRNA-specific qRT-PCR analysis.

RNAs	Primer	Sequence (5' to 3')
15:3279732|3280203 (circRNA)	Forward primer	TGGAAGCCAATATGGTAGATTTCTC
	Reverse primer	TCATTTTCTCTCCCCAACTCAGTC
17:39848416|39848682 (circNA)	Forward primer	CCCTCGTAGACACGGAAGAGC
	Reverse primer	CTTTTCTGGCCTCGCCACC
mmu-miR-1247-3p (miRNA)	Forward primer	GGAACGTCGAGACTGGAGCA
mmu-miR-339-5p (miRNA)	Forward primer	TGTCCTCCAGGAGCTCACGA
mmu-miR-379-5p (miRNA)	Forward primer	TGGTAGACTATGGAACGTAGGA
mmu-miR-146b-5p (miRNA)	Forward primer	TGAGAACTGAATTCCATAGGCTA

Results

Differentially expressed CircRNAs and miRNAs

Compared with the control group, a total of 265 DE circRNAs and 171 DE miRNAs were identified at the acute infection stage,

and 97 DE circRNAs and 77 DE miRNAs were detected in the livers at the chronic infection stage (Figure 1 and Supplementary Table S1). A total of 19 circRNAs and 46 miRNAs were commonly dysregulated between the acute and chronic *T. gondii*-infected groups (Figure 2). Among DE transcripts, the mmu-miR-147-3p was up-regulated 32.94 folds at the acute infection stage, however, it was down-regulated to 3.66 folds at the chronic infection stage. Moreover, mmu-miR-342-3p was up-regulated 8.23 folds at the acute infection stage. Furthermore, mmu-miR-143-3p was down-regulated 4.05 folds and 2.11 folds at the acute and chronic infection stages, respectively (Supplementary Table S1).

GO annotation and KEGG pathway analysis

To find the potential biological associations of DE miRNAs, GO and KEGG pathway enrichment analyses for infection-associated transcripts were predicted. The top 30 GO terms were shown in Figure 3. Most of predicted genes were involved in the "fatty acid metabolic process", "positive regulation of cytokine production", "positive regulation of response to external stimulus" and "regulation of T cell activation" at the acute infection stage (Figure 3A).

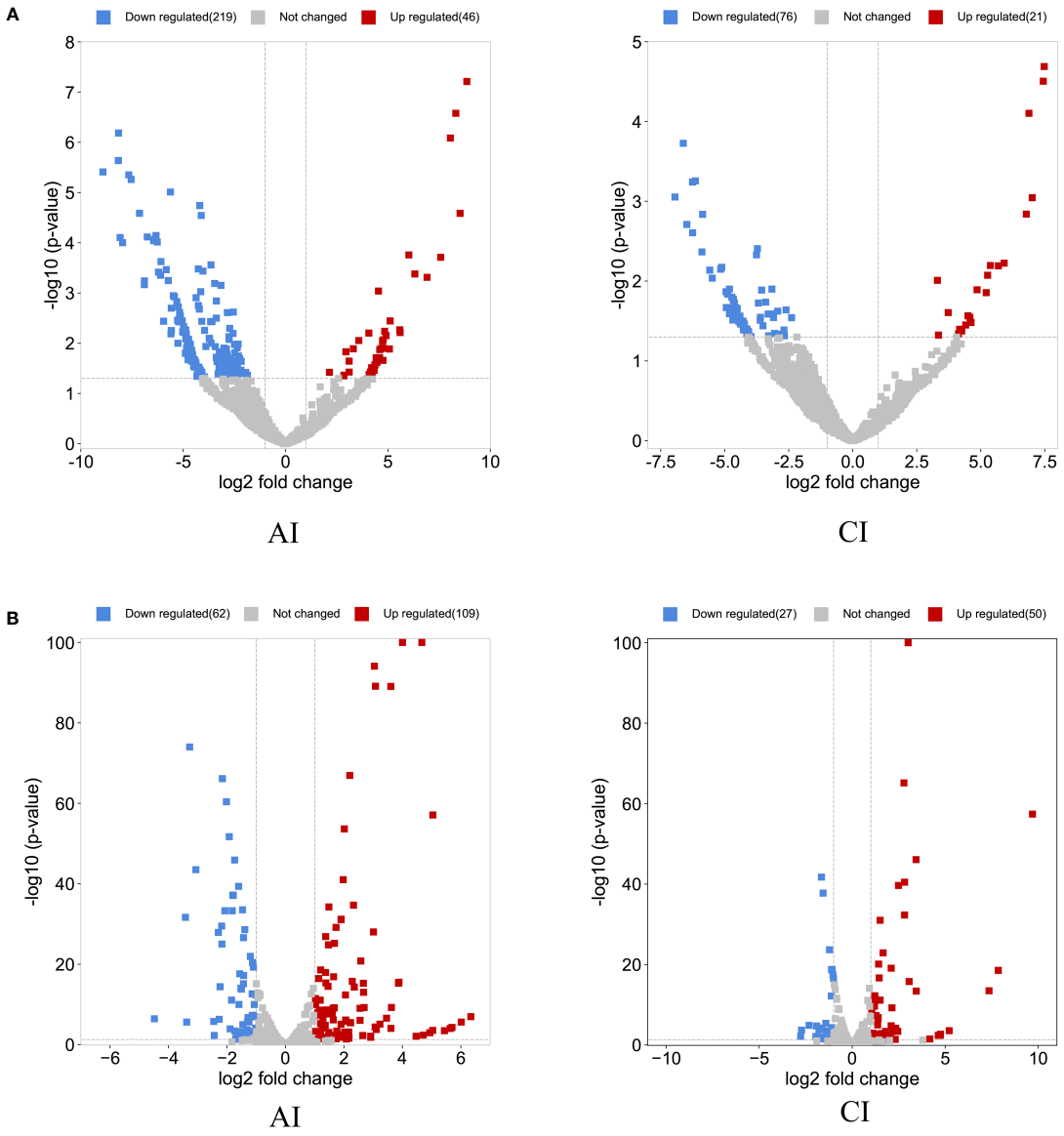

FIGURE 1
Overview of the differentially expressed (DE) circRNAs and DEmiRNAs. The volcano plots of DEcircRNAs **(A)** and DEmiRNAs **(B)** at acute infection (AI) and chronic infection (CI) stages. The horizontal-axis shows the log2 fold change, and the vertical-axis shows the -log10 p-value. The up-regulated are marked in red and the down-regulated RNAs are in blue.

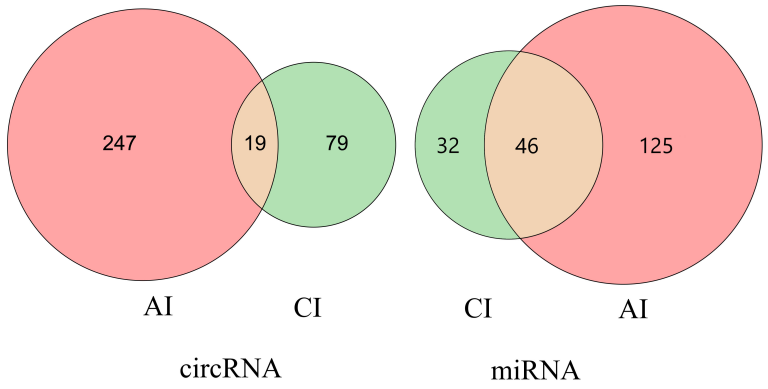

FIGURE 2
Venn diagram of the differentially expressed (DE) circRNAs and DEmiRNAs. the number of the common or unique DEcircRNAs and DEmiRNAs at two infection stages.

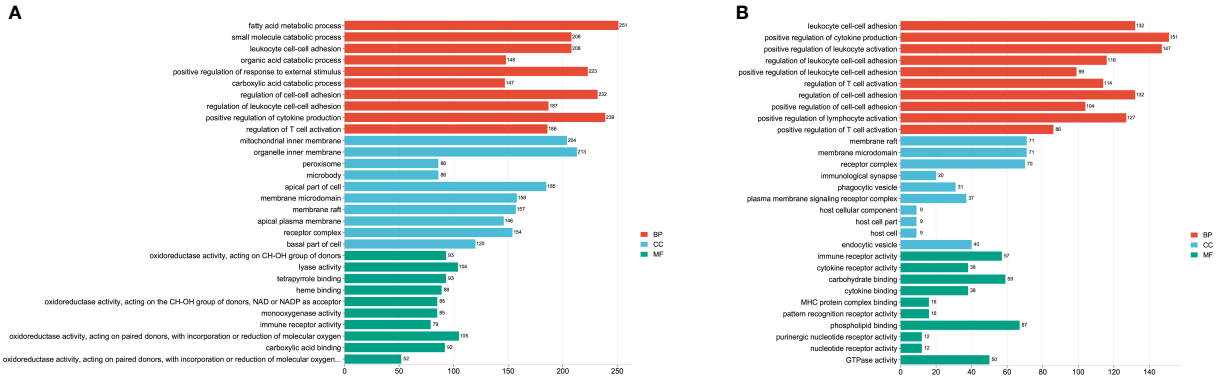

FIGURE 3
The top 30 GO terms of target genes of the differentially expressed (DE) miRNAs at acute infection **(A)** and chronic infection **(B)** stages. The vertical-axis represents the GO terms. The horizontal-axis represents numbers of target genes. The BP represents biological process, CC represents cellular component, and MF represents molecular function.

Furthermore, the biological process mainly included "leukocyte cell-cell adhesion", "positive regulation of cytokine production", and "positive regulation of leukocyte activation". The cellular component included "membrane raft" and "membrane microdomain", the molecular function included "immune receptor activity" and "phospholipid binding" at the chronic infection stage (Figure 3B).

KEGG enrichment analysis showed that pathways mainly included "Valine, leucine, and isoleucine degradation", "Fatty acid metabolism", "Glycine, serine and threonine metabolism", and "Tryptophan metabolism" (Figure 4A) at the acute infection stage. These results showed the hepatic metabolism affected the acute infection stage of *T. gondii*. Moreover, some pathways were related to immunity and inflammation, such as "Cytokine-cytokine receptor interaction", "Cell adhesion molecules", "NF-kappa B signaling pathway", "Primary immunodeficiency", "Inflammatory bowel disease", "Th1 and Th2 cell differentiation", "Th17 cell differentiation", and "NOD-like receptor signaling pathway". Interestingly, some pathways were related with intestinal flora, e.g. "Inflammatory bowel disease" and "Intestinal immune network for IgA production" (Figure 4B).

Co-expression networks of DEcircRNAs and DEmiRNAs

To further reveal the mechanisms underlying the DEcircRNAs and DEmiRNAs in the livers during *T. gondii* infection, a network was constructed (Figure 5 and Supplementary Table S2). In this network, the DEcircRNA 6:124519352|124575359 was related to

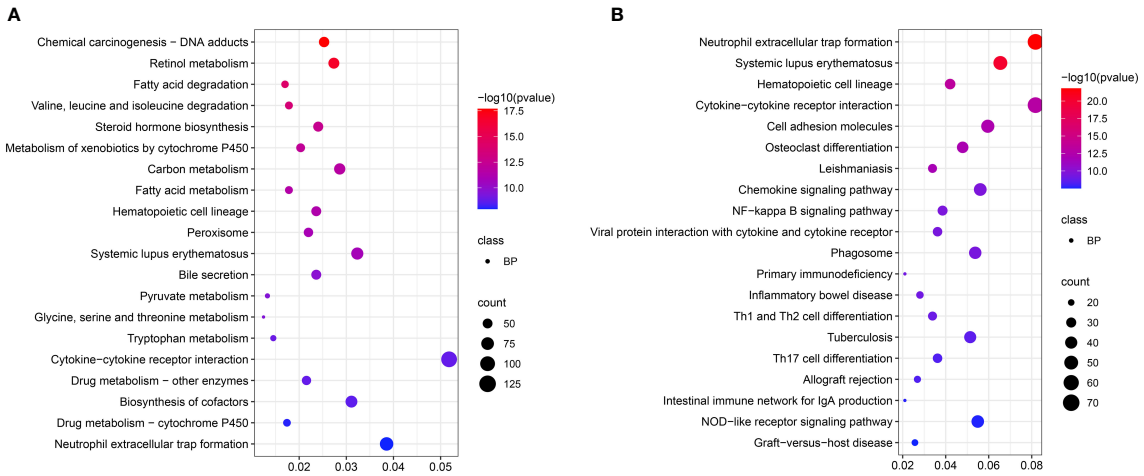

FIGURE 4
Scatter plots showing KEGG pathway of the target genes. The top 20 enriched pathways at acute infection **(A)** and chronic infection **(B)** stages, respectively. The vertical-axis represent pathways, and the horizontal-axis numbers represent the rich factor.

DE miRNAs mmu-miR-132-3p, mmu-miR-146a-5p, mmu-miR-150-5p, and other DEmiRNAs (n = 42, Supplementary Table S2). Moreover, DEcircRNA 4:61958498|62052011 was associated with DEmiRNAs (mmu-miR-146a-5p) and 45 other DEmiRNAs. Moreover, DEmiRNA mmu-miR-1247-3p shared 5 DEcircRNAs, including 12:103731961|103897311, 12:103854668|103947209, 5:145708877|145868684, 4:61958498|62052011, and 7:13832577|13909898 (Figure 5). The networks showed that multiple miRNAs were regulated by several circRNAs at the two infection stages, thus suggesting a complex regulatory relationship between DEcircRNAs and DEmiRNAs.

Verification of the DEcircRNAs and DEmiRNAs by qRT-PCR

To evaluate the reliability of RNA-sequence results, the expression profiles of the randomly selected DEcircRNAs and DEmiRNAs were successfully confirmed by qRT-PCR. The results obtained by RNA-Seq and qRT-PCR were consistent in the trend and magnitude of the expression (Supplementary Figure S1).

Discussion

Previous omics studies have provided a wealth of resources that improved understanding of the pathogenesis of *T. gondii* (Garfoot et al., 2019; Antil et al., 2021; Menard et al., 2021; Antil et al., 2022), and many studies mainly focused on mRNAs (He et al., 2016; Zhou et al., 2016; Lutshumba et al., 2020). Recently, Zhou and colleagues revealed putative functions of miRNAs and circRNAs in brains of mice after an infection with *T. gondii* (Zhou et al., 2020). However, the expression levels of circRNAs and miRNAs specific to *T. gondii* infection in livers of mice were unclear. Thus, the present study explored the expression profiles of circRNAs and miRNAs in the livers of mice at acute and chronic stages after *T. gondii* infection by using RNA-seq technique.

MiR-147-3p (mmu-miR-147-3p) has been reported to dampen Toll-like receptor (TLR)-signaling in murine macrophages (Liu et al., 2009). It can limit excessive inflammation in the hosts response to influenza A virus infection (Preusse et al., 2017). The miR-147 plays an important role in the negative regulation of TLR/NF-κB-mediated proinflammatory cytokines, and inhibits the expression of proinflammatory cytokines (Zuo et al., 2020). In this study, the miR-147-3p was up-regulated 32.94 folds at the acute infection stage. *T. gondii* infection triggered liver inflammation at an early infection stage, and the up-regulation of miR-147-3p could limit excessive inflammation for protecting the hosts. Further protection was attenuated with increasing duration of infection, as the expression of miR-147-3p decreased to 3.66-fold during the chronic infection stage. Interestingly, miR-342-3p (up-regulated 8.23 fold) seemed to have the same effect as miR-147-3p at the acute infection stage. Overexpression of miR-342-3p can suppress inflammation response in THP-1 cells (Wang et al., 2019). Moreover, miR-342-3p was considered to be significantly relative with regulating metabolic profiles of Treg cells (Kim et al., 2020), which may explain for its role in inflammation inhibition. Moreover, miR-143-3p could participate in inflammatory pain responses in fibromyalgia patients (Jiang et al., 2015). A previous study showed that miR-143-3p might inhibit inflammatory factors' levels through

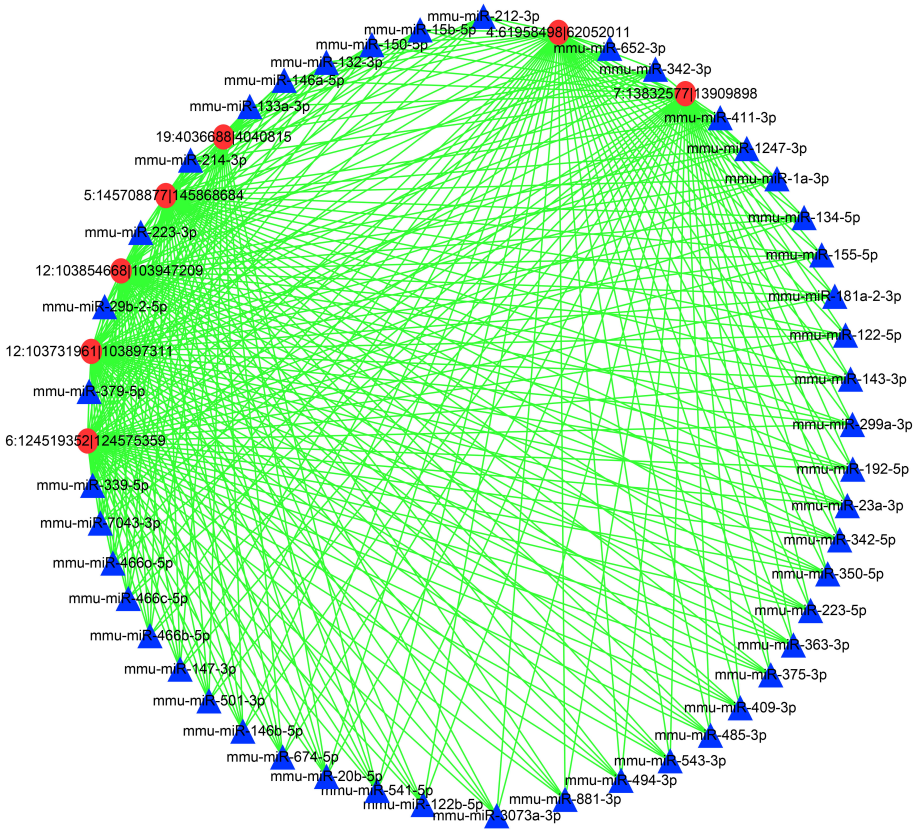

FIGURE 5
A network of the commonly DEcircRNAs with their associate DEmiRNAs. Different colors show different RNA, with red for DEcircRNAs and blue for DEmiRNAs.

regulating the MyD88/NF-κB signaling pathway (Wang et al., 2020). In this study, the miR-143-3p (mmu-miR-143-3p) was down-regulated 4.05 folds and 2.11 folds at the acute and chronic infection stages, respectively. Thus, these findings suggest that miR-143-3p may participate in the inflammation reaction of livers during *T. gondii* infection, and the down-regulation of miR-143-3p can increase the inflammation of livers for resisting infection. In addition, these findings reveal mediation of pro-inflammatory and anti-inflammatory mechanisms in the livers in *T. gondii* pathogenesisis.

In this study, some immunity-related GO terms were enriched at the two infection stages, such as "positive regulation of cytokine production", "regulation of T cell activation", "leukocyte cell-cell adhesion", "positive regulation of leukocyte activation", and "immune receptor activity" (Figure 3), indicating that *T. gondii* induced the liver immunity reaction of hosts. KEGG analysis showed that a series of pathways (e.g. "Valine, leucine and isoleucine degradation", "Fatty acid metabolism", and "Glycine, serine and threonine metabolism") were involved in liver disease. The reductions of valine, leucine, and isoleucine are considered to be related to hepatic encephalopathy pathogenesis, and impair liver regeneration (Fischer et al., 1975; Marchesini et al., 2003; Nakaya et al., 2007; Urata et al., 2007). Moreover, TNF-α and IL-6 activate branched-chain keto acid dehydrogenase increased valine, leucine, and isoleucine catabolism (Nawabi et al., 1990; Holecek, 1996). IL-6 and TNF-α are proinflammatory cytokines, and metabolic disturbances are strongly related to increased levels of these two cytokines (Popko et al., 2010), thus suggesting *T. gondii* causes the metabolic disturbance of the livers at the acute infection stage. The other metabolism pathways enriched in the livers at the acute infection stage indicated disorders of metabolic function of the host livers induced by *T. gondii* infection. The cell adhesion molecules are considered as targets for the bacterial pathogens in establishing intimate contact with the cells and tissues of hosts (Hauck et al., 2006). A previous study reported that targeted disruption of *SAG3* gene in *T. gondii* results in a partial decrease in host cell adhesion, and drastic reduction of virulence in mice (Dzierszinski et al., 2000). The "Cell adhesion molecules" pathway enriched at the chronic infection stage indicated potential relationships between cell adhesion molecules and *T. gondii* infection. The NF-κB family of transcription factors was closely related to the mediation of innate and adaptive immunities against

infection (Caamaño et al., 1999). A previous study showed that the NF-κB2$^{-/-}$ mice could resist *T. gondii* infection during the acute phase of toxoplasmosis, but displayed a protracted pattern of mortality during the chronic stage of infection (Franzoso et al., 1998). These findings suggest NF-κB signaling pathway is essential for *T. gondii* infection in livers. Th17 produces AMPs that prevent the dysbiosis and bacterial translocation related to the pathogenic infection through secreting IL-17, and Th17 is crucial for host survival after *T. gondii* (type II strain) infection (Cervantes-Barragan et al., 2019). Moreover, a few studies reported that IL-17 signaling played a protective role during *T. gondii* infection (Kelly et al., 2005; Moroda et al., 2017). Thus, the "Th17 cell differentiation" pathway was observed in the livers at the chronic infection stage. An early *T. gondii* infection can disrupt the resident microbial communities and induce acute inflammation in the ileum (Heimesaat et al., 2006; Raetz et al., 2013). *T. gondii* infection also induces the increment of abundance of proinflammatory proteobacteria, and decrement of beneficially bacterial communities, causing disruption of the microbial community composition that persists at the chronic infection stage (French et al., 2022). These findings support that *T. gondii* infection causes microbial imbalance. Notably, "Inflammatory bowel disease" and "Intestinal immune network for IgA production" pathways were also enriched in the livers at the chronic infection stage. These two pathways are significantly associated with microbiota (Federici et al., 2022; Tan et al., 2022; Tchitchek et al., 2022). Thus, we suspect that *T. gondii* infection could mediate hepatic metabolism, and further affecting microbial balance in mice. How this mechanism works remains to be investigated.

CircRNAs act as miRNA decoys or sponges in regulating gene expression (Panda, 2018). Thus, a correlation analysis of the expression profiles from the DEcircRNAs and DEmiRNAs predictive interactions was performed. In the network, DE miRNAs mmu-miR-146a-5p and mmu-miR-150-5p were regulated by DEcircRNA 6:124519352|124575359. miR-146a-5p plays a role in different disease contexts and acts as a negative regulator of inflammatory and immune responses (Xu et al., 2012). A previous study reported that HCV-induced increment of miR-146a-5p promoted viral infection and metabolic pathways related to pathogenesis of hepatic disease (Bandiera et al., 2016). Thus, miR-146a-5p is associated with liver immunity and pathogenesis of liver disease. The upregulation of miR-146a-5p at both two infection stages (Supplementary Table S1) revealed a potential role in the *T. gondii* infection induced liver disease. However, the DEcircRNA 6:124519352|124575359 mediates this process. miR-150-5p regulates target genes IL-10 and PIM1, having an anti-inflammatory effect (Neamah et al., 2019). It was also increased at both acute and chronic infection stages, and was regulated by DEcircRNA 6:124519352|124575359. This illustrates both circRNA 6:124519352|124575359 and miR-150-5p have protective effects on *T. gondii*-induced liver excessive inflammation. Moreover, mmu-miR-1247-3p was regulated by multiple circRNAs. The treatment of HCC with miR-1247-3p would increase the expression levels of IL-1β, IL-6, and IL-8, thus suggesting the proinflammatory role of miR-1247-3p (Fang et al., 2018). The DEmiRNA mmu-miR-1247-3p was regulated by DEcircRNAs 12:103731961|103897311, 12:103854668|103947209, 5:145708877|145868684, 4:61958498|62052011, and 7:13832577|13909898 in the network, indicating that these DEcircRNAs participated in liver inflammation caused by *T. gondii* infection. In this study, RNA-seq was performed to detect the differential expression profiles of circRNAs and miRNAs in the livers of mice infected with *T. gondii*. However, some limits should be addressed, including other organizations of expression profiles should be added, and the potential interaction between circRNA-miRNA and mRNA is needed to validate in the future work.

Conclusions

This study explored the differential expression levels of circRNAs and miRNAs in the livers of mice infected with *T. gondii* at the acute and chronic stages. The functional enrichment analysis showed that many DEcirciRNAs and DE miRNAs were associated with the inflammation responses of the livers after *T. gondii* infection. Our results provided valuable data for the understanding of the circRNAs and miRNAs involved in the molecular basis of the hepatic responses to *T. gondii* infection. The functions of DEcircRNAs and DEmiRNAs in the pathogenesis of *T. gondii* infection in livers will be further verified.

Data availability statement

The datasets presented in this study can be found in online repositories. The names of the repository/repositories and accession number(s) can be found in the article/Supplementary Material.

Ethics statement

The animal study was reviewed and approved by the Animal Ethics Committee of Qingdao Agricultural University.

Author contributions

X-XZ and H-WC conceived and designed the experiments. J-XM and X-YM performed the experiments. X-YG, X-YW, J-XM, CC and H-LC contributed reagents/materials/analysis tools. YZ analyzed the data and wrote the paper. X-YW, J-XM, L-HY, X-XZ and HW-C critically revised the manuscript. All authors read and approved the final version of the manuscript.

Funding

This work was supported by the National Natural Science Foundation of China (Grant No. 31902238), Research Foundation for Distinguished Scholars of Qingdao Agricultural University (665-1120044).

Conflict of interest

The authors declare that the research was conducted in the absence of any commercial or financial relationships that could be construed as a potential conflict of interest.

Publisher's note

All claims expressed in this article are solely those of the authors and do not necessarily represent those of their affiliated organizations, or those of the publisher, the editors and the reviewers. Any product that may be evaluated in this article, or claim that may be made by its manufacturer, is not guaranteed or endorsed by the publisher.

Supplementary material

The Supplementary Material for this article can be found online at: https://www.frontiersin.org/articles/10.3389/fcimb.2022.1037586/full#supplementary-material

SUPPLEMENTARY FIGURE 1
Validation for the expression of the DEcircRNAs and DEmiRNAs by qRT-PCR at acute infection (AI) and chronic infection (CI) stages.

SUPPLEMENTARY TABLE 1
The expression profile of differentially expressed circRNAs and miRNAs in the liver at acute infection and chronic infection stages.

SUPPLEMENTARY TABLE 2
The data of DEcircRNA-DEmiRNA network analysis.

References

Anders, S., and Huber, W. (2010). Differential expression analysis for sequence count data. *Genome. Biol.* 11, R106. doi: 10.1186/gb-2010-11-10-r106

Antil, N., Arefian, M., Kandiyil, M. K., Awasthi, K., Keshava Prasad, T. S., and Raju, R. (2022). The core human microRNAs regulated by *Toxoplasma gondii*. *Microrna* doi: 10.2174/2211536611666220428130250

Antil, N., Kumar, M., Behera, S. K., Arefian, M., Kotimoole, C. N., Rex, D. A. B., et al. (2021). Unraveling GT1 strain virulence and new protein-coding genes with proteogenomic analyses. *OMICS* 25, 591–604. doi: 10.1089/omi.2021.0082

Balasundaram, M. B. (2010). Outbreak of acquired ocular toxoplasmosis involving 248 patients. *Arch. Ophthalmol.* 128, 28. doi: 10.1001/archophthalmol.2009.354

Bandiera, S., Pernot, S., El Saghire, H., Durand, S. C., Thumann, C., Crouchet, E., et al. (2016). Hepatitis c virus-induced upregulation of microRNA miR-146a-5p in hepatocytes promotes viral infection and deregulates metabolic pathways associated with liver disease pathogenesis. *J. Virol.* 90, 6387–6400. doi: 10.1128/JVI.00619-16

Caamaño, J., Alexander, J., Craig, L., Bravo, R., and Hunter, C. A. (1999). The NF-kappa b family member RelB is required for innate and adaptive immunity to *Toxoplasma gondii*. *J. Immunol.* 163, 4453–4461.

Cervantes-Barragan, L., Cortez, V. S., Wang, Q., McDonald, K. G., Chai, J. N., Di Luccia, B., et al. (2019). CRTAM protects against intestinal dysbiosis during pathogenic parasitic infection by enabling Th17 maturation. *Front. Immunol.* 10. doi: 10.3389/fimmu.2019.01423

Chomczynski, P., and Sacchi, N. (2006). The single-step method of RNA isolation by acid guanidinium thiocyanate-phenol-chloroform extraction: Twenty-something years on. *Nat. Protoc.* 1, 581–585. doi: 10.1038/nprot.2006.83

Conn, S. J., Pillman, K. A., Toubia, J., Conn, V. M., Salmanidis, M., Phillips, C. A., et al. (2015). The RNA binding protein quaking regulates formation of circRNAs. *Cell.* 160, 1125–1134. doi: 10.1016/j.cell.2015.02.014

Dhamija, S., and Menon, M. B. (2018). Non-coding transcript variants of protein-coding genes - what are they good for? *RNA Biol.* 15, 1025–1031. doi: 10.1080/15476286.2018

Doğan, N., Kabukçuoğlu, S., and Vardareli, E. (2007). Toxoplasmic hepatitis in an immunocompetent patient. *Turkiye Parazitol. Derg.* 31, 260–263.

Dubey, J. P. (2008). The history of toxoplasma gondii–the first 100 years. *J. Eukaryot. Microbiol.* 55, 467–475. doi: 10.1111/j.1550-7408.2008.00345.x

Dzierszinski, F., Mortuaire, M., Cesbron-Delauw, M. F., and Tomavo, S. (2000). Targeted disruption of the glycosylphosphatidylinositol-anchored surface antigen *SAG3* gene in *Toxoplasma gondii* decreases host cell adhesion and drastically reduces virulence in mice. *Mol. Microbiol.* 37, 574–582. doi: 10.1046/j.1365-2958.2000.02014.x

Fang, T., Lv, H., Lv, G., Li, T., Wang, C., Han, Q., et al. (2018). Tumor-derived exosomal miR-1247-3p induces cancer-associated fibroblast activation to foster lung metastasis of liver cancer. *Nat. Commun.* 9, 191. doi: 10.1038/s41467-017-02583-0

Federici, S., Kredo-Russo, S., Valdés-Mas, R., Kviatcovsky, D., Weinstock, E., Matiuhin, Y., et al. (2022). Targeted suppression of human IBD-associated gut microbiota commensals by phage consortia for treatment of intestinal inflammation. *Cell* 185, 2879–2898.e24. doi: 10.1016/j.cell.2022.07.003

Fischer, J. E., Funovics, J. M., Aguirre, A., James, J. H., Keane, J. M., Wesdorp, R. I., et al. (1975). The role of plasma amino acids in hepatic encephalopathy. *Surgery* 78, 276–290.

Franzoso, G., Carlson, L., Poljak, L., Shores, E. W., Epstein, S., Leonardi, A., et al. (1998). Mice deficient in nuclear factor (NF)-kappa B/p52 present with defects in humoral responses, germinal center reactions, and splenic microarchitecture. *J. Exp. Med.* 187, 147–159. doi: 10.1084/jem.187.2.147

French, T., Steffen, J., Glas, A., Osbelt, L., Strowig, T., Schott, B. H., et al. (2022). Persisting microbiota and neuronal imbalance following infection reliant on the infection route. *Front. Immunol.* 13. doi: 10.3389/fimmu.2022.920658

Friedländer, M. R., Mackowiak, S. D., Li, N., Chen, W., and Rajewsky, N. (2012). miRDeep2 accurately identifies known and hundreds of novel microRNA genes in seven animal clades. *Nucleic. Acids Res.* 40, 37–52. doi: 10.1093/nar/gkr688

Gao, Y., Wang, J., and Zhao, F. (2015). CIRI: an efficient and unbiased algorithm for *de novo* circular RNA identification. *Genome Biol.* 16, 4. doi: 10.1186/s13059-014-0571-3

Garfoot, A. L., Wilson, G. M., Coon, J. J., and Knoll, L. J. (2019). Proteomic and transcriptomic analyses of early and late-chronic *Toxoplasma gondii* infection shows novel and stage specific transcripts. *BMC Genomics* 20, 859. doi: 10.1186/s12864-019-6213-0

Granados-Riveron, J. T., and Aquino-Jarquin, G. (2016). The complexity of the translation ability of circRNAs. *Biochim. Biophys. Acta* 1859, 1245–1251. doi: 10.1016/j.bbagrm.2016.07.009

Griffiths-Jones, S. (2016). miRBase: the microRNA sequence database. *Methods. Mol. Biol.* 342, 129–38. doi: 10.1385/1-59745-123-1:129

Hassan, M. M., Farghaly, A. M., Gaber, N. S., Nageeb, H. F., Hegab, M. H., and Galal, N. (1996). Parasitic causes of hepatomegaly in children. *J. Egypt. Soc Parasitol.* 26, 177–189.

Hauck, C. R., Agerer, F., Muenzner, P., and Schmitter, T. (2006). Cellular adhesion molecules as targets for bacterial infection. *Eur. J. Cell Biol.* 85, 235–242. doi: 10.1016/j.ejcb.2005.08.002

Heimesaat, M. M., Bereswill, S., Fischer, A., Fuchs, D., Struck, D., Niebergall, J., et al. (2006). Gram-negative bacteria aggravate murine small intestinal Th1-type immunopathology following oral infection with *Toxoplasma gondii*. *J. Immunol.* 177, 8785–8795. doi: 10.4049/jimmunol.177.12.8785

He, J. J., Ma, J., Li, F. C., Song, H. Q., Xu, M. J., and Zhu, X. Q. (2016). Transcriptional changes of mouse splenocyte organelle components following acute infection with *Toxoplasma gondii*. *Exp. Parasitol.* 167, 7–16. doi: 10.1016/j.exppara.2016.04.019

Holecek, M. (1996). Leucine metabolism in fasted and tumor necrosis factor-treated rats. *Clin. Nutr.* 15, 91–93. doi: 10.1016/s0261-5614(96)80028-8

Hu, R. S., He, J. J., Elsheikha, H. M., Zhang, F. K., Zou, Y., Zhao, G. H., et al. (2018). Differential brain microRNA expression profiles after acute and chronic infection of mice with oocysts. *Front. Microbiol.* 9. doi: 10.3389/fmicb.2018.02316

Jiang, Q., Yi, M., Guo, Q., Wang, C., Wang, H., Meng, S., et al. (2015). Protective effects of polydatin on lipopolysaccharide-induced acute lung injury through TLR4-MyD88-NF-κB pathway. *Int. Immunopharmacol.* 29, 370–376. doi: 10.1016/j.intimp.2015.10.027

Karasawa, T., Shikata, T., Takizawa, I., Morita, K., and Komukai, M. (1981). Localized hepatic necrosis related to cytomegalovirus and *Toxoplasma gondii*. *Acta Pathol. Jpn.* 31, 527–534.

Kelly, M. N., Kolls, J. K., Happel, K., Schwartzman, J. D., Schwarzenberger, P., Combe, C., et al. (2005). Interleukin-17/interleukin-17 receptor-mediated signaling is important for generation of an optimal polymorphonuclear response against *Toxoplasma gondii* infection. *Infect. Immun.* 73, 617–621. doi: 10.1128/IAI.73.1.617-621.2005

Kim, D., Nguyen, Q. T., Lee, J., Lee, S. H., Janocha, A., Kim, S., et al. (2020). Anti-inflammatory roles of glucocorticoids are mediated by Foxp3 regulatory T cells *via* a miR-342-dependent mechanism. *Immunity.* 53, 581–596.e5. doi: 10.1016/j.immuni.2020.07.002

Langmead, B., and Salzberg, S. L. (2012). Fast gapped-read alignment with bowtie 2. *Nat. Methods* 9, 357–359. doi: 10.1038/nmeth.1923

Lei, B., Tian, Z., Fan, W., and Ni, B. (2019). Circular RNA: a novel biomarker and therapeutic target for human cancers. *Int. J. Med. Sci.* 16, 292–301. doi: 10.7150/ijms.28047

Liu, G., Friggeri, A., Yang, Y., Park, Y. J., Tsuruta, Y., and Abraham, E. (2009). miR-147, a microRNA that is induced upon toll-like receptor stimulation, regulates murine macrophage inflammatory responses. *Proc. Natl. Acad. Sci. U.S.A.* 106, 15819–15824. doi: 10.1073/pnas.0901216106

Livak, K. J., and Schmittgen, T. D. (2001). Analysis of relative gene expression data using real-time quantitative PCR and the 2(-delta delta C(T)) method. *Methods* 25, 402–408. doi: 10.1006/meth.2001.1262

Lutshumba, J., Ochiai, E., Sa, Q., Anand, N., and Suzuki, Y. (2020). Selective upregulation of transcripts for six molecules related to T cell costimulation and phagocyte recruitment and activation among 734 immunity-related genes in the brain during perforin-dependent, CD8 T cell-mediated elimination of *Toxoplasma gondii* cysts. *mSystems* 5, e00189-20. doi: 10.1128/mSystems.00189-20

Mao, X., Cai, T., Olyarchuk, J. G., and Wei, L. (2005). Automated genome annotation and pathway identification using the KEGG orthology (KO) as a controlled vocabulary. *Bioinformatics* 21, 3787–3793. doi: 10.1093/bioinformatics/bti430

Marchesini, G., Bianchi, G., Merli, M., Amodio, P., Panella, C., Loguercio, C., et al. (2003). Nutritional supplementation with branched-chain amino acids in advanced cirrhosis: a double-blind, randomized trial. *Gastroenterology* 124, 1792–1801. doi: 10.1016/s0016-5085(03)00323-8

Memczak, S., Jens, M., Elefsinioti, A., Torti, F., Krueger, J., Rybak, A., et al. (2013). Circular RNAs are a large class of animal RNAs with regulatory potency. *Nature* 495, 333–338. doi: 10.1038/nature11928

Menard, K. L., Bu, L., and Denkers, E. Y. (2021). Transcriptomics analysis of *Toxoplasma gondii*-infected mouse macrophages reveals coding and noncoding signatures in the presence and absence of MyD88. *BMC Genomics* 22, 130. doi: 10.1186/s12864-021-07437-0

Meng, S., Zhou, H., Feng, Z., Xu, Z., Tang, Y., Li, P., et al. (2017). CircRNA: functions and properties of a novel potential biomarker for cancer. *Mol. Cancer.* 16, 94. doi: 10.1186/s12943-017-0663-2

Montoya, J. G., and Liesenfeld, O. (2004). Toxoplasmosis. *Lancet* 363, 1965–1976. doi: 10.1016/S0140-6736(04)16412-X

Moroda, M., Takamoto, M., Iwakura, Y., Nakayama, J., and Aosai, F. (2017). Interleukin-17A-deficient mice are highly susceptible to *Toxoplasma gondii* infection due to excessively induced *T. gondii* HSP70 and interferon gamma production. *Infect. Immun.* 85, e00399-17. doi: 10.1128/IAI.00399-17

Nakaya, Y., Okita, K., Suzuki, K., Moriwaki, H., Kato, A., Miwa, Y., et al. (2007). BCAA-enriched snack improves nutritional state of cirrhosis. *Nutrition* 23, 113–120. doi: 10.1016/j.nut.2006.10.008

Nawabi, M. D., Block, K. P., Chakrabarti, M. C., and Buse, M. G. (1990). Administration of endotoxin, tumor necrosis factor, or interleukin 1 to rats activates skeletal muscle branched-chain alpha-keto acid dehydrogenase. *J. Clin. Invest.* 85, 256–263. doi: 10.1172/JCI114421

Neamah, W. H., Singh, N. P., Alghetaa, H., Abdulla, O. A., Chatterjee, S., Busbee, P. B., et al. (2019). AhR activation leads to massive mobilization of myeloid-derived suppressor cells with immunosuppressive activity through regulation of CXCR2 and microRNA miR-150-5p and miR-543-3p that target anti-inflammatory genes. *J. Immunol.* 203, 1830–1844. doi: 10.4049/jimmunol.1900291

Ortego, T. J., Robey, B., Morrison, D., and Chan, C. (1990). Toxoplasmic chorioretinitis and hepatic granulomas. am. J. *Gastroenterology* 85, 1418–1420.

Panda, A. C. (2018). Circular RNAs act as miRNA sponges. *Adv. Exp. Med. Biol.* 1087, 67–79. doi: 10.1007/978-981-13-1426-1_6

Pertea, M., Kim, D., Pertea, G. M., Leek, J. T., and Salzberg, S. L. (2016). Transcript-level expression analysis of RNA-seq experiments with HISAT, StringTie and ballgown. *Nat. Protoc.* 11, 1650–1667. doi: 10.1038/nprot.2016.095

Popko, K., Gorska, E., Stelmaszczyk-Emmel, A., Plywaczewski, R., Stoklosa, A., Gorecka, D., et al. (2010). Proinflammatory cytokines il-6 and TNF-α and the development of inflammation in obese subjects. *Eur. J. Med. Res.* 15 Suppl 2, 120–122. doi: 10.1186/2047-783x-15-s2-120

Preusse, M., Schughart, K., and Pessler, F. (2017). Host genetic background strongly affects pulmonary microRNA expression before and during influenza a virus infection. *Front. Immunol.* 8. doi: 10.3389/fimmu.2017.00246

Raetz, M., Hwang, S.-H., Wilhelm, C. L., Kirkland, D., Benson, A., Sturge, C. R., et al. (2013). Parasite-induced TH1 cells and intestinal dysbiosis cooperate in IFN-γ-dependent elimination of paneth cells. *Nat. Immunol.* 14, 136–142. doi: 10.1038/ni.2508

Smith, N. C., Goulart, C., Hayward, J. A., Kupz, A., Miller, C. M., and van dooren, G. G. (2021). Control of human toxoplasmosis. *Int. J. Parasitol.* 51, 95–121. doi: 10.1016/j.ijpara.2020.11.001

Stauffer, W. M., Magill, A., and Kain, K. C. (2006). Parasitic central nervous system infections in immunocompromised hosts: clarification of malaria diagnosis. *Clin. Infect. Dis.* 43, 114–115. doi: 10.1086/504951

Tang, Y., Jiang, M., Jiang, H. M., Ye, Z. J., Huang, Y. S., Li, X. S., et al. (2020). The roles of circRNAs in liver cancer immunity. *Front. Oncol.* 10. doi: 10.3389/fonc.2020.598464

Tan, J., Ni, D., Taitz, J., Pinget, G. V., Read, M., Senior, A., et al. (2022). Dietary protein increases T-cell-independent sIgA production through changes in gut microbiota-derived extracellular vesicles. *Nat. Commun.* 13, 4336. doi: 10.1038/s41467-022-31761-y

Tchitchek, N., Nguekap Tchoumba, O., Pires, G., Dandou, S., Campagne, J., Churlaud, G., et al. (2022). Low-dose interleukin-2 shapes a tolerogenic gut microbiota that improves autoimmunity and gut inflammation. *JCI. Insight.* 7, e159406. doi: 10.1172/jci.insight.159406

Tenter, A. M., Heckeroth, A. R., and Weiss, L. M. (2000). *Toxoplasma gondii*: from animals to humans. *Int. J. Parasitol.* 30, 1217–1258. doi: 10.1016/s0020-7519(00)00124-7

Urata, Y., Okita, K., Korenaga, K., Uchida, K., Yamasaki, T., and Sakaida, I. (2007). The effect of supplementation with branched-chain amino acids in patients with liver cirrhosis. *Hepatol. Res.* 37, 510–516. doi: 10.1111/j.1872-034X.2007.00081.x

Wang, Y., Li, H., Shi, Y., Wang, S., Xu, Y., Li, H., et al. (2020). miR-143-3p impacts on pulmonary inflammatory factors and cell apoptosis in mice with mycoplasmal pneumonia by regulating TLR4/MyD88/NF-κB pathway. *Biosci. Rep.* 40, BSR20193419. doi: 10.1042/BSR20193419

Wang, L., Xia, J. W., Ke, Z. P., and Zhang, B. H. (2019). Blockade of NEAT1 represses inflammation response and lipid uptake *via* modulating miR-342-3p in human macrophages THP-1 cells. *J. Cell. Physiol.* 234, 5319–5326. doi: 10.1002/jcp.27340

Wen, M., Shen, Y., Shi, S., and Tang, T. (2012). miREvo: an integrative microRNA evolutionary analysis platform for next-generation sequencing experiments. *BMC Bioinf.* 13, 140. doi: 10.1186/1471-2105-13-140

Xu, W. D., Lu, M. M., Pan, H. F., and Ye, D. Q. (2012). Association of microRNA-146a with autoimmune diseases. *Inflammation* 35, 1525–1529. doi: 10.1007/s10753-012-9467-0

Yao, T., Chen, Q., Fu, L., and Guo, J. (2017). Circular RNAs: Biogenesis, properties, roles, and their relationships with liver diseases. *Hepatol. Res.* 47, 497–504. doi: 10.1111/hepr.12871

Young, M. D., Wakefield, M. J., Smyth, G. K., and Oshlack, A. (2010). Gene ontology analysis for RNA-seq: accounting for selection bias. *Genome Biol.* 11, R14. doi: 10.1186/gb-2010-11-2-r14

Zhou, C. X., Ai, K., Huang, C. Q., Guo, J. J., Cong, H., He, S. Y., et al. (2020). miRNA and circRNA expression patterns in mouse brain during toxoplasmosis development. *BMC Genomics* 21, 46. doi: 10.1186/s12864-020-6464-9

Zhou, L., Chen, J., Li, Z., Li, X., Hu, X., Huang, Y., et al. (2010). Integrated profiling of microRNAs and mRNAs: microRNAs located on Xq27.3 associate with

clear cell renal cell carcinoma. *PLoS One* 5, e15224. doi: 10.1371/journal.pone.0015224

Zhou, C. X., Elsheikha, H. M., Zhou, D. H., Liu, Q., Zhu, X. Q., and Suo, X. (2016). Dual identification and analysis of differentially expressed transcripts of porcine PK-15 cells and *Toxoplasma gondii* during *in vitro* infection. *Front. Microbiol.* 7. doi: 10.3389/fmicb.2016.00721

Zhou, J., Xiong, Q., Chen, H., Yang, C., and Fan, Y. (2017). Identification of the spinal expression profile of non-coding RNAs involved in neuropathic pain following spared nerve injury by sequence analysis. *Front. Mol. Neurosci.* 10. doi: 10.3389/fnmol.2017.00091

Zhu, S., Wang, J., He, Y., Meng, N., and Yan, G. R. (2018). Peptides/proteins encoded by non-coding RNA: A novel resource bank for drug targets and biomarkers. *Front. Pharmacol.* 9. doi: 10.3389/fphar.2018.01295

Zuo, X., Wang, L., Bao, Y., and Sun, J. (2020). The ESX-1 virulence factors downregulate miR-147-3p in *Mycobacterium marinum*-infected macrophages. *Infect. Immun.* 88, e00088-20. doi: 10.1128/IAI.00088-20

frontiers | Frontiers in Cellular and Infection Microbiology

TYPE Original Research
PUBLISHED 02 November 2022
DOI 10.3389/fcimb.2022.1021464

OPEN ACCESS

EDITED BY
William Harold Witola,
University of Illinois at Urbana–Champaign, United States

REVIEWED BY
Iraj Sharifi,
Kerman University of Medical Sciences, Iran
Daniel A. Abugri,
Alabama State University, United States

*CORRESPONDENCE
Syamal Roy
drsyamalroy@yahoo.com
Madhumita Manna
madhumita.manna09@gmail.com

†PRESENT ADDRESS
Supriya Khanra,
Institute of Infection, Immunity and Inflammation, University of Glasgow, Main campus, Glasgow, United Kingdom
Nibedeeta Rani Sarraf,
Department of Zoology, Bidhannagar College, Kolkata, India
Sanchita Datta,
Department of Pharmaceutical Technology, Jadavpur University, Kolkata, India
Madhumita Manna,
WBSES Education Directorate, Department of Higher Education, Govt. of West Bengal, Kolkata, India

SPECIALTY SECTION
This article was submitted to Parasite and Host, a section of the journal Frontiers in Cellular and Infection Microbiology

RECEIVED 17 August 2022
ACCEPTED 06 October 2022
PUBLISHED 02 November 2022

CITATION
Khanra S, Das S, Sarraf NR, Datta S, Das AK, Manna M and Roy S (2022) Antimony resistance mechanism in genetically different clinical isolates of Indian Kala-azar patients.
Front. Cell. Infect. Microbiol.
12:1021464.
doi: 10.3389/fcimb.2022.1021464

Antimony resistance mechanism in genetically different clinical isolates of Indian Kala-azar patients

Supriya Khanra[1†], Shantanabha Das[2], Nibedeeta Rani Sarraf[1†], Sanchita Datta[1†], Anjan Kumar Das[3], Madhumita Manna[1*†] and Syamal Roy[4*]

[1]Department of Zoology, Barasat Government College, Kolkata, India, [2]Department of Zoology, Diamond Harbour Women's University, Sarisha, West Bengal, India, [3]Department of Medicine, Calcutta National Medical College, Kolkata, India, [4]Department of Infectious Diseases and Immunology, Indian Institute of Chemical Biology, Kolkata, India

The central theme of this enterprise is to find common features, if any, displayed by genetically different antimony (Sb)-resistant viscerotropic *Leishmania* parasites to impart Sb resistance. In a limited number of clinical isolates (n = 3), we studied the breadth of variation in the following dimensions: (a) intracellular thiol content, (b) cell surface expression of glycan having N-acetyl-D-galactosaminyl residue as the terminal sugar, and (c) gene expression of thiol-synthesizing enzymes (CBS, MST, gamma-GCS, ODC, and TR), antimony-reducing enzymes (TDR and ACR2), and antimonial transporter genes (AQP1, MRPA, and PRP1). One of the isolates, T5, that was genotypically characterized as *Leishmania tropica*, caused Indian Kala-azar and was phenotypically Sb resistant (T5-LT-SSG-R), while the other two were *Leishmania donovani*, out of which one isolate, AG83, is antimony sensitive (AG83-LD-SSG-S) and the other isolate, T8, is Sb resistant (T8-LD-SSG-R). Our study showed that the Sb-resistant parasites, regardless of their genotype, showed significantly higher intracellular thiol compared with Sb-sensitive AG83-LD-SSG-S. Seemingly, T5-LT-SSG-R showed about 1.9-fold higher thiol content compared with T8-LD-SSG-R which essentially mirrored cell surface N-acetyl-D-galactosaminyl expression. Except TR, the expression of the remaining thiol-synthesizing genes was significantly higher in T8-LD-SSG-R and T5-LT-SSG-R than the sensitive one, and between the Sb-resistant parasites, the latter showed a significantly higher expression. Furthermore, the genes for Sb-reducing enzymes increased significantly in resistant parasites regardless of genotype compared with the sensitive one, and between two resistant parasites, there was hardly any difference in expression. Out of three antimony transporters, AQP1 was decreased with the concurrent increase in MRPA and PRP1 in resistant isolates when compared with the sensitive counterpart. Interestingly, no difference in expression of the above-mentioned transporters was noted between two Sb-resistant isolates. The

enduring image that resonated from our study is that the genetically diverse Sb-resistant parasites showed enhanced thiol-synthesizing and antimony transporter gene expression than the sensitive counterpart to confer a resistant phenotype.

KEYWORDS

drug resistance, Indian Kala-azar, clinical isolates, *Leishmania donovani*, *L. tropica*

Introduction

Drug resistance is a serious problem in controlling any kind of infection, be it viral, bacterial, fungal, or protozoan or any other parasitic infection (WHO, 2021). Leishmaniases are no exception. Leishmaniases are neglected tropical diseases that have diversified epidemiology, pathogenesis, and clinical symptoms. Among all leishmaniases disease manifestations, mainly cutaneous, mucocutaneous, and visceral form, visceral leishmaniasis (VL) or Kala-azar (KA) is the most severe type if left untreated (Sundar, 2001). Approximately 20 million people are infected with leishmaniases worldwide (Bhargava and Singh, 2012). KA is endemic in the Indian subcontinent spanning across India, Bangladesh, Brazil, Iran, Nepal, and Sudan (Ostyn et al., 2013). Post-Kala-azar dermal leishmaniasis may develop in about 5–10% of apparently cured KA patients (Gasim et al., 2000). In the Indian subcontinent, KA is caused not only by *L. donovani* (Manna et al., 2005) but also by *L. tropica* (Sacks et al., 1995; Khanra et al., 2012). Among different species belonging to the *Leishmania* genus, the species *L. donovani* and *L tropica* show an anthroponotic nature of transmission (Steverding, 2017). This anthroponotic mode of transmission facilitates the emergence of drug-resistant isolates in these species, unlike the other zoonotic *Leishmania* spp. (ZVL and ZCL) in the Old World (Bamorovat et al., 2021). The main strategies to control the diseases associated with *L. donovani* and *L. tropica* are by developing effective control measures for primary human host infection (Bamorovat et al., 2021), early case detection (Oliaee et al., 2018), and prompt effective treatment (Singh and Sundar, 2015). According to the WHO, all cases must be treated because humans are reservoirs for transmitting the disease to others *via* sandfly vectors (WHO, 2022).

The emergence and progression of resistance of parasites to the commonly used antimonials and other drugs (Purkait et al., 2011; Khanra et al., 2017) made the control strategy inadequate (Capela et al., 2019). Researchers in the field emphasized that the emergence of antimonial resistance in *Leishmania* parasites may be related to sodium stibogluconate (SSG) treatment failure in the Indian state of Bihar (Rijal et al., 2003; Dube et al., 2005), and in the year 2000, the percentage of treatment failure cases had rose up to 60–70% in that region (Sundar et al., 2000). Amphotericin B, pentamidine, paromomycin, and miltefosine are other alternative drugs used for the disease, and they have their own limitations (Sundar, 2001; Moore and Lockwood, 2010).

The mechanism of parasite resistance towards the drug SSG is primarily *via* reduced drug concentration within the parasite, either by a low level of drug uptake or by a high level of drug efflux, and there are some other possible resistance mechanisms. These are related to the inefficiency in the conversion of pentavalent to trivalent antimony and the high level of trivalent antimony detoxification (Decuypere et al., 2005). All of these events related to SSG resistance are governed either by the thiol-metabolizing genes or by antimony transporter genes (Croft et al., 2006). Several types of ATP binding cassette (ABC) transporters are reported to be related to multi-drug resistance (MDR), and the MDR-related protein named multidrug-resistant protein A has been amplified in different *Leishmania* spp. in response to drugs *in vitro* (El Fadili et al., 2005; Coelho et al., 2007). A previous investigation demonstrated that thiol metabolism plays an essential role to preserve the intracellular reducing environment, and as a result, parasites can avoid the harm caused by oxidative stress within the macrophages (Wyllie et al., 2004). Altered levels of thiol have also been reported in Indian field isolates (Mandal et al., 2007; Singh et al., 2014).

The primary aim of our study was to investigate the drug resistance mechanism of genotypically diverse sodium stibogluconate-resistant (SSG-R) clinical isolates (T5 and T8) with respect to a sodium stibogluconate-sensitive (SSG-S) reference isolate (AG83). By the word "genotypically diverse field isolates", we meant both T8 and T5 are SSG-R and collected from confirmed Kala-azar patients, but their species status is completely different. T8 is the classical *L. donovani* isolate, while T5 belongs to *L. tropica* species (Khanra et al., 2016). As stated above, the third isolate (AG83) taken here for comparison is *L. donovani* and SSG-S. The purpose is to examine the relationship between the evolution of molecular mechanism and genetic background in the heterogeneous field isolates.

To our knowledge, this is the first such kind of report in which the antimony resistance mechanism of two resistant

isolates belonging to two different *Leishmania* species causing the same disease condition has been evaluated, and the results were expressed in comparison with antimony-sensitive *L. donovani*.

Materials and methods

Ethics statements

Bone marrow aspirates collected from Kala-azar patients were approved by the Ethical Committee of the Calcutta National Medical College, Kolkata. Patient details and the Human Ethics Clearance related statements have already been published previously (Khanra et al., 2012; Sarraf et al., 2021).

Animal ethics statements

BALB/c mice (*Mus musculus*) and hamsters (*Mesocricetus auratus*) were maintained and bred under pathogen-free conditions. Animal use was approved by the Institutional Animal Ethics Committees of the Indian Institute of Chemical Biology, Kolkata, India. Animal infections to maintain the parasites *in vivo* were performed according to the National Regulatory Guidelines issued by the Committee for the Purpose of Supervision of Experiments on Animals (IICB/AEC-15-2008, 10.06.2008), Ministry of Environment and Forest, Government of India.

Leishmania parasite culture

The present study has been carried out with three (n = 3) clinical isolates of KA patients, from which one is the *L. donovani* isolate AG83 (MHOM/IN/1983/AG83), which is used as a reference strain for the present study. The other two named as T5 (MHOM/IN/2010/T5) and T8 (MHOM/IN/2012/T8) were collected in the year between 2010 and 2012 from the confirmed VL patients, and the respective patients' details were reported previously (Khanra, 2015; Khanra et al., 2016; Sarraf et al., 2021) and are delineated in Supplementary Table S1. T5 and T8 parasites were isolated from bone marrow aspirates. Briefly, the sternum or iliac crest was punctured by a special type of needle, and marrow was aspirated using a syringe containing an anticoagulant, such as heparin or EDTA. Only two to three drops were added to each culture tube containing Schneider's *Drosophila* medium with 20% fetal calf serum (FCS). The *Leishmania* amastigotes were confirmed by Giemsa staining, and after the transformation of amastigotes to promastigotes, the parasites were maintained in M199 medium (St. Louis, MO, USA) with 10% fetal bovine serum. The other one is the *L. donovani* isolate AG83 (MHOM/IN/1983/AG83), which was collected in the year 1983, maintained in M199 medium with 10% FCS, and used here as a reference strain. All the isolates were maintained in infected mice/hamster, and heavily infected animals were sacrificed, with their infected organs cultured to get large numbers of promastigotes. The promastigotes (1×10^6) were kept frozen in the vials. Depending on our need the frozen vial was thawed and propagated one or two cycles in M199 containing 10% FCS to conduct experiments. Our earlier report based on PCR-RFLP and SSCP analysis revealed the genotyping status of T8 and T5, where T5 was found to be *L. tropica* and T8 was found to be *L. donovani*, and our *in vitro* amastigote–macrophage model data shows that both of the parasites are less sensitive towards the drug SSG, with EC_{50} values of 45.17 ± 3.55 and 18.77 ± 4.84 μg/ml for T5 and T8, respectively (Khanra et al., 2016). The SSG unresponsiveness of the T8 parasite was further supported by whole genome analysis (Sarraf et al., 2021). On the other hand, the reference AG83 parasite has been reported as SSG-sensitive parasite (Mukhopadhyay et al., 2011; Palit et al., 2012). Hence, we named T5 and T8 as T5-LT-SSG-R and T8-LD-SSG-R, respectively, and AG83 as AG83-LD-SSG-S in the present study.

Measurement of non-protein thiol content in *Leishmania* parasites

The promastigotes (2×10^6 each/ml) were washed with phosphate-buffered saline (PBS) thrice and then incubated for 20 min at 37°C with the addition of 5 μM 5-chloromethylfluorescein-diacetate (Molecular Probes, CA, USA) (Sarkar et al., 2009). The labeled promastigotes were subjected to BDFACSAria II cell sorter for cytometric measurement, and the analyses were performed using FACSDIVA software (BD Biosciences, San Jose, CA, USA).

Measurement of surface sugar residue in *Leishmania* parasites

The expression of surface glycan in promastigotes was carried out as described previously (Mukhopadhyay et al., 2011). Briefly, the promastigotes were washed three times with 1X sterile PBS and incubated with FITC-labeled horsegram (*Dolichos biflorus*) lectin at a dilution of 1:50 for 30 min in FACS buffer. After labeling, flow cytometric measurement of the FITC-labeled promastigotes was performed using BDFACSAria II cell sorter. The mean fluorescence intensity was analyzed by FACSDIVA software (BD Biosciences, San Jose, CA, USA) to determine the expression of surface sugar.

RNA isolation, cDNA synthesis, and semi-quantitative reverse transcription-PCR

RNA extractions were carried out from all of the harvested promastigotes by disrupting in Trizol solution (Khanra et al., 2017). For the synthesis of cDNA, the total RNA (2 µg/reaction) was first incubated with gene-specific reverse primers, heated at 75°C for 10 min, and immediately kept in ice. A common master mixture (2 µl of 0.1 M DTT, 5 µl of 5X FS buffer, 2 µl of 10 mM dNTP, and 0.5 µl of mouse Moloney leukemia virus reverse transcriptase) was added to the ice-cold RNA mixture and then incubated at 37°C for 90 min, followed by 70°C for 15 min (Banerjee et al., 2009). The freshly prepared cDNA was then amplified in a reaction mixture containing 0.5 µl of cDNA with 1 µl 10 mM dNTP, 1.5 µl 50 mM $MgCl_2$, and 0.5 µl Taq polymerase as well as gene-specific primers (Supplementary Table S2). Amplification reactions were performed with an Applied Biosystems thermocycler. The cycling conditions for genes of interest were 5 min at 95°C, followed by 30 cycles of denaturation at 95°C for 30 s, annealing at 55–60°C for 3 0s, and extension at 72°C for 30 s. The identities of the PCR-amplified respective gene products were checked by agarose gel electrophoresis. Identical aliquots were investigated in parallel without reverse transcriptase to eliminate the presence of residual genomic DNA contamination in PCR amplification preparations. Densitometry analyses were performed using ImageJ software (v1.41o) (Mukherjee et al., 2012). For the densitometric calculations, the same band area was used to determine the band intensity and normalized for GAPDH. GAPDH was used as the internal control gene.

Statistical analyses for the *in vitro* study

Each experiment was performed at least three times. The results are expressed as mean ± SD. GraphPad prism software was used to perform Student's *t*-test for significance analysis, and a *P*-value <0.05 was considered to be significant. The correlation between the EC_{50} and other parameters was measured by the Spearman rank correlation coefficient and represented by R (Khanra et al., 2017).

Results

Intracellular thiol content

The thiol content was determined in the promastigotes. It was observed that there was a significantly increased thiol content in resistant parasites than in sensitive parasites. It was about 30-fold ($P < 0.0001$) and 16-fold ($P = 0.0002$) increase in thiol content in Sb-resistant T5-LT-SSG-R and T8-LD-SSG-R, respectively, compared with Sb-sensitive AG83-LD-SSG-S. Between the two genetically diverse parasites, T5-LT-SSG-R showed about 1.9-fold ($P = 0.0006$) higher thiol content than T8-LD-SSG-R. Our data revealed a high correlation ($R = 0.99$) between intracellular thiol content and SSG resistance (Figure 1, Supplementary Figure S1).

Expression of terminal N-acetyl-D-galactosaminyl on cell surface glycan

The expression of N-acetyl-D-galactosaminyl as the terminal sugar on the cell surface glycan was determined using fluorescence-labeled horse gram (*Dolichos biflorus*) lectin. The binding of lectin was significantly higher in resistant parasites compared with the sensitive counterpart. It was observed that the expression of N-acetyl-D-galactosaminyl as the terminal sugar was about 28-fold ($P < 0.0001$) and ninefold ($P = 0.0009$) higher in Sb-resistant T5-LT-SSG-R and T8-LD-SSG-R, respectively, compared with Sb-sensitive AG83-LD-SSG-S. Between the two genetically diverse parasites, T5-LT-SSG-R showed about threefold ($P = 0.0003$) higher N-acetyl-D-galactosaminyl terminal sugar expression than T8-LD-SSG-R. There was a high correlation ($R = 0.99$) between the expression of N-acetyl-D-galactosaminyl and the SSG sensitivities of the isolates (Figure 2, Supplementary Figure S2).

Expression of genes of thiol-synthesizing enzymes

The expression of cystathionine-ß synthase (CBS), mercaptopyruvate sulfurtransferase (MST), gamma-glutamylcysteine synthase (ϒ-GCS), ornithine decarboxylase (ODC), and trypanothione reductase (TR) was studied both in Sb-resistant and Sb-sensitive parasites, and the results were expressed as fold increase compared with the sensitive counterpart. The gel pictures of the gene expression profiling experiments are provided in Supplementary Figure S3. It was observed that CBS expression was about sixfold higher in T5-LT-SSG-R ($P < 0.0001$) and 2.8-fold higher in T8-LD-SSG-R ($P = 0.0007$) (Figure 3A) than in AG83-LD-SSG-S (and the positive correlation value between CBS expressions and EC_{50} of the isolates was determined to be $R = 0.99$). MST expression was 3.9-fold higher in T5-LT-SSG-R ($P < 0.0001$) and 2.9-fold higher in T8-LD-SSG-R ($P = 0.0002$) than in AG83-LD-SSG-S, with a positive correlation value $R = 0.95$ (Figure 3A). The other gene ϒ-GCS was about fivefold over-expressed in T5-LT-SSG-R ($P < 0.0001$) and approximately 3.3-fold over-expressed in T8-LD-SSG-R ($P = 0.0004$) compared with AG83-LD-SSG-S, with a positive correlation between EC_{50} and ϒ-GCS expression ($R = 0.97$, Figure 3A). Similarly, ODC expression was upregulated approximately 3.9-fold in T5-LT-SSG-R ($P = 0.0003$) and 2.8-

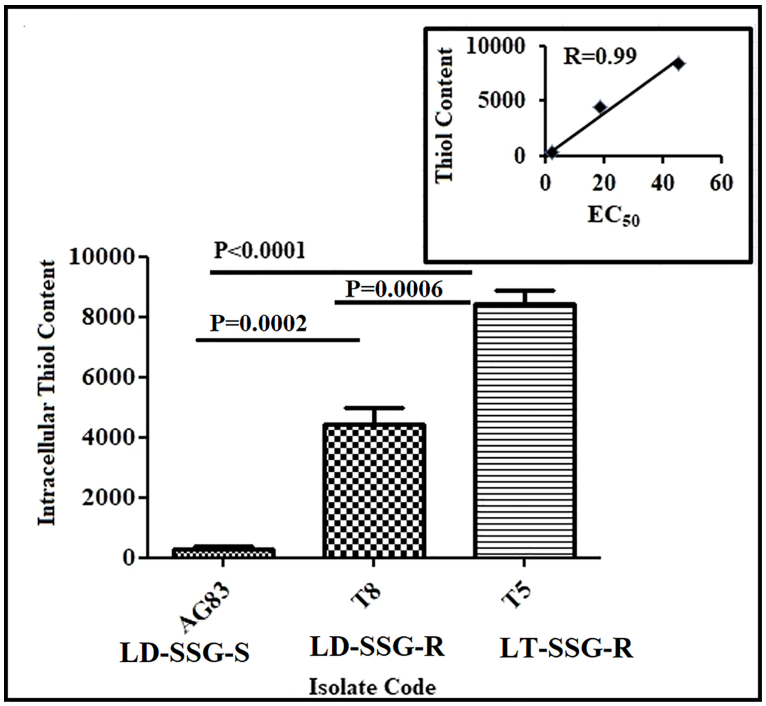

FIGURE 1
Analysis of thiol content in SSG-S (AG83-LD-SSG-S) and SSG-R (T5-LT-SSG-R and T8-LD-SSG-R) *Leishmania* promastigotes by flow cytometry. The thiol content was measured using a fluorescence probe 5-chloromethylfluorescein-diacetate and presented in terms of mean fluorescence intensity values. The inset shows the scatter plot representing the correlation between EC_{50} values against sodium stibogluconate and the intracellular thiol content of each isolate.

fold in T8-LD-SSG-R ($P = 0.0008$) compared with that in AG83-LD-SSG-S, with a positive correlation value $R = 0.96$ (Figure 3A). TR expression (Figure 3B) showed approximately 2.6- and 2.2-fold higher expressions in SSG-R isolates (T5-LT-SSG-R; $P = 0.0006$, T8-LD-SSG-R; $P = 0.0003$, $R = 0.80$) than in the SSG-sensitive counterpart (AG83-LD-SSG-S). These results have also pointed out the enhanced over-expression of those four genes (CBS, ϒ-GCS, MST, and ODC) except TR in T5-LT-SSG-R (SSG-R *L. tropica*), which ranged from approximately 1.3- to 2.2-fold compared with T8-LD-SSG-R (SSG-R *L. donovani*) (Figures 3A, B).

Expression of genes for antimony reduction

The expression level of thiol-dependent reductase (TDR) and arsenate reductase2 (ACR2) was studied and normalized for GAPDH (Figure 4). ACR2 expression (Figure 4) was approximately 3.8-fold higher ($P = 0.0001$) in T5-LT-SSG-R and 3.2-fold higher ($P = 0.0007$) in T8-LD-SSG-R than in AG83-LD-SSG-S with $R = 0.84$, whereas TDR expression (Figure 4) showed around 3.5 fold higher ($P = 0.0003$) expression in T5-LT-SSG-R and 3.2 fold higher ($P = 0.0004$) expression in T8-LD-SSG-R than in AG83-LD-SSG-S with R = 0.82. The respective gel pictures of the gene expression profiling experiments can be found in Supplementary Figure S3.

Expression of genes for antimony transport

The expression levels of genes for antimony transport such as aquaglyceroporin (AQP1), multidrug-resistant protein A (MRPA), and pentamidine resistance protein 1 (PRP1) are significantly altered between SSG-S (AG83-LD-SSG-S) and SSG-R isolates (T5-LT-SSG-R, T8-LD-SSG-R) but not considerably more pronounced between T5-LT-SSG-R and T8-LD-SSG-R relative to the genes stated above. The expression level of AQP1 was found to be upregulated approximately four times ($P < 0.0001$) in AG83-LD-SSG-S parasite compared with that of T5-LT-SSG-R and T8-LD-SSG-R isolates, respectively, and a negative correlation exists between EC_{50} and AQP1 expression ($R = -0.81$) (Figure 5; Supplementary Figure S3). On the other hand, the MRPA expression (Figure 5; Supplementary Figure S3) was approximately fourfold ($P =$

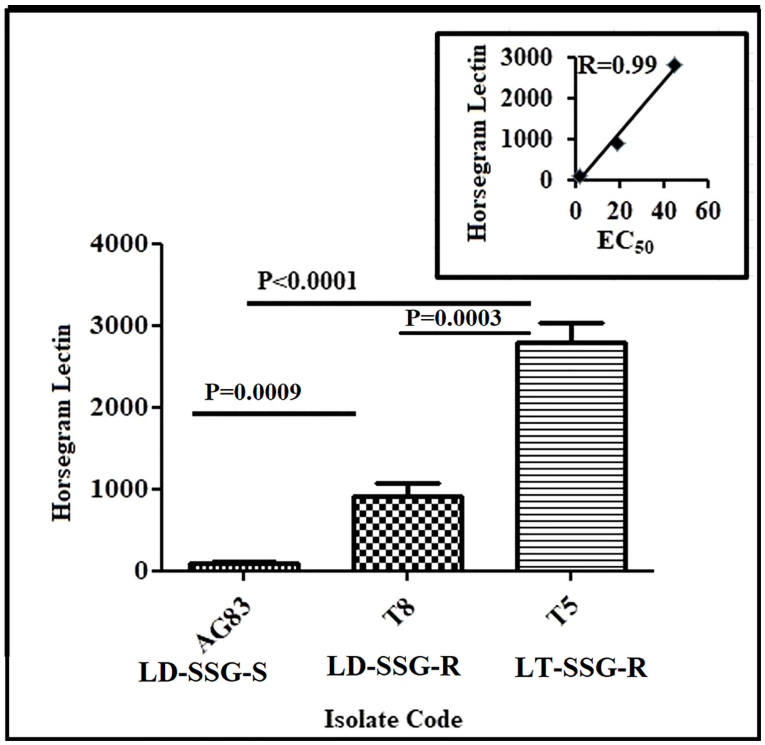

FIGURE 2
Flow cytometric analysis of the differential expressions of terminal N-acetyl- D-galactosaminyl residue in promastigotes of SSG-R (T5-LT-SSG-R and T8-LD-SSG-R) and SSG-S (AG83-LD-SSG-S) field isolates. The plot shows the binding of FITC-labeled horsegram lectin (*Dolichos biflorus*) in SSG-R and SSG-S isolates. Each scatter plot in the inset represents the correlation between the EC_{50} of the isolates with the presence of surface sugar residue.

0.0001) and 4.4-fold ($P < 0.0001$) over-expressed in T8-LD-SSG-R and T5-LT-SSG-R isolates, respectively, compared with AG83-LD-SSG-S with $R = 0.85$. Similarly, the PRP1 expression was also approximately 4.6- and 4.2-fold upregulated in T5-LT-SSG-R ($P < 0.0001$) and T8-LD-SSG-R ($P < 0.0001$), respectively, with $R = 0.86$ (Figure 5; Supplementary Figure S3).

Discussion

An understanding of drug resistance mechanism in respective field isolates is essential because it may offer clues to determine the drug regimen to go for, *e.g.*, either single drug therapeutics or combination therapy for the treatment of patients. It also helps us to evaluate the progress and extent of resistance in the field (Ashutosh et al., 2007).

Multifactorial determinants are responsible for variations in the drug susceptibility of the field isolates of KA (Croft et al., 2006). A divergence in membrane sterol (Goad et al., 1984; Beach et al., 1988) and lipid (Beach et al., 1979) contents has been established to lead to various drug susceptibility profiles. The wide use of SSG in areas of hyper-endemicity may have changed the biochemical composition of these parasite membranes in ways that might affect drug susceptibility (Kumar et al., 2009). An earlier report demonstrated a variety of biochemical and biophysical changes in SSG-resistant *Leishmania* parasites (Mukhopadhyay et al., 2011) and also delineated the association between the expression level of terminal glycoconjugates and IL-10 induction (Mukherjee et al., 2013).

Our previous investigation based on the *in vitro* amastigote–macrophage model revealed that 46.2% of our studied field isolates were SSG resistant—among them is *L. tropica*, and the others were *L. donovani* (Khanra et al., 2016). A recent report from our group furthermore confirmed the genetic characteristics of some of those SSG-resistant isolates by whole genome analysis (Sarraf et al., 2021). We have taken the SSG R -*L. tropica* (T5-LT-SSG-R; $EC_{50} = 45.17 \pm 3.55$, μg/ml) and one SSG-R *L. donovani* (T8-LD-SSG-R; $EC_{50} = 18.77 \pm 4.84$, μg/ml) clinical isolate along with one SSG-S *L. donovani* (AG83-LD-SSG-S; $EC_{50} = 1.87 \pm 0.07$, μg/ml) isolate for our present study to investigate the relationship between the evolution of molecular mechanism and SSG-resistant phenotype in genetically heterogeneous field isolates.

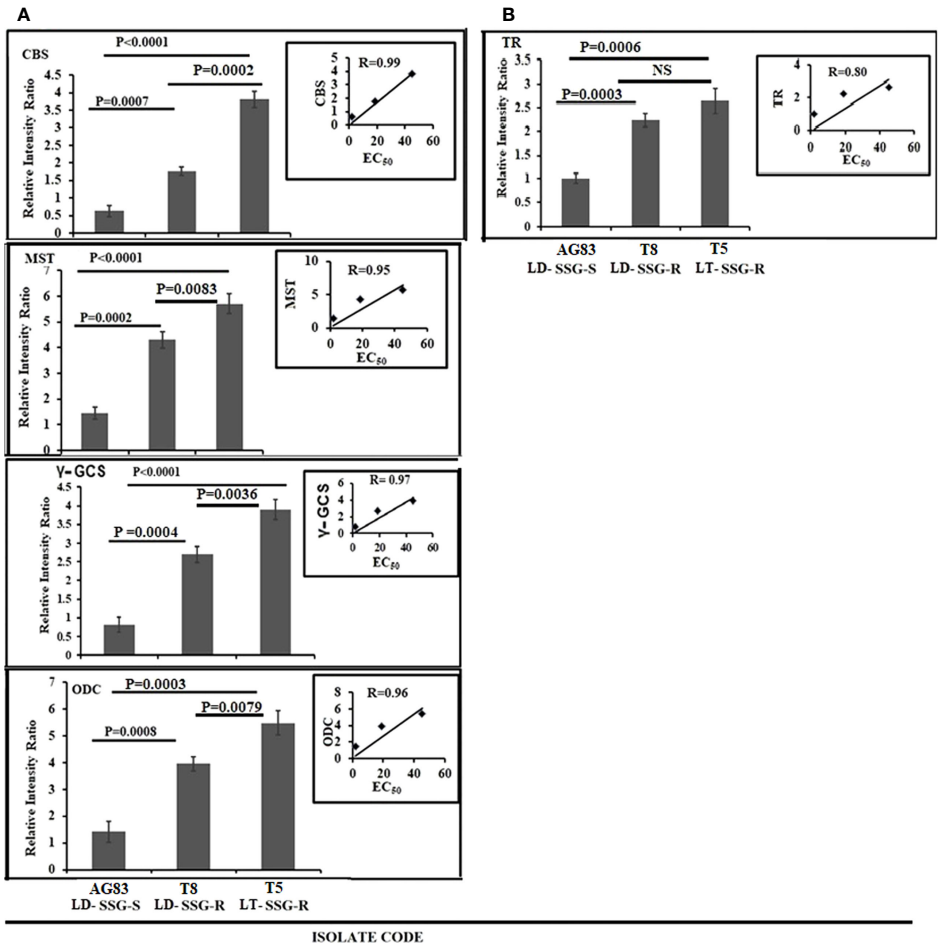

FIGURE 3
Graphical representation of the densitometric data. **(A)** Expression levels of thiol-metabolizing enzymes CBS, MST, γ-GCS, and ODC were expressed as a ratio of CBS, MST, γ-GCS, and ODC mRNA levels to GAPDH mRNA level, respectively. Data were expressed as the mean ± SD of three independent experiments. Each scatter plot in the inset represents the correlation between the EC_{50} of the isolates against sodium stibogluconate and the respective gene expressions. **(B)** The expression level of another thiol-metabolizing enzyme (TR) was expressed as a ratio of TR mRNA level to GAPDH mRNA level. Data were expressed as the mean ± SD of three independent experiments. Each scatter plot in the inset represents the correlation between the EC_{50} of the isolates against sodium stibogluconate and the respective gene expression. NS, Non-significant.

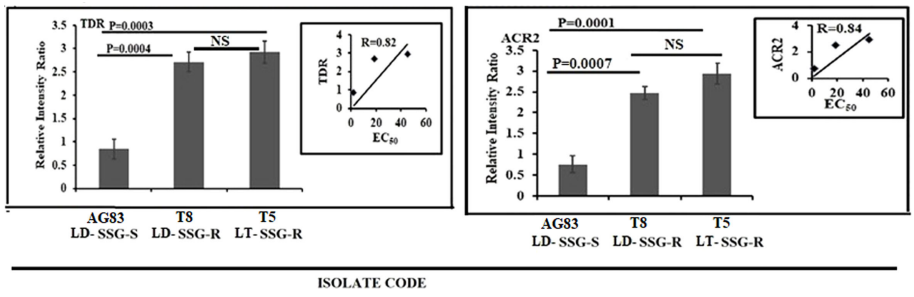

FIGURE 4
Graphical representation of the densitometric data of the genes responsible for the reduction of pentavalent to trivalent antimony. The expressions of ACR2 and TDR were expressed as the ratio of ACR2 and TDR mRNA levels to GAPDH mRNA level, respectively. Data were expressed as the mean ± SD of three independent experiments. Each scatter plot in the inset represents the correlation between the EC_{50} of the isolates against sodium stibogluconate and the respective gene expression. NS, Non-significant.

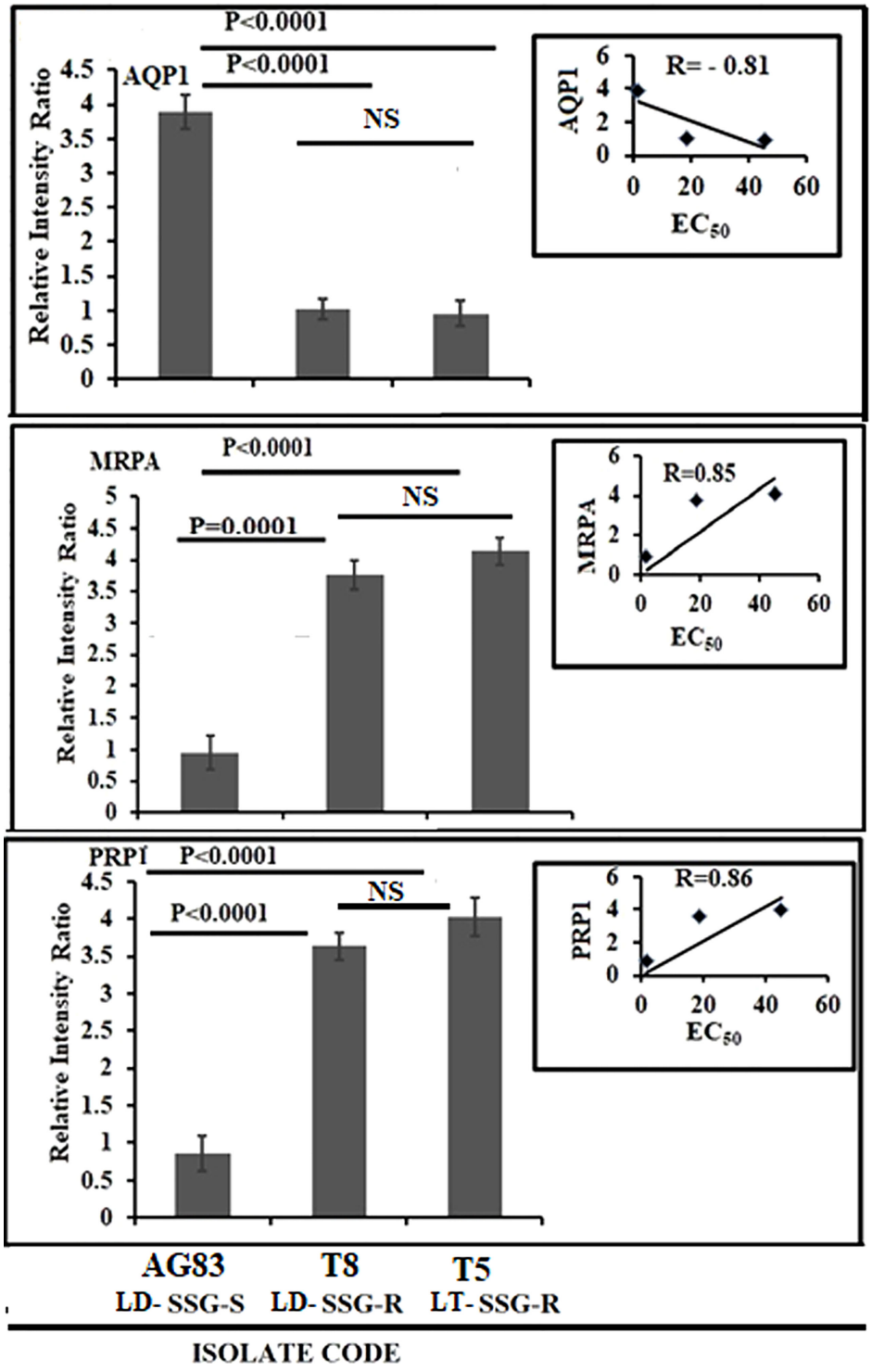

FIGURE 5
Graphical representation of the densitometric data of sodium stibogluconate (SSG)-transporting enzyme and ABC transporter. The expression level of AQP1 was expressed as a ratio of AQP1 mRNA level to GAPDH mRNA level. Data were expressed as the mean ± SD of three independent experiments. Each scatter plot in the inset represents the correlation between the EC_{50} of the isolates against SSG and the respective gene expression. The expression levels of MRPA and PRP1 were expressed as the ratio of MRPA and PRP1 mRNA levels to GAPDH mRNA level, respectively. Data were expressed as the mean ± SD of three independent experiments. Each scatter plot in the inset represents the correlation between the EC_{50} of the isolates against SSG and the respective gene expression. NS, Non-significant.

Leishmania produce huge, glycosylated proteins and proteoglycans that have a significant role in parasite virulence (Merida-de-Barros et al., 2018). It is demonstrated that the metacyclogenesis in *Leishmania* parasites is connected with alterations of surface glycoconjugates (Monteiro Tínel et al., 2014) that, in the resistant isolates, were found to be upregulated (Vanaerschot et al., 2010). We have observed significantly higher terminal glycan levels in T5-LT-SSG-R and T8-LD-SSG-R, respectively, than in AG83-LD-SSG-S.

It is documented that the thiol content in the SSG-R isolate is higher than that of the SSG-S isolate (Singh et al., 2014), and our results are offering credence to such a notion. The present study also revealed a very high correlation coefficient ($r = 0.99$) between SSG resistance and intracellular non-protein thiol content in the isolates studied here. Interestingly, our data revealed that the thiol content of the T5-LT-SSG-R isolate is approximately 30.98-fold higher than in AG83-LD-SSG-S and 1.9-fold higher than that of T8-LD-SSG-R isolate. Our data also revealed that T8-LD-SSG-R had approximately 16.30 fold ($P < 0.0001$) higher intracellular thiol content than that of AG83-LD-SSG-S. This observation prompted us to search the potential association between the intracellular thiol content and the expression of genes of thiol-metabolizing enzymes.

Our study demonstrated the over-expression of AQP1 in AG83-LD-SSG-S isolate with respect to T5-LT-SSG-R and T8-LD-SSG-R isolates. AQP1 facilitates SSG uptake into the cell (Haldar et al., 2011; Decuypere et al., 2012). The rest of the genes that are responsible for thiol metabolism and antimony transport were all significantly upregulated in all the SSG-R isolates (T5-LT-SSG-R and T8-LD-SSG-R). Among all of the genes studied, the four genes (CBS, ϒ-GCS, MST, and ODC) showed a considerable over-expression in SSG-R *L. tropica* isolate (T5-LT-SSG-R) whose range of over-expression varied from 3.8- to 6.1-fold compared with SSG-S *L. donovani* isolate (AG83-LD-SSG-S), whereas it was 1.3- to 2.2-fold higher in the other SSG-R isolate (T8-LD-SSG-R) than in the sensitive counterpart. It has been reported earlier that the pronounced expressions of ODC and ϒ-GCS in drug-resistant parasites help in the production of trypanothione precursors such as glutathione and spermidine (Grondin et al., 1997; Haimeur et al., 1999) and are also related to an increased thiol level in the antimony-resistant parasites (Mukherjee et al., 2007; Mittal et al., 2007). The other two genes, MST and CBS, also play key roles in the production of cysteine, the other thiol source of trypanosomatids (Nozaki et al., 2001). At this point, it could be strongly postulated that our SSG-R *L. tropica* isolate would show a stronger SSG-resistant phenotype than SSG-R *L. donovani* isolate due to the pronounced expressions of those four specific thiol-metabolizing genes (CBS, ϒ-GCS, MST, and ODC). This observation also supported our earlier report that showed the higher EC_{50} value of the *L. tropica* isolate, T5-LT-SSG-R (EC_{50} = 45.17 ± 3.55, μg/ml), towards SSG compared with that of other isolates (Khanra et al., 2016). The rest of the genes studied, such as ACR2 and TDR1, have the ability to catalyze the reduction of anti-leishmanial pentavalent antimony to trivalent antimony, and two other genes (MRPA and PRP1) are reported as ABC transporters (Denton et al., 2004; Wyllie et al., 2004; Decuypere et al., 2012). Our present study revealed that the expressions of those genes (ACR2, TDR, TR, MRPA, and PRP1) are not statistically different between two SSG-resistant isolates, T5-LT-SSG-R and T8-LD-SSG-R, but significantly different from SSG-sensitive isolate AG83-LD-SSG-S, which is in congruence with earlier reports stating that the upregulation of MRPA, PRP1, ACR2, TDR, and TR genes may contribute in conferring resistance to the antimonial drug (Mukhopadhyay et al., 2011; Ponte-Sucre et al., 2017).

Our results showed that thiol-metabolizing genes play a crucial role in determining the antimony resistance phenotype in genetically divergent clinical isolates of Indian Kala-azar.

Conclusion

We may conclude that the altered levels of expression of thiol-metabolizing genes are responsible for the antimony-resistant phenotype in genetically different resistant isolates causing Indian Kala-azar.

Limitation and strength of the study

The limitation of the present study is the small sample size ($n = 3$). The strength of the present study is that it depicted the comparative profiles of the antimony resistance mechanism of two recent clinical isolates identified as *L. donovani* (T8-LD-SSG-R) and *L. tropica* (T5-LT-SSG-R), which are both resistant to SSG. The results were compared with their SSG-sensitive counterpart (AG83-LD-SSG-S). To the best of our knowledge, this is the first report in which we showed that the antimony resistance mechanism of two field isolates belonging to two different *Leishmania* species causing the same disease is essentially similar.

Data availability statement

The original contributions presented in the study are included in the article/Supplementary Material. Further inquiries can be directed to the corresponding authors.

Ethics statement

The bone marrow aspirates collected from Kala-azar patients were approved by the Ethical Committee of the Calcutta National Medical College, Kolkata. Written consents were obtained from every patient and guardian (in the case of minors) prior to the study. The patients/participants provided their written informed

consent to participate in this study. The animal study was reviewed and approved by the Committee for the Purpose of Supervision of Experiments on Animals (IICB/AEC-15-2008, 10.06.2008), Ministry of Environment and Forest, Government of India.

Author contributions

SK, ShD, NS, SaD, and AD have worked under this project. MM and SR have designed the problem and written the manuscript. All authors contributed to the article and approved the submitted version.

Funding

We sincerely acknowledge the Department of Biotechnology (DBT Twinning Program, BCIL/NER-BPMC/2013), New Delhi, India, and the University Grant Commission (UGC), New Delhi, India [35/57/2009 (SR)] for financial help. We further acknowledge the Council of Scientific and Industrial Research, New Delhi, India, for the fellowship of SK. This work was also supported by the Network Project (Project NWP 0005), J.C. Bose Fellowship (SB/S2/JCB-65/2014), and ICMR Emeritus Fellowship to SR.

Acknowledgments

We are thankful to the Director of Public Instruction, Higher Education Dept. Govt. of West Bengal, the Principal, Barasat Govt. College, Kolkata, India, and the Director, Indian Institute of Chemical Biology, Kolkata. We thank Mr. Connor Tennant, doctoral student, Wellcome Centre for Integrative Parasitology, Institute of Infection, Immunity and Inflammation, University of Glasgow for reading and correcting the manuscript.

Conflict of interest

The authors declare that the research was conducted in the absence of any commercial or financial relationships that could be construed as a potential conflict of interest.

Publisher's note

Supplementary material

The Supplementary Material for this article can be found online at: https://www.frontiersin.org/articles/10.3389/fcimb.2022.1021464/full#supplementary-material

SUPPLEMENTARY FIGURE 1
Flow cytometric analysis of thiol content in *Leishmania*. Analyses of the thiol content in promastigotes of SSG-S *L. donovani* (**A**: AG83-LD-SSG-S), SSG-R *L. donovani* (**B**: T8-LD-SSG-R), and SSG-R *L. tropica* (**C**: T5-LT-SSG-R) were performed with fluorescence probe 5-chloromethylfluorescein-diacetate. Our result denoted that the thiol content has been varied among the SSG-S and SSG-R isolates studied here.

SUPPLEMENTARY FIGURE 2
Flow cytometric analysis of surface sugar in *Leishmannia* promastigotes. Terminal N-acetyl-D galactosaminyl residues in *Leishmannia* promastigotes were measured by the binding of FITC-labeled horsegram (*Dolichos biflorus*) lectin in SSG-R and SSG-S isolates. Our data revealed the differential expressions of the terminal N-acetyl-D-galactosaminyl residue in the promastigotes of SSG-S *Leishmania donovani* (**A**: AG83-LD-SSG-S) and SSG-R *Leishmania donovani* (**B**: T8-LD-SSG-R) and SSG-R *Leishmania tropica* (**C**: T5-LT-SSG-R).

SUPPLEMENTARY FIGURE 3
Gel images of the studied gene expressions. GAPDH mRNA expressions: lane 1, AG83-LD-SSG-S; lane 2, T8-LD-SSG-R; lane 3, T5-LT-SSG-R. AQP1 mRNA expressions: lane 1, T8-LD-SSG-R; lane 2, T5-LT-SSG-R; lane 3, AG83-LD-SSG-S. ACR2 mRNA expressions: lane 1, T5-LT-SSG-R; lane 2, T8-LD-SSG-R; lane 3, AG83-LD-SSG-S. CBS mRNA expressions: lane 1, T5-LT-SSG-R; lane 2, T8-LD-SSG-R; lane 3, AG83-LD-SSG-S. γ-GCSmRNA expressions: lane 1, T5-LT-SSG-R; lane 2, T8-LD-SSG-R; lane 3, AG83-LD-SSG-S. MST mRNA expressions: lane 1, AG83-LD-SSG-S; lane 2, T5-LT-SSG-R; lane 3, T8-LD-SSG-R. ODC mRNA expressions: lane 1, T8-LD-SSG-R; lane 2, T5-LT-SSG-R; lane 3, AG83-LD-SSG-S. MRPA mRNA expressions: lane 1, AG83-LD-SSG-S; lane 2, T5-LT-SSG-R; lane 3, T8-LD-SSG-R. PRP1 mRNA expressions: lane 1, T5-LT-SSG-R; lane 2, T8-LD-SSG-R; lane 3, AG83-LD-SSG-S. TDR mRNA expressions: lane 1, AG83-LD-SSG-S; lane 2, T5-LT-SSG-R; lane 3, T8-LD-SSG-R. TR mRNA expressions: lane 1, T8-LD-SSG-R; lane 2, AG83-LD-SSG-S; lane 3, T5-LT-SSG-R.

References

Ashutosh,, Sundar., S., and Goyal, N. (2007). Molecular mechanisms of antimony resistance in leishmania. *J. Med. Microbiol.* 56, 143–153. doi: 10.1099/jmm.0.46841-0

Bamorovat, M., Sharifi, I., Oliaee, R. T., Jafarzadeh, A., and Khosravi, A. (2021). Determinants of unresponsiveness to treatment in cutaneous leishmaniasis: A focus on anthroponotic form due to leishmania tropica. *Front. Microbiol.* 12, 638957. doi: 10.3389/fmicb.2021.638957

Banerjee, S., Ghosh, J., Sen, S., Guha, R., Dhar, R., Ghosh, M., et al. (2009). Designing therapies against experimental visceral leishmaniasis by modulating the membrane fluidity of antigen-presenting cells. *Infect. Immun.* 77, 2330–2342. doi: 10.1128/IAI.00057-09

Beach, D. H., Goad, L. J., and Holz, G. G.Jr. (1988). Effects of antimycotic azoles on growth and sterol biosynthesis of leishmania promastigotes. *Mol. Biochem. Parasitol.* 31, 149–162. doi: 10.1016/0166-6851(88)90166-1

Beach, D. H., Holz, G. G.Jr., and Anekwe, G. E. (1979). Lipids of leishmania promastigotes. *J. Parasitol.* 65, 201–216. doi: 10.2307/3280147

Bhargava, P., and Singh, R. (2012). Developments in diagnosis and antileishmanial drugs. *Inter. Discip. Perspect. Infect. Dis.* 2012, 626838. doi: 10.1155/2012/626838

Capela, R., Moreira, R., and Lopes, F. (2019). An overview of drug resistance in protozoal diseases. *Int. J. Mol. Sci. 15* 20 (22), 5748. doi: 10.3390/ijms20225748

Coelho, A. C., Messier, N., Ouellette, M., and Cotrim, P. C. (2007). Role of the ABC transporter PRP1 (ABCC7) in pentamidine resistance in leishmania amastigotes. *Antimicrob. Agents. Chemother.* 51, 3030–3032. doi: 10.1128/AAC.00404-07

Croft, S. L., Sundar, S., and Fairlamb, A. H. (2006). Drug resistance in leishmaniasis. *Clin. Microbiol. Rev.* 19, 111–126. doi: 10.1128/CMR.19.1.111-126.2006

Decuypere, S., Rijal, S., Yardley, V., De Doncker, S., Laurent, T., Khanal, B., et al. (2005). Gene expression analysis of the mechanism of natural Sb(V) resistance in leishmania donovani isolates from Nepal. *Antimicrob. Agents. Chemother.* 49, 4616–4621. doi: 10.1128/AAC.49.11.4616-4621.2005

Decuypere, S., Vanaerschot, M., Brunker, K., Imamura, H., Mu¨ller, S., Khanal, B., et al. (2012). Molecular mechanisms of drug resistance in natural leishmania populations vary with genetic background. *PLoS. Negl. Trop. Dis.* 6, e1514. doi: 10.1371/journal.pntd.0001514

Denton, H., McGregor, J. C., and and Coombs, G. H. (2004). Reduction of antileishmanial pentavalent antimonial drugs by a parasite-specific thiol-dependent reductase, TDR1. *Biochem. J.* 15, 405–412. doi: 10.1042/BJ20040283

Dube, A., Singh, N., Sundar, S., and Singh, N. (2005). Refractoriness to the treatment of sodium stibogluconate in Indian kala-azar field isolates persist in *in vitro* and *in vivo* experimental models. *Parasitol. Res.* 96, 216–223. doi: 10.1007/s00436-005-1339-1

El Fadili, K., Messier, N., Leprohon, P., Roy, G., Guimond, C., Trudel, N., et al. (2005). Role of the ABC transporter MRPA (PGPA) in antimony resistance in leishmania infantum axenic and intracellular amastigotes. *Antimicrob. Agents. Chemother.* 49, 1988–1993. doi: 10.1128/AAC.49.5.1988-1993.2005

Gasim, S., Elhassan, A. M., Kharazmi, A., Khalil, E. A., Ismail, A., and Theander, T. G. (2000). The development of post-kala-azar dermal leishmaniasis (PKDL) is associated with acquisition of leishmania reactivity by peripheral blood mononuclear cells (PBMC). *Clin. Exp. Immunol.* 119 (3), 523–529. doi: 10.1046/j.1365-2249.2000.01163.x

Goad, L. J., Holz, G. G., and Beach, D. H. (1984). Sterols of leishmania species. implications for biosynthesis. *Mol. Biochem. Parasitol.* 10, 161–170. doi: 10.1016/0166-6851(84)90004-5

Grondin, K., Haimeur, A., Mukhopadhyay, R., Rosen, B. P., and Ouellette, M. (1997). Coamplification of the gamma-glutamylcysteine synthetase gene gsh1 and of theABC transporter gene pgpA in arsenite-resistant leishmania tarentolae. *EMBO. J.* 16, 3057–3065. doi: 10.1093/emboj/16.11.3057

Haimeur, A., Guimond, C., Pilote, S., Mukhopadhyay, R., Rosen, B. P., Poulin, R., et al. (1999). Elevated levels of polyamines and trypanothione resultingfrom overexpression of the ornithine decarboxylase gene in arsenite resistant leishmania. *Mol. Microbiol.* 34, 726–735. doi: 10.1046/j.1365-2958.1999.01634.x

Haldar, A. K., Sen, P., and Roy, S. (2011). Use of antimony in the treatment of leishmaniasis: current status and future directions. *Mol. Biol. Int.* 2011, 571242. doi: 10.4061/2011/571242

Khanra, S. (2015). *Analysis of the genome and genetic markers of the clinical isolates of Indian kala-azar for molecular taxonomical purpose* (Kolkata, India: Jadavpur University).

Khanra, S., Datta, S., Mondal, D., Saha, P., Bandopadhyay, S. K., Roy, S., et al. (2012). RFLPs of ITS, ITS1 and hsp70 amplicons and sequencing of ITS1 of recent clinical isolates of kala-azar from India and Bangladesh confirms the association of l. tropica with the disease. *Acta Trop.* 124, 229–234. doi: 10.1016/j.actatropica.2012.08.017

Khanra, S., Sarraf, N. R., Das, S., Das, A. K., Roy, S., and Manna, M. (2016). Genetic markers for antimony resistant clinical isolates differentiation from Indian kala-azar. *Acta Trop.* 164, 177–184. doi: 10.1016/j.actatropica.2016.09.012

Khanra, S., Sarraf, N. R., Das, A. K., Roy, S., and Manna, M. (2017). Miltefosine resistant field isolate from Indian kala-azar patient shows similar phenotype in experimental infection. *Sci. Rep.* 7 (1), 10330. doi: 10.1038/s41598-017-09720-1

Kumar, D., Kulshrestha, A., Singh, R., and Salotra, P. (2009). *In vitro* susceptibility of field isolates of leishmania donovani to miltefosine and amphotericin b: Correlation withsodium antimony gluconate susceptibility and implications for treatment in areas of endemicity. *Antimicrob. Agents. Chemother.* 53, 835–838. doi: 10.1128/AAC.01233-08

Mandal, G., Wyllie, S., Singh, N., Sundar, S., Fairlamb, A. H., and Chatterjee, M. (2007). Increased levels of thiols protect antimony unresponsive leishmania donovani field isolate against reactive oxygen species generated by trivalent antimony. *Parasitology* 134, 1679–1687. doi: 10.1017/S0031182007003150

Manna, M., Majumder, H. K., Sunder, S., and Bhaduri, A. N. (2005). The molecular characterization of clinical isolatesfrom Indian kala-azar patients by MLEE and RAPD-PCR. *Med. Sci. Monit.* 11 (7), BR220–BR227.

Merida-de-Barros, D. A., Chaves, S. P., Belmiro, C. L. R., and Wanderley, J. L. M. (2018). Leishmaniasis and glycosaminoglycans: a future therapeutic strategy? *Parasit. Vectors.* 11 (1), 536. doi: 10.1186/s13071-018-2953-y

Mittal, M. K., Rai, S., Ashutos.,, Ravinder.,, Gupta, S., Sundar, S., et al. (2007). Characterization of natural antimony resistance in leishmania donovani isolates. *Am. J. Trop. Med. Hyg.* 76, 681–688. doi: 10.4269/ajtmh.2007.76.681

Monteiro Tínel, J. M., Benevides, M. F., Frutuoso, M. S., Rocha, C. F., Arruda, F. V., Vasconcelos, M. A., et al. (2014). A lectin from dioclea violacea interacts with midgut surface of lutzomyia migonei, unlike its homologues, cratylia floribunda lectin and canavalia gladiata lectin. *Sci. World J.* 2014, 239208. doi: 10.1155/2014/239208

Moore, E. M., and Lockwood, D. N. (2010). Treatment of visceral leishmaniasis. *J. Glob. Infect. Dis.* 2 (2), 151–158. doi: 10.4103/0974-777X.62883

Mukherjee, S., Mukherjee, B., Mukhopadhyay, R., Naskar, K., Sundar, S., Dujardin, J. C., et al. (2012). Imipramine is an orally active drug against both antimony sensitive and resistant leishmania donovani clinical isolates in experimental infection. *PLoS. Negl. Trop. Dis.* 6, e1987. doi: 10.1371/journal.pntd.0001987

Mukherjee, B., Mukhopadhyay, R., Bannerjee, B., Chowdhury, S., Mukherjee, S., Naskar, K., et al. (2013). Antimony-resistant but not antimony-sensitive leishmania donovani up-regulates host IL-10 to overexpress multidrug-resistant protein 1. *Proc. Natl. Acad. Sci. U. S. A.* 110, E575–E582. doi: 10.1073/pnas.1213839110

Mukherjee, A., Padmanabhan, P. K., Singh, S., Roy, G., Girard, I., Chatterjee, M., et al. (2007). Role ofABC transporter MRPA, gamma-glutamylcysteine synthetase and ornithinedecarboxylase in natural antimony-resistant isolates of leishmania donovani. *J. Antimicrob. Chemother.* 59, 204–211. doi: 10.1093/jac/dkl494

Mukhopadhyay, R., Mukherjee, S., Mukherjee, B., Naskar, K., Mondal, D., Decuypere, S., et al. (2011). Characterization of antimony-resistant leishmania donovani isolates: Biochemical and biophysical studies and interaction with host cells. *Int. J. Parasitol.* 41, 1311–1321. doi: 10.1016/j.ijpara.2011.07.013

Nozaki, T., Shigeta, Y., Saito-Nakano, Y., Imada, M., and Kruger, W. D. (2001). Characterization of transsulfuration and cysteine biosynthetic pathways inthe protozoan hemoflagellate, trypanosoma cruzi. isolation and molecularcharacterization of cystathionine beta-synthase and serine acetyltransferasefrom trypanosoma. *J. Biol. Chem.* 276, 6516–6523. doi: 10.1074/jbc.M009774200

Oliaee, R. T., Sharifi, I., Afgar, A., Kareshk, A. T., Asadi, A., Heshmatkhah, A., et al. (2018). Unresponsiveness to meglumine antimoniate in anthroponotic cutaneous leishmaniasis field isolates: analysis of resistance biomarkers by gene expression profiling. *Trop. Med. Int. Health* 23 (6), 622–633. doi: 10.1111/tmi.13062

Ostyn, B., Malaviya, P., Hasker, E., Uranw, S., Singh, R. P., Rijal, S., et al. (2013). Retrospective quarterly cohort monitoring for patientswith visceral leishmaniasis in the Indian subcontinents: outcomes of apilot project. *Trop. Med. Int. Health* 18 (6), 725–733. doi: 10.1111/tmi.12092

Palit, P., Hazra, A., Maity, A., Vijayan, R. S., Manoharan, P., Banerjee, S., et al. (2012). Discovery of safe and orally effective 4-aminoquinaldine analogues as apoptotic inducers with activity against experimental visceral leishmaniasis. *Antimicrob. Agents Chemother.* 56 (1), 432–445. doi: 10.1128/AAC.00700-11

Ponte-Sucre, A., Gamarro, F., Dujardin, J. C., Barrett, M. P., López-Vélez, R., García-Hernández, R., et al. (2017). Drug resistance and treatment failure in leishmaniasis: A 21st century challenge. *PloS Negl. Trop. Dis.* 11 (12), e0006052. doi: 10.1371/journal.pntd.0006052

Purkait, B., Kumar, A., Nandi, N., Sardar, A. H., Das, S., Kumar, S., et al. (2011). Mechanism of amphotericin b resistance in clinical isolates of leishmania donovani. *Antimicrob. Agents Chemother.* 56, 1031–1041. doi: 10.1128/AAC.00030-11

Rijal, S., Chappuis, F., Singh, R., Bovier, P. A., Acharya, P., Karki, B. M., et al. (2003). Treatment of visceral leishmaniasis in south-eastern Nepal: decreasing efficacy of sodium stibogluconate and need for a policy to limit further decline. *Trans. R. Soc Trop. Med. Hyg.* 97 (3), 350–354. doi: 10.1016/S0035-9203(03)90167-2

Sacks, D. L., Kenney, R. T., Neva, F. A., Kreutzer, R. D., Jaffe, C. L., Gupta, A. K., et al. (1995). Indian Kala-azar caused by leishmania tropica. *Lancet* 345, 959–961. doi: 10.1016/S0140-6736(95)90703-3

Sarkar, A., Mandal, G., Singh, N., Sundar, S., and Chatterjee, M. (2009). Flow cytometric determination of intracellular non-protein thiols in leishmania promastigotes using 5-chloromethyl fluorescein diacetate. *Exp. Parasitol.* 122, 299–305. doi: 10.1016/j.exppara.2009.04.012

Sarraf, N. R., Mukhopadhyay, S., Banerjee, A., Das, A. K., Roy, S., Chakrabarti, S., et al. (2021). Genome wide comparison of leishmania donovani strains from Indian visceral leishmaniasis and para-kala-azar dermal leishmaniasis patients. *Acta Trop.* 223, 106086. doi: 10.1016/j.actatropica.2021.106086

Singh, N., Chatterjee, M., and Sundar, S. (2014). The overexpression of genes of thiol metabolism contribute to drug resistance in clinical isolates of visceral leishmaniasis (Kala-azar) in India. *Parasitol. Vectors* 7, 596. doi: 10.1186/s13071-014-0596-1

Singh, O. P., and Sundar, S. (2015). Developments in diagnosis of visceral leishmaniasis in the elimination era. *J. Parasitol. Res.* 2015, 239469. doi: 10.1155/2015/239469

Steverding, D. (2017). The history of leishmaniasis. *Parasites Vectors* 10, 82. doi: 10.1186/s13071-017-2028-5

Sundar, S. (2001). Drug resistance in Indian visceral leishmaniasis. *Trop. Med. Int. Health* 6, 849–854. doi: 10.1046/j.1365-3156.2001.00778.x

Sundar, S., More, D. K., Singh, M. K., Singh, V. P., Sharma, S., Makharia, A., et al. (2000). Failure of pentavalent antimony in visceral leishmaniasis in India: report from the center of the Indian epidemic. *Clin. Infect. Dis.* 31, 1104–1107. doi: 10.1086/318121

Vanaerschot, M., Maes, I., Ouakad, M., Adaui, V., Maes, L., De Doncker, S., et al. (2010). Linking *in vitro* and *in vivo* survival of clinical leishmania donovani strains. *PloS One* 5 (8), e12211. doi: 10.1371/journal.pone.0012211

WHO (2021) *Antimicrobial resistance*. Available at: https://www.who.int/news-room/fact-sheets/detail/antimicrobial-resistance.

WHO (2022) *Leishmaniasis*. Available at: https://www.who.int/news-room/fact-sheets/detail/leishmaniasis.

Wyllie, S., Cunningham, M. L., and Fairlamb, A. H. (2004). Dual action of antimonial drugson thiol redox metabolism in the human pathogen leishmania donovani. *J. Biol. Chem.* 279, 39925–39932. doi: 10.1074/jbc.M405635200

frontiers | Frontiers in Cellular and Infection Microbiology

TYPE Original Research
PUBLISHED 14 November 2022
DOI 10.3389/fcimb.2022.1042279

OPEN ACCESS

EDITED BY
William Harold Witola,
University of Illinois at Urbana–Champaign, United States

REVIEWED BY
Yurong Yang,
Henan Agricultural University, China
Dong-Hui Zhui,
Fujian Agriculture and Forestry University, China

*CORRESPONDENCE
Caroline F. Frey
caroline.frey@vetsuisse.unibe.ch
Ragab M. Fereig
Ragab.feraeg2@vet.svu.edu.eg

SPECIALTY SECTION
This article was submitted to Parasite and Host, a section of the journal Frontiers in Cellular and Infection Microbiology

RECEIVED 12 September 2022
ACCEPTED 31 October 2022
PUBLISHED 14 November 2022

CITATION
Fereig RM, Abdelbaky HH, El-Alfy E-S, El-Diasty M, Elsayed A, Mahmoud HYAH, Ali AO, Ahmed A, Mossaad E, Alsayeqh AF and Frey CF (2022) Seroprevalence of *Toxoplasma gondii* and *Neospora caninum* in camels recently imported to Egypt from Sudan and a global systematic review.
Front. Cell. Infect. Microbiol. 12:1042279.
doi: 10.3389/fcimb.2022.1042279

Seroprevalence of *Toxoplasma gondii* and *Neospora caninum* in camels recently imported to Egypt from Sudan and a global systematic review

Ragab M. Fereig[1*], Hanan H. Abdelbaky[2], El-Sayed El-Alfy[3], Mohamed El-Diasty[4], Ahmed Elsayed[5], Hassan Y. A. H. Mahmoud[6], Alsagher O. Ali[6], Abdulrahman Ahmed[6], Ehab Mossaad[7], Abdullah F. Alsayeqh[8] and Caroline F. Frey[9*]

[1]Division of Internal Medicine, Department of Animal Medicine, Faculty of Veterinary Medicine, South Valley University, Qena, Egypt, [2]Doctor of Veterinary Sciences, Veterinary Clinic, Eterinary Directorate, Qena, Egypt, [3]Department of Parasitology, Faculty of Veterinary Medicine, Mansoura University, Mansoura, Egypt, [4]Agricultural Research Center (ARC), Animal Health Research Institute-Mansoura Provincial Lab, (AHRI-Mansoura), Cairo, Egypt, [5]Agricultural Research Center (ARC), Animal Health Research Institute-Al Shalateen Provincial Lab (AHRI-Al Shalateen),Giza, Cairo, Egypt, [6]Division of Infectious Diseases, Department of Animal Medicine, Faculty of Veterinary Medicine, South Valley University, Qena, Egypt, [7]Department of Pathology, Parasitology and Microbiology, College of Veterinary Medicine, Sudan University of Science and Technology, Khartoum, Sudan, [8]Department of Veterinary Medicine, College of Agriculture and Veterinary Medicine, Qassim University, Buraidah, Qassim, Saudi Arabia, [9]Institute of Parasitology, Department of Infectious Diseases and Pathobiology, Vetsuisse-Faculty, University of Bern, Bern, Switzerland

Introduction: Toxoplasma gondii and Neospora caninum are closely related intracellular protozoan parasites of medical and veterinary concern by causing abortions and systemic illness. Limited or ambiguous data on the prevalence of T. gondii and N. caninum in camels triggered us to conduct this study.

Methods: Camels (n = 460) recently imported from Sudan and destined mainly for human consumption, were tested for specific antibodies against these protozoans using commercially available ELISAs. From the two only quarantine stations for camels from Sudan, 368 camels were sampled between November 2015 and March 2016 in Shalateen, Red Sea governorate, and 92 samples were collected between September 2018 and March 2021 from Abu Simbel, Aswan governorate.

Results & Discussion: Overall, seropositive rates in camels were 25.7%, 3.9% and 0.8% for T. gondii, N. caninum and mixed infection, respectively. However, marked differences were found between the two study sites and/or the two sampling periods: For T. gondii, a higher rate of infection was recorded in the Red Sea samples (31.5%, 116/368; odds ratio 20.7, 5.0-85.6; P<0.0001) than in those collected in Aswan (2.2%, 2/92). The opposite was found for N. caninum with a lower rate of infection in the Red Sea samples (0.82%, 3/368; odds ratio 23.7, 6.7-83.9; P<0.0001) than in the samples from Aswan (16.3%, 15/92). Additionally, our systematic review revealed that the overall published

seroprevalence of T. gondii and N. caninum was 28.6% and 14.3% in camels worldwide, respectively. To the best of our knowledge, this study provides the first record of seroprevalence of both T. gondii and N. caninum in recently imported camels kept under quarantine conditions before delivery to other Egyptian cities and regions. In addition, our review provides inclusive data on the prevalence of T. gondii and N. caninum in camel globally. This knowledge provides basic data for the implementation of strategies and control measures against neosporosis and toxoplasmosis.

KEYWORDS

toxoplasmosis, neosporosis, camel, dromedary, ELISA, Egypt

Introduction

Globally, the population size of large camelids (dromedary, *Camelus dromedarius*, and Bactrian camel, *C. bactrianus*) is estimated at over 35.5 million heads; dromedaries constitute 95% of them with the largest populations being reared in Africa and the Middle East (Zhu et al., 2019; FAOSTAT, 2020; Faye, 2020; Khalafalla and Hussein, 2021). Camels are vital to many countries' economies, primarily those in the Arabian Peninsula, Sudan, Somalia and Ethiopia, wherein they are being used to produce milk, meat, wool, and hides, and as draught and racing animals (Zarrin et al., 2020; Khalafalla and Hussein, 2021). However, camels have been well documented to transmit a number of zoonotic diseases to humans, among others the protozoan parasite *Toxoplasma gondii* (Sazmand et al., 2019; Zhu et al., 2019; Hughes and Anderson, 2020; Mohammadpour et al., 2020). Transmission of *T. gondii* to humans may occur by eating raw or undercooked camel meat or offal, such as the liver, which is widely consumed by pastoralists (Gebremedhin et al., 2014). Another source of transmission might be unpasteurized camel milk (Boughattas, 2017; Sazmand et al., 2019), which is consumed for its higher vitamin C and iron content than cow's milk, and for attributed important therapeutic effects for type 1 diabetes as well as allergy reduction in children.

Toxoplasma gondii and *Neospora caninum* are obligate intracellular protozoan parasites that infect a wide variety of domestic and wild animals as well as humans in case of *T. gondii* (Dubey, 2003; Dubey et al., 2007; Dubey, 2010). *Toxoplasma gondii* affects most warm-blooded animals and is implicated in abortion cases in women, ewes and sows. Similarly, *N. caninum* is an abortifacient agent in many mammalian species, particularly in cattle. Natural *T. gondii* and/or *N. caninum* infections of livestock are mainly acquired through the consumption of oocysts contaminating food and/or water (Elamin et al., 1992; Dubey, 2003; Dubey et al., 2007; Moore and Venturini, 2018), or through intrauterine infection.

Clinical and congenital toxoplasmosis in camels is limited to a few reports and likely underestimated in dromedaries; clinical manifestation was described as hemorrhagic enterocolitis and toxoplasmic peritonitis (Hagemoser et al., 1990; Riley et al., 2017; Sazmand et al., 2019), and more recently, abortion related to *T. gondii* was documented in a Bactrian Camel (Komnenou et al., 2022). Despite instances of anti-*N. caninum* antibodies in camels' sera, clinical illness in large camelids has not yet been reported (Sazmand and Joachim, 2017).

In Egypt, some reports have investigated the seroprevalence of *T. gondii* and *N. caninum* in camels using different serological tests and on animals selected from different regions with special interest for those in Greater Cairo and Nile Delta regions (reviewed by Rouatbi et al., 2019; Abbas et al., 2020). Reported seroprevalence rates varied widely between 3.3% and 96.4% (Kuraa and Malek, 2016; Saad et al., 2018). Only two studies detected anti-*N. caninum* antibodies in camels in Egypt so far; Hilali et al. (1998) in Cairo using *Neospora* agglutination test found a seroprevalence of 3.7%, while Selim and Abdelhady (2020) in various Egyptian governorates using ELISA determined 11% seropositive animals, respectively. Nothing is known about the seroprevalence of these protozoans in camels imported to Egypt and destined for human consumption.

The global pooled seroprevalence of *T. gondii* infection in the Camelidae family was found to be 28.16% by a meta-analysis based on 42 studies that included large camelids (dromedary and Bactrian camels) and small camelids (guanaco, llamas, vicunas, and alpacas) (Maspi et al., 2021). As there was no particular focus on large camelids, and as some articles on *T. gondii* seroprevalence have been published in regional journals, we performed a systematic search using different databases for a comprehensive assessment of infections. Furthermore, there was no literature review of *N. caninum* prevalence in camels. Thus, we aimed to review the studies conducted on *T. gondii* and *N. caninum* infections in large camelids globally. This work had thus two aims: First, to establish the seroprevalence of *T. gondii*

and *N. caninum* in recently imported camels from Sudan and kept at Shalateen quarantine, Red Sea governorate and Abu Simbel quarantine, Aswan governorate, Southern Egypt. Second, to conduct a systematic review including all published prevalence and genotyping data in large camels worldwide. The extending cross-comparisons between our results and resources from Egyptian and global studies can be used to address this serious public health issue in order to better understand the parasite epidemiology in large camelids.

Materials and methods

Ethical statement

This study was conducted according to instructions established by the "Research Board" of the Faculty of Veterinary Medicine, South Valley University, Qena, Egypt. The protocols were approved by Research Code of Ethics at South Valley University number 36 (RCOE-36). Blood samples were collected by a group of highly trained veterinarians and staff after consultation with the officials and animal owners.

Animal population and geographic locations

A total of 460 blood samples were randomly collected from recently imported camels at the only two Egyptian quarantine stations for camels imported from Sudan. Shalateen quarantine station belongs to the Red Sea governorate and is situated in southeastern Egypt, while Abu Simbel quarantine station, Aswan governorate, is situated in central south Egypt (Figure 1). Camels arriving at these quarantine points are usually imported in a way known as Dabuka journey, in which about 100-200 camels led by an expert man are walking for several days through the Sudanese and Egyptian desert. These camels are usually collected from different regions in Sudan, with camels of Eastern Sudan arriving at Shalateen and those of Western Sudan arriving at Abu Simbel (Figure 1B). At the Egyptian-Sudanese border, camels pass Argeen port before being sent to Abu Simbel, or Ras Hadarba port before arriving in Shalateen, respectively, where they are quarantined for 14 days or less (Figure 1B). During this period, camels are routinely checked for Rift valley fever and Corona virus infections by specific laboratory tests, and examined for apparent clinical abnormalities before permitting entrance to

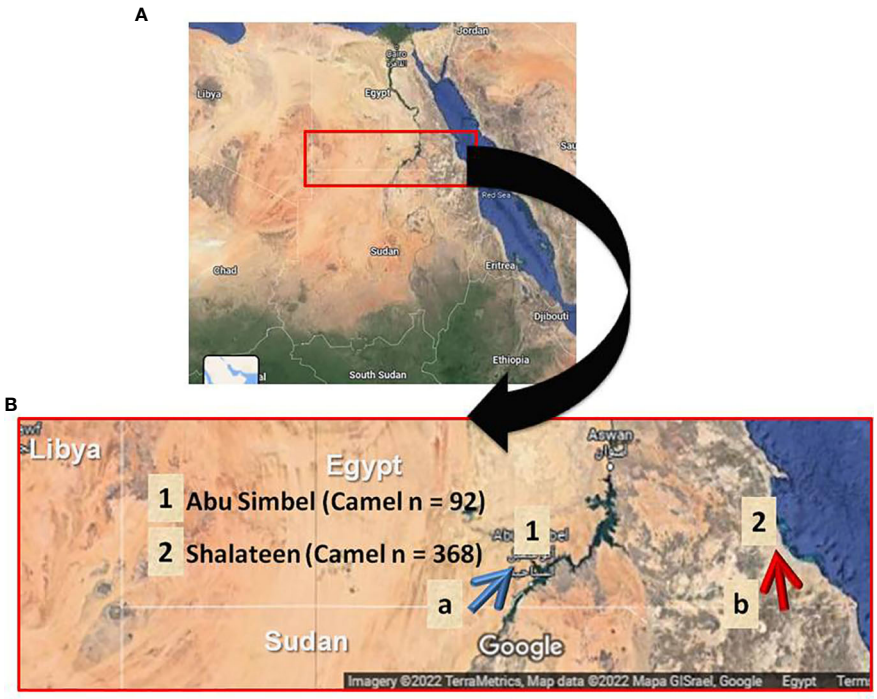

FIGURE 1
Geographical location of sample collection. **(A)** Map of Egypt illustrating the collection sites for camel samples in Southern Egypt. **(B)** Landscape enlarged area of testing samples. Blue arrow indicates the journey route of camel herds after crossing the Sudanese-Egyptian border at Argeen checking point (a) until reaching Abu Simbel quarantine (1). Red arrow shows the journey path of camel herds after crossing the Sudanese-Egyptian border at Ras Hadarba checking point (b) until reach Shalateen quarantine (2).

different Egyptian cities. Screening for *T. gondii* or *N. caninum* infection is not part of the mandated protocol. Most if not all of the imported camels are adult males, and they are primarily destined for human consumption and some for use as transport animals. In Shalateen, 368 samples were collected from November 2015 to March 2016 with two separate visits, one from November to December 2015 (n = 100 samples) and another from February to March 2016 (n = 268 samples). In Abu Simbel, 92 samples were collected from September 2018 to March 2021.

Serum sample collection and preparation

Blood samples were collected *via* puncture of the jugular vein using glass tubes without anticoagulant. All blood samples were kept in an icebox during transportation until separation of serum at Shalateen Laboratory for those collected at Shalateen quarantine, and our laboratory at South Valley University for those collected from Abu Simbel. Serum samples from Shalateen laboratory were sent in an icebox to our laboratory and all samples were stored at −20°C at the Faculty of Veterinary Medicine, South Valley University, Qena, until use in ELISA testing.

ELISA testing and interpretation of results

Serum samples of camels were tested for anti-*T. gondii* and anti-*N. caninum* antibodies, respectively, using commercial Multi-species ELISA kits (ID Screen® Toxoplasmosis Indirect Multi-species and ID Screen® *Neospora caninum* Competition, both ID Vet, Grables, France). Positive and negative control sera were provided in the kits and the tests were done following the manufacturer's instructions. The optical density (OD) of ELISA results was read at 450 nm measured with an Infinite® F50/Robotic ELISA reader (Tecan Group Ltd., Männedorf, Switzerland).

The Toxoplasmosis kit detects specific immunoglobulin G (IgG) antibodies against the P30 *T. gondii* protein using a peroxidase-conjugated anti-multi-species secondary antibody. The percentage sample (*S*) to positive (*P*) ratio (S/P %) for each of the test samples was calculated according to the following formula:

$$S/P\% \ \frac{\text{OD sample} - \text{OD negative control}}{\text{OD positive control} - \text{OD negative control}} \times 100$$

The samples with *S*/*P*% values greater than 50% were considered to be positive, those between 40 and 50% were classified as doubtful, and measurements less than or equal to 40% were considered to be negative as per the manufacturer.

The *N. caninum* kit detects specific antibodies against a purified *N. caninum* extract, using an anti-*N. caninum*-peroxidase-conjugated competing antibody. The percentage sample (*S*) to negative (*N*) ratio (S/N %) for each of the test samples was calculated according to the following formula:

$$S/N\% \ \frac{\text{OD sample}}{\text{OD negative control}} \times 100$$

The samples with *S*/*N*% values less than or equal to 50% were considered to be positive, those greater than 50% and less than or equal to 60% were classified as doubtful, and measurements greater than 60% were considered to be negative as per the manufacturer.

Statistical analysis

The significance of the differences in the prevalence rates was analyzed with Chi-square (Pearson) test, 95% confidence intervals (including continuity correction) and odds ratios using an online statistical website www.vassarstats.net (accession dates; 01-02 July, 2022) as described previously (Fereig et al., 2016a; Fereig et al., 2016b). *P*-values and odds ratio were confirmed also with GraphPad Prism version 5 (GraphPad Software Inc., La Jolla, CA, USA). The results were considered significant when the *p*-value was< 0.05 (*) or highly significant when *p*-value was< 0.0001 (**).

Data searching strategy

PubMed, Scopus, Web of Science, ScienceDirect, and Google Scholar were searched for studies on camel toxoplasmosis and neosporosis published in English up to 2022 (May, 2022). In addition, the Egyptian knowledge bank's website (http://www.ekb.eg) was searched to collect papers from Egypt published in local journals. *Toxoplasma gondii* and *Neospora caninum* were used as search terms, along with the keyword "camel(s)." Studies were considered eligible for inclusion if they found positive samples for toxoplasmosis and neosporosis in both the one-humped dromedary camels (*Camelus dromedarius*) and the two-humped Bactrian camels (*Camelus bactrianus*).

Articles on both serodiagnosis and molecular investigations of either parasite using serum, milk and meat samples were eligible. Data from eligible studies on infections of camels was organized in a database, and the following information was extracted: sub-region/country, sample size, number of positives (%), detection methods, study year (date of samples collection), cut-off values, genetic markers and revealed genotypes (where recorded), and references with publication date. Different serological tests were included to study the prevalence of both parasites. Even in a single article, two tests may have been used, all of which were included in our literature review. Studies with more than one test were also combined with others after selection of the test with highest number of positives for

estimating the pooled prevalence of both parasites either in Egypt or worldwide.

Results

Seroprevalence for *T. gondii* and *N. caninum* infection in camels imported to Egypt

In this study, specific antibodies against *T. gondii* were detected in 118 of the 460 surveyed animals (25.7%; 95% CI: 21.8-29.9). Consistently, 18 camels tested positive for *N. caninum* antibodies (3.9%; 95% CI: 2.4-6.2), and mixed infection was determined in 3 animals (0.65%; 95% CI: 0.17-2.1) (Table 1).

Based on available data, the location and period of sample collection were identified to have a significant influence on the presence of *T. gondii* and *N. caninum* antibodies in recently imported camels in Egypt. A significantly higher seroprevalence rate for *T. gondii* was recorded in animals sampled at Shalateen Quarantine, Red Sea governorate (31.5%; odds ratio = 20.7; *P* =<0.0001) compared to camel samples collected at Abu Simbel Quarantine, Aswan governorate (2.2%). Samples in Shalateen were collected between November to December 2015 and between February to March 2016, and those in Aswan between January 2018 to January 2021. Thus, the same effect was seen when univariable analysis of period of sample collection was performed. Samples collected between November to December 2015 and between February to March 2016 showed higher seropositive rates (27%; OR = 16.6; *P* =<0.0001, and 33.2%; OR = 26.3; *P* =<0.0001), respectively) than those collected between Jan 2018 to Jan 2021 (2.2%) set as a reference group (Table 2).

In case of *N. caninum* in camels, the seroprevalence rate recorded in animals sampled at Shalateen quarantine (0.82%; OR = 23.7; *P* =<0.0001) was significantly lower than that reported in camel samples collected at Abu Simbel Quarantine (16.3%). Again, this was also reflected when the collection periods were compared. The seropositive rates of samples collected between November to December 2015 and between February to March 2016 were lower (1%; OR = 19.3; *P* = 0.00013, and 0.7%; OR = 25.9; *P* =<0.0001), respectively) than in the samples collected between September 2018 to March 2021 (16.3%) set as a reference group (Table 3).

Global systematic review data

A total of 79 studies were included and reviewed in this article comprising 74 articles on large camels' toxoplasmosis and 14 articles conducted on neosporosis, respectively, of which 9 articles investigated both parasites. For Egypt, a pooled prevalence rate of 38.5% for antibodies against *T. gondii* was found in 1,444 serum samples of dromedaries collected from various governorates and tested with various assays (Table 4). Furthermore, 71 milk samples from camels tested for *T. gondii* antibodies revealed a pooled prevalence of 18.3% in this matrix (Table 4). For antibodies against *N. caninum*, a pooled prevalence of 8.4% was found in 443 serum samples (Table 5). Globally, 12,092 serum samples collected from large camels were investigated for *T. gondii* antibodies, of which 3,457 were found

TABLE 1 Seroprevalence of *Toxoplasma gondii, Neospora caninum* and mixed infection in camels in Egypt.

Type of infection	No. of tested	No. of negative (%)	No. of doubtful (%)	No. of positive (%)	95% CI*
T. gondii	460	332 (72.2)	10 (2.2)	118 (25.7)	21.8-29.9
N. caninum	460	438 (95.2)	4 (0.87)	18 (3.9)	2.4-6.2
Mixed infection	460	457 (99.4)	0	3 (0.65)	0.17-2.1

* 95% CI calculated according to method described by (http://vassarstats.net/).

TABLE 2 Factors influencing anti-*Toxoplasma gondii* antibodies in camels in Egypt.

Analyzed factor	No. of tested	No. of negative (%)	No. of positive (%)	OR (95% CI)#	*P*-value[x]
Collection region					<0.0001**
Shalateen (Red Sea)	368	252 (68.5)	116 (31.5)	20.7 (5.0-85.6)	Ref
Abu Simbel (Aswan)	92	90 (97.8)	2 (2.2)	Ref	
Collection time					<0.0001** <0.0001**
Nov 2015 – Dec 2015	100	73 (73)	27 (27)	16.6 (3.8-72.3)	Ref
Feb 2016 – Mar 2016	268	152 (56.7)	89 (33.2)	26.3 (6.3-109.6)	
Sep 2018 – Mar 2021	92	90 (97.8)	2 (2.2)	Ref	

Odds ratio at 95% confidence interval as calculated by http://vassarstats.net/.
[x]P value was evaluated by Chi square test (Pearson test) using online statistics software http://vassarstats.net/ and GraphPad Prism version 5.
** The result is significant at P< 0.0001.
Ref.; value used as a reference.

TABLE 3 Factors influencing anti-*Neospora caninum* antibodies in camels in Egypt.

Analyzed factor	No. of tested	No. of negative (%)	No. of positive (%)	OR (95% CI)[#]	*P*-value[x]
Collection region					<0.0001**
Shalateen (Red Sea)	368	365 (68.5)	3 (0.82)	23.7 (6.7-83.9)	Ref
Abu Simbel (Aswan)	92	77 (97.8)	15 (16.3)	Ref	
Collection time					0.00013* <0.0001**
Nov 2015 – Dec 2015	100	99 (99)	1 (1)	19.3 (2.5-149.2)	Ref
Feb 2016 – Mar 2016	268	266 (99.3)	2 (0.7)	25.9 (5.8-115.8)	
Sep 2018 - Mar 2021	92	77 (83.7)	15 (16.3)	Ref	

Odds ratio at 95% confidence interval as calculated using http://vassarstats.net/.
[x]P value was evaluated by Chi square test (Pearson test) using online statistics software http://vassarstats.net/ and GraphPad Prism version 5.
* The result is significant at P < 0.05.
**The result is significant at P < 0.0001.Ref.; value used as a reference.

TABLE 4 Seroprevalence of anti-*Toxoplasma gondii* antibodies in camels (*Camelus dromedarius* and *Camelus bactrianus*) worldwide.

Country	Region	Study Year	No. tested	No. positive (%)	Diagnostic methods	Cut-off	Reference
Afghanistan*	Kabul	1974	19	14 (73.7)	IHA	1:64	Kozojed et al. (1976)
Algeria	Biskra, El- Oued, Ouargla, and Ghardaia	2018	320	48 (15)	ELISA	MI	Abdallah et al. (2020)
China©	Qinghai	2010–2011	234	7 (2.99)	IHA	1:64	Wang et al. (2013)
Czech Republic©	–	2001–2011	36	22 (61) 25 (69)	IFAT ELISA	1:50 MI	Bártová et al. (2017)
Egypt	Different	–	49	3 (6.1)	IFA		Maronpot and Botros (1972)[a]
	Ismailia	–	43	29 (67.4)	DT	1:8	Rifaat et al. (1977)[a]
	Assiut	–	80	12 (15.0)	DT	1:16	Michael et al. (1977)[a]
	Menoufiya	–	80	15 (18.7)			
	Matrouh	–	80	40 (50.0)			
	Menoufiya	–	30	17 (56.7)	DT	1:8	Rifaat et al. (1978)[a]
	Assiut	–	119	30 (24.4)	DT	1:4	Fahmy et al. (1979)[a]
	Sharkia	–	19	5 (26.3)	IHA		El-Ridi et al. (1990)[a]
	Gharbia	–	36	6 (16.7)	IHA	1:64	Ibrahim et al. (1997)[a]
	Cairo	NS	166	29 (17.4)	MAT	1:25	Hilali et al. (1998)
	Cairo	NS	150	[1] 27 (18.0), [2] 30 (20.0), [3] 46 (30.7), [4] 41 (27.3)	MAT#	1:25	Shaapan and Khalil (2008)
	Cairo	NS	60	40 (66.7)	ELISA[¥]	NS	Toaleb et al. (2013)
	Assiut	2014-2016	56	20 (35.7) 54 (96.4)	LAT ELISA	1:2 MI	Kuraa and Malek (2016)
	Cairo, Giza	NS	34	9 (26.5)	ELISA	NS	Elfadaly et al. (2017)
	Mersa Matrooh	2014	53	32 (60.37)	LAT	MI	Osman et al. (2016)
	Qalyubia	2014-2015	120	6 (5) 63 (52.5)	IHA iELISA	MI	Ahmed et al. (2017)
	Upper Egypt	NS	30-Milk	1 (3.33)	ELISA	MI	Saad et al. (2018)
	Aswan	2017	37	12 (32.4)	LAT	MI	Sameeh et al. (2021)
	Matrouh	2016-2017	124	80 (64.51)	ELISA	MI	Khattab et al. (2022)
	Beni Suef, Giza, Monufa, Alexandria, Sharqia, Matruh, and Faiyum	2019-2021	108 41-Milk	34 (31.48) 12 (29.26)	ELISA	MI	Zeedan et al. (2022)
Ethiopia	Fentale	2012-2013	455[b] 451[b]	220 (49.62) 179 (40.49)	DAT iELISA	1:40 MI	Gebremedhin et al. (2014)

(Continued)

TABLE 4 Continued

Country	Region	Study Year	No. tested	No. positive (%)	Diagnostic methods	Cut-off	Reference
	Afar	NS	384	262 (72.9)	MAT	1:40	Hadush et al. (2015)
	Borana	2013-2014	396	33 (8.33)	DAT	1:40	Gebremedhin et al. (2016)
	Oromia	2011-2013	292	42 (14.38)	iELISA	MI	Tilahun et al. (2018)
India	Rajasthan	NS	108 231	12 (11.1) 25 (10.8)	SFDT IHA	1:4 1:16	Gill and Prakash (1969)
Iraq	Al-Najaf	2011-2012	360 91	91 (25.2) 15 (16.4)	LAT ELISA	MI	Mahmoud et al. (2014)
	Wasit	NS	92	19 (20.6)	ELISA	NS	Asal and Al Zubaidy (2016)
	Al-Najaf	2014-2015	227 70	70 (30.8) 16 (22.8)	LAT iELISA	MI	Al-Dhalimy and Mahmoud (2019)
	Kirkuk	2018	76	20(26.3)	SFDT	1:16	Yawoz et al. (2021)
Iran	Mashhad	2004-2005	120	5 (4.16)	IFAT	1:20	Sadrebazzaz et al. (2006)
	Isfahan	–	310	87 (28.06)	IFAT	1:16	Hosseininejad et al. (2010)
	Tehran, Isfahan, and Fars	2011-2012	160-Milk	3 (1.87)	cELISA	–	Dehkordi et al. (2013)
	Yazd	2008-2009	254	37 (14.56)	MAT	1:20	Hamidinejat et al. (2013)
	southern provinces	2013-2014	493	49 (9.93)	ELISA	MI	Azma et al. (2015)
	Kerman, Razavi Khorasan, and south Khorasan	2015	50	13 (26)	MAT	1:20	Tavakoli Kareshk et al. (2018)
Italy	Southern	2014	9[©] 5	2 (22) 2 (40)	IFAT	1:50	Marková et al. (2019)
Nigeria	Kano	NS	159	0 (0)	IHA	1:64	Okoh et al. (1981)
Pakistan	Bahawalpur	NS	100	10 (10)	LAT	1:16	Chaudhry et al. (2014)
	Punjab	2015	201	36 (17.91)	LAT	MI	Lashari et al. (2018)
	Punjab	2016	897	360 (40.1)	iELISA	1:100	Fatima et al. (2019)
	Mianwali	2017-2018	350	133 (38.0)	iELISA	NS	Shehzad et al. (2022)
Saudi Arabia	–	NS	46	0	IHA	1:64	Hossain et al. (1987)
	–	NS	227	36 (16)	IHA	1:64	Hussein et al. (1988)
	Riyadh	2010	412	27 (6.5%)	IFAT	1:20	Al-Anazi (2011)
	Al-Riyadh, Alharig, Al- Solyl, Dar- maa and Wady Al- Dawaser	2009-2010	482	219 (45.44)	iELISA	MI	Al-Khatib (2011)
	Al-Ahsa	2010	210	17 (8)	ELISA	MI	Al-Mohammed (2011)
	Ad-Dawadimi, Shaqra, Afif, Al-Quwayiyah	NS	713	94 (13.1)	LAT	1:8	Al-Anazi (2012)
	Riyadh	NS	182	43 (23.6)	IFAT	1:32	Alanazi (2013)
	Najran	2014	90	22 (24.4) 19 (21.1)	IHA ELISA	1:80 1:80	Mosa et al. (2015)
	Qassim	NS	141	0 (0)	ELISA	MI	Derar et al. (2017)
	Hofuf, Riyadh, Tabuk, Jizan, Taif	NS	199	68 (34.2)	ELISA		Mohammed et al. (2020)
Somalia	Benadir	NS	64	4 (6.3)	LAT	1:2	Kadle (2014)
Spain	Canary Islands	2012	96	35 (36.5)	MAT	1:25	Mentaberre et al. (2013)
Sudan	Kordofan and central regions	1982-1983	204	111 (54.4)	IHA	1:40	Zain Eldin et al. (1985)
	Tamboul and Butana plains	NS	95	11 (11.57)	IHA	1:64	Abbas et al. (1987)
	Tampoul	NS	102	23 (22.5)	MSF	1:5	Bornstein and Musa (1987)
	Butana plains	NS	482	323 (67)	LAT	1:8	Elamin et al. (1992)

(Continued)

TABLE 4 Continued

Country	Region	Study Year	No. tested	No. positive (%)	Diagnostic methods	Cut-off	Reference
	Butana area, north and south Kordofan	NS	153	34 (22.2)	LAT	1:4	Khalil et al. (2007)
	Khartoum	NS	70	14 (20)	LAT	1:8	Khalil and Elrayah (2011)
	Tumbool	2009	100	44 (44)	LAT	NS	Basheir et al. (2012)
	Khartoum	2012-2014	61	33 (54.1)	LAT	1:2	Ibrahim et al. (2014); Ibrahim et al. (2015)
	Tamboul	NS	150	47 (31.3)	LAT	NS	Elias et al. (2017)
	West Kordofan, and Blue Nile states	NS	45	6 (13.3)	LAT	1:32	Abdelbaset et al. (2020)
Turkey	Nevsehir	2010	11	10 (90.9)	SFDT	1:16	Utuk et al. (2012)
UAE	Abu Dhabi	NS	97 143	30 (30.9) 52 (36.4)	DAT IHA	1:24 1:220	Afzal and Sakkir (1994)
	NS	NS	100	18 (18)	LAT	1:64	Chaudhary et al. (1996)

ELISA, enzyme-linked immunosorbent assay; DAT, direct agglutination test; IHA, indirect hemagglutination; LAT, latex agglutination test; MAT, modified agglutination test; MSF, modified Sabin-Feldman dye test; SFDT, Sabin-Feldman Dye Test; cELISA, Capture Enzyme-Linked Immunosorbent Assay; MI; Data results interpretations were done according to Manufacturer's Instructions; NS, not stated.
[a]Studies were reviewed by Abbas et al., 2020.
[b]Samples were from the same animals but different sample size for the two used tests.
* The species of camels were not indicated.
# MAT was conducted using formalin-treated whole tachyzoites from different antigen; [1] RH strain, [2] local equine strain, [3] local camel strain and [4] local sheep strain.
¥ ELISA using T. gondii camel strain isolated fraction.
© Bactrian camels.

to be positive giving an estimated overall prevalence of 28.6% (Table 4). Meanwhile, 2,654 serum samples were investigated for *N. caninum* antibodies, of which 380 samples were positive, resulting in an estimated pooled prevalence of 14.3% (Table 5). *Toxoplasma gondii* type I, II, and III were identified in meat, blood and milk samples from camels using different molecular markers (Table 6).

Discussion

In the present study, we investigated the seroprevalence of *T. gondii* and *N. caninum* in camels recently imported to Egypt from Sudan. The quarantine stations of Shalateen, Red Sea governorate, and Abu Simbel, Aswan governorate, are the only gates for importing camels to Egypt coming from Sudan. These

TABLE 5 Seroprevalence of anti-*Neospora caninum* antibodies in camels (*Camelus dromedarius* and *Camelus bactrianus*) worldwide.

Country	Region	Study Year	No. tested	No. positive (%)	Diagnostic methods	Cut-off	Reference
Czech Republic	–	2001–2011	36	17 (47) 11 (31)	IFAT cELISA	1:50 MI	Bártová et al. (2017)
Egypt	Cairo	NS	161	6 (3.7)	NAT	1:40	Hilali et al. (1998)
	Red Sea, Qalyubia, Kafr ElSheikh	2018–2019	282	31 (11)	ELISA	MI	Selim and Abdelhady (2020)
Iran	Mashhad	2004-2005	120	7 (5.83)	IFAT	1:20	Sadrebazzaz et al. (2006)
	Isfahan	2008	310	10 (3.22)	IFAT	1:50	Hosseininejad et al. (2009)
	Yazd	2008-2009	254	10 (3.94)	NAT	1:20	Hamidinejat et al. (2013)
	Bushehr	NS	92	25 (27)	NAT	1:20	Namavari et al. (2017)
Italy	Southern	2014	9[©] 5	0 (0) 0 (0)	IFAT	1:50	Marková et al. (2019)
Pakistan	Punjab	2014-2015	81	9 (11.1)	cELISA	MI	Nazir et al. (2017)
Spain	Canary Islands	2012	100	86 (86)	cELISA	MI	Mentaberre et al. (2013)
Saudi Arabia	Riyadh	2010	412	23 (5.6)	IFAT	1:20	Al-Anazi (2011)
	variable	2013	532	117 (21.99)	ELISA	MI	Aljumaah et al. (2018)
	Hofuf, Riyadh, Tabuk, Jizan, Taif	NS	199	33 (16.6)	ELISA	MI	Mohammed et al. (2020)
Sudan	Khartoum	2013-2014	61	6 (9.8)	cELISA	NS	Ibrahim et al. (2015)

ELISA, enzyme-linked immunosorbent assay; cELISA, competitive ELISA; IFAT, indirect fluorescent antibody test; NAT, Neospora agglutination test; MI; Data results interpretations were done according to Manufacturer's Instructions; NS, not stated.

TABLE 6 Summary of molecular detection and genotyping reports for *T. gondii* and *N. caninum* infecting camels worldwide.

Country	Region	Type of samples	Study Year	Marker#	No. tested	No. positive (%)	Isolates (no.)	Genotyping method	Protozoan species/ Remarks	Reference
Egypt	Qalyubia	Blood	2014-2015	NC-5	50	12 (24)	4	–	–	Ahmed et al. (2017)
	Cairo, Giza	Diaphragm and thigh muscles	NS	B1	9	5 (55.5)	2	PCR-RFLP (5′-SAG2, 3′-SAG2)	*T. gondii* (type II, III)	Elfadaly et al. (2017)
	Cairo	Cardiac muscles	2017-2018	B1	90	1 (1.1)	1	PCR-RFLP (5′-SAG2, 3′-SAG2, alt. SAG2)	*T. gondii* (type II)	El-Alfy et al. (2019)
	Aswan	Meat samples	2017	B1	12	6 (50)	–	–	–	Sameeh et al. (2021)
	Matrouh	Buffy coat	2016-2017	B1 & P30	80	–	1	–	–	Khattab et al. (2022)
	7 provinces	Blood Milk	2019-2021	B1	108 41	18(16.6) 2 (4.8)	–	–	–	Zeedan et al. (2022)
Iran	Tehran, Isfahan, and Fars	Milk	2011-2012	B1	160	4 (2.5)	–	–	–	Dehkordi et al. (2013)
	Isfahan	Blood	2013	18srRNA	122	8 (6.6)	–	–	–	Khamesipour et al. (2014)
	Sabzevar	Diaphragm and heart muscles	2014	B1	40	26 (65)	9	PCR-RFLP B1	*T. gondii* (type II, III)	Aliabadi and Ziaali (2016)*
	Kerman, Razavi Khorasan, and south Khorasan	Diaphragm heart muscles	2015	B1	50 50	7 (14) 6 (12)	3	PCR-RFLP (GRA6)	*T. gondii* (type I, II, III)	Tavakoli Kareshk et al. (2018)
Mongolia©	Tuv and Omnigovi	Milk samples	NS	ITS-1 and B1	9	5 (55.5)	4	–	–	Iacobucci et al. (2019)
UAE*	Abu Dhabi	Blood and milk	–	–	53	13	13	PCR-RFLP (SAG2)	*T. gondii* (type I, II)	Sharif et al. (2017)

Target gene used for the pathogen detection using PCR.
* This study did not mention the camel genus (dromedary or Bactrian).
©Bactrian camels.
NS, not stated.

animals are quarantined and subjected to numerous veterinary examinations including clinical and laboratory procedures, but not including *T. gondii* or *N. caninum* screening. Data on the seroprevalence of these important parasites is therefore missing, which is particularly concerning as these animals from Sudan are mainly destined for human consumption. We now determined an overall seroprevalence of *T. gondii* of 25.7%, which could represent a considerable infection risk for consumers. The seroprevalence for *N. caninum* and mixed infections was much lower with 3.9% and 0.65%, respectively. These results fall within the ranges of seroprevalence established in previous serological studies in large camels for *T. gondii* and/or *N. caninum* (Tables 4 and 5).

Our tested camels are short-lived in Egypt, and most if not all of them are adult males as the Sudanese government restricts the export of female camels for human consumption. The dromedaries are usually transported in a way known as "Dabuka journey" which means travelling from Sudan to Egyptian border ports by a long walk. This journey usually takes several days to weeks before arriving to Egypt, and thus Sudan might be suspicious as the original country of infection. Indeed, numerous reports revealed the high prevalence and endemicity of *T. gondii* and *N. caninum* among camels in various Sudanese regions (Zain Eldin et al., 1985; Abbas et al., 1987; Bornstein and Musa, 1987; Elamin et al., 1992; Khalil et al., 2007; Ibrahim et al., 2015; Elias et al., 2017; see Tables 4 and 5). However, we found marked differences in the seroprevalence of *T. gondii* and *N. caninum* between the two quarantine stations. While we cannot rule out that these differences were caused by the difference in sampling years, we would argue that the different origin in Sudan and differences in travel routes of the camels in the two quarantine stations played a crucial role. Camels arriving in Shalateen made a long journey from Eastern Sudan to Southeastern Egypt where wild cats such as leopard *(Panthera pardus)* were already reported (Soultan et al., 2017). Moreover, camels from Eastern Sudan, before being exported to Egypt, are quarantined in the Sudanese government quarantine near Kassala city, around which many stray domesticated cats

are usually seen. In addition, in Eastern Sudan, wild cats (Civet cat; *Civetticitis civetta* and Serval cats; *Leptailurus serval*) are abundant (Khalid, 2016). As camels are probably mainly infected by ingestion of *T. gondii* oocysts, the presence of wild and stray cats could explain the higher seroprevalence for *T. gondii* in camels from Eastern Sudan. However, more studies are needed for the detection of *Toxoplasma* oocysts in the feces of the wild and stray cats in the area. On the other hand, the higher seroprevalence for *N. caninum* recorded in the camels that have entered Egypt through Abu Simbel region, could be explained by the fact that these animals are originally from Western Sudan and owned by nomad tribes. Common animal husbandry practice in that area is the use of guard dogs (at least 10 dogs per camel herd of 100 animals). This co-herding of camels and dogs can be considered as a major risk factor for many diseases including trypanosomosis (Mossaad et al., 2017), hydatidiosis (Ibrahim et al., 2011) and also *N. caninum* infection, as seen in the current study. It remains to be investigated whether *N. caninum* may also cause abortions in dromedaries, and the prevalence of *N. caninum* in dogs in the area should also be studied. In addition, camels with free access to pasture might have a greater opportunity of ingesting *T. gondii* or *N. caninum* oocysts compared to those raised in intensive and semi-intensive breeding systems (Venturoso et al., 2021).

As we explained in our systematic review, data on seroprevalence of *T. gondii* and *N. caninum* in camels is scarce and further studies are needed whether in Egypt or other countries. Our review also revealed a significant limitation regarding the overall number of camels (n = 443) that had been tested in all previous studies for *N. caninum* which is lower than the camels tested in this study (n = 460). Our seroprevalences for *T. gondii* and *N. caninum* in camels were lower than in the calculated pooled prevalence from previous studies Egypt for *T. gondii* (556/1144, 38.5%), and *N. caninum* (37/443, 8.4%), respectively. However, our positive rate for *T. gondii* in camel was similar to that reported globally from a pooled prevalence rate (3451/12047, 28.6%) but our positive rate for *N. caninum* was lower than that estimated worldwide (380/2654, 14.3%). These variable observations can be explained by the vast differences depending on the country, region, age, sex, season, breed of the animals, and type of serological test used (Dubey and Lindsay, 2006).

In conclusion, we provide novel data on the seroprevalence of *T. gondii* and *N. caninum* in recently imported camels from Sudan, quarantined in Shalateen and Abu Simbel, Southern Egypt. Our results demonstrated a high exposure of camels to *T. gondii* and *N. caninum* infection either in Egypt or in Sudan. Also, our study revealed the substantial lack of data on camel toxoplasmosis and neosporosis in Egypt and worldwide, demonstrating the need for further studies.

Data availability statement

The raw data supporting the conclusions of this article will be made available by the authors, without undue reservation.

Ethics statement

The animal study was reviewed and approved by Research Code of Ethics at South Valley University number 36 (RCOE-36).

Author contributions

Conceptualization and design: RF, CF. Experiments, formal analysis, investigation: RF, HA, E-SE-A, ME-D. Resources and shared materials: RF, HA, E-SE-A, ME-D, AE, HM, AOA, AA, EM, AA, CF. Writing—original draft, RF, HA, E-SE-A, CF. Writing—review and editing: RF, HM, AOA, EM, AA, CF. Project administration: RF, CF. All authors contributed to the article and approved the submitted version.

Acknowledgments

We thank all veterinarians and officials who helped in collection of samples of recently imported quarantined camels and the animal owners for their cooperation in providing animals and required data and information. We appreciate the great help of our colleagues at Department of Animal Medicine, Faculty of Veterinary Medicine, South Valley University, Qena, Egypt, for their cooperation and technical assistance.

Conflict of interest

The authors declare that the research was conducted in the absence of any commercial or financial relationships that could be construed as a potential conflict of interest.

Publisher's note

References

Abbas, B., El Zubeir, A. E. A., and Yassin, T. T. M. (1987). Survey for certain zoonotic diseases in camels in Sudan. *Rev. Elev Med. Vet. Pays Trop.* 40 (3), 231–233. doi: 10.19182/remvt.8635

Abbas, I. E., Villena, I., and Dubey, J. P. (2020). A review on toxoplasmosis in humans and animals from Egypt. *Parasitology* 147 (2), 135–159. doi: 10.1017/S0031182019001367

Abdallah, M. C., Kamel, M., Karima, B., Samir, A., Hocine, B. M., Djamel, K., et al. (2020). First report of *Toxoplasma gondii* infection and associated risk factors in the dromedary camel (*Camelus dromedarius*) population in south East Algeria. *Vet. Parasitol: Reg. Stud. Rep.* 22, 100475. doi: 10.1016/j.vprsr.2020.100475

Abdelbaset, A. E., Mossaad, E., Ismail, A. A., Ibrahim, A. M., Xuan, X., Suganuma, K., et al. (2020). Seroprevalence of *Toxoplasma gondii* in farm animals in West kordofan, and blue Nile states, Sudan. *J. Protozool Res.* 30 (1-2), 31–37. doi: 10.32268/jprotozoolres.30.1-2_31

Afzal, M., and Sakkir, M. (1994). Survey of antibodies against various infectious disease agents in racing camels in Abu Dhabi, united Arab Emirates. *Rev. Scientifique Technique (International Office Epizootics)* 13 (3), 787–792. doi: 10.20506/rst.13.3.794

Ahmed, N. E., Al–Akabway, L. M., Ramadan, M. Y., El-Gawad, A., Mohamed, S., and Moustafa, M. (2017). Serological and PCR-sequencing assays for diagnosis of *Toxoplasma gondii* and *Neospora caninum* infecting camels in Egypt. *Benha Vet. Med. J.* 33 (2), 200–210. doi: 10.21608/bvmj.2017.30466

Al-Anazi, A. D. (2011). Prevalence of *Neospora caninum* and *Toxoplasma gondii* antibodies in sera from camels (*Camelus dromedarius*) in Riyadh province, Saudi Arabia. *J. Egypt Soc. Parasitol.* 41 (2), 245–250.

Al-Anazi, A. D. (2012). Antibodies in sera from camels (*Camelus dromedarius*) in western and southern regions of central province, Saudi Arabia. *J. Egypt Soc. Parasitol.* 42 (3), 659–664. doi: 10.12816/0006349

Alanazi, A. D. (2013). Determination of seropositivity for *Toxoplasma gondii* in sheep, goats and camels slaughtered for food and human consumptions in Riyadh municipal abattoirs, Saudi Arabia. *J. Egypt Soc. Parasitol.* 43 (3), 569–576. doi: 10.12816/0006414

Al-Dhalimy, A. M. B., and Mahmoud, M. H. S. (2019). Serological detection of infection rate with toxoplasmosis in camels at Al-najaf governorate, Iraq. *Biochem. Cell Arch.* 19 (1), 79–81.

Aliabadi, J., and Ziaali, P. N. (2016). Survey of *Toxoplasma gondii* in livestocks' meat (sheep, goat, camel), using nested PCR method in sabzavar district. *Euro Online J. Nat. Soc. Sci.* 5 (2), 368–376.

Aljumaah, R. S., Alshaikh, M. A., Jarelnabi, A., Abdelrahman, M. M., and Hussein, M. F. (2018). Serological prevalence of *Neospora caninum* in indigenous dromedary camels (*Camelus dromedarius*) in Saudi Arabia. *Pakistan J. Zool.* 25 (46), 74–19. doi: 10.17582/journal.pjz/2018.50.4.1199.1203

Al-Khatib, R. M. (2011). Serological studies of *Toxoplasma gondii* infection in camels (*Camelus dromedarius*). *Assiut Vet. Med. J.* 57 (130), 1–10.

Al-Mohammed, H. I. (2011). Seroprevalence of *Toxoplasma gondii* infection in cats, dogs and ruminant animals in Al-ahsa area in Saudi Arabia. *Res. J. Med. Sci.* 5 (4), 190–192.

Asal, S. N., and Al Zubaidy, I. A. (2016). Seroprevelance study of *Toxoplasma gondii* in horses and camels animal in wasit province. *Iraq J. Vet. Med.* 40 (1), 147–150. doi: 10.30539/iraqijvm.v40i1.152

Azma, F., Razavi, S. M., Nazifi, S., Rakhshandehroo, E., and Sanati, A. R. (2015). A study on the status of inflammatory systems in camels naturally infected with *Toxoplasma gondii*. *Trop. Anim. Health Prod.* 47 (5), 909–914. doi: 10.1007/s11250-015-0807-6

Bártová, E., Kobédová, K., Lamka, J., Kotrba, R., Vodička, R., and Sedlák, K. (2017). Seroprevalence of *Neospora caninum* and *Toxoplasma gondii* in exotic ruminants and camelids in the Czech republic. *Parasitol. Res.* 116 (7), 1925–1929. doi: 10.1007/s00436-017-5470-6

Basheir, H. M. E., Elias, S., and Abdel-Aziz, B. E. (2012). Serosurveillance of *Toxoplasma gondii* antibodies in camels at tumbool slaughterhouse, central Sudan. *Sudan J. Vet. Res.* 27, 65–67.

Bornstein, S., and Musa, B. E. (1987). Prevalence of antibodies to some viral pathogens, *Brucella abortus* and *Toxoplasma gondii* in serum from camels (*Camelus dromedarius*) in Sudan. *J. Vet. Med. Ser. B* 34 (1-10), 364–370. doi: 10.1111/j.1439-0450.1987.tb00409.x

Boughattas, S. (2017). *Toxoplasma* infection and milk consumption: Meta-analysis of assumptions and evidences. *Crit. Rev. Food Sci. Nutr.* 57 (13), 2924–2933. doi: 10.1080/10408398.2015.1084993

Chaudhary, Z. I., Iqbal, J., Raza, M., and Kandeel, M. I. (1996). Haematological and biochemical studies on toxoplasmosis in racing camels-a preliminary report. *J. Camel Pract. Res.* 3 (1), 7–9.

Chaudhry, U. N., Ali, A. A., Ashraf, S., Khan, M. T., Nadeem, S. M., and Ashraf, K. (2014). Seroprevalence of *Toxoplasma gondii* infection in camels (*Camelus dromedarius*) in and around bahawalpur region of Pakistan. *J. Infect. Mol. Biol.* 2, 16–18. doi: 10.14737/jimb.2307-5465/2.1.16.18

Dehkordi, F. S., Haghighi Borujeni, M. R., Rahimi, E., and Abdizadeh, R. (2013). Detection of *Toxoplasma gondii* in raw caprine, ovine, buffalo, bovine, and camel milk using cell cultivation, cat bioassay, capture ELISA, and PCR methods in Iran. *Foodborne Pathog. Dis.* 10 (2), 120–125. doi: 10.1089/fpd.2012.1311

Derar, D. R., Ali, A., Osman, S. A., Al-Sobayil, F. A., Saeed, E., Hassanein, K., et al. (2017). Potential pathogens in infertile male dromedary camels and their association with the spermiogram and clinical findings. *Comp. Clin. Pathol.* 26 (4), 965–970. doi: 10.1007/s00580-017-2461-z

Dubey, J. P. (2003). Review of *Neospora caninum* and neosporosis in animals. *Kor J. Parasitol.* 41 (1), 1. doi: 10.3347/kjp.2003.41.1.1

Dubey, J. P. (2010). *Toxoplasmosis in animals and man. 2nd ed* (Boca Raton: CRC Press).

Dubey, J. P., and Lindsay, D. S. (2006). Neosporosis, toxoplasmosis, and sarcocystosis in ruminants. *Vet. Clin. N Am. - Food Anim. Pract.* 22 (3), 645–671. doi: 10.1016/j.cvfa.2006.08.001

Dubey, J. P., Schares, G., and Ortega-Mora, L. (2007). Epidemiology and control of neosporosis and *Neospora caninum*. *Clin. Microbiol. Rev.* 20 (2), 323–367. doi: 10.1128/CMR.00031-06

El-Alfy, E. S., Abu-Elwafa, S., Abbas, I., Al-Araby, M., Al-Kappany, Y., Umeda, K., et al. (2019). Molecular screening approach to identify protozoan and trichostrongylid parasites infecting one-humped camels (*Camelus dromedarius*). *Acta Trop.* 197, 105060. doi: 10.1016/j.actatropica.2019.105060

Elamin, E. A., Elias, S., Daugschies, A., and Rommel, M. (1992). Prevalence of *Toxoplasma gondii* antibodies in pastoral camels (*Camelus dromedarius*) in the butana plains, mid-Eastern Sudan. *Vet. Parasitol.* 43 (3-4), 171–175. doi: 10.1016/0304-4017(92)90158-6

Elfadaly, H. A., Hassanain, N. A., Shaapan, R. M., Hassanain, M. A., Barakat, A. M., and Abdelrahman, K. A. (2017). Molecular detection and genotyping of *Toxoplasma gondii* from Egyptian isolates. *Asian J. Epidemiol.* 10 (1), 37–44. doi: 10.3923/aje.2017.37.44

Elias, H. M., Tagwa, M. B., and Abdalla, H. S. (2017). Seroprevalence of *Toxoplasma gondii* in camels in tamboul area, Sudan. *J. Vet. Med. Anim. Prod.* 8 (1), 74–75.

El-Ridi, A. M., Nada, S. M., Aly, A. S., Habeeb, S. M., and Aboul-Fattah, M. M. (1990). Serological studies on toxoplasmosis in zagazig slaughterhouse. *J. Egypt Soc. Parasitol.* 20, 677–681.

Fahmy, M. A., Mandour, A. M., Arafa, M. S., and Abdel Rahman, B. M. (1979). Toxoplasmosis of camels in assiut governorate. *J. Egypt Vet. Med. Assoc.* 39, 27–31.

FAOSTAT (2020). Available at: http://www.fao.org/faostat/en/#data/QA.

Fatima, T., Mehnaz, S., Wang, M., Yang, J., Sajid, M. S., and Shen B. Zhao, J. (2019). Seroprevalence of *Toxoplasma gondii* in one-humped camels (*Camelus dromedarius*) of thal and cholistan deserts, punjab, Pakistan. *Parasitol. Res.* 118 (1), 307–316. doi: 10.1007/s00436-018-6124-z

Faye, B. (2020). How many large camelids in the world? a synthetic analysis of the world camel demographic changes. *Pastoralism* 10 (1), 1–20. doi: 10.1186/s13570-020-00176-z

Fereig, R. M., AbouLaila, M. R., Mohamed, S., Mahmoud, H., Ali, A. O., Ali, A. F., et al. (2016b). Serological detection and epidemiology of *Neospora caninum* and *Cryptosporidium parvum* antibodies in cattle in southern Egypt. *Acta Trop.* 162, 206–211. doi: 10.1016/j.actatropica.2016.06.032

Fereig, R. M., Mahmoud, H., Mohamed, S., AbouLaila, M. R., Abdel-Wahab, A., Osman, S. A., et al. (2016a). Seroprevalence and epidemiology of *Toxoplasma gondii* in farm animals in different regions of Egypt. *Vet. Parasitol Reg. Stud. Rep.* 3–4, 1–6. doi: 10.1016/j.vprsr.2016.05.002

Gebremedhin, E. Z., Dima, N., Beyi, A. F., Dawo, F., Feyissa, N., Jorga, E., et al. (2016). Toxoplasmosis in camels (*Camelus dromedarius*) of borana zone, oromia region, Ethiopia: seroprevalence and risk factors. *Trop. Anim. Health Prod.* 48 (8), 1599–1606. doi: 10.1007/s11250-016-1133-3

Gebremedhin, E. Z., Yunus, H. A., Tesfamaryam, G., Tessema, T. S., Dawo, F., Terefe, G., et al. (2014). First report of *Toxoplasma gondii* in camels (*Camelus dromedarius*) in Ethiopia: bioassay and seroepidemiological investigation. *BMC Vet. Res.* 10 (1), 1–12. doi: 10.1186/s12917-014-0222-7

Gill, H. S., and Prakash, O. (1969). Toxoplasmosis in India: prevalence of antibodies in camels. *Ann. Trop. Med. Parasitol.* 63 (2), 265–267. doi: 10.1080/00034983.1969.11686626

Hadush, A., Gebru, M. U., Zeru, F., Hadush, T., Tesfamaryam, G., and Feleke, A. (2015). Sero-epidemiology of camel toxoplasmosis and public awareness on its

zoonotic importance in central afar region, north East Ethiopia. *World Appl. Sci. J.* 33 (12), 1880–1887. doi: 10.5829/idosi.wasj.2015.33.12.10192

Hagemoser, W. A., Dubey, J. P., and Thompson, J. R. (1990). Acute toxoplasmosis in a camel. *J. Am. Vet. Med. Assoc.* 196 (2), 347–347.

Hamidinejat, H., Ghorbanpour, M., Rasooli, A., Nouri, M., Hekmatimoghaddam, S., Namavari, M. M., et al. (2013). Occurrence of anti-*Toxoplasma gondii* and *Neospora caninum* antibodies in camels (*Camelus dromedarius*) in the center of Iran. *Turkish J. Vet. Anim. Sci.* 37 (3), 277–281. doi: 10.3906/vet-1110-21

Hilali, M., Romand, S., Thulliez, P., Kwok, O. C. H., and Dubey, J. P. (1998). Prevalence of *Neospora caninum* and *Toxoplasma gondii* antibodies in sera from camels from Egypt. *Vet. Parasitol.* 75 (2-3), 269–271. doi: 10.1016/S0304-4017(97)00181-7

Hossain, A., Bolbol, A. S., Bakir, T. M. F., and Bashandi, A. M. (1987). A serological survey of the prevalence of *Toxoplasma gondii* in slaughtered animals in Saudi Arabia. *Ann. Trop. Med. Parasitol.* 81 (1), 69–70. doi: 10.1080/00034983.1987.11812094

Hosseininejad, M., Pirali-Kheirabadi, K., Ebrahimi, A., and Hosseini, F. (2010). *Toxoplasma gondii* infection in camels (*Camelus dromedarius*): a serologic assay in Iran. *J. Camel Pract. Res.* 17 (1), 35–36.

Hosseininejad, M., Pirali-Kheirabadi, K., and Hosseini, F. (2009). Seroprevalence of *Neospora caninum* infection in camels (*Camelus dromedarius*) in isfahan province, center of Iran. *Iran J. Parasitol.* 4 (4), 61–64.

Hughes, E. C., and Anderson, N. E. (2020). Zoonotic pathogens of dromedary camels in Kenya: a systematised review. *Vet. Sci.* 7 (3), 103. doi: 10.3390/vetsci7030103

Hussein, M. F., Bakkar, M. N., Basmaeil, S. M., and El Nabi, A. G. (1988). Prevalence of toxoplasmosis in Saudi Arabian camels (*Camelus dromedarius*). *Vet. Parasitol.* 28 (1-2), 175–178. doi: 10.1016/0304-4017(88)90030-1

Iacobucci, E., Taus, N. S., Ueti, M. W., Sukhbaatar, L., Bastsukh, Z., Papageorgiou, S., et al. (2019). Detection and genotypic characterization of *Toxoplasma gondii* DNA within the milk of Mongolian livestock. *Parasitol. Res.* 118 (6), 2005–2008. doi: 10.1007/s00436-019-06306-w

Ibrahim, A. M., Ismail, A. A., Angara, T. E. E., and Osman, M. O. (2014). Area-wide detection of anti-*Toxoplasma gondii* antibodies in dairy animals from the Khartoum state, Sudan. *J. Life Sci.* 8 (9), 723–730.

Ibrahim, A. M., Ismail, A. A., Angara, E., and Osman, O. M. (2015). Detection of antibodies against *Toxoplasma gondii* and *Neospora caninum* in dairy camels from the Khartoum state, Sudan. *Sudan J. Sci. Technol.* 1, 19–28. Available at: http://repository.sustech.edu/handle/123456789/16391

Ibrahim, B. B., Salama, M. M., Gawish, N. I., and Haridy, F. M. (1997). Serological and histopathological studies on *Toxoplasma gondii* among the workers and the slaughtered animals in tanta abattoir, gharbia governorate. *J. Egypt Soc. Parasitol.* 27, 273–278.

Ibrahim, K., Thomas, R., Peter, K., and Omer, R. A. (2011). A molecular survey on cystic echinococcosis in sinnar area, blue Nile state (Sudan). *Chin. Med. J. (Engl).* 124 (18), 2829–2833. doi: 10.3760/cma.j.issn.0366-6999.2011.18.006

Kadle, A. A. H. (2014). Sero-prevalence of toxoplasmosis in domestic animals in benadir region, Somalia. *Open J. Vet. Med.* 4, 170–174. doi: 10.4236/ojvm.2014.48019

Khalafalla, A. I., and Hussein, M. F. (2021). *Infectious diseases of dromedary camels*. (Cham, Switzerland: Springer International Publishing). doi: 10.1007/978-3-030-79389-0

Khalid, O. H. H. (2016). *Parasitological and molecular detection of echinococcosis in some wild animal species* (Animal Resources Research Council, Sudan Academy of Sciences Animal Resources Research Council).

Khalil, K. M., and Elrayah, I. E. (2011). Seroprevalence of *Toxoplasma gondii* antibodies in farm animals (camels, cattle, and sheep) in Sudan. *J. Vet. Med. Anim. Health* 3 (3), 36–39.

Khalil, K. M., Gadir, A. E. A., Rahman, M. M. A., Yassir Mohammed, O., Ahmed, A. A., and Elrayah, I. E. (2007). Prevalence of *Toxoplasma gondii* antibodies in camels and their herders in three ecologically different areas in Sudan. *J. Camel Pract. Res.* 14 (1), 11–13.

Khamesipour, F., Doosti, A., Mobarakeh, H. I., and Komba, E. V. (2014). *Toxoplasma gondii* in cattle, camels and sheep in isfahan and chaharmahal va bakhtiary provinces, Iran. *Jundishapur J. Microbiol.* 7 (6), e17460. doi: 10.5812/jjm.17460

Khattab, R. A. H., Barghash, S. M., Mostafa, O. M. S., Allam, S. A., Taha, H. A. H., and Ashour, A. A. E. B. (2022). Seroprevalence and molecular characterization of *Toxoplasma gondii* infecting ruminants in the north-West of Egypt. *Acta Trop.* 225, 106139. doi: 10.1016/j.actatropica.2021.106139

Komnenou, A. T., Giadinis, N. D., Kritsepi-Konstantinou, M., Angelos-Loris, T., Danika, S., Terpsidis, K., et al. (2022). Abortion related to *Toxoplasma gondii* infection in a bactrian camel (*Camelus bactrianus*) in Greece: A case report. *Iran J. Parasitol.* 17 (1), 111. doi: 10.18502/ijpa.v17i1.9033

Kozojed, V., Blazek, K., and Amin, A. (1976). Incidence of toxoplasmosis in domestic animals in Afghanistan. *Folia Parasitologica* 23 (3), 273–275.

Kuraa, H. M., and Malek, S. S. (2016). Seroprevalence of *Toxoplasma gondii* in ruminants by using latex agglutination test (LAT) and enzyme-linked immunosorbent assay (ELISA) in assiut governorate. *Trop. Biomed.* 33 (4), 711–725.

Lashari, M. H., Ghouri, M. T., Akhtar, M. S., Kamran, Z., Chaudhari, M. S., Ayaz, M., et al. (2018). Hematological and biochemical alterations associated with toxoplasmosis in dromedaries (*Camelus dromedarius*) habitating in cholistan desert of bahawalpur, punjab, pakistan. JAPS. *J. Anim. Plant Sci.* 28 (4), 1043–1048.

Mahmoud, M. H., Al-Rubaie, A. E. S., and Al-Jeburii K.O and Taha, A. K. A. (2014). Serosurvillance on toxoplasmosis in camels (*Camelus dromedarius*) at Al-najaf province. *Kufa J. Vet. Med. Sci.* 5 (2), 204–210.

Marková, J., Machačová, T., Bártová, E., Sedlák, K., Budíková, M., Silvestre, P., et al. (2019). *Toxoplasma gondii*, *Neospora caninum* and *Encephalitozoon cuniculi* in animals from captivity (zoo and circus animals). *J. Eukaryotic Microbiol.* 66 (3), 442–446. doi: 10.1111/jeu.12688

Maronpot, R. R., and Botros, B. A. M. (1972). *Toxoplasma* serologic survey in man and domestic animals in Egypt. *J. Egypt Pub Health Assoc.* 47, 58–67.

Maspi, N., Nayeri, T., Moosazadeh, M., Sarvi, S., Sharif, M., and Daryani, A. (2021). Global seroprevalence of *Toxoplasma gondii* in camelidae: A systematic review and meta-analysis. *Acta Parasitol.* 66 (3), 733–744. doi: 10.1007/s11686-020-00333-9

Mentaberre, G., Gutiérrez, C., Rodríguez, N. F., Joseph, S., González-Barrio, D., Cabezón, O., et al. (2013). A transversal study on antibodies against selected pathogens in dromedary camels in the canary islands, Spain. *Vet. Microbiol.* 167 (3-4), 468–473. doi: 10.1016/j.vetmic.2013.07.029

Michael, S. A., El Reaii, A. H., and Morsy, T. A. (1977). Incidence of *Toxoplasma* antibodies among camels in Egypt. *J. Egypt Soc. Parasitol.* 7, 129–132.

Mohammadpour, R., Champour, M., Tuteja, F., and Mostafavi, E. (2020). Zoonotic implications of camel diseases in Iran. *Vet. Med. Sci.* 6 (3), 359–381. doi: 10.1002/vms3.239

Mohammed, O. B., Amor, N., and Omer S.A and Alagaili, A. N. (2020). Seroprevalence of *Toxoplasma gondii* and *Neospora caninum* in dromedary camels (*Camelus dromedarius*) from Saudi Arabia. *Rev. Bras. Parasitol. Vet.* 29 (1), e019119. doi: 10.1590/s1984-29612020008

Moore, D. P., and Venturini, M. C. (2018). "Neospora," in *Parasitic Protozoa of farm animals and pets* (Cham: Springer), 125–148.

Mosa, M., El-Shahawy, I. S., and Fawzi, E. M. (2015). Comparative analysis of toxoplasmosis in farm animals by indirect hemagglutination assay and enzyme linked immunosorbent assay. *Alex J. Vet. Sci.* 46, 90–94.

Mossaad, E., Satti, R. A., Fadul, A., Suganuma, K., Salim, B., Elamin, E. A., et al. (2017). The incrimination of three trypanosome species in clinically affected German shepherd dogs in Sudan. *Parasitol. Res.* 116 (11), 2921–2925. doi: 10.1007/s00436-017-5598-4

Namavari, M., Tavanaei, H. R., Abbasifar, A., Manavian, M., and Niko, D. (2017). High seroprevalence of *Neospora caninum* antibodies in camels (*Camelus dromedarius*) in the south of Iran. *Appl. Anim. Sci. Res. J.* 6 (24), 57–62. doi: 10.22092/AASRJ.2017.115836

Nazir, M. M., Oneeb, M., Ayaz, M. M., Bibi, F., Ahmad, A. N., Waheed, A., et al. (2017). Prevalence of antibodies to *Neospora caninum* in the serum of camels (*Camelus dromedarius*) from central punjab, Pakistan. *Trop. Anim. Health Prod.* 49 (5), 1081–1084. doi: 10.1007/s11250-017-1300-1

Okoh, A. E. J., Agbonlahor, D. E., and Momoh, M. (1981). Toxoplasmosis in Nigeria–a serological survey. *Trop. Anim. Health Prod.* 13 (1), 137–140. doi: 10.1007/BF02237910

Osman, A. O., EL-Metwaly, H. A., Wahba, A. A., and Hefny, S. F. (2016). Studies on causes of abortion in maghrabian camels. *Egypt J. Agric. Res.* 94 (4), 955–967. doi: 10.21608/ejar.2016.153236

Rifaat, M. A., Morsy, T. A., Sadek, M. S. M., Khalid, M. L. M., Azab, M. E., Makled, M. K., et al. (1977). Incidence of toxoplasmosis among farm animals in Suez canal governorates. *J. Egypt Soc. Parasitol.* 7, 135–140.

Rifaat, M. A., Morsy, T. A., Sadek, M. S. M., Khalid, M. L. M., Azab, M. E., and Safar, E. H. (1978). Prevalence of *Toxoplasma* antibodies among slaughtered animals in lower Egypt. *J. Egypt Soc. Parasitol.* 8, 339–345.

Riley, J., Garner, M. M., and Kiupel M and Hammond, E. E. (2017). Disseminated toxoplasmosis in a captive adult dromedary camel (*Camelus dromedarius*). *J. Zoo Wildl Med.* 48 (3), 937–940. doi: 10.1638/2016-0057.1

Rouatbi, M., Amairia, S., Amdouni, Y., Boussaadoun, M. A., Ayadi, O., Al-Hosary, A., et al. (2019). *Toxoplasma gondii* infection and toxoplasmosis in north Africa: a review. infection par toxoplasma gondii et toxoplasmose en afrique du nord : synthèse. *Parasite (Paris France)* 26, 6. doi: 10.1051/parasite/2019006

Saad, N. M., Hussein, A. A., and Ewida, R. M. (2018). Occurrence of *Toxoplasma gondii* in raw goat, sheep, and camel milk in upper Egypt. *Vet. World* 11 (9), 1262. doi: 10.14202/vetworld.2018.1262-1265

Sadrebazzaz, A., Haddadzadeh, H., and Shayan, P. (2006). Seroprevalence of *Neospora caninum* and *Toxoplasma gondii* in camels (*Camelus dromedarius*) in mashhad, Iran. *Parasitol. Res.* 98 (6), 600–601. doi: 10.1007/s00436-005-0118-3

Sameeh, S., Mahmoud, A. E., Monib, M. M., and M El-Salahy and Eldeek, H. E. (2021). Latex agglutation test and PCR assays for diagnosis of *Toxoplasma gondii* infection in red meat producing animals in Aswan governorate, southern Egypt. *Slov Vet. Res.* 58, 281–288.

Sazmand, A., and Joachim, A. (2017). Parasitic diseases of camels in Iran, (1931–2017)–a literature review. *Parasite* 24, 1–15. doi: 10.1051/parasite/2017024

Sazmand, A., Joachim, A., and Otranto, D. (2019). Zoonotic parasites of dromedary camels: so important, so ignored. *Parasit Vectors* 12 (1), 1–10. doi: 10.1186/s13071-019-3863-3

Selim, A., and Abdelhady, A. (2020). Neosporosis among Egyptian camels and its associated risk factors. *Trop. Anim. Health Prod* 52 (6), 3381–3385. doi: 10.1007/s11250-020-02370-y

Shaapan, R. M., and Khalil, A. F. (2008). Evaluation of different *Toxoplasma gondii* isolates as antigens used in the modified agglutination test for the detection of toxoplasmosis in camels and donkeys. *Am-Eurasian J. Agr Environ. Sci.* 3, 837–841.

Sharif, M., Amouei, A., Sarvi, S., Mizani, A., Aarabi, M., Hosseini, S. A., et al. (2017). Genetic diversity of *Toxoplasma gondii* isolates from ruminants: a systematic review. *Int. J. Food Microbiol.* 258, 38–49. doi: 10.1016/j.ijfoodmicro.2017.07.007

Shehzad, ,. A., Masud, A., Fatima, T., Khan, F. M., Rehman, S., Effendi, M. H., et al. (2022). Seroprevalence of *Toxoplasma gondii* and associated alterations in hematology and serum biochemistry of one-humped camels (*Camelus dromedarius*) in Pakistan. *Vet. World* 15 (1), 110–118. doi: 10.14202/vetworld.2022.110-118

Soultan, A., Attum, O., Hamada, A., Hatab, E., Ahmed, S. E., Eisa, A., et al. (2017). Recent observation for leopard *Panthera pardus* in Egypt. *Mammalia* 81, 115–117. doi: 10.1515/mammalia-2015-0089

Tavakoli Kareshk, A., Oliaee, R. T., Mahmoudvand, H., Keyhani, A., Mohammadi, M. A., Bamorovat, M., et al. (2018). The first survey of isolation and molecular typing of *Toxoplasma gondii* by bioassay and PCR method in BALB/c mice in camels (*Camelus dromedarius*) from eastern Iran. *Iran J. Parasitol.* 13 (3), 382.

Tilahun, B., Tolossa, Y. H., Tilahun, G., Ashenafi, H., and Shimelis, S. (2018). Seroprevalence and risk factors of *Toxoplasma gondii* infection among domestic ruminants in East hararghe zone of oromia region, Ethiopia. *Vet. Med. Int.* 2018:4263470. doi: 10.1155/2018/4263470

Toaleb, N. I., Shaapan, R. M., Hassan, S. E., and El Moghazy, F. M. (2013). High diagnostic efficiency of affinity isolated fraction in camel and cattle toxoplasmosis. *World Med. Sci. J.* 8 (1), 61–66. doi: 10.5829/idosi.wjms.2013.8.1.72161

Utuk, A. E., Kirbas, A., Babur, C., and Balkaya, I. (2012). Detection of *Toxoplasma gondii* antibodies and some helminthic parasites in camels from nevsehir province of Turkey. *Isr. J. Vet. Med.* 67 (2), 106–108.

Venturoso, S., Venturoso, J., Silva, G., and Maia, O. (2021). Risk factor analysis associated with *Neospora caninum* in dairy cattle in Western Brazilian Amazon. *Braz. J. Vet. Parasitol.* 30 (1), 1–11. doi: 10.1590/s1984-296120201088

Wang, M., Wang, Y. H., Meng, P., Ye, Q., and Zhang, D. L. (2013). *Toxoplasma gondii* infection in bactrian camel (*Camelus bactrianus*) in China. *Vet. Parasitol.* 192 (1-3), 288–289. doi: 10.1016/j.vetpar.2012.09.028

Yawoz, M., Jaafar, S. E., Alali, F., and Babur, C. (2021). Seroprevalence of camels listeriosis, brucellosis and toxoplasmosis from kirkuk province-Iraq. *Pak Vet. J.* 41 (3), 335–340. doi: 10.29261/pakvetj/2021.030

Zain Eldin, E. A., Elkhawad, S. E., and Kheir, H. S. M. (1985). A serological survey for *Toxoplasma* antibodies in cattle, sheep, goats and camels (*Camelus dromedarius*) in the Sudan. *Rev. d'Elevage Med. Vet. Des. Pays Tropicaux (France)* 38 (3), 247–249.

Zarrin, M., Riveros, J. L., Ahmadpour, A., de Almeida, A. M., Konuspayeva, G., Vargas-Bello-Pérez, E., et al. (2020). Camelids: new players in the international animal production context. *Trop. Anim. Health Prod.* 52 (3), 903–913. doi: 10.1007/s11250-019-02197-2

Zeedan, G. S., Abdalhamed, A. M., Shaapan, R. M., and El-Namaky, A. H. (2022). Rapid diagnosis of *Toxoplasma gondii* using loop-mediated isothermal amplification assay in camels and small ruminants. *Beni-Suef Univ J. Basic Appl. Sci.* 11 (1), 1–10. doi: 10.1186/s43088-021-00184-x

Zhu, S., Zimmerman, D., and Deem, S. L. (2019). A review of zoonotic pathogens of dromedary camels. *Ecohealth* 16 (2), 356–377. doi: 10.1007/s10393-019-01413-7

frontiers | Frontiers in Cellular and Infection Microbiology

TYPE Brief Research Report
PUBLISHED 14 November 2022
DOI 10.3389/fcimb.2022.1048962

OPEN ACCESS

EDITED BY
Kayode K. Ojo,
University of Washington,
United States

REVIEWED BY
Reginaldo G. Bastos,
Washington State University,
United States
Pratap Vydyam,
Yale University, United States

*CORRESPONDENCE
Mingming Liu
lmm_2010@hotmail.com
Xuenan Xuan
gen@obihiro.ac.jp

SPECIALTY SECTION
This article was submitted to Parasite and Host, a section of the journal Frontiers in Cellular and Infection Microbiology

RECEIVED 20 September 2022
ACCEPTED 25 October 2022
PUBLISHED 14 November 2022

CITATION
Ji S, Galon EM, Amer MM, Zafar I, Yanagawa M, Asada M, Zhou J, Liu M and Xuan X (2022) Phosphatidylinositol 4-kinase is a viable target for the radical cure of *Babesia microti* infection in immunocompromised hosts. *Front. Cell. Infect. Microbiol.* 12:1048962.
doi: 10.3389/fcimb.2022.1048962

Phosphatidylinositol 4-kinase is a viable target for the radical cure of *Babesia microti* infection in immunocompromised hosts

Shengwei Ji[1], Eloiza May Galon[1], Moaz M. Amer[1,2], Iqra Zafar[1], Masashi Yanagawa[3], Masahito Asada[1], Jinlin Zhou[4], Mingming Liu[5]* and Xuenan Xuan[1]*

[1]National Research Center for Protozoan Diseases, Obihiro University of Agriculture and Veterinary Medicine, Obihiro, Hokkaido, Japan, [2]Biotechnology Department, Animal Health Research Institute, Dokki, Egypt, [3]Department of Veterinary Medicine, Obihiro University of Agriculture and Veterinary Medicine, Obihiro, Hokkaido, Japan, [4]Shanghai Veterinary Research Institute, Chinese Academy of Agricultural Sciences, Shanghai, China, [5]School of Basic Medicine, Hubei University of Arts and Science, Xiangyang, China

Human babesiosis is a global emerging tick-borne disease caused by infection with intra-erythrocytic parasites of the genus *Babesia*. With the rise in human babesiosis cases, the discovery and development of new anti-*Babesia* drugs are essential. Phosphatidylinositol 4-kinase (PI4K) is a widely present eukaryotic enzyme that phosphorylates lipids to regulate intracellular signaling and trafficking. Previously, we have shown that MMV390048, an inhibitor of PI4K, showed potent inhibition against *Babesia* species, revealing PI4K as a druggable target for babesiosis. However, twice-administered, 7-day regimens failed to clear *Babesia microti* parasites from the immunocompromised host. Hence, in this study, we wanted to clarify whether targeting PI4K has the potential for the radical cure of babesiosis. In a *B. microti*-infected SCID mouse model, a 64-day-consecutive treatment with MMV390048 resulted in the clearance of parasites. Meanwhile, an atovaquone (ATO) resistant parasite line was isolated from the group treated with ATO plus azithromycin. A nonsynonymous variant in the Y272C of the *cytochrome b* gene was confirmed by sequencing. Likewise, MMV390048 showed potent inhibition against ATO-resistant parasites. These results provide evidence of PI4K as a viable drug target for the radical cure of babesiosis, which will contribute to designing new compounds that can eradicate parasites.

KEYWORDS

***Babesia microti*, babesiosis, phosphatidylinositol 4-kinase, treatment, MMV390048**

Introduction

Human babesiosis is a tick-borne disease caused by several *Babesia* species, of which *Babesia microti* is one of the main agents (Vannier et al., 2015). *B. microti* infection shows a wide spectrum of symptoms from asymptomatic to fatal disease, particularly in immunocompromised or elderly patients (Vannier et al., 2015). Most cases occur in the United States (U.S.), especially in the northeastern and northern midwestern regions (Krause, 2019). For the time being, the treatment of human babesiosis, as recommended by Centers for Disease Control and Prevention (CDC), usually involves the combination of atovaquone (ATO) plus azithromycin (AZI) for 1-2 weeks, which exhibits fewer side effects compared to an alternative combined therapy of clindamycin and quinine (Vannier and Krause, 2012). The treatment period for babesiosis may extend to six weeks or more in severely immunocompromised patients, and *cytochrome b* (*Cytb*) and *ribosomal protein subunit L4* (*rpl4*) mutations were associated with parasite resistance to ATO and AZI, respectively, resulting in treatment failure (Krause et al., 2008; Wormser et al., 2010; Vannier and Krause, 2012; Simon et al., 2017). Another recommended regimen for babesiosis, clindamycin combined with quinine, is frequently associated with side effects, such as hearing loss, vertigo, and tinnitus (Renard and Ben Mamoun, 2021). Due to limited options, this treatment is still recommended for patients with severe babesiosis (Renard and Ben Mamoun, 2021). Moreover, previous reports revealed that monotherapy with quinine, clindamycin, or AZI was ineffective against *B. microti* infection in immunocompromised hosts (Lawres et al., 2016). Therefore, the buildout of new drug candidates or targets is urgently needed for the control and treatment of human babesiosis. Phosphatidylinositol 4-kinase (PI4K) is a ubiquitous eukaryotic lipid kinase involved in the production of phosphatidylinositol 4-phosphate (PI4P) (Li et al., 2021). PI4K has been reported to play a key role in the occurrence and development of cancer, viral infections, and malaria (Li et al., 2021). PI4K not only exhibits the potential for eliminating malaria (McNamara et al., 2013; Paquet et al., 2017), but also possesses an inhibitory effect against *Babesia* species, as we recently reported (Ji et al., 2022). The 2-aminopyridine MMV390048, a representative of a new chemical class of *Plasmodium* PI4K inhibitor (Paquet et al., 2017), showed potent inhibition against *B. gibsoni in vitro*, and against *B. rodhaini* and *B. microti in vivo* (Ji et al., 2022). However, twice-administered, short-time treatment did not eliminate the parasite from immunocompromised hosts. Hence, the purpose of this study was to test whether uninterrupted treatment targeting *B. microti* PI4K could eradicate *B. microti* infection in immunocompromised hosts.

Materials and methods

Chemical reagents

MMV390048, sesame oil (SO), atovaquone (ATO), and azithromycin (AZI) were purchased from Sigma-Aldrich (Tokyo, Japan). MMV390048, ATO, and AZI were dissolved in SO to prepare a stock solution with a concentration of 40 mg/ml and kept at 4°C before use. KOD FX Neo DNA polymerase was purchased from Toyobo (Tokyo, Japan). The Big Dye Terminator v3.1 cycle sequencing kit was purchased from Applied Biosystems (Tokyo, Japan).

Parasites and mice

Babesia microti Peabody mjr strain (ATCC® PRA-99™) was purchased from ATCC and stocked in our laboratory. For the maintenance of *B. microti*, cryopreserved parasitized RBCs were passaged by intraperitoneal (i.p.) injection in donor mice. Six-week-old female severe combined immunodeficiency (SCID) mice and BALB/c mice were purchased from CLEA Japan (Tokyo, Japan) and used for *in vivo* studies.

Mouse infection and drug administration

To confirm the efficacy of uninterrupted treatment targeting PI4K, 15 SCID mice were randomly divided equally into 3 groups and intraperitoneally injected with 1×10^7 *B. microti*. Blood smears were prepared every other day, and the hematocrit (HCT) was measured every four days. Treatment was initiated at 4 days post-infection (DPI) when mouse parasitemia is ~1%. This timeline was followed since early clinical manifestations are observed when parasitemia exceeds 1% in babesiosis patients (Akel and Mobarakai, 2017). Daily treatment with 20 mg/kg MMV390048, 20 mg/kg ATO plus 20 mg/kg AZI, and 0.2 ml vehicle (sesame oil) was given orally to each group, respectively (Batiha et al., 2020; Tuvshintulga et al., 2022). These treatments were discontinued when mice tested negative by PCR detection of *B. microti* 18S ribosomal RNA (18S-rRNA) gene. To isolate the *B. microti Cytb* mutant strain, parasites from the SCID mouse treated with ATO plus AZI were collected and passaged in a donor SCID mouse. To evaluate the efficacy of PI4K inhibitor on ATO-resistant parasites, 15 BALB/c mice were randomly divided equally into 3 groups and intraperitoneally injected with 1×10^7 *B. microti Cytb* mutant strain. A 7-day treatment was given to mouse groups as described above and the parasitemia and HCT levels were monitored.

Detection of *B. microti* 18S-rRNA gene and surveillance of gene variants

Blood samples were collected from the tail vein and were diluted in PBS, followed by incubation at 100°C for 5 min. After incubation, the samples were centrifuged at 10,000 rpm for 5 min and the supernatants were collected and used for detection. To rule out false negative results, the samples were checked using Qubit™ 1 × dsDNA BR assay kit (Thermo Fisher Scientific) and Qubit® 2.0 fluorometer (Thermo Fisher Scientific) before running the PCR assay to ensure that genomic DNA was present. Detection of the 18S-rRNA gene started 16 DPI and was used to evaluate whether the parasites were cleared from the SCID mice. Gene amplification was performed following a previously described protocol (Persing et al., 1992). The *Cytb* and *rpl4* mutations were determined by Sanger sequencing (Tuvshintulga et al., 2022). The obtained sequence was aligned with the wild type sequence. A genetic variant was detected in *Cytb* gene and deposited in GenBank database with accession no. ON815034.

Statistical analysis

The differences in parasitemia and HCT between control and treated groups were analyzed using the one-way analysis of variance using GraphPad Prism (La Jolla, CA, USA). A *P* value of < 0.05 was considered to be statistically significant.

Results

Radical cure of human babesiosis by uninterrupted treatment targeting phosphatidylinositol 4-kinase

Treatment with MMV390048 showed potent efficacy against *B. microti*, evidenced by abated parasitemia from 5 DPI and undetectable parasites in blood smears from 8 DPI (Figure 1A). Moreover, parasites were no longer detectable by PCR from 64 DPI to 92 DPI (Figure 2). At 10 DPI, parasites in the vehicle-treated group reached the highest parasitemia (average 60.6%), with a transient and slight decline at 14 DPI, and maintained

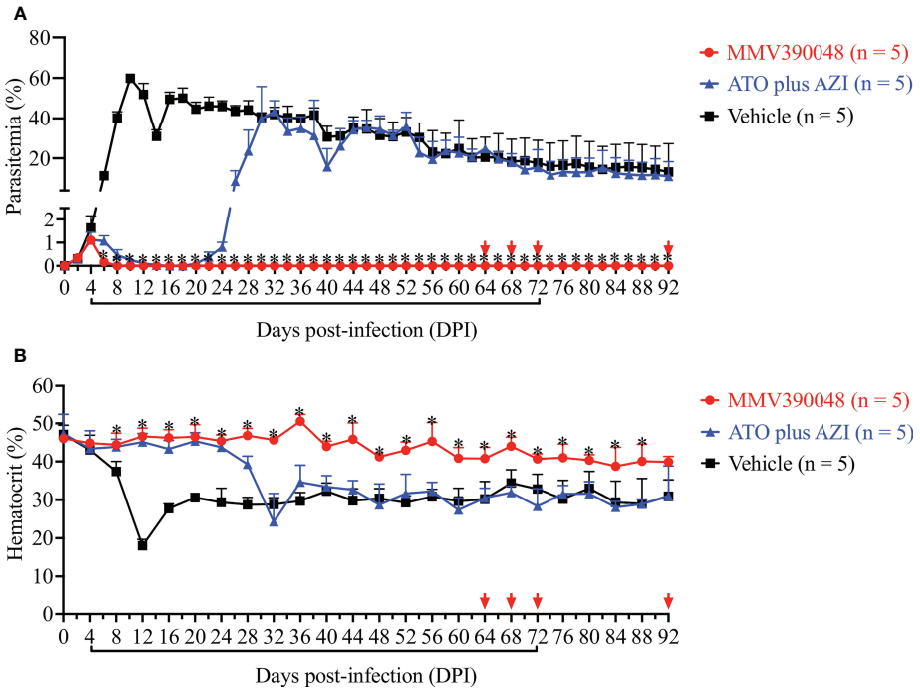

FIGURE 1
The efficacy of consecutive treatment with MMV390048 in *Babesia microti*-infected severe combined immunodeficiency (SCID) mice. **(A)** Course of parasitemia in vehicle-, or atovaquone (ATO) plus azithromycin- (AZI), or MMV390048-treated groups. **(B)** Hematocrit changes in *B. microti*-infected SCID mice treated with vehicle, or ATO plus AZI, or MMV390048. Treatment was given orally starting from 4 days post-infection (DPI). The black lines indicate time of treatment and the red arrows indicate testing negative in PCR assay. The asterisks indicate a significant difference ($P < 0.05$) between the drug-treated groups and vehicle-treated group. Parasitemia was calculated by counting infected RBCs among 3,000 RBCs using Giemsa-stained blood smears.

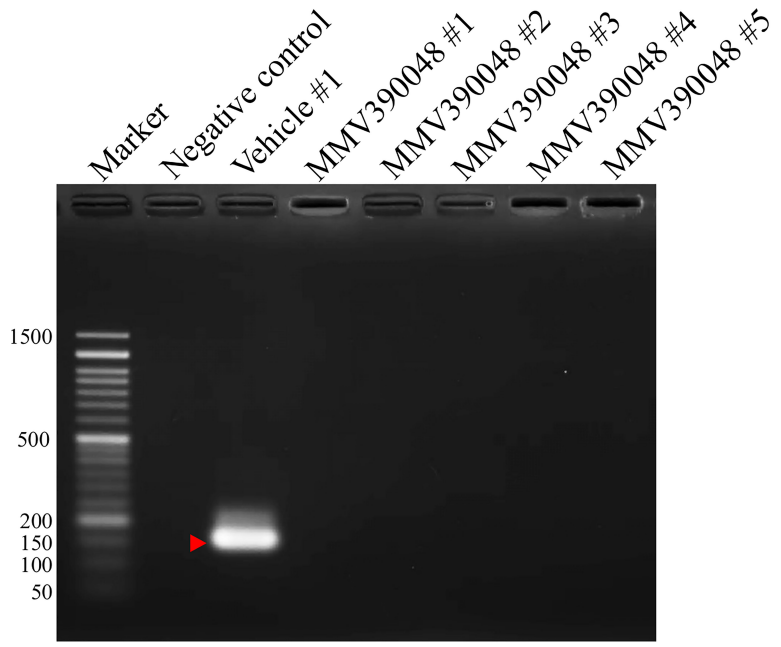

FIGURE 2
Molecular detection of parasite DNA in the blood of MMV390048-treated group (#1-5) at 92 DPI. The red arrow shows the expected band length of 154 bp for the *B. microti* 18S-rRNA gene.

fluctuating parasitemia until the end of the trial. The mean parasitemia significantly differed between the vehicle-treated and MMV390048-treated groups from 6 DPI (Figure 1A). In ATO plus AZI-treated group, parasites were initially inhibited until 22 DPI, but the parasitemia rapidly increased from 24 DPI and reached its peak at 32 DPI (average 40.1%) (Figure 1A). From 30 DPI, the ATO plus AZI was ineffective on parasite growth as no significant difference in parasitemia was observed when compared to the vehicle-treated group. In addition, markedly lower HCT levels were recorded in vehicle-treated and ATO plus AZI-treated groups from 8 DPI and 32 DPI, respectively (Figure 1B). The *Cytb* and *rpl4* genes were sequenced from relapsed parasites and a single nucleotide variant (SNV) of the *Cytb* gene was detected as a non-synonymous coding change at position 272 (Y272C) (Figure 3). Meanwhile, there was no mutation detected in the *rpl4* gene.

Inhibitory efficacy of MMV390048 against ATO-resistant *B. microti* strain

The next step was to evaluate the sensitivity of *B. microti Cytb* mutant strain to MMV390048. In the vehicle-treated group, *B. microti Cytb* mutant strain rapidly increased in mice and reached peak parasitemia at 10 DPI (average 36.7%) and a lower HCT level was observed from 12 DPI (Figure 4). As expected, ATO plus AZI was ineffective against the *B. microti Cytb* mutant strain (Figure 4A). No significant difference in the level of parasitemia was observed between vehicle- and ATO plus AZI-treated groups. In contrast, the growth of *B. microti Cytb* mutant strain and the development of anemia were significantly inhibited upon treating mice with MMV390048 (Figure 4B).

Discussion

To avoid developing drug resistance, the treatment for human babesiosis usually consists of a two-drug combination, such as ATO plus AZI (Krause et al., 2000). Despite this, acquired drug resistance is well documented in some severe cases in immunocompromised patients (Krause et al., 2008; Wormser et al., 2010; Vannier and Krause, 2012; Simon et al., 2017). Hence, the radical cure of babesiosis remains challenging in severely immunocompromised patients. In the recent past, a few compounds have been reported as promising drugs against human babesiosis, namely endochin-like quinolones (ELQs) (Lawres et al., 2016; Chiu et al., 2021), tafenoquine (Mordue and Wormser, 2019; Liu et al., 2021), and clofazimine (Tuvshintulga et al., 2022). ELQs showed inhibitory effects against apicomplexan parasites by targeting *Cytb* (Doggett et al., 2012; Stickles et al., 2015). In babesiosis, a 7-day treatment of

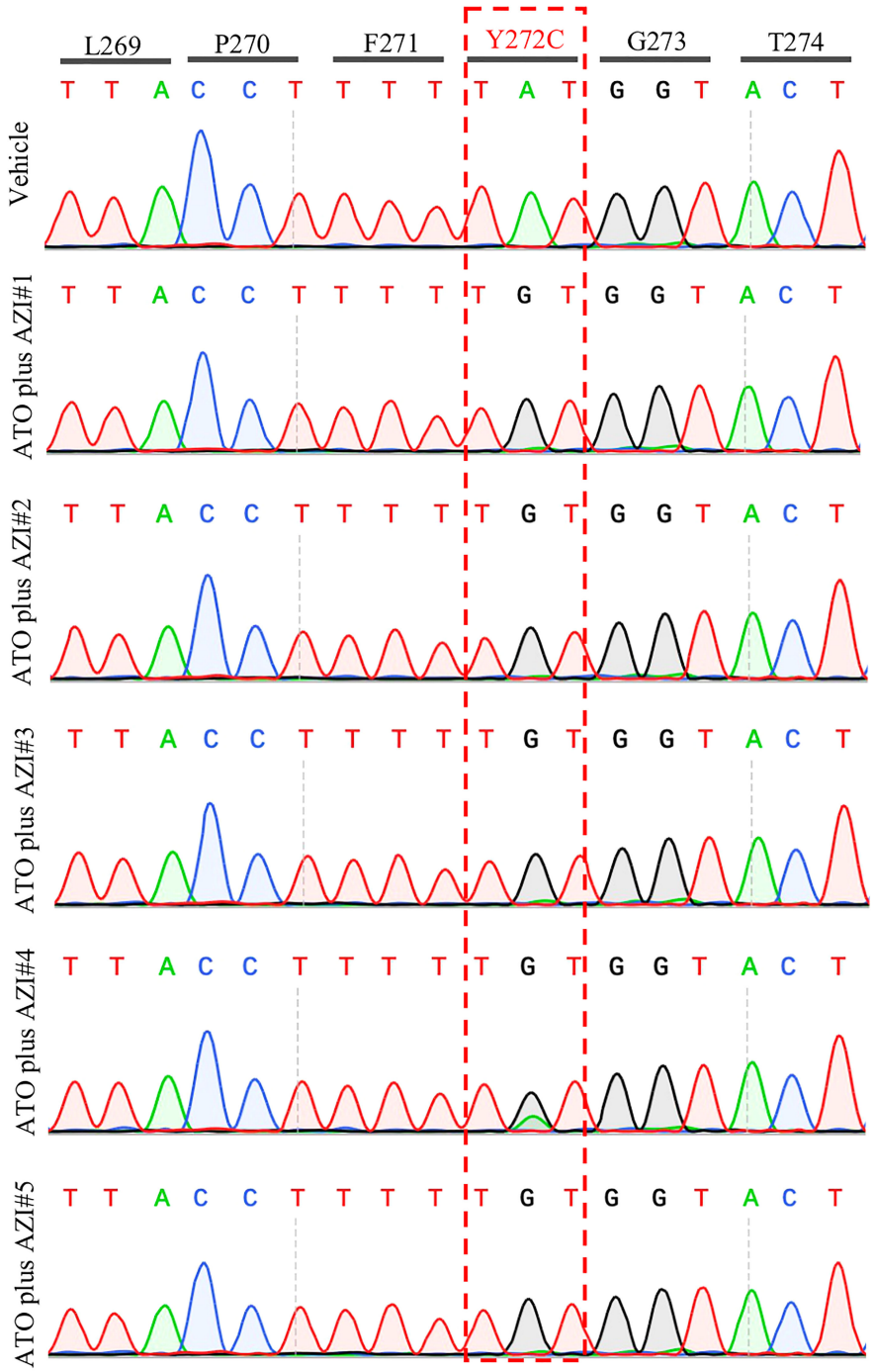

FIGURE 3
Representative sequencing chromatogram of *cytochrome b* (*Cytb*) gene in recrudescent parasites. The parasite DNA of vehicle #1 and ATO plus AZI (#1-5) were extracted from a blood sample at 92 days post-infection and was used to amplify and sequence the *B. microti Cytb* gene.

ELQ-334 plus ATO prevented the recrudescence in the SCID mouse model of *B. microti* infection (Lawres et al., 2016). Similarly, a 10-day treatment of ELQ-502 monotherapy or in combination with ATO resulted in the radical cure of babesiosis with no recrudescence in the mouse model (Chiu et al., 2021). Tafenoquine was approved by U. S. Food and Drug Administration (FDA) in 2018 for the radical cure of *Plasmodium vivax* infection and chemoprophylaxis of malaria

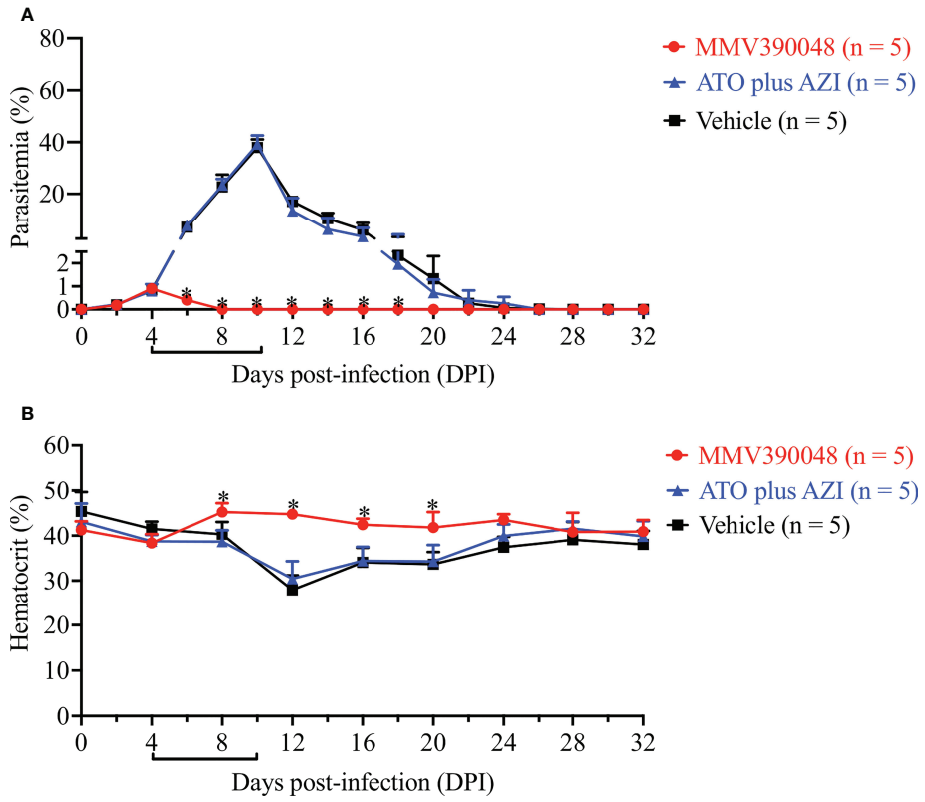

FIGURE 4
The efficacy of MMV390048 against *B. microti Cytb* mutant strain in BALB/c mice. **(A)** Course of parasitemia of vehicle- or ATO plus AZI-, or MMV390048-treated BALB/c mouse groups. **(B)** Hematocrit changes of *B. microti Cytb* mutant strain in mice treated with vehicle, or ATO plus AZI, or MMV390048. The black lines indicate the time of treatment. The asterisks indicate a significant difference ($P < 0.05$) between the drug-treated groups and vehicle-treated group. Parasitemia was calculated by counting infected RBCs among 3,000 RBCs using Giemsa-stained blood smears.

(Watson et al., 2021). In SCID mice, tafenoquine showed strong inhibition against *B. microti* infection, evident from the single dose requirement (Mordue and Wormser, 2019; Liu et al., 2021). Tafenoquine treatment in cases of relapsing babesiosis caused by drug-resistant *B. microti* is followed by resolution of parasitemia and symptoms in the patient, demonstrating tafenoquine's excellent effectivity in clinical settings (Marcos et al., 2022; Rogers et al., 2022). However, the use of tafenoquine entails the risk of inducing severe hemolytic anemia in G6PD-deficient patients (Peters and Van Noorden, 2009). Clofazimine combined with ATO was also evaluated as a candidate for human babesiosis. Uninterrupted treatment of clofazimine with ATO resulted in the radical cure of *B. microti*-infected SCID mice in 44 days (Tuvshintulga et al., 2022). Phosphatidylinositol kinases (PIKs) are essential in the regulation of cell proliferation, survival, and membrane trafficking (Hassett and Roepe, 2018). Currently, six *P. falciparum* genes are hypothesized to encode PIKs, while in *Babesia* species, these genes are still unidentified (Hassett and Roepe, 2018). In *Plasmodium*, PI4K phosphorylates lipids to regulate intracellular signaling and trafficking, making it a druggable target to eliminate malaria (McNamara et al., 2013). In blood stages, the inhibitor prevents the parasite's development by disrupting plasma membrane ingression around the developing daughter merozoites. *B. microti* PI4K shares an identity value of 62.8% with *P. falciparum* and is highly conserved among *Babesia* species (Ji et al., 2022). Hence, we speculate that the mechanism in *Plasmodium* also applies to *Babesia* species. MMV390048 is an inhibitor of *Plasmodium* PI4K which was under evaluation in human clinical trials (Sinxadi et al., 2020). A previous study reported MMV390048 has potent inhibition against *Babesia* species by targeting PI4K, revealing a promising druggable target (Ji et al., 2022). In light of this, we further examined if targeting PI4K by monotherapy is sufficient to achieve the radical cure of *B. microti* infection in SCID mice. In this study, we used MMV390048 as an inhibitor for *B. microti* PI4K (*Bm*PI4K) and a 64-day uninterrupted treatment with MMV390048 succeeded in curing babesiosis in *B. microti*-

infected SCID mice. Although this therapy was longer than in ELQ-502 (10 days) and clofazimine with ATO (44 days), we have confirmed that PI4K is a promising target for the clearance of parasites. Meanwhile, in ATO plus AZI-treatment group, the parasite established resistance to ATO and AZI, in addition to the development of a single amino acid mutation (Y272C) in the *B. microti Cytb* gene. Y272 is highly conserved among apicomplexan parasites and the site mutation of Y272 will confer a high degree of resistance to the drug (Fisher and Meunier, 2008; Lemieux et al., 2016). Moreover, *B. microti* Y272C mutation has been described in a clinical case and caused treatment failure (Simon et al., 2017). MMV390048 also demonstrated potent inhibition of *B. microti Cytb* mutant strain. Despite MMV390048 exhibiting a good inhibitory effect, *Babesia* tends to be more tolerant than *Plasmodium* when treated with MMV390048. Hence, if MMV390048 were to be used for treating human babesiosis, the recommended dose should be higher than 120 mg (a safety dose test in human clinical trials) (Sinxadi et al., 2020; Ji et al., 2022). Moreover, the accompanying safety issues should be considered and future work can focus on developing and designing *Babesia* PI4K-specific inhibitors, as well as the development of MMV390048-combined therapeutics. This will accelerate the development of next-generation anti-babesiosis therapeutics to eliminate *Babesia* infection. In summary, results from the present study revealed that targeting *Bm*PI4K not only suppresses parasite growth but also eradicates parasites in immunocompromised hosts, especially in relapsing infections caused by ATO-resistant *B. microti* strain.

Conclusion

Based on the preceding findings, we conclude that *Bm*PI4K is a feasible and promising drug target for the elimination of *B. microti* infection. This study opens new avenues to rationally design inhibitors with improved drug-like properties against *Babesia* species.

Data availability statement

The datasets presented in this study can be found in online repositories. The names of the repository/repositories and accession number(s) can be found below: https://www.ncbi.nlm.nih.gov/nuccore/ON815034.

Ethics statement

The animal study was reviewed and approved by the Research Ethics Review Committee of the Obihiro University of Agriculture and Veterinary Medicine.

Author contributions

SJ, ML, and XX designed the study. SJ carried out the experiments. IZ contributed reagents/materials preparation. SJ, EG, MMA, MY, MA, and JZ wrote the manuscript. All authors read and approved the final manuscript.

Funding

This project was funded by a Grant-in-Aid for Scientific Research (18H02336 and 18KK0188) and the Japan Society for the Promotion of Science Core-to-Core program, (both grants are from the Ministry of Education, Culture, Sports, Science and Technology of Japan), in addition to a grant from Strategic International Collaborative Research Project (JPJ008837) promoted by the Ministry of Agriculture, Forestry and Fisheries of Japan. This research was also partially funded by the Central Public-interest Scientific Institution Basal Research Fund of China (Y2021GH01-3).

Conflict of interest

The authors declare that the research was conducted in the absence of any commercial or financial relationships that could be construed as a potential conflict of interest.

Publisher's note

References

Akel, T., and Mobarakai, N. (2017). Hematologic manifestations of babesiosis. *Ann. Clin. Microbiol. Antimicrob.* 16, 6. doi: 10.1186/s12941-017-0179-z

Batiha, G. E., Beshbishy, A. M., Alkazmi, L. M., Nadwa, E. H., Rashwan, E. K., Yokoyama, N., et al. (2020). *In vitro* and *in vivo* growth inhibitory activities of cryptolepine hydrate against several babesia species and theileria equi. *PLoS Negl. Trop. Dis.* 14, e0008489. doi: 10.1371/journal.pntd.0008489

Chiu, J. E., Renard, I., Pal, A. C., Singh, P., Vydyam, P., Thekkiniath, J., et al. (2021). Effective therapy targeting cytochrome bc1 prevents babesia erythrocytic

development and protects from lethal infection. *Antimicrob. Agents Chemother.* 65, e0066221. doi: 10.1128/AAC.00662-21

Doggett, J. S., Nilsen, A., Forquer, I., Wegmann, K. W., Jones-Brando, L., Yolken, R. H., et al. (2012). Endochin-like quinolones are highly efficacious against acute and latent experimental toxoplasmosis. *Proc. Natl. Acad. Sci. U. S. A* 109, 15936–15941. doi: 10.1073/pnas.1208069109

Fisher, N., and Meunier, B. (2008). Molecular basis of resistance to cytochrome bc1 inhibitors. *FEMS Yeast Res.* 8, 183–192. doi: 10.1111/j.1567-1364.2007.00328.x

Hassett, M. R., and Roepe, P. D. (2018). PIK-ing new malaria chemotherapy. *Trends Parasitol.* 34, 925–927. doi: 10.1016/j.pt.2018.06.003

Ji, S., Galon, E. M., Rizk, M. A., Yi, Y., Zafar, I., Li, H., et al. (2022). Efficacy of the antimalarial MMV390048 against babesia infection reveals phosphatidylinositol 4-kinase as a druggable target for babesiosis. *Antimicrob. Agents Chemother.* 66 e0057422. doi: 10.1128/aac.00574-22

Krause, P. J. (2019). Human babesiosis. *Int. J. Parasitol.* 49, 165–174. doi: 10.1016/j.ijpara.2018.11.007

Krause, P. J., Gewurz, B. E., Hill, D., Marty, F. M., Vannier, E., Foppa, I. M., et al. (2008). Persistent and relapsing babesiosis in immunocompromised patients. *Clin. Infect. Dis.* 46, 370–376. doi: 10.1086/525852

Krause, P. J., Lepore, T., Sikand, V. K., Gadbaw, J.Jr., Burke, G., Telford, S. R.3rd., et al. (2000). Atovaquone and azithromycin for the treatment of babesiosis. *N Engl. J. Med.* 343, 1454–1458. doi: 10.1056/NEJM200011163432004

Lawres, L. A., Garg, A., Kumar, V., Bruzual, I., Forquer, I. P., Renard, I., et al. (2016). Radical cure of experimental babesiosis in immunodeficient mice using a combination of an endochin-like quinolone and atovaquone. *J. Exp. Med.* 213, 1307–1318. doi: 10.1084/jem.20151519

Lemieux, J. E., Tran, A. D., Freimark, L., Schaffner, S. F., Goethert, H., Andersen, K. G., et al. (2016). A global map of genetic diversity in babesia microti reveals strong population structure and identifies variants associated with clinical relapse. *Nat. Microbiol.* 1, 16079. doi: 10.1038/nmicrobiol.2016.79

Li, Y. P., Mikrani, R., Hu, Y. F., Faran Ashraf Baig, M. M., Abbas, M., Akhtar, F., et al. (2021). Research progress of phosphatidylinositol 4-kinase and its inhibitors in inflammatory diseases. *Eur. J. Pharmacol.* 907, 174300. doi: 10.1016/j.ejphar.2021.174300

Liu, M., Ji, S., Kondoh, D., Galon, E. M., Li, J., Tomihari, M., et al. (2021). Tafenoquine is a promising drug candidate for the treatment of babesiosis. *Antimicrob. Agents Chemother.* 65, e0020421. doi: 10.1128/AAC.00204-21

Marcos, L. A., Leung, A., Kirkman, L., and Wormser, G. P. (2022). Use of tafenoquine to treat a patient with relapsing babesiosis with clinical and molecular evidence of resistance to azithromycin and atovaquone. *IDCases.* 27, e01460. doi: 10.1016/j.idcr.2022.e01460

McNamara, C. W., Lee, M. C., Lim, C. S., Lim, S. H., Roland, J., Simon, O., et al. (2013). Targeting plasmodium PI (4)K to eliminate malaria. *Nature.* 504, 248–253. doi: 10.1038/nature12782

Mordue, D. G., and Wormser, G. P. (2019). Could the drug tafenoquine revolutionize treatment of babesia microti infection? *J. Infect. Dis.* 220, 442–447. doi: 10.1093/infdis/jiz119

Paquet, T., Le Manach, C., Cabrera, D. G., Younis, Y., Henrich, P. P., Abraham, T. S., et al. (2017). Antimalarial efficacy of MMV390048, an inhibitor of plasmodium phosphatidylinositol 4-kinase. *Sci. Transl. Med.* 9, eaad9735. doi: 10.1126/scitranslmed.aad9735

Persing, D. H., Mathiesen, D., Marshall, W. F., Telford, S. R., Spielman, A., Thomford, J. W., et al. (1992). Detection of babesia microti by polymerase chain reaction. *J. Clin. Microbiol.* 30, 2097–2103. doi: 10.1128/jcm.30.8.2097-2103.1992

Peters, A. L., and Van Noorden, C. J. (2009). Glucose-6-phosphate dehydrogenase deficiency and malaria: cytochemical detection of heterozygous G6PD deficiency in women. *J. Histochem Cytochem* 57, 1003–1011. doi: 10.1369/jhc.2009.953828

Renard, I., and Ben Mamoun, C. (2021). Treatment of human babesiosis: Then and now. *Pathogens.* 10, 1120. doi: 10.3390/pathogens10091120

Rogers, R., Krause, P. J., Norris, A. M., Ting, M. H., Nagami, E. H., Cilley, B., et al. (2022). Broad antimicrobial resistance in a case of relapsing babesiosis successfully treated with tafenoquine. *Clin. Infect. Dis.* 10, ciac473. doi: 10.1093/cid/ciac473

Simon, M. S., Westblade, L. F., Dziedziech, A., Visone, J. E., Furman, R. R., Jenkins, S. G., et al. (2017). Clinical and molecular evidence of atovaquone and azithromycin resistance in relapsed babesia microti infection associated with rituximab and chronic lymphocytic leukemia. *Clin. Infect. Dis.* 65, 1222–1225. doi: 10.1093/cid/cix477

Sinxadi, P., Donini, C., Johnstone, H., Langdon, G., Wiesner, L., Allen, E., et al. (2020). Safety, tolerability, pharmacokinetics, and antimalarial activity of the novel plasmodium phosphatidylinositol 4-kinase inhibitor MMV390048 in healthy volunteers. *Antimicrob. Agents Chemother.* 64, e01896–e01819. doi: 10.1128/AAC.01896-19

Stickles, A. M., de Almeida, M. J., Morrisey, J. M., Sheridan, K. A., Forquer, I. P., Nilsen, A., et al. (2015). Subtle changes in endochin-like quinolone structure alter the site of inhibition within the cytochrome bc1 complex of plasmodium falciparum. *Antimicrob. Agents Chemother.* 59, 1977–1982. doi: 10.1128/AAC.04149-14

Tuvshintulga, B., Sivakumar, T., Nugraha, A. B., Ahedor, B., Batmagnai, E., Otgonsuren, D., et al. (2022). Combination of clofazimine and atovaquone as a potent therapeutic regimen for the radical cure of babesia microti infection in immunocompromised hosts. *J. Infect. Dis.* 225, 238–242. doi: 10.1093/infdis/jiab537

Vannier, E. G., Diuk-Wasser, M. A., Ben Mamoun, C., and Krause, P. J. (2015). Babesiosis. *Infect. Dis. Clin. North Am.* 29, 357–370. doi: 10.1016/j.idc.2015.02.008

Vannier, E., and Krause, P. J. (2012). Human babesiosis. *N Engl. J. Med.* 36, 2397–2407. doi: 10.1056/NEJMra1202018

Watson, J. A., Nekkab, N., and White, M. (2021). Tafenoquine for the prevention of plasmodium vivax malaria relapse. *Lancet Microbe* 2, e175–e176. doi: 10.1016/S2666-5247(21)00062-8

Wormser, G. P., Prasad, A., Neuhaus, E., Joshi, S., Nowakowski, J., Nelson, J., et al. (2010). Emergence of resistance to azithromycin-atovaquone in immunocompromised patients with babesia microti infection. *Clin. Infect. Dis.* 50, 381–386. doi: 10.1086/649859

frontiers | Frontiers in Cellular and Infection Microbiology

TYPE Original Research
PUBLISHED 25 November 2022
DOI 10.3389/fcimb.2022.1072385

OPEN ACCESS

EDITED BY
Mingming Liu,
Hubei University of Arts and Science, China

REVIEWED BY
Ding Jing,
Jilin University, China
Fei Liu,
Jilin Agriculture University, China

*CORRESPONDENCE
Jing Liu
liuliang9983@163.com
Gang Liu
gangliu@qau.edu.cn

†These authors have contributed equally to this work

SPECIALTY SECTION
This article was submitted to Parasite and Host, a section of the journal Frontiers in Cellular and Infection Microbiology

RECEIVED 17 October 2022
ACCEPTED 08 November 2022
PUBLISHED 25 November 2022

CITATION
Li X-M, Geng H-L, Wei Y-J, Yan W-L, Liu J, Wei X-Y, Zhang M, Wang X-Y, Zhang X-X and Liu G (2022) Global prevalence and risk factors of *Cryptosporidium* infection in *Equus*: A systematic review and meta-analysis. *Front. Cell. Infect. Microbiol.* 12:1072385.
doi: 10.3389/fcimb.2022.1072385

Global prevalence and risk factors of *Cryptosporidium* infection in *Equus*: A systematic review and meta-analysis

Xiao-Man Li[1†], Hong-Li Geng[1†], Yong-Jie Wei[1], Wei-Lan Yan[1], Jing Liu[2*], Xin-Yu Wei[3], Miao Zhang[1], Xiang-Yu Wang[1], Xiao-Xuan Zhang[1] and Gang Liu[1*]

[1]College of Veterinary Medicine, Qingdao Agricultural University, Qingdao, Shandong, China, [2]College of Life Science, Changchun Sci-Tech University, Shuangyang, Jilin, China, [3]College of Animal Science and Veterinary Medicine, Heilongjiang Bayi Agricultural University, Daqing, Heilongjiang, China

Intoduction: Cryptosporidiosis is a zoonotic disease caused by Cryptosporidium infection with the main symptom of diarrhea. The present study performed a metaanalysis to determine the global prevalence of Cryptosporidium in Equus animals.

Methods: Data collection was carried out using Chinese National Knowledge Infrastructure (CNKI), VIP Chinese journal database (VIP), WanFang Data, PubMed, and ScienceDirect databases, with 35 articles published before 2021 being included in this systematic analysis. This study analyzed the research data through subgroup analysis and univariate regression analysis to reveal the factors leading to high prevalence. We applied a random effects model (REM) to the metadata.

Results: The total prevalence rate of Cryptosporidium in Equus was estimated to be 7.59% from the selected articles. The prevalence of Cryptosporidium in female Equus was 2.60%. The prevalence of Cryptosporidium in Equus under 1-year-old was 11.06%, which was higher than that of Equus over 1-year-old (2.52%). In the experimental method groups, the positive rate detected by microscopy was the highest (10.52%). The highest Cryptosporidium prevalence was found in scale breeding Equus (7.86%). The horses had the lowest Cryptosporidium prevalence (7.32%) among host groups. C. muris was the most frequently detected genotype in the samples (53.55%). In the groups of geographical factors, the prevalence rate of Cryptosporidium in Equus was higher in regions with low altitude (6.88%), rainy (15.63%), humid (22.69%), and tropical climates (16.46%).

Discussion: The search strategy use of five databases might have caused the omission of some researches. This metaanalysis systematically presented the global prevalence and potential risk factors of Cryptosporidium infection in Equus. The farmers should strengthen the management of young and female Equus animals, improve water filtration systems, reduce stocking densities, and harmless treatment of livestock manure.

KEYWORDS

***Cryptosporidium*, *Equus*, meta-analysis, prevalence, zoonotic diseases**

Introduction

Cryptosporidium is a zoonotic coccidian parasite, which mainly parasitizes in the epithelial cells of the small intestine in vertebrates (Xue, 2021). The life cycle of *Cryptosporidium* in hosts comprises asexual and sexual phases, and finally, the oocysts were shed with faeces. The oocyst containing infective sporozoites can survive for months in moist conditions (Chalmers et al., 2019). The *Cryptosporidium*-infected patients usually display signs of diarrhea and abdominal pain, and other clinical features include nausea, vomiting, and low-grade fever. The occasional signs include myalgia, weakness, malaise, headache, and anorexia. The severity, persistence, and eventual outcome of infection generally depend on the characteristics of *Cryptosporidium* and host factors (Bouzid et al., 2013).

Cryptosporidium was examined in mucosal tissues of mice by Tyzzer in 1907 (Zhang and Jiang, 2001). *Cryptosporidium* was the first detection happened to be in immunodeficient Arabian horse foals in 1978 (Snyder et al., 1978). People didn't pay attention to the disease at first. At the end of the nineteenth century, the events of death of AIDS patients who were infected with *Cryptosporidium* caused a full attention of cryptosporidiosis (Current et al., 1983). *Cryptosporidium* is worldwide distributed, and the infections of *Cryptosporidium* in organisms have been reported in more than 70 countries (Xue, 2021).

Equus animals are mainly distributed in Eurasia and Africa, roughly divided into three species: horse, donkey and zebra. Horses are now mainly used for entertainment or competition, donkeys are kept as companions or used as working or production animals, whereas mules are mainly used for working purposes (Jian, 2012). Because they are maintained in a close association with their owners and veterinary personnel, *Equus* animals are the important reservoirs for transmission of pathogens (such as *Cryptosporidium hominis* and *Toxoplasma gondii*) to humans and other animals (Alvarado-Esquivel et al., 2015; Jian et al., 2016). The cases of *Equus* cryptosporidiosis have been reported in many countries around the world, such as China, Italy, and United States. (Veronesi et al., 2010; Qi et al., 2015; Wagnerová et al., 2016).

At present, the systematic evaluation and analysis of *Equus* cryptosporidiosis are still absent. Therefore, a systematic review and meta-analysis were conducted to evaluate the prevalence of *Equus* cryptosporidiosis in the world. The collected information was used to discuss the factors affecting the infection of *Cryptosporidium* in *Equus* (Page et al., 2021).

Materials and methods

Search strategy

To evaluate the prevalence of *Cryptosporidium* infections in *Equus* around the world, we performed a comprehensive review of literatures both in Chinese and English published from the beginning of the creation to October 1, 2021. The articles were derived from five databases, including CNKI, VIP Chinese Journal Database, Wanfang Data, PubMed, and ScienceDirect. In the three Chinese databases, the advanced search was carried out using "*Equus* (in Chinese)" and "*Cryptosporidium* (in Chinese)" as keywords. In Science Direct, the keywords "*Cryptosporidium*" and "*Equus*" were used for a search. We used MeSH terms "*Cryptosporidium*" and "Equine" and their entry terms, such as "Horse", "Horse, Domestic", "Domestic Horse", "Domestic Horses", "Horses, Domestic", "*Equus*" "caballus", and "*Equus* przewalskii" in PubMed. We used boolean operators "AND" to connect MeSH terms and "OR" to connect the entry terms. Finally, the search formula was "((*Cryptosporidium*) OR *Cryptosporidiums*) AND (((((((Horse) OR Horse, Domestic) OR Domestic Horse) OR Horses, Domestic) OR *Equus* caballus) OR *Equus* przewalskii) OR Horse genus) ". Endnote (X9.2 version) was employed to organize the obtained article information. A protocol for the literature review was devised (Figure 1) in accordance with the PRISMA guidelines.

Inclusion and exclusion criteria

As part of the eligibility for inclusion, titles that suggested the topic *Cryptosporidium* in *Equus* were selected. The abstracts from the selected reference titles were reviewed by two independent reviewers to determine if the studies met the inclusion criteria and, if so, the entire articles were reviewed in full. The inclusion criteria for the systematic review and meta-analysis were as follows: (1) the object of research was *Equus*; (2) the diseased individuals were positive for *Cryptosporidium* in the research; (3) the research contained clear information, including the number of sick individuals and the population, the number of positive samples, the location of the test, and the location of sampling; (4) the article should contain a full text; (5) the research must be designed for a cross-sectional extension. Articles that do not meet these criteria were excluded. Unpublished reports, comments and copies were also excluded.

Data extraction

The extracted data included article title, first author, publication year, detection method, breeding environment, breeding method, genotypes, sampling year, article quality, detailed geographic and climatic factors, total number, number of positives, age and gender of the research object, geographic location (latitude and longitude), altitude, relative humidity, annual average temperature, annual precipitation, climate, and detection method type. The meteorological data of the years involved were from the China Meteorological Data Service Center (CMDC, http://data.cma.cn/) and national centers of

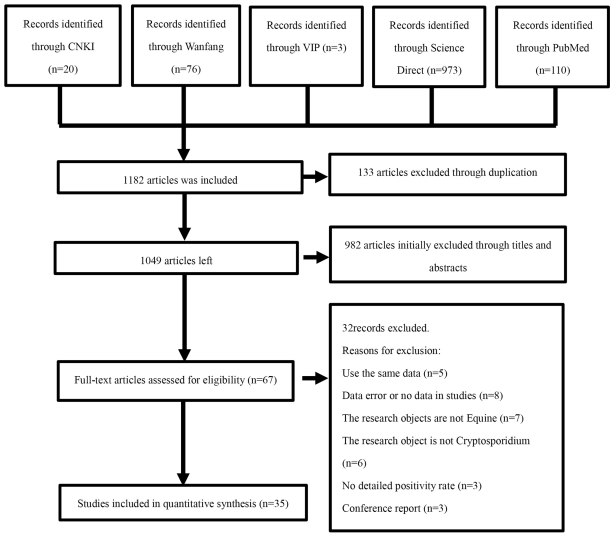

FIGURE 1
Flow diagram of literature search and selection.

environmental information (https://www.ncei.noaa.gov/maps/monthly/), such as temperature, rainfall, longitude, latitude, humidity and altitude. The database was established by using Microsoft Excel (version 16.32). Two authors independently extracted and recorded data from each selected study. The differences derived from reviewers or uncertainty about the qualifications of the research were further assessed by another author of this paper. The grouping method is based on previous studies (Wei et al., 2021a; Wei et al., 2021b).

Quality assessment

The quality of the included studies was evaluated according to the criteria based on the recommended grading evaluation, formulation, and the Grading of Recommendations Assessment, Development and Evaluation (GRADE) (Xie and Machado, 2021). The scoring criteria were as follows: (1) whether a clear detection method was employed; (2) whether the sampling animal was clear; (3) whether three or more influencing factors were included; (4) the sample size was greater than enough; and (5) whether the sampling year was clear. Therefore, the studies could be scored between 0 and 5 points.

Statistical analyses

The meta package in R software version 4.0.3 ("R core team, R: A language and environment for statistical computing" R core team 2018) was employed to analyze the data in this study (Zeng et al., 2020). Before performing the meta-analysis, we tested five transformation methods to bring the data closer to a Gaussian distribution, namely no transformation (PRAW), logarithmic transformation (PLN), logit transform (PLOGIT), arcsine transform (PAS), and double arcsine transform (PFT) (Table 1). The conversion rate was based on a Shapiro-Wilk normal test. The W-value close to 1 and the *P*-value greater than 0.05 was close to the Gaussian distribution criterion. The heterogeneity between studies was calculated by *Cochran*-Q, I^2 statistics, and χ^2 test, the *P*-value < 0.05 and I^2 = 50% was used to define the degree of heterogeneity with a statistical significance. According to the heterogeneity of the included articles, a random effect model was selected for analysis (Ni et al., 2020). The forest plots were used for a comprehensive analysis. The funnel plot and Egger's test were used to evaluate publication bias of studies. When there is publication bias in the included articles, the funnel plot is asymmetric, and the distribution is skewed (Egger et al., 1997). The Egger's test is expected to have a regression intercept of 0 in the absence of bias (Lin and Chu, 2018). The stability of a study was evaluated by the trim and fill analysis and sensitivity analysis (Wang et al., 2021).

To further study the potential sources of heterogeneity, the individual and multivariate model factors were analyzed to determine factors that affected heterogeneity. The factors included sampling surveys (before 2008 vs. others), diagnostic methods (molecular diagnostics vs. other methods), age ≤ 1year vs. age >1year, genotype (*C. parvum* vs. others), gender (female vs. male), feeding method (cage-free vs. scale breeding), host (horse vs. others), country (China vs. others), the quality level of publications (5 points vs. others), longitude (<50° vs. others), latitude (<30° vs. others), annual average rainfall (< 500 mm vs. ≥ 500 mm), annual average temperature (< 10°C vs. ≥ 10°C),

annual average humidity (40%-50% vs. others), altitude (<50 m vs. others), and climate (temperate climate vs. others)

Results

Search results

In this study, 1,182 related articles were identified after searching five databases, and 67 articles were selected after the initial screening and removal of duplicates. According to the selection criteria described in section, an additional 32 indeterminate articles were excluded after checking the full text. Finally, 35 articles were selected for the meta-analysis. (Figure 1; Table 2).

Qualification research and publication bias

The included articles involved 13 countries. In the 35 studies, the total number of samples was 9,817, and the number of positives was 816 (Table 3). According to our quality criteria, 11 articles were considered to be 5 points, 21 were of medium-quality (three or four points), and the remaining 3 articles were deemed to be of low-quality (zero to two points; Table 3).

In the included studies, the forest plot showed the degree of heterogeneity of all data (χ^2 = 0.0267, I^2 = 96.0%, P < 0.01) (Figure 2). According to the funnel chart, the distribution of points was observed to be incompletely symmetrical, which might be due to a publication bias (0.6344) or a small sample bias (Figure 3). Six supplementary studies were found in trim and fill analysis, which changed the aggregate estimate (Figure 4). The Egger's test was used to assess the potential publication bias in the analysis with a P-value (0.7398) greater than 0.05, thus indicating that no publication bias was present in the data (Figure 5). The sensitivity test showed that the reorganized data were not significantly affected after excluding any study, and the results were consistent (Figure 6), which verified the rationality and reliability of this analysis. Figure 7 is a map of *Cryptosporidium* prevalence in *Equus* worldwide. A chord diagram shows the relationship between the prevalence of *Cryptosporidium* in *Equus* species and epidemiological variables (stripe width indicates prevalence) (Figure 8). *C. parvum* genotype had a larger proportion in North America in the geographic area grouping. Genotype *C. hominis* accounted for a large proportion of donkey in the host group. Genotype *C. andersoni* accounted for more than 1- year-old in the age group.

Meta-analysis of *Equus Cryptosporidium* worldwide

According to the data obtained from the selected articles, the global combined prevalence of *Equus Cryptosporidium* infection was 7.59% (95% CI: 4.86-10.87) (Table 3). Before 2008, the prevalence of *Cryptosporidium* in *Equus* was 10.77% (95% CI: 3.92-20.32), which was significantly higher than that in other time periods (P < 0.01). The highest positive rate of *Equus Cryptosporidium* was 17.91% (95% CI: 9.73-27.92) in Oceania. Among the detection methods, microscopic examination had the highest rate of 10.52% (95% CI: 4.99-17.19). The prevalence of *Cryptosporidium* in *Equus* ≤ 1-year-old was 11.06% (95% CI: 6.13-17.22), which was significantly higher than in other age groups (P < 0.01). The highest prevalence of *Cryptosporidium* in female *Equus* was 2.60% (95% CI: 0.78-5.44). The highest prevalence of *Cryptosporidium* among the rearing method groups was 7.86% (95% CI: 4.39-12.22) for collectivized breeding. Among the host groups, mules had the highest rate of 20.00% (95% CI: 10.20-32.09). The highest prevalence of *Equus Cryptosporidium* was 19.58% (95% CI: 6.03–38.43) in Italy, which was significantly higher than that in other countries (Table 4). The highest genotype prevalence of *Cryptosporidium* in *Equus* was *C. muris* (53.55%; 95% CI: 11.65-92.51), followed by *C. hominis*, with a rate of 43.94% (95% CI: 23.11–65.95) (Table 5).

Among the analyzed geographical factors, the positive rate of *Cryptosporidium* in *Equus* at northern latitude < 30° was the highest (8.77%; 95% CI: 2.88-17.44). The positive rate of *Cryptosporidium* in *Equus* with longitude > 100° was the highest (9.03%, 95% CI: 3.15-17.53). The information for other geographical latitude subgroup analyses included precipitation range (≥ 500 mm; 15.63%; 95% CI: 8.60-24.28), temperature range (≥ 10°C; 8.04%, 95% CI: 3.30-14.60), humidity range

TABLE 1 Normal distribution tests for normal rates and different transitions.

Conversion form	W	P
PRAW	0.8277	7.482e-05
PLN	NaN	NA
PLOGIT	NaN	NA
PAS	0.94712	0.09241
PFT	0.94693	0.09118

"PRAW": raw exchange rate; PLN: log conversion. "PLOGIT": logit transformation; "PAS": arcsine transformation; "PFT": double arcsine transformation; "NaN": meaningless number; NA: data is missing.

(70%-80%; 22.69%; 95% CI: 13.76-33.10) and altitude range (< 50 m; 6.88%; 95% CI: 2.70-12.78). According to the analysis of climatic factors, we found that tropical climate had the highest positive rate of *Equus Cryptosporidium* (16.46%; 95% CI: 0.48-48.11; Table 6).

Discussion

Cryptosporidium is a waterborne pathogen that infects livestock, poultry, and companion animals, thus posing a great threat to public health (Gao et al., 2021). Many large *Cryptosporidium* outbreaks were caused by contamination of water sources with animal feces (Rodríguez et al., 2012). Cryptosporidiosis can cause slow growth of sick animals, extreme weight loss, decreased resistance, and huge losses to the animal husbandry (Han et al., 2020). In this study, a publication bias was observed according to the Egger's test. Pass I^2 statistics results, the prevalence of *Cryptosporidium* in *Equus* species in the world was highly heterogeneous in the eligible studies, which may be caused by differences in detection methods, age, gender, geographic factors, and countries.

The prevalence of *Cryptosporidium* in female *Equus* was identified to be higher than that in male *Equus*. This is

TABLE 2 Studies in the analysis.

Study ID	Sampling time	Country	Test method	Event	Positive rate
Xiao L et al. (1994)	1992.3-1992.10	America	Direct immunofluorescence staining method	16/222	0.072
Johnson et al. (1997)	1994.8-1994.10	America	Direct fluorescent antibody	0/91	0.000
Olson et al. (1997)	1996.7	Canada	Microscopic examination	6/35	0.171
Majewska et al. (1999)	NA	Poland	Enzyme immunoassay	10/106	0.094
Majewska et al. (2004)	NA	Poland	Microscopic examination	11/318	0.035
Grinberg et al. (2009)	2005-2007	New Zealand	Microscopic examination	12/67	0.179
De Souza et al. (2009)	NA	Brazil	Microscopic examination	3/396	0.008
Veronesi et al. (2010)	2007.2-4	Italy	DFA	12/150	0.080
Burton et al. (2010)	2009.2-5	America	DFA	16/349	0.046
Perrucci et al. (2011)	2006-2008	NA	ELISA	2/74	0.027
Jian (2012)	2008.7-2013.9	China	Microscopic examination	222/1302	0.171
Inácio et al. (2012)	2010.11-2011.3	NA	Microscopic examination	39/196	0.199
Caffara et al. (2013)	NA	Italy	PCR	14/37	0.378
Laatamna et al. (2013)	2010-2011	Algeria	PCR	4/138	0.029
Guo P et al. (2014)	2001.9-2003.10	China	PCR	161/436	0.369
Qi et al. (2015)	2013.8-9	China	PCR	7/262	0.027
Liu A et al. (2015)	NA	China	PCR	3/29	0.103
Laatamna et al. (2015)	2011.11-2013.5	Algeria	PCR	7/343	0.020
Kostopoulou et al. (2015)	NA	Belgium et al.	PCR	8/398	0.020
Zhou H. (2015)	2013.3-2014.5	China	Microscopic examination	30/508	0.059
Galuppi et al. (2015)	2011.12-2012.12	Italy	PCR	14/73	0.192
Wagnerová et al. (2015)	2011-2012	NA	PCR	12/352	0.034
Wagnerová et al. (2016)	NA	America	PCR	28/84	0.333
Hijjawi et al. (2016)	2014.10-2015.5	NA	PCR	6/74	0.081
Song Y et al. (2017)	NA	China	PCR	1/10	0.100
Deng L et al. (2017)	2015.8-2016.4	NA	PCR	6/333	0.018
Inácio et al. (2017)	2010.11-2011.3	Brazil	PCR	20/92	0.217
Raue et al. (2017)	2004-2012	Germany	Microscopic examination	4/21	0.190
Deng (2018)	2015.7-2017.5	China	PCR	6/441	0.014
Zhang Q et al. (2019)	2018.5-7	China	PCR	0/32	0.000
Li F et al. (2019)	2015-2019	China	PCR	90/878	0.103
Wei Z. (2020)	2016.2018.6	China	PCR	11/621	0.018
Couso-Pérez et al. (2020)	NA	Portugal,Spain	IFAT	10/79	0.127
Wang (2020)	2016.2-2018.12	China	Microscopic examination	16/680	0.024
Zhang (2021)	2018-2020	China	PCR	9/590	0.015

NA, data is missing; PCR, Polymerase Chain Reaction; IFAT, International Federationt for Alternative Trade; DFA, Direct Immunofluorescence Assay; ELISA, Enzyme-linked Immunosorbent Assay.

TABLE 3 Summary of global equine *Cryptosporidium* infection rates.

Variable	Category	No. studies	No. examined	No. positive	% (95% CI*)	Heterogeneity			Univariate meta-regression	
						χ^2	*P*-value	I^2 (%)	*P*-value*	Coefficient (95% CI)
Detection methods	Molecular diagnostics	21	5982	430	7.49% (3.77-12.35)	603.44	< 0.01	96.7	0.3555	-0.0679(-0.2121 to 0.0762)
	Microscopic examination	8	2843	327	10.52% (4.99-17.79)	200.33	< 0.01	96.5		
	Immunological detection	7	1071	59	4.37% (1.83-7.95)	27.32	< 0.01	78.0		
Gender	Female	12	1564	52	2.60% (0.78-5.44)	61.96	< 0.01	82.2	0.8605	-0.0124 (-0.1506 to 0.1258)
	Male	6	452	12	2.36% (0.04-8.07)	21.05	< 0.01	76.2		
Year	≤1year	19	3257	394	11.06% (6.13-17.22)	346.09	< 0.01	94.8	0.0014	-0.1792(-0.2889 to -0.0695)
	> 1year	16	3602	131	2.52% (0.97-4.77)	156.63	< 0.01	90.4		
Geographic area	Asia	14	5088	366	5.44% (2.24-9.94)	465.79	< 0.01	97.2	0.1730	0.2025(-0.0888 to 0.4938)
	Oceania	1	67	12	17.91% (9.73-27.92)	0.00	NA	NA		
	Europe	9	1534	95	10.15% (4.77-17.24)	74.19	< 0.01	89.2		
	Africa	2	481	11	2.27% (1.13-3.79)	0.30	0.58	0.00		
	North America	4	746	60	7.37% (0.08-24.78)	69.68	< 0.01	95.7		
	South America	4	719	68	12.45% (2.84 -27.51)	101.94	< 0.01	97.1		
Sampling year	Before 2008	9	1361	241	10.77% (3.99-20.32)	214.05	< 0.01	96.3	0.0125	-0.1615 (-0.2883 to -0.0348
	2009-2012	10	2580	306	10.73% (5.79-16.95)	200.18	< 0.01	95.5		
	After or 2013	10	4419	181	3.04% (1.52-5.06)	114.57	< 0.01	92.1		
Feeding method	Cage-free	3	555	48	5.09% (0.00–20.00)	64.51	< 0.01	96.9	0.5752	-0.0584(-0.2628 to 0.1459)
	Scale breeding	18	4995	546	7.86% (4.39-12.22)	500.57	< 0.01	96.6		
Host	Zebra	1	10	1	10.00% (0.01-34.87)	0.00	NA	NA	0.6247	0.1419(-0.4267 to 0.7105)
	Horse	32	6851	480	7.32% (4.49-10.78)	684.18	< 0.01	95.5		
	Mule	1	50	10	20.00% (10.20-32.09)	0.00	NA	NA		
	Donkey	5	2906	333	7.52% (2.25-15.54)	196.58	< 0.01	98.0		
Fraction	middle	21	3138	193	7.44% (4.05-11.74)	224.33	< 0.01	91.1	0.0939	0.1839 (-0.0313 to 0.3990)
	high	11	6410	575	5.93% (2.17-11.37)	606.89	< 0.01	98.4		
	low	3	269	48	17.36% (5.92-33.15)	18.76	< 0.01	89.3		
Total		35	9817	816	7.59% (4.86-10.87)					

CI*: confidence interval; NA*: not applicable; P value *: P < 0.05 was statistically significant.
Quality *: High: 5 points; Medium: 3 or 4; Low: 2.

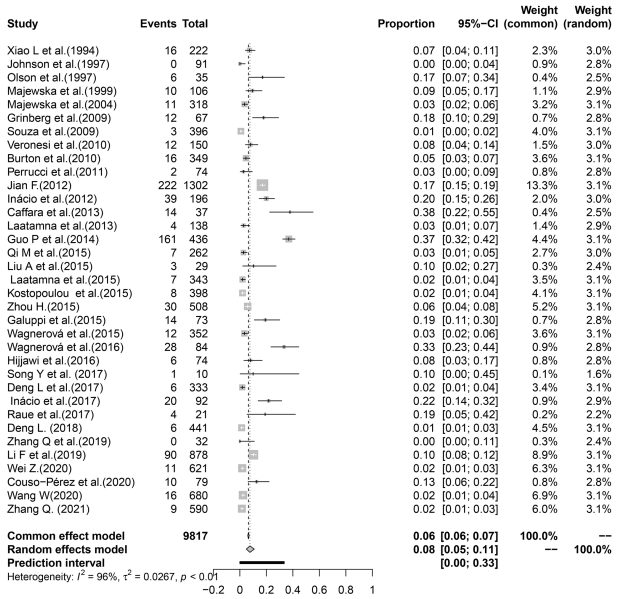

FIGURE 2
Forest map of global cryptosporidiosis in *Equus* epidemic.

probably due to a weaker body resistance of female *Equus* than males, especially after giving birth, and more susceptible to *Cryptosporidium* infection (Chen et al., 2013). The mare is considered to be a carrier of *Cryptosporidium*, and the young animals could be infected with *Cryptosporidium* by sharing a pasture or barn with the foals (Qi and Zhang, 2018). The eggs of *Cryptosporidium* in infected female *Equus* have no obvious shedding phenomenon, but the amount of shedding during the perinatal period increases (Skerrett and Holland, 2001).

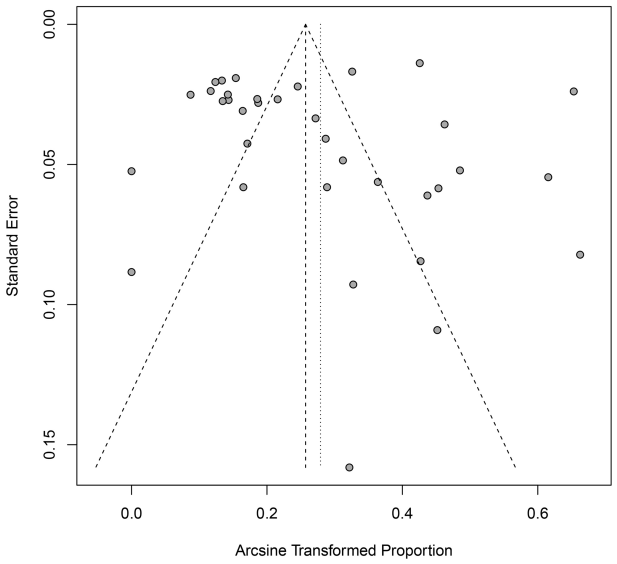

FIGURE 3
Funnel plot with pseudo 95% confidence interval for publication bias test.

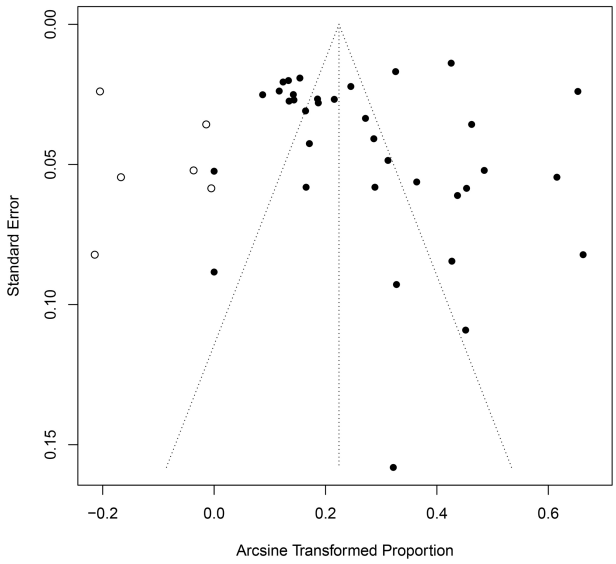

FIGURE 4
Shear complement graph and pseudo 95% confidence interval publication bias test.

This significantly increases the probability of young animals being infected with *Cryptosporidium*.

In this study, the prevalence of *Cryptosporidium* in *Equus* of ≤ 1 year was higher than that of *Equus* > 1 year, which is basically in line with the previous reports (Langkjaer et al., 2007; Wang, 2020). The maternal antibodies in the young animals will lose protective effects in 2-6 months, resulting in a decreased resistance of the young animals (Lu et al., 2008). In addition, the weaning stress response in young animals will lead to changes at hormone levels and immune function, thus causing immune system suppression, and thereby increasing the possibility of being infected with *Cryptosporidium* (Ren et al., 2018). Therefore, the breeding of dams and cubs needs to be strengthened to improve the resistance of animals, and the dams can be isolated during the breeding period.

Poor sanitary conditions increase the infection risk of *Cryptosporidium* in animals and expand the spread of

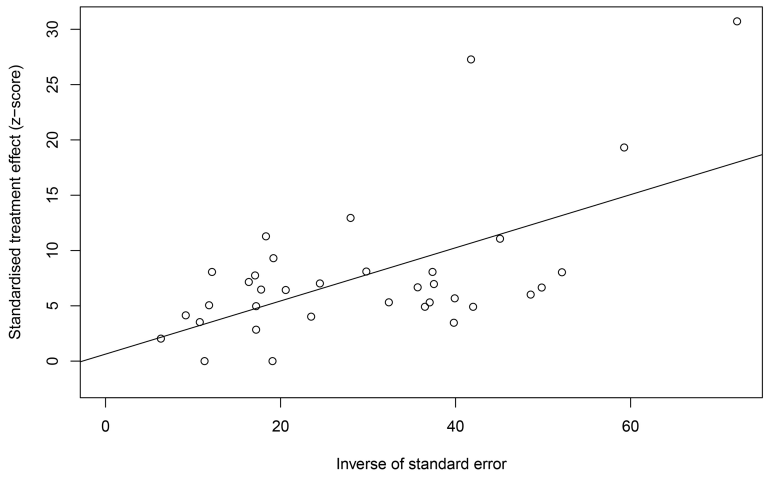

FIGURE 5
Egger's test for publication bias.

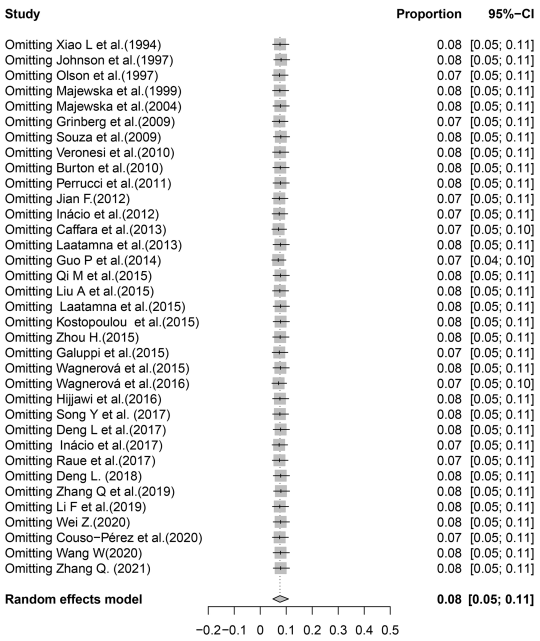

FIGURE 6
Sensitivity analysis.

Cryptosporidium species (Gao et al., 2021). Our study of the rearing group showed that mules and donkeys had higher rates of *Cryptosporidium* infection than horses. The living environment of mules and donkeys is relatively complicated, and they usually suffer from poor harness, lack of veterinary care, improper nutrition, and low status and value, in spite of their usefulness (Davis, 2019). Meanwhile, the feces cannot be cleaned in time, which is more likely to cause the transmission and infection of *Cryptosporidium* in animals (Jian, 2012). An analysis of the breeding environment also showed that the

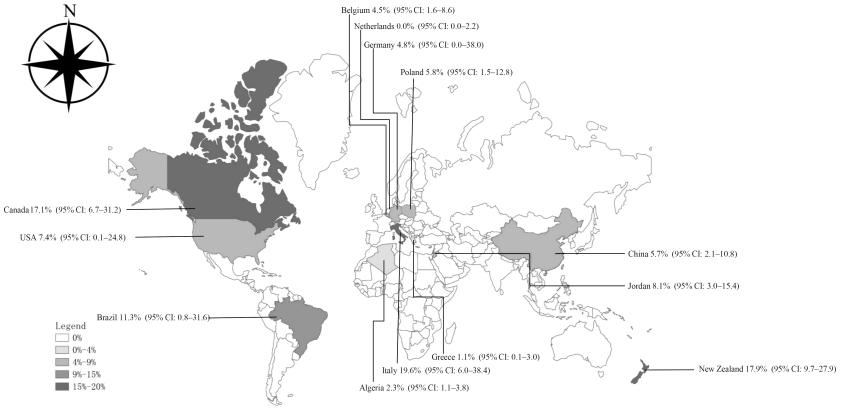

FIGURE 7
Map of *Cryptosporidium* prevalence in *Equus* worldwide.

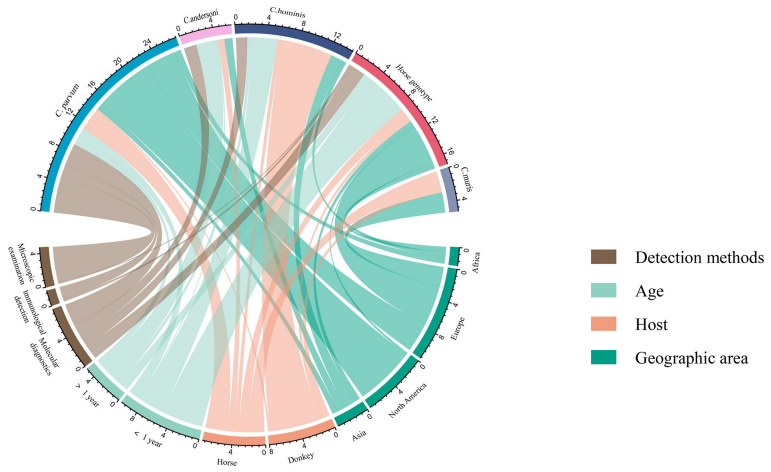

FIGURE 8
Distribution of *Cryptosporidium* species/genotypes.

prevalence of *Cryptosporidium* was higher in *Equus* than that farmed on scale breeding. The high stocking densities of large-scale farming might result in high rates of *Cryptosporidium* infection in high-density captive equines. This may be due to the facts that more oocysts are scattered in high-density pens and the transmission speed is fast (Wang et al., 2008). Therefore, we recommend reducing stocking density and enhancing the animal welfare of donkeys and mules.

TABLE 4 Concentrated prevalence of equine *Cryptosporidium* in different countries.

Variable	Category	No. studies	No. examined	No. positive	% (95% CI*)
Country	Algeria	2	481	11	2.27% (1.13–3.79)
	America	4	746	60	7.37% (0.08–24.78)
	Belgium	1	134	6	4.48% (1.64–8.61)
	Brazil	3	684	62	11.28% (0.76–31.64)
	Canada	1	35	6	17.14% (6.67–31.19)
	China	13	6122	562	5.65% (2.08–10.83)
	Germany	2	51	4	4.84% (0.00–38.02)
	Greece	1	190	2	1.05% (0.10–2.99)
	Italy	3	260	40	19.58% (6.03–38.43)
	Netherlands	1	44	0	0.00% (0.00–2.17)
	New Zealand	1	67	12	17.91% (9.73–27.92)
	Poland	2	424	21	5.81% (1.47–12.76)
	Jordan	1	74	6	8.11% (3.03–15.36)

TABLE 5 The prevalence of *Cryptosporidium* in different genotypes.

Variable	Category	No. studies	No. examined	No. positive	% (95% CI*)
Genotype	*C. parvum*	17	348	80	31.95% (15.53–51.11)
	C. andersoni	5	34	12	38.83% (12.50–69.36)
	C. hominis	8	165	103	43.94% (23.11–65.95)
	C. muris	2	19	11	53.55% (11.65–92.51)
	Horse genotype	10	245	41	29.24% (9.47–54.44)

The investigation of sampling year in the selected articles showed that the prevalence of *Cryptosporidium* in *Equus* animals before 2012 was higher. In 2008, a worldwide economic crisis occurred and started to recover until 2010 (Zhang, 2018). The sluggish world economy may make people slack in *Equus* breeding, which may be one of the reasons for the high prevalence of *Cryptosporidium*. After 2013, the world economy gradually recovered, and many countries began to pay more attention to the animal husbandry. The gradually increased animal welfare may contributed to the lower prevalence of *Cryptosporidium* in *Equus*.

In the continent and country groups, the highest positive rate of *Cryptosporidium* was found in Oceania and the lowest was in Africa. Among them, New Zealand in Oceania had the highest positive rate, and Algeria in Africa had the lowest positive rate. New Zealand has a temperate maritime climate, with a warm and humid climate throughout the year, and its long coastline and abundant water resources make it more suitable for *Cryptosporidium* to survive. The frequent rainfall may lead to the transmission of *Cryptosporidium* in animal feces from fields to surface waters, thus resulting in a higher

TABLE 6 A subgroup analysis of the prevalence of *Cryptosporidium* in equine genus by geographical location, climate and other variables.

Variable	Category	No. studies	No. examined	No. positive	% (95% CI*)	Heterogeneity			Univariate meta-regression	
						χ^2	*P*-value	I^2 (%)	*P*-value*	Coefficient (95% CI)
Latitude	< 30°	7	794	45	8.77% (2.88-17.44)	70.94	<0.01	91.5	0.1377	-0.1346(-0.3122 to 0.0431)
	30°-35°	3	809	56	3.67% (0.02-13.11)	60.19	<0.01	96.7		
	35°-40°	7	2357	213	2.70% (0.10-8.61)	281.98	<0.01	97.9		
	40°-45°	7	1283	52	5.17% (0.74-13.23)	70.21	<0.01	91.5		
	> 45°	8	1597	121	7.45% (3.77-12.26)	79.96	<0.01	91.2		
Longitude	< 50°	7	1383	66	5.62% (1.27-12.79)	76.48	<0.01	92.2	0.2230	-0.1085 (-0.2830 to 0.0660)
	50°-100°	6	2108	39	1.75% (0.7-3.26)	17.72	<0.01	71.8		
	> 100°	9	3282	370	9.03% (3.15-17.53)	305.79	<0.01	97.4		
Altitude(m)	< 50	15	3717	372	6.88% (2.70-12.78)	365.84	<0.01	96.2	0.2367	-0.1096(-0.2913 to 0.0720)
	50-100	6	858	21	2.41% (0.07-7.87)	31.02	<0.01	83.9		
	100-150	8	1722	73	4.23% (1.08-9.32)	72.01	<0.01	90.3		
	> 150	6	543	21	4.94% (0.06-16.98)	63.07	<0.01	92.1		
Rainfall (mm)	< 500	3	620	20	1.71% (0.06-5.54)	56.80	<0.01	84.2	0.0004	-0.2751 (-0.4277 to 0.1225)
	≥ 500	2	1436	220	15.63% (8.60-24.28)	117.90	<0.01	93.2		
Temperature (°C)	< 10	14	744	32	3.95% (0.34-11.25)	97.30	<0.01	86.6	0.3395	0.0872 (-0.0918 to 0.2662)
	≥ 10	11	1599	217	8.04% (3.30-14.60)	173.21	<0.01	94.2		
Humidity (%)	40-50	3	183	8	1.26% (0.00-8.59)	6.95	0.03	71.2	0.0367	0.3927 (0.0243 to 0.7610)
	50-60	10	581	33	4.41% (0.07-14.98)	93.76	<0.01	90.4		
	60-70	8	661	50	5.02% (0.94-12.07)	69.96	<0.01	90.0		
	70-80	3	569	142	22.69% (13.76-33.10)	10.57	<0.01	81.1		
Climate	Plateau alpine climate	2	52	9	12.71% (0.00-78.20)	26.62	<0.01	96.2	0.5059	-0.0998 (-0.3937 to 0.1942)
	Subtropical climate	15	2701	255	7.82% (3.27-14.10)	413.23	<0.01	96.6		
	Temperate climate	16	6251	455	5.81% (3.61-8.49)	359.24	<0.01	94.7		
	Tropical climate	3	567	55	16.46% (0.48-48.11)	123.02	<0.01	98.4		

CI*, Confidence interval; NA*, not applicable; P-value*: P < 0.05 is statistically significant.

prevalence of *Cryptosporidium* in this genus of horses (Sterk et al., 2016). In contrast, the Algerian coast has a Mediterranean climate, with high temperature and rainy winter, while the central and southern parts have a savanna and tropical desert climate, which is dry and rainy, with cold winter and hot summer. The increase of temperature will reduce the life activity of the worms on the land surface (Moriarty et al., 2012). Therefore, the prevalence of *Cryptosporidium* in *Equus* in Africa is low.

In the geographical groups, the positive rate of *Cryptosporidium* was the highest in regions with longitude > 100° and latitude < 30°. These two factors are mainly concentrated in the central and southern parts of China. The central and southern parts of China belong to the temperate monsoon climate and the subtropical monsoon climate. The rainfall types of these two climates are high temperature and rainy in summer, low temperature and less rain in winter (Wang, 2009). Meanwhile, the positive rate of *Cryptosporidium* in *Equus* that live in areas with humidity 70%-80%, rainfall > 500 mm, temperature ≥ 10°C, and altitude < 50 m was higher than that in other regions. High rainfall will increase the pollution of water sources, and *Cryptosporidium* is mainly transmitted through water sources, thereby increasing the prevalence of *Cryptosporidium* (Young et al., 2015). As altitude decreases, the temperature gradually increases (Zhu et al., 2013). Suitable temperature and hot and humid weather are the reasons for an increase in the prevalence of *Cryptosporidium*. This is in line with previous reports (Burton et al., 2010; Lv et al., 2021).

The genotypes of *Cryptosporidium* in infected *Equus* were analyzed. The main genotypes of *Equus Cryptosporidium* were *C. parvum*, *horse genotype*, *C. andersoni, C. muris, C. hominis*, and *C. cuniculus* (Wang, 2015; Wagnerová et al., 2016; Deng, 2018; Zhang, 2021). Among them, *C. parvum, C. andersoni, and C. hominis* are the genotypes that infect humans. In this study, the positive rates of *C. muris* and *C. hominis* genotypes were higher. Therefore, strengthening the feeding, management, and control of *Equus Cryptosporidium* are of great importance to the public safety of humans and animals.

The included articles mainly employed three types of detection methods, including molecular detection, immunological detection, and microscopic detection. Molecular examination is mainly based on PCR. Immunological tests include IFAT, DAF, and ELISA. Among them, the positive rate detected by IFAT technology is the highest, followed by microscopy and PCR. The microscopic detection of *Cryptosporidium* is easily operated and has a low cost but may lead to misdiagnosis and increase the probability of false positives (Robinson and Chalmers, 2020a). For immunological detection, although ELISA has the advantages of high sensitivity and specificity, it cannot perform species identification (Mittal et al., 2014). IFAT is prone to false positive, thus resulting in a high positive rate (Robinson et al., 2020b). The PCR detection method have high sensitivity and specificity than that of microscopy, has become the optimal method for *Cryptosporidium* detection (Zhang et al., 2017). It is recommended to use PCR method to detect *Cryptosporidium* in epidemiological investigations.

These results reflect the prevalence of *Cryptosporidium* in *Equus* to a certain extent around the world. In this meta-analysis, the reasons for losing points in some studies are: (1) less than 3 risk factors; (2) limited samples; (3) unclear sampling year; and (4) absence of specific sampling location. It is recommended that researchers should take more samples and explore more influencing factors to provide more data that support for the prevention and treatment of *Cryptosporidium* infection in *Equus*.

The advantages of this study are rigorous method and lots of risk factors. The publication bias was tested by using funnel chart and more accurate Egger's test. The subgroup analysis and regression analysis correctly identified the influence of heterogeneity on the results. The combination of multiple data analysis methods made our findings reasonable. A comprehensive analysis of subgroups can replenish the previous articles and provide more complete data for follow-up research. However, this study also has some limitations. First, we searched in five databases, and the search strategy might have caused the omission of some researches. Second, the data in some subgroups, such as Italy in the city subgroup, are covered only by one article, which can lead to unstable outcomes.

Concluding remarks

A systematic review and meta-analysis of 35 articles provided a comprehensive overview of the global epidemiology of *Equus Cryptosporidium*. The results showed that cryptosporidiosis was widespread in *Equus*, and cryptosporidiosis was prone to occur in the areas with warm climate. *Equus* under 1 year were more susceptible to *Cryptosporidium* infection. In view of the high incidence of cryptosporidiosis, correct prevention and control measures should be taken in time for specific age groups and regions. During the breeding process, good hygiene habits should be developed, regional prevention and control should be strengthened, and water pollution should be minimized.

Data availability statement

The original contributions presented in the study are included in the article/Supplementary Material. Further inquiries can be directed to the corresponding authors.

Ethics statement

Ethical review and approval was not required for the animal study.

Author contributions

X-ML and H-LG: Data curation, Methodology, Supervision, Writing-review and editing. W-LY and X-XZ: Writing-review and editing. Y-JW, Xin-YW: Data curation, Resources, Software. MZ and Xia-YW: Data curation, Methodology, Visualization. JL and GL: Conceptualization, Supervision, Funding acquisition. All authors contributed to the article and approved the submitted version.

Funding

This work was supported by the Research Foundation for Distinguished Scholars of Qingdao Agricultural University (grant no. 665-1120044 and 665-1122009).

Conflict of interest

The authors declare that the research was conducted in the absence of any commercial or financial relationships that could be construed as a potential conflict of interest.

Publisher's note

All claims expressed in this article are solely those of the authors and do not necessarily represent those of their affiliated organizations, or those of the publisher, the editors and the reviewers. Any product that may be evaluated in this article, or claim that may be made by its manufacturer, is not guaranteed or endorsed by the publisher.

References

Alvarado-Esquivel, C., Alvarado-Esquivel, D., and Dubey, J. P. (2015). Prevalence of toxoplasma gondii antibodies in domestic donkeys (*Equus asinus*) in durango, mexico slaughtered for human consumption. *BMC Vet. Res.* 11, 6. doi: 10.1186/s12917-015-0325-9

Bouzid, M., Hunter, P. R., Chalmers, R. M., and Tyler, K. M. (2013). *Cryptosporidium* pathogenicity and virulence. *Clin. Microbiol. Rev.* 26 (1), 115–134. doi: 10.1128/CMR.00076-12

Burton, A. J., Nydam, D. V., Dearen, T. K., Mitchell, K., Bowman, D. D., and Xiao, L. (2010). The prevalence of *Cryptosporidium*, and identification of the *Cryptosporidium* horse genotype in foals in new York state. *Vet. Parasitol.* 174 (1-2), 139–144. doi: 10.1016/j.vetpar.2010.08.019

Caffara, M., Piva, S., Pallaver, F., Iacono, E., and Galuppi, R. (2013). Molecular characterization of *Cryptosporidium* spp. from foals in Italy. *Vet. J.* 198 (2), 531–533. doi: 10.1016/j.tvjl.2013.09.004

Chalmers, R. M., Davies, A. P., and Tyler, K. (2019). Cryptosporidium. *Microbiol. (Reading)* 165 (5), 500–502. doi: 10.1099/mic.0.000764

Chen, J., Shen, K. F., and Ren, H. X. (2013). Investigation of goats *Cryptosporidium* infection in some breeding farms of chongqing. *Chin. J. Vet. Med.* 48 (12), 15–17.

Couso-Pérez, S., de Limia, F. B., Ares-Mazás, E., and Gómez-Couso, H. (2020). First report of zoonotic *Cryptosporidium parvum* GP60 subtypes IIaA15G2R1 and IIaA16G3R1 in wild ponies from the northern Iberian Peninsula. *Parasitol. Res.* 119 (1), 249–254. doi: 10.1007/s00436-019-06529-x

Current, W. L., Reese, N. C., Ernst, J. V., Bailey, W. S., Heyman, M. B., and Weinstein, W. M. (1983). Human cryptosporidiosis in immunocompetent and immunodeficient persons. studies of an outbreak and experimental transmission. *N Engl. J. Med.* 308 (21), 1252–1257. doi: 10.1056/NEJM198305263082102

Davis, E. (2019). Donkey and mule welfare. *Vet. Clin. North Am. Equine Pract.* 35 (3), 481–491. doi: 10.1016/j.cveq.2019.08.005

De Souza, P. N., Bomfim, T. C., Huber, F., Abboud, L. C., and Gomes, ,. R. S. (2009). Natural infection by *Cryptosporidium* sp., *Giardia* sp. and *Eimeria leuckarti* in three groups of equines with different handlings in Rio de Janeiro, Brazil. *Vet. Parasitol.* 160 (3-4), 327–333. doi: 10.1016/j.vetpar.2008.10.103

Deng, L. (2018). Phylogenetic and multilocus genotypes of *Cryptosporidium* and *Enterocytozoon bieneusi* in horses. *Sichuan Agric. Univ* 2, 1–63.

Deng, L., Li, W., Zhong, Z., Gong, C., Cao, X., Song, Y., et al. (2017). Occurrence and Genetic Characteristics of *Cryptosporidium hominis* and *Cryptosporidium andersoni* in Horses from Southwestern China. *J. Eukaryot Microbiol.* 64 (5), 716–720. doi: 10.1111/jeu.12399

Egger, M., Davey, S. G., Schneider, M., and Minder, C. (1997). Bias in meta-analysis detected by a simple, graphical test. *BMJ.* 315 (7109), 629–634. doi: 10.1136/bmj.315.7109.629

Galuppi, R., Piva, S., Castagnetti, C., Iacono, E., Tanel, S., Pallaver, F., et al. (2015). Epidemiological survey on *Cryptosporidium* in an Equine Perinatology Unit. *Vet. Parasitol.* 210 (1-2), 10–18. doi: 10.1016/j.vetpar.2015.03.021

Gao, H. H., Wang, J. D., Kang, X. D., Wang, P. Z., Wu, X. Q., and Li, Y. K. (2021). Prevalence and risk factors of *Cryptosporidium* in sheep and goat of China. *Chin. J. Vet. Sci.* 41 (2), 401–406.

Grinberg, A., Pomroy, W. E., Carslake, H. B., Shi, Y., Gibson, I. R., and Drayton, ,. B. M. (2009). A study of neonatal cryptosporidiosis of foals in New Zealand. *N Z Vet. J.* 57 (5), 284–289. doi: 10.1080/00480169.2009.58622

Guo, P. F., Chen, T. T., Tsaihong, J. C., Ho, G. D., Cheng, P. C., Tseng, Y. C., et al. (2014). Prevalence and species identification of *Cryptosporidium* from fecal samples of horses in Taiwan. *Southeast Asian J. Trop. Med. Public Health* 45 (1), 6–12.

Han, M. N., Ma, L., Zhou, L. L., Ren, M., Wang, D., and Lin, Q. (2020). Cryptosporidiosis and its prevalence in yak. *Prog. Vet. Med.* 41 (1), 10812.

Hijjawi, N., Mukbel, R., Yang, R., and Ryan, U. (2016). Genetic characterization of *Cryptosporidium* in animal and human isolates from Jordan. *Vet. Parasitol.* 228, 116–120. doi: 10.1016/j.vetpar.2016.08.015

Inácio, S. V., de Brito, R. L., Zucatto, A. S., Coelho, W. M., de Aquino, M. C., Aguirre, ,. A., et al. (2012). *Cryptosporidium* spp. infection in mares and foals of the northwest region of São Paulo State, Brazil. *Rev. Bras. Parasitol. Vet.* 21 (4), 355–358. doi: 10.1590/s1984-29612012005000003

Inácio, S. V., Widmer, G., de Brito, R. L., Zucatto, A. S., de Aquino, M. C., Oliveira, B. C., et al. (2017). First description of *Cryptosporidium hominis* GP60 genotype IkA20G1 and *Cryptosporidium parvum* GP60 genotypes IIaA18G3R1 and IIaA15G2R1 in foals in Brazil. *Vet. Parasitol.* 233, 48–51. doi: 10.1016/j.vetpar.2016.11.021

Jian, F. (2012). Molecular epidemiology of *Cryptosporidium* and *Giardia* of equine in some regions of China. *Henan Agric. Univ* 7, 1–9.

Jian, F., Liu, A., Wang, R., Zhang, S., Qi, M., Zhao, W., et al. (2016). Common occurrence of *Cryptosporidium hominis* in horses and donkeys. *Infect. Genet. Evol.* 43, 261–266. doi: 10.1016/j.meegid.2016.06.004

Johnson, E., Atwill, E. R., Filkins, M. E., and Kalush, J. (1997). The prevalence of shedding of *Cryptosporidium* and *Giardia* spp. based on a single fecal sample collection from each of 91 horses used for backcountry recreation. *J. Vet. Diagn. Invest.* 9 (1), 56–60. doi: 10.1177/104063879700900110

Kostopoulou, D., Casaert, S., Tzanidakis, N., van Doorn, D., Demeler, J., von Samson-Himmelstjerna, G., et al. (2015). The occurrence and genetic characterization of *Cryptosporidium* and *Giardia* species in foals in Belgium, The Netherlands, Germany and Greece. *Vet. Parasitol.* 211 (3-4), 170–174. doi: 10.1016/j.vetpar.2015.04.018

Laatamna, A. E., Wagnerová, P., Sak, B., Květoňová, D., Aissi, M., Rost, M., et al. (2013). Equine cryptosporidial infection associated with *Cryptosporidium* hedgehog genotype in Algeria. *Vet. Parasitol.* 197 (1-2), 350–353. doi: 10.1016/j.vetpar.2013.04.041

Laatamna, A. E., Wagnerová, P., Sak, B., Květoňová, D., Xiao, L., Rost, M., et al. (2015). Microsporidia and *Cryptosporidium* in horses and donkeys in Algeria: detection of a novel *Cryptosporidium hominis* subtype family (Ik) in a horse. *Vet. Parasitol.* 208 (3-4), 135–142. doi: 10.1016/j.vetpar.2015.01.007

Langkjaer, R. B., Vigre, H., Enemark, H. L., and Maddox-Hyttel, C. (2007). Molecular and phylogenetic characterization of *Cryptosporidium* and *Giardia* from pigs and cattle in Denmark. *Parasitology*. 134 (3), 339. doi: 10.1017/S0031182006001533

Li, F., Su, J., Chahan, B., Guo, Q., Wang, T., Yu, Z., et al. (2019). Different distribution of *Cryptosporidium* species between horses and donkeys. *Infect. Genet. Evol.* 75, 103954. doi: 10.1016/j.meegid.2019.103954

Lin, L., and Chu, H. (2018). Quantifying publication bias in meta-analysis. *Biometrics.* 74 (3), 785–794. doi: 10.1111/biom

Liu, A., Zhang, J., Zhao, J., Zhao, W., Wang, R., and Zhang, L. (2015). The first report of *Cryptosporidium andersoni* in horses with diarrhea and multilocus subtype analysis. *Parasit Vectors.* 8, 483. doi: 10.1186/s13071-015-1102-0

Lu, Q. B., Qiu., S. X., and Ru, B. R. (2008). Epidemiological investigation of cryptosporidiosis in dairy calves in some prefectures of henan province. *Vet. Sci. China* 2008 (3), 261–267.

Lv, X. Q., Qin, S. Y., Lyu, C., Leng, X., Zhang, J. F., and Gong, Q. L. (2021). A systematic review and meta-analysis of *Cryptosporidium* prevalence in deer worldwide. *Microb. Pathog.* 157, 105009. doi: 10.1016/j.micpath.2021.105009

Majewska, A. C., Solarczyk, P., Tamang, L., and Graczyk, ,. T. K. (2004). Equine Cryptosporidium parvum infections in western Poland. *Parasitol. Res.* 93 (4), 274–278. doi: 10.1007/s00436-004-1111-y

Majewska, A. C., Werner, A., Sulima, P., and Luty, T. (1999). Survey on equine cryptosporidiosis in Poland and the possibility of zoonotic transmission. *Ann. Agric. Environ. Med.* 6 (2), 161–165.

Mittal, S., Sharma, M., Chaudhary, U., and Yadav, A. (2014). Comparison of ELISA and microscopy for detection of *Cryptosporidium* in stool. *J. Clin. Diagn. Res.* 8 (11), DC07–DC08. doi: 10.7860/JCDR/2014/9713.5088

Moriarty, E. M., Weaver, L., Sinton, L. W., and Gilpin, B. (2012). Survival of *Escherichia coli*, *Enterococci* and *Campylobacter* jejuni in Canada goose faeces on pasture. *Zoonoses Public Health* 59 (7), 490–497. doi: 10.1111/zph.12014

Ni, H. B., Gong, Q. L., Zhao, Q., Li, X. Y., and Zhang, X. X. (2020). Prevalence of *Haemophilus parasuis* "*Glaesserella parasuis*" in pigs in China: A systematic review and meta-analysis. *Prev. Vet. Med.* 182, 105083. doi: 10.1016/j.prevetmed.2020.105083

Olson, M. E., Thorlakson, C. L., Deselliers, L., Morck, D. W., and McAllister, ,. T. A. (1997). *Giardia* and *Cryptosporidium* in Canadian farm animals. *Vet. Parasitol.* 68 (4), 375–381. doi: 10.1016/s0304-4017(96)01072-2

Page, M. J., McKenzie, J. E., Bossuyt, P. M., Boutron, I., Hoffmann, T. C., Mulrow, C. D., et al. (2021). The PRISMA 2020 statement: an updated guideline for reporting systematic reviews. *BMJ* 74 (9), 790–799. doi: 10.1136/bmj.n71

Perrucci, S., Buggiani, C., Sgorbini, M., Cerchiai, I., Otranto, D., and Traversa, D. (2011). *Cryptosporidium parvum* infection in a mare and her foal with foal heat diarrhoea. *Vet. Parasitol.* 182 (2-4), 333–336. doi: 10.1016/j.vetpar.2011.05.051

Qi, M., and Zhang, L. X. (2018). Advance of research on *Cryptosporidium* and cryptosporidiosis of equine. *Chin. J. Zoonoses.* 34 (3), 267–271.

Qi, M., Zhou, H., Wang, H., Wang, R., Xiao, L., Arrowood, M. J., et al. (2015). Molecular identification of cryptosporidium spp. and *Giardia duodenalis* in grazing horses from xinjiang, China. *Vet. Parasitol.* 209 (3-4), 169–172. doi: 10.1016/j.vetpar.2015.02.030

Raue, K., Heuer, L., Böhm, C., Wolken, S., Epe, C., and Strube, C. (2017). 10-year parasitological examination resultto 2012) of faecal samples from horses, ruminants, pigs, dogs, cats, rabbits and hedgehogs. *Parasitol. Res.* 116 (12), 3315–3330. doi: 10.1007/s00436-017-5646-0

Ren, G. J., Wang, X. T., Jing, S., Song, J. K., and Zhao, G. H. (2018). Infection status of cryptosporidium spp.in post-weaned qinchuan calves in partial regions of shanxi province. *Chin. J. Vet. Sci.* 38 (7), 1355–1358.

Robinson, G., and Chalmers, R. M. (2020a). *Cryptosporidium* diagnostic assays: Microscopy. *Methods Mol. Biol.* 2052, 1–10. doi: 10.1007/978-1-4939-9748-0_1

Robinson, G., Elwin, K., and Chalmers, R. M. (2020b). *Cryptosporidium* diagnostic assays: Molecular detection. *Methods Mol. Biol.* 2052, 11–22. doi: 10.1007/978-1-4939-9748-0_2

Rodríguez, D. C., Pino, N., and Peñuela, G. (2012). Microbiological quality indicators in waters of dairy farms: Detection of pathogens by PCR in real time. *Sci. Total Environ.* 427-8, 314–318. doi: 10.1016/j.scitotenv.2012.03.052

Skerrett, H. E., and Holland, C. V. (2001). Asymptomatic shedding of *Cryptosporidium* oocysts by red deer hinds and calves. *Vet. Parasitol.* 94 (4), 239–246. doi: 10.1016/s0304-4017(00)00405-2

Snyder, S. P., England, J. J., and McChesney, A. E. (1978). Cryptosporidiosis in immunodeficient arabian foals. *Vet. Pathol.* 15 (1), 12–17. doi: 10.1177/030098587801500102

Song, Y., Li, W., Zhong, Z. J., Peng, J. L., Xie, N., and Huang, X. M. (2017). Investigation and identification of *Cryptosporidium* from animals in Guiyang Zoo. *Vet. Sci. China* 47 (3), 295–300. doi: 10.16656/j.issn.1673-4696.2017.03.004

Sterk, A., Schijven, J., de, Roda, Husman, A. M., and de, Nijs, T. (2016). Effect of climate change on runoff of *Campylobacter* and *Cryptosporidium* from land to surface water. *Water Res.* 95, 90–102. doi: 10.1016/j.watres.2016.03.005

Veronesi, F., Passamonti, F., Cacciò, S., Diaferia, M., Piergili,, and Fioretti, D. (2010). Epidemiological survey on equine *Cryptosporidium* and *Giardia* infections in Italy and molecular characterization of isolates. *Zoonoses Public Health* 57 (7-8), 510–517. doi: 10.1111/j.1863-2378.2009.01261.x

Wagnerová, P., Sak, B., McEvoy, J., Rost, M., Sherwood, D., Holcomb, K., et al. (2016). *Cryptosporidium parvum* and *Enterocytozoon bieneusi* in American mustangs and chincoteague ponies. *Exp. Parasitol.* 162, 24–27. doi: 10.1016/j.exppara.2015.12.004

Wang, B. J. (2009). Use comparative methods to fully grasp climate knowledge. *Test questions Res.* 36), 38–46.

Wang, H. (2015). Molecular epidemiology of three intestinal protozoas on livestock in henan province. *China Agric. Univ* 8, 1–106.

Wagnerová, P., Sak, B., McEvoy, J., Rost, M., Matysiak, A. P., Ježková, J., et al. (2015). Genetic diversity of Cryptosporidium spp. including novel identification of the *Cryptosporidium muris* and *Cryptosporidium tyzzeri* in horses in the Czech Republic and Poland. *Parasitol. Res.* 114 (4), 1619–1624. doi: 10.1007/s00436-015-4353-y

Wang, W. (2020). Investigation of intestinal parasites infection in donkey in parts of xinjiang [D]. *Tarim Univ*.

Wang, Y. L., Cui, B., Jian, F. C., Zhang, L. X., Ning, C. S., Dong, H. P., et al. (2008). Epidemiological investigation of ovine cryptosporidiosis in henan province. *Vet. Sci. China.* 2), 160–164.

Wang, W., Gong, Q. L., Zeng, A., Li, M. H., Zhao, Q., and Ni, H. B. (2021). Prevalence of *Cryptosporidium* in pigs in China: A systematic review and meta-analysis. *Transbound Emerg. Dis.* 68 (3), 1400–1413. doi: 10.1111/tbed.13806

Wei, X. Y., Gao, Y., Lv, C., Wang, W., Chen, Y., Zhao, Q., et al. (2021a). The global prevalence and risk factors of *Toxoplasma gondii* among foxes: A systematic review and meta-analysis. *Microb. Pathog.* 150, 104699. doi: 10.1016/j.micpath.2020.104699

Wei, X. Y., Gong, Q. L., Zeng, A., Wang, W., Wang, Q., and Zhang, X. X. (2021b). Seroprevalence and risk factors of *Toxoplasma gondii* infection in goats in China from 2010 to 2020: A systematic review and meta-analysis. *Prev. Vet. Med.* 186, 105230. doi: 10.1016/j.prevetmed.2020.105230

Wei, Z. L. (2020). Investigation of intestinal parasites infection in racehorses in parts of China. *Tarim Univ.* 11, 1–52. doi: 10.27708/d.cnki.gtlmd.2020.000054

Xiao, L., and Herd, ,. R. P. (1994). Epidemiology of equine *Cryptosporidium* and *Giardia* infections. *Equine Vet. J.* 26 (1), 14–17. doi: 10.1111/j.2042-3306.1994.tb04323.x

Xie, C. X., and Machado, G. C. (2021). Clinimetrics: Grading of recommendations, assessment, development and evaluation (GRADE). *J. Physiother.* 67 (1), 66. doi: 10.1016/j.jphys.2020.07.003

Xue, N. Y. (2021). Molecular epidemiological investigation and genotype analysis of four kinds of intestinal protozoa in longjiang wagyu cattle in heilongjiang province. *Heilongjiang Bayi Agric. Univ* 9, 1–74.

Young, I., Smith, B. A., and Fazil, A. (2015). A systematic review and meta-analysis of the effects of extreme weather events and other weather-related variables on *Cryptosporidium* and *Giardia* in fresh surface waters. *J. Water Health* 13 (1), 1–17. doi: 10.2166/wh.2014.079

Zeng, A., Gong, Q. L., Wang, Q., Wang, C. R., and Zhang, X. X. (2020). The global seroprevalence of toxoplasma gondii in deer from 1978 to 2019: A systematic review and meta-analysis. *Acta Trop.* 208, 105529. doi: 10.1016/j.actatropica.2020.105529

Zhang, B. L. (2018). Main trends of contemporary world economic development. *Forum Leadership Sci.* 2018 (8), 65–77.

Zhang, Q. Y. (2021). Dynamic investigation of *Cryptosporidium* infection in foals in parts of xinjiang. *Tarim Univ* 8, 1–50.

Zhang, Q., Zhang, Z., Ai, S., Wang, X., Zhang, R., and Duan, Z. (2019). *Cryptosporidium* spp., *Enterocytozoon bieneusi*, and *Giardia duodenalis* from animal sources in the Qinghai-Tibetan Plateau Area (QTPA) in China. *Comp. Immunol. Microbiol. Infect. Dis.* 67, 101346. doi: 10.1016/j.cimid.2019.101346

Zhang, L. X., and Jiang, J. S. (2001). Research progress of *Cryptosporidium* and cryptosporidiosis. *Acta Parasitol. Et Med. Entomologica Sinica.* 2001 (3), 184–192.

Zhang, Y. X., Zhou, M. J., Yu, Z. J., Chen, S. Y., Wang, L. Y., and Yu, Y. L. (2017). Investigation on infection of *Cryptosporidium* in domestic dogs of Beijing. *Prog. Vet. Med.* 38 (6), 120–123.

Zhou, H. (2015). A Survey of Intestinal Parasites in Donkeys of animal-exchange market in Jiaxiang County, Shandong and Multilocus Sequence Typing of *Cryptosporidium* Donkey Genotype. *Henan Agric. Univ.* 7, 1–59.

Zhu, L. Y., Pan, J. J., and Zhang, W. (2013). Study on soil organic carbon pools and turnover characteristics along an elevation gradient in qilian mountain. *Environ. Sci.* 34 (2), 668–675.

frontiers | Frontiers in Cellular and Infection Microbiology

TYPE Original Research
PUBLISHED 25 November 2022
DOI 10.3389/fcimb.2022.1039197

OPEN ACCESS

EDITED BY
William Harold Witola,
University of Illinois at Urbana–Champaign, United States

REVIEWED BY
Juan Mosqueda,
Universidad Autónoma de Querétaro, Mexico
Albert Mulenga,
Texas A&M University, United States

*CORRESPONDENCE
Choukri Ben Mamoun
choukri.benmamoun@yale.edu

SPECIALTY SECTION
This article was submitted to Parasite and Host, a section of the journal Frontiers in Cellular and Infection Microbiology

RECEIVED 07 September 2022
ACCEPTED 07 November 2022
PUBLISHED 25 November 2022

CITATION
Chand M, Choi J-Y, Pal AC, Singh P, Kumari V, Thekkiniath J, Gagnon J, Timalsina S, Gaur G, Williams S, Ledizet M and Mamoun CB (2022) Epitope profiling of monoclonal antibodies to the immunodominant antigen BmGPI12 of the human pathogen *Babesia microti*. *Front. Cell. Infect. Microbiol.* 12:1039197.
doi: 10.3389/fcimb.2022.1039197

Epitope profiling of monoclonal antibodies to the immunodominant antigen BmGPI12 of the human pathogen *Babesia microti*

Meenal Chand[1], Jae-Yeon Choi[1], Anasuya C. Pal[1], Pallavi Singh[1], Vandana Kumari[1], Jose Thekkiniath[1], Jacqueline Gagnon[2], Sushma Timalsina[2], Gauri Gaur[2], Scott Williams[3], Michel Ledizet[2] and Choukri Ben Mamoun[1]*

[1]Department of Internal Medicine, Section of Infectious Diseases, Yale School of Medicine, New Haven, CT, United States, [2]L2 Diagnostics, LLC, New Haven, CT, United States, [3]Department of Forestry and Horticulture, Connecticut Agricultural Experiment Station, New Haven, CT, United States

The significant rise in the number of tick-borne diseases represents a major threat to public health worldwide. One such emerging disease is human babesiosis, which is caused by several protozoan parasites of the *Babesia* genus of which *B. microti* is responsible for most clinical cases reported to date. Recent studies have shown that during its intraerythrocytic life cycle, *B. microti* exports several antigens into the mammalian host using a novel vesicular-mediated secretion mechanism. One of these secreted proteins is the immunodominant antigen BmGPI12, which has been demonstrated to be a reliable biomarker of active *B. microti* infection. The major immunogenic determinants of this antigen remain unknown. Here we provide a comprehensive molecular and serological characterization of a set of eighteen monoclonal antibodies developed against BmGPI12 and a detailed profile of their binding specificity and suitability in the detection of active *B. microti* infection. Serological profiling and competition assays using synthetic peptides identified five unique epitopes on the surface of BmGPI12 which are recognized by a set of eight monoclonal antibodies. ELISA-based antigen detection assays identified five antibody combinations that specifically detect the secreted form of BmGPI12 in plasma samples from *B. microti*-infected mice and humans but not from other *Babesia* species or *P. falciparum*.

KEYWORDS

human babesiosis, apicomplexan parasite, *Babesia microti*, antigen capture, ELISA, BmGPI12, antibodies, epitope mapping

Introduction

Recent epidemiological reports have raised concerns about the rapid increase in tick-borne diseases in the United States and worldwide and the threat they pose to public health (Rosenberg et al., 2018; Kumar et al., 2021; Renard and Ben Mamoun, 2021). Major factors influencing this rise include anthropogenic alterations of the ecosystem, socio-economic changes, and climate change, as well as improved diagnostic methods and better notification (Gilbert, 2021). More than 75% of all vector-borne related illnesses reported in the United States between 2004 and 2016 were caused by tick-borne pathogens (Rosenberg et al., 2018; Renard and Ben Mamoun, 2021).

One such emerging tick-borne disease is human babesiosis, which has a global distribution and remains an endemic disease in the United States (Renard and Ben Mamoun, 2021). The disease is caused by several protozoan parasites of the *Babesia* genus (Renard and Ben Mamoun, 2021; Pal et al., 2022). Depending on the pathogen and the host immune status, the infection can lead to moderate or severe life-threatening illness, especially among immunocompromised hosts such as asplenic, cancer, and HIV patients, individuals on immunosuppressive drugs such as Rituximab, neonates as well as individuals over the age of 50 (Kumar et al., 2021).

Of the 8 species of *Babesia* that are associated with documented clinical reports of human babesiosis worldwide, *Babesia microti* accounts for the vast majority of mild, complicated or fatal clinical cases (Renard and Ben Mamoun, 2021). This eukaryotic pathogen is a member of the *Apicomplexa* phylum which also includes *Plasmodium* parasites, the causative agents of human malaria (Renard and Ben Mamoun, 2021). *Ixodes scapularis* ticks, which also transmit Lyme disease, anaplasmosis and Powassan encephalitis, are the main vectors of *B. microti*. However other modes of transmission have also been reported and include blood transfusion, organ transplantation, and perinatal transmission (Bloch et al., 2021; Krause et al., 2021; Meredith et al., 2021; Renard and Ben Mamoun, 2021). Approved treatment for human babesiosis include the use of drug combinations consisting of atovaquone and azithromycin for mild disease, and quinine and clindamycin for severe disease (Krause et al., 2021; Renard and Ben Mamoun, 2021). The emergence of drug-resistant parasites following treatment, and the commonly reported side effects associated with some of these drugs have led to the use of other antimalarial drugs such as proguanil and tafenoquine in the treatment of human babesiosis (Vyas et al., 2007; Carvalho et al., 2020). More specific drugs tailored to *Babesia* parasites, which have been evaluated in animal models of human babesiosis, have also been developed and include endochin-like quinolones ELQ-502, ELQ-331 and ELQ468, which alone or in combination with atovaquone have shown strong efficacy (Chiu et al., 2021; Chiu et al., 2022; Pal et al., 2022).

Following tick injection of *B. microti* sporozoites, the parasites invade human red blood cells, develop into mature ring and filamentous forms, and then divide to produce 4 daughter parasites per infected erythrocyte (Thekkiniath et al., 2018). Unlike *P. falciparum*, *B. microti* does not degrade hemoglobin and relies heavily on host plasma as a nutrient source for survival (Cornillot et al., 2012; Silva et al., 2016). Recent studies have shown that *B. microti* uses a unique mechanism of protein secretion to deliver its proteins into the host (Thekkiniath et al., 2019). Electron microscopy analysis showed that during its intraerythrocytic cycle, the parasite produces a string of attached vesicles that emerge out of the parasite plasma membrane and contain most of the parasite cytoplasm including proteins and ribosomes (Thekkiniath et al., 2019). Immunoproteomic analyses, using sera from *B. microti*-infected mice and humans, identified several antigens whose IgM and IgG profiles correlate with the early and late stages of infection, respectively (Cornillot et al., 2016; Silva et al., 2016). Interestingly, several of these immune-reactive antigens have been found to be associated with these vesicles and include BmGPI12, a member of the BMN1 multigene family of antigens, and BmIPA48, a constituent of the rhoptry organelle (Thekkiniath et al., 2019; Bastos et al., 2021). Transcription analyses showed that *BmGPI12* is one of the most highly expressed genes of *B. microti* (Cornillot et al., 2012; Carpi et al., 2016; Silva et al., 2016). Fractionation and immunoelectron microscopy studies have shown that BmGPI12 protein can be found in three major fractions: the parasite fraction where the protein was found to be associated with the parasite plasma membrane; the red blood cytoplasm fraction; and the extracellular fraction where the protein is readily detected by immunoblot and ELISA assays (Thekkiniath et al., 2018). The unique profile of this protein has made it an excellent choice for detection of active *B. microti* infection (Thekkiniath et al., 2018).

In this study, we aimed to characterize the epitope map of eighteen monoclonal antibodies developed against BmGPI12 (Gagnon et al., 2022) with the goal to develop specific antigen capture ELISA-based assays for detection of active *B. microti* infection. Our study identified five antibody combinations that specifically detect secreted BmGPI12 in *B. microti*-infected plasma but not in plasma from *B. duncani*-infected mice or supernatants of *B. duncani*, *B. divergens* and *P. falciparum in vitro* cultures in human red blood cells.

Materials and methods

Ethics statement

All animal experiments were approved by the Institutional Animal Care and Use Committees (IACUC) at Yale University (Protocol #2020-07689). Animals were acclimatized for one

week after arrival before the start of an experiment. Animals that showed signs of distress or appeared moribund were humanly euthanized using approved protocols.

Parasite strains and mouse infections

5-6 weeks old female C.B-17.SCID (Severe Combined immunodeficient) (C.B-17/IcrHsd-Prkdc^{scid}) mice obtained from Envigo, NJ, and 5-6 weeks old female Balb/cJ mice purchased from Jackson Laboratories were used in this study. Mouse infections were established by intravenous injection of previously cryo-preserved *B. microti* (LabS1 strain)-infected blood. For studies involving *B. duncani*-infected mice, C3H/HeJ mice from Jackson Laboratories were infected with 10^6-*B. duncani* (WA-1) red blood cells as previously described (Pal et al., 2022).

BmGPI12 monoclonal antibodies

The anti-BmGPI12 monoclonal antibodies (MAbs) described in this study have been generated and purified as described by Gagnon and colleagues (Gagnon et al., 2022). These antibodies and the concentration used in this study are listed in Table 1.

Production of recombinant sub fragments of BmGPI12

Codon-optimized DNA fragments encoding the full length BmGPI12 and sub-fragments F1 (amino acids 1-100), F2 (amino acids 50-150), F3 (amino acids 100 to 200), F4 (amino acids 150 to 250) and F5 (amino acids 200 to 328) were synthesized (Genscript Inc.), cloned into the *BamHI* and *XhoI* sites of the pGEX-6p expression plasmid (GE Healthcare) and the resulting plasmids were introduced into *E. coli* BL21 strain. Expression and purification of the recombinant proteins was conducted as described previously (Thekkiniath et al., 2018) with some modifications. Briefly, the *E. coli* strains harboring the plasmids were pre-grown overnight in Luria-Bertani (LB) Broth containing ampicillin (100 µg/ml). The cells were diluted by 100-fold in 200 ml of fresh medium and grown to OD_{600} of 0.5. Expression of the recombinant proteins was induced by adding 0.1 mM isopropyl-β-d-thiogalactopyranoside (IPTG) (I56000-25.0, RPI) to the cell culture and continued by incubation for 5h at 30°C while shaking at 230 rpm. Cells were spun down by centrifugation at 2,900 x g for 20 min at 4°C and the pellets were re-suspended in 5 ml of phosphate buffered saline (PBS, pH 7.3) buffer supplemented with protease inhibitor cocktail (Mini-cOmplete™ EDTA-free (11836170001, Roche). The cell free extracts were obtained by sonication using an Omni Sonic Ruptor 400 Ultrasonic Homogenizer (15 sec burst at 30% amplitude, 10 times, with 15 sec cooling on ice after each burst), followed by centrifugation at 16,000 g for 20 min. GST tagged recombinant proteins were purified by affinity chromatography on a 1 ml of glutathione sepharose high performance column (17-5279-01, Cytiva) by following the manufacturer's instructions (Cytiva, 71502754 AC). Proteins bound to the column were eluted by applying 1 ml of elution buffer (50 mM Tris-HCl, 100 mM NaCl, 5 mM DTT, and 10 mM reduced glutathione, pH 8.0) to the column 3 times and glutathione was removed from the purified protein solutions using PD-10 desalting columns containing Sephadex G-25 resin (17085101, Cytiva). The purified proteins were used in the western blot, dot blot and ELISA assays described in this study.

TABLE 1 List of BmGPI12 mouse monoclonal antibodies and their concentrations.

BmGPI12 MAb	Concentration (µg/mL)
1A5	1030
1B10	3160
1E11	1070
1G11	2310
2A7	1789
2H6	2135
3A12	2400
3B1	1850
3B6	1020
3D4	2575
4B12	995
4C8	1090
4C12	350
4E1	1517
4F8	1648
4H5	1430
5C11	840
5D11	2545

BmGPI12 peptide library

A library of 19 overlapping peptides covering a portion of the BmGPI12 protein between amino acids 50 and 200 were synthesized by Genscript, Inc. Each peptide consists of 11 amino acids with the last 3 amino acids of one peptide overlapping with the first 3 amino acids of the next peptide. Table 2 includes the list of all the peptides used in this study.

Babesia microti short-term *in-vitro* culture

Short-term *in-vitro* culture of *B. microti* was performed as previously described (Thekkiniath et al., 2018). Under these conditions, the parasite develops from ring to tetrad stages (Lawres et al., 2016) and secretes antigens such as BmGPI12 and BmIPA48, which are also detected in plasma from *B. microti*-

TABLE 2 Primary sequences of the BmGPI12 peptides.

BmGPI12 peptide	Amino acid position	Peptide sequence	kDa
P1	50-60	SNPTGAGG**QPN**	1
P2	58-68	**QPN**NEAKK**KAV**	1.2
P3	66-76	**KAV**KLDLD**LMK**	1.3
P4	74-84	**LMK**ETKNV**CTT**	1.3
P5	82-92	**CTT**VNTKL**VGK**	1.2
P6	90-100	**VGK**AKSKL**NKL**	1.2
P7	98-108	**NKL**EGESH**KEY**	1.3
P8	106-116	**KEY**VAEKT**KEI**	1.3
P9	114-124	**KEI**DEKNK**KFN**	1.4
P10	122-132	**KFN**ENLVK**IEK**	1.4
P11	130-140	**IEK**RKKIK**VPA**	1.3
P12	138-148	**VPA**DTGAE**VDA**	1
P13	146-156	**VDA**VDDGV**AGA**	1
P14	154-164	**AGA**LSDLS**SDI**	1
P15	162-172	**SDI**SAIKT**LTD**	1.2
P16	170-180	**LTD**DVSEK**VSE**	1.2
P17	178-188	**VSE**NLKDD**EAS**	1.2
P18	186-196	**EAS**ATEHT**DIK**	1.2
P19	190-200	**TEH**TDIKEKAT	1.3

Overlapping amino acids are indicated by bold letters.

infected animals (Thekkiniath et al., 2019). Briefly, one C.B-17.SCID mouse (Cornillot et al., 2016) was infected with the *B. microti Lab S1* strain and 50 µL of infected blood (at 15% parasitemia) was mixed with 100 µL of uninfected human RBC (A^+, 50% hematocrit) and allowed to grow in complete DMEM-F12-based cell culture medium (850 µL) (BE04-687F/U1, Lonza) supplemented with 20% heat-inactivated fetal bovine serum (HI-FBS, F4135, Sigma), 1X-antibiotic/antimycotic solution (15240-062, GIBCO), 2% 50X HT Media Supplement Hybri-Max 230 TM (H0137, Sigma), 1% 200 mM L-Glutamine (25030-081, GIBCO) for 24h at 37°C under hypoxic condition (2% O_2) (Singh et al., 2022). 1 ml culture volume was centrifuged at 400 x g at room temperature for 10 min, and a 1ml culture supernatant (S) was collected. The cell pellet was further treated with 1% saponin (100 µl) and incubated on ice for 30 min. Hemolysate (H) and parasite pellet (P) fractions were collected after centrifugation at 9,300 x g for 10 min at 4°C. The parasite pellet was resuspended in 30µl of 1X Laemmli sample buffer. The collected S, H, and P fractions were used for immunoblot analysis.

Immunodetection of BmGPI12

Supernatant (S), hemolysate (H), and parasite pellet (P) fractions from a short-term *in vitro* culture of *B. microti* (iRBCs) and similar fractions from non-infected human RBCs (uRBCs, control) were used in western blots. Sample (S, H and P) were mixed with Laemmli sample buffer (1610747, BIO-RAD), boiled at 80°C for 5 min, separated on 12% mini-protean gels, and transferred onto nitrocellulose membranes. The membrane was blocked with 5% non-fat skim milk (AB10109-01000, American Bio) in Tris-buffered saline (TBS) containing 0.02 M Tris base, 0.15 M NaCl, and 0.1% Tween 20 (1X TBST) for 1h at room temperature followed by incubation with 18 anti-BmGPI12 MAbs (1:250 dilution in blocking buffer) at 4°C overnight. Following treatment with primary antibodies, the membranes were washed three times with 1X TBST (10 min each) and incubated with HRP-conjugated goat anti-mouse IgG (1: 5,000 dilution) (31466, Thermo Fisher) for 1h at room temperature. Subsequently, the membranes were washed twice with 1X TBST and once with 1X PBS and developed using Super signal™ West Pico PLUS chemiluminescent substrate (34577, Thermo Scientific). The blot was imaged using LI-COR Odyssey-Fc imaging system.

Immunofluorescence assay

Thin blood smears from uninfected and *B. microti*-infected C.B-17.SCID mice RBCs were prepared on glass slides (640-001T, DOT scientific) and fixed with chilled methanol (9070-05, JT Baker) for 15 min at -20°C. The smears were air-dried and blocked in 3% BSA in PBS buffer (A9418, Sigma) for 1h at room temperature. Following this step, the smears were incubated with the mouse monoclonal anti-BmGPI12 antibody 5C11 at 1:500 dilution for 1h at room temperature. This was followed by three

washes in 1X PBS containing 0.05% Tween and three washes in 1X PBS, 5 min each. Subsequently, the smears were incubated with goat anti-mouse IgG antibodies conjugated to Alexa Fluor 488 (1:500 dilution) (A-11001, Life Technologies) for 1h at room temperature. This was followed by three washes in 1X PBST and three washes in 1X PBS. The smears were further incubated with Phycoerythrin (PE)-conjugated anti-mouse TER-119 (1:200 dilution) (116207, BioLegend) for 1h at room temperature followed by three washes in 1X PBST and three washes in 1X PBS. Coverslips were then mounted on glass slides using Vectashield mounting medium containing DAPI (H-1200-10, Vector Laboratories) and examined using a Nikon ECLIPSE TE2000-E microscope. A 100X oil immersion objective was used for image acquisition. Excitation at 465-495 nm was used to detect Alexa Fluor 488 positive cells; excitation at 510-560 nm was used to detect PE positive cells, and excitation at 340-380 nm was used to detect DAPI positive cells. The images were acquired using MetaVue with 1,392 x 1,040 pixel as the chosen image size and subsequently analyzed using ImageJ.

Immunoelectron microscopy

Sample preparation, immune labeling and image processing for immunoelectron microscopic analysis of *B. microti LabS1*–infected mouse (CB.17-SCID) red blood cells (mRBCs) were performed as previously described by Thekkiniath et al. (Thekkiniath et al., 2019). Briefly, *B. microti*-infected mRBCs were fixed in 4% PFA and frozen using a Leica HMP100 at 2,000 psi. The frozen samples were then freeze-substituted using a Leica Freeze AFS unit starting at −95°C using 1% osmium tetroxide, 1% glutaraldehyde, and 1% water in acetone for 10h, warmed to −20° C for 12h and then to 4°C for 2h. The samples were rinsed in 100% acetone and infiltrated with Durcupan resin (Electron Microscopy Science) and baked at 60°C for 24h. Hardened blocks were cut using a Leica UltraCut UC7, and 60-nm sections were collected on formvar/carbon–coated nickel grids. Resin sections were incubated with anti-BmGPI12 monoclonal antibodies at 1: 100 dilution (overnight), rinsed in buffer, and then incubated with the secondary antibody 10 nm protein A gold (UtrechtUMC) for 30 min. The grids were rinsed and fixed using 1% glutaraldehyde for 5 min, rinsed well in distilled water, and contrast-stained using 2% uranyl acetate and lead citrate. The grids were viewed in an FEI Tencai Biotwin TEM at 80 kV. Images were taken using Morada CCD and iTEM (Olympus) software.

Dot blot analysis of BmGPI12

Dot blot analysis was used to detect specific interactions of the various MAbs with the sub-fragments of BmGPI12 or individual peptides (11 amino acids each). Samples (100 ng) were spotted on a nitrocellulose membrane and dried at room temperature for 1h. The membrane was then blocked by application of 200 µl of blocking buffer (5% BSA in TBS with 0.05% Tween-20 (TBST-0.05%)) (Singh et al., 2022) into each well for 1h at room temperature. Following this step, the blocking buffer solution was replaced with 200 µl of 0.1% BSA in TBST-0.05% buffer and kept for 1h at room temperature or overnight at 4°C. Primary antibodies were diluted 1:1000 in 0.1% BSA in TBST-0.05% buffer and added to the membranes for 1h at room temperature, followed by incubation with HRP-conjugated goat anti-mouse IgG (1: 5,000 dilution) (31466, Thermo Fisher) secondary antibody for 45 min at room temperature. The blots were washed three times with TBST-0.05%, once with PBS (5 min), and then developed using the Super signal™ West Pico PLUS chemiluminescent substrate (34577, Thermo Scientific) and imaged using the Odyssey Fc imaging system.

Detection of anti-BmGPI12 antibodies in sera or plasma samples from *B. microti* infected Balb/c mice and field mice

Immunoreactivity of mouse plasma or sera to full length BmGPI12 or its sub fragments (F1, F2, F3, F4 and F5) were determined by indirect ELISA. Recombinant BmGPI12 or sub-fragments were coated (50 ng/well) in 96-well Nunc Maxisorp plates and incubated overnight at 4°C. Plates were then blocked with 5% BSA in PBS containing 0.05% Tween 20 (PBST) for 1.5h at 37°C. All sera and plasma dilutions were made in 1% BSA in PBST. Following this step, plates were incubated with sera and plasma from *B. microti*-infected or uninfected mice at 1: 200 dilution for 1.5h at room temperature. For studies involving sera collected from field mice, similar antigen coated plates were incubated with CDC-confirmed *B. microti* PCR positive or negative mouse sera at 1: 200 dilution. Following plasma/sera incubation, plates were washed 4 times with PBST, then incubated for 1h with goat anti-mouse HRP conjugated secondary antibody (1: 5000) (31466, Thermo Fisher). The plates were then washed 4 times with PBST and 100 µL TMB substrate (3,3,5,5,-tetramethylbenzidine (KPL 5120-0083, SeraCare Life Sciences) was added to each well. After a 5 min incubation at room temperature (in the dark), the reaction was stopped by adding 100 µl of 0.1N HCl. Optical density (OD) was measured at 450 nm on a BioTek PowerWave HT plate reader. Standard Deviation (SD) was calculated using Graphpad Prism 9.3 software. The cut-off OD_{450} was determined as mean + 2 x SD of uninfected/ negative samples.

Detection of BmGPI12 in human plasma samples

Plasma samples from blood collected in EDTA from individuals that were either negative or positive for *B. microti* nucleic acid by PCR or transcription-mediated amplification

(TMA) were obtained as de-identified samples from the American Red Cross (ARC) under an approved agreement (Tonnetti et al., 2020). 96-well Nunc Maxisorp plates were coated with purified BmGP12-Full length (FL) or sub-fragments F1, F2, F3, F4 or F5 at 50 ng/well (diluted in coating buffer (20 mM Tris-HCl pH 8.5 + 0.1M NaCl)), overnight at 4°C. Wells with only coating buffer were used as controls. Antigen coated wells were blocked with 200 µl ChonBlocking sample dilution ELISA Buffer (9068, Chondrex, Inc.) for 2h at 37°C. Following blocking, *B. microti* positive or negative plasma samples added at 1:250 dilution in 1% BSA in PBST for 1.5h at room temperature. The plates were subsequently washed four times with PBST and incubated with HRP-conjugated Fc gamma fragment specific goat anti-human IgG (32935, Cell Signaling) at 1:10,000 dilution for 1h at room temperature. After four washes with PBST, 100 µL of TMB substrate was added to each well and incubated for approximately 5 min at room temperature in the dark. The reaction was stopped by adding 100 µl of 0.1N HCl. The OD was measured at 450 nm using Bio-Tek Power Wave HT plate reader. Each experiment was independently repeated with two technical replicates each. Standard Deviation (SD) was calculated using Graphpad Prism 9.3 software. The cut-off OD_{450} value was determined as mean + 2 x SD of the OD_{450} value of the negative/uninfected samples.

mGPAC assay with monoclonal antibody combinations

Sandwich ELISA using monoclonal antibody combinations to detect *B. microti* infection in mice were performed as previously described (Gagnon et al., 2022) with slight modifications. Briefly, 96-well plates were coated with 200 ng/well of capture MAbs (2H6, 1E11, and 4C8), and incubated at room temperature for 2h. The wells were then blocked with 5% BSA in PBST (0.05% Tween-20) and incubated at room temperature for 1h. Following this, plates were incubated overnight at 4°C with either recombinant BmGPI12 (100 ng/well) or with heat inactivated (30 min at 56°C) plasma from uninfected or *B. microti* (LabS1) infected C.B-17.SCID mouse at 1:100 dilution. The plates were then washed 4 times with PBST followed by addition of 2 µg/ml biotinylated detection MAbs (2H6, 1E11, 4C8, 5C11, or 1A5) and incubated at room temperature for 2h. The plates were then washed with PBST and incubated with HRP conjugated streptavidin (KPL 474-3000, SeraCare Life Sciences) at 1:5000 dilution for 1h at room temperature. Finally, the plates were washed four times with PBST, and 100 µl TMB substrate was added, incubated for 5 min at room temperature and 100 µl of 0.1N HCl was added to stop the reaction. The optical density at 450 nm was measured on a BioTek PowerWave HT plate reader. Results were analyzed using the Graphpad Prism 9.3 software and statistical significances were calculated using two-way ANOVA.

The specificity of the MAb combinations was evaluated by using culture supernatants from *B. duncani WA-1* (25% parasitemia), *B. divergens Rouen87* (10% parasitemia), *P. falciparum* 3D7 (10% parasitemia), and *P. falciparum* HB3 (10% parasitemia)-infected human erythrocytes as well as heat inactivated plasma from uninfected or *B. duncani*-infected C3H/HeJ mice (34% parasitemia). *B. duncani* and *B. divergens* were propagated *in vitro* in complete DMEM-F12 (cF12) (Singh et al., 2022) whereas *P. falciparum* strains were propagated in complete RPMI (cRPMI) medium (El Bissati et al., 2006). Plasma from *B. microti* infected or uninfected SCID mice were used as positive and negative controls, respectively. Statistical significances were calculated using one way ANOVA test using the Graphpad Prism 9.3 software. For each sample type the cut-off OD_{450} value was determined as the mean + 2 x SD of the OD_{450} value of the corresponding uninfected sample. Any signal above the cut-off limit was considered a positive result.

Results

BmGPI12 cellular distribution in *B. microti*-infected erythrocytes using specific monoclonal antibodies

Eighteen monoclonal antibodies (MAbs) developed against BmGPI12 were recently characterized by ELISA using recombinant BmGPI12 as a target antigen (Gagnon et al., 2022) (Table 1). The specificity of these antibodies was assessed by immunoblotting using supernatant (S), hemolysate (H) and free parasites (P) fractions from *B. microti*-infected erythrocytes. Fourteen of the eighteen MAbs recognized the native BmGPI12 in all three fractions (Figure 1); the remaining four MAbs, 2A7, 2H6, 3A12, and 4E1, showed weak signal in this analysis. As a control, no signal could be detected using similar fractions from uninfected erythrocytes (Figure 1). Immunofluorescence microscopy analyses using these MAbs identified 16 MAbs, which were specific and presented a localization profile for BmGPI12 (Supplementary Figure S1; Figure 2A) identical to that previously reported using polyclonal antibodies raised against the full-length protein (Thekkiniath et al., 2019). As shown in Figure 2A, BmGPI12 could be detected using MAb 5C11 in *B. microti*-infected erythrocytes both on the parasite plasma membrane and the vesicular network produced by the parasite and exported into the erythrocyte cytoplasm (Thekkiniath et al., 2019). Five of the monoclonal antibodies (1G11, 1E11, 5C11, 4C8 and 1A5) were further used in immunoelectron microscopy (IEM) analyses. However, only 5C11 showed a specific signal by IEM in *B. microti*-infected erythrocytes with BmGPI12 localized to the plasma membrane of *B. microti* as well as to the surface of the secreted vesicles (Figures 2B, C) as previously reported using polyclonal antibodies (Thekkiniath et al., 2019)

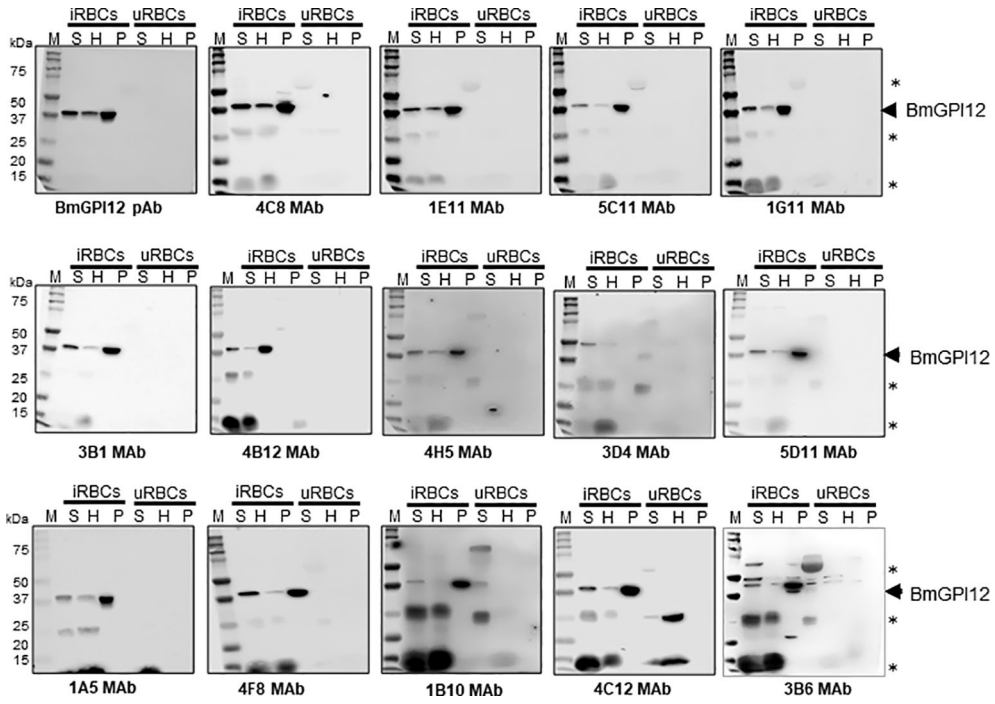

FIGURE 1
Detection and localization of BmGPI12 using anti-BmGPI12 polyclonal and monoclonal antibodies. Immunoblot analysis of secreted (S), hemolysate (H) and parasite (P) fractions isolated from *B microti* short-term *in vitro* culture (iRBC) or uninfected human RBCs (uRBCs) using α-BmGPI12 polyclonal (pAb) and different monoclonal antibodies (MAbs). Samples were analyzed on a 12% mini protein gel, transferred to nitrocellulose membrane and probed with BmGPI12 poly or monoclonal antibodies as indicated. * indicates nonspecific bands or degradation products.

Anti-BmGPI12 MAbs map to highly immunogenic regions of the secreted antigen

To identify the specific regions in BmGPI12 that are recognized by the various monoclonal antibodies, the full-length protein (FL: amino acids 28-328) as well as five overlapping fragments F1 (amino acids 1 to 100 of BmGPI12), F2 (amino acids 50 to 150 of BmGPI12), F3 (amino acids 100 to 200 of BmGPI12), F4 (amino acids 150 to 250 of BmGPI12) and F5 (amino acids 200 to 328 of BmGPI12) were purified as recombination fusion proteins using an N-terminal GST tag and used in dot blot and immunoblot assays with each of the 18 MAbs. A schematic representation of the BmGPI12 FL and sub-fragments are shown in Figure 3A. As shown in Figure 3B, 13 MAbs were found to bind to either a specific fragment or 2 overlapping fragments of BmGPI12. Monoclonal antibodies 5D11, 2H6, 3D4, 3B6, 4C12, 3A12, and 1E11 specifically recognized the F2 fragment; 4C8, and 1G11 mapped specifically to both F2 and F3 fragments; whereas 5C11 and 1A5 MAbs mapped specifically to the F3 and F4 fragments. The F1 and the F5 fragments showed low reactivity with the MAbs in immunoblot and dot blot (data not shown). The antigenicity profile of the F1, F2, F3, F4 and F5 fragments of BmGPI12 were further characterized using serum and plasma samples from uninfected and *B. microti*-infected mice as well as human plasma from *B. microti* positive or -negative individuals in indirect ELISA. As shown in Figures 4A–F, 5A–F, both sera and plasma from *B. microti*-infected mice reacted strongly with the recombinant antigens with optimal immunoreactivity achieved with the full length BmGPI12 (OD at 450 nm ranged between 2.5 and 3.7) followed by the F2 and F3 fragments whereas the F4 fragment showed only a modest reactivity. As a control, no reactivity could be found using sera and plasma from uninfected mice (Figures 4A–F, 5A–F). Similarly, the immunoreactivity of human plasma samples from *B. microti* positive individuals reacted with all the fragments of BmGPI12 with the highest reactivity recorded with fragments F2 and F3 (Figures 6A–F). No reactivity could be detected with plasma from *B. microti*-negative individuals (Figure 6). Both plasma and serum samples from mice and humans that showed the strongest immunoreactivity using the full length recombinant BmGPI12 were also those that reacted strongly with the F2 and F3 fragments.

To further assess whether a similar immunoreactivity profile could be seen in reservoir animals, we screened 62 serum samples obtained from field mice from various regions in Connecticut, USA. These samples were previously characterized by PCR to detect *B. microti* 18S rDNA and separated into 31 PCR-positive and 31 PCR-negative samples. As shown in Figures 7A–D, the immunoreactivity of the majority of *B. microti* PCR-positive samples were found to be

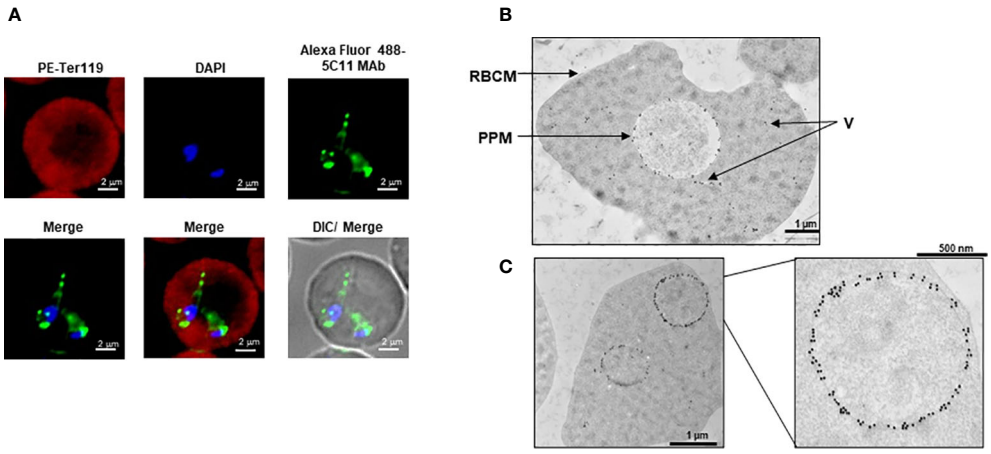

FIGURE 2
Subcellular localization of BmGPI12. **(A)** Immunofluorescence staining of BmGPI12 using 5C11 monoclonal antibody (raised in mouse) followed by staining with Alexa Fluor (AF)-488 conjugated anti-rabbit secondary antibody (AF488-BmGPI12 pAb, Green) in *B microti*-infected mouse RBCs (Bm-iRBC). Mouse RBCs were stained with Phycoerythrin (PE)-conjugated anti-mouse Ter 119 (PE-Ter119, Red). DAPI (Blue) was used to label parasite DNA. Bars, 2μm. **(B, C)** Transmission immunoelectron microscopic analysis of *B microti* LabS1–infected mouse red blood cells (mRBCs). Ultrathin sections of high-pressure frozen and Durcupan resin–embedded infected RBCs were immunolabeled with anti-BmGPI12 monoclonal antibody (5C11) coupled to 10 nm gold particle. Portion of image **(C)** is magnified to show enlarged parasite showing localization of BmGPI12 in the parasite plasma membrane (PPM). RBCM: red blood cell membrane; V, vesicles. Bars, 1μm and 500 nm.

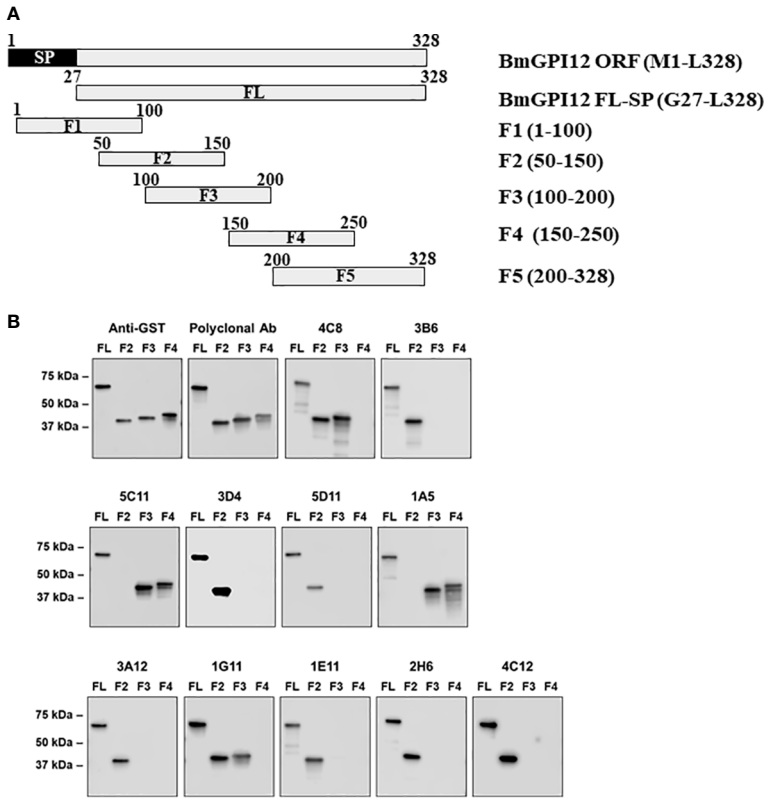

FIGURE 3
Mapping of MAb binding to specific BmGPI12 fragments. **(A)** Schematic diagram of BmGPI12 and its sub-fragments. **(B)** Western blot analysis using anti-GST or different anti-BmGPI12 MAbs against full length (FL) BmGPI12 or sub-fragments F2, F3 and F4.

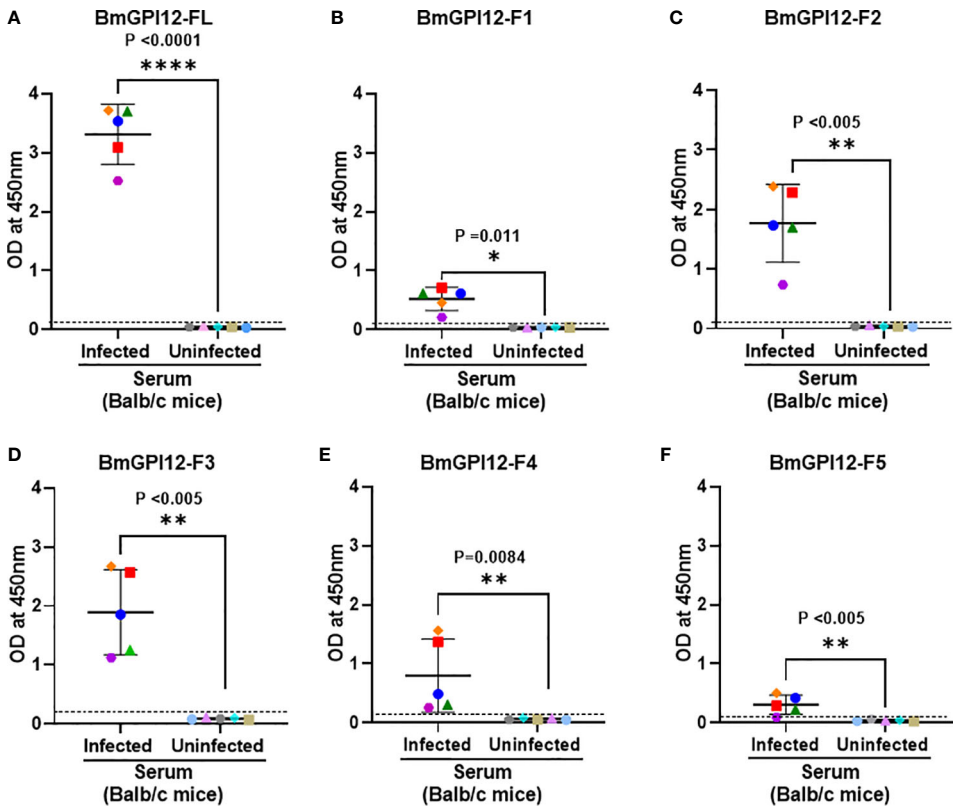

FIGURE 4
Detection of full length BmGPI12 or its sub-fragments by indirect ELISA using uninfected or *B microti*-infected mouse sera. Heat inactivated sera from *B microti*-infected or uninfected Balb/c mice were used (1:200 dilution) to detect recombinant BmGPI12-FL or sub-fragments F1, F2, F3, F4 or F5 coated on ELISA plates at 50 ng/well. In all graphs, one color represents the reactivity of each mouse serum sample to different BmGPI12 antigens- FL **(A)**, F1 **(B)**, F2 **(C)**, F3 **(D)**, F4 **(E)** and F5 **(F)**. Each assay was conducted more than once with at least two technical replicates per assay. Error bars denote the standard deviation (SD) calculated using the Graphpad Prism 9.3 software. OD_{450} cut-off (dashed line) was determined as the mean + 2 x SD of the OD_{450} value of the uninfected samples. ****: statistically significant (p<0.0001, by two-way ANOVA); **: statistically significant (p<0.005, by two-way ANOVA); *: statistically significant (p=0.011, by two-way ANOVA).

above the OD_{450} cut-off value of the full-length antigen (>97%) as well as the F2 (80%), and F3 (71%) fragments (p values ≤ 0.0001 by 2-way ANOVA). The cut-off OD_{450} value was determined as the mean + 2 x SD of the OD_{450} value of the corresponding negative/uninfected sera samples for each antigen. Consistent with the PCR data, all sera from PCR-negative field mice showed no signals above the OD_{450} cut-off (Figure 7).

Epitope mapping of MAbs to BmGPI12

The finding that the F2, F3, and F4 fragments of BmGPI12 are the most immunogenic regions of the antigen led us to investigate the exact binding sites of the monoclonal antibodies by epitope mapping (Figure 8A). A set of 19 small overlapping peptides (11 amino acids in length with 3 amino acid overlaps between adjacent peptides) covering the F2 to F4 fragments of the BmGPI12 antigen were synthesized (Table 2) and coated into nitrocellulose membranes. Specific interactions of the peptides with the 13 MAbs were determined using a dot blot-based direct binding. The specific binding of MAbs to individual peptides was further validated by examining the ability of the peptides to interfere with the binding of MAbs to the F2, F3 and F4 fragments (Figures 8A, B). As shown in Figure 8B, peptide P3 effectively blocked the binding of the F2 fragment to 3A12, 3B6, 3D4, and 2H6 MAbs; peptides P6 and P10 blocked the binding of F2 domain to 1E11 and 4C8 MAbs, respectively; and peptide P15 blocked the binding of the F3 domain to 1A5 MAb. Taken together, 3A12, 3B6, 3D4 and 2H6 MAbs mapped to P3 (KAVKLDLDLMK, BmGPI12$^{66\text{-}76}$); 1E11 MAb to P6 (VG KAKSKLNKL, BmGPI12$^{90\text{-}100}$); 4C8 MAb to P10 (KFNENL VKIEK, BmGPI12$^{122\text{-}}$132), 5C11 MAb to P13 (VDAVD DGVAGA, BmGPI12$^{136\text{-}156}$); and 1A5 MAb to P15 (SDISAIK TLTD BmGPI12$^{162\text{-}172}$) (Figure 8A; Table 3).

To gain further insights into the immunogenicity profile of BmGPI12 at the structural level, the 3-dimensional structure of protein was generated using the AlphaFold Protein Structure Database (https://alphafold.com/entry/A0A0K3AT66)

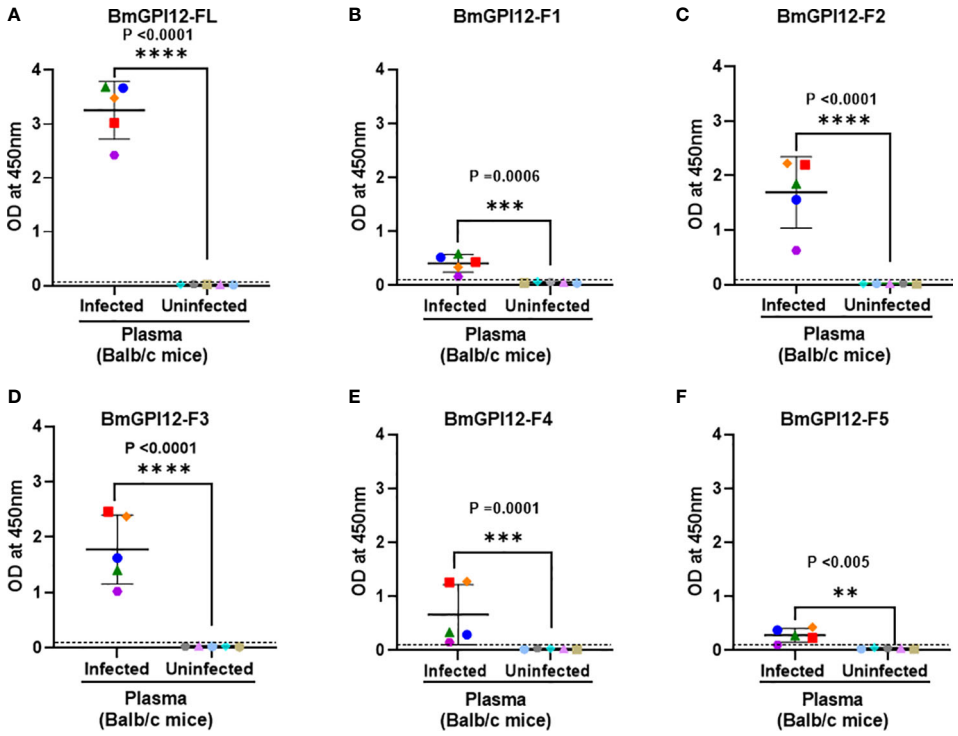

FIGURE 5
Detection of full length BmGPI12 or its sub-fragments by indirect ELISA using uninfected or *B microti*-infected mouse plasma. Heat inactivated plasma from *B microti*-infected or uninfected Balb/c mice were used (1:200 dilution) to detect recombinant BmGPI12-FL or sub-fragments F1, F2, F3, F4 or F5 coated on ELISA plates at 50 ng/well. In all graphs, one color represents the reactivity of each mouse plasma sample to different BmGPI12 antigens- FL **(A)**, F1 **(B)**, F2 **(C)**, F3 **(D)**, F4 **(E)** and F5 **(F)**. Each assay was conducted more than once with at least two technical replicates per assay. Error bars denote the standard deviation calculated using the Graphpad Prism 9.3 software. OD_{450} cut-off (dashed line) was determined as the mean + 2 x SD of the OD_{450} value of the uninfected samples. ****: statistically significant (p<0.0001, by two-way ANOVA); ***: statistically significant (p<0.0006, by two-way ANOVA); **: statistically significant (p<0.005, by two-way ANOVA).

(Figure 8C). While the N-terminal 58 amino acids (including 27 amino acids of the cleaved signal peptide sequence) and the C-terminal 19 amino acids were found to be unstructured, most of the sequences between the two extremities were modeled with high accuracy scores. The predicted protein structure showed 2 distinct bundles of helices, one with 3 helices in the N-terminal region and the other with 4 helices in the C-terminal region. The N-terminal 3 helices encompass the F2 and the F3 fragments consistent with their highly immunogenic profile. Interestingly, peptides P3, P6, P10, P13 and P15, which are within these 2 fragments, were found to be on the surface of the protein with P3, P6, P10, and P13 directly exposed to the surface of the helices (Figure 8C), making them easily accessible to antibody binding.

Specificity of ELISA assays based on anti-BmGPI12 MAbs

Our finding that 4C8, 1E11, 5C11, 1A5 and 2H6 map to specific epitopes on BmGPI12 led us to evaluate specific combinations of monoclonal antibodies that can be used to detect this antigen using antigen capture ELISA assays (mGPAC assay). Figure 9A shows the schematic representation of the mGPAC assay that was used to evaluate different monoclonal antibody combinations. All 5 monoclonal antibodies were found to be suitable as detection antibodies, whereas only 2H6, 1E11 and 4C8 were found to be suitable as capture antibodies (Figure 9). Whereas all 12 possible combinations of capture and detection antibodies detected the purified recombinant BmGPI12, only 7 of these combinations detected the native secreted antigen in plasma from *B. microti*-infected mice (Figure 9B). When using recombinant protein in the capture assay, capture MAb 2H6 worked best with detection MAbs 1E11, 4C8, 5C11, and 1A5 (Figures 9B–E), while capture MAb 1E11 was most suitable in combination with detection MAbs 4C8, 5C11 and 1A5 (Figures 9F–I). Similarly, 4C8 as a capture antibody worked best with detection MAbs 1E11, 5C11 and 1A5, while the 4C8-2H6 combination showed a comparatively weaker detection (Figures 9J–M). When *B. microti*-infected mouse plasma was used as the antigen source, the signal was mostly similar to that obtained for the recombinant protein when capture MAbs 1E11 and 4C8 were used (Figures 9F–M). In contrast, the capture MAb 2H6 detected BmGPI12 in the plasma only in combination with 4C8

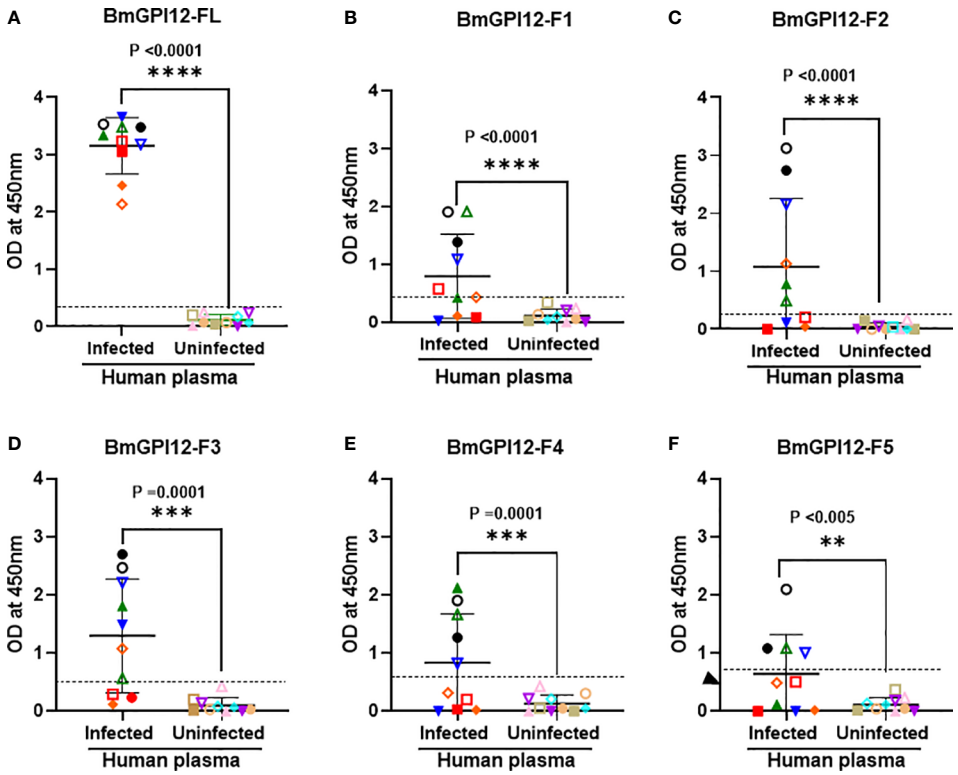

FIGURE 6
Detection of recombinant BmGPI12 or its sub-fragments using plasma from *B microti* PCR-positive and -negative humans. Graphs show the detection of full length BmGPI12 or its sub fragments (F1-F5) with *B microti* positive (by PCR or TMA) or negative (by TMA) human plasma samples. ELISA plates were coated with 50 ng/well of BmGPI12 FL **(A)** or fragments F1 **(B)**, F2 **(C)**, F3 **(D)**, F4 **(E)**, F5 **(F)**. Human plasma samples were used at 1:250 dilution. Each assay was conducted more than once with at least two technical replicates per assay. Error bars denote the standard deviation(SD) calculated using the Graphpad Prism 9.3 software. In all graphs, each color/symbol represents the reactivity of individual human plasma sample to different BmGPI12 antigens. Statistical significance was calculated using two-way ANOVA. The OD_{450} cut-off (dashed line) denotes the mean + 2 x SD of the OD_{450} value of the negative samples. ****: statistically significant (p<0.0001, by two-way ANOVA); ***: statistically significant (p=0.0001, by two-way ANOVA); **: statistically significant (p<0.005, by two-way ANOVA).

(Figures 9C) but poorly detected the protein when combined with MAbs 1E11, 5C11 or 1A5 (Figures 9B, D, E). As a control, no significant signal could be detected with the MAb combinations using plasma from uninfected mice (Figures 9B–M). Overall, we identified 7 different combinations of capture and detection antibodies (2H6-4C8, 1E11-4C8, 1E11-5C11, 1E11-1A5, 4C8-1E11, 4C8-5C11, 4C8-1A5) that were optimal for detection of secreted BmGPI12 protein in plasma from *B. microti*-infected mice using antigen capture ELISA. Noteworthy, the combination 1E11 +4C8 has recently been validated in a capture assay using plasma samples from *B. microti*-infected humans (Gagnon et al., 2022). The specificity of these antibody combinations was further tested using plasma from *B. duncani*-infected mice as well as supernatants from cultures of other *Babesia* species (*B. duncani* WA-1 isolate and *B. divergens Rouen87* strain) as well as two *Plasmodium falciparum strains* 3D7 and HB3) and we found strong specificity with the following combinations - 2H6-4C8, 1E11-4C8, 1E11-5C11, 4C8-1E11 and 4C8-5C11, where no significant signal above background could be detected (Figures 10A–E; Supplementary Figure S2).

Discussion

Mapping the binding sites of antibodies to proteins can be an invaluable tool in various fields including immunology, cellular biology, structural biology and pharmacology by unraveling important cellular processes such as immune signaling, receptor binding and pathogen invasion. Determining the sites of these antibody interactions could also facilitate the development of specific therapeutic and diagnostic strategies to fight pathogens and detect active infections. In this study, we have used this approach to map the specific sites of several monoclonal antibodies that bind to the most important immunogenic regions of the major antigen, BmGPI12, of the human pathogen *B. microti*.

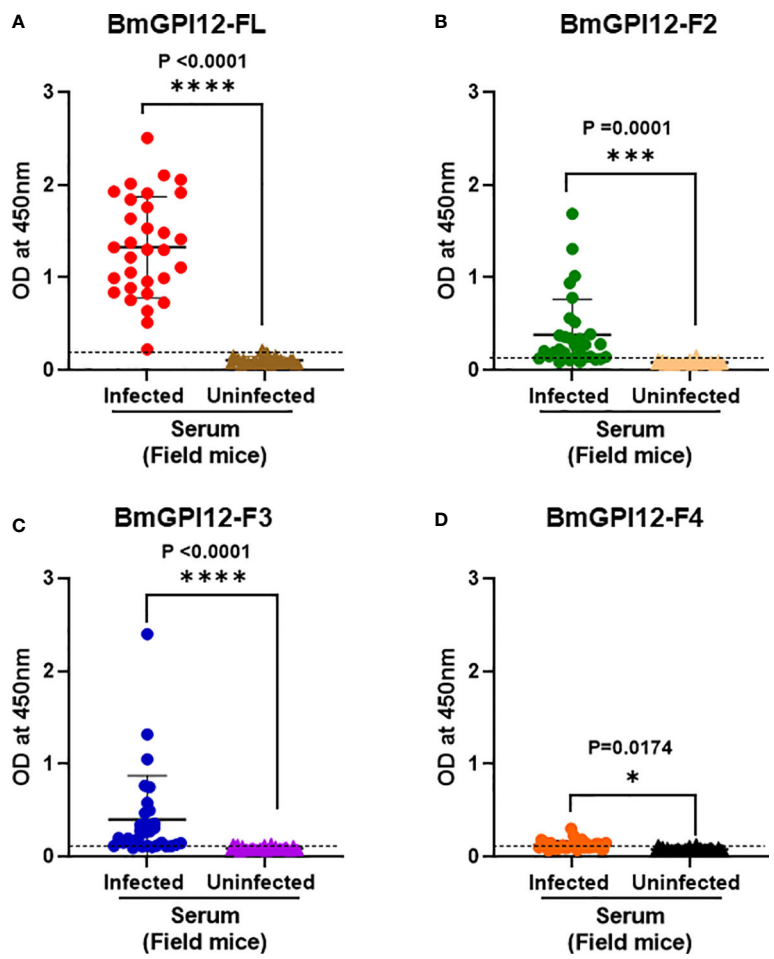

FIGURE 7
Immunodetection of recombinant BmGPI12 or sub-fragments using serum samples from wild mice. ELISA plates were coated with recombinant BmGPI12- full length (FL) **(A)**, sub-fragments F2 **(B)**, F3 **(C)** and F4 **(D)** at 50 ng/well. Graphs represent immunoreactivity of *Babesia* positive and negative wild mice sera (used at 1:200 dilution) to respective coated antigens. Red, green, blue and orange solid circles represent responses of *B microti* PCR positive samples to recombinant BmGPI12-FL, F2, F3 and F4 sub-fragments respectively. Brown, peach, purple and black solid triangles represent responses of *B microti* PCR negative samples to recombinant BmGPI12- FL, F2, F3 and F4 sub-fragments respectively. Each assay was conducted more than once with at least two technical replicates per assay. Error bars denote the standard deviation calculated using the Graphpad Prism 9.3 software. The OD_{450} cut-off (dashed line) denotes the mean + 2 x SD of the OD_{450} value of the negative samples. ****: statistically significant (p<0.0001, by two-way ANOVA); ***: statistically significant (p=0.0001, by two-way ANOVA); *: statistically significant (p=0.017, by two-way ANOVA).

Of 18 monoclonal antibodies characterized in this study, 14 showed strong signals by immunoblotting whereas the other 4 showed weak signal in this assay. On the other hand, only 2 antibodies (3B1 and 3A12) failed to detect the native BmGPI12 antigen by immunofluorescence. While we did not test all the antibodies by immunoelectron microscopy, out of 5 monoclonal antibodies tested (1G11, 1E11, 5C11, 4C8 and 1A5), only 5C11 showed the predicted localization of the antigen to the parasite plasma membrane as well as to the vesicular network produced by the parasite from this membrane as was previously demonstrated using polyclonal antibodies raised against the full length protein (Thekkiniath et al., 2019). The differences in the reactivity of these antibodies in different assays could be due to differences in epitope conformation in the native versus denatured antigen and the types of assays used.

Our strategy to map the specific sites of binding of monoclonal antibodies to BmGPI12 involved first identifying specific regions in the protein that are recognized by these antibodies and then designing overlapping 11 amino acid peptides covering these regions. Using 5 overlapping 100 amino acid sub-fragments (F1-F5) of BmGPI12, we were able to map 14 monoclonal antibodies to specific regions of the protein. Using plasma and sera from uninfected and *B. microti*-infected inbred mice, as well as sera samples from field mice

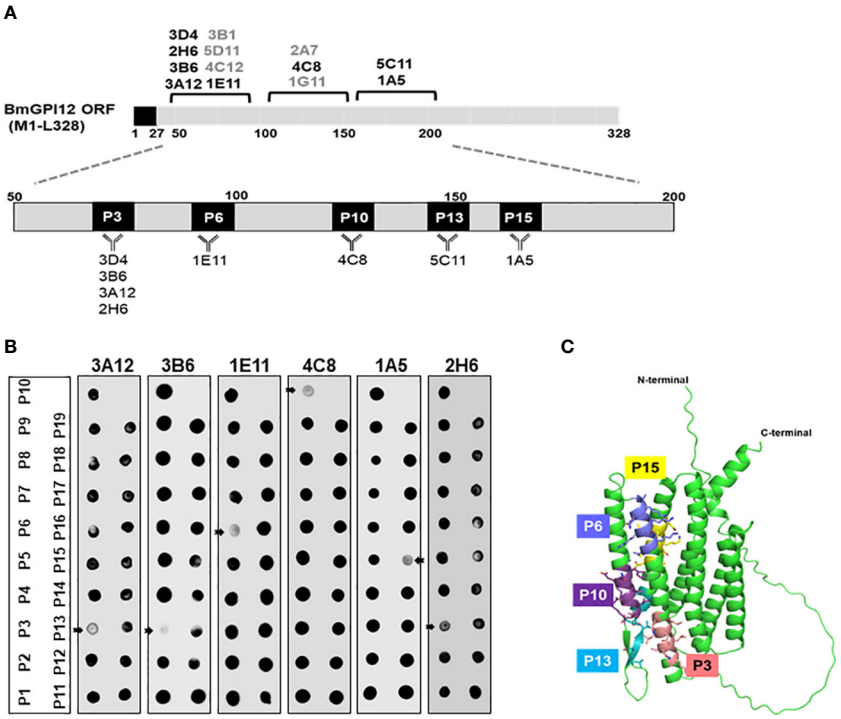

FIGURE 8
Epitope mapping of BmGPI12 monoclonal antibodies using overlapping peptides and localization of the peptides on the predicted BmGPI12 structure. **(A)** Schematic representation of the binding sites of 13 monoclonal antibodies to the BmGPI12 antigen. The specific 11-amino acid binding sites (P3, P6, P10, P13 and P15) recognized by the 8 monoclonal antibodies on BmGPI12 are highlighted. **(B)** Panels represent dot blot-based competition assays used to examine the interaction between the BmGPI12 antigen and various monoclonal antibodies in the presence of each of the overlapping nineteen 11-amino acid peptides (P1-19). The panel shows the analysis for 3A12, 3B6, 1E11, 4C8, 1A5 and 2H6 monoclonal antibodies. Arrows indicate where specific peptides block the binding of the MAb to the antigen. **(C)** Predicted three-dimensional structure of BmGPI12 and the location of the P3, P6, P10, P13 and P15 peptides.

(reservoir animals), we found that F2 and F3 were the most immunogenic fragments of the protein. Our results using sera from *B. microti*-infected field mice showed stronger serum immunoreactivity (97%) to recombinant full-length BmGPI12 protein compared to the F2 (80%) and F3 fragments (71%). This could be attributed to the presence of more epitopes on the full-length protein than on the individual fragments.

We also found that the immunogenic profile of BmGPI12 using sera from *B. microti*-infected field mice (reservoir) varied between individual mice. The differences are likely due to

TABLE 3 Primary sequences of the 5 BmGPI12 peptides recognized by a set of monospecific monoclonal antibodies.

BmGPI12 peptide #	Amino acid position	Peptide sequence	Monoclonal Antibodies
			3D4
			3B6
P3	66-76	KAVKLDLDLMK	3A12
			2H6
P6	90-100	VGKAKSKLNKL	1E11
P10	122-132	KFNENLVKIEK	4C8
P13	146-156	VDAVDDGVAGA	5C11
P15	162-172	SDISAIKTLTD	1A5

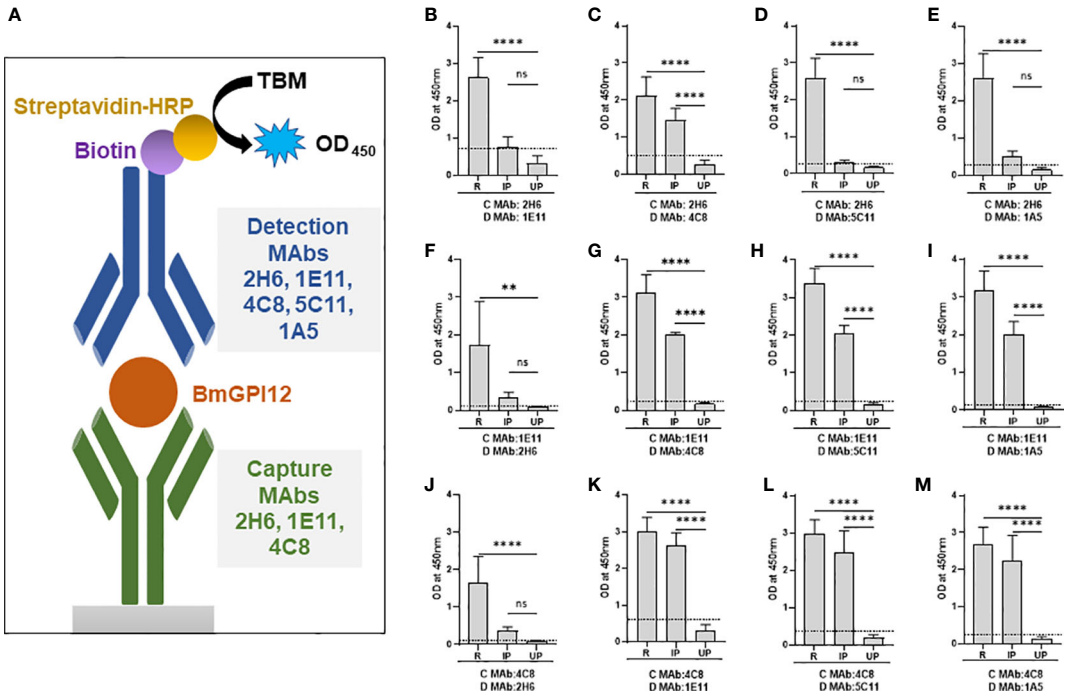

FIGURE 9
Monoclonal antibody combinations for detection of recombinant and native BmGPI12. **(A)** Schematic representation of the mGPAC antigen capture assay. MAb, monoclonal antibody; TMB, 3,3′,5,5′-Tetramethylbenzidine; HRP, Horseradish Peroxidase; OD_{450}, Optical Density at 450 nm. **(B-M)** mGPAC antigen capture ELISA was performed with different combinations of 2H6, 1E11, 4C8, 5C11 and 1A5 as either capture or detection antibodies. Assays were conducted using either recombinant BmGPI12 (R), plasma from uninfected (UP) or *B microti*-infected mice (IP). C: capture antibody; D: detection antibody. Each data set represents the mean of 3 independent experiments each performed in duplicates. Error bars denote the standard deviation calculated using the Graphpad Prism 9.3 software. ****, statistically significant ($p<0.0001$, by one-way ANOVA); **, statistically significant ($p=0.0015$, by one-way ANOVA); ns, non-significant. The OD_{450} cut-off (dashed line) denotes the mean + 2 x SD of the OD_{450} value of the uninfected plasma.

differences in parasitemia in the field mice and the immune response of each mouse to infection.

Our analysis of human plasma samples from *B. microti* positive and negative individuals showed a response profile similar to that observed in mouse. While the range of antibody reactivity varied between the full-length recombinant BmGPI12 and the F2 and F3 fragments, blood samples that displayed the strongest immunoreactivity to the full-length protein were also those that displayed the strongest reactivity to the F2 and F3 fragments. Competition studies using overlapping 11 amino acid peptides further mapped 8 of the anti-BmGPI12 monoclonal antibodies to 5 specific peptides within the highly immunogenic region of the antigen encompassing the F2 and F3 fragments. The predicted three dimensional structure of BmGPI12, which was generated using AlphaFold Protein Structure Database (Jumper et al., 2021; Varadi et al., 2022), showed that the N-terminal triple helix structures encompassing the F2 and F3 fragments contain the majority of the antigenic sites of the protein consistent with the high immunogenicity of this region. Noteworthy, the immunoreactivity of F1 and F4 with plasma from *B. microti*-infected humans was much higher than that from infected mice, highlighting differences between the two mammalian hosts in their response to *B. microti* infection.

While the exact role of BmGPI12 in *B. microti* virulence remains unknown, this protein has been demonstrated to be an excellent biomarker of active infection (Thekkiniath et al., 2018) and is highly conserved among six *B. microti* isolates examined by whole genome sequencing (Silva et al., 2016). Our epitope mapping of a set of BmGPI12 monoclonal antibodies that detect the native secreted antigen with high specificity was critical to our design of optimal antibody combinations for ELISA-based antigen capture assays and rapid detection of active *B. microti* infection. One such combination consisting of two MAbs, 1E11and 4C8, was found to be optimal for detection of *B. microti* infection in human blood (Gagnon et al., 2022). In addition to their use in the detection of active *B. microti* infection, these antibodies may serve as useful resources to understanding the biological function of this important antigen, unraveling its mode of secretion, and determining its host targets.

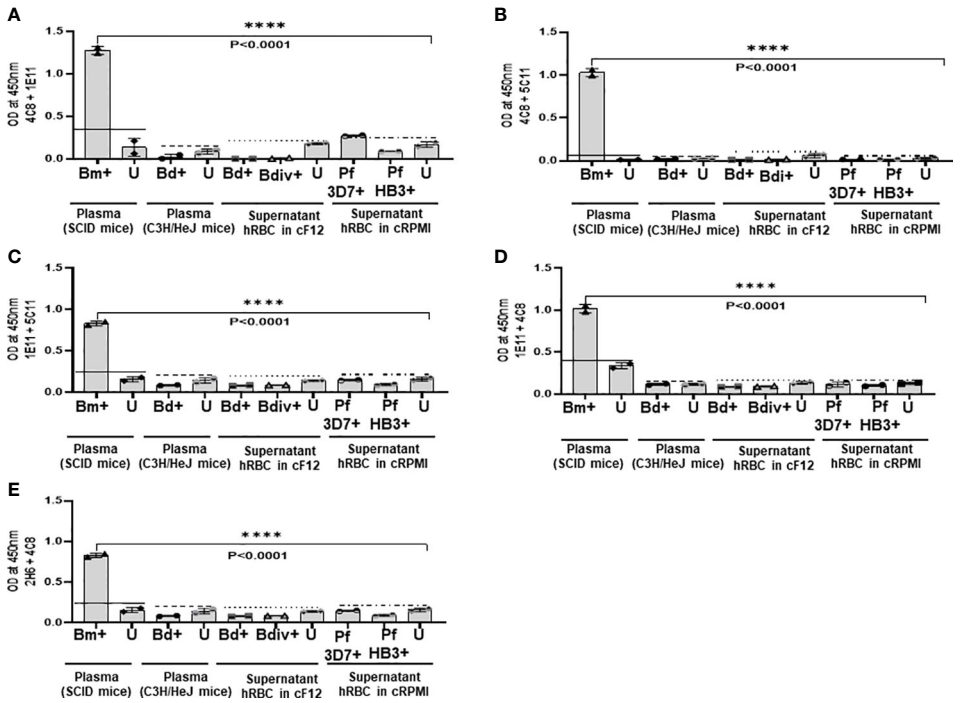

FIGURE 10
Specificity of the mGPAC assay. Antigen capture assays with different combinations **(A–E)** of anti-BmGPI12 monoclonal antibodies were conducted using culture supernatants from *B duncani WA-1* (25% parasitemia), *B divergens Rouen87* (10% parasitemia), *P. falciparum* 3D7 (10% parasitemia), and *P. f*alciparum HB3 (10% parasitemia)-infected human erythrocytes as well as heat inactivated plasma from uninfected or *B duncani*-infected C3H/HeJ mice (34% parasitemia). Plasma from *B microti* infected or uninfected SCID mice were used as positive and negative controls, respectively. Parasite cultures that were available in the laboratory at the time of the experiments were used. Error bars denote the standard deviation (SD) calculated using the Graphpad Prism 9.3 software. For each sample type, the OD_{450} cut-off (dashed line) denotes the mean + 2 x SD of the OD_{450} value of the corresponding uninfected sample. ****, statistically significant (p<0.0001, by one-way ANOVA). Bm, *B microti*; Bd, *B duncani*; Bdiv, *B >divergens*; Pf, *P. falciparum*; +: infected; U, uninfected; hRBCs, human red blood cells; cF12, complete DMEM-F12; cRPMI, complete RPMI.

Data availability statement

The original contributions presented in the study are included in the article/Supplementary Material. Further inquiries can be directed to the corresponding author.

Ethics statement

The animal study was reviewed and approved by Institutional Animal Care and Use Committees (IACUC) at Yale University.

Author contributions

MC, J-YC, PS, VK and AP: Investigation, methodology, formal analysis, visualization, writing original draft, review and editing. JG, ST, GG and JT: Investigation, methodology, review and editing. SW: Sample collection and analysis. CB and ML: Conceptualization, supervision, funding acquisition, project administration, writing original draft, review and editing. All authors have read and agreed to the published version of the manuscript. All authors contributed to the article and approved the submitted version.

Funding

The research described herein was supported by NIH grant A136118 to ML and CB. CB research is also supported by NIH grants AI138139, AI123321, AI152220 and AI153100 and AI136118; the Steven and Alexandra Cohen Foundation (Lyme 62 2020); the Global Lyme Alliance and The Blavatnik Family Foundation. The content is solely the responsibility of the authors and does not necessarily represent the official views of the National Institute of Health.

Acknowledgments

We thank Isaline Renard for providing blood samples from infected mice to use in some of the assays described in this study, Pratap Vydyam for doing short-term *in-vitro* culture of *B. microti*, Shalev Gihaz for generating the three-dimensional protein structure, Morven Graham and Xinran Liu for help with the IEM analyses, and Sara Mootien for her initial analysis of the monoclonal antibodies used in this study. We would also like to thank Dr. Laura Tonnetti and the American Red Cross for providing the blood samples for these studies.

Conflict of interest

Authors JG, ST, GG and ML are employed by L2 Diagnostics, United States.

The remaining authors declare that the research was conducted in the absence of any commercial or financial relationships that could be construed as a potential conflict of interest.

Publisher's note

All claims expressed in this article are solely those of the authors and do not necessarily represent those of their affiliated organizations, or those of the publisher, the editors and the reviewers. Any product that may be evaluated in this article, or claim that may be made by its manufacturer, is not guaranteed or endorsed by the publisher.

Supplementary material

The Supplementary Material for this article can be found online at: https://www.frontiersin.org/articles/10.3389/fcimb.2022.1039197/full#supplementary-material

References

Bastos, R. G., Thekkiniath, J., Ben Mamoun, C., Fuller, L., Molestina, R. E., Florin-Christensen, M., et al. (2021). Babesia microti immunoreactive rhoptry-associated protein-1 paralogs are ancestral members of the piroplasmid-confined RAP-1 family. *Pathogens* 10(11):1384–1398. doi: 10.3390/pathogens10111384

Bloch, E. M., Krause, P. J., and Tonnetti, L. (2021). Preventing transfusion-transmitted babesiosis. *Pathogens* 10(9):1176–1190. doi: 10.3390/pathogens10091176

Carpi, G., Walter, K. S., Mamoun, C. B., Krause, P. J., Kitchen, A., Lepore, T. J., et al. (2016). Babesia microti from humans and ticks hold a genomic signature of strong population structure in the united states. *BMC Genomics* 17, 888. doi: 10.1186/s12864-016-3225-x

Carvalho, L. J. M., Tuvshintulga, B., Nugraha, A. B., Sivakumar, T., and Yokoyama, N. (2020). Activities of artesunate-based combinations and tafenoquine against babesia bovis *in vitro* and babesia microti *in vivo*. *Parasit. Vectors* 13, 362. doi: 10.1186/s13071-020-04235-7

Chiu, J. E., Renard, I., George, S., Pal, A. C., Alday, P. H., Narasimhan, S., et al. (2022). Cytochrome b drug resistance mutation decreases babesia fitness in the tick stages but not the mammalian erythrocytic cycle. *J. Infect. Dis.* 225, 135–145. doi: 10.1093/infdis/jiab321

Chiu, J. E., Renard, I., Pal, A. C., Singh, P., Vydyam, P., Thekkiniath, J., et al. (2021). Effective therapy targeting cytochrome bc1 prevents babesia erythrocytic development and protects from lethal infection. *Antimicrob. Agents Chemother.* 65, e0066221. doi: 10.1128/AAC.00662-21

Cornillot, E., Dassouli, A., Pachikara, N., Lawres, L., Renard, I., Francois, C., et al. (2016). A targeted immunomic approach identifies diagnostic antigens in the human pathogen babesia microti. *Transfusion* 56, 2085–2099. doi: 10.1111/trf.13640

Cornillot, E., Hadj-Kaddour, K., Dassouli, A., Noel, B., Ranwez, V., Vacherie, B., et al. (2012). Sequencing of the smallest apicomplexan genome from the human pathogen babesia microti. *Nucleic Acids Res.* 40, 9102–9114. doi: 10.1093/nar/gks700

El Bissati, K., Zufferey, R., Witola, W. H., Carter, N. S., Ullman, B., and Ben Mamoun, C. (2006). The plasma membrane permease PfNT1 is essential for purine salvage in the human malaria parasite plasmodium falciparum. *Proc. Natl. Acad. Sci. U.S.A.* 103, 9286–9291. doi: 10.1073/pnas.0602590103

Gagnon, J., Timalsina, S., Choi, J. Y., Chand, M., Singh, P., Lamba, P., et al. (2022). Specific and sensitive diagnosis of babesia microti active infection using monoclonal antibodies to the immunodominant antigen BmGPI12. *J. Clin. Microbiol.*, 60(9)e0092522. doi: 10.1128/jcm.00925-22

Gilbert, L. (2021). The impacts of climate change on ticks and tick-borne disease risk. *Annu. Rev. Entomol.* 66, 373–388. doi: 10.1146/annurev-ento-052720-094533

Jumper, J., Evans, R., Pritzel, A., Green, T., Figurnov, M., Ronneberger, O., et al. (2021). Highly accurate protein structure prediction with AlphaFold. *Nature* 596, 583–589. doi: 10.1038/s41586-021-03819-2

Krause, P. J., Auwaerter, P. G., Bannuru, R. R., Branda, J. A., Falck-Ytter, Y. T., Lantos, P. M., et al. (2021). Clinical practice guidelines by the infectious diseases society of America (IDSA): 2020 guideline on diagnosis and management of babesiosis. *Clin. Infect. Dis.* 72, e49–e64. doi: 10.1093/cid/ciaa1216

Kumar, A., O'bryan, J., and Krause, P. J. (2021). The global emergence of human babesiosis. *Pathogens* 10(11): 1447–1470. doi: 10.3390/pathogens10111447

Lawres, L. A., Garg, A., Kumar, V., Bruzual, I., Forquer, I. P., Renard, I., et al. (2016). Radical cure of experimental babesiosis in immunodeficient mice using a combination of an endochin-like quinolone and atovaquone. *J. Exp. Med.* 213, 1307–1318. doi: 10.1084/jem.20151519

Meredith, S., Oakley, M., and Kumar, S. (2021). Technologies for detection of babesia microti: Advances and challenges. *Pathogens* 10(12):1563–1578. doi: 10.3390/pathogens10121563

Pal, A. C., Renard, I., Singh, P., Vydyam, P., Chiu, J. E., Pou, S., et al. (2022). Babesia duncani as a model organism to study the development, virulence and drug susceptibility of intraerythrocytic parasites *in vitro* and *in vivo*. *J. Infect. Dis* 226 (7):1267–1275. doi: 10.1093/infdis/jiac181

Renard, I., and Ben Mamoun, C. (2021). Treatment of human babesiosis: Then and now. *Pathogens* 10(9): 1120–1137. doi: 10.3390/pathogens10091120

Rosenberg, R., Lindsey, N. P., Fischer, M., Gregory, C. J., Hinckley, A. F., Mead, P. S., et al. (2018). Vital signs: Trends in reported vectorborne disease cases - united states and territories 2004-2016. *MMWR Morb Mortal Wkly Rep.* 67, 496–501. doi: 10.15585/mmwr.mm6717e1

Silva, J. C., Cornillot, E., Mccracken, C., Usmani-Brown, S., Dwivedi, A., Ifeonu, O. O., et al. (2016). Genome-wide diversity and gene expression profiling of babesia microti isolates identify polymorphic genes that mediate host-pathogen interactions. *Sci. Rep.* 6, 35284. doi: 10.1038/srep35284

Singh, P., Pal, A. C., and Ben Mamoun, C. (2022). An alternative culture medium for continuous *In vitro* propagation of the human pathogen *Babesia duncani* in human erythrocytes. *Pathogens* 11, 599. doi: 10.3390/pathogens11050599

Thekkiniath, J., Kilian, N., Lawres, L., Gewirtz, M. A., Graham, M. M., Liu, X., et al. (2019). Evidence for vesicle-mediated antigen export by the human pathogen babesia microti. *Life Sci. Alliance* 2(3):e201900382. doi: 10.26508/lsa.201900382

Thekkiniath, J., Mootien, S., Lawres, L., Perrin, B. A., Gewirtz, M., Krause, P. J., et al. (2018). BmGPAC, an antigen capture assay for detection of active babesia microti infection. *J. Clin. Microbiol.* 56(10):e00067–18. doi: 10.1128/JCM.00067-18

Tonnetti, L., Young, C., Kessler, D. A., Williamson, P. C., Reik, R., Proctor, M. C., et al. (2020). Transcription-mediated amplification blood donation screening for babesia. *Transfusion* 60, 317–325. doi: 10.1111/trf.15630

Varadi, M., Anyango, S., Deshpande, M., Nair, S., Natassia, C., Yordanova, G., et al. (2022). AlphaFold protein structure database: massively expanding the structural coverage of protein-sequence space with high-accuracy models. *Nucleic Acids Res.* 50, D439–D444. doi: 10.1093/nar/gkab1061

Vyas, J. M., Telford, S. R., and Robbins, G. K. (2007). Treatment of refractory babesia microti infection with atovaquone-proguanil in an HIV-infected patient: case report. *Clin. Infect. Dis.* 45, 1588–1590. doi: 10.1086/523731

frontiers | Frontiers in Cellular and Infection Microbiology

TYPE Original Research
PUBLISHED 28 November 2022
DOI 10.3389/fcimb.2022.1071988

OPEN ACCESS

EDITED BY
Mingming Liu,
Hubei University of Arts and Science, China

REVIEWED BY
Jixu Li,
Qinghai University, China
Xiao-Xuan Zhang,
Qingdao Agricultural University, China

*CORRESPONDENCE
Songrui Liu
srui_liu@163.com
Rong Hou
405536517@qq.com

†These authors have contributed equally to this work and share first authorship

SPECIALTY SECTION
This article was submitted to Parasite and Host, a section of the journal Frontiers in Cellular and Infection Microbiology

RECEIVED 17 October 2022
ACCEPTED 11 November 2022
PUBLISHED 28 November 2022

CITATION
Yue C, Yang W, Fan X, Lan J, Huang W, Zhang D, Li Y, Liao L, Ayala JE, Wu K, Liu Y, Zheng W, Li L, Zhang H, Su X, Yan X, Hou R and Liu S (2022) Seroprevalence and risk factors of *Toxoplasma gondii* infection in captive giant panda (*Ailuropoda melanoleuca*). *Front. Cell. Infect. Microbiol.* 12:1071988.
doi: 10.3389/fcimb.2022.1071988

Seroprevalence and risk factors of *Toxoplasma gondii* infection in captive giant panda (*Ailuropoda melanoleuca*)

Chanjuan Yue[1†], Wanjing Yang[1†], Xueyang Fan[1], Jingchao Lan[1], Wenjun Huang[1], Dongsheng Zhang[1], Yunli Li[1], Lihui Liao[1], James Edward Ayala[1], Kongju Wu[1], Yiyan Liu[1,2], Weichao Zheng[3], Lin Li[1], Hongwen Zhang[1], Xiaoyan Su[1], Xia Yan[1], Rong Hou[1*] and Songrui Liu[1*]

[1]Sichuan Key Laboratory of Conservation Biology for Endangered Wildlife, Chengdu Research Base of Giant Panda Breeding, Chengdu, Sichuan, China, [2]College of Veterinary Medicine, Sichuan Agricultural University, Chengdu, Sichuan, China, [3]Rare and Endangered Species Reintroduction and Species Monitoring Research Center, Schuan Academy of Giant Panda, Chengdu, Sichuan, China

Introduction: Toxoplasma gondii, a globally zoonotic protozoan parasite, infects most warm-blooded animals including the giant panda, and poses a serious threat to the giant panda conservation. However, the seroprevalence and the risk factors for toxoplasmosis in giant pandas are unknown. Here we aimed to determine the seroprevalence of *T. gondii* in the captive population of giant pandas and analyze the factors associated with the increased risk of infection.

Methods: A total of 203 serum samples were collected from 157 (95 females and 62 males) captive giant pandas from 2007 to 2022, antibodies against *T. gondii* were screened using commercial ELISA and MAT kits.

Results: The results showed 56 (35.67%) giant pandas were seropositive, age and transfer history between institutions were identifiified as risk factors for *T. gondii* infection. It is suggested that age-related seroprevalence was the main factor, and housing multiple species in the same environment may increase the chance of cross-infection of *T. gondii*.

Discussion: This study can provide research data for developing policies for the prevention and control of *T. gondii* and protecting the health of captive giant pandas and other wildlife.

KEYWORDS

***Toxoplasma gondii*, giant panda (ailuropoda melanoleuea), seroprevalence, wildlife conservation, zoonosis**

Introduction

Toxoplasma gondii is a globally distributed intracellular parasite capable of infecting almost all known warm-blooded animals, including giant pandas (*Ailuropoda melanoleuca*). Felines, especially feral domestic cats, are definitive/intermediate hosts of *T. gondii*, and contamination of the environment with fecal-containing oocysts from felines, is the main cause of toxoplasmosis transmission (Dubey, 2009). Toxoplasmosis can cause reproductive disorders in captive animals as well as livestock (Zhang et al., 2016), such as infertility, abortion, stillbirth, and weak fetuses, in addition, severe acute infection can even cause the death of the host (Dubey, 2022) with several infections and deaths of wildlife reported worldwide (Hollings et al., 2013; Lv et al., 2021).

The giant panda is considered a Class One protected species in China and is currently categorized as "vulnerable" by the International Union for Conservation of Nature (IUCN). One of the leading causes of death for both captive and wild giant pandas is parasitic diseases (Wang et al., 2018). It was reported that a captive giant panda in Zhengzhou zoo died of acute infection of *T. gondii* which showed that *T.* gondii can be an important factor in the health of giant pandas (Ma et al., 2015). However, to date, there are no reports about the prevalence of toxoplasmosis in giant pandas, and the major risk factors for the prevalence of *T. gondii* are also unknown. Therefore, this study aimed to estimate the seroprevalence and risk factors of *T. gondii* in captive giant pandas. Additionally, the association among age, season, and seroprevalence of *T. gondii* was investigated. Understanding the seroprevalence and risk factors associated with *T. gondii* can broaden our knowledge of the conservation of giant pandas, as well as guide us to formulate an appropriate plan for disease prevention and control within the population of this vulnerable species.

Materials and methods

Animal information and sampling

A total of 203 serum samples were collected from 157 (95 females and 62 males) giant panda individuals in four zoos, five breeding centers, and two nature reserves from 2007 to 2022 as part of a larger biomedical survey. One serum sample from each of the 157 giant pandas was selected for the serological investigation of *T. gondii* in this study. We classified giant pandas by the following age groups as described by Zhang and Wei (2006): cubs (0.5-2 years); sub-adults (3-5 years); adults (6-20 years); seniors (> 20 years). The dry and rainy seasons are divided according to the local statistics website of the national bureau of statistics (National Bureau of Statistics, 2022). In addition, to further study the correlation between age and the prevalence of *T. gondii*, nine adult giant panda individuals were selected from the Chengdu Research Base of Giant Panda Breeding (CRBGPB). For this subset, at least five serum samples were collected from each of the individuals during discontinuous or continuous years, with a total of 55 serum samples for this group. The nine adult giant pandas summary information was listed in Table 1.

TABLE 1 The summary information of the subset of nine adult giant pandas and the number of samples by year.

No.	Sex	Birth year	Source	Sample collected time			
A	Female	+/- 2006	Wild	2012	2013	2015	2017
				2018	2020		
B	Female	2005	Captive	2007	2012	2013	2013
				2018	2021		
C	Female	1999	Captive	2007	2012	2015	2016
				2018	2021		
D	Female	2007	Captive	2012	2013	2015	2016
				2018	2020		
E	Male	2004	Captive	2007	2012	2013	2015
				2016	2017	2018	2020
F	Male	2008	Captive	2015	2017	2018	2020
				2022			
G	Male	2008	Captive	2015	2017	2018	2020
				2022			
H	Male	2001	Captive	2012	2013	2015	2016
				2018	2022		
I	Female	2006	Captive	2007	2012	2013	2015
				2018	2020	2022	

This study took place in four regions of China (Sichuan, Shaanxi, Zhejiang, and Taiwan). The geographical distribution of giant pandas was as follows: 97.45% (153/157) of the samples were collected in Sichuan province; The remaining samples were collected from Zhejiang province (1/157), Shaanxi province (2/157) and Taiwan province (1/157). Among them, the largest captive population of giant pandas is in Sichuan province, with this province considered the conservation management center for the species. Therefore, the majority of the samples were collected from this region. However, the number of animals sampled per location depended on the number of transferred giant pandas (Figure 1).

Sample collection

The animal handling and sampling procedures were approved by the Institutional Animal Care and Use Committee (CRBGPB) (NO. 2020006). The samples were collected from the forelimb vein of a giant panda without anesthesia, taken in the anticoagulant-free vacuum blood collection tube, and then centrifuged at 3500 rpm for 10 mins for serum separation after coagulation, and the sera were stored at -80°C after divided and labeled for the following test. All serum samples were transported to the CRBGPB, Sichuan, China, for serological testing under low-temperature storage.

Serological analysis

A *T. gondii* MAT kit with a cut-off titer of 25 (University of Tennessee Research Foundation, Technology Transfer & Licensing, Memphis, USA) and a *T. gondii* ELISA kit (for multi-species, Haitai Biological Pharmaceuticals Co., Ltd, Zhuhai, China) were selected for detection of the giant panda *T. gondii* IgG antibody, the experimental procedure was performed according to the manufacturer's instructions. If both two tests showed positive, the result was judged as positive, otherwise, it was negative. If the two tests showed different results, the sample needed further verification. All of the tests were performed according to the methods described in our previous study (Yue et al., 2022).

Data analysis

Due to the small sample size of the cub age group, to better understand the relationship between the prevalence of toxoplasmosis in giant pandas, we used the following classification for statistical analysis: age (≦ 10 years old, 11-20 years old or ≧ 20 years old). We then compared these with age groups, sex (male or female), season condition (dry or rainy season) and transfer history (yes or no) were assessed using the Chi-square (χ^2) test or Fisher's exact test with "stats" package in R statistical software (version 4.1.2) (R Core Team, 2021). Multiple

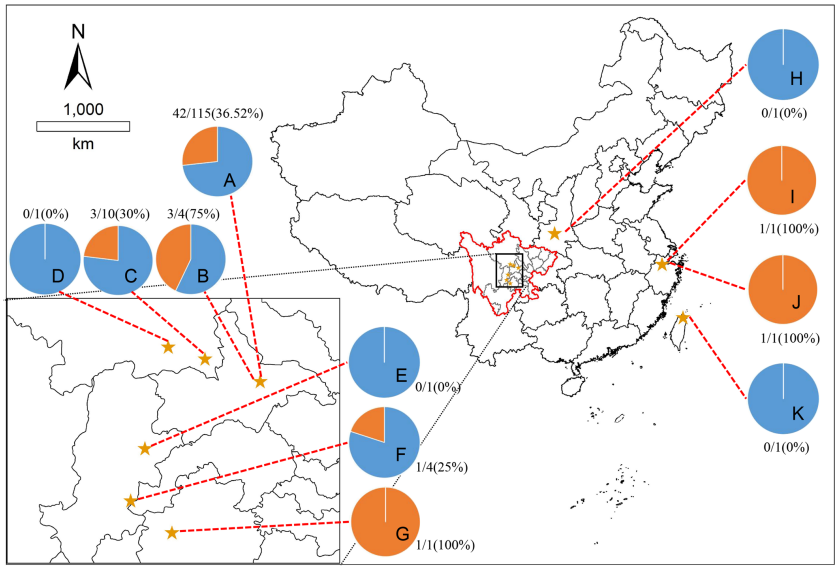

FIGURE 1
Map showing eleven sampling sites. The pie charts showed the seroprevalence of giant pandas for *T. gondii* in different sampling sites, the blue part is negative, and the orange part is positive. The locations represented by the letters: **(A)**, Chengdu Research Base of Giant Panda Breeding, Chengdu, Sichuan; **(B)**, Chengdu Zoo, Chengdu, Sichuan; **(C)**, Chengdu Field Research Center for Giant Panda-Panda Valley; **(D)**, China Conservation Research Center for Giant Panda, Wolong, Sichuan; **(E)**, China Conservation Research Center for Giant Panda, Yaan, Sichuan; **(F)**, Sichuan Daxiangling Research Base of Giant Panda Reintroduction, Sichuan; **(G)**, Heizhugou National Nature Reserve, Leshan, Sichuan; **(H)**, Shanxi Rare Wildlife Research Center Zhouzhi, Shaanxi; **(I)**, Hangzhou Zoo, Hangzhou, Zhejiang; **(J)**, Anji Bamboo Expo Park, Anji, Zhejiang; **(K)**, Taibei Zoo, Taibei, Taiwan.

logistic regression was performed by the Wald test with the "glm" function from the "stats" package in R to assess the effect of the above five variables on the prevalence of toxoplasmosis. A probability (p) value <0.05 was considered statistical significance in this study. The adjusted odds ratios (ORs) and 95% confidence intervals (CIs) revealed the associations between the risk factors and the presence of *T. gondii* in giant pandas.

The McNemar Chi-square test was used to analyze the difference in agreement between MAT and ELISA tests (P < 0.05 was considered a significant difference). The degree of agreement between MAT and ELISA was evaluated by Cohen kappa coefficient statistics (κ), the values of κ were interpreted as follows: 0.0-0.20 = slight agreement; 0.21-0.40 = fair agreement; 0.41-0.60= moderate agreement; 0.61-0.80 = substantial agreement; 0.81-0.1 = near perfect agreement.

A total of 55 serum samples from nine adult giant pandas were used to study the correlations between age and the prevalence of *T. gondii*. The data from August was removed from the analysis since there was only one sample. Statistically significant differences were set at p-value < 0.05.

Results

Evaluation of detection methods

Following the cut-off titer provided by the commercial kits, 157 serum samples were randomly selected from giant pandas and tested using the two methods. The antibodies titer to *T. gondii* of the MAT test is shown in Table 2. Among the 157 serum samples, 54 (34.4%, 95% CI: 26.96-41.83) were positive by ELISA, and 56 (35.67%, 95% CI: 28.18-43.16) by MAT (Table 3). The degree of agreement between MAT and ELISA was calculated using the Cohen kappa coefficient (κ), the κ of ELISA showed near perfect agreement (κ = 0.97, 95% CI: 0.93-1.00), and there was no significant difference between MAT and ELISA tests (P > 0.05). The seroprevalence was 34.40% (95% CI: 26.96-41.83) in ELISA (Table 3). After repeated experiments on samples with inconsistent results of the two tests, 56 of 157 samples were finally determined as positive.

Seroprevalence of *T. gondii* in giant panda

The results of the geographical distribution analysis showed that the seroprevalence was 32.69% for *T. gondii* of giant pandas in Sichuan province, 0% (0/1) in Shaanxi Province, 100% (2/2) in Zhejiang province, 0% (0/1) in Taiwan province; 73.25% (115/157) of the total samples were collected from the CRBGPB, and the seroprevalence of these samples was 36.52% (Figure 1).

In regards to seroprevalence in different age groups, seropositivity of *T. gondii* increased with age (Table 4). There was an increasing trend of the seropositivity, which was highest in seniors (73.33%, 11/15), followed by adults (49.32%, 36/73), sub-adults (4.55%, 2/44), and lastly cubs (4%, 1/25) (Figure 2). This suggested that increasing age is one of the important influencing factors of seroprevalence of *T. gondii* in giant pandas. To further study the changing trend of antibodies to *T. gondii* by age, a subset of nine individuals for which serum samples were collected over a period of at least five years were selected. As age increased, the antibodies to *T. gondii* changed from negative to positive in most of the giant pandas (6/9, panda A, B, C, D, G, H); one panda tested positive during the entire sample period (panda F), while the other two tested negative during the sample period (panda E and panda I) (Figure 3).

The seroprevalence of *T. gondii* for giant pandas which were transferred between other institutions, was higher (47.5%, 36.56-58.44% than giant pandas without transfer history (23.38%, 13.93-32.83%) (Table 4). The seroprevalence of *T. gondii* in giant pandas in different months was also studied among one hundred and fifty-seven individuals. The seroprevalence of *T. gondii* in giant pandas was highest in autumn, followed by spring, winter and summer; Meanwhile, the seroprevalence of *T. gondii* reached the peak in November, and the second peak was in March (Figure 4).

TABLE 2 Antibody titers to *T. gondii* of the MAT test.

MAT titer					Total
<25	1:25	1:50	1:100	1:200	
101	12	19	2	23	157

Risk factors

Univariate analysis of variance for the explanatory variables showed age (p < 0.01) and travel history (p < 0.01) were the two main factors strongly associated with the seropositivity of *T. gondii* (Table 4). However, factors like age < 10 years old, sex, and season were not classified as risk factors because the observed differences were not statistically significant. Furthermore, the results of multivariate logistic regression revealed that the >20 years of age group (OR = 7.87, 95% CI 2.31-31.86), the 11-20 age group (OR = 4.31, 95% CI 1.90-10.06), and the giant pandas that had transfer history (OR = 2.69, 95%CI 1.28-5.81) contributed to the high *T. gondii* seropositivity in this study (p < 0.05, Table 4).

Discussion

Toxoplasmosis is a disease that results from infection with the *Toxoplasma gondii*, which can cause death in wildlife (Rouatbi et al., 2019; Wilson et al., 2021). It is also a potentially serious threat to giant pandas, which can cause reproductive disorder and even death. As infected individuals

TABLE 3 The cross-classification and inter-agreement between MAT and ELISA for the detection of *T.gondii* antibodies in giant panda serum.

	MAT	ELISA		Total (Rate)
		+	-	
Cross-classification	+	54	2	56 (35.67%)
	–	0	101	101 (64.33%)
Total (Rate)		54 (34.40%)	103 (65.60%)	157
False negative rate (%)				0.00
False positive rate (%)				3.60
κ (95%CI)				0.97 (0.93-1.00)

$\chi 2$ = 148.45, P=0.500.
**P < 0.01, The difference is highly significant.
*0.01 < P < 0.05, difference significant.
P > 0.05, no significant difference.
κ ≤ 0.20, The degree of agreement between two methods is slight;
0.21 < κ ≤ 0.40, The degree of agreement between two methods is fair;
0.41 < κ ≤ 0.60, The degree of agreement between two methods is moderate;
0.61 < κ ≤ 0.80, The degree of agreement between two methods is substantial;
0.81 < κ ≤ 1, The degree of agreement between two methods is near perfect.

TABLE 4 Seroprevalence and risk factors associated with seropositivity of *T. gondii* in the giant panda.

Variable	Categories	n	Seroprevalence(%)	Differences 95% (%)		P-value	OR	Differences 95% CI		P-value
				Lower	Upper			Lower	Upper	
Sex	Female	95	33.68	24.18	43.18	0.64	baseline	–	–	–
	Male	62	38.71	26.59	50.85		1.24	0.58	2.64	0.58
Age	≦10	105	22.86	30.89	14.83	<0.01	baseline	–	–	–
	11-20	37	56.76	72.72	40.90		4.31	1.90	10.06	<0.01
	>20	15	73.33	95.71	50.96		7.87	2.31	31.86	<0.01
Season	Dry season	72	38.89	50.15	27.63	0.54	baseline	–	–	–
	Rainy season	85	32.94	42.93	22.95		1.036	0.381	2.84	0.945
Transfer history	No	77	23.38	32.83	13.93	<0.01	baseline	–	–	–
	Yes	80	47.5	58.44	36.56		2.69	1.28	5.81	0.01

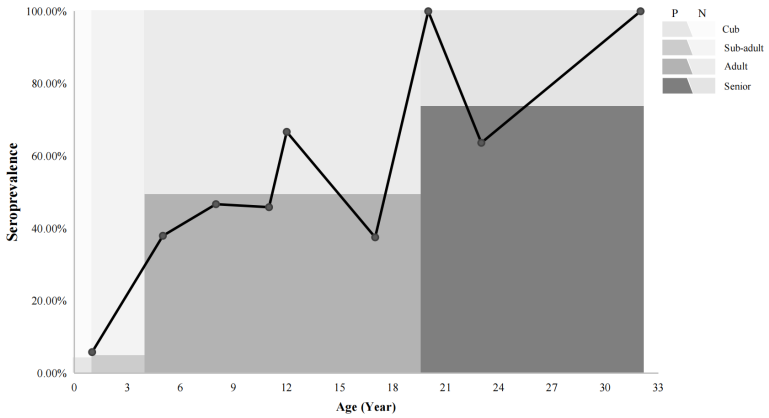

FIGURE 2
The relationships between the prevalence of giant pandas and age trends. P: positive, N: negative. The line chart shows the seroprevalence in different ages. The colors in the background indicated the percentage of the seroprevalence (The dark color: positive; The light color: negative) in different age groups.

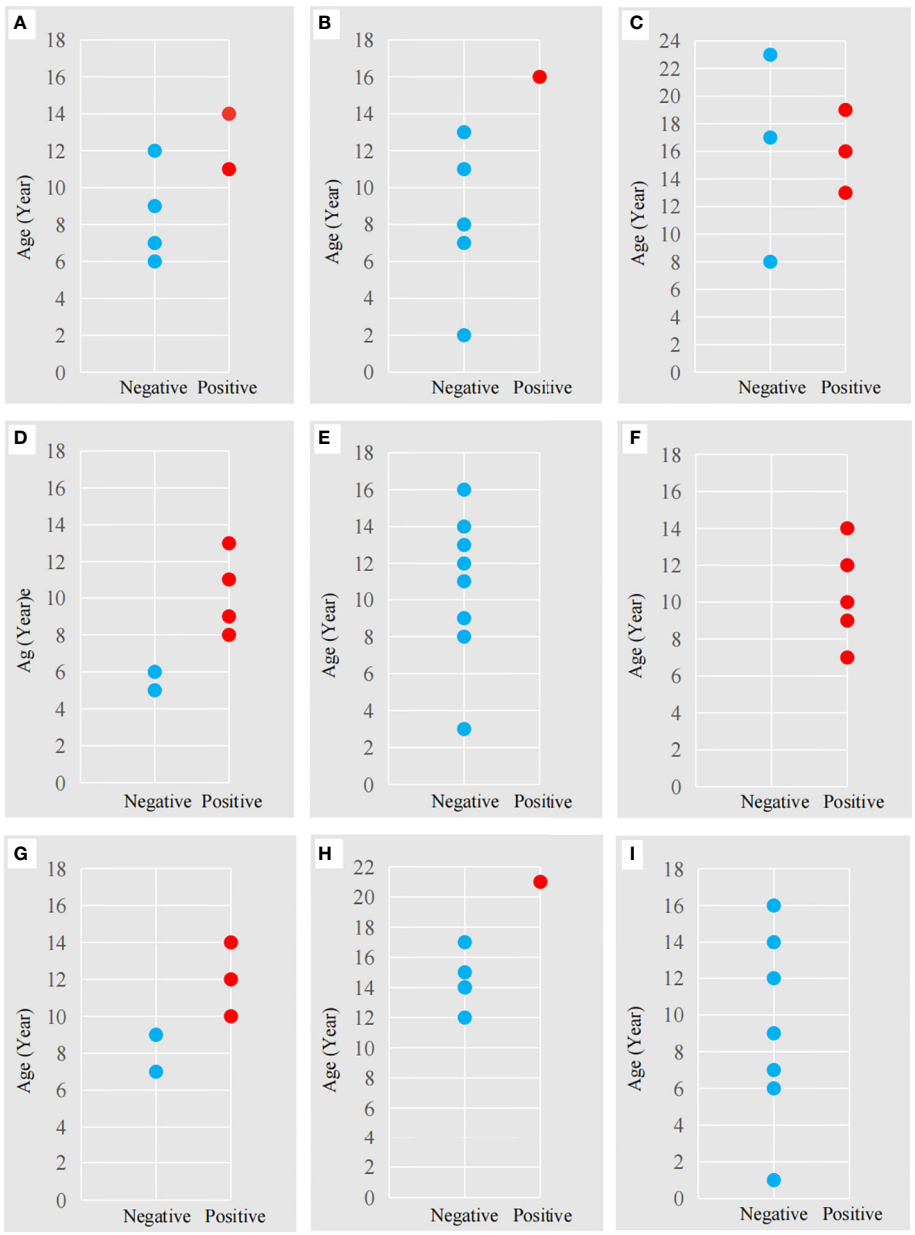

FIGURE 3
The antibodies to *T. gondii* in nine adult giant pandas at different ages. The letters **(A-I)** correspond to the nine adult giant pandas (Table 1) for which 55 serum samples were collected. Red dot: antibody-positive, Blue dot: antibody-negative. The abscissa represents a negative or positive result; The ordinate represents the age of the panda at the time of sample collection.

can be asymptomatic further investigation of this disease is necessary. Despite the risk of toxoplasmosis in giant pandas, there is limited data on the seroprevalence of *T. gondii* in the captive population of this vulnerable species. To the best of our knowledge, this is the first large-scale study to survey the seroprevalence and analyze the risk factors for the presence of *T. gondii* in the captive panda population. As the detection of the *T. gondii* infection in host primarily relies on serological assays, the serological methods used in this study were selected from our previous studies by comparing five commercial kits (Yue et al., 2022).

Our results showed the seroprevalence of *T. gondii* in giant pandas was 35.67%, which was consistent with Loeffler et al. (2007) (31.58%, 6/19), but was higher than Zhong et al. (2014)

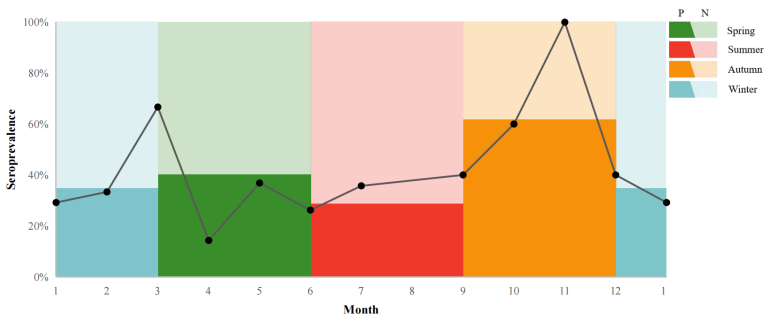

FIGURE 4
T. gondii seroprevalence giant pandas in different months. P: positive, N: negative. The line chart shows the seroprevalence in a different month. The colors in the background indicated the percentage of the seroprevalence (The dark color: positive; The light color: negative) in spring, summer, autumn, and winter.

(1.45%, 1/69), these differences may be due to the different diagnostic methods and study designs. These similar differences were found in other wildlife studies, such as in Ursidae species. In the US, previous studies have often used ELISA or MAT to detect *T. gondii* antibodies in different Ursidae species, with the seropositivity rates of black bears (*Ursus americanus*) ranging from 14.2% to 84.5%; the brown bears (*Ursus arctos*) ranged from 24.7% to 44.0%, and polar bears (*Ursus maritimus*) ranged from 18.5% to 45.6% (Dubey, 2022).

In the present study, we found that the seropositivity of *T. gondii* increased with age. Higher infection rates were found in the senior age group, and an age-related seroprevalence was seen in giant pandas, the seropositivity became high with increased age. Moreover, the old individuals may have some underlying diseases which enhanced their susceptibility to *T. gondii* infection. This result is in agreement with previous studies (Brandon-Mong et al., 2015; Deshmukh et al., 2021). In addition, our findings demonstrated that acquired infection may be the main rountion giant panda are infected with *T. gondii*. These results are consistent with previous findings in ursids (Briscoe et al. (1993), in which the prevalence of *T. gondii* in American black bears was found to increases with age.

Felines are the definitive host of *T. gondii*, infected cats can excrete oocysts into the environment, which could become a potential source of infection. Moreover, cats are popular pets in many households in both urban and rural areas, and the problem of disease transmission by stray cats has become increasingly prominent. Therefore, stray cats may be the main threat of *T. gondii* infection to the giant panda. Furthermore, rodents play an essential role in the life cycle of *T. gondii* and the epidemiology of toxoplasmosis because they are considered the primary source of infection (food and reservoir) for cats (Galeh et al., 2020). Both stray cats and rats often appear in or around the captive enclosures of giant pandas, and are difficult to control. Unfortunately, we did not collect enough data about *T. gondii* infection in stray cats and rats, so we cannot assess how serious a threat they pose to the health of captive giant pandas, this is also an important factor that needs to be investigated in the future.

As an iconic flagship species for wildlife conservation, the giant panda is considered a national treasure in China and plays a significant role not only as an umbrella species but also in national diplomacy and cultural communication. For cultural exchange, science popularization, and public education, some giant pandas will be transferred between zoos or breeding centers in different cities for exhibition. Based on our results, transferring the giant pandas between facilities was identified as one of the risk factors for *T. gondii* infection (OR = 2.69, $p < 0.05$). This result could be due to the zoos often keeping various species of animals, and as almost all known warm-blooded animals can be the intermediate host of *T. gondii*, infection rates may be higher. Therefore, managing multi-species in one area, such as in a zoo compared to breeding centers, which only have one species, may likely increase the risk of infection of *T. gondii*. Furthermore, the act of transferring giant panda or any animal is very stressful (Tang et al., 2019). This stress of moving to a new place, combined with acclimating to a new environment may reduce immune function and make the animal more vulnerable to infection.

Non-statistically significant associations were found between antibodies to *T. gondii* and sex and season. In addition, many studies showed there is no association between *T. gondii* and sex (Dubey, 2009; Must et al., 2015). The season was not an associated risk factor affecting the prevalence of *T. gondii* in giant pandas in this study. We also studied the trend of seroprevalence of *T. gondii* in giant pandas with month, and the seroprevalence was highest in November. However, other previous studies showed that the prevalence of *T. gondii* in the rainy season or monsoon associated with mild temperatures seems to be higher (Du et al., 2012), one study also mentioned the prevalence of *T. gondii* in foxes was lower at higher elevations with the cooler and drier area (Wei et al., 2021). Due to the rarity

and particularity of giant pandas, the collection of serum samples is often limited and few samples in some months, such as November (three samples), resulting in the fluctuation of seroprevalence. The trend of the seroprevalence of *T. gondii* with the month in giant pandas needs further investigation.

Conclusions

The *T.gondii* antibodies of 203 serum samples in giant pandas from 2007 to 2022 were detected and the distribution patterns of *T.gondii* infections were determined. The results showed 56 (35.67%) giant pandas were seropositive, age and transfer history between institutions were identified as risk factors for *T. gondii* infection. It is suggested that age-related seroprevalence was the main factor, and zoo housing, where multiple species are kept, may increase the chance of cross-infection of *T. gondii*. As an iconic flagship species and an umbrella species, the giant panda plays a vital role in wildlife conservation within China. It is hoped that these data can provide baseline information for developing policies and protecting the health of giant pandas and other wildlife.

Data availability statement

The raw data supporting the conclusions of this article will be made available by the authors, without undue reservation.

Ethics statement

The animal study was reviewed and approved by the Institutional Animal Care and Use Committee (CRBGPB) (NO. 2020006).

Author contributions

SL, RH, and CY contributed to conception and design of the study. WY, WH, DZ, KW, and LHL collected samples. JL, XS, HZ, and YYL organized the database. XF, WY, XY, YLL and WZ performed the statistical analysis. CY, LL, and WY wrote the first draft of the manuscript. CY, SL and JA wrote sections of the manuscript. All authors contributed to the article and approved the submitted version.

Funding

This research was supported by the Research Project of the Science and Technology Department of Sichuan Province (2020YJ0489), Chengdu Research Base of Giant Panda Breeding (2021CPB-B11, 2021CPB-B08) and National Forestry and Grassland Administration and Sichuan Province Finance Department (project title: study on main epidemiological investigation and prevention of giant panda).

Acknowledgment

We sincerely thank the veterinary staff and keepers of the Chengdu Research Base of Giant Panda Breeding and Zoos for their participation in the sample collection work, and James Edward Ayala for reviewing the manuscript.

Conflict of interest

The authors declare that the research was conducted in the absence of any commercial or financial relationships that could be construed as a potential conflict of interest.

Publisher's note

References

Brandon-Mong, G. J., Che Mat Seri, N. A., Sharma, R. S., Andiappan, H., Tan, T. C., Lim, Y. A., et al. (2015). Seroepidemiology of toxoplasmosis among people having close contact with animals. *Front. Immuno.* 6. doi: 10.3389/fimmu.2015.00143

Briscoe, N., Humphreys, J. G., and Dubey, J. P. (1993). Prevalence of *Toxoplasma gondii* infections in Pennsylvania black bears, *Ursus americanus*. *J. Wildl. Dis.* 29, 599–601. doi: 10.7589/0090-3558-29.4.599

Deshmukh, A. S., Hebbar, B. K., Mitra, P., Shinde, S., Chaudhari, S., and Barbuddhe, S. B. (2021). Seroprevalence and risk factors of *Toxoplasma gondii* infection among veterinary personnel and abattoir workers in central India. *Parasitol. Int.* 84, 102402. doi: 10.1016/j.parint.2021.102402

Dubey, J. P. (2009). History of the discovery of the life cycle of *Toxoplasma gondii*. *Int. J. Parasito* 39 (8), 877–882. doi: 10.1016/j.ijpara.2009.01.005

Dubey, J. P. (2022). *Toxoplasmosis of animals and humans. 3rd edition* (Boca Raton: CRC Press).

Du, F., Feng, H. L., Nie, H., Tu, P., Zhang, Q. L., Hu, M., et al. (2012). Survey on the contamination of *Toxoplasma gondii* oocysts in the soil of public parks of wuhan, China. *Vet. Parasitol.* 184 (2-4), 141–146. doi: 10.1016/j.vetpar.2011.08.025

Galeh, T. M., Sarvi, S., Montazeri, M., Moosazadeh, M., Nakhaei, M., Shariatzadeh, S. A., et al. (2020). Global status of toxoplasma gondii seroprevalence in rodents: A systematic review and meta-analysis. *Front. Vet. Sci.* 7. doi: 10.3389/fvets.2020.00461

Hollings, T., Jones, M., Mooney, N., and McCallum, H. (2013). Wildlife disease ecology in changing landscapes: Mesopredator release and toxoplasmosis. *Int. J. Parasitol. Parasites Wildl.* 2, 110–118. doi: 10.1016/j.ijppaw.2013.02.002

Loeffler, I. K., Howard, J., Montali, R. J., Hayek, L. A., Dubovi, E., Zhang, Z., et al. (2007). Serosurvey of ex-situ giant pandas (*Ailuropoda melanoleuca*) and red pandas (*Ailurus fulgens*) in China with implications for species conservation. *J. Zoo Wildl. Med.* 38 (4), 559–566. doi: 10.1638/2006-0008R.1

Lv, Q. B., Zeng, A., Xie, L. H., Qiu, H. Y., Wang, C. R., and Zhang, X. X. (2021). Prevalence and risk factors of toxoplasma gondii infection among five wild rodent species from five provinces of China. *Vector Borne Zoonotic Dis.* 21 (2), 105–109. doi: 10.1089/vbz.2020.2658

Ma, H. Y., Wang, Z. D., Wang, C. D., Li, C. W., Wei, F., and Liu, Q. (2015). Fatal *Toxoplasma gondii* infection in the giant panda. *Parasite* 22, 30. doi: 10.1051/parasite/2015030

Must, K., Lassen, B., and Jokelainen, P. (2015). Seroprevalence of and risk factors for *Toxoplasma gondii* infection in cats in Estonia. *Vector Borne Zoonotic Dis.* 15 (10), 597–601. doi: 10.1089/vbz.2015.1809

National Bureau of Statistics (2022) *Local statistics website*. Available at: http://www.stats.gov.cn/tjgz/wzlj/dftjwz/ (Accessed October 15, 2022).

R Core Team (2021). *R: A language and environment for statistical computing* (Vienna: R Foundation for Statistical Computing). Available at: https://www.R-project.org.

Rouatbi, M., Amairia, S., Amdouni, Y., Boussaadoun, M. A., Ayadi, O., Al-Hosary, A., et al (2019). *Toxoplasma gondii* infection and toxoplasmosis in north Africa: a review. infection par *Toxoplasma gondii* et toxoplasmose en afrique du nord : synthèse. *Parasit.* 26, 6. doi: 10.1051/parasite/2019006

Tang, D., Yang, B., Zhang, Z. Z., Wang, Y., Zhu, T., Wu, D. F., et al. (2019). Assessing transport stress on captive giant pandas by fecal steroids assay. *Chin. J. Wildl.* 40 (3), 753–757. doi: 10.3969/j.issn.1000-0127.2019.03.031

Wang, T., Xie, Y., Zheng, Y., Wang, C., Li, D., Koehler, A. V., et al. (2018). Parasites of the giant panda: A risk factor in the conservation of a species. *Adv. Parasitol.* 99, 1–33. doi: 10.1016/bs.apar.2017.12.003

Wei, X. Y., Gao, Y., Lv, C., Wang, W., Chen, Y., Zhao, Q., et al. (2021). The global prevalence and risk factors of *Toxoplasma gondii* among foxes: A systematic review and meta-analysis. *Microb. Pathog.* 150, 104699. doi: 10.1016/j.micpath.2020.104699

Wilson, A. ,. G., Wilson, S., Alavi, N., and Lapen, D. R. (2021). Human density is associated with the increased prevalence of a generalist zoonotic parasite in mammalian wildlife. *Proc. Biol. Sci.* 288 (1961), 20211724. doi: 10.1098/rspb.2021.1724

Yue, C. J., Yang, W. J., Li, Y. L., Zhang, D. S., Lan, J. C., Su, X. Y., et al. (2022). Comparison of a commercial ELISA and indirect hemagglutination assay with the modified agglutination test for detection of *Toxoplasma gondii* antibodies in giant panda (*Ailuropoda melanoleuca*). *Int. J. Parasitol. Parasites Wildl.* 18, 287–291. doi: 10.1016/j.ijppaw.2022.07.001

Zhang, X. X., Cong, W., Ma, J. G., Lou, Z. L., Zhao, Q., Meng, Q. F., et al. (2016). First genetic characterization of toxoplasma gondii infection in Arctic foxes (Vulpes lagopus) in China. *Infect. Genet. Evol.* 44, 127–129. doi: 10.1016/j.meegid.2016.06.042

Zhang, Z. H., and Wei, F. W. (2006). *Giant panda ex-situ conservation theory and practice* (Beijing: Science Press), 65.

Zhong, Z. J., Huang, X. M., Yang, Y., Wu, K. J., Xu, X. Y., Cao, X. F., et al. (2014). Serology analysis of Brucellosis,Toxoplasmosis and heartworm in giant pandas. *Sichuan J. Zool.* 33 (6), 836–839. doi: 10.3969/j.issn.1000-7083.2014.06.005

frontiers | Frontiers in Cellular and Infection Microbiology

TYPE Original Research
PUBLISHED 15 December 2022
DOI 10.3389/fcimb.2022.1029768

OPEN ACCESS

EDITED BY
Ningbo Xia,
South China Agricultural University, China

REVIEWED BY
Veeranoot Nissapatorn,
Walailak University, Thailand
Hong-Juan Peng,
Southern Medical University, China

*CORRESPONDENCE
Jixu Li
lijixu@qhu.edu.cn

†These authors have contributed equally to this work and share first authorship

SPECIALTY SECTION
This article was submitted to Parasite and Host, a section of the journal Frontiers in Cellular and Infection Microbiology

RECEIVED 27 August 2022
ACCEPTED 05 December 2022
PUBLISHED 15 December 2022

CITATION
Qi T, Ai J, Sun Y, Ma H, Kang M, You X and Li J (2022) Application of *Toxoplasma gondii*-specific SAG1, GRA7 and BAG1 proteins in serodiagnosis of animal toxoplasmosis. *Front. Cell. Infect. Microbiol.* 12:1029768. doi: 10.3389/fcimb.2022.1029768

Application of *Toxoplasma gondii*-specific SAG1, GRA7 and BAG1 proteins in serodiagnosis of animal toxoplasmosis

Tongsheng Qi[1,2†], Jingkai Ai[1,2†], Yali Sun[1,2,3], Hejia Ma[1,2], Ming Kang[1,2], Xiaoqian You[4] and Jixu Li[1,2,3*]

[1]State Key Laboratory of Plateau Ecology and Agriculture, Qinghai University, Xining, China, [2]College of Agriculture and Animal Husbandry, Qinghai University, Xining, China, [3]Qinghai Provincial Key Laboratory of Pathogen Diagnosis for Animal Diseases and Green Technical Research for Prevention and Control, Qinghai University, Xining, China, [4]Qinghai Animal Disease Control Center, Department of Agriculture and Rural Affairs of Qinghai Province, Xining, China

Toxoplasmosis is a zoonotic disease caused by the obligate intracellular protozoan parasite *T. gondii* which is widely prevalent in humans and animals worldwide. The diagnosis of toxoplasmosis and distinguishing acute or chronic *T. gondii* infections have utmost importance for humans and animals. The *Tg*SAG1, *Tg*GRA7, and *Tg*BAG1 proteins were used in the present study to develop the serological rSAG1-ELISA, rGRA7-ELISA and rBAG1-ELISA methods for the testing of *T. gondii* specific IgG and IgM antibodies and differentiating acute or chronic toxoplasmosis in 3733 animals, including Tibetan sheep, yaks, pigs, cows, cattle, horses, chickens, camels and donkeys from the Qinghai-Tibetan Plateau. The ELISA tests showed that the overall positivity of IgG antibody was 21.1% (786/3733), 15.3% (570/3733) and 18.2% (680/3733) for rSAG1-, rGRA7- and rBAG1-ELISA, respectively, and the positivity of IgM antibody was 11.8% (439/3733), 13.0% (486/3733) and 11.8% (442/3733) for rSAG1-, rGRA7- and rBAG1-ELISA, respectively. A total of 241 animals (6.5%) positive for all rSAG1-, rGRA7- and rBAG1-IgG were found in this study, and the 141 animals (3.8%) tested were anti-*T. gondii* IgM positive in all three ELISAs. Moreover, the 338, 284 and 377 animals were IgG positive in rSAG1 + rGRA7-, rBAG1 + rGRA7- and rSAG1 + rBAG1- ELISAs respectively, and the 346, 178 and 166 animals in rSAG1 + rGRA7-, rBAG1 + rGRA7- and rSAG1 + rBAG1-ELISAs were IgM positive respectively. The results confirmed that the application of SAG1, GRA7, and BAG1 recombinant antigens could successfully be used in the detection of specific IgG and IgM antibodies for distinguishing between acute or chronic *T. gondii* infections. It is inferred that the forms in which current animal species in the plateau area were infected with *T. gondii*, and the period

of infection or the clinical manifestations of the current infections may be different. The present study provides substantial clinical evidence for the differential diagnosis of toxoplasmosis, and the classification of acute and chronic *T. gondii* infections.

KEYWORDS

Toxoplasma gondii, SAG1, GRA7, BAG1, IgG, IgM, animals

1 Introduction

Toxoplasmosis is a zoonotic disease caused by the obligate intracellular protozoan parasite *T. gondii* which is widely prevalent among humans and animals worldwide (Robert-Gangneux and Dardé, 2012; Halonen and Weiss, 2013; Liu et al., 2015; Matta et al., 2021). Humans and animals can become the intermediate hosts of *T. gondii* through the ingestion of foods or water contaminated with oocysts of *T. gondii* shed with definitive host cats, or by eating undercooked or raw meats that contain tissue cysts of *T. gondii* (Robert-Gangneux and Dardé, 2012; Halonen and Weiss, 2013; Liu et al., 2015; Matta et al., 2021). *T. gondii* infections are characterized by significant morbidity and mortality in immunocompromised patients, such as individuals with AIDS, and serious congenital immune defects (Tenter et al., 2000). Common toxoplasmosis among both weakened humans and animals leads to neurological, ocular, and systemic diseases or abortion, stillbirths, and abnormalities or becoming carrier (Tenter et al., 2000). Thus, the infection of *T. gondii* is divided into acute infection caused by oocysts (sporozoite form) or tachyzoites and chronic infection caused by bradyzoites in a long-term presence in the host tissues (Dubey et al., 1998; Lyons et al., 2002). This chronic or latent infection generally exhibits a benign course in the immunocompetent population but can reactivate in people with weak immune systems (Montoya and Liesenfeld, 2004; Robert-Gangneux and Dardé, 2012; Saadatnia and Golkar, 2012; Lourido, 2019). Therefore, the diagnosis of toxoplasmosis and distinguishing acute or chronic *T. gondii* infections are important for humans and animals.

The diagnosis of toxoplasmosis can be achieved using microscopic examination, *in vitro* culture, animal inoculation, and molecular and serological methods, while the common approach is the serological assays using *T. gondii* tachyzoite lysate antigen or specific antigens (Terkawi et al., 2013; Döşkaya et al., 2014). ELISAs are reliable serological tests that have been developed for the detection of *T. gondii* infection in animals, and the key component of these methods is the selection of antigens with strong specificity and high sensitivity (Terkawi et al., 2013; Döşkaya et al., 2014). Recently, ELISA methods based on recombinant proteins have been developed to diagnose acute toxoplasmosis, such as surface-related proteins (SRS family), dense granule proteins (GRAs), and rhoptry proteins (ROPs) (Pietkiewicz et al., 2004; Terkawi et al., 2013; Döşkaya et al., 2014; Holec-Gąsior et al., 2014; Xicoténcatl-García et al., 2019; Teimouri et al., 2021). Among these *T. gondii* specific antigens, *Tg*SAG1 and *Tg*GRA7 are highlighted and have been widely used serologically to diagnose *T. gondii* infection (Terkawi et al., 2013; Xicoténcatl-García et al., 2019; Teimouri et al., 2021). *Tg*SAG1 is expressed on the surface of tachyzoites, which is a highly antigenic protein widely used for the diagnosis of *T. gondii* infection (Holec-Gąsior et al., 2014; Xicoténcatl-García et al., 2019; Teimouri et al., 2021). *Tg*GRA7 is a secreted protein and expressed by sporozoites, tachyzoites and early-stage bradyzoites, and GRA7 produces a very strong antibody response in the acute phase of infection caused by all three parasite forms (Terkawi et al., 2013; Xicoténcatl-García et al., 2019; Teimouri et al., 2021). Moreover, *Tg*BAG1 which is only expressed in bradyzoites, is a specific and characterized protein of the bradyzoite form and is a marker of *T. gondii* cyst infections (Döşkaya et al., 2014). The specific *T. gondii* antigens to sporozoite, tachyzoite and bradyzoite forms could be used to predict the infection stage.

Distinguishing between acute and chronic *T. gondii* infections could be achieved based on serological detection of immunoglobulin M (IgM) and immunoglobulin G (IgG) data (Montoya and Remington, 2008; Dhakal et al., 2015). Hence, the current study utilized the *Tg*SAG1, *Tg*GRA7, and *Tg*BAG1 proteins to develop serological rSAG1-, rGRA7- and rBAG1-ELISAs to test *T. gondii* specific IgG and IgM antibodies for distinguishing acute or chronic *T. gondii* infections in Tibetan sheep (*Ovis aries*), yaks (*Bos grunniens*), pigs (*Sus domesticus*), cows (*Bos taurus*), cattle (*Bos taurus domestica*), horses (*Equus ferus caballus*), chickens (*Gallus gallus domesticus*), camels (*Camelus bactrianus*) and donkeys (*Equus asinus*) from the Qinghai-Tibetan Plateau area.

2 Materials and methods

2.1 Serum collection from various animals in the Qinghai-Tibetan Plateau

In this study, a total of 3733 animal blood samples were collected from Tibetan sheep, yaks, pigs, cows, cattle, horses, chickens, camels and donkeys at 49 sampling sites in the 5 states and 2 cities in the Qinghai-Tibetan Plateau area (QTPA) with geographical coordinates of 31°36′-39°19′ N and 89°35′-103°04′ E from June 2021 to February 2022 as shown in Figure S1 and Table S1. Centrifugation of the fresh blood from different animals was performed at 5000 rpm for 10 minutes. The serum from the supernatant was transferred to new collection tubes. After excluding the unqualified serum (such as hemolytic samples), animal serum samples were frozen and stored at -80°C until assayed. All procedures were carried out according to the ethical guidelines of Qinghai University.

2.2 Cloning and expression of *T. gondii* specific-SAG1, GRA7 and BAG1 proteins

Amino acid sequence alignment and phylogenetic analyses for *Tg*SAG1, *Tg*GRA7, and *Tg*BAG1 with the related cycle-forming organizations (*Neospora caninum*, *Besnoitia species*, *Sarcocystis* species, etc.) were constructed using the maximum lifestyle statistical method and bootstrap analysis with 500 replications in MEGA7, and the sequences included *T. gondii* SAG1 (AFO54849.1), *N. caninum* SAG1 (AAD25091.1), *Sarcocystis neurona* SAG1 (AAK40366.1), *T. gondii* GRA7 (ABE69193.1), *N. caninum* GRA7 (AFB77190.1), *Besnoitia besnoiti* GRA7 (XP_029218567.1), *T. gondii* BAG1 (XP_002365116.1), *N. caninum* BAG1 (BAI44436.1), and *B. besnoiti* BAG1 (XP_029221932.1). The pGEX-4T-3-SAG1 and pGEX-4T-3-GRA7 plasmids from previous studies were used to produce recombinant *Tg*SAG1-GST and *Tg*GRA7-GST proteins (Kimbita et al., 2001; Masatani et al., 2013). The *BAG1* gene (*Toxoplasma* Genomics Resource TGME49_259020) was amplified by PCR from the cDNA of *T. gondii*. The primers that included a BamHI site (underlined) in the forward primer 5'- CGC GGATCC ATG GCG CCG TCA GCA TCG CAT -3' and a NotI site (underlined) in the reverse primer 5'- ATAAGAAT GCGGCCGC CTA CTT CAC GCT GAT TTG TTG CT-3' for the *BAG1* gene were used. The PCR products were digested with BamH I and Not I, and inserted into the pGEX-4T-1 plasmid vector treated with the same restriction enzymes (Roche, Switzerland). The recombinant pGEX-4T-1 empty vector, pGEX-4T-3-SAG1, pGEX-4T-3-GRA7, and pGEX-4T-1-BAG1 were expressed as glutathione s-transferase (GST) fusion proteins in *Escherichia coli* BL21(DE3) (New England BioLabs, USA) and purified with Glutathione-Sepharose 4B beads (GE Healthcare Life Sciences, USA) according to the manufacturer's instructions. The final concentrations of GST, r*Tg*SAG1-GST, r*Tg*GRA7-GST, and r*Tg*BAG1-GST proteins were measured with a bicinchoninic acid protein assay kit (Thermo Fisher Scientific, USA) before being used.

2.3 Development of indirect ELISAs based on rSAG1, rGRA7 and rBAG1 proteins

In this study, the r*Tg*SAG1-GST, r*Tg*GRA7-GST, and r*Tg*BAG1-GST proteins were used to establish the indirect rSAG1-ELISA, rGRA7-ELISA and rBAG1-ELISA to detect both IgG and IgM antibodies against *T. gondii* in the 3733 animals, including the 904 in Tibetan sheep, 752 in yaks, 496 in cows, 456 in pigs, 451 in cattle, 389 in horses, 199 in chickens, 49 in camels and 37 in donkeys. Briefly, the 1 μg/mL recombinant proteins were diluted in coating buffer (0.05 M carbonate-bicarbonate, pH 9.6). The animal sera were diluted by 1:100, and the secondary antibodies of anti-bovine, cow, sheep, horse, pig, chicken, donkey, and camel IgG or IgM as listed in Table S2, were diluted 1:3000-4000. The ABTS, (2,2'-azino-bis(3-ethylbenzothiazoline-6-sulfonic acid)) substrate, was used to show the OD 415 nm values. The soluble GST protein was used as the control under consistent experimental conditions with three ELISAs. In this study, the 5 positive and negative mouse sera for anti-*T. gondii*, *Neospora caninum* and *Sarcocystis gigantea* were used to assess the specificity of IgG-ELISA and IgM-ELISA based on GRA7, SAG1, BAG1, and GST proteins, respectively. Moreover, the coated *Tg*GRA7, *Tg*SAG1, *Tg*BAG1, and GST proteins at 2, 1, 0.5, 0.25, 0.125, and 0.0625 μg/mL, or anti-*T. gondii* positive and negative sera diluted 1:100, 200, 400, 800, 1600, 3200, 6400, 12800 and 25600, were used to develop the IgG-ELISAs and IgM-ELISAs for analyzing the sensitivity of the current tests, respectively. Moreover, the positive and negative animal serum samples for *T. gondii* IgG and IgM antibodies confirmed by the commercial ID Screen® Toxoplasmosis Indirect Multi-species ELISA kit (ID.vet, France) and our previous study (Li et al., 2021) were used as controls. All controls were re-confirmed using the ELISA tests based on tachyzoite and bradyzoite lysate antigens under the current protocol. Furthermore, the commercial kit (ID Screen® Toxoplasmosis Indirect Multi-species ELISA, ID.vet, Grabels, France) was used to confirm the currently determined seropositive and seronegative samples from at least one animal species.

2.4 Data analysis

For the resulting judgment, the cut-off points were calculated as the mean values of OD 415 nm for the negative sera (including the serum samples of 30 Tibetan sheep, 30 yaks, 30 cows, 30 pigs, 30 cattle, 20 horses, 20 chickens, 5 camels, and 5 donkeys) kept in our lab (Qinghai University, Xining, China) (Li et al., 2021) plus three times the standard deviations of OD 415 nm values of these negative controls: the mean (X) and standard

deviation (SD) of the negative control results were calculated, and the X+3SD was the cut-off values. The OD 415 values of the tested animals were greater than the respective cut-off values assessed as positive. For the weak positive samples with similar cut-off values or lighter colors were repeated with the second doubtful result being treated as negative samples. To graph and analyze the data, GraphPad Prism 8 software (GraphPad Software Inc., USA) was used. The prevalence and 95% confidence intervals per pathogen species were calculated using the OpenEpi program (http://www.openepi.com/Proportion/Proportion.htm). The chi-squared test was used to compare the proportions of determined seropositivity in animals from different regions. The differences were considered to be statistically significant when the resulting *P*-values were < 0.05.

3 Results

3.1 Establishment of rSAG1-ELISA, rGRA7-ELISA and rBAG1-ELISA tests

In this study, the amino acid sequence alignment analysis was performed on the SAG1, GRA7, and BAG1 proteins of *T. gondii* with the related cyst-forming organisms (*Neospora caninum*, *Besnoitia* species, *Sarcocystis* species, etc.), and shared the homology of 5.0-86.8% (Figure S2). The r*Tg*SAG1-GST, r*Tg*GRA7-GST, and r*Tg*BAG1-GST proteins were expressed (Figure 1), and used to establish the indirect rSAG1-ELISA, rGRA7-ELISA and rBAG1-ELISA methods for identifying the carrier animals of *T. gondii* specific-IgG and IgM antibodies, and comparing the differences among three antigens in the serodiagnosis of animal toxoplasmosis in various animals from the Qinghai-Tibetan Plateau.

The IgG-ELISAs (Figure S3A) and IgM-ELISAs (Figure S3B) based on *Tg*GRA7, *Tg*SAG1, *Tg*BAG1, and GST proteins were performed to detect mouse anti-*T. gondii*, *N. caninum*, and *S. gigantea* positive sera to analyze the specificity of the current ELISA tests in this study respectively. The results showed that GRA7-, SAG1-, and BAG1-ELISAs only reacted with the positive sera of *T. gondii* but did not respond to the positive sera of *N. caninum* and *S. gigantea* (Figure S3). The GST protein did not react with any serum (Figure S3). In addition, the results show that the current ELISA reactions could occur when the concentration of coated proteins was very low under a positive serum dilution of 1:100 (Figure S4). Moreover, the OD values at the serum dilution of 1:800-6400 were still greater than the cut-off values (calculated using the OD values of negative controls), while GST protein did not demonstrate any response (Figure S5). These results suggest that the detection methods employed were highly specific and sensitive.

The 5-30 negative sera confirmed by our previous study (Li et al., 2021) and the commercial kits were used to detect OD 415 values in the different animal species, and calculate the cut-off values for IgG and IgM determination in Tibetan sheep, yaks, cows, pigs, cattle, horses, chickens, camels, and donkeys as shown in Figures 2A, B. The glutathione s-transferase (GST)-ELISA tests showed no-reaction with *T. gondii* positive sera under the same experimental conditions (Figure S3).

3.2 Detection of *T. gondii* IgG and IgM antibodies in animals

As shown in Figure 3 and Table 1, rSAG1-ELISA, rGRA7-ELISA and rBAG1-ELISA were used to detect *T. gondii* IgG and IgM antibodies in the same animals. The results showed that the overall positivity of IgG antibody was 21.1% (786/3733), 15.3% (570/3733) and 18.2% (680/3733) for rSAG1-ELISA, rGRA7-ELISA and rBAG1-ELISA respectively (Figures 3A, B), and the 11.8% (439/3733), 13.0% (486/3733) and 11.8% (442/3733) of

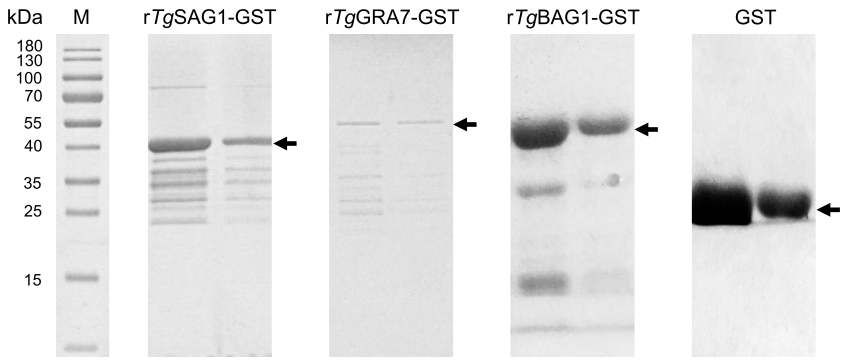

FIGURE 1
The recombinant SAG1, GRA7 and BAG1 proteins of *T. gondii* was expressed. SDS-PAGE analysis showed the rSAG1, rGRA7, rBAG1 and GST proteins.

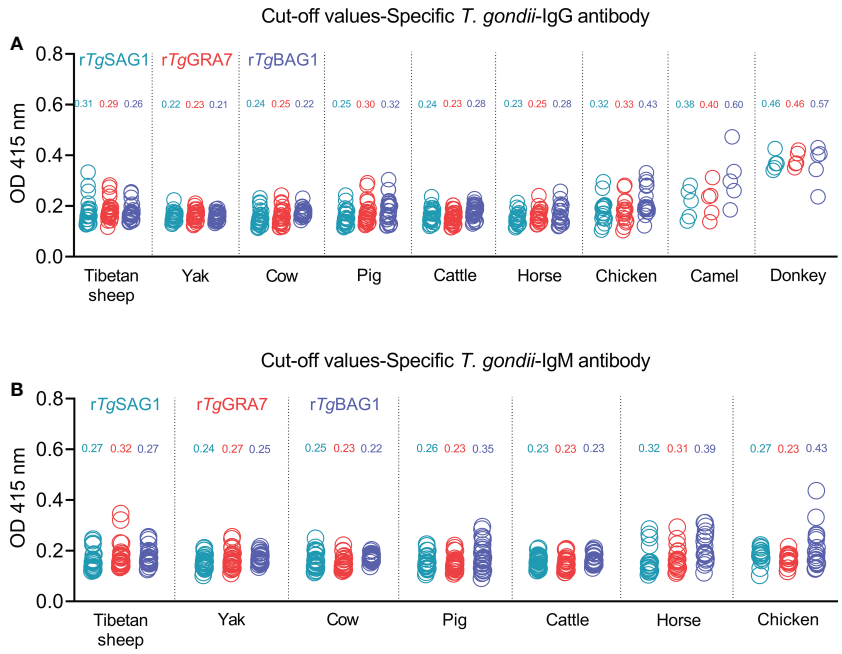

FIGURE 2
Establishment of rSAG1-ELISA, rGRA7-ELISA and rBAG1-ELISA tests and calculating the cut-off values for *T. gondii* IgG **(A)** and IgM **(B)** antibodies.

the animals were IgM antibody-positive for rSAG1-ELISA, rGRA7-ELISA and rBAG1-ELISA respectively (Figures 3C, D).

In ELISA tests, the pig was the most prevalent animal in both rSAG1-ELISA and rGRA7-ELISA and the donkey was the most prevalent animal in rBAG1-ELISA for IgG positivity, while horses had the highest IgM positivity according to all three methods (Figure 3 and Table 1). Specifically, our results revealed that the animals with the next highest IgG positivity rates in the rSAG1-tests were donkeys, chickens, camels, Tibetan sheep, yaks, cattle and cows; those with the next highest rates in the rGRA7- tests were donkeys, chickens, camels, Tibetan sheep, yaks, cattle, horses and cows; and those with the next highest rates in the rBAG1-IgG tests were pigs, camels, chickens, cows, yaks, Tibetan sheep, cattle and horses. However, the results showed that the animals with the next

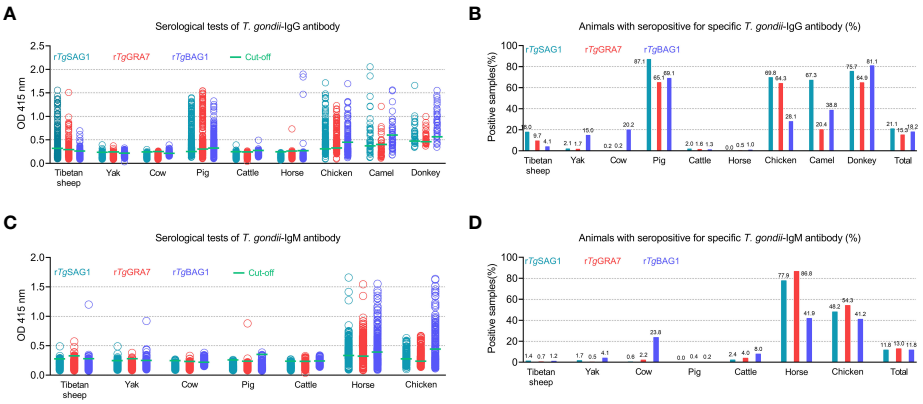

FIGURE 3
Detection of *T. gondii* IgG **(A, B)** and IgM **(C, D)** antibodies in various animals in the Qinghai-Tibet Plateau by the indirect ELISA methods based on SAG1, GRA7 and BAG1 antigens in this study.

10.3389/fcimb.2022.1029768

TABLE 1 Seroprevalence of specific-*T. gondii* IgG and IgM antibodies in various animals.

Animal	No. tested	IgG-SAG1 (%, 95% CI)	IgG-GRA7 (%, 95% CI)	IgG-BAG1 (%, 95% CI)	IgM-SAG1 (%, 95% CI)	IgM-GRA7 (%, 95% CI)	IgM-BAG1 (%, 95% CI)
Tibetan sheep	904	163 (18.0, 15.5-20.5)	88 (9.7, 7.8-11.7)	37 (4.1, 2.8-5.4)	13 (1.4, 0.7-2.2)	6 (0.7, 0.1-1.2)	11 (1.2, 0.5-1.9)
Yak	752	16 (2.1, 1.1-3.2)	13 (1.7, 0.8-2.7)	113 (15.0, 12.5-17.6)	13 (1.7, 0.8-2.7)	4 (0.5, 0.0-1.1)	31 (4.1, 2.7-5.5)
Cow	496	1 (0.2, 0.2-0.6)	1 (0.2, 0.2-0.6)	100 (20.2, 16.6-23.7)	3 (0.6, 0.1-1.3)	11 (2.2, 0.9-3.5)	118 (23.8, 20.0-27.5)
Pig	456	397 (87.1, 84.0-90.1)	297 (65.1, 60.8-69.5)	315 (69.1, 64.8-73.3)	0	2 (0.4, 0.2-1.0)	1 (0.2, 0.2-0.6)
Cattle	451	9 (2.0. 0.7-3.3)	7 (1.6, 0.4-2.7)	6 (1.3, 0.3-2.4)	11 (2.4, 1.0-3.9)	18 (4.0, 2.2-5.8)	36 (8.0, 5.5-10.5)
Horse	389	0	2 (0.5, 0.2-1.2)	4 (1.0, 0.0-2.0)	303 (77.9, 73.8-82.0)	337 (86.8, 83.3-90.0)	163 (41.9, 37.0-46.8)
Chicken	199	139 (69.8, 63.5-76.2)	128 (64.3, 57.7-71.0)	56 (28.1, 21.9-34.4)	96 (48.2, 41.3-55.2)	108 (54.3, 47.3-61.2)	82 (41.2, 34.4-48.0)
Camel	49	33 (67.3, 54.2-80.5)	10 (20.4, 9.1-31.7)	19 (38.8, 25.1-52.4)	/	/	/
Donkey	37	28 (75.7, 61.9-89.5)	24 (64.9, 49.5-80.2)	30 (81.1, 68.5-93.7)	/	/	/
Total	3733	786 (21.1, 19.7-22.4)	570 (15.3, 14.1-16.4)	680 (18.2, 17.0-19.5)	439 (11.8, 10.7-12.8)	486 (13.0, 11.9-14.1)	442 (11.8, 10.8-12.9)

%, Prevalence. 95% CI, 95% Confidence Interval./, no tested.

highest positivity rates of IgM antibodies in the rSAG1- tests were followed by chickens, cattle, yaks, Tibetan sheep and cows; those in the rGRA7- tests were followed by chickens, cattle, cows, Tibetan sheep, yaks and pigs; those in the rBAG1-IgG tests were followed by chickens, cows, cattle, yaks, Tibetan sheep and pigs. Moreover, the results of the analysis of the positivity of animals for both IgG and IgM antibodies based on the same antigen, revealed that 2.0%, 2.5% and 1.5% of the animals exhibited both IgG and IgM positivity in the rSAG1-ELISA, rGRA7-ELISA and rBAG1-ELISA tests, respectively (Table 2).

In order to confirm the current ELISAs, the 50 seropositive and 50 seronegative samples determined with the current IgG-ELISA based on SAG1 in pigs were selected to compare with the commercial kits based on *Tg*SAG1 protein. The results showed an 82% match rate between the kits and the current SAG1-IgG ELISA, including a 68% match rate for positive and 92% for negative samples (Table S3). According to these results (Table S3), we calculated that the serological *T. gondii* IgG-ELISA assay based on the SAG1 protein established in pigs in this study had a sensitivity of 89.7% and a specificity of 75.4%.

TABLE 2 Animals with seropositive for both IgG and IgM antibodies in rSAG1-ELISA, rGRA7-ELISA and rBAG1-ELISA tests.

Animal	No. tested	rSAG1-ELISA (%, 95% CI)	rGRA7-ELISA (%, 95% CI)	rBAG1-ELISA (%, 95% CI)
Tibetan sheep	904	3 (0.3, 0.0-0.7)	4 (0.4, 0.0-0.9)	2 (0.2, 0.1-0.5)
Yak	752	0	0	7 (0.9, 0.2-1.6)
Cow	496	0	0	44 (8.9, 6.4-11.4)
Pig	456	0	2 (0.4, 0.2-1.0)	0
Cattle	451	0	2 (0.4, 0.2-1.1)	0
Horse	389	0	1 (0.3, 0.2-0.8)	1 (0.3, 0.2-0.8)
Chicken	199	71 (35.7, 29.0-42.3)	83 (41.7, 34.9-48.6)	3 (1.5, 0.2-3.2)
Camel	49	/	/	/
Donkey	37	/	/	/
Total	3733	74 (2.0, 1.5-2.4)	92 (2.5, 2.0-3.0)	57 (1.5, 1.1-1.9)

%, Prevalence. 95% CI, 95% Confidence Interval./, no tested.

3.3 Analysis of animal co-positive for rSAG1-ELISA, rGRA7-ELISA and rBAG1-ELISA

A total of 241 animals (6.5%) with all rSAG1-, rGRA7- and rBAG1-IgG positivity were found in this study (Table 3), and the 141 animals (3.8%) tested which included 130 horses and 11 chickens were anti-*T. gondii* IgM positive in all three ELISAs (Table 4). Moreover, a total of 338, 284 and 377 animals were IgG positive in the rSAG1 + rGRA7-, rBAG1 + rGRA7- and rSAG1 + rBAG1- ELISAs respectively (Table 3), and 346, 178 and 166 animals in the rSAG1 + rGRA7-, rBAG1 + rGRA7- and rSAG1 + rBAG1-ELISAs were IgM positive respectively (Table 4). Furthermore, the 1796 animals (48.1%) were positive animals for IgG and IgM antibodies in at least one specific *T. gondii* antigen, and 29.8% of animals (1111/3733) were IgG-positive for at least one specific *T. gondii* antigen and a total of 825 animals (22.1%) were IgM-positive for at least one antigen (Table 5).

3.4 Analysis of the effect of altitude on the animal seropositive for *T. gondii*-specific antibodies

To determine the influence of altitude on the positivity of *T. gondii* IgG and IgM antibodies, all animals were differentiated into three groups, including 2000-3000, 3000-4000, and 4000-5000 m altitudes (Table S4). The results revealed that significant differences ($P < 0.05$) were found in Tibetan sheep, cattle, yaks and horses from different altitudes (Table S4).

4 Discussion

In this study, serological ELISA diagnostic methods based on *Tg*SAG1, *Tg*GRA7 and *Tg*BAG1 antigens present in the different *T. gondii* forms were established to analyze the positivity rates of specific *T. gondii* IgG and IgM antibodies in Tibetan sheep, yaks, pigs, cows, cattle, horses, chickens, camels and donkeys from the Qinghai-Tibetan Plateau. The differences in IgG or IgM antibody levels in the serum of the same animal were detected among rSAG1-ELISA, rGRA7-ELISA and rBAG1-ELISA. Moreover, there were also large differences in the overall positivity rates of antibodies detected by the three antigens in 3733 serum samples. Therefore, we infer that the parasite forms in which current animal species in the QTPA were infected with *T. gondii*, and the period of infection or the clinical manifestations of the current infection may be different.

Usually, the animals are infected with *T. gondii* by accidentally ingesting oocysts and tissue cysts while eating or drinking (Dubey, 2009; Cenci-Goga et al., 2011; Hill and Dubey, 2013). Sporozoites and bradyzoites were released after the ingestion of oocysts or tissue cysts, invaded the intestinal cells, and quickly differentiated into tachyzoites in 12 and 18 hours, respectively (Dubey, 1997; Dubey et al., 1997). When subjected to strong immune resistance, tachyzoites will transform into bradyzoites to form tissue cysts that persist in the body for a long time. Therefore, throughout the transition process, the bodies of humans and animals will produce specific antibodies against the antigens of the different forms of *T. gondii*. Current specific *T. gondii* antigens used, including SAG1 expressed in the tachyzoite form, GRA7 expressed in sporozoite, tachyzoite and bradyzoite forms, and BAG1 expressed in the bradyzoite form, should be markers for the different parasite stages.

TABLE 3 Specific-*T. gondii* IgG-positive animals based on among SAG1, GRA7 and BAG1 proteins.

Animal	No. tested	Both IgG-SAG1 and IgG-GRA7 positive (%, 95% CI)	Both IgG-BAG1 and IgG-GRA7 positive (%, 95% CI)	Both IgG-SAG1 and IgG-BAG1 positive (%, 95% CI)	Among IgG-SAG1, -GRA7 and-BAG1 positive (%, 95% CI)
Tibetan sheep	904	28 (3.1, 2.0-4.2)	5 (0.6, 0.1-1.0)	10 (1.1, 0.4-1.8)	2 (0.2, 0.1-0.5)
Yak	752	0	1 (0.1, 0.1-0.4)	3 (0.4, 0.1-0.8)	0
Cow	496	0	0	0	0
Pig	456	187 (41.0, 36.5-45.5)	208 (45.6, 41.0-50.2)	279 (61.2, 56.7-65.7)	182 (39.9, 35.4-44.4)
Cattle	451	0	0	1 (0.2, 0.2-0.7)	0
Horse	389	0	0	0	0
Chicken	199	98 (49.2, 42.3-56.2)	47 (23.6, 17.7-29.5)	46 (23.1, 17.3-29.0)	39 (19.6, 14.1-25.1)
Camel	49	7 (14.3, 4.5-24.1)	4 (8.2, 0.5-15.8)	15 (30.6, 17.7-43.5)	3 (6.1, 0.6-12.8)
Donkey	37	18 (48.6, 32.5-64.8)	19 (51.4, 35.2-67.5)	23 (62.2, 46.5-77.8)	15 (40.5, 24.7-56.4)
Total	3733	338 (9.1, 8.1-10.0)	284 (7.6, 6.8-8.5)	377 (10.1, 9.1-11.1)	241 (6.5, 5.7-7.2)

%, Prevalence. 95% CI, 95% Confidence Interval.

TABLE 4 Specific-*T. gondii* IgM-positive animals based on among SAG1, GRA7 and BAG1 proteins.

Animal	No. tested	Both IgM-SAG1 and IgM-GRA7 positive (%, 95% CI)	Both IgM-BAG1 and IgM-GRA7 positive (%, 95% CI)	Both IgM-SAG1 and IgM-BAG1 positive (%, 95% CI)	Among IgM-SAG1, -GRA7 and-BAG1 positive (%, 95% CI)
Tibetan sheep	904	0	0	0	0
Yak	752	0	0	0	0
Cow	496	0	3 (0.6, 0.1-1.3)	2 (0.4, 0.2-1.0)	0
Pig	456	0	0	0	0
Cattle	451	0	0	1 (0.2, 0.2-0.7)	0
Horse	389	275 (70.7, 66.2-75.2)	145 (37.3, 32.5-42.1)	143 (36.8, 32.0-41.6)	130 (33.4, 28.7-38.1)
Chicken	199	71 (35.7, 29.0-42.3)	30 (15.1, 10.1-20.0)	20 (10.1, 5.9-14.2)	11 (5.5, 2.4-8.7)
Camel	49	/	/	/	/
Donkey	37	/	/	/	/
Total	3733	346 (9.3, 8.3-10.2)	178 (4.8, 4.1-5.5)	166 (4.4, 3.8-5.1)	141 (3.8, 3.2-4.4)

%, Prevalence. 95% CI, 95% Confidence Interval./, no tested.

TABLE 5 Animals with seropositive for at least one specific-*T. gondii* antigen in animals.

Animal	No. tested	Positive animals for at least one specific-*T. gondii* antigen (%, 95% CI)	IgG positive animals for at least one specific antigen (%, 95% CI)	IgM positive animals for at least one specific antigen (%, 95% CI)
Tibetan sheep	904	260 (28.8, 25.8-31.7)	245 (27.1, 24.2-30.0)	30 (3.3, 2.2-4.5)
Yak	752	176 (23.4, 20.4-26.4)	137 (18.2, 15.5-21.0)	47 (6.3, 4.5-8.0)
Cow	496	182 (36.7, 32.5-40.9)	102 (20.6, 17.0-24.1)	129 (26.0, 22.1-29.9)
Pig	456	453 (99.3, 98.6-100.1)	453 (99.3, 98.6-100.1)	3 (0.7, 0.1-1.4)
Cattle	451	82 (18.2, 14.6-21.7)	21 (4.7, 2.7-6.6)	64 (14.2, 11.0-17.4)
Horse	389	372 (95.6,93.6-97.7)	6 (1.5, 0.3-2.8)	373 (95.9, 93.9-97.9)
Chicken	199	195 (98.0, 96.0-99.9)	171 (85.9, 81.1-90.8)	179 (89.9, 85.8-94.1)
Camel	49	39 (79.6, 68.3-90.9)	39 (79.6, 68.3-90.9)	/
Donkey	37	37 (100.0, 100.0)	37 (100.0, 100.0)	/
Total	3733	1796 (48.1, 46.5-49.7)	1111 (29.8, 28.3-31.2)	825 (22.1, 20.8-23.4)

%, Prevalence. 95% CI, 95% Confidence Interval./, no tested.

During the natural course of infections, sporozoite- and bradyzoite-specific immune responses are the markers for the diagnosis of cases of firstly acute toxoplasmosis (Döşkaya et al., 2014). Tachyzoite presence indicates that the animal is suffering from acute *T. gondii* infection (Lyons et al., 2002). Moreover, during *T. gondii* infections, the positivity for IgM antibody is proposed to be a marker of acute infection due to the occurrence of IgM antibody within days to a couple of weeks, and IgG antibodies are often interpreted as rising to protective levels after infection and remaining detectable for years, while the positivity for both IgG and IgM antibodies resulted is generally considered to indicate chronic reactivated cases (Kimbita et al., 2001; Döşkaya et al., 2014; Dhakal et al., 2015). IgM antibodies may be detected in humans or animals for a long time following primary *T. gondii* infections (Del Bono et al., 1989; Fricker-Hidalgo et al., 2013; Dhakal et al., 2015; Ybanez et al., 2020; Teimouri et al., 2021), and the natural IgM antibody may interact with parasite antigens in the absence of the *Toxoplasma* infection (Potasman et al., 1986; Sensini et al., 1996.; Liesenfeld et al., 1997; Dhakal et al., 2015; Teimouri

et al., 2021). In the current study, the application of specific antigens from different *T. gondii* forms may serve as reliable laboratory tools to confirm the doubts raised by these traditional methods. For the diagnosis of toxoplasmosis in this study, the *Tg*SAG1, *Tg*GRA7, and *Tg*BAG1 antigens from the different parasite forms were used to further analyze both IgG and IgM antibodies. Therefore, these present positive results may represent: the IgG antibody test, rSAG1 + rGRA7 positivity indicates that animals have been infected or are infected currently by tachyzoites, rBAG1 + rGRA7 positivity indicates that animals have been infected by bradyzoites or present tissue cysts, and rSAG1 + rGRA7 + rBAG1 indicates that animals have been infected by parasites or are chronic infections of *T. gondii* currently. The rSAG1 + rGRA7 positivity in IgM antibody tests indicates that the animal is suffering from acute toxoplasmosis caused by tachyzoites; rBAG1 + rGRA7 positivity indicates that the animal is being infected and is in the acute stage of infection caused by bradyzoites; rSAG1 + rGRA7 + rBAG1 indicates that the animal is suffering from acute toxoplasmosis caused by sporozoites, tachyzoites or bradyzoites.

In this work, although it is shown that Tibetan sheep, yaks, cows, and cattle were overall low both for *T. gondii* IgG and IgM positivity, there was no significant difference among rSAG1-, rGRA7-, and rBAG1-ELISAs. These results indicate that *T. gondii* may be infected at low titers in the animals collected in this study. However, the positive rates of 4.1% in yaks, 23.8% in cows and 8.0% in cattle in rBAG1-IgM were found, suggesting the possibility of elevated IgM antibody levels due to vertical infection or sexual transmission in these animal populations cannot be ruled out (Montoya and Remington, 2008; Lopes et al., 2013; Paquet et al., 2013; Beder and Esenkaya Taşbent, 2020).

Interestingly, three current ELISAs were used to test the serum samples of camels, horses and donkeys. It was found that all ELISAs revealed more than 20.4% IgG positivity in camels and 64.9% IgG positivity in donkeys. However, the positivity rates of the three IgG tests in horses were almost zero, but the positivity rates of IgM were 77.9% for rSAG1-, 86.8% for rGRA7- and 41.9% for rBAG1-ELISA. Moreover, in horse testing, 70.7%, 37.3%, 36.8% and 33.4% high IgM positivity was found in the rSAG1 + rGRA7-, rBAG1 + rGRA7-, rSAG1 + rBAG1- and rSAG1 + rGRA7 + rBAG1-ELISAs, respectively. Therefore, horses in the current study may be suffering from sporozoites, tachyzoites or bradyzoite reactivated-caused acute *Toxoplasma* infection, while camels and donkeys may have experienced acute toxoplasmosis or become long-term carriers of tissue cysts. At the same time, such a high positivity rate of IgG or IgM also indicates that the grass or water for horses, donkeys and camels in the sampling area has been polluted by oocysts excluded by wild or stray cats (Tenter et al., 2000; Cenci-Goga et al., 2011; Robert-Gangneux and Dardé, 2012; Saadatnia and Golkar, 2012; Halonen and Weiss, 2013; Liu et al., 2015; Lourido, 2019; Matta et al., 2021).

Furthermore, the rSAG1-ELISA, rGRA7-ELISA and rBAG1-ELISA tests showed high IgG positivity in current pigs, but for IgM antibody, only three pigs presented IgM positivity (two pigs for IgM-GRA7- and one pig for IgM-BAG1-ELISA), suggesting that current pigs may become long-term carriers of tissue cysts of *T. gondii*. Moreover, the seropositive and seronegative samples based on the current SAG1-IgG in pigs were selected to perform the comparative analysis with the commercial ELISA kits based on *Tg*SAG1 protein. The results revealed an 82% match rate with the commercial kits, and a sensitivity of 89.7% and a specificity of 75.4% of the serological *T. gondii* IgG-ELISA assay based on the SAG1 protein established in pigs in this study. These provide confirmations for currently establishing IgG-ELISA and IgM-ELISA based on the proteins that could apply for the serodiagnosis of *T. gondii* infections.

However, it was found that the results were different from those of other animal species in the toxoplasmosis detection of chickens, that is, the positivity rates of IgG and IgM were very high in all tests. This result demonstrates the fact that acute toxoplasmosis occurred in chickens, as well as the soil, water and food (containing animal meats with oocysts) in the chicken's surroundings are contaminated with oocysts. Moreover, the chicken's habit of pecking the soil may lead to greater exposure to the threat of oocysts (Wang et al., 2015). Certainly, in areas with the prevalence of toxoplasmosis, the definitive-host cats, especially stray cats, play a key role in frequently exposing other animals to the infectious source and causing *T. gondii* infections in the Qinghai-Tibetan Plateau (Xia et al., 2022; Yang et al., 2022).

In conclusion, the current study confirmed that the application of *Tg*SAG1, *Tg*GRA7, and *Tg*BAG1 recombinant antigens could successfully be used in the detection of specific IgG and IgM antibodies for the serodiagnosis of *T. gondii* infections in Tibetan sheep, yaks, pigs, cows, cattle, horses, chickens, camels and donkeys from the Qinghai-Tibetan Plateau. However, the limitations of the present study include the lack of application of specific antigens of sporozoites and testing of IgG avidity. Future studies need to develop serodetection tests for IgG and IgM against sporozoite antigens and should also test definitive host cats that live around these animals in this plateau area.

Data availability statement

The original contributions presented in the study are included in the article/Supplementary Material, further inquiries can be directed to the corresponding authors.

Ethics statement

The animal study was reviewed and approved by Ethics Committee of Qinghai University (License number: SL-2021061). Written informed consent was obtained from the owners for the participation of their animals in this study.

Author contributions

TQ: Collection of animal samples, Data curation, Formal analysis, Investigation, Writing-review and editing. JA: Investigation. YS: Writing-review and editing. HM: Investigation. MK: Writing-review and editing. XY: Collection of animal samples. JL: Conceptualization, Funding acquisition, Resources, Writing-original draft, Writing-review and editing. All authors contributed to the article and approved the submitted version.

Funding

This study was supported by the Natural Science Foundation of Qinghai Province of China (grant numbers 2022-ZJ-956Q).

Acknowledgments

This is a short text to acknowledge the contributions of specific colleagues, institutions, or agencies that aided the efforts of the authors.

Conflict of interest

The authors declare that the research was conducted in the absence of any commercial or financial relationships that could be construed as a potential conflict of interest.

Publisher's note

All claims expressed in this article are solely those of the authors and do not necessarily represent those of their affiliated organizations, or those of the publisher, the editors and the reviewers. Any product that may be evaluated in this article, or claim that may be made by its manufacturer, is not guaranteed or endorsed by the publisher.

Supplementary material

The Supplementary Material for this article can be found online at: https://www.frontiersin.org/articles/10.3389/fcimb.2022.1029768/full#supplementary-material

SUPPLEMENTARY FIGURE 1
The geographical location and quantity of sampling in various animals in Qinghai province for serodiagnosis of toxoplasmosis based on *T. gondii*-specific SAG1, GRA7 and BAG1 proteins. The graph shows the average altitudes of sampling sites in the 5 states and 2 cities from which the samples were collected and the number of samples of the different animals in each region. HX, Haixi Mongol and Tibetan Autonomous Prefecture. YS, Yushu Tibetan Autonomous Prefecture. HB, Haibei Tibetan Autonomous Prefecture. HN, Hainan Tibetan Autonomous Prefecture. HUN, Huangnan Tibetan Autonomous Prefecture. GL: Guoluo Tibetan Autonomous Prefecture. XN, Xining city. HD, Haidong city.

SUPPLEMENTARY FIGURE 2
Amino acid sequence alignment and phylogenetic analyses for *Tg*SAG1, *Tg*GRA7, and *Tg*BAG1 with the related cycle-forming organizations. The sequences included *T. gondii* SAG1 (AFO54849.1), *N. caninum* SAG1 (AAD25091.1), *Sarcocystis neurona* SAG1 (AAK40366.1), *T. gondii* GRA7 (ABE69193.1), *N. caninum* GRA7 (AFB77190.1), *Besnoitia besnoiti* GRA7 (XP_029218567.1), *T. gondii* BAG1 (XP_002365116.1), *N. caninum* BAG1 (BAI44436.1), and *B. besnoiti* BAG1 (XP_029221932.1).

SUPPLEMENTARY FIGURE 3
The specificity of the current ELISA tests was established in this study. IgG-ELISAs **(A)** and IgM-ELISAs **(B)** based on *Tg*GRA7, *Tg*SAG1, *Tg*BAG1, and GST proteins were performed using mouse anti-*T. gondii*, *N. caninum*, and *S. gigantea* positive sera. At least 5 positive sera were used. The coating concentration of the proteins was 1 μg/mL, and the serum dilutions were 1:100. The results showed that GRA7-, SAG1-, and BAG1-ELISAs only reacted with the positive sera of *T. gondii* but did not respond to the positive sera of *N. caninum* and *S. gigantea*. The GST protein did not react with any serum. *Tg*, *T. gondii*. *Nc*, *N. caninum*. *Sg*, *S. gigantea*.

SUPPLEMENTARY FIGURE 4
The sensitivity assay of the protein concentration under a positive serum dilution of 1:100. In this study, the coated *Tg*GRA7, *Tg*SAG1, *Tg*BAG1, and GST proteins were diluted 2, 1, 0.5, 0.25, 0.125, and 0.0625 μg/mL, and IgG-ELISAs and IgM-ELISAs were developed at a positive serum dilution of 1:100, 200, 400, 800, 1600 and 3200. The 5 positive mouse sera were used. The results show that the reactions could also occur when the concentration of coated proteins was very low under a positive serum dilution of 1:100. P, positive sera. N, negative sera.

SUPPLEMENTARY FIGURE 5
The sensitivity assay for the serum dilution. Here, mouse anti-*T. gondii* positive and negative sera were diluted with 1:100, 200, 400, 800, 1600, 3200, 6400, 12800 and 25600 for IgG-ELISAs and IgM-ELISAs based on 1 μg/mL *Tg*GRA7, *Tg*SAG1, *Tg*BAG1, and GST proteins. The 5 positive or negative mouse sera were used. The results showed that the OD values at the serum dilution 1:800-6400 were still greater than the cut-off values (calculated using the OD values of negative controls), while GST protein did not show any response.

References

Beder, D., and Esenkaya Taşbent, F. (2020). General features and laboratory diagnosis of *Toxoplasma gondii* infection. *Turkiye. Parazitol. Derg.* 44, 94–101. doi: 10.4274/tpd.galenos.2020.6634

Cenci-Goga, B. T., Rossitto, P. V., Sechi, P., McCrindle, C. M., and Cullor, J. S. (2011). *Toxoplasma* in animals, food, and humans: An old parasite of new concern. *Foodborne. Pathog. Dis.* 8, 751–762. doi: 10.1089/fpd.2010.0795

Del Bono, V., Canessa, A., Bruzzi, P., Fiorelli, M. A., and Terragna, A. (1989). Significance of specific immunoglobulin M in the chronological diagnosis of 38 cases of toxoplasmic lymphadenopathy. *J. Clin. Microbiol.* 27, 2133–2135. doi: 10.1128/jcm.27.9.2133-2135.1989

Dhakal, R., Gajurel, K., Pomares, C., Talucod, J., Press, C. J., and Montoya, J. G. (2015). Significance of a positive *Toxoplasma* immunoglobulin M test result in the united states. *J. Clin. Microbiol.* 53, 3601–3605. doi: 10.1128/JCM.01663-15

Döşkaya, M., Caner, A., Can, H., Gülçe İz, S., Gedik, Y., Döşkaya, A. D., et al. (2014). Diagnostic value of a rec-ELISA using *Toxoplasma gondii* recombinant SporoSAG, BAG1, and GRA1 proteins in murine models infected orally with tissue cysts and oocysts. *PLoS One* 9, e108329. doi: 10.1371/journal.pone.0108329

Dubey, J. P. (1997). Bradyzoite-induced murine toxoplasmosis: Stage conversion, pathogenesis, and tissue cyst formation in mice fed bradyzoites of different strains of *Toxoplasma gondii*. *J. Eukaryot. Microbiol.* 44, 592–602. doi: 10.1111/j.1550-7408.1997.tb05965.x

Dubey, J. P. (2009). Toxoplasmosis in sheep–the last 20 years. *Vet. Parasitol.* 163, 1–14. doi: 10.1016/j.vetpar.2009.02.026

Dubey, J. P., Lindsay, D. S., and Speer, C. A. (1998). Structures of *Toxoplasma gondii* tachyzoites, bradyzoites, and sporozoites and biology and development of tissue cysts. *Clin. Microbiol. Rev.* 11, 267–299. doi: 10.1128/CMR.11.2.267

Dubey, J. P., Speer, C. A., Shen, S. K., Kwok, O. C., and Blixt, J. A. (1997). Oocyst-induced murine toxoplasmosis: Life cycle, pathogenicity, and stage conversion in mice fed *Toxoplasma gondii* oocysts. *J. Parasitol.* 83, 870–882. doi: 10.2307/3284282

Fricker-Hidalgo, H., Cimon, B., Chemla, C., Darde, M. L., Delhaes, L., L'Ollivier, C., et al. (2013). *Toxoplasma* seroconversion with negative or transient immunoglobulin m in pregnant women: Myth or reality? A French multicenter retrospective study. *J. Clin. Microbiol.* 51, 2103–2111. doi: 10.1128/JCM.00169-13

Halonen, S. K., and Weiss, L. M. (2013). Toxoplasmosis. *Handb. Clin. Neurol.* 114, 125–145. doi: 10.1016/B978-0-444-53490-3.00008-X

Hill, D. E., and Dubey, J. P. (2013). *Toxoplasma gondii* prevalence in farm animals in the United States. *Int. J. Parasitol.* 43, 107–113. doi: 10.1016/j.ijpara.2012.09.012

Holec-Gąsior, L., Ferra, B., Hiszczyńska-Sawicka, E., and Kur, J. (2014). The optimal mixture of *Toxoplasma gondii* recombinant antigens (GRA1, P22, ROP1) for diagnosis of ovine toxoplasmosis. *Vet. Parasitol.* 206, 146–152. doi: 10.1016/j.vetpar.2014.09.018

Kimbita, E. N., Xuan, X., Huang, X., Miyazawa, T., Fukumoto, S., Mishima, M., et al. (2001). Serodiagnosis of *Toxoplasma gondii* infection in cats by enzyme-linked immunosorbent assay using recombinant SAG1. *Vet. Parasitol.* 102, 35–44. doi: 10.1016/s0304-4017(01)00522-2

Liesenfeld, O., Press, C., Montoya, J. G., Gill, R., Isaac-Renton, J. L., Hedman, K., et al. (1997). False-positive results in immunoglobulin m (IgM) *Toxoplasma* antibody tests and importance of confirmatory testing: The platelia *Toxo* IgM test. *J. Clin. Microbiol.* 35, 174–178. doi: 10.1128/jcm.35.1.174-178.1997

Liu, Q., Wang, Z. D., Huang, S. Y., and Zhu, X. Q. (2015). Diagnosis of toxoplasmosis and typing of *Toxoplasma gondii*. *Parasitol. Vectors.* 8, 292. doi: 10.1186/s13071-015-0902-6

Li, G., Zheng, W., Yang, J., Qi, T., He, Y., Chen, W., et al. (2021). Seroprevalence and epidemiology of *Toxoplasma gondii* in animals in the qinghai-Tibetan plateau area, China. *Pathogens.* 10, 432. doi: 10.3390/pathogens10040432

Lopes, W. D., Rodriguez, J. D., Souza, F. A., dos Santos, T. R., dos Santos, R. S., Rosanese, W. M., et al. (2013). Sexual transmission of *Toxoplasma gondii* in sheep. *Vet. Parasitol.* 195, 47–56. doi: 10.1016/j.vetpar.2012.12.056

Lourido, S. (2019). Toxoplasma gondii. *Trends. Parasitol.* 35, 944–945. doi: 10.1016/j.pt.2019.07.001

Lyons, R. E., McLeod, R., and Roberts, C. W. (2002). *Toxoplasma gondii* tachyzoite-bradyzoite interconversion. *Trends. Parasitol.* 18, 198–201. doi: 10.1016/s1471-4922(02)02248-1

Masatani, T., Matsuo, T., Tanaka, T., Terkawi, M. A., Lee, E. G., Goo, Y. K., et al. (2013). *Tg*GRA23, a novel *Toxoplasma gondii* dense granule protein associated with the parasitophorous vacuole membrane and intravacuolar network. *Parasitol. Int.* 62, 372–379. doi: 10.1016/j.parint.2013.04.003

Matta, S. K., Rinkenberger, N., Dunay, I. R., and Sibley, L. D. (2021). *Toxoplasma gondii* infection and its implications within the central nervous system. *Nat. Rev. Microbiol.* 19, 467–480. doi: 10.1038/s41579-021-00518-7

Montoya, J. G., and Liesenfeld, O. (2004). Toxoplasmosis. *Lancet.* 363, 1965–7196. doi: 10.1016/S0140-6736(04)16412-X

Montoya, J. G., and Remington, J. S. (2008). Management of *Toxoplasma gondii* infection during pregnancy. *Clin. Infect. Dis.* 47, 554–566. doi: 10.1086/590149

Paquet, C., Yudin, M. H.Society of Obstetricians and Gynaecologists of Canada (2013). Toxoplasmosis in pregnancy: Prevention, screening, and treatment. *J. Obstet. Gynaecol. Can.* 35, 78–81. doi: 10.1016/s1701-2163(15)31053-7

Pietkiewicz, H., Hiszczyńska-Sawicka, E., Kur, J., Petersen, E., Nielsen, H. V., Stankiewicz, M., et al. (2004). Usefulness of *Toxoplasma gondii*-specific recombinant antigens in serodiagnosis of human toxoplasmosis. *J. Clin. Microbiol.* 42, 1779–1781. doi: 10.1128/JCM.42.4.1779-1781.2004

Potasman, I., Araujo, F. G., and Remington, J. S. (1986). *Toxoplasma* antigens recognized by naturally occurring human antibodies. *J. Clin. Microbiol.* 24, 1050–1054. doi: 10.1128/jcm.24.6.1050-1054.1986

Robert-Gangneux, F., and Dardé, M. L. (2012). Epidemiology of and diagnostic strategies for toxoplasmosis. *Clin. Microbiol. Rev.* 25, 264–296. doi: 10.1128/CMR.05013-11

Saadatnia, G., and Golkar, M. (2012). A review on human toxoplasmosis. *Scand. J. Infect. Dis.* 44, 805–814. doi: 10.3109/00365548.2012.693197

Sensini, A., Pascoli, S., Marchetti, D., Castronari, R., Marangi, M., Sbaraglia, G., et al. (1996). IgG avidity in the serodiagnosis of acute *Toxoplasma gondii* infection: A multicenter study. *Clin. Microbiol. Infect.* 2, 25–29. doi: 10.1111/j.1469-0691.1996.tb00196.x

Teimouri, A., Abbaszadeh Afshar, M. J., Mohtasebi, S., Jafarpour Azami, S., Alimi, R., and Keshavarz, H. (2021). Assessment of an in-house enzyme-linked immunosorbent assay and IgG avidity test based on SAG1 and GRA7 proteins for discriminating between acute and chronic toxoplasmosis in humans. *J. Clin. Microbiol.* 59, e0041621. doi: 10.1128/JCM.00416-21

Tenter, A. M., Heckeroth, A. R., and Weiss, L. M. (2000). *Toxoplasma gondii*: from animals to humans. *Int. J. Parasitol.* 30, 1217–1258. doi: 10.1016/s0020-7519(00)00124-7

Terkawi, M. A., Kameyama, K., Rasul, N. H., Xuan, X., and Nishikawa, Y. (2013). Development of an immunochromatographic assay based on dense granule protein 7 for serological detection of *Toxoplasma gondii* infection. *Clin. Vaccine Immunol.* 20, 596–601. doi: 10.1128/CVI.00747-12

Wang, S., Zhao, G. W., Wang, W., Zhang, Z. C., Shen, B., Hassan, I. A., et al. (2015). Pathogenicity of five strains of *Toxoplasma gondii* from different animals to chickens. *Korean. J. Parasitol.* 53, 155–162. doi: 10.3347/kjp.2015.53.2.155

Xia, N., Ji, N., Li, L., Huang, Y., Yang, C., Guo, X., et al. (2022). Seroprevalence and risk factors of *Toxoplasma gondii* in urban cats from China. *BMC. Vet. Res.* 18, 331. doi: 10.1186/s12917-022-03427-w

Xicoténcatl-García, L., Enriquez-Flores, S., and Correa, D. (2019). Testing new peptides from *Toxoplasma gondii* SAG1, GRA6, and GRA7 for serotyping: better definition using GRA6 in mother/newborns pairs with risk of congenital transmission in Mexico. *Front. Cell. Infect. Microbiol.* 9. doi: 10.3389/fcimb.2019.00368

Yang, J., Ai, J., Qi, T., Ni, X., Xu, Z., Guo, L., et al. (2022). *Toxoplasma gondii* and *Neospora caninum* infections in stray cats and dogs in the qinghai-Tibetan plateau area, China. *Anim. (Basel).* 12, 1390. doi: 10.3390/ani12111390

Ybanez, R. H. D., Ybanez, A. P., and Nishikawa, Y. (2020). Review on the current trends of toxoplasmosis serodiagnosis in humans. *Front. Cell. Infect. Microbiol.* 8. doi: 10.3389/fcimb.2020.00204

frontiers | Frontiers in Cellular and Infection Microbiology

TYPE Original Research
PUBLISHED 16 December 2022
DOI 10.3389/fcimb.2022.1058081

OPEN ACCESS

EDITED BY
William Harold Witola,
University of Illinois at Urbana–Champaign, United States

REVIEWED BY
Jian Li,
Hubei University of Medicine, China
Paula Mello De Luca,
Oswaldo Cruz Foundation (FIOCRUZ), Brazil

*CORRESPONDENCE
Nobuko Arisue
arisue.nobuko@twmu.ac.jp
Nirianne Marie Q. Palacpac
nirian@biken.osaka-u.ac.jp

SPECIALTY SECTION
This article was submitted to Parasite and Host, a section of the journal Frontiers in Cellular and Infection Microbiology

RECEIVED 30 September 2022
ACCEPTED 17 November 2022
PUBLISHED 16 December 2022

CITATION
Arisue N, Palacpac NMQ, Ntege EH, Yeka A, Balikagala B, Kanoi BN, Bougouma EC, Tiono AB, Nebie I, Diarra A, Houard S, D'Alessio F, Leroy O, Sirima SB, Egwang TG and Horii T (2022) African-specific polymorphisms in *Plasmodium falciparum* serine repeat antigen 5 in Uganda and Burkina Faso clinical samples do not interfere with antibody response to BK-SE36 vaccination. *Front. Cell. Infect. Microbiol.* 12:1058081.
doi: 10.3389/fcimb.2022.1058081

African-specific polymorphisms in *Plasmodium falciparum* serine repeat antigen 5 in Uganda and Burkina Faso clinical samples do not interfere with antibody response to BK-SE36 vaccination

Nobuko Arisue[1,2]*, Nirianne Marie Q. Palacpac[3]*, Edward H. Ntege[4], Adoke Yeka[5], Betty Balikagala[6], Bernard N. Kanoi[7], Edith Christiane Bougouma[8,9], Alfred B. Tiono[8,9], Issa Nebie[8,9], Amidou Diarra[8,9], Sophie Houard[10], Flavia D'Alessio[10], Odile Leroy[10,11], Sodiomon B. Sirima[8,9], Thomas G. Egwang[12] and Toshihiro Horii[3]

[1]Research Center for Infectious Disease Control, Research Institute for Microbial Diseases, Osaka University, Suita, Osaka, Japan, [2]Section of Global Health, Division of Public Health, Department of Hygiene and Public Health, Tokyo Women's Medical University, Tokyo, Japan, [3]Department of Malaria Vaccine Development, Research Institute for Microbial Diseases, Osaka University, Suita, Osaka, Japan, [4]Department of Plastic and Reconstructive Surgery, University of the Ryukyus, Graduate School of Medicine and Hospital, Okinawa, Japan, [5]Makerere University School of Public Health, Kampala, Uganda, [6]Department of Tropical Medicine and Parasitology, School of Medicine, Juntendo University, Tokyo, Japan, [7]Centre for Malaria Elimination (CME) and Centre for Research in Infectious Diseases (CRID), Directorate of Research and Innovation, Mount Kenya University, Thika, Kenya, [8]Public Health Department, Institut National de Santé Publique/Centre National de Recherche et de Formation sur le Paludisme (INSP/CNRFP), Ouagadougou, Burkina Faso, [9]Groupe de Recherche Action en Santé (GRAS), Ouagadougou, Burkina Faso, [10]European Vaccine Initiative (EVI), Universitäts Klinikum Heidelberg, Heidelberg, Germany, [11]Sorekara-x consultant, Paris, France, [12]Med Biotech Laboratories, Kampala, Uganda

BK-SE36, based on *Plasmodium falciparum* serine repeat antigen 5 (SERA5), is a blood-stage malaria vaccine candidate currently being evaluated in clinical trials. Phase 1 trials in Uganda and Burkina Faso have demonstrated promising safety and immunogenicity profiles. However, the genetic diversity of *sera5* in Africa and the role of allele/variant-specific immunity remain a major concern. Here, sequence analyses were done on 226 strains collected from the two clinical trial/follow-up studies and 88 strains from two cross-sectional studies in Africa. Compared to other highly polymorphic vaccine candidate antigens, polymorphisms in *sera5* were largely confined to the repeat regions of the gene. Results also confirmed a SERA5 consensus sequence with African-specific polymorphisms. Mismatches with the vaccine-type SE36 (BK-SE36) in the octamer repeat, serine repeat, and flanking regions, and single-nucleotide polymorphisms in non-repeat regions could compromise vaccine response and efficacy. However, the haplotype

diversity of SERA5 was similar between vaccinated and control participants. There was no marked bias or difference in the patterns of distribution of the SE36 haplotype and no statistically significant genetic differentiation among parasites infecting BK-SE36 vaccinees and controls. Results indicate that BK-SE36 does not elicit an allele-specific immune response.

KEYWORDS

BK-SE36 malaria vaccine, Plasmodium falciparum, serine repeat antigen 5, polymorphism, clinical trial

Introduction

Despite unprecedented gains in malaria control, progress has stalled in recent years. Children under 5 years old in sub-Saharan Africa continue to shoulder a disproportionate share of the malaria burden (Weiss et al, 2019; WHO, 2021). In a historic move, the World Health Organization (WHO) endorsed the first-ever malaria vaccine, RTS,S (Maxmen, 2021). RTS,S, based on the circumsporozoite protein (CSP), has a modest efficacy of 36% against malaria over 4 years of follow-up (Laurens, 2020). After pilot implementation studies that confirmed safety as well as its feasible deployment, modeling studies show that 4 doses will avert 116,480 cases of clinical malaria and 484 deaths per 100,000 vaccinated children (Laurens, 2020). The contribution of a more effective second-generation malaria vaccine cannot be overemphasized.

One major impediment to the elusive goal of a highly efficacious vaccine is the polymorphic nature of antigens that alter epitope antibody responses, leading to low or limited vaccine efficacy (Palacpac and Horii, 2020). In phase 3 trials, RTS,S had a better overall efficacy at protecting against malaria caused by vaccine-strain than non-vaccine strain CSP in 5–17-month-old children (Neafsey et al., 2015). Efficacy was approximately 10–15% lower against non-vaccine (mismatched) type parasite infections. Other candidate vaccines based on polymorphic merozoite surface protein 1 (MSP: FMP1/AS02) (Ogutu et al., 2009) and apical membrane antigen 1 (AMA1: FMP2.1/AS02$_A$, AMA1-C1, AMA1-FVO) (Takala et al., 2009; Thera et al., 2011) did not show significant overall protection in proof-of-concept trials but had allele-specific efficacy against clinical malaria. Sequence analyses of *ama1* genes obtained in a phase 2 trial revealed that the AMA1 vaccine reduced the risk of clinical malaria only when the infecting parasite had identical amino acid residues to the vaccine type at a key position in the AMA1 cluster 1 loop (Ouattara et al., 2013). These studies highlight the need for molecular epidemiological studies to identify and determine the roles of polymorphisms in natural populations and during vaccine trials, particularly in cases of genetic and antigenic diversity and vaccine failure.

BK-SE36 is a formulation based on the serine repeat antigen 5 (SERA5) of *Plasmodium falciparum*. SERA5 is a blood-stage antigen (Arisue et al., 2020) expressed during the late trophozoite and schizont stages as a 120-kDa precursor and secreted into the parasitophorous vacuole after removal of the signal peptide (Debrabant et al., 1992). The protein is cleaved by subtilisin-like serine protease 1 into 47-, 56-, and 18-kDa fragments (Yeoh et al., 2007) (Figure 1). The 47-kDa fragment is linked to the 18-kDa fragment *via* a disulfide bond and localizes to the merozoite surface (Li et al., 2002). The 56-kDa fragment containing the papain-like catalytic domain is further cleaved by an unknown protease to 50- and 6-kDa fragments just before parasite egress (Li et al., 2002; Yeoh et al., 2007; Stallmach et al., 2015). SE36 is identical to the 47-kDa fragment (P47) except for the serine repeats which were removed to improve the hydrophilicity of the protein.

The N-terminal fragment, SE36, was selected for clinical development based on the findings that (i) antibodies against the P47 domain (SE36 with the serine repeat region) inhibited parasite growth *in vitro* (Fox et al., 1997; Pang and Horii, 1998; Pang et al., 1999; Aoki et al., 2002; Yagi et al., 2014); (ii) seroepidemiological studies in malaria-endemic areas showed a negative correlation between parasitemia and anti-P47 antibody titers (Okech et al., 2001; Horii et al., 2010); and (iii) high anti-SE36 antibody titers were associated with protection from severe malaria outcomes (Okech et al., 2006; Owalla et al., 2013). BK-SE36, which is SE36 adsorbed to aluminum hydroxide gel, is a malaria vaccine candidate currently in clinical trials. The phase 1b randomized trial and follow-up study in Uganda, conducted in 2010–2012, showed that the vaccine was safe and immunogenic; and the 6–20-year-olds that received the vaccine had a reduced risk of time-to-first episodes and all episodes of high parasitemia (>5000 parasites/μL) and fever at 130–365 days post-second vaccination (Palacpac et al., 2013). A clinical trial in Burkina Faso with 12–60-month-old children was also completed (Bougouma et al., 2022).

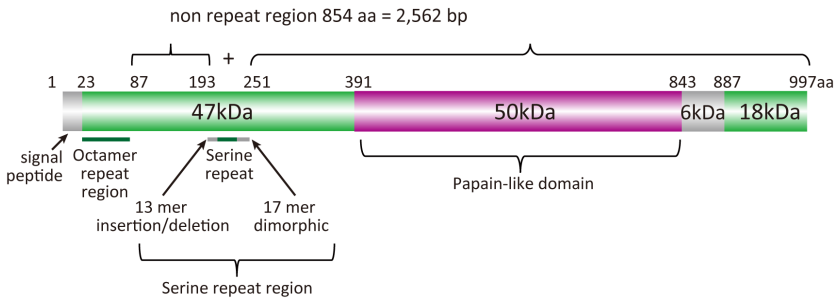

FIGURE 1
Schematic representation of the SERA5 structure. *Plasmodium falciparum* 3D7 strain was used as a reference for the illustration.

Epitope mapping of the SE36 region in SERA5 using serum samples from a malaria endemic area indicated that the intrinsically unstructured N-terminal octamer repeat region possessed inhibitory epitopes (Yagi et al., 2014). Sequence analyses of SERA5 genes using 445 P. *falciparum* isolates collected from nine endemic countries in Africa, Southeast Asia, Oceania, and South America revealed variations in the (i) number and motifs of octamer amino acid units in the SERA5 N-terminal domain, (ii) number of serine repeats and polymorphisms in the 13-mer insertion/deletion region and 17-mer dimorphic sequence flanking these repeats, and (iii) area-specific single-nucleotide polymorphisms (SNPs) in non-repeat regions of the gene (Tanabe et al., 2012). Thus, although no strong signature for positive selection was detected in the non-repeat sequence regions (2,562 bp), protective epitopes were located in predicted disordered regions of the protein. Whether these polymorphisms are involved in allele-specific immunity remains unclear. Furthermore, information on SERA5 polymorphisms in *P. falciparum* isolates circulating in Africa is limited. Here, the different features of the polymorphism in *sera5* and other antigen and housekeeping genes were examined. Patterns of genetic variation were compared for parasites isolated within Africa and for those vaccinated with BK-SE36 and saline. Variations in *sera5* did not appear to influence the effectiveness of BK-SE36 to elicit an immune response.

Materials and methods

Ethics approval

Ethical approval for the Ugandan trial and follow-up study were obtained from the ethical institutional review committees of Med Biotech Laboratories (Ref# IRB-00003990-MBL-BIOMEDICAL, IRB-00003995-MBL-BIOMEDICAL), Uganda National Council for Science and Technology (Ref# HS635, HS866), Osaka University (Ref# 20-3, 287), and Research Foundation for Microbial Diseases of Osaka University.

Approval for the Burkina Faso trial was obtained from Comité d'Éthique pour la Recherche en Santé du Burkina Faso (Ref# 2014-12-144), Comité Institutionnel de Bioéthique du INSP/CNRFP (previous name: CNRFP) (Ref# N°2014/071/MS/SG/CNRFP/CIB, N°2016/000008/MS/SG/CNRFP/CIB), Agence Nationale de Régulation Pharmaceutique (ANRP, previous name: Direction Générale de la Pharmacie, du Médicament et des Laboratoires [DGPML], Ref# N°2015_658/MS/CAB), Scientific Committee/Institutional Review Committee of the Research Institute for Microbial Diseases (Ref# 26), Osaka University (Ref# 574); and London School of Hygiene and Tropical Medicine Research Ethics Committee (Ref# 9175).

Consent, either by signature or thumbprint, was obtained from the children and/or children's parents or guardians prior to sampling and other trial-related procedures. In Uganda, for subjects 8–17 years old, assent by the child took precedence over consent from the parents or guardians.

All studies were conducted in compliance with the protocol, International Council for Harmonisation of Technical Requirements for Pharmaceuticals for Human Use (ICH), Good Clinical Practices, the Declaration of Helsinki 2013, and country-specific laws and regulations.

Clinical trial in Uganda

The details of the randomized, single-blind, safety and immunogenicity phase 1b trial (Current Controlled trials ISRCTN71619711 https://doi.org/10.1186/ISRCTN71619711) and follow-up study in Lira, northern Uganda have been previously described (Palacpac et al., 2013; Yagi et al., 2016). The clinical trial site, Lira Medical Centre, is in a region with intense transmission and bimodal rainfall pattern from April to May and September to October (Proietti et al., 2011). Blood samples and data on malaria incidence were obtained from healthy children and young adults aged 6–20 years old (n = 84). Participants in 3 age cohorts (6–10, 11–15, and 16–20 years old) were randomized to be administered twice with either half- (0.5 mL, n=11) or full-

(1.0 mL, n=6) dose BK-SE36 or saline (n=6). Subcutaneous vaccination was performed 21-days apart. During the follow-up study (130–440 days post-second vaccination), 50 additional children (as unvaccinated controls) were recruited. Recruitment of the additional control group used the same inclusion and exclusion criteria as in the clinical trial and was age-, gender-, and locality-matched as much as possible. The paired control participants visited the trial center on the same scheduled day as trial participants to undergo assessments for vital signs, physical examination, monthly questionnaire, and blood smear. Blood samples for filter blots, thick and thin blood smears, were obtained at 28-day intervals (active surveillance) or whenever the child was sick (passive surveillance). In this study, any blood smear-positive samples (any parasitemia) were used for analyses.

Clinical trial in Burkina Faso

The Burkina Faso trial was a double-blind, randomized, controlled, age de-escalation safety and immunogenicity trial and follow-up study conducted in Banfora, south western Burkina Faso (Pan African Clinical Trials Registry: PACTR201411000934120; https://pactr.samrc.ac.za/TrialDisplay.aspx?TrialID=934) (Bougouma et al., 2022). The trial site, Unité de Recherche Clinique de Banfora, is in a region where transmission occurs throughout the year with a peak for clinical malaria occurring within the 4 months (June–September) of the rainy season of May–November (Tiono et al., 2014). Samples and data of clinical malaria episodes were obtained from healthy children aged 12–60 months (n = 108). Participants in two age cohorts (12–24 and 25–60-months-old) were randomized for administration of Synflorix® (0.5 mL, control arm, n = 18); or BK-SE36 (1.0 mL) *via* either the subcutaneous route (n = 18), or the intramuscular route (n = 18). Two administrations were performed 28 days apart, and a third dose was administered at week 26 (Day 182). The control group was vaccinated with Synflorix® at Days 0 and 182, and with saline at Day 28 to comply with the manufacturer's recommendation of at least a 2-month interval between the 2 primary Synflorix® doses while ensuring that the trial was performed in a double-blinded manner. Clinical malaria episodes, defined as ≥5000 parasites/μL + tympanic temperature ≥38°C, from Day 56 (4 weeks after dose 2) until the final visit (Day 477, 42 weeks after dose 3) were assessed. Two thick and thin blood smears were prepared for malaria diagnosis and blood samples spotted onto Whatman™ 903 Protein Saver Card (GE Healthcare Life Sciences, MA, USA) were dried and stored until use.

DNA preparation, SERA5 gene amplification, and nucleotide sequencing

The BioRobot EZ1 DNA investigator kit (QIAGEN, Hilden, Germany) was used to extract parasite DNA from the filter paper blood spots. Four pieces of a 3-mm-diameter circle, corresponding to a 20-μL volume of blood, were punched out from 1-2 blood spots for downstream reactions. The extracted DNA was resuspended in 50 μL TE solution, and stored at -20°C until use.

Exon regions II-IV of the SERA5 gene, covering approximately 3.3 kb, were amplified using specific primers sera5-F1 and sera5-R1 (Supplementary Table S1). Exon I encoding the signal peptide was not analyzed because of sequencing difficulties. Amplification was carried out in a 25-μL reaction mixture containing 0.4 μM each of forward and reverse primers, 0.4 mM each of dNTP, 0.5 units of KOD FX Neo polymerase (TOYOBO, Osaka, Japan), 12.5 μL of 2x PCR buffer, and 1 μL of genomic DNA solution. PCR conditions were as follows: 95°C for 2 min, 35 cycles of 95°C for 15 sec, 59°C for 30 sec, and 68°C for 2 min. A 2-μL aliquot of the PCR product was used as template for a second PCR amplification in a 25-μL reaction mixture using the primers sera5-F2 and sera5-R2 (Supplementary Table S1) under the same thermocycler conditions. In case of failure with the first set of primers, other primer pairs were also tested: sera5-F1 and sera5-R1 for the 1st PCR and sera5-F3 and sera5-R2 for the 2nd PCR or sera5-F2 and sera5-R1 for the 1st PCR and sera5-F3 and sera5-R2 for the 2nd PCR. PCR products were purified using the QIAquick PCR Purification kit (QIAGEN) according to the manufacturer's instructions. Purified DNA fragments were eluted in 30 μL TE. Optical density was measured with a NanoDrop (Thermo Fisher Scientific, Waltham, MA, USA) and the DNA concentration was adjusted to 0.026 μg/μL using TE. At this concentration, 1 μL was suitable for performing one sequencing reaction.

DNA sequencing was performed directly using the BigDye® Terminator v3.1 Cycle Sequencing Kit and 3130xI Genetic Analyzer (Applied Biosystems, Foster City, CA, USA). Sequencing primers were designed to cover target regions in both directions (Supplementary Table S1). If inconsistencies were obtained after two independent amplifications, a third round of PCR/sequencing reaction was performed. Only isolates showing a single genotype infection, without overlapping peaks on the electropherograms, were used for further analysis. To compare the nucleotide diversity of SERA5 with other antigens and housekeeping genes, the sequences of apical membrane antigen 1 (*ama1*), circumsporozoite protein (*csp*), Ca2+-transporting ATPase (*serca*), and adenylosuccinate lyase (*adsl*) genes were determined using the Ugandan isolates. The PCR and sequencing strategies were the same as those used for *sera5* except that the PCR conditions were adjusted to be suitable for each gene. The PCR sequencing primers are listed in (Supplementary Table S1).

Accession numbers

The newly determined nucleotide sequences in this study have been deposited in the DNA Data Bank of Japan (accession nos. LC580441– LC581218). Samples from a previous study

were used to compare polymorphisms found in Africa. The Tanzania and Ghana isolates were described previously (Tanabe et al., 2010). Briefly, Tanzania blood samples (n = 55) were collected from residents of Nyamisati village in the Rufiji River Delta, eastern coastal Tanzania in February and March 1993, 1998, and January 2003. Asymptomatic donors had a mean age of 14.2 years (range, 1–78), 16.8 years (range, 1–63), and 13.8 years (range, 10–19) in 1993, 1998, and 2003, respectively. Ghana isolates (n = 33) were collected during malaria surveys in 0–15-year-old children from three villages near Winneba (Okyereko, Mpota, and Apam), a western coastal region, in November 2004. The accession numbers of *sera5*, *ama1*, *csp*, *serca*, and *adsl* are summarized in Supplementary Table S2.

Sequence alignment and genetic analyses

The nucleotide sequences of *sera5* were aligned using CLUSTALW implemented in GENETYX® ver. 15 (GENETYX Corporation, Tokyo, Japan) with manual corrections. According to our previous analyses (Tanabe et al., 2012), the SERA5 sequence was categorically divided into an octamer repeat (OR) region, serine repeat (SR) region, and non-repeat regions (2,562 bp) (Figure 1). The number of haplotypes, haplotype diversity (Hd), and nucleotide diversity (θ_π) were calculated using DnaSP v5.10.01 (Librado and Rozas, 2009). The difference between the numbers of synonymous substitutions per synonymous site (dS) and nonsynonymous substitutions per nonsynonymous site (dN) was calculated by the Nei and Gojobori method (Nei and Gojobori, 1986) with Jukes and Cantor correction as implemented in MEGA X (Kumar et al., 2018). The statistical significance of the difference between dN and dS was estimated with MEGA Z-test. If dN was greater than dS, positive selection was predicted. Genetic differentiation of SERA5 among the parasite population was examined using *Fst*, the Wright's fixation index (Wright, 1965) of inter-population variance in allele frequencies. Pairwise *Fst* between parasite populations was calculated using Arlequin v3.5 (Excoffier and Lischer, 2010). These programs had built-in statistical analyses which were performed automatically, however, when statistical analyses were not supported, Mann-Whitney test for differences between two independent groups, the Kruskal-Wallis test for differences between multiple groups, and the chi-square ($\chi 2$) test for proportions between group were used.

Results

Sample description

In the trial conducted in Uganda, of the 247 infection events recorded, sequence information from 172 infections was obtained (75 were mixed infections and excluded from further analyses). Parasitemia ranged from 16 to 151,680 parasites/μL and 4 samples had *P. falciparum* gametocyte. Of the 172 available sequences, 33 were from subjects who had only one infection and 66 were from participants who had at least two infections during the follow-up period. In summary, 77 isolates were from the BK-SE36 vaccine arm and 95 from the control group. The samples were collected from March 2011 to February 2012, covering 2 malaria transmission seasons.

For the Burkina Faso trial, of 78 clinical malaria events, sequence information was obtained from 54 cases (24 were mixed infections and excluded from further analyses). Parasitemia ranged from 6,527 to 253,900 parasites/μL. Of the 54 available sequences, 29 sequences were from subjects who had only one infection and 10 were from subjects who had at least two infections during the follow-up period. Twenty-nine sequences were from the BK-SE36 vaccine arm and 25 from the control group. Samples were obtained from July 2015 to January 2017, covering the rainy season of May–November. Each subject had a total follow-up period of 16 months.

Comparison of SERA5 polymorphism with major antigen genes and housekeeping genes

P. falciparum isolates from the four African countries were used to compare polymorphisms in 3 antigen genes (*sera5*, *ama1* and *csp*) and 2 housekeeping genes (*serca* and *adsl*) (Figure 2, Supplementary Table S3). As expected, the degree of polymorphism varied between antigen-coding genes and housekeeping genes. Notably, the level of polymorphism in all African isolates within each gene was similar. The Hd of the three antigen genes *ama1*, *csp*, and *sera5* (Supplementary Table S4A) were extremely high (close to 1.0), demonstrating that most sequences were distinct from each other. The Hd of the concatenated housekeeping genes of *adsl* and *serca* (*adsl+serca*) was slightly lower than that of the antigen genes. In the antigen genes, the number of sequence variations was almost the same in both the nucleotide and amino acid sequences; however, in the housekeeping genes, the amino acid sequence showed far fewer variations compared to the nucleotide sequences. Nucleotide substitutions in the antigen genes mainly occurred at non-synonymous sites which resulted in amino acid changes, whereas in housekeeping genes, nucleotide substitutions tend to occur at synonymous sites without amino acid changes.

Nucleotide diversity was estimated as θ_π, the average pairwise nucleotide difference (Figure 2A). The θ_π of the antigen genes *ama1* and *csp* were very high, whereas that of the antigen gene *sera5* was much lower and comparable to the concatenated gene sequences of *adsl+serca*. Among the three antigen genes, *ama1* and *csp* showed a signature of diversifying selection with a significant excess of dN over dS (Figure 2B). The

10.3389/fcimb.2022.1058081

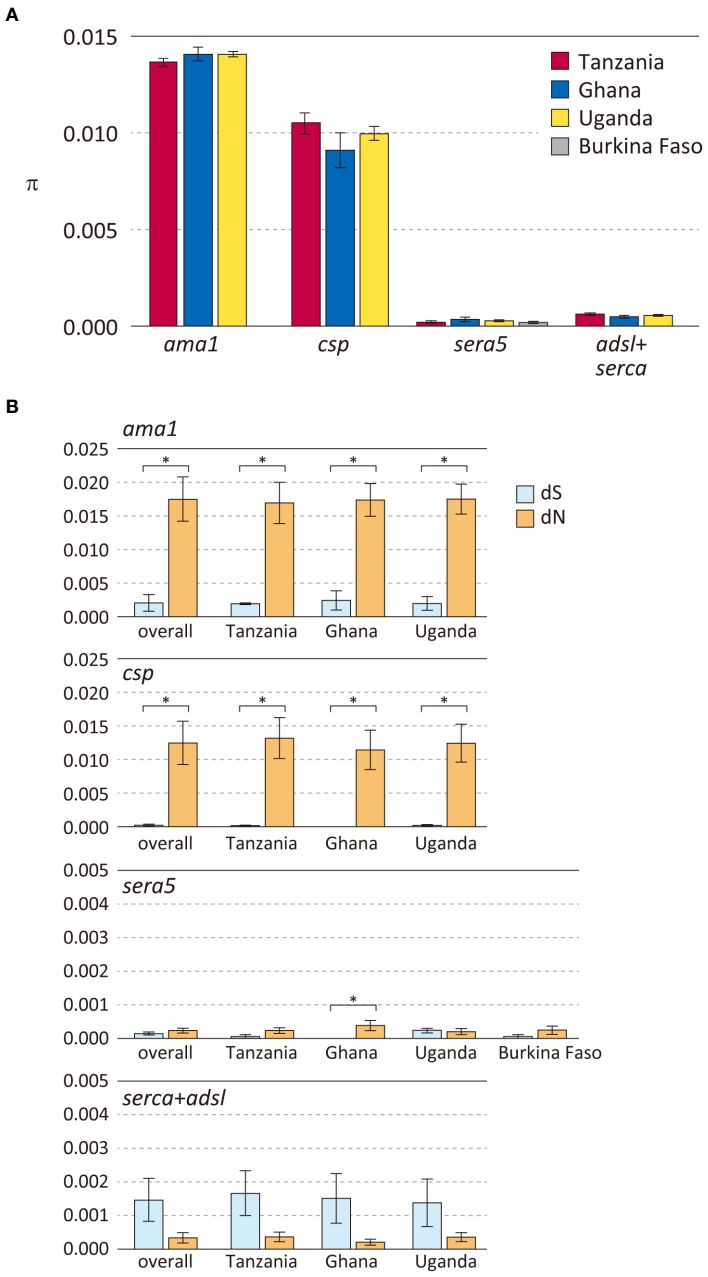

FIGURE 2
Polymorphisms in three *P. falciparum* vaccine candidate genes and housekeeping genes in parasite populations from Africa. **(A)** Nucleotide diversities (θ_π) are shown. Error bars reflect standard deviation. **(B)** Number of synonymous substitutions per synonymous site (dS) and number of non-synonymous substitutions per non-synonymous site (dN) are shown. Error bars reflect the standard error. For details, see Supplementary Table S3. Differences between dS and dN that were significant (dN>dS, $p < 0.01$), denoting positive selection, are indicated in asterisk.

high values of θ_π and dN in *ama1* and *csp* indicate large differences between the sequences, and dN>dS is likely due to host immune evasion. In contrast, the values of θ_π, dN, and dS of *sera5* were much lower than those of *ama1* and *csp*. Although dN was significantly larger than dS in *sera5* from the Ghana isolates, the differences between the amino acid sequences were small compared to either *ama1* or *csp* (Figure 2B). For each of these genes, analyses for θ_π, dS, and dN were performed to compare Hd with (Supplementary Table S4A) or without regions containing insertions and deletions (Supplementary Table S4B). The comparison provides insight into the various processes involved in generating alleles in antigen genes. The

excluded regions would refer to the 'NANP' repeat region in *ama1*; the eight-mer amino acid repeat units in *csp*; the serine repeat region, the 13-mer insertion/deletion region, and the 17-mer dimorphic region in *sera5*; and the asparagine repeat region in *adsl+serca*. When Hd of *sera5* was analyzed using the same dataset which excluded insertions and deletions, the value of Hd was much smaller than that obtained using full-length *sera5* (Supplementary Table S4). The Hd of *ama1* was similar, as there were no insertions or deletions in the gene. The Hd of *csp* was also similar despite the exclusion of NANP repeat regions. The lower Hd of *sera* when regions of insertions and deletions are removed suggests that sequence variations in *sera5* are mainly introduced by recombination rather than by point mutation. In *ama1*, all polymorphisms are produced by point mutation, whereas in *csp*, both point mutation and recombination resulting in different numbers of NANP units act to generate sequence variations.

Sequence comparison of SE36 region in SERA5

The consensus sequence of SE36 in SERA5 was inferred from 314 sequences obtained from four African countries: Uganda (n = 172), Burkina Faso (n = 54), Tanzania (n = 55), and Ghana (n = 33). The consensus sequence in African isolates (Af-cons) was aligned with the SE36 sequence based on Honduras-1 and two representative laboratory strains, 3D7 and FCR3. The BK-SE36 candidate vaccine was designed with reference to the SERA5 sequence of the Honduras-1 strain (Sugiyama et al., 1996). As shown in Figure 3, there were several sequence mismatch regions, particularly between the vaccine-type SE36 variant and Af-cons.

At the N-terminal, of the 314 SERA5 sequences, there were 76 variations in the OR region (Supplementary Figure S1). The number of octamer units varied widely: seven octamer units (23 OR variations) were detected in 196 SERA5 sequences across Africa (62.4%), eight octamer units (16 OR variations) were found in 47 sequences (15.0%), and six octamer units (8 OR variations) were found in 14 sequences (4.5%). In all four African countries, seven octamer units were the most frequently detected. The number of OR units detected from SERA5 sequences was not significantly different among the four countries ($p > 0.05$, Kruskal-Wallis test). Vaccine-type SE36 has six octamer units, made up of one Ib subunit; and an identical OR sequence was found only in 5 *P. falciparum* isolates (1.6%): 4 from Uganda and 1 isolate from Ghana (Table 1; Supplementary Figure S1). The seven octamer units found predominantly in Af-cons contain two Ib subunits (Figure 3).

The SR region has three distinct sequence components: a 13-mer insertion/deletion, stretch of serine repeats, and a 17-mer dimorphic region (Morimatsu et al., 1997; Tanabe et al., 2012). A total of 69 amino acid sequence variations was identified in the SR region (Supplementary Figure S2). The 13-mer deletion in the SR region of the FCR3 strain (Figure 3) was observed in Oceania and South America, but not in Africa (Tanabe et al.,

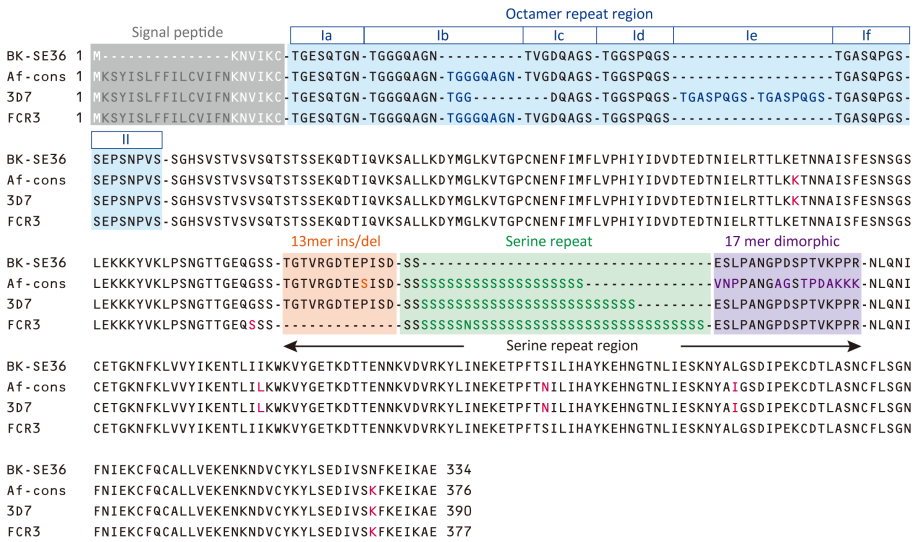

FIGURE 3
Sequence comparison of SE36 region in SERA5. The African consensus sequence (Af-cons) of the SE36 region was derived from sequence comparison of 314 SERA5 sequences from four African countries. Amino acid sequences of the corresponding SE36 region were compared among vaccine-type variants (the vaccine candidate based on *P. falciparum* Honduras 1), 3D7 and FCR3 strains, and Af-cons. Characteristic regions are shaded in color: signal peptide, octamer repeat region, serine repeat region. Amino acids that differ from vaccine-type SE36 are shown in red font. Octamer repeat sequence was classified into Ia to If and II according to a previous study (Tanabe et al., 2012).

2012). In vaccine-type SE36 and Af-cons, the 13-mer sequence contained a serine/proline variation at position 203: a proline residue was found in the vaccine-type and 3D7 strain but a serine residue was mostly found in all isolates from the four African countries. SERA sequences did not differ significantly among the four African countries in terms of serine/proline ratios at position 203 ($p > 0.05$, χ^2-test) (Table 2).

For the stretch of serine tandem repeats from which SERA5 was named, vaccine-type SE36 contains only two serine residues (Figure 3). This stretch of serine tandem repeats was mostly deleted from the vaccine construct to improve the hydrophilicity of the protein and make it amenable for large-scale Good Manufacturing Practices (GMP) production (Palacpac et al., 2011). Among the 314 African isolates, the number of poly-serine residues varied from 5 to 43, with 21 repeats as the most common in all 4 African countries (Table 3). The difference in the number of serine residues among the four countries was statistically significant ($p < 0.05$, Kruskal-Wallis test). Notably, the amino acids isoleucine, asparagine, glycine, and arginine were also found in the serine stretch in eight of the 314 African isolates (Supplementary Figure S2).

Just after the poly-serine repeat is a 17-mer dimorphic region (Figure 3) containing four major sequence variations (Tanabe et al., 2012): 'VNPPANGAGSTPDAKKK' (Type I), 'ESLPANGPDSPTVKPPR' (Type IV), and recombination forms 'VNPPANGAGSTPDAKKR` (Type II) and 'VNPPANGPDSPTVKPPR' (Type III). Vaccine-type SE36 has the Type IV sequence, whereas all African isolates had Type I as dominant sequence (Table 4). For the four African countries, the ratio of Type I to Type IV sequence was significantly different ($p < 0.01$, χ2-test); and notably, no Type II and Type III sequences were found in Burkina Faso isolates. There were also sequence variations in Type IV. Substitutions at position 241 of proline to leucine and position 244 of proline to leucine were found in one Ugandan and Tanzanian isolate, respectively (Supplementary Table S2, Supplementary Figure S2).

In non-repeat regions, amino acid mismatches were observed in Af-cons at five positions (Figure 3). Those were at positions 159, 275, 308, 330, and 383 of the SERA5 amino acid sequence of *P. falciparum* strain 3D7. Among them, glutamic acid at position 159 and leucine at position 330 were also found in Uganda (n=1), Tanzania (n=1), and Ghana (n=1) isolates, although their frequencies were very low (Figure 4). In the vaccine-type SE36, at positions 275, 308, and 383, isoleucine, serine, and lysine were found, whereas African isolates exclusively showed leucine, asparagine, and lysine, respectively.

According to the above results, there are multiple differences between the vaccine-type SE36 and the corresponding SERA5 sequence from African isolates. The occurrence of identical sequences to the vaccine-type variant was rare.

Sequence variation in SE36 of *P. falciparum* clinical isolates obtained from vaccinated and control groups

If BK-SE36 confers allele-specific immune response or shows efficacy targeting only vaccine-type parasites or closely related variants, then vaccinated individuals may be selectively infected with *P. falciparum* strains whose SERA5 sequences are less identical/heterologous to vaccine-type variant. Additionally, if sequence-dependent selection occurs, the haplotype diversity of SERA5 in the vaccinated group may be lower than that of SERA5 in the control group. To explore these possibilities, the haplotype diversity of SE36; OR and SR regions of SERA5 were compared between isolates from the BK-SE36 arm and isolates

TABLE 1 Number and frequency of octamer units found in SERA5 sequences from 314 African isolates.

No of octamer unit	total n = 314	Uganda n = 172	Burkina Faso n = 54	Tanzania n = 55	Ghana n = 33
2	2 (0.6)	N.D.	N.D.	1 (1.8)	1 (3.0)
5	1 (0.3)	1 (0.6)	N.D.	N.D.	N.D.
6	14 (4.5)	7 (4.1)	5 (9.3)	1 (1.8)	1 (3.0)
7	196 (62.4)	119 (69.2)	23 (42.6)	38 (69.1)	16 (48.5)
8	47 (15.0)	17 (9.9)	15 (27.8)	5 (9.1)	10 (30.3)
9	17 (5.4)	9 (5.2)	4 (7.4)	4 (7.3)	N.D.
10	6 (1.9)	2 (1.2)	2 (3.7)	N.D.	2 (6.1)
11	10 (3.2)	4 (2.3)	4 (7.4)	2 (3.6)	N.D.
12	10 (3.2)	7 (4.1)	1 (1.9)	N.D.	2 (6.1)
13	4 (1.3)	1 (0.6)	N.D.	3 (5.5)	N.D.
14	4 (1.3)	3 (1.7)	N.D.	1(1.8)	N.D.
15	2 (0.6)	1 (0.6)	N.D.	N.D.	1 (3.0)
35	1 (0.3)	1 (0.6)	N.D.	N.D.	N.D.

The frequency is shown as a percentage in parentheses.
For details, see Supplementary Figure S1.
N.D. not detected.

10.3389/fcimb.2022.1058081

TABLE 2 Frequency of serine/proline residues at position 203 in the 13-mer insertion/deletion region of SERA5.

		position 203	
	n	Serine	Proline
Uganda	172	125 (72.7)	47 (27.3)
Burkina Faso	54	41 (75.9)	13 (24.1)
Tanzania	55	35 (63.6)	20 (36.4)
Ghana	33	18 (54.5)	15 (45.5)

The amino acid position is numbered after the 3D7 sequence.
The frequency is shown as a percentage in parentheses.

from the control arm in Uganda and Burkina Faso trials (Supplementary Table S5). The haplotype diversity of SERA5 was similar between the vaccinated and control groups at the two trial sites. In the OR and SR regions, haplotype diversity was slightly higher in the vaccinated group than in the control group.

Four Ugandan isolates showed the same amino acid sequence as the OR region of vaccine-type SE36; three were from the BK-SE36 vaccine arm and one from the control arm. No isolate from Burkina Faso showed an identical OR sequence (Supplementary Figure S1). In terms of the number of OR repeat units, seven Ugandan isolates and five Burkina Faso isolates had six OR units, similar to the vaccine-type variant (Table 5). There was no significant difference in the frequency of the six OR units between the vaccinated and control groups, both in Uganda and Burkina Faso isolates ($p > 0.05$, χ2-test). As inferred above, from the African samples, seven OR units were the most common in both Uganda and Burkina Faso isolates, although overall no marked differences in OR frequencies can be seen between the vaccinated and control groups.

For the serine/proline substitution in the 13-mer insertion/deletion part of the SR region, the frequency of proline substitution was not biased between the vaccinated and control groups in both the Uganda and Burkina Faso isolates ($p > 0.05$, χ2-test) (Table 6). For the 17-mer dimorphic region where the vaccine type is Type IV, the frequency of Type IV isolates did not greatly differ from those obtained from the BK-SE36 vaccine group and control subjects ($p > 0.05$, χ2-test) (Table 6). Considering the number of serine residues between the vaccinated and control groups (Figure 5, Supplementary Table S6), the variation in the length of the serine stretch also did not differ between the two treatment arms (BK-SE36 or control arms) ($p > 0.05$, Mann-Whitney test). However, it is noted that the number of serine residues was

TABLE 3 Number of serine repeats/amino acid residues in the stretch of serine tandem repeats of the SERA5 SR region.

No. of amino acid	Uganda n = 172	Burkina Faso n = 54	Tanzania n = 55	Ghana n = 33
5	1 (0.6)	N.D.	1 (1.8)	1 (3.0)
11	1 (0.6)	N.D.	1 (1.8)	N.D.
15	7 (4.1)	3(5.6)	6 (10.9)	2 (6.1)
17	3 (1.7)	N.D.	N.D.	N.D.
19	1 (0.6)	1 (1.9)	1 (1.8)	N.D.
21	44 (25.6)	21 (38.9)	16 (29.1)	8 (24.2)
23	21 (12.2)	10 (18.5)	6 (10.9)	3 (9.1)
25	16 (9.3)	7 (13.0)	4 (7.3)	2 (6.1)
27	12 (7.0)	3 (5.6)	4 (7.3)	1 (3.0)
29	7 (4.1)	1 (1.9)	3 (5.5)	4 (12.1)
31	43 (25.0)	5 (9.3)	11 (20.0)	5 (15.2)
33	8 (4.7)	3 (5.6)	1 (1.8)	3 (9.1)
35	3 (1.7)	N.D.	N.D.	2 (6.1)
37	1 (0.6)	N.D.	N.D.	N.D.
39	2 (1.2)	N.D.	N.D.	N.D.
41	2 (1.2)	N.D.	N.D.	1 (3.0)
43	N.D.	N.D.	1 (1.8)	1 (3.0)

The frequency is shown as a percentage in parentheses.
N.D. not detected.

10.3389/fcimb.2022.1058081

TABLE 4 Frequency of Type I to Type IV sequence types in the 17-mer dimorphic sequence of SERA5 SR region.

		17 mer dimorphic sequence			
	n	Type I	Type II	Type III	Type IV
Uganda	172	90 (52.3)	10 (5.8)	37 (21.5)	35 (20.3)
Burkina Faso	54	46 (85.2)	N.D.	N.D.	8 (14.8)
Tanzania	55	21 (38.2)	9 (16.4)	11 (20.0)	14 (25.5)
Ghana	33	21 (63.6)	1 (3.0)	1 (3.0)	10 (30.3)

The frequency is shown as a percentage in parentheses.
N.D. not detected.

relatively greater (*i.e.* longer stretch of serine residues) in the Ugandan isolates than those isolated from Burkina Faso ($p < 0.05$, Mann-Whitney test).

Genetic differentiation in the SE36 region of SERA5 was examined using *Fst*, the Wright's fixation index of inter-population variance in allele frequencies (Wright, 1965) (Table 7). The *Fst* value suggested a significant difference in the SE36 region of SERA5 and SR region between the Ugandan and Burkina Faso isolates ($p < 0.05$). However, no significant differentiation was detected between isolates from two vaccination arms (BK-SE36 or control). The OR region did not significantly differ between the Uganda and Burkina Faso isolates.

Discussion

Antigen polymorphisms driving allele-specific efficacy are a common limitation in malaria vaccine development (Thera

Amino acid position	1559	2758	3083	3380	3883
3D7	K	L	N	I	K
BK-SE36	E	I	S	L	N
Uganda n=172	K	L	N	I	K
	E			L	
Burkina Faso n=54	K	L	N	I	K
Tazania n=55	K	L	N	I	K
	E			L	
Ghana n=33	K	L	N	I	K
	E			L	

FIGURE 4
Amino acid variation in vaccine-type SE36 with the octamer and serine repeat regions removed from the analyses. Amino acid positions are numbered after the *P. falciparum* 3D7 sequence. The gray background shows a minor allele with only one allele found in each population.

TABLE 5 Number and frequency of octamer units found in the SERA5 sequence from clinical trial sites.

No. of octamer unit	Uganda			Burkina Faso		
	total n = 172	vaccinated n = 77	controls n = 95	total n = 54	vaccinated n = 29	controls n = 25
5	1 (0.6)	1 (1.3)	N.D.	N.D.	N.D.	N.D.
6	**7 (4.1)**	**3 (3.9)**	**4 (4.2)**	**5 (9.3)**	**3 (10.3)**	**2 (8.0)**
7	119 (69.2)	55 (71.4)	64 (67.4)	23 (42.6)	14 (48.3)	9 (36.0)
8	17 (9.9)	8 (10.4)	9 (9.5)	14 (25.9)	8 (27.6)	6 (24.0)
9	9 (5.2)	5 (6.5)	4 (4.2)	5 (9.3)	1 (3.4)	4 (16.0)
10	2 (1.2)	1 (1.3)	1 (1.1)	2 (3.7)	1 (3.4)	1 (4.0)
11	4 (2.3)	1 (1.3)	3 (3.2)	4 (7.4)	1 (3.4)	3 (12.0)
12	7 (4.1)	2 (2.6)	5 (5.3)	1 (1.9)	1 (3.4)	N.D.
13	1 (0.6)	N.D.	1 (1.1)	N.D.	N.D.	N.D.
14	3 (1.7)	1 (1.3)	2 (2.1)	N.D.	N.D.	N.D.
15	1 (0.6)	N.D.	1 (1.1)	N.D.	N.D.	N.D.
35	1 (0.6)	N.D.	1 (1.1)	N.D.	N.D.	N.D.

The frequency is shown as a percentage in parentheses.
The octamer unit that is the same as BK-SE36 is shown in bold.
N.D. not detected.

et al., 2011; Ouattara et al., 2013; Neafsey et al., 2015). Early-stage clinical trials demonstrated that the BK-SE36 vaccine had acceptable reactogenicity, had no unexpected safety concerns, and was immunogenic. As a blood-stage vaccine, BK-SE36 is expected to reduce morbidity and mortality from *P. falciparum* infections. Indeed, in the longitudinal study following the clinical trial in Uganda, the BK-SE36 vaccine arm showed substantial differences in the hazard ratio to first episodes of high parasitemia + fever (0.28, 95% CI: 0.12-0.66, $p < 0.01$) and against all malaria episodes of high parasitemia + fever (0.34, 95% CI: 0.15-0.76, $p = 0.01$) (Palacpac et al., 2013). This promising efficacy could be due to the high frequency of identical/homologous alleles to vaccine-type SE36 at the clinical trial site, however, the current analysis indicates that the frequency of homologous alleles was very low, not only in Uganda (where promising data were obtained) but also in Burkina Faso as well as other African countries such as Tanzania and Ghana. When SERA5 sequences from the BK-SE36 vaccinated and control group were compared, the difference between the frequency of the identical or homologous allele to vaccine-type SE36 was within statistical error, showing no evidence of vaccination-induced allele selection. In addition, no selection of the SERA5 haplotype was evident in the BK-SE36 treatment arm.

SERA5 has markedly fewer SNPs than the malaria vaccine candidates AMA1 and CSP, although it is the recombination events that generated much of the diversity in the number of octamer repeats and number of serine residues in the serine stretch in SERA5. The consensus sequence of SERA5 was identical in the four African countries. The genetic

TABLE 6 Frequency of proline in 13-mer insertion/deletion sequence and frequency of Type IV sequence in the 17-mer dimorphic sequence of the SERA5 SR region in Uganda and Burkina Faso.

	n	No. of Proline	frequency (%)	No. of Type IV	frequency (%)
Uganda + Burkina Faso	226	60	26.5	43	19.0
Vaccinated	106	29	27.4	21	19.8
Controls	120	31	25.8	22	18.3
Uganda	172	47	27.3	35	20.3
Vaccinated	77	21	27.3	16	20.8
Controls	95	26	27.4	19	20.0
Burkina Faso	54	13	24.1	8	14.8
Vaccinated	29	8	27.6	5	17.2
Controls	25	5	20.0	3	12.0

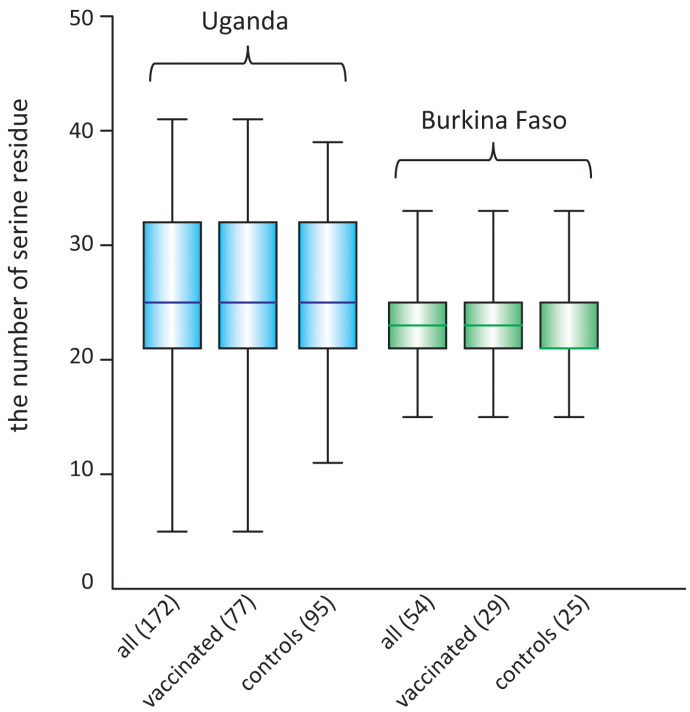

FIGURE 5
Box plot showing the number of poly-serine residues in the stretch of serine tandem repeats in the SR region of SERA5, in isolates from two clinical trial sites. The number of analyzed sequences is shown in parentheses.

differentiation in SERA5 (observed in SNPS and repeat variants found in the OR and SR regions) among isolates from Uganda and Burkina Faso may be due to geographical distance. This finding was similar to an earlier inference using worldwide isolates from 9 countries, albeit isolates from Africa were sourced only from 2 countries (Tanabe et al., 2012). The biased geographical distribution for SNPs and repeat variants may possibly be a result of gene flow barriers or divergent selection in different populations resulting in high-level sequence conservation of *sera5*, except for the insertion/deletion and repeat regions.

TABLE 7 Genetic differentiation (*Fst*) of the vaccine-type SE36 in SERA5 among isolates from clinical trial sites.

	***Fst* (*p*-value)**
***Fst* of SERA5 BK-SE36 region**	
Uganda vs Burkina Faso	0.0248 (0.000)
Uganda: vaccinated group vs control group	-0.0028 (0.613)
Burkina Faso: vaccinated group vs control group	-0.0017 (0.396)
***Fst* of SERA5 octamer repeat region**	
Uganda vs Burkina Faso	0.0073 (0.099)
Uganda: vaccinated group vs control group	-0.0032 (0.622)
Burkina Faso: vaccinated group vs control group	0.0040 (0.351)
***Fst* of SERA5 serine repeat region**	
Uganda vs Burkina Faso	0.0615 (0.000)
Uganda: vaccinated group vs control group	-0.0018 (0.414)
Burkina Faso: vaccinated group vs control group	-0.0172 (0.703)

Both OR and SR regions, hot spots of recombination, are characterized as intrinsically unstructured (Yagi et al., 2014). The epitope mapping data suggest that (i) intrinsically unstructured regions allow some flexibility for the epitopes to interact with other molecules/proteins; (ii) the regions adjacent to the repeats are not strictly disordered as they showed a tendency to form a secondary structure; (iii) the protective epitopes of BK-SE36 are located in the N-terminal region where the repeat number of octamer units varied among alleles; and (iv) serum from mice and squirrel monkeys vaccinated with BK-SE36 also showed a broad range of reactivity against peptides covering the SR region (Yagi et al., 2014). Indeed, serum samples from clinical trial participants that received BK-SE36 preferentially recognized epitopes corresponding to the SR and flanking regions (including 13-mer insertion/deletion, polyserine residue and 17-mer dimorphic region) (Ezoe et al., 2020; Bougouma et al., 2022). Thus, these indicate that the antibodies induced by BK-SE36 vaccination bound, with reproducibility, to epitopes located in the disordered regions of the protein. Further studies with larger sample size, in combination with protective efficacy data, would

fine-tune which epitopes would be immunologically important with respect to vaccine development.

Limited polymorphism of SERA5 could be attributed a to low seropositive population even in malaria-endemic regions. For example, a seroepidemiology study in the Solomon Islands showed that <50% of adults and <10% of children under 10 years were seropositive to anti-SE36, although higher seropositivity to MSP-1 was observed in the population (Horii et al., 2010). In the phase 1b BK-SE36 trial in Uganda, almost no seroconversion was evident in vaccinated adults (18-32 years old), but notably, around 70% of 6-10-year-old in the BK-SE36 arm were seropositive after two BK-SE36 vaccinations (i.e. seropositivity is defined as having ≥2-fold increase in anti-SE36 antibody titers compared to baseline) (Palacpac et al., 2013). The low seroconversion rate observed in adult subjects living in malaria-endemic areas is in contrast to an early-stage trial in malaria naïve Japanese adults where 100% seroconversion was achieved after two or three vaccinations of BK-SE36 (Horii et al., 2010). These data suggest that immune tolerance occurs in malaria-endemic areas through repeated infections. Recently, SE36 was demonstrated to tightly bind the host protein vitronectin and the resulting complex cloaks the merozoite surface allowing the parasite to circumvent host immunity (Tougan et al., 2018). We contend that the repeated presentation of vitronectin-bound-SE36, as a result of infection, was exploited by the parasite such that SE36 disguises itself as a host antigen, avoiding clearance by phagocytosis and leading to the gradual acquisition of immune tolerance. If this interpretation is true, young children or individuals with limited malaria infection history would respond better to BK-SE36 vaccination similar to malaria naïve Japanese adults. Indeed, the seroconversion rate was higher in the 24–60-month-old and 12–24-month-old Burkinabe children (79–83% after two- and 89–97% after three-vaccinations) (Bougouma et al., 2022). This immune tolerance could also explain why SERA5 is less likely to be under substantial immune selection pressure compared to other blood-stage malaria vaccine antigens such as AMA1 and CSP. Moving forward, an important caveat to our data interpretation would be how to overcome immune tolerance in hyporesponsive populations.

Overall, despite polymorphism and mismatches observed in SERA5 repeat regions and in some SNPs between Af-cons and vaccine-type SE36, BK-SE36 is a promising vaccine candidate, especially for infants and malaria naïve travelers. In the current analyses, samples with multiple *P. falciparum* infections were excluded, so a direct comparison of the number of infections is not possible based solely on the number of SERA5 sequences. In the Ugandan follow-up study, based on different parasite density thresholds, BK-SE36 may likely have a disease ameliorating effect rather than preventing infection per se (Palacpac et al., 2013). Differences were observed among isolates from the four African countries in the number of consecutive serine residues in the SR region and the frequency of Type I to IV sequences in the 17-mer dimorphic region. How these differences could affect the efficacy of the vaccine is not known. Larger efficacy proof-of-concept trials are needed.

Data availability statement

The datasets presented in this study can be found in online repositories. The names of the repository/repositories and accession number(s) can be found in the article/ Supplementary Materials

Ethics statement

The studies involving human 1: participants were reviewed and approved by for the Ugandan trial and follow-up study the ethical institutional review committees of Med Biotech Laboratories (Ref# IRB-00003990-MBL-BIOMEDICAL, IRB-00003995-MBL-BIOMEDICAL), Uganda National Council for Science and Technology (Ref# HS635, HS866), Osaka University (Ref# 20-3, 287), and Research Foundation for Microbial Diseases of Osaka University. 2: Approval for the Burkina Faso trial was obtained from Comité d'Éthique pour la Recherche en Santé du Burkina Faso (Ref# 2014-12-144), Comité Institutionnel de Bioéthique du INSP/CNRFP (previous name: CNRFP) (Ref# N° 2014/071/MS/SG/CNRFP/CIB, N°2016/000008/MS/SG/CNRFP/CIB), Agence Nationale de Régulation Pharmaceutique (ANRP, previous name: Direction Générale de la Pharmacie, du Médicament et des Laboratoires [DGPML], Ref# N°2015:658/MS/CAB), Scientific Committee/Institutional Review Committee of the Research Institute for Microbial Diseases (Ref# 26), Osaka University (Ref# 574); and London School of Hygiene and Tropical Medicine Research Ethics Committee (Ref# 9175). Written informed consent to participate in this study was provided by the participants' legal guardian/next of kin.

Author contributions

Conceptualization, NA, NP and TH. methodology, validation and formal analysis, NA. investigation and resources, NA, AY, BB, EN, BK, TE, EB, AT, IN, AD, SS, SH, FD, OL, TH. data curation, NA, NP, SH, and SS. writing—original draft preparation, NA, NP, and TH. writing—review and editing, BK, EN, BB, EB, SH, FD. visualization, NA, NP, and TH. funding acquisition, NP, SH, OL, SS, TE and TH. All authors contributed to the article and approved the submitted version.

Funding

This work was supported by the Global Health Innovative Technology Fund (GHIT 2013-105) to TH; (G2014-109, G2016-106, G2019-208) to the EVI-RIMD-Burkina Faso consortium. MEXT KAKENHI Grant Numbers 15651988, 24249024; Funds for Integrated Promotion of Social System Reform and Research and Development (38201103-01), Grant for Translational Research Network Program (JP20lm0203135, AMED) (C-13); Grant for Clinical Application of Innovative Medical Seeds (AMED) to TH; Support Program for Orphan Drug Prior to the Designation (AMED) (17nk0101206j0003) to Nobelpharma Co., Ltd (NPC); and Irish Aid to EVI. The funders had no role in study design, data collection and analysis, interpretation of data, decision to publish, or preparation of the manuscript.

Acknowledgments

We would like to thank all participants and their families in Lira, Uganda and Banfora, Burkina Faso for taking part in the clinical trials. The Research Foundation for Microbial Diseases of Osaka University, Nobelpharma Co. Ltd., the research teams from Med Biotech Laboratories (Uganda); Unité de Recherche Clinique de Banfora and Institut National de Santé Publique/Centre National de Recherche et de Formation sur le Paludisme (Burkina Faso); European Vaccine Initiative (Germany); Research Institute for Microbial Diseases (including laboratory assistance of Hideko Yoshikawa, Sawako Itagaki) (Japan). We also would like to thank Editage (www.editage.jp) for English language editing.

Conflict of interest

TH is the inventor of BK-SE36 and all rights have now been turned over to NPC. NP, EN, AY, BB, BK, and TE received remuneration from BIKEN for the Ugandan trial and follow-up.

For the Burkina Faso clinical trial/follow-up study, the following received some support from NPC: EB, AD, SH, FD, OL, and NP. TH and NP are currently supported by a research fund from NPC.

The remaining authors declare that the research was conducted in the absence of any commercial or financial relationships that could be construed as a potential conflict of interest.

Publisher's note

Supplementary material

The Supplementary Material for this article can be found online at: https://www.frontiersin.org/articles/10.3389/fcimb.2022.1058081/full#supplementary-material

References

Aoki, S., Li, J., Itagaki, S., Okech, B. A., Egwang, T. G., Matsuoka, H., et al. (2002). Serine repeat antigen (SERA5) is predominantly expressed among the SERA multigene family of *Plasmodium falciparum*, and the acquired antibody titers correlate with serum inhibition of the parasite growth. *J. Biol. Chem.* 277, 47533–47540. doi: 10.1074/jbc.M207145200

Arisue, N., Palacpac, N. M. Q., Tougan, T., and Horii, T. (2020). Characteristic features of the SERA multigene family in the malaria parasite. *Parasitol. Vectors.* 13, 170. doi: 10.1186/s13071-020-04044-y

Bougouma, E. C., Palacpac, N. M. Q., Tiono, A. B., Nebie, I., Ouédraogo, A., Houard, S., et al. (2022). Safety and immunogenicity of BK-SE36 in a blinded, randomized, controlled, age de-escalating phase ib clinical trial in Burkinabe children. *Front. Immunol.* 13, 978591. doi: 10.3389/fimmu.2022.978591

Debrabant, A., Maes, P., Delplace, P., Dubremetz, J. F., Tartar, A., and Camus, D. (1992). Intramolecular mapping of *Plasmodium falciparum* p126 proteolytic fragments by n-terminal amino acid sequencing. *Mol. Biochem. Parasitol.* 53, 89–96. doi: 10.1016/0166-6851(92)90010-h

Excoffier, L., and Lischer, H. E. (2010). Arlequin suite ver 3.5: a new series of programs to perform population genetics analyses under Linux and windows. *Mol. Ecol. Resour.* 10, 564–567. doi: 10.1111/j.1755-0998.2010.02847.x

Ezoe, S., Palacpac, N. M. Q., Tetsutani, K., Yamamoto, K., Okada, K., Taira, M., et al. (2020). First-in-human randomised trial and follow-up study of *Plasmodium falciparum* blood-stage malaria vaccine BK-SE36 with CpG-ODN(K3). *Vaccine.* 38, 7246–7257. doi: 10.1016/j.vaccine.2020.09.056

Fox, B. A., Xing-Li, P., Suzue, K., Horii., T., and Bzik, D. J. (1997). *Plasmodium falciparum*: An epitope within a highly conserved region of the 47-kDa amino-terminal domain of the serine repeat antigen is a target of parasite-inhibitory antibodies. *Exp. Parasitol.* 85, 121–134. doi: 10.1006/expr.1996.4118

Horii, T., Shirai, H., Li, J., Ishii, K. J., Palacpac, N. Q., Tougan, T., et al. (2010). Evidences of protection against blood-stage infection of *Plasmodium falciparum* by the novel protein vaccine SE36. *Parasitol. Int.* 59, 380–386. doi: 10.1016/j.parint.2010.05.002

Kumar, S., Stecher, G., Li, M., Knyaz, C., and Tamura, K. (2018). MEGA X: Molecular evolutionary genetics analysis across computing platforms. *Mol. Biol. Evol.* 35, 1547–1549. doi: 10.1093/molbev/msy096

Laurens, M. B. (2020). RTS,S/AS01 vaccine (Mosquirix™): An overview. *Hum. Vaccin. Immunother.* 16, 480–489. doi: 10.1080/21645515.2019.1669415

Librado, P., and Rozas, J. (2009). DnaSP v5: a software for comprehensive analysis of DNA polymorphism data. *Bioinformatics.* 25, 1451–1452. doi: 10.1093/bioinformatics/btp187

Li, J., Matsuoka, H., Mitamura, T., and Horii, T. (2002). Characterization of proteases involved in the processing of *Plasmodium falciparum* serine repeat antigen (SERA). *Mol. Biochem. Parasitol.* 120, 177–186. doi: 10.1016/s0166-6851(01)00452-2

Maxmen, A. (2021). Scientists hail historic malaria vaccine approval - but point to challenges ahead. *Nature*. doi: 10.1038/d41586-021-02755-5

Morimatsu, K., Morikawa, T., Tanabe, K., Bzik, D. J., and Horii, T. (1997). Sequence diversity in the amino-terminal 47 kDa fragment of the *Plasmodium falciparum* serine repeat antigen. *Mol. Biochem. Parasitol.* 86, 249–254. doi: 10.1016/s0166-6851(97)00038-8

Neafsey, D. E., Juraska, M., Bedford, T., Benkeser, D., Valim, C., Griggs, A., et al. (2015). Genetic diversity and protective efficacy of RTS,S/AS01 malaria vaccine. *N. Engl. J. Med.* 373, 2025–2037. doi: 10.1056/NEJMoa1505819

Nei, M., and Gojobori, T. (1986). Simple methods for estimating the numbers of synonymous and nonsynonymous nucleotide substitutions. *Mol. Biol. Evol.* 3, 418–426. doi: 10.1093/oxfordjournals.molbev.a040410

Ogutu, B. R., Apollo, O. J., McKinney, D., Okoth, W., Siangla, J., Dubovsky, F., et al. (2009). Blood stage malaria vaccine eliciting high antigen-specific antibody concentrations confers no protection to young children in Western Kenya. *PloS One* 4, e4708. doi: 10.1371/journal.pone.0004708

Okech, B., Mujuzi, G., Ogwal, A., Shirai, H., Horii, T., and Egwang, T. G. (2006). High titers of IgG antibodies against *Plasmodium falciparum* serine repeat antigen 5 (SERA5) are associated with protection against severe malaria in Ugandan children. *Am. J. Trop. Med. Hyg.* 74, 191–197. doi: 10.4269/ajtmh.2006.74.191

Okech, B. A., Nalunkuma, A., Okello, D., Pang, X. L., Suzue, K., Li, J., et al. (2001). Natural human immunoglobulin G subclass responses to *Plasmodium falciparum* serine repeat antigen in Uganda. *Am. J. Trop. Med. Hyg.* 65, 912–917. doi: 10.4269/ajtmh.2001.65.912

Ouattara, A., Takala-Harrison, S., Thera, M. A., Coulibaly, D., Niangaly, A., Saye, R., et al. (2013). Molecular basis of allele-specific efficacy of a blood-stage malaria vaccine: vaccine development implications. *J. Infect. Dis.* 207, 511–519. doi: 10.1093/infdis/jis709

Owalla, T. J., Palacpac, N. M., Shirai, H., Horii, T., and Egwang, T. G. (2013). Association of naturally acquired IgG antibodies against *Plasmodium falciparum* serine repeat antigen-5 with reduced placental parasitemia and normal birth weight in pregnant Ugandan women: a pilot study. *Parasitol. Int.* 62, 237–239. doi: 10.1016/j.parint.2013.01.006

Palacpac, N. M., Arisue, N., Tougan, T., Ishii, K. J., and Horii, T. (2011). *Plasmodium falciparum* serine repeat antigen 5 (SE36) as a malaria vaccine candidate. *Vaccine.* 29, 5837–5845. doi: 10.1016/j.vaccine.2011.06.052

Palacpac, N. M. Q., and Horii, T. (2020). Malaria vaccines: Facing unknowns. *F1000Res.* 9, F1000 Faculty Rev–296. doi: 10.12688/f1000research.22143.1

Palacpac, N. M., Ntege, E., Yeka, A., Balikagala, B., Suzuki, N., Shirai, H., et al. (2013). Phase 1b randomized trial and follow-up study in Uganda of the blood-stage malaria vaccine candidate BK-SE36. *PloS One* 8, e64073. doi: 10.1371/journal.pone.0064073

Pang, X. L., and Horii, T. (1998). Complement-mediated killing of *Plasmodium falciparum* erythrocytic schizont with antibodies to the recombinant serine repeat antigen (SERA). *Vaccine.* 16, 1299–1305. doi: 10.1016/s0264-410x(98)00057-7

Pang, X. L., Mitamura, T., and Horii, T. (1999). Antibodies reactive with the N-terminal domain of *Plasmodium falciparum* serine repeat antigen inhibit cell proliferation by agglutinating merozoites and schizonts. *Infect. Immun.* 67, 1821–1827. doi: 10.1128/IAI.67.4.1821-1827.1999

Proietti, C., Pettinato, D. D., Kanoi, B. N., Ntege, E., Crisanti, A., and Riley, E. M. (2011). Continuing intense malaria transmission in northern Uganda. *Am. J. Trop. Med. Hyg.* 84, 830–837. doi: 10.4269/ajtmh.2011.10-0498

Stallmach, R., Kavishwar, M., Withers-Martinez, C., Hackett, F., Collins, C. R., Howell, S. A., et al. (2015). *Plasmodium falciparum* SERA5 plays a non-enzymatic role in the malarial asexual blood-stage lifecycle. *Mol. Microbiol.* 96, 368–387. doi: 10.1111/mmi.12941

Sugiyama, T., Suzue, K., Okamoto, M., Inselburg, J., Tai., K., and Horii, T. (1996). Production of recombinant SERA proteins of *Plasmodium falciparum* in *Escherichia coli* by using synthetic genes. *Vaccine.* 14, 1069–1076. doi: 10.1016/0264-410x(95)00238-v

Takala, S. L., Coulibaly, D., Thera, M. A., Batchelor, A. H., Cummings, M. P., Escalante, A. A., et al. (2009). Extreme polymorphism in a vaccine antigen and risk of clinical malaria: implications for vaccine development. *Sci. Transl. Med.* 1, 2ra5. doi: 10.1126/scitranslmed.3000257

Tanabe, K., Arisue, N., Palacpac, N. M., Yagi, M., Tougan, T., Honma, H., et al. (2012). Geographic differentiation of polymorphism in the *Plasmodium falciparum* malaria vaccine candidate gene SERA5. *Vaccine.* 30, 1583–1593. doi: 10.1016/j.vaccine.2011.12.124

Tanabe, K., Mita, T., Jombart, T., Eriksson, A., Horibe, S., Palacpac, N., et al. (2010). *Plasmodium falciparum* accompanied the human expansion out of Africa. *Curr. Biol.* 20, 1283–1289. doi: 10.1016/j.cub.2010.05.053

Thera, M. A., Doumbo, O. K., Coulibaly, D., Laurens, M. B., Ouattara, A., Kone, A. K., et al. (2011). A field trial to assess a blood-stage malaria vaccine. *N. Engl. J. Med.* 365, 1004–1013. doi: 10.1056/NEJMoa1008115

Tiono, A. B., Kangoye, D. T., Rehman, A. M., Kargougou, D. G., Kaboré, Y., Diarra, A., et al. (2014). Malaria incidence in children in south-West Burkina Faso: comparison of active and passive case detection methods. *PloS One* 9, e86936. doi: 10.1371/journal.pone.0086936

Tougan, T., Edula, J. R., Takashima, E., Morita, M., Shinohara, M., Shinohara, A., et al. (2018). Molecular camouflage of *Plasmodium falciparum* merozoites by binding of host vitronectin to P47 fragment of SERA5. *Sci. Rep.* 8, 5052. doi: 10.1038/s41598-018-23194-9

Weiss, D. J., Lucas, T. C. D., Nguyen, M., Nandi, A. K., Bisanzio, D., Battle, K. E., et al. (2019). Mapping the global prevalence, incidence, and mortality of *Plasmodium falciparum*, 2000-17: A spatial and temporal modelling study. *Lancet*, 394, 322–331. doi: 10.1016/S0140-6736(19)31097-9

WHO (2021) *World malaria report*. Available at: https://www.who.int/teams/global-malaria-programme/reports/world-malaria-report-2021 (Accessed August 15, 2022).

Wright, S. (1965). The interpretation of population structure by F-statistics with special regard to systems of mating. *Evolution.* 19, 395–420. doi: 10.1111/j.1558-5646.1965.tb01731.x

Yagi, M., Bang, G., Tougan, T., Palacpac, N. M., Arisue, N., Aoshi, T., et al. (2014). Protective epitopes of the *Plasmodium falciparum* SERA5 malaria vaccine reside in intrinsically unstructured n-terminal repetitive sequences. *PloS One* 9, e98460. doi: 10.1371/journal.pone.0098460

Yagi, M., Palacpac, N. M., Ito, K., Oishi, Y., Itagaki, S., Balikagala, B., et al. (2016). Antibody titres and boosting after natural malaria infection in BK-SE36 vaccine responders during a follow-up study in Uganda. *Sci. Rep.* 6, 34363. doi: 10.1038/srep34363

Yeoh, S., O'Donnell, R. A., Koussis, K., Dluzewski, A. R., Ansell, K. H., Osborne, S. A., et al. (2007). Subcellular discharge of a serine protease mediates release of invasive malaria parasites from host erythrocytes. *Cell.* 131, 1072–1083. doi: 10.1016/j.cell.2007.10.049

frontiers | Frontiers in Cellular and Infection Microbiology

TYPE Review
PUBLISHED 24 January 2023
DOI 10.3389/fcimb.2023.1115522

OPEN ACCESS

EDITED BY
Sudhir Kumar,
Seattle Children's Research Institute,
United States

REVIEWED BY
Franziska Dengler,
University of Veterinary Medicine Vienna,
Austria
Praveen Kumar,
Institute of Medical Sciences, Banaras
Hindu University, India

*CORRESPONDENCE
William H. Witola
whwit35@illinois.edu

SPECIALTY SECTION
This article was submitted to
Parasite and Host,
a section of the journal
Frontiers in Cellular and
Infection Microbiology

RECEIVED 04 December 2022
ACCEPTED 09 January 2023
PUBLISHED 24 January 2023

CITATION
Khan SM and Witola WH (2023) Past,
current, and potential treatments for
cryptosporidiosis in humans and farm
animals: A comprehensive review.
Front. Cell. Infect. Microbiol. 13:1115522.
doi: 10.3389/fcimb.2023.1115522

Past, current, and potential treatments for cryptosporidiosis in humans and farm animals: A comprehensive review

Shahbaz M. Khan and William H. Witola*

Department of Pathobiology, College of Veterinary Medicine, University of Illinois Urbana-Champaign, Urbana, IL, United States

The intracellular protozoan parasite of the genus *Cryptosporidium* is among the leading causes of waterborne diarrheal disease outbreaks throughout the world. The parasite is transmitted by ingestion of infective oocysts that are highly stable in the environment and resistant to almost all conventional disinfection methods and water treatments. Control of the parasite infection is exceedingly difficult due to the excretion of large numbers of oocysts in the feces of infected individuals that contaminate the environment and serve as a source of infection for susceptible hosts including humans and animals. Drug development against the parasite is challenging owing to its limited genetic tractability, absence of conventional drug targets, unique intracellular location within the host, and the paucity of robust cell culture platforms for continuous parasite propagation. Despite the high prevalence of the parasite, the only US Food and Drug Administration (FDA)-approved treatment of *Cryptosporidium* infections is nitazoxanide, which has shown moderate efficacy in immunocompetent patients. More importantly, no effective therapeutic drugs are available for treating severe, potentially life-threatening cryptosporidiosis in immunodeficient patients, young children, and neonatal livestock. Thus, safe, inexpensive, and efficacious drugs are urgently required to reduce the ever-increasing global cryptosporidiosis burden especially in low-resource countries. Several compounds have been tested for both *in vitro* and *in vivo* efficacy against the disease. However, to date, only a few experimental compounds have been subjected to clinical trials in natural hosts, and among those none have proven efficacious. This review provides an overview of the past and present anti-*Cryptosporidium* pharmacotherapy in humans and agricultural animals. Herein, we also highlight the progress made in the field over the last few years and discuss the different strategies employed for discovery and development of effective prospective treatments for cryptosporidiosis.

KEYWORDS

***Cryptosporidium*, cryptosporidiosis, treatment, prevention, drug discovery, protozoa, diarrhea**

1 Introduction

1.1 History

The intracellular protozoan parasite *Cryptosporidium* is one of the most common parasitic pathogens causing enteric disease in humans and in a broad range of animals worldwide (Chalmers, 2014). First recognized and described briefly in 1907 by Ernest Tyzzer in the gastric glands of the common mouse (Tyzzer, 1907), *Cryptosporidium* was later described in greater detail in 1910, again from histological preparations from the murine gastric mucosa (Tyzzer, 1910). Tyzzer proposed the name *Cryptosporidium muris* for the parasite (Tyzzer, 1907; Tyzzer, 1910). In 1912, Tyzzer described another species with smaller oocysts than those of *C. muris* in the small intestine of experimentally infected laboratory mice, which he named *Cryptosporidium parvum* (Tyzzer, 1912). Although *Cryptosporidium* was subsequently identified in a wide range of domesticated animals, this genus of parasites only gained importance in the 1970s (after almost 7 decades from its initial discovery), when the parasite was found to be linked to gastrointestinal disease in humans and farm animals (Panciera et al., 1971; Meuten et al., 1974; Meisel et al., 1976; Nime et al., 1976). In the 1980s, cryptosporidiosis gained more widespread recognition after reports of fatal cryptosporidiosis in AIDS patients (Soave et al., 1984), zoonotic cryptosporidiosis in immunocompetent and immunodeficient humans (Current et al., 1983), waterborne human diarrheal outbreaks (D'Antonio et al., 1985; Hayes et al., 1989), and diarrheal disease in children (Sallon et al., 1988) and animals (Tzipori et al., 1980; Moon and Bemrick, 1981; Angus et al., 1982). In 1993, *Cryptosporidium* caused the largest documented drinking water outbreak in US history, which affected an estimated 403,000 people in Milwaukee, Wisconsin, and resulted in over $96 million in combined healthcare costs and productivity losses (Mac Kenzie et al., 1994; Hoxie et al., 1997; Corso et al., 2003). The enormity of the Milwaukee outbreak sparked concern among the public and attracted generous funds for *Cryptosporidium* research from governmental agencies all over the world during the next decade. This resulted in further advances in our knowledge about the basic biology of the parasite and the development of reliable molecular detection tools for estimating the global burden of the disease.

1.2 Life cycle

The life cycle of *Cryptosporidium* is direct and complex (Figure 1), consisting of both asexual multiplication and sexual reproduction phases within a single host that culminate in the production of environmentally resistant oocysts (Current and Garcia, 1991). Following ingestion of sporulated thick-walled oocysts, four infectious sporozoites are released from each oocyst that attach to the apical surface of intestinal epithelial cells, and then actively invade the host cell membrane to form an intracellular but extracytoplasmic parasitophorous vacuole (Current and Reese, 1986). Within the vacuole, sporozoites mature into trophozoites, which undergo three rounds of asexual proliferation, followed by a single generation of sexual stages to generate either thin-walled or thick-walled oocysts,

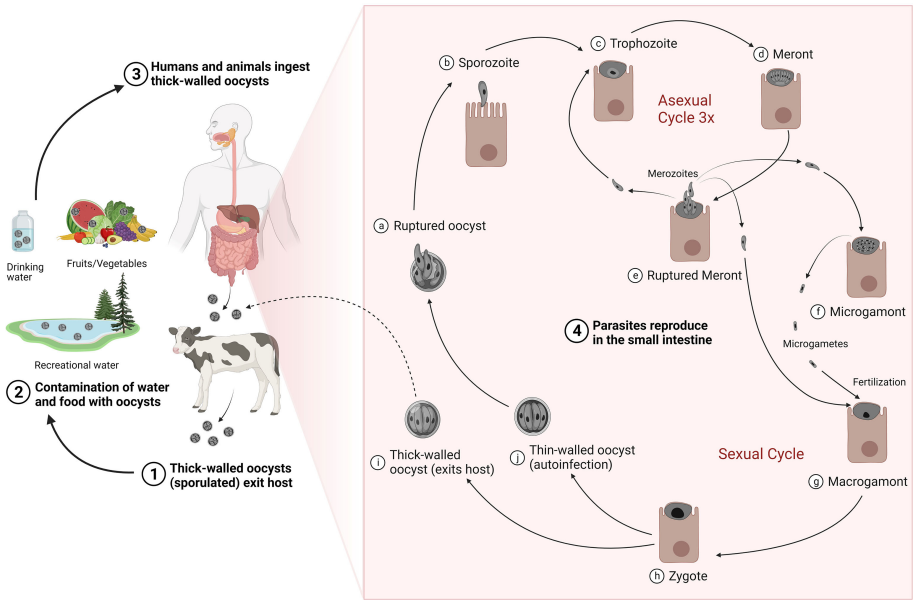

FIGURE 1
Life cycle and transmission of *Cryptosporidium*. Thick-walled sporulated oocysts are released in the feces of infected hosts (1) that contaminate food and water sources (2). Transmission occurs mainly by ingestion of contaminated water or food by susceptible hosts (3). Following ingestion, oocyst ruptures (4a) to release four sporozoites (4b). Sporozoites exhibit gliding motility, enter the host epithelial cells and mature into trophozoites (4c), which undergo three rounds of asexual multiplication to produce meronts (4d) that invariably release eight merozoites (4e). Merozoites released from the third round of asexual proliferation give rise to the sexual stages upon reinvasion of host cells: the male microgamonts (4f) and the female macrogamonts (4g). Microgametes released from the microgamont penetrate and fertilize macrogamonts to form diploid zygotes (4h). The zygotes undergo meiosis and sporogony generating either thin-walled (4i) or thick-walled (4j) oocysts, each containing four haploid sporozoites. Thick-walled oocysts are released into the lumen of the intestine and excreted into the environment, where they are instantly infectious. The thin-walled oocysts, in contrast, excyst to cause autoinfection in the same host. Adapted with modification from (CDC, 2019). Created with BioRender.com.

each containing four haploid sporozoites (Current and Reese, 1986; English et al., 2022). Thick-walled oocysts containing two-layered membranes are environmentally resistant and are passed out of the body in feces, where they are immediately infectious for other susceptible hosts. Thin-walled oocysts rupture in the intestinal lumen, releasing naked infectious sporozoites that autoinfect other enteric cells to ensure continued infection of the same host.

1.3 Transmission

In general, cryptosporidiosis is transmitted through the fecal-oral route (Figure 1) and contact with animals, manure or contaminated food and water is believed to lead to infections in humans (Xiao et al., 2004). Transmission in animals mainly occurs *via* ingestion of oocysts excreted by infected animals especially neonates in overcrowded or mixed housing facilities. Manure produced by livestock, especially cattle, is an important source of infection to both animals and people and it has been estimated that the global *Cryptosporidium* load in livestock manure is approximately 3.2×10^{23} oocysts per year (Vermeulen et al., 2017). Oocysts are highly stable in the environment and resistant to almost all conventional disinfection methods and water treatments such as chlorination (Fayer et al., 2000). Indeed, these persistent parasites have been found to be responsible for majority of the global protozoal water outbreaks that occurred from 2004–2010 (Karanis, 2018) and pose the biggest pathogen threat to the water industry (Chalmers, 2012). In the United States, exposure to treated recreational water such as swimming pools and water playgrounds was responsible for nearly 35% of the reported cryptosporidiosis outbreaks resulting in almost 57% cases during 2009–2017 (Gharpure et al., 2019). In addition to treated recreational water, contact with infected cattle (~15%), and contact with infected persons in childcare settings (~13%) were the other predominant causes of these outbreaks (Gharpure et al., 2019). *Cryptosporidium* is also recognized as an important foodborne pathogen, being responsible for more than 40 documented foodborne outbreaks to date, and more than 8 million cases of foodborne illnesses annually (Zahedi and Ryan, 2020). However, these numbers may be highly under-reported due to the lack of proper surveillance and the difficulties in tracing the source of foodborne disease outbreaks. Food can be contaminated at any point along the food production chain (during processing, distribution, or preparation) by direct contact with infected food handlers or by indirect exposure to water, preparation surfaces, equipment, or utensils contaminated with oocysts. Raw unpasteurized milk, unpasteurized apple cider, and salads are most associated with foodborne outbreaks of cryptosporidiosis (Gharpure et al., 2019; Zahedi and Ryan, 2020).

2 Cryptosporidiosis global disease burden in humans and animals

Cryptosporidium spp. enjoy high parasitic success due to their wide host range, low infective threshold, high excretion of resistant oocysts from infected individuals, and water-borne route of transmission (Innes et al., 2020). Protozoa of this genus are associated with diarrheal disease throughout the world with a higher incidence in developing countries (Shirley et al., 2012). Cryptosporidiosis is a major cause of public health concern in developed countries as well, with reported cases on the rise mainly due to the leading role of *Cryptosporidium* in causing waterborne outbreaks (Gharpure et al., 2019). Unfortunately, the global burden of cryptosporidiosis is likely to be underestimated, due to the lack of cheap and consistent methods of diagnosis, under-recognized disease in immunocompetent patients, lack of proper surveillance in developed countries, and difficulties observed in measuring the impact of the disease in poor-resource areas. Many infected individuals either do not exhibit symptoms or exhibit mild symptoms due to a self-limiting illness, and such infections often go unrecognized. There is a wide range of disease severity that is affected by the host's age, nutritional, and immune status, and perhaps by the parasite species and subtype (Shirley et al., 2012). Differences in sensitivity of methods, type of diagnostics used, and study populations have resulted in a large variation in burden estimates for diarrhea from *Cryptosporidium* infection in humans and animals. However, the recent advances in knowledge and the development of highly sensitive and superior diagnostic and typing tools have improved our understanding of the epidemiology and true burden of the disease.

2.1 Humans

Out of the currently documented 44 species of *Cryptosporidium*, *Cryptosporidium hominis* (*C. hominis*) and *Cryptosporidium parvum* (*C. parvum*) are responsible for most human infections (Ryan et al., 2021). While *C. hominis* is primarily anthroponotic and only infects humans, *C. parvum* is a zoonotic parasite that can be transmitted between humans and animals. Apart from *C. hominis* and *C. parvum*, 21 other *Cryptosporidium* species and genotypes including *C. meleagridis*, *C. felis*, *C. canis*, *C. ubiquitum*, *C. cuniculus*, *C. ditrichi*, *C. erinacei*, *C. fayeri*, *C. scrofarum*, *C. tyzzeri*, *C. viatorum*, *C. muris*, *C. andersoni*, *C. suis*, *C. bovis*, *C. occultus*, *C. xiaoi*, horse genotype, chipmunk genotype I, skunk genotype, and mink genotype have also been reported in humans (Ryan et al., 2021).

Cryptosporidiosis is considered a high-risk and often lethal opportunistic disease for patients with compromised immune systems such as those suffering from HIV/AIDS (O'Connor R et al., 2011) or those receiving organ transplants (Danziger-Isakov, 2014; Bhadauria et al., 2015). The global prevalence of *Cryptosporidium* in HIV/AIDS patients was 10.09% during the period from 2007 to 2017 (Wang et al., 2018). However, the greatest burden of cryptosporidiosis occurs among young children living in less developed countries. *Cryptosporidium* prevalence is higher in such areas that lack proper sanitation facilities, mainly drinking water and sewage, which led the World Health Organization (WHO) to include it in the water sanitation and health program (WHO, 2009). Several epidemiological studies conducted in the previous decade have estimated the disease burden of diarrheal pathogens in developing countries. In the Global Enteric Multicenter Study (GEMS) conducted at seven sites in sub-Saharan Africa and South Asia, *Cryptosporidium* was found to be the main cause of linear growth faltering and the

second leading cause of moderate-to-severe diarrhea in infants (0–11 months of age) (Kotloff et al., 2013; Nasrin et al., 2021). *Cryptosporidium* infection was also associated with a higher risk of mortality in diarrheic children aged 12–23 months who were admitted to hospitals (Kotloff et al., 2013). The 2016 Global Burden of Diseases, Injuries, and Risk Factors study (GBD) identified *Cryptosporidium* as a leading cause of diarrheal mortality in children younger than 5 years old with an estimated loss of 4.2 million disability-adjusted life years (DALYs) (Troeger et al., 2018). However, this study focused on acute illness alone, and as such, the number increased to 12.9 million DALYs, when long-term-effects of cryptosporidiosis such as growth retardation and cognitive defects were also considered (Khalil et al., 2018). Furthermore, the MAL-ED (Etiology, Risk Factors, and Interactions of Enteric Infections and Malnutrition and the Consequences for Child Health and Development Project) study carried out at eight sites in South America, sub-Saharan Africa, and Asia, found that *Cryptosporidium* along with four other pathogens exhibited the highest attributable burdens of diarrhea in community clinics in the first year of life (Platts-Mills et al., 2015).

2.2 Cattle

At least four main *Cryptosporidium* species infect cattle: *C. parvum*, *C. bovis*, *C. ryanae*, and *C. andersoni* (Lindsay et al., 2000; Santin et al., 2004; Fayer et al., 2005; Fayer et al., 2008), although other species have also been reported in sporadic cases, including *C. felis, C. hominis*, *C. suis, C. canis*, *C. scrofarum, C. tyzzeri, C. serpentis*, and *C. occultus* (formerly known as the *C. suis*-like genotype) (Robertson et al., 2014; Santin, 2020). The occurrence of *C. parvum*, *C. bovis*, *C. ryanae*, and *C. andersoni* in cattle follows an age-related pattern: the zoonotic *C. parvum* infects mostly pre-weaned calves, *C. bovis* and *C. ryanae* are found mostly in post-weaned calves, whereas *C. andersoni* is the predominant species found in heifers and adults (de Graaf et al., 1999; Santin et al., 2004; Fayer et al., 2006; Santin et al., 2008; Khan et al., 2010).

Cryptosporidiosis is one of the most important global causes of diarrhea in neonatal farm ruminants including calves. *Cryptosporidium* parasites invade intestinal epithelial cells and cause severe mucosal erosion resulting in villus shortening and fusion, and hypertrophy of crypts at small intestinal sites that lead to impaired digestion and increased intestinal permeability (Tzipori et al., 1983). The resulting diarrhea causes high production losses including mortality, reduced live weight gain, veterinary costs, and the added feeding and rearing costs for affected animals with slowed growth rates (Innes et al., 2020; Santin, 2020; Shaw et al., 2020). Cryptosporidiosis is recognized as endemic in cattle worldwide and the prevalence of bovine cryptosporidiosis varies substantially between countries, age groups, and studies, ranging from 11.7 to 78%, with the highest incidence reported in pre-weaned calves (Santin et al., 2004; Watanabe et al., 2005; Fayer et al., 2006; Maddox-Hyttel et al., 2006; Trotz-Williams et al., 2007; Khan et al., 2010; Amer et al., 2013; Thomson et al., 2017; Hatam-Nahavandi et al., 2019). An 18-month longitudinal study that focused on 2,545 dairy heifer calves from birth to weaning at 104 dairy operations in 13 US states identified at least 1 calf positive for *Cryptosporidium* at almost all operations (Urie et al., 2018b). Furthermore, the overall prevalence of *Cryptosporidium* in pre-weaned heifer calves was 43.1% with the disease more prevalent among young calves less than 2 weeks of age (63.3%) compared with calves older than 6 weeks (9.1%) (Urie et al., 2018a).

2.3 Small ruminants

Of the species infecting small ruminants, *C. parvum*, *C. ubiquitum*, *and C. xiaoi* are the most frequently detected species (Fayer and Santin, 2009; Fayer et al., 2010; Santin, 2020). In addition, *C. andersoni*, *C. bovis*, *C. ryanae*, *C. hominis*, *C. fayeri*, *C. baileyi*, and *C. suis* have been identified sporadically in sheep and goats (Hatam-Nahavandi et al., 2019; Santin, 2020).

Cryptosporidium causes significant morbidity and mortality in neonatal lambs and goat kids (de Graaf et al., 1999; Wright and Coop, 2007). Diarrhea resulting in reduced productivity and growth has been associated with *Cryptosporidium* infections in lambs and kids (Paraud and Chartier, 2012; Jacobson et al., 2016; Jacobson et al., 2018). *Cryptosporidium* shedding was also associated with less carcass weight and lowered dressing percentage in both symptomatic and apparently asymptomatic sheep on Australian farms (Jacobson et al., 2016). A wide range of *Cryptosporidium* prevalence based on microscopy and molecular detection methods has been reported in small ruminants worldwide ranging from 12.5% to 77.4% in lambs (Causape et al., 2002; Ryan et al., 2005; Castro-Hermida et al., 2007; Goma et al., 2007; Santin et al., 2007; Geurden et al., 2008) and from 4.8% to 70.8% in goat kids (Noordeen et al., 2001; Watanabe et al., 2005; Castro-Hermida et al., 2007; Goma et al., 2007; Geurden et al., 2008). As in cattle, *Cryptosporidium* oocysts are found mostly in feces of very young animals (1–3 weeks of age), with a lower incidence in older animals (de Graaf et al., 1999; Noordeen et al., 2001; Causape et al., 2002; Santín and Trout, 2007).

2.4 Pigs

The most common species and subtypes found in pigs are *C. parvum*, *C. suis*, and *C. scrofarum* formerly known as *Cryptosporidium* pig genotype II (Zahedi and Ryan, 2020), although *C. muris* and *C. tyzzeri* have also been reported occasionally (Robertson et al., 2014). As seen in ruminants, *Cryptosporidium* species tend to generally follow an age-related pattern: *C. suis* is more commonly found in piglets whereas starter pigs and fatteners primarily host *C. scrofarum* (Petersen et al., 2015).

There is a huge disparity in prevalence rates (0.1% to 100%) reported from all over the world (Robertson et al., 2014). Nonetheless, it is obvious that prevalence and intensity of infection is predominant in younger animals than older ones (Maddox-Hyttel et al., 2006; Petersen et al., 2015). While natural or experimental infections with the pig-adapted species, *C. suis* and *C. scrofarum*, are usually asymptomatic and cause mild or no illness (Robertson et al., 2014), experimental infection of piglets with either *C. parvum* or *C. hominis* results in watery diarrhea, anorexia, mucosal lesions, and increased mortality (Tzipori et al., 1994; Theodos et al., 1998; Lee et al., 2017).

3 Treatment options in humans and animals: The past and current state of affairs

Immunocompromised patients, neonatal animals, and young children especially malnourished ones are the most vulnerable to cryptosporidiosis, and hence, are the ones in most urgent need for effective therapeutics. Although cryptosporidiosis causes a self-limiting diarrheal illness in immunocompetent humans, patients do face a considerable risk for longer-term sequelae, especially in low-income countries. Additionally, *Cryptosporidium* infections in adult animals can lead to reduced production and result in economic losses to the livestock and food industry. As such, there is an urgent need for the development of safe, inexpensive, and efficacious drugs to reduce the ever-increasing worldwide burden of this disease. However, despite the widespread occurrence of the parasite, current effective treatment and prophylactic options for human and animal *Cryptosporidium* infections are virtually non-existent.

3.1 Humans

Several drugs with *in vitro* and *in vivo* anti-*Cryptosporidium* activity have been tested against human cases of cryptosporidiosis in uncontrolled/controlled clinical trials, open label/blinded studies, and case reports. These include macrolides, rifamycin derivatives, letrazuril, paromomycin, nitazoxanide, clofazimine, and other pharmacological agents (Table 1). In addition to drugs

TABLE 1 Efficacies of treatments tested against cryptosporidiosis in human patients.

Drug	Age and health status of patients	Number of individuals	Study type	Reference	Treatment type	Efficacy	
						Clinical Cure	Parasitological Cure
Albendazole	Adults with advanced AIDS (CD4+ cell counts >200/mm^3)	4	OL	(Zulu et al., 2002)	Therapeutic	+	+
Azithromycin	Adults with AIDS	85	R, DB, PC	(Soave et al., 1993)	Therapeutic	±	±
	Children on chemotherapy for cancer	2	CR	(Vargas et al., 1993)	Therapeutic	+	±
	Children with AIDS	4	CR	(Hicks et al., 1996)	Therapeutic	+	+
	Adults with AIDS	14	OL	(Blanshard et al., 1997)	Therapeutic	–	–
		13	OL, DC	(Dionisio et al., 1998)	Therapeutic	±	±
		54	RCR	(Holmberg et al., 1998)	Prophylactic	–	–
		41	R, OL, DC	(Kadappu et al., 2002)	Therapeutic	+	±
	Immunocompetent children	43	OL, AC	(Allam and Shehab, 2002)	Therapeutic	+	+
	Children on chemotherapy for cancer	2	CR	(Trad et al., 2003)	Therapeutic	+	+
Clarithromycin	Adults with AIDS	353	RCR	(Jordan, 1996)	Prophylactic	+	+
	Adults with AIDS	312	RCR	(Holmberg et al., 1998)	Prophylactic	+	+
	Adults with advanced AIDS	530	RCR	(Fichtenbaum et al., 2000)	Prophylactic	–	–
Clofazimine	Adults with advanced AIDS	20	R, DB, PC	(Iroh Tam et al., 2021)	Therapeutic	–	–
Diclazuril	Adults with AIDS	9	OL	(Connolly et al., 1990)	Therapeutic	–	–
		1	CR	(Menichetti et al., 1991)	Therapeutic	±	±
Letrazuril	Adults with advanced AIDS	1	CR	(Murdoch et al., 1993)	Therapeutic	+	+

(Continued)

TABLE 1 Continued

Drug	Age and health status of patients	Number of individuals	Study type	Reference	Treatment type	Efficacy	
						Clinical Cure	Parasitological Cure
		14	OL	(Harris et al., 1994)	Therapeutic	±	±
		35	OL	(Loeb et al., 1995)	Therapeutic	±	±
		10	OL	(Blanshard et al., 1997)	Therapeutic	±	±
Miltefosine	Malnourished adults with AIDS	7	OL	(Sinkala et al., 2011)	Therapeutic	±	–
Nitazoxanide	Adults with advanced AIDS	12	OL	(Doumbo et al., 1997)	Therapeutic	±	±
	Adults with AIDS	66	R, DB, PC	(Rossignol et al., 1998)	Therapeutic	±	±
	Immunocompetent adults and children	99	R, DB, PC	(Rossignol et al., 2001)	Therapeutic	+	±
	Malnourished HIV-seronegative children	47	R, DB, PC	(Amadi et al., 2002)	Therapeutic	±	±
	Malnourished HIV-seropositive children	49				–	–
	Adults with AIDS	207	R, DB, PC	(Zulu et al., 2005)	Therapeutic	–	–
	Immunocompetent adults and adolescents	86	R, DB, PC	(Rossignol et al., 2006)	Therapeutic	+	+
	Children and adults with AIDS	357	CU, OL	(Rossignol, 2006)	Therapeutic	±	±
	Children with AIDS	3	CU, CR	(Abraham et al., 2008)	Therapeutic	+	+
	Children with AIDS	52	R, DB, PC	(Amadi et al., 2009)	Therapeutic	–	–
	Pediatric solid organ transplant recipients	6	RCR	(Krause et al., 2012)	Therapeutic	+	+
	Immunocompetent children	135	R, OL, AC, PC	(Hussien et al., 2013)	Therapeutic	+	+
	Immunocompetent adults	58	OL	(Ali et al., 2014)	Therapeutic	±	±
	Adult renal transplant recipients	13	RCR	(Bhadauria et al., 2015)	Therapeutic	±	±
	Immunocompetent children	60	R, DB, PC	(Abaza et al., 2016)	Therapeutic	+	+
	Immunocompromised children	60				±	±
	Adults on chemotherapy for cancer	2	CR	(Demonchy et al., 2021)	Therapeutic	±	±
Paromomycin	Adults with AIDS	12	RCR	(Gathe et al., 1990)	Therapeutic	±	±
		5	CR	(Clezy et al., 1991)	Therapeutic	±	±
		5	CR	(Armitage et al., 1992)	Therapeutic	±	±
		1	CR	(Danziger et al., 1993)	Therapeutic	±	±
		7	RCR	(Fichtenbaum et al., 1993)	Therapeutic	±	±

(Continued)

TABLE 1 Continued

Drug	Age and health status of patients	Number of individuals	Study type	Reference	Treatment type	Efficacy	
						Clinical Cure	Parasitological Cure
		6	CR	(Wallace et al., 1993)	Therapeutic	±	±
		24	OL	(Bissuel et al., 1994)	Therapeutic	±	±
		35	OL	(Scaglia et al., 1994)	Therapeutic	±	±
		10	R, DB, PC	(White et al., 1994)	Therapeutic	+	+
		44	OL	(Flanigan et al., 1996)	Therapeutic	±	±
		20	OL	(Blanshard et al., 1997)	Therapeutic	±	±
		70	RCR	(Hashmey et al., 1997)	Therapeutic	±	±
		35	R, DB, PC	(Hewitt et al., 2000)	Therapeutic	–	–
	Children on chemotherapy for cancer	3	CR	(Trad et al., 2003)	Therapeutic	+	±
	Immunocompetent children	38	OL	(Vandenberg et al., 2012)	Therapeutic	±	±
		135	R, OL, AC, PC	(Hussien et al., 2013)	Therapeutic	±	±
Roxithromycin	Adults with AIDS	24	OL	(Sprinz et al., 1998)	Therapeutic	+	±
		22	OL	(Uip et al., 1998)	Therapeutic	+	±
Rifabutin	Adults with AIDS	214	RCR	(Holmberg et al., 1998)	Prophylactic	+	+
	Adults with advanced AIDS	650	RCR	(Fichtenbaum et al., 2000)	Prophylactic	+	+
Rifaximin	Adults and children infected with HIV (CD4+ cell counts >200/mm^3)	10	OL	(Amenta et al., 1999)	Therapeutic	+	+
	Adult solid organ transplant recipient	1	CR	(Burdese et al., 2005)	Therapeutic	+	+
	Adults with AIDS (CD4+ cell counts <50 cells/mm^3)	5	CR	(Gathe et al., 2008)	Therapeutic	+	+
Spiramycin	Adult with AIDS	1	N of 1 trial	(Woolf et al., 1987)	Therapeutic	–	–
	Immunocompromised adults	37	CU, OL	(Moskovitz et al., 1988)	Therapeutic	+	±
	Immunocompetent infants	44	DB, PC	(Saez-Llorens et al., 1989)	Therapeutic	+	+
	Malnourished infants	39	R, DB, PC	(Wittenberg et al., 1989)	Therapeutic	–	–
	Adults with AIDS	31	CR	(Weikel et al., 1991)	Therapeutic	–	–

1. AC, active-controlled; DB, double-blind; CU, compassionate use; CR, case report; DC, dose comparison; OL, open-label; PC, placebo-controlled; R, randomized; RCR, retrospective case review.
2. "+" = complete resolution; "-" = no demonstrable activity; "±" = partial resolution or relapse after treatment discontinuation.

having direct anti-parasitic activity, other medications that augment the host immunity or ameliorate the symptoms/pathology of cryptosporidiosis have also been tested for the management of the disease (Table 2). However, unfortunately most of these treatments showed limited efficacy and inconsistent results when tested in the most susceptible target population including immunocompromised individuals and young children.

TABLE 2 Other immunological and supportive treatments tested for efficacy against cryptosporidiosis in human patients.

Drug	Age and health status of patients	Number of individuals	Study type	Reference	Treatment type	Efficacy	
						Clinical Cure	Parasitological Cure
Bovine leukocyte extract	Adults and a child with AIDS	8	CR	(Louie et al., 1987)	Therapeutic	±	±
	Adults with AIDS	14	R, DB, PC	(McMeeking et al., 1990)	Therapeutic	+	+
Human serum immune globulin	Child on chemotherapy for cancer	1	CR	(Borowitz and Saulsbury, 1991)	Therapeutic	+	+
Hyperimmune bovine colostrum	Immunocompromised children and adult	3	CR	(Tzipori et al., 1987)	Therapeutic	+	±
	Adults with AIDS	5	R, DB, PC	(Nord et al., 1990)	Therapeutic	±	±
		1	CR	(Ungar et al., 1990)	Therapeutic	+	+
	Immunodeficient children and adults	7	OL	(Rump et al., 1992)	Therapeutic	+	+
	Adults with AIDS	7	OL	(Plettenberg et al., 1993)	Therapeutic	±	±
	Child infected with HIV	1	CR	(Shield et al., 1993)	Therapeutic	+	+
	Adults with AIDS	20	OL	(Greenberg and Cello, 1996)	Therapeutic	±	–
	Immunocompetent adults	16	R, DB, PC	(Okhuysen et al., 1998)	Prophylactic	±	±
	Adults with AIDS	20	OL	(Floren et al., 2006)	Therapeutic	+	NR
Somatostatin analogs (octreotide and vapreotide)	Adults with AIDS	1	CR	(Cook et al., 1988)	Therapeutic	+	–
		1	CR	(Katz et al., 1988)	Therapeutic	+	–
		4	CR	(Clotet et al., 1989)	Therapeutic	±	–
		15	OL	(Cello et al., 1991)	Therapeutic	±	–
		18	OL	(Romeu et al., 1991)	Therapeutic	±	–
		21	OL	(Girard et al., 1992)	Therapeutic	±	–
		4	OL	(Liberti et al., 1992)	Therapeutic	±	–
		13	OL	(Moroni et al., 1993)	Therapeutic	±	–
HIV protease inhibitor (indinavir or saquinavir)	Adults with advanced AIDS (CD4+ count < 50/mm^3)	1	CR	(Grube et al., 1997)	Therapeutic	+	+
		5	OL	(Bobin et al., 1998)	Therapeutic	+	+
		2	R, OL	(Foudraine et al., 1998)	Therapeutic	+	+
HAART including HIV protease inhibitor	Adults with AIDS (CD4+ count < 400/mm^3)	4	OL	(Carr et al., 1998)	Therapeutic	+	+
HAART including HIV protease inhibitor	Adults with advanced AIDS (CD4+ count < 50/mm^3)	3	CR	(Miao et al., 1999; Miao et al., 2000)	Therapeutic	+	+

1. DB, double-blind; CR, case report; NR, not reported; OL, open-label; PC, placebo-controlled; R, randomized.
2. "+" = complete resolution; "-" = no demonstrable benefit; "±" = partial resolution or relapse after treatment discontinuation.

3.1.1 Nitazoxanide

Thus far, nitazoxanide is the only drug approved by the United States Food and Drug Administration (FDA) for the treatment of cryptosporidiosis in immunocompetent human patients (Checkley et al., 2015). Nitazoxanide is a member of the thiazole class of drugs that was initially developed as a veterinary anthelmintic but was later reported to have broad-spectrum activity against parasites, viruses, and bacteria. This drug acts by inhibiting the pyruvate:ferredoxin/flavodoxin oxidoreductase (PFOR), an enzyme essential for the anaerobic energy metabolism of various microorganisms (Hoffman et al., 2007). However, the exact mechanism of action against *Cryptosporidium* remains questionable since these parasites encode a unique PFOR with a fused C-terminal cytochrome P450 domain (Rotte et al., 2001). Interestingly, nitazoxanide was shown to inhibit the growth of *C. parvum* by more than 90% at a concentration of 10 μg/ml (32 μM) in cell culture but was ineffective in the anti-IFN-γ-conditioned SCID mouse model of cryptosporidiosis even at high doses (Theodos et al., 1998). Furthermore, nitazoxanide has also been found to be ineffective in other immunodeficient or immunocompromised animal models of cryptosporidiosis, questioning the true efficacy of the drug (Lee et al., 2017; Jumani et al., 2018).

Various randomized placebo-controlled studies have found nitazoxanide to be helpful in treating cryptosporidiosis in adults and children without HIV resulting in reduced duration of both diarrhea and oocyst shedding (Rossignol et al., 2001; Amadi et al., 2002; Rossignol et al., 2006; Hussien et al., 2013; Abaza et al., 2016). Studies conducted in Egyptian immunocompetent adults and children demonstrated significantly higher clinical and parasitological cure rates compared with the placebo-treated groups (Rossignol et al., 2001; Rossignol et al., 2006). In a randomized controlled trial involving malnourished children in Zambia, nitazoxanide treatment for 3 days yielded a partial but significantly better cure than placebo (Amadi et al., 2002). Recent controlled trials have also reported complete clinical and parasitological recovery in most immunocompetent children with cryptosporidiosis (Hussien et al., 2013; Abaza et al., 2016).

However, a meta-analysis of seven randomized controlled trials involving 169 participants with cryptosporidiosis confirmed the absence of obvious evidence of efficacy of nitazoxanide in HIV-seropositive patients (Abubakar et al., 2007). A course of nitazoxanide does not appear to improve the resolution of diarrhea and parasitological outcome in HIV-infected and immunocompromised patients (Doumbo et al., 1997; Rossignol et al., 1998; Amadi et al., 2002; Zulu et al., 2005; Amadi et al., 2009; Abaza et al., 2016). In the first randomized controlled trial of this drug in adult HIV patients with cryptosporidiosis, better overall parasite clearance rates were seen in the treated group compared with the placebo one, but significant differences were only seen in those with CD4+ T-cell counts above 50/mm^3 (Rossignol et al., 1998). Other randomized placebo-controlled trials conducted by Amadi and others in HIV-positive children in Zambia have also documented no beneficial effect of nitazoxanide over placebo in terms of clinical and parasitological cure rates or mortality (Amadi et al., 2002; Amadi et al., 2009). Moreover, only moderate efficacy was achieved in a study of cryptosporidiosis in immunocompromised children even after prolonged nitazoxanide treatment of up to 28 days (Abaza et al., 2016). While prolonged therapy with higher doses of the drug is somewhat effective in treating cryptosporidiosis in patients with compromised immunity, normal prescribed doses and short-term duration of therapy are inadequate for preventing recurrence of disease symptoms after treatment discontinuation (Abraham et al., 2008; Krause et al., 2012; Ali et al., 2014; Bhadauria et al., 2015; Demonchy et al., 2021). Therefore, it is evident that nitazoxanide therapy is clearly futile in treating cryptosporidiosis in advanced AIDS patients and other severely immunocompromised patients.

Lack of efficacy in immunocompromised animal models and humans suggests that a healthy host immune system is essential to the effectiveness of nitazoxanide. Nitazoxanide treatment has been recently shown to result in broad amplification of the host cell innate immune response to viral infections, including an increase in interferon activities (Jasenosky et al., 2019). If an immune defect renders the host incapable of generating an interferon-γ-dependent response, nitazoxanide would be expected to be ineffective in such immunocompromised hosts (Theodos et al., 1998; Jumani et al., 2018), given the importance of these innate responses in controlling *Cryptosporidium* at its initial stages of infection (McDonald et al., 2013). Similarly, lack of curative effect of nitazoxanide in advanced AIDS patients (with low CD4+ T-cell counts) suffering from chronic cryptosporidiosis can be explained by the fact that adaptive immunity plays a crucial role in clearing the parasites completely from the infected host (Mead, 2014). Thus, the efficacy of nitazoxanide seems to be closely related to both the innate and adaptive immune status of the host.

3.1.2 Paromomycin

Another well studied drug, a poorly absorbed aminoglycoside paromomycin, has been investigated against cryptosporidiosis in three published controlled trials (White et al., 1994; Hewitt et al., 2000; Hussien et al., 2013), but results have been highly divergent and mostly discouraging. Paromomycin, like other aminoglycoside antibiotics, inhibits protein synthesis by binding to the 30S ribosomal subunit and shows broad spectrum activity against bacteria and some protozoa (Lin et al., 2018). Several uncontrolled trials and case studies in AIDS patients suffering from cryptosporidiosis have reported favorable clinical outcomes after paromomycin treatment (Gathe et al., 1990; Clezy et al., 1991; Armitage et al., 1992; Danziger et al., 1993; Fichtenbaum et al., 1993; Wallace et al., 1993; Bissuel et al., 1994; Scaglia et al., 1994; Hashmey et al., 1997). However, the patient responses in most cases were short-lived and continuous maintenance therapy was required to prevent frequent relapses after treatment discontinuation suggesting that complete parasitological cure was not achieved in these cases. Children suffering from cryptosporidiosis have been reported to respond favorably after treatment with paromomycin, although the overall clinical and parasitological response is reduced as compared to nitazoxanide or azithromycin (Trad et al., 2003; Vandenberg et al., 2012; Hussien et al., 2013).

3.1.3 Macrolides

Macrolides are a class of antibiotics that disrupt bacterial protein synthesis by binding to the 50S subunit of the ribosome (Lin et al., 2018). Among the macrolides tested for efficacy against human cryptosporidiosis, azithromycin remains the most studied. In a multi-center, placebo-controlled, double-blind study, preliminary data analysis revealed no significant improvement in clinical

symptoms and oocyst numbers in azithromycin-treated AIDS patients with cryptosporidiosis (Soave et al., 1993). Interestingly, however, a statistically significant decrease in cryptosporidial oocyst shedding was reported in patients with appropriate azithromycin serum concentrations (Soave et al., 1993). By contrast, azithromycin was found to have no therapeutic or prophylactic efficacy in the management of cryptosporidial diarrhea in AIDS patients (Blanshard et al., 1997; Holmberg et al., 1998). While short-term azithromycin treatment for cryptosporidiosis was unable to achieve total parasitological clearance and prevent relapses in AIDS patients, long-term and low dose maintenance therapy was associated with noticeable clinical and parasitological benefits (Dionisio et al., 1998; Kadappu et al., 2002). Nevertheless, azithromycin seems to be more effective in treating children with cryptosporidiosis. Prompt clinical improvement and high parasite clearance rates have been reported after azithromycin therapy in both immunocompetent and immunocompromised children (Vargas et al., 1993; Hicks et al., 1996; Allam and Shehab, 2002; Trad et al., 2003).

Clarithromycin has been tested in humans with AIDS for prophylactic effectiveness against cryptosporidiosis. But studies have reported conflicting results with some indicating a highly protective effect against the development of cryptosporidiosis (Jordan, 1996; Holmberg et al., 1998) while others concluding that the drug is not useful in preventing cryptosporidiosis in this patient population (Fichtenbaum et al., 2000). Similarly, spiramycin has also shown inconsistent results in treating cryptosporidiosis in controlled and uncontrolled trials involving infants (Saez-Llorens et al., 1989; Wittenberg et al., 1989) and adult patients (Woolf et al., 1987; Moskovitz et al., 1988) with reports of acute intestinal injury in some patients receiving high doses of the drug (Weikel et al., 1991). Another macrolide, roxithromycin has proven effective in uncontrolled studies of AIDS patients with cryptosporidial enteritis. However, complete parasite clearance was only achieved in half of the treated patients and the results were not compared with a placebo-treated control group (Sprinz et al., 1998; Uip et al., 1998).

3.1.4 Rifamycin derivatives

Rifamycins are a group of drugs that are highly active against mycobacterial infections. Members of this antibiotic class inhibit RNA synthesis by selective binding of the bacterial DNA-dependent RNA polymerase (Hartmann et al., 1967). Several uncontrolled studies have evaluated rifamycin derivatives, namely rifabutin and rifaximin, for prophylactic and therapeutic efficacy respectively, against cryptosporidiosis in HIV-infected humans. Rifabutin has been found to be highly effective in preventing the development of cryptosporidiosis in AIDS patients receiving chemoprophylaxis for *Mycobacterium avium* complex infection (Holmberg et al., 1998; Fichtenbaum et al., 2000). Similarly, some studies have demonstrated a significant clinical and parasitological benefit of rifaximin, a poorly absorbed rifamycin, in the treatment of cryptosporidiosis in solid organ transplant recipient patients (Burdese et al., 2005) and a small number of HIV-infected adults and children with CD4+ T-cell counts ranging from <50 cells/mm^3 to >200 cells/mm^3 (Amenta et al., 1999; Gathe et al., 2008). Thus, these results warrant the testing of these drugs in larger randomized controlled clinical trials for confirmation of anti-*Cryptosporidium* efficacy.

3.1.5 Benzene acetonitrile derivatives

Diclazuril and letrazuril have been both shown to be active against *Eimeria* species, parasites closely related to *Cryptosporidium*, although the exact mode of action of these drugs is currently unknown. Yet, diclazuril failed to show any obvious effect in severe cryptosporidiosis in adults with HIV infection (Connolly et al., 1990). In another study, a single patient showed both clinical and parasitological response to diclazuril treatment but the infection was less severe and the patient also received antiretroviral therapy during and after the treatment course (Menichetti et al., 1991). Additionally, letrazuril, the p-fluor analog of diclazuril, shows only partial efficacy against advanced AIDS-related cryptosporidial diarrhea (Harris et al., 1994; Loeb et al., 1995; Blanshard et al., 1997) and treated patients develop temporary drug-related side-effects including abnormal liver function tests and skin rashes that tend to resolve after treatment discontinuation (Murdoch et al., 1993; Harris et al., 1994; Loeb et al., 1995).

3.1.6 Miscellaneous antimicrobials

3.1.6.1 Clofazimine

Clofazimine, an FDA-approved antimycobacterial drug primarily used to treat leprosy, was found to be effective against both *C. parvum* and *C. hominis in vitro* and showed promising efficacy against *C. parvum* in a mouse model (Love et al., 2017). Interestingly, the mechanism of action of clofazimine as an anti-mycobacterial drug is not well understood. A recent randomized controlled clinical trial tested the efficacy of the drug in enrolled patients with advanced HIV infection and *Cryptosporidium*-associated diarrhea. The findings of the study, however, failed to demonstrate any effectiveness of clofazimine in reducing fecal parasite shedding and stool frequency in immunocompromised patients (Iroh Tam et al., 2021). Moreover, unexpected adverse events were higher in the clofazimine-treated patients as compared to the placebo control group.

3.1.6.2 Miltefosine

Like clofazimine, miltefosine an anti-*Leishmania* drug, has also shown promising *in vitro* efficacy against *C. parvum* as per anecdotal observations but its specific mode of action is not entirely known. This drug, however, showed modest clinical improvement without evidence of oocyst clearance in treated HIV-infected malnourished individuals (Sinkala et al., 2011). Furthermore, adverse events including hepatic dysfunction and renal failure were observed in some patients, leading to premature termination of the phase-1–phase-2 trial.

3.1.6.3 Albendazole

Albendazole is a broad-spectrum anthelmintic drug that is known to bind to β-tubulin and inhibit microtubule assembly in helminth worms (Lacey, 1988). This benzimidazole derivative was shown to have a significant effect on the duration of diarrhea in a randomized, controlled trial in HIV-seropositive patients with persistent diarrhea (Kelly et al., 1996). Later, another study assessed the effect of albendazole on *C. parvum* and other intracellular protozoa including *Isospora* and microsporidia in HIV-positive patients and found the drug to exhibit complete *C. parvum* clearance when used at doses higher than the normal prescribed dose (Zulu et al., 2002).

However, the number of HIV patients with cryptosporidiosis in this study was very small as compared to patients infected with other protozoa, and the results cannot be considered credible due to the lack of an untreated control group for comparison. Nevertheless, it does seem that albendazole has some activity against *Cryptosporidium* at high doses (Fayer and Fetterer, 1995), but, to the best of our knowledge, no other study has evaluated albendazole for anti-*Cryptosporidium* efficacy in immunocompromised humans.

3.1.7 Other treatments

Although most studies on the treatment of cryptosporidiosis have been carried out by repurposing the use of antibacterial drugs, some studies have tested other treatments with alternate modes of action such as immune cell extracts, immunoglobulins, hyperimmune colostrum, somatostatin analogs, and highly active antiretroviral therapy (HAART) (Table 2).

3.1.7.1 Immunotherapy

Passive immunotherapy by oral administration of immunoglobulins derived from bovine colostrum or human serum was shown to be effective in *Cryptosporidium*-infected immunosuppressed humans in several open-label uncontrolled studies and case reports (Tzipori et al., 1987; Ungar et al., 1990; Borowitz and Saulsbury, 1991; Rump et al., 1992; Shield et al., 1993; Floren et al., 2006), but results obtained from randomized double-blind controlled studies have been disappointing (Nord et al., 1990; Okhuysen et al., 1998). Similarly, treatment of AIDS-associated cryptosporidial diarrhea by oral administration of cellular extracts prepared from lymphocytes obtained from immunized calves produced mixed results (Louie et al., 1987; McMeeking et al., 1990).

3.1.7.2 Somatostatin analogs

Somatostatin analogs including octreotide and vapreotide have been reported to improve secretory diarrhea by inhibiting the motility and secretions of the gastro-intestinal tract. Patients with AIDS-related chronic diarrhea, especially those without specific pathogens, may benefit from treatment with this class of drugs. However, these agents have mostly been ineffective or partially effective in reducing the fecal output in *Cryptosporidium*-associated diarrhea in HIV-infected patients and show no parasitological cure (Cook et al., 1988; Katz et al., 1988; Clotet et al., 1989; Cello et al., 1991; Romeu et al., 1991; Girard et al., 1992; Liberti et al., 1992; Moroni et al., 1993).

3.1.7.3 Highly active antiretroviral therapy

Cryptosporidiosis is typically a self-limiting illness in immunocompetent individuals, and therefore, immune reconstitution by restoring CD4+ T-cell levels in particular, is an essential part of the disease management strategy in the immunocompromised (Flanigan et al., 1992). HIV-infected patients with CD4+ T-cell counts below 200/mm^3 tend to be susceptible to a higher frequency of cryptosporidial infections highlighting the relationship of these opportunistic pathogens with the immune status of an individual (de Oliveira-Silva et al., 2007; Tuli et al., 2008; Adamu et al., 2013; Nsagha et al., 2016; Cerveja et al., 2017; Amoo et al., 2018). The use of HAART in HIV-infected patients has significantly reduced the global frequency and severity of cryptosporidiosis in this patient population (Le Moing et al., 1998; Call et al., 2000; Conti et al., 2000; Ives et al., 2001; Babiker et al., 2002; Bachur et al., 2008; Missaye et al., 2013). HAART re-establishes CD4+ T-cell counts and inhibits viral replication using a combination of nucleoside reverse transcriptase inhibitors (NRTIs), non-nucleoside reverse transcriptase inhibitors (NNRTIs), and HIV protease inhibitors. However, chronic diarrhea at initiation of HAART in HIV-positive patients has been associated with increased early mortality, emphasizing the need for early anti-retroviral therapy before the onset of diarrhea (Dillingham et al., 2009). Most studies involving HAART for the treatment of cryptosporidiosis have used HIV protease inhibitors either individually or in combination with other antiretrovirals to successfully treat the disease with major clinical and parasitological benefits (Grube et al., 1997; Bobin et al., 1998; Carr et al., 1998; Foudraine et al., 1998; Miao et al., 1999; Miao et al., 2000). Such a therapy may exert its pharmacological effect against AIDS-associated cryptosporidiosis both by restoration of circulating CD4+ T-cell counts and direct inhibition of *Cryptosporidium* proteases (Mele et al., 2003; Pantenburg et al., 2009). But individuals with other causes of weakened immunity, including primary immunodeficiency, immunosuppressive therapy in organ transplant recipients, and chemotherapy in cancer patients, remain at high risk of severe cryptosporidiosis.

3.1.8 Combination therapy

Several combination therapies involving the use of either nitazoxanide or paromomycin in conjunction with macrolides, rifamycin derivatives, or HAART have shown promising efficacy for cryptosporidiosis in small uncontrolled trials and case studies with both clinical improvement and parasite elimination in a range of affected immunocompromised individuals (Table 3). However, these results need to be replicated in large, controlled trials before any definite conclusions can be drawn regarding the efficacy of such combinations. Huang and colleagues conducted a randomized placebo-controlled trial to investigate the therapeutic effects of acetylated spiramycin and garlicin on *Cryptosporidium* infection in institutionalized drug users. Although the combination treatment achieved high parasitological cure rates, this study was carried out in asymptomatic *Cryptosporidium* carriers without ascertaining the HIV/immune status of the enrolled individuals, and therefore has limited clinical significance (Huang et al., 2015).

Certain clinical case reports have documented favorable clinical and parasitological outcomes in HIV-infected and organ transplant recipient patients diagnosed with extra-intestinal and intestinal cryptosporidiosis, after antimicrobial combination therapy with azithromycin and paromomycin (Palmieri et al., 2005; Meamar et al., 2006; Denkinger et al., 2008). In a small open-label, uncontrolled study, patients with AIDS (<100 CD4+ T-cells/mm^3) and chronic cryptosporidiosis, showed a marked improvement in stool frequency and a significant decrease in fecal excretion of *Cryptosporidium* oocysts in response to azithromycin/paromomycin combination therapy (Smith et al., 1998). However, follow-up study after the completion of treatment revealed the persistence of chronic, mild diarrhea in some patients.

TABLE 3 Efficacies of various combination therapies tested against human cryptosporidiosis.

Drug combination	Age and health status of patients	Number of individuals	Study type	Reference	Treatment type	Efficacy	
						Clinical Cure	Parasitological Cure
Acetylspiramycin + garlicin	Asymptomatic adult drug users	151	R, PC	(Huang et al., 2015)	Therapeutic	–	+
Azithromycin + paromomycin	Adults with AIDS	11	OL	(Smith et al., 1998)	Therapeutic	+	±
	Adult with AIDS	1	CR	(Palmieri et al., 2005)	Therapeutic	+	+
	Adult with AIDS	1	CR	(Meamar et al., 2006)	Therapeutic	+	+
	Adult liver transplant recipient	1	CR	(Denkinger et al., 2008)	Therapeutic	+	+
Azithromycin + paromomycin + nitazoxanide	Pediatric renal transplant recipient	1	CR	(Hong et al., 2007)	Therapeutic	+	+
Azithromycin + nitazoxanide	Adult allogeneic hematopoietic stem cell transplant recipients	5	OL	(Legrand et al., 2011)	Therapeutic	+	+
	Child on chemotherapy for cancer	1	CR	(Bakliwal et al., 2021)	Therapeutic	+	+
	Immunosuppressed child with CD40L deficiency	1	CR	(Dupuy et al., 2021)	Therapeutic	+	+
Azithromycin + nitazoxanide + rifaximin	Adult renal transplant recipient	1	CR	(Tomczak et al., 2022)	Therapeutic	+	+
Clarithromycin + rifabutin	Adults with advanced AIDS	451	RCR	(Fichtenbaum et al., 2000)	Prophylactic	±	±
Antiretrovirals + Paromomycin, Spiramycin, or Azithromycin	Adults with AIDS (CD4+ count < 180/mm^3)	45	RCR	(Maggi et al., 2000)	Therapeutic	+	+
HAART + Paromomycin	Adults with advanced AIDS (CD4+ count < 50/mm^3)	1	CR	(Schmidt et al., 2001)	Therapeutic	+	+
HAART + Glutamine + Azithromycin + Paromomycin		1	CR	(Moling et al., 2005)	Therapeutic	+	±
Nitazoxanide + fluoroquinolone	Adult renal transplant recipients	21	RCR	(Bhadauria et al., 2015)	Therapeutic	+	+
Spiramycin + paromomycin + nitazoxanide	Pediatric renal transplant recipient	1	CR	(Acikgoz et al., 2012)	Therapeutic	+	+

1. DB, double-blind; CR, case report; OL, open-label; PC, placebo-controlled; R, randomized; RCR, retrospective case review.
2. "+" = complete resolution; "-" = no demonstrable activity; "±" = partial resolution or relapse after treatment discontinuation.

Complete resolution of diarrhea as well as elimination of the parasite has been reported in immunosuppressed children and adults suffering from cryptosporidiosis after dual therapy with azithromycin and nitazoxanide (Legrand et al., 2011; Bakliwal et al., 2021; Dupuy et al., 2021). Additionally, triple therapy involving azithromycin, nitazoxanide, and paromomycin or rifaximin led to complete clinical and parasitological cure with no relapse in renal transplant patients (Hong et al., 2007; Tomczak et al., 2022). Another study successfully treated cryptosporidiosis in a pediatric renal transplant patient using a triple therapy consisting of spiramycin, nitazoxanide, and paromomycin (Acikgoz et al., 2012).

Moreover, quite a few small uncontrolled studies suggest that a combination of antimicrobials and HAART (especially with protease inhibitors) dramatically accelerates the clinical response in AIDS patients suffering from cryptosporidiosis (Maggi et al., 2000; Schmidt et al., 2001; Moling et al., 2005). But data from randomized controlled trials is required to support these results given the self-limiting nature of the disease. Nevertheless, increasing evidence has demonstrated that combination therapy achieves better clinical and microbiological resolution rates than monotherapy for the treatment of cryptosporidiosis in immunocompromised patients (Maggi et al., 2000; Bhadauria et al., 2015; Lanternier et al., 2017; Bakliwal et al., 2021; Tomczak et al., 2022).

3.2 Animals

Numerous antimicrobial compounds have been screened and evaluated for efficacy against naturally acquired and experimentally

induced cryptosporidiosis in animals (Table 4), albeit with limited success. Most of the tested drugs exhibit only partial prophylactic and therapeutic efficacy in reducing oocyst excretion and disease severity in affected animals. Thus far, no effective currently licensed therapeutics are available in the United States for *Cryptosporidium* infections in animals (Santin, 2020; Zahedi and Ryan, 2020). Alternatively, several supportive and immunological therapies have also been tested for the management of cryptosporidiosis in livestock (Table 5), but none have shown promise in changing the course of the disease.

3.2.1 Anticoccidials

3.2.1.1 Halofuginone lactate

Halofuginone lactate, a prolyl-tRNA synthetase inhibitor, is a synthetic quinazolinone coccidiostat primarily used in veterinary

TABLE 4 Anti-cryptosporidial efficacies of various antimicrobial and novel treatments in farm animals and natural host animal models.

Therapeutic agent	Animal species and age	Number of individuals	Type of infection	Reference	Treatment type	Efficacy	
						Clinical Cure	Parasitological Cure
Aminoacyl-tRNA synthetase inhibitor Compound 2093	Neonatal calves	6	Experimental	(Hasan et al., 2021)	Therapeutic	±	±
Azithromycin	Neonatal calves	50	Natural	(Elitok et al., 2005)	Therapeutic	+	±
		25	Natural	(Nasir et al., 2013)	Therapeutic	NR	±
	Gnotobiotic piglets	40	Experimental	(Lee et al., 2017)	Therapeutic	±	–
	Buffalo calf	1	Natural	(Maurya et al., 2016)	Therapeutic	+	NR
Benzoxaborole AN7973	Neonatal calves	17	Experimental	(Lunde et al., 2019)	Therapeutic	+	+
Bumped Kinase Inhibitor 1294	Neonatal calves	18	Experimental	(Lendner et al., 2015)	Prophylactic	±	±
		24	Experimental	(Schaefer et al., 2016)	Therapeutic	±	+
Bumped Kinase Inhibitor 1369	Neonatal calves	7	Experimental	(Hulverson et al., 2017)	Therapeutic	+	+
	Gnotobiotic piglets	18	Experimental	(Lee et al., 2018)	Therapeutic	+	+
Decoquinate	Neonatal calves	30	Experimental	(Redman and Fox, 1993)	Prophylactic	±	±
		43	Experimental	(Moore et al., 2003)	Prophylactic	–	–
		90	Natural	(Lallemand et al., 2006)	Prophylactic	–	–
	Neonatal goat kids	20	Experimental	(Mancassola et al., 1997)	Prophylactic	+	±
		64	Natural	(Ferre et al., 2005)	Prophylactic	±	±
Halofuginone lactate	Neonatal calves	150	Natural	(Villacorta et al., 1991)	Prophylactic	+	±
		20	Experimental	(Naciri et al., 1993)	Prophylactic	+	±
		70	Natural and experimental	(Peeters et al., 1993)	Prophylactic	+	±
		158	Natural	(Lefay et al., 2001)	Prophylactic	+	±
		152	Natural	(Joachim et al., 2003)	Metaphylactic	±	±
		31	Natural		Prophylactic	±	±

(Continued)

TABLE 4 Continued

Therapeutic agent	Animal species and age	Number of individuals	Type of infection	Reference	Treatment type	Efficacy	
						Clinical Cure	Parasitological Cure
				(Jarvie et al., 2005)			
		90	Natural	(Lallemand et al., 2006)	Prophylactic	–	±
		260	Natural	(Klein, 2008)	Prophylactic	±	±
					Therapeutic	±	±
		32	Natural	(De Waele et al., 2010)	Prophylactic	+	±
		513	Natural	(Trotz-Williams et al., 2011)	Prophylactic	±	±
		45	Natural	(Almawly et al., 2013)	Prophylactic	–	–
		149	Natural	(Keidel and Daugschies, 2013)	Metaphylactic	±	±
		530	Natural	(Meganck et al., 2015)	Prophylactic	±	±
		144	Natural	(Niine et al., 2018)	Prophylactic	±	–
		20	Natural	(Aydogdu et al., 2018)	Therapeutic	±	±
		123	Natural	(Velez et al., 2019)	Prophylactic	–	±
	Neonatal lambs	12	Experimental	(Naciri and Yvore, 1989)	Prophylactic	+	+
		5			Therapeutic	+	±
		28	Natural	(Causapé et al., 1999)	Prophylactic	–	±
					Therapeutic	±	±
		1170	Natural	(Giadinis et al., 2007)	Prophylactic	+	±
					Therapeutic	+	+
	Neonatal goat kids	69	Natural	(Chartier et al., 1999)	Prophylactic	±	±
		2240	Natural	(Giadinis et al., 2008)	Prophylactic	+	+
					Therapeutic	+	+
		44	Experimental	(Petermann et al., 2014)	Prophylactic	±	±
Lasalocid	Neonatal calves	10	Experimental	(Moon et al., 1982)	Prophylactic	±	±
		11	Natural	(Sahal et al., 2005)	Therapeutic	+	±
		12	Natural	(Murakoshi et al., 2014)	Prophylactic	+	±
Nitazoxanide	Neonatal calves	20	Experimental	(Ollivett et al., 2009)	Therapeutic	+	±
		9	Experimental	(Schnyder et al., 2009)	Prophylactic	–	–
					Therapeutic	–	–
	Neonatal goat kids	47	Experimental	(Viel et al., 2007)	Prophylactic	NR	±

(Continued)

TABLE 4 Continued

Therapeutic agent	Animal species and age	Number of individuals	Type of infection	Reference	Treatment type	Efficacy	
						Clinical Cure	Parasitological Cure
	Gnotobiotic piglets	31	Experimental	(Theodos et al., 1998)	Therapeutic	–	±
		40	Experimental	(Lee et al., 2017)	Therapeutic	±	±
Paromomycin	Neonatal calves	16	Experimental	(Fayer and Ellis, 1993)	Prophylactic	+	+
		20	Natural	(Grinberg et al., 2002)	Prophylactic	±	±
		20	Natural	(Aydogdu et al., 2018)	Therapeutic	±	±
	Neonatal goat kids	19	Experimental	(Mancassola et al., 1995)	Prophylactic	+	+
		30	Natural	(Chartier et al., 1996)	Prophylactic	+	±
		55	Natural	(Johnson et al., 2000)	Prophylactic	+	+
	Neonatal lambs	36	Natural	(Viu et al., 2000)	Therapeutic	±	+
	Gnotobiotic piglets	21	Experimental	(Tzipori et al., 1994)	Therapeutic	±	±
		31	Experimental	(Theodos et al., 1998)	Therapeutic	+	±
Triazolopyradizine MMV665917	Neonatal calves	13	Experimental	(Stebbins et al., 2018)	Therapeutic	+	+
	Gnotobiotic piglets	28	Experimental	(Lee et al., 2019)	Therapeutic	+	±
Pyrazolopyridine KDU731	Neonatal calves	13	Experimental	(Manjunatha et al., 2017)	Therapeutic	+	+
Sulfonamides	Neonatal calves	59	Natural	(Fischer, 1983)	Prophylactic	–	–
					Therapeutic	–	–
		13	Experimental	(Fayer, 1992)	Prophylactic	–	–
		152	Natural	(Joachim et al., 2003)	Metaphylactic	–	–
		25	Natural	(Nasir et al., 2013)	Therapeutic	NR	–
	Neonatal goat kids	24	Experimental	(Koudela and Bokova, 1997)	Prophylactic	–	–
					Therapeutic	–	–
Tilmicosin	Neonatal goat kids	22	Natural	(Paraud et al., 2010)	Prophylactic	–	–
Tylosin	Neonatal calves	23	Natural	(Duru et al., 2013)	Therapeutic	+	±

1. NR, not reported.
2. "+" = complete cure; "-" = no demonstrable effect; "±" = partial cure or relapse after treatment discontinuation.

medicine for the prevention and treatment of *Eimeria* infections in avian species. This medication is licensed for veterinary use in cattle against cryptosporidiosis in several European countries as well as Canada, although it is not labeled for use in the United States. Halofuginone lactate has a narrow safety index and is contraindicated in dehydrated animals suffering from diarrhea: clinical signs typical of cryptosporidiosis in neonatal animals. Hence, this drug is not suitable for therapeutic purposes and is generally used as a prophylactic to prevent cryptosporidial diarrhea in newborn farm animals. Recently, Brainard and others conducted a systematic review of literature and used meta-analysis to evaluate key outcomes such as oocyst shedding, diarrhea, mortality, and weight gain for the treatment

TABLE 5 Alternate treatments tested for efficacy against cryptosporidiosis in farm animals and natural host animal models.

Drug	Animal species and age	Number of individuals	Type of infection	Study	Treatment type	Efficacy	
						Clinical Cure	Parasitological Cure
α-cyclodextrin	Neonatal goat kids	20	Experimental	(Castro-Hermida et al., 2004)	Prophylactic	±	±
β-cyclodextrin	Neonatal calves	12	Natural	(Castro-Hermida et al., 2001a)	Prophylactic	+	±
					Therapeutic	±	±
	Neonatal lambs	53	Natural	(Castro-Hermida et al., 2001b)	Prophylactic	+	+
					Therapeutic	+	±
Activated charcoal	Neonatal calves	258	Natural	(Ross et al., 2021)	Therapeutic	±	±
Activated charcoal + wood vinegar	Neonatal calves	6	Experimental	(Watarai et al., 2008)	Therapeutic	+	+
	Neonatal goat kids	40	Natural	(Paraud et al., 2011)	Prophylactic	±	±
Anti-IL-10 egg yolk antibody	Neonatal calves	133	Natural	(Raabis et al., 2018)	Prophylactic	–	–
Artificial sweetener/ Glucagon-like peptide	Neonatal calves	24	Experimental	(Connor et al., 2017)	Prophylactic	±	±
Bobel-24 (anti-inflammatory drug)	Neonatal lambs	37	Experimental	(Castro-Hermida et al., 2008)	Prophylactic	±	±
					Therapeutic	±	–
Bovine/Ovine colostrum	Neonatal calves	12	Experimental	(Fayer et al., 1989)	Prophylactic	±	±
		30	Experimental	(Slacek et al., 1996)	Prophylactic	±	±
		12	Experimental	(Perryman et al., 1999)	Prophylactic	+	+
		10	Experimental	(Askari et al., 2016)	Prophylactic	+	+
		30	Natural	(Kacar et al., 2022)	Prophylactic	+	+
	Neonatal lambs	32	Experimental	(Naciri et al., 1994)	Prophylactic	+	±
	Gnotobiotic piglets	21	Experimental	(Tzipori et al., 1994)	Therapeutic	–	–
Bovine interleukin-12 (recombinant)	Neonatal calves	20	Experimental	(Pasquali et al., 2006)	Prophylactic	–	–
Bovine serum concentrate	Neonatal calves	24	Experimental	(Hunt et al., 2002)	Prophylactic	±	±
Bovine leukocyte extract	Neonatal calves	9	Experimental	(Fayer et al., 1987)	Prophylactic	–	–
Clinoptilolite	Neonatal lambs	30	Experimental	(Dinler Ay et al., 2021)	Prophylactic	+	+
					Therapeutic	+	+
Chitosan	Neonatal lambs	32	Experimental	(Aydogdu et al., 2019)	Therapeutic	±	±
Phytogenic extracts and essential oils	Neonatal calves	43	Experimental	(Olson et al., 1998)	Prophylactic	–	–
		41	Natural	(Weyl-Feinstein et al., 2014)	Prophylactic	+	±
		91	Natural	(Katsoulos et al., 2017)	Prophylactic	±	–
		30	Natural	(Volpato et al., 2019)	Prophylactic	–	–
		26	Experimental	(Mendonca et al., 2021)	Prophylactic	±	±
Probiotics (lactic acid producing bacteria)	Neonatal calves	134	Natural	(Harp et al., 1996)	Prophylactic	–	–

(Continued)

TABLE 5 Continued

Drug	Animal species and age	Number of individuals	Type of infection	Study	Treatment type	Efficacy	
						Clinical Cure	Parasitological Cure
		30	Natural	(Fernandez et al., 2020)	Prophylactic	±	–
		44	Natural	(Stefańska et al., 2021)	Prophylactic	±	±
Yeast fermentation products	Neonatal calves	123	Natural	(Velez et al., 2019)	Prophylactic	–	–

"+" = complete cure; "-" = no demonstrable effect; "±" = partial cure or relapse after treatment discontinuation.

of calf cryptosporidiosis with halofuginone lactate. The authors concluded that prophylactic halofuginone treatment was associated with significantly lower incidence of oocyst shedding, diarrhea burden, and mortality especially when the treatment was started early in life (Brainard et al., 2021). Furthermore, Giadinis et al. conducted two extensive field trials in Greece and found the drug to be effective in preventing and treating cryptosporidiosis, and reducing deaths associated with the disease in neonatal lambs and goat kids (Giadinis et al., 2007; Giadinis et al., 2008).

A number of early reports suggested that halofuginone showed effectiveness in protecting young ruminants from severe cryptosporidiosis, but relapses occurred after treatment discontinuation in calves (Villacorta et al., 1991; Naciri et al., 1993; Peeters et al., 1993; Lefay et al., 2001), lambs (Naciri and Yvore, 1989; Causapé et al., 1999), and goat kids (Chartier et al., 1999), questioning the effectiveness of the preventative treatment. Moreover, although halofuginone lactate treatment reduces oocyst shedding in infected animals, it fails to provide complete protection and cure, implying that treatment along with good animal husbandry practices including individual housing, proper hygiene measures, and suitable disinfection are required to prevent environmental contamination and disease transmission among animals on farms (Joachim et al., 2003; Jarvie et al., 2005; Klein, 2008; De Waele et al., 2010; Trotz-Williams et al., 2011; Keidel and Daugschies, 2013). Likewise, a few studies also showed some efficacy in reducing excretion of *Cryptosporidium* oocysts in treated animals as compared to untreated controls, but no significant effect on the prevalence of diarrhea or body weight gain was noted (Causapé et al., 1999; Lallemand et al., 2006; Trotz-Williams et al., 2011; Almawly et al., 2013). Interestingly, preventive treatment with halofuginone lactate was also found to be associated with reduced weight gain in calves (Niine et al., 2018; Velez et al., 2019). Thus, the preventive and therapeutic effectiveness of halofuginone lactate in animals remains controversial.

3.2.1.2 Decoquinate

Decoquinate is a quinolone coccidiostat most used for controlling coccidiosis in ruminants and poultry. This drug inhibits the mitochondrial respiration by blocking electron transport in *Eimeria* parasites (Wang, 1976). Decoquinate produces limited-to-no clinical and parasitological response when used preventatively before the development of signs and symptoms of cryptosporidiosis in experimentally or naturally infected calves (Redman and Fox, 1993; Moore et al., 2003; Lallemand et al., 2006). However, it significantly reduces oocyst shedding and severity of cryptosporidiosis in neonatal kids, but without complete eradication of infection (Mancassola et al., 1997; Ferre et al., 2005).

3.2.1.3 Lasalocid

Lasalocid is an ionophore antibiotic and a coccidiostat that is commonly used as a feed additive for promoting growth and preventing coccidiosis in ruminants. This drug has been used as a prophylactic or therapeutic to treat *Cryptosporidium* infections in calves. Based on anecdotal reports, short-term dosing (3-4 days) of lasalocid (6-15 mg/kg/day) was effective in treating severe cryptosporidiosis in calves (Gobel, 1987a; Gobel, 1987b; Sahal et al., 2005). However, mortality and serious side effects resulting from lasalocid toxicosis have been described in animals when long-term therapy or a dose higher than the label dose was used as a preventative for cryptosporidiosis (Moon et al., 1982; Benson et al., 1998). More recently however, Murakoshi and others demonstrated a highly beneficial effect of lasalocid, without any side effects, when used at a lower dose (3 mg/kg/day) to prevent calf cryptosporidiosis. But the treatment was not found to be protective after the 7-day dosing period (Murakoshi et al., 2014).

3.2.1.4 Sulfonamides

Sulfonamides are broadly active antimicrobial agents that inhibit dihydropteroate synthase, an enzyme involved in folate synthesis (Henry, 1943). They have been widely used in veterinary medicine to prevent coccidiosis and treat bacterial infections in animals and poultry. However, prophylactic or therapeutic treatment of natural or experimental cryptosporidiosis with a variety of sulfonamides and potentiated sulfonamides including sulfadimidine, sulfadimethoxine, and cotrimoxazole (trimethoprim in combination with sulfamethoxazole) has failed miserably in calves (Moon et al., 1982; Fischer, 1983; Fayer, 1992; Joachim et al., 2003; Nasir et al., 2013) and goat kids (Naciri et al., 1984; Koudela and Bokova, 1997).

3.2.2 Paromomycin

In addition to humans, paromomycin has also been extensively tested for anti-*Cryptosporidium* efficacy in various food animals. However, as has been the case in humans, results have been varied

and the treatment failed to achieve complete parasitological cure in most studies. Prophylactic administration of paromomycin was found to decrease the duration and severity of diarrhea as well as the duration and intensity of oocyst shedding in calves experimentally infected with *C. parvum* (Fayer and Ellis, 1993). Similar positive results were reported in a controlled-blind field trial of natural infection in calves, but the treated group started shedding oocysts and developed diarrhea after the treatment withdrawal (Grinberg et al., 2002). However, paromomycin does seem to be more effective in small ruminants. Treatment has been shown to reduce both cryptosporidial oocyst output and severity of clinical signs, when used prophylactically in neonatal goat kids (Mancassola et al., 1995; Chartier et al., 1996; Johnson et al., 2000) and therapeutically in neonatal lambs (Viu et al., 2000). This agent was also proven to be therapeutically effective against moderate cryptosporidiosis but ineffective against severe cryptosporidiosis in infected gnotobiotic piglets (Tzipori et al., 1994; Theodos et al., 1998). However, paromomycin, like many aminoglycosides, is potentially nephrotoxic and detrimental effects on growth have been observed after treatment in young animals (Viu et al., 2000). In addition, the drug is expensive and therefore, its use in agricultural animals is impractical.

3.2.3 Nitazoxanide

Nitazoxanide, the only licensed treatment available in humans, has also been tested for efficacy in animal cryptosporidiosis, although reports on treatment outcomes have been conflicting. While Ollivett and others found this medication to significantly reduce the duration of oocyst shedding and clinical severity in experimentally infected calves as compared to the placebo treated group (Ollivett et al., 2009), another controlled study found no prophylactic or therapeutic effect of nitazoxanide on clinical appearance or oocyst excretion in calves infected with *C. parvum* (Schnyder et al., 2009). Furthermore, while nitazoxanide reduced oocyst shedding in experimentally challenged newborn goat kids, no reduction in mortality rates or improvement in weight gains were recorded in the treated groups compared with the control group (Viel et al., 2007). Importantly, the authors of this study suggested that the mortalities seen in kid neonates in the nitazoxanide treated groups were caused by severe drug toxicity (Viel et al., 2007). In the gnotobiotic piglet diarrhea model, nitazoxanide demonstrated only partial efficacy at high doses in reducing *C. parvum* oocyst shedding, induced drug-related diarrhea, and was not as effective as paromomycin (Theodos et al., 1998). In another study performed in the same animal model but infected with *C. hominis*, nitazoxanide reduced diarrhea and oocyst shedding in only the initial phase of treatment and had no clinical or parasitological effect at the later stages of the disease (Lee et al., 2017).

3.2.4 Macrolides

Macrolides have been evaluated as anti-*Cryptosporidium* agents in a range of animals. Azithromycin significantly suppressed *Cryptosporidium* oocyst shedding and resulted in significant clinical improvement and weight gain in naturally infected dairy calves when used as a therapeutic at high doses, but high costs of treatment are a concern (Elitok et al., 2005). Similar reports of azithromycin efficacy against *C. parvum* infection in calves (Nasir et al., 2013) and a buffalo calf (Maurya et al., 2016) have also been published. Treatment of gnotobiotic neonatal piglets infected with *C. hominis* alleviated clinical disease only for the first few days and azithromycin treated piglets exhibited no reduction of oocyst excretion compared with untreated animals (Lee et al., 2017). In combination with nitazoxanide, azithromycin led to significant clinical improvement in infected piglets but did not eliminate oocyst excretion after producing a transient initial reduction in oocyst shedding in treated animals (Lee et al., 2017).

Experience with other macrolides has also been mixed. While tilmicosin failed to prevent severe cryptosporidiosis in newborn kids raised on a commercial dairy goat farm (Paraud et al., 2010), tylosin was found to be therapeutically effective in reducing fecal oocyst excretion and clinical signs of disease in naturally infected calves (Duru et al., 2013).

3.2.5 Other treatments

3.2.5.1 Immunotherapy

Passive immunotherapy using bovine colostrum or bovine serum concentrate containing specific antibodies to *Cryptosporidium* provided only partial protection against cryptosporidiosis by reducing duration of diarrhea and oocyst shedding in experimentally infected calves (Fayer et al., 1989; Slacek et al., 1996; Hunt et al., 2002). However, much better protection from *Cryptosporidium* infection was noted in some studies after prophylactic oral administration of bovine/ovine colostrum comprising of anti-cryptosporidial antibodies in infected calves and lambs (Naciri et al., 1994; Perryman et al., 1999; Askari et al., 2016; Kacar et al., 2022). Moreover, therapeutic administration of hyperimmune colostrum-immunoglobulin in experimentally infected gnotobiotic piglets reduced oocyst shedding but had little-to-no effect on diarrhea and intestinal mucosal damage caused by the parasite (Tzipori et al., 1994). Similarly, preventive treatment of experimentally induced calf cryptosporidiosis by recombinant bovine interleukin-12 (rBoIL-12) or lymphocyte extracts from immunized calves failed to provide prophylaxis (Fayer et al., 1987; Pasquali et al., 2006).

3.2.5.2 Adsorbents

Oral intestinal adsorbents have been used worldwide as a remedy to treat diarrhea of various causes. A product consisting of activated charcoal and wood vinegar was found to be highly effective in treating experimental *C. parvum* infection in calves (Watarai et al., 2008) and provided partial protection to newborn kids against natural infection (Paraud et al., 2011). More recently, activated charcoal also showed a partial curative effect on neonatal calf diarrhea caused mainly by *C. parvum* at a commercial calf-raising farm (Ross et al., 2021). Similarly, another adsorbent clinoptilolite also demonstrated a good prophylactic and therapeutic effect against *C. parvum* in experimentally infected lambs (Dinler Ay et al., 2021). These adsorbents seem to be effective against cryptosporidial infections probably because of their potential to adsorb and thereby trap parasites and prevent host cell invasion. Although this adsorption principle has been demonstrated in an *in vitro* adsorption test

(Watarai et al., 2008), the same needs to be confirmed in further *in vivo* studies.

3.2.5.3 Polysaccharides

Cyclodextrins are cyclic oligosaccharides that are commonly used as drug excipients to enhance the solubility, safety, stability, and bioavailability of drugs. After showing some unexpected activity against *C. parvum* experimental infection in mice, β-cyclodextrin has been tested for both prophylactic as well as therapeutic efficacy against cryptosporidiosis in young ruminants with results showing that the preventive effect is greater than the curative one. While β-cyclodextrin showed partial efficacy in reducing diarrhea and oocyst shedding in naturally infected calves (Castro-Hermida et al., 2001a), this drug reduced mortality and produced an even better clinical and parasitological response in infected lambs under field conditions (Castro-Hermida et al., 2001b). Another drug of this class, α-cyclodextrin was tested for prophylactic effectiveness in experimentally infected neonatal kids and showed some reduction in the intensity of infection and oocyst shedding, but almost half treated kids died probably due to drug-related side effects (Castro-Hermida et al., 2004).

Chitosan, a natural linear polysaccharide has also been investigated for efficacy in *C. parvum* infected lambs. Therapeutic treatment after the onset of disease improved clinical signs and fecal consistency, and reduced oocyst excretion, but did not eliminate cryptosporidiosis completely in treated lambs (Aydogdu et al., 2019).

Researchers have suggested various modes of action of polysaccharides such as cyclodextrins and chitosan in controlling viral, bacterial, and parasitic infections that involve use of their antimicrobial properties, osmotic properties, and cholesterol-sequestering ability, among others (Aydogdu et al., 2019; Braga, 2019). It is likely that, in the case of *Cryptosporidium*, these polysaccharides might form a protective film over the intestinal surface due to their adhesive properties, which may act as a physical barrier and prevent cell invasion by parasites. However, to date, the exact mechanism of action of these pharmaceutical agents against *Cryptosporidium* remains unknown.

3.2.5.4 Natural plant-based products

Various natural products like phytogenic extracts, essential oils, and phytobiotics have been used to treat animal cryptosporidiosis, but with unconvincing results. A randomized controlled study evaluated allicin, a sulfur-containing component of garlic, in experimentally infected neonatal calves and found it to have no effect on the duration of diarrhea or weight gain in treated calves (Olson et al., 1998). Another study conducted in Israel showed that a concentrated pomegranate extract feed supplement partially reduced clinical signs and fecal oocyst counts in natural calf cryptosporidiosis (Weyl-Feinstein et al., 2014). Similarly, experimentally infected calves receiving plant-based isoquinoline alkaloids as feed additive suffered from less intense diarrhea for a shorter period but shed similar number of oocysts daily compared with the control group (Mendonca et al., 2021). Furthermore, administration of essential oils or essential oil-based phytogenic products to newborn calves also failed to produce any preventive effect on parasite shedding in infected calves (Katsoulos et al., 2017; Volpato et al., 2019).

3.2.5.5 Probiotics

A few animal studies suggest some potential for the use of probiotics for prophylactic treatment of cryptosporidiosis, though bacterial mechanisms involved in protection against *Cryptosporidium* infection are not known. Daily oral administration of lactic acid producing bacteria for 10 consecutive days to *C. parvum* infected dairy calves had limited effect on clinical signs and no effect on parasite abundance (Harp et al., 1996; Fernandez et al., 2020), although a partial reduction in the severity of diarrhea, prevalence of cryptosporidial infection, and oocyst excretion was noted when probiotics combined with phytobiotics were dispensed to calves under field conditions (Stefańska et al., 2021). Likewise, feeding of yeast fermentation products had no clinical and parasitological benefits in bovine cryptosporidiosis (Velez et al., 2019).

3.2.5.6 Miscellaneous treatments

Apart from drugs that have a direct anti-parasitic effect, other medications that have no known anti-*Cryptosporidium* activity but act by improving the symptoms of cryptosporidiosis have also been tested in animals. Such drugs might show some reduction of parasite load in young animals probably by relieving the symptoms of disease and allowing natural host immunity to develop and act against the infection. One such anti-inflammatory drug, Bobel-24, was unable to completely prevent or treat experimentally induced *C. parvum* infection in neonatal lambs but showed some prophylactic efficacy in reducing the duration and intensity of oocyst shedding and the presence of diarrhea (Castro-Hermida et al., 2008). Also, preventive administration of anti-IL-10 egg yolk antibodies for 11 days had no effect on the prevalence of *Cryptosporidium* infection in calves reared under field conditions (Raabis et al., 2018). In another study, administration of glucagon-like peptide 2 or artificial sweetener therapy before a low-level experimental *C. parvum* exposure reduced severity of diarrhea, fecal oocyst excretion, and intestinal pathology in neonatal calves (Connor et al., 2017).

4 New potential treatments for humans and animals

So far, no satisfactory prophylactics or therapeutics are available for the prevention or treatment of severe cryptosporidiosis in humans and animals. The limited progress made in this field can be directly attributed to the limited genetic tractability of *Cryptosporidium*, lack of conventional apicomplexan targets, as well as the unique intracellular but extracytoplasmic location within the host cells. Furthermore, the lack of reliable cell culture platforms and limited availability of technical tools to study the parasite in biological systems, lead to an inadequate knowledge about the host-parasite interactions (Checkley et al., 2015; Innes et al., 2020). Nevertheless, breakthrough genetic modification of the parasite that has been made recently has advanced *Cryptosporidium* research, although the approach is complicated compared to methods developed for other apicomplexan parasites, as it requires the passage of the transgenic parasites in laboratory animals (Vinayak et al., 2015). Importantly, some significant progress has been made in generating genetically modified *C. parvum* strains *in vitro*, using mouse-derived intestinal

organoid cultures grown in a modified air-liquid-interface system, that enables the completion of the life cycle and produces viable oocysts that are infectious in cell culture and immunocompromised mice (Wilke et al., 2019; Wilke et al., 2020). Indeed, recent advances in genetic manipulation and culture of *Cryptosporidium* have resulted in substantial progress in anti-*Cryptosporidium* drug discovery in recent years, and several compounds of preclinical, lead, and late lead status have emerged from target-based and phenotypic screens and are currently in development (Love and Choy, 2021).

C. parvum infects both humans and cattle as natural hosts, with the human disease closely resembling the one found in neonatal calves (Santín and Trout, 2007). Thus, the use of the neonatal calf infection model is highly recommended for assessment of efficacy of candidate compounds before advancement to human clinical trials and should ensure the safety and efficacy of promising compounds in both humans and livestock. Recently some compounds have shown promising efficacy in treating cryptosporidiosis in natural animal host models including the neonatal calf model without any major safety issues. These include bumped kinase inhibitors (BKIs), pyrazolopyridine-based KDU731, triazolopyradizine MMV665917, benzoxaborole AN7973, and compound 2093 (Table 4).

BKIs inhibit the *Cryptosporidium parvum* calcium-dependent protein kinase 1 (CpCDPK1), an enzyme that is essential for host cell invasion and does not have any mammalian analogs (Van Voorhis et al., 2021). Recent studies have assessed novel BKIs as a possible cure for cryptosporidiosis. In one study, Lendner et al. evaluated a bumped kinase inhibitor BKI-1294 for efficacy against *C. parvum* in experimentally infected neonatal calves and concluded that BKI-1294 reduced oocyst shedding but had no effect on diarrhea and dehydration in treated calves (Lendner et al., 2015). In another study, Schaefer and others demonstrated that BKI-1294 significantly improved clinical appearance, diarrhea, and parasitological outcomes but failed to eliminate diarrhea and other clinical symptoms of bovine cryptosporidiosis (Schaefer et al., 2016). Nonetheless, another CpCDPK1 inhibitor, BKI-1369, has emerged as an encouraging lead compound for anti-*Cryptosporidium* therapy in animals (Van Voorhis et al., 2021). This compound has shown promising efficacy against cryptosporidiosis in both the *C. parvum* infected neonatal calf, and the *C. hominis* infected gnotobiotic piglet models (Hulverson et al., 2017; Lee et al., 2018). Unfortunately, these BKIs possess potent human *Ether-à-go-go*-Related *Gene* (hERG) inhibitory activity, which is associated with a potentially fatal disorder called long QT syndrome and cardiotoxicity in humans, effectively removing them from the anti-cryptosporidial drug development pipeline for humans (Van Voorhis et al., 2021). Nevertheless, BKI-1369 displayed both efficacy and safety in the neonatal calf model with a 30-fold reduction in total oocyst excretion and, therefore, calls for additional development as an anti-*Cryptosporidium* therapeutic for cattle (Hulverson et al., 2017).

The pyrazolopyridine derivative KDU731 is another promising anti-cryptosporidial drug candidate that inhibits the enzymatic activity of *Cryptosporidium* lipid kinase PI(4)K (phosphatidylinositol-4-OH-kinase) and is active against both *C. parvum* and *C. hominis*. Oral treatment with KDU731 resulted in significant reduction in oocyst shedding, duration of severe diarrhea, and dehydration without any adverse drug-related effects in neonatal calves experimentally infected with *C. parvum* (Manjunatha et al., 2017). Intriguingly, KDU731 displayed limited systemic exposure in pharmacokinetic analysis of the drug in *C. parvum*-infected calves, suggesting that systemic exposure may not be important for therapeutic efficacy.

Recently, a piperazine derivative MMV665917 with an unknown molecular mechanism of action (MMOA), was identified within the open access "Malaria Box" collection of antimalarial compounds and found to have potent *in vitro* activity against both *C. parvum* and *C. hominis* in addition to excellent *in vivo* anti-*Cryptosporidium* efficacy in mouse models of acute (IFN-γ KO) and chronic (NSG) cryptosporidiosis (Jumani et al., 2018). This compound was later tested in the neonatal calf model of cryptosporidiosis by Stebbins and colleagues and treatment resulted in rapid resolution and reduced duration of diarrhea, as well as a 94% reduction in total fecal excretion of cryptosporidial oocysts in treated calves compared with the control group (Stebbins et al., 2018). In another study conducted in the gnotobiotic piglet model, MMV665917 was shown to significantly reduce fecal *C. hominis* oocyst shedding, intestinal lesions, parasite colonization, and severity of diarrhea, compared with untreated control piglets (Lee et al., 2019). Unfortunately, like BKIs, this promising compound shows partial hERG inhibition and is potentially cardiotoxic in humans. However, similarities between the modes of action of BKIs and MMV665917 cannot be drawn based on this finding since hERG inhibition is generally an off-target effect and several compounds with diverse structures and modes of action are known to promiscuously block this channel (Witchel, 2011). Hence, studies to determine the MMOA of MMV665917 are needed to aid further lead optimization efforts to reduce the affinity for hERG binding.

Another compound that has been discovered by phenotypic screening of an antimalarial compound library for *Cryptosporidium* growth inhibitors is the 6-carboxamide benzoxaborole AN7973 (Lunde et al., 2019). Like MMV665917, AN7973 is active against both *C. parvum* and *C. hominis* in cell culture and shows promising efficacy in both the acute and chronic murine models of cryptosporidiosis but does not have a validated target in *Cryptosporidium*. In the calf clinical model of cryptosporidiosis, AN7973 demonstrated exceptional efficacy in reducing the total parasite fecal excretion by >90% with complete elimination of diarrhea and significant reduction in dehydration in treated calves. Furthermore, the compound possesses favorable safety, stability, and pharmacokinetic characteristics and does not inhibit hERG, a major liability for development of other potential anti-cryptosporidial therapeutics including BKIs and MMV665917 for the human disease (Lunde et al., 2019).

Aminoacyl-tRNA synthetase inhibitors have emerged as promising therapeutic candidates for targeting protein synthesis in *Cryptosporidium* for the development of anti-cryptosporidial drugs (Jain et al., 2017; Baragana et al., 2019; Buckner et al., 2019; Vinayak et al., 2020). Amongst these compounds, only the potent *Cryptosporidium parvum* methionyl-tRNA synthetase (CpMetRS) inhibitor, compound 2093, has been tested in the neonatal calf efficacy model of cryptosporidiosis so far (Hasan et al., 2021). In dairy calves experimentally infected with *C. parvum*, compound 2093 initially reduced total oocyst shedding, diarrhea, and dehydration during the first 4 days of infection but most treated calves relapsed

later with a severe progressive disease indicating the likely emergence of drug resistance. Sequencing analysis of parasite DNA extracted from feces of relapsed animals revealed the presence of two mutant parasite strains with different single amino acid substitutions in the *CpMetRS* genomic locus that potentially conferred MetRS inhibitor resistance. Further genome editing, structural modeling, and enzymatic studies confirmed the spontaneous emergence of drug resistant *Cryptosporidium* parasites, an alarming finding that demands immediate attention (Hasan et al., 2021).

In addition to the above discussed compounds, several other promising compounds have been unveiled in the last few years and found to be effective in both *in vitro* and mouse models of cryptosporidial infection. These include but are not limited to benzoxaboroles (Swale et al., 2019; Bellini et al., 2020), 5-aminopyrazole-4-carboxamide-based BKIs (Huang et al., 2019), *C. parvum* prolyl-tRNA synthetase (CpPRS) inhibitors (Jain et al., 2017), *C. parvum* lysyl-tRNA synthetase (CpKRS) inhibitors (Baragana et al., 2019), *C. parvum* phenylalanyl-tRNA synthetase (CpPheRS) inhibitors (Vinayak et al., 2020), piperazine derivatives (Oboh et al., 2021), and glycolytic enzyme inhibitors (Li et al., 2019; Khan et al., 2022b). However, demonstration of efficacy and safety of these compounds in the neonatal calf and gnotobiotic piglet infection models is essential before further advancement to the next stages of development. Nevertheless, availability of multiple potential anti-cryptosporidial compounds is advantageous as a diverse pool of candidate compounds would be needed to account for the high attrition rate that is typical of drug development programs.

5 Vaccine development

Since efficacious anti-cryptosporidial drug options are currently lacking, vaccines could be a relevant option for the control of this disease. However, there are currently no vaccines available to prevent cryptosporidiosis. In any case, humans and animals with healthy immune systems suffer from a mild self-limiting illness and improve without treatment. Therefore, it is unclear whether vaccination is justified in these patient groups. However, vaccination could be particularly useful in preventing cryptosporidiosis in neonatal animals, immunocompromised individuals, and malnourished children living in underdeveloped countries. An effective vaccine should provide rapid long-lasting immunity in vaccinated individuals and minimize disease in livestock with a reduction in shedding of oocysts in feces thereby preventing the spread of the disease. A degree of cross-protective immunity against multiple species and subtypes, albeit less possible, will also be beneficial. The most viable strategy would be to vaccinate cattle, as they are the most significant contributors to contaminated manure globally (Vermeulen et al., 2017). However, it might be difficult to generate protective immunity in neonatal calves rapidly enough through active vaccination (Thomson et al., 2017). Therefore, passive immunization by transfer of anti-*Cryptosporidium* antibodies from immunized dams to calves through colostrum is a feasible alternate approach to protect them during the early days of life (Innes et al., 2020). Several immunogenic *Cryptosporidium* antigens, such as gp15, Cp15, and Cp23 that are involved in attachment or penetration of host cells, are being explored as vaccine candidates especially in the form of a multivalent vaccine, incorporating multiple antigens or antigenic epitopes (Mead, 2014; Innes et al., 2020). However, a major obstacle to the development of vaccines is our current limited understanding of the protective immune response against *Cryptosporidium* infection (Checkley et al., 2015).

6 Concluding remarks

The target patient population for anti-*Cryptosporidium* drug development is mainly comprised of young children, neonatal calves, and immunocompromised patients. These groups frequently suffer from co-morbidities due to their underdeveloped immunity or immunodeficiency and thus, there is an increased likelihood of such patients receiving other treatments. A highly safe pharmacological profile with a minimal risk of drug-drug interactions is, therefore, a key selection criterion for anti-*Cryptosporidium* drug candidates. Establishment of *in vitro* safety profiles of candidate compounds early in the drug development process is also crucial as it can help researchers filter out compounds with potential toxicity issues before they enter the costlier late stages of drug development. In addition to safety-related pharmacological properties, assessment of the absorption, distribution, metabolism, and excretion (ADME) properties of a lead compound is also critical to its initial selection and clinical success. Failure of translation of excellent *in vitro* efficacy into *in vivo* clinical potency may be caused by insufficient drug concentrations at the target site. Because cryptosporidiosis is primarily an enteric disease, optimal local gastrointestinal concentrations, in addition to systemic concentrations, might be essential for *in vivo* anti-*Cryptosporidium* efficacy of the compounds (Hulverson et al., 2017; Manjunatha et al., 2017; Stebbins et al., 2018; Lunde et al., 2019).

Modern drug-discovery projects utilize either a phenotype-based or target-based screening approach to identify lead candidate compounds for further development. *Cryptosporidium* drug discovery programs in the recent past have mostly used phenotypic screening methods to successfully discover or repurpose compounds with *in vitro* and *in vivo* activity against the parasite (Love et al., 2017; Jumani et al., 2018; Lunde et al., 2019; Li et al., 2020; Khan et al., 2022a). However, such an approach invariably results in the identification of candidate compounds that are difficult to optimize as their MMOA and structure-activity relationships (SAR) are generally unknown. This inflexibility typically leads to higher failure rates once a roadblock is reached in the drug development process. As such, molecular target identification and validation by various genetic and molecular "target deconvolution" methodologies are essential for hits identified from phenotype-based screens (Swinney and Anthony, 2011).

Another approach to anti-cryptosporidial drug discovery is to target biochemical pathways that are unique to the parasite and at the same time, essential for its survival, infection, or multiplication within the host. This strategy has also been used for anti-*Cryptosporidium* drug discovery, albeit less commonly than the phenotypic one. In the

last few years, several enzymes have been identified as potential drug targets, including calcium-dependent protein kinases (Van Voorhis et al., 2021), aminoacyl-tRNA synthetases (Jain et al., 2017; Baragana et al., 2019; Buckner et al., 2019; Vinayak et al., 2020), lipid kinase PI (4)K (Manjunatha et al., 2017), and glycolytic enzymes (Witola et al., 2017; Eltahan et al., 2018; Zhang et al., 2018; Eltahan et al., 2019; Li et al., 2019; Velez et al., 2021; Khan et al., 2022b), among others. The advantage with this approach is that discovery of drug candidates with known MMOA and clearer SAR will create better opportunities for structure-based drug optimization. Indeed, while phenotypic screening has historically had more success in identifying first-in-class drugs, target-based screening has produced more best-in-class drugs (Swinney and Anthony, 2011). However, both approaches need to go hand in hand to identify safe and efficacious anti-*Cryptosporidium* lead compounds for further development.

Finally, the field will need to leverage the advantages of combination therapy for animal and human cryptosporidiosis to 1) increase the efficacy of treatment, 2) reduce the chances of host toxicity, and 3) prevent the inevitable rise of drug resistance in the future. As pointed out earlier in this review (Table 3), several drug combinations tested in the past have yielded superior results than monotherapy for treating *Cryptosporidium* infections in humans, though the number of studies evaluating drug combinations in animals is too small to draw a similar conclusion. Besides, given the success of combination therapies for other related apicomplexan diseases such as malaria, babesiosis, and toxoplasmosis, and the alarming acquisition of spontaneous drug resistant mutations during anti-cryptosporidial therapy by parasites in a recent study, more focus should be put on testing drug combinations against cryptosporidiosis in at-risk individuals.

Author contributions

SK: conceptualization, literature review, and manuscript writing (original draft and revision). WW: conceptualization, supervision, manuscript writing (proof-reading, corrections, editing, and revision). All authors contributed to the article and approved the submitted version.

Funding

The work to compile this review and for open access publications was funded by University of Illinois Urbana-Champaign indirect cost recovery funds to WW.

Conflict of interest

The authors declare that the research was conducted in the absence of any commercial or financial relationships that could be construed as a potential conflict of interest.

Publisher's note

References

Abaza, B. E., Hamza, R. S., Farag, T. I., Abdel-Hamid, M. A., and Moustafa, R. A. (2016). Assessing the efficacy of nitazoxanide in treatment of cryptosporidiosis using pcr examination. *J. Egypt Soc. Parasitol.* 46 (3), 683–692.

Abraham, D. R., Rabie, H., and Cotton, M. F. (2008). Nitazoxanide for severe cryptosporidial diarrhea in human immunodeficiency virus infected children. *Pediatr. Infect. Dis. J.* 27 (11), 1040–1041. doi: 10.1097/inf.0b013e318186257b

Abubakar, I., Aliyu, S. H., Arumugam, C., Hunter, P. R., and Usman, N. K. (2007). Prevention and treatment of cryptosporidiosis in immunocompromised patients. *Cochrane Database Syst. Rev.* 1), CD004932. doi: 10.1002/14651858.CD004932.pub2

Acikgoz, Y., Ozkaya, O., Bek, K., Genc, G., Sensoy, S. G., and Hokelek, M. (2012). Cryptosporidiosis: a rare and severe infection in a pediatric renal transplant recipient. *Pediatr. Transplant.* 16 (4), E115–E119. doi: 10.1111/j.1399-3046.2011.01473.x

Adamu, H., Wegayehu, T., and Petros, B. (2013). High prevalence of diarrhoegenic intestinal parasite infections among non-ART HIV patients in fitche hospital, Ethiopia. *PloS One* 8 (8), e72634. doi: 10.1371/journal.pone.0072634

Ali, S., Mumar, S., Kalam, K., Raja, K., and Baqi, S. (2014). Prevalence, clinical presentation and treatment outcome of cryptosporidiosis in immunocompetent adult patients presenting with acute diarrhoea. *J. Pak Med. Assoc.* 64 (6), 613–618.

Allam, A. F., and Shehab, A. Y. (2002). Efficacy of azithromycin, praziquantel and mirazid in treatment of cryptosporidiosis in school children. *J. Egypt Soc. Parasitol.* 32 (3), 969–978.

Almawly, J., Prattley, D., French, N. P., Lopez-Villalobos, N., Hedgespeth, B., and Grinberg, A. (2013). Utility of halofuginone lactate for the prevention of natural cryptosporidiosis of calves, in the presence of co-infection with rotavirus and *Salmonella* typhimurium. *Vet. Parasitol.* 197 (1-2), 59–67. doi: 10.1016/j.vetpar.2013.04.029

Amadi, B., Mwiya, M., Musuku, J., Watuka, A., Sianongo, S., Ayoub, A., et al. (2002). Effect of nitazoxanide on morbidity and mortality in Zambian children with cryptosporidiosis: a randomised controlled trial. *Lancet* 360 (9343), 1375–1380. doi: 10.1016/S0140-6736(02)11401-2

Amadi, B., Mwiya, M., Sianongo, S., Payne, L., Watuka, A., Katubulushi, M., et al. (2009). High dose prolonged treatment with nitazoxanide is not effective for cryptosporidiosis in HIV positive Zambian children: a randomised controlled trial. *BMC Infect. Dis.* 9 (1), 195. doi: 10.1186/1471-2334-9-195

Amenta, M., Dalle Nogare, E. R., Colomba, C., Prestileo, T. S., Di Lorenzo, F., Fundaro, S., et al. (1999). Intestinal protozoa in HIV-infected patients: effect of rifaximin in *Cryptosporidium parvum* and *Blastocystis hominis* infections. *J. Chemother.* 11 (5), 391–395. doi: 10.1179/joc.1999.11.5.391

Amer, S., Zidan, S., Adamu, H., Ye, J., Roellig, D., Xiao, L., et al. (2013). Prevalence and characterization of cryptosporidium spp. in dairy cattle in Nile river delta provinces, Egypt. *Exp. Parasitol.* 135 (3), 518–523. doi: 10.1016/j.exppara.2013.09.002

Amoo, J. K., Akindele, A. A., Amoo, A. O. J., Efunshile, A. M., Ojurongbe, T. A., Fayemiwo, S. A., et al. (2018). Prevalence of enteric parasitic infections among people living with HIV in abeokuta, Nigeria. *Pan Afr Med. J.* 30, 66. doi: 10.11604/pamj.2018.30.66.13160

Angus, K. W., Tzipori, S., and Gray, E. W. (1982). Intestinal lesions in specific-pathogen-free lambs associated with a cryptosporidium from calves with diarrhea. *Vet. Pathol.* 19 (1), 67–78. doi: 10.1177/030098588201900110

Armitage, K., Flanigan, T., Carey, J., Frank, I., MacGregor, R. R., Ross, P., et al. (1992). Treatment of cryptosporidiosis with paromomycin. a report of five cases. *Arch. Intern. Med.* 152 (12), 2497–2499. doi: 10.1001/archinte.1992.00400240111018

Askari, N., Shayan, P., Mokhber-Dezfouli, M. R., Ebrahimzadeh, E., Lotfollahzadeh, S., Rostami, A., et al. (2016). Evaluation of recombinant P23 protein as a vaccine for passive immunization of newborn calves against *Cryptosporidium parvum*. *Parasite Immunol.* 38 (5), 282–289. doi: 10.1111/pim.12317

Aydogdu, U., Coskun, A., Atas, A. D., Basbug, O., and Agaoglu, Z. T. (2019). The determination of treatment effect of chitosan oligosaccharide in lambs with experimentally cryptosporidiosis. *Small Rumin Res.* 180, 27–34. doi: 10.1016/j.smallrumres.2019.09.021

Aydogdu, U., Isik, N., Ekici, O. D., Yildiz, R., Sen, I., and Coskun, A. (2018). Comparison of the effectiveness of halofuginone lactate and paromomycin in the treatment of calves naturally infected with *Cryptosporidium parvum*. *Acta Scientiae Veterinariae* 46 (1), 9. doi: 10.22456/1679-9216.81809

Babiker, A., Darbyshire, J., Pezzotti, P., Porter, K., Rezza, G., Walker, S. A., et al. (2002). Changes over calendar time in the risk of specific first AIDS-defining events following HIV seroconversion, adjusting for competing risks. *Int. J. Epidemiol.* 31 (5), 951–958. doi: 10.1093/ije/31.5.951

Bachur, T. P., Vale, J. M., Coelho, I. C., Queiroz, T. R., and Chaves Cde, S. (2008). Enteric parasitic infections in HIV/AIDS patients before and after the highly active antiretroviral therapy. *Braz. J. Infect. Dis.* 12 (2), 115–122. doi: 10.1590/s1413-86702008000200004

Bakliwal, A., Nath, U. K., Mohanty, A., and Gupta, P. (2021). Life-threatening *Cryptosporidium* diarrhea in a child on induction chemotherapy for acute lymphoblastic leukemia. *Cureus* 13 (9), e18340. doi: 10.7759/cureus.18340

Baragana, B., Forte, B., Choi, R., Nakazawa Hewitt, S., Bueren-Calabuig, J. A., Pisco, J. P., et al. (2019). Lysyl-tRNA synthetase as a drug target in malaria and cryptosporidiosis. *Proc. Natl. Acad. Sci. U.S.A.* 116 (14), 7015–7020. doi: 10.1073/pnas.1814685116

Bellini, V., Swale, C., Brenier-Pinchart, M. P., Pezier, T., Georgeault, S., Laurent, F., et al. (2020). Target identification of an antimalarial oxaborole identifies AN13762 as an alternative chemotype for targeting CPSF3 in apicomplexan parasites. *iScience* 23 (12), 101871. doi: 10.1016/j.isci.2020.101871

Benson, J. E., Ensley, S. M., Carson, T. L., Halbur, P. G., Janke, B. H., and Quinn, W. J. (1998). Lasalocid toxicosis in neonatal calves. *J. Vet. Diagn. Invest.* 10 (2), 210–214. doi: 10.1177/104063879801000224

Bhadauria, D., Goel, A., Kaul, A., Sharma, R. K., Gupta, A., Ruhela, V., et al. (2015). *Cryptosporidium* infection after renal transplantation in an endemic area. *Transpl Infect. Dis.* 17 (1), 48–55. doi: 10.1111/tid.12336

Bissuel, F., Cotte, L., Rabodonirina, M., Rougier, P., Piens, M. A., and Trepo, C. (1994). Paromomycin: an effective treatment for cryptosporidial diarrhea in patients with AIDS. *Clin. Infect. Dis.* 18 (3), 447–449. doi: 10.1093/clinids/18.3.447

Blanshard, C., Shanson, D. C., and Gazzard, B. G. (1997). Pilot studies of azithromycin, letrazuril and paromomycin in the treatment of cryptosporidiosis. *Int. J. STD AIDS* 8 (2), 124–129. doi: 10.1258/0956462971919543

Bobin, S., Bouhour, D., Durupt, S., Boibieux, A., Girault, V., and Peyramond, D. (1998). Importance of antiproteases in the treatment of microsporidia and/or cryptosporidia infections in HIV-seropositive patients. *Pathol. Biol. (Paris)* 46 (6), 418–419.

Borowitz, S. M., and Saulsbury, F. T. (1991). Treatment of chronic cryptosporidial infection with orally administered human serum immune globulin. *J. Pediatr.* 119 (4), 593–595. doi: 10.1016/s0022-3476(05)82412-6

Braga, S. S. (2019). Cyclodextrins: Emerging medicines of the new millennium. *Biomolecules* 9 (12), 801. doi: 10.3390/biom9120801

Brainard, J., Hammer, C. C., Hunter, P. R., Katzer, F., Hurle, G., and Tyler, K. (2021). Efficacy of halofuginone products to prevent or treat cryptosporidiosis in bovine calves: a systematic review and meta-analyses. *Parasitology* 148 (4), 408–419. doi: 10.1017/S0031182020002267

Buckner, F. S., Ranade, R. M., Gillespie, J. R., Shibata, S., Hulverson, M. A., Zhang, Z., et al. (2019). Optimization of methionyl tRNA-synthetase inhibitors for treatment of *Cryptosporidium* infection. *Antimicrob. Agents Chemother.* 63 (4), e02061–e02018. doi: 10.1128/AAC.02061-18

Burdese, M., Veglio, V., Consiglio, V., Soragna, G., Mezza, E., Bergamo, D., et al. (2005). A dance teacher with kidney-pancreas transplant and diarrhoea: what is the cause? *Nephrol. Dial Transplant.* 20 (8), 1759–1761. doi: 10.1093/ndt/gfh881

Call, S. A., Heudebert, G., Saag, M., and Wilcox, C. M. (2000). The changing etiology of chronic diarrhea in HIV-infected patients with CD4 cell counts less than 200 cells/mm3. *Am. J. Gastroenterol.* 95 (11), 3142–3146. doi: 10.1111/j.1572-0241.2000.03285.x

Carr, A., Marriott, D., Field, A., Vasak, E., and Cooper, D. A. (1998). Treatment of HIV-1-associated microsporidiosis and cryptosporidiosis with combination antiretroviral therapy. *Lancet* 351 (9098), 256–261. doi: 10.1016/S0140-6736(97)07529-6

Castro-Hermida, J. A., Garcia-Presedo, I., Gonzalez-Warleta, M., Mezo, M., Fenoy, S., Rueda, C., et al. (2008). Activity of an anti-inflammatory drug against cryptosporidiosis in neonatal lambs. *Vet. Parasitol.* 155 (3-4), 308–313. doi: 10.1016/j.vetpar.2008.05.012

Castro-Hermida, J. A., Gonzalez-Losada, Y., Freire-Santos, F., Mezo-Menendez, M., and Ares-Mazas, E. (2001a). Evaluation of beta-cyclodextrin against natural infections of cryptosporidiosis in calves. *Vet. Parasitol.* 101 (2), 85–89. doi: 10.1016/s0304-4017(01)00505-2

Castro-Hermida, J. A., Gonzalez-Warleta, M., and Mezo, M. (2007). Natural infection by *Cryptosporidium parvum* and *Giardia duodenalis* in sheep and goats in Galicia (NW Spain). *Small Ruminant Res.* 72 (2-3), 96–100. doi: 10.1016/j.smallrumres.2006.08.008

Castro-Hermida, J. A., Pors, I., Otero-Espinar, F., Luzardo-Alvarez, A., Ares-Mazas, E., and Chartier, C. (2004). Efficacy of alpha-cyclodextrin against experimental cryptosporidiosis in neonatal goats. *Vet. Parasitol.* 120 (1-2), 35–41. doi: 10.1016/j.vetpar.2003.12.012

Castro-Hermida, J. A., Quilez-Cinca, J., Lopez-Bernad, F., Sanchez-Acedo, C., Freire-Santos, F., and Ares-Mazas, E. (2001b). Treatment with beta-cyclodextrin of natural *Cryptosporidium parvum* infections in lambs under field conditions. *Int. J. Parasitol.* 31 (10), 1134–1137. doi: 10.1016/s0020-7519(01)00220-x

Causape, A. C., Quilez, J., Sanchez-Acedo, C., del Cacho, E., and Lopez-Bernad, F. (2002). Prevalence and analysis of potential risk factors for *Cryptosporidium parvum* infection in lambs in zaragoza (northeastern Spain). *Vet. Parasitol.* 104 (4), 287–298. doi: 10.1016/s0304-4017(01)00639-2

Causapé, A. C., Sanchez-Acedo, C., Quilez, J., Del Cacho, E., and Viu, M. (1999). Efficacy of halofuginone lactate against natural *Cryptosporidium parvum* infections in lambs. *Res. Rev. Parasitol.* 59, 41–46.

CDC (2019)DPDx cryptosporidiosis. In: *Centers for disease control and prevention*. Available at: https://www.cdc.gov/dpdx/cryptosporidiosis/index.html (Accessed December 30 2022).

Cello, J. P., Grendell, J. H., Basuk, P., Simon, D., Weiss, L., Wittner, M., et al. (1991). Effect of octreotide on refractory AIDS-associated diarrhea. a prospective, multicenter clinical trial. *Ann. Intern. Med.* 115 (9), 705–710. doi: 10.7326/0003-4819-115-9-705

Cerveja, B. Z., Tucuzo, R. M., Madureira, A. C., Nhacupe, N., Langa, I. A., Buene, T., et al. (2017). Prevalence of intestinal parasites among HIV infected and HIV uninfected patients treated at the 1 degrees de maio health centre in Maputo, Mozambique. *EC Microbiol.* 9 (6), 231–240.

Chalmers, R. M. (2012). Waterborne outbreaks of cryptosporidiosis. *Ann. Ist Super Sanita*. (San Diego, CA, USA: Academic Press, Elsevier) 48 (4), 429–446. doi: 10.4415/ANN_12_04_10

Chalmers, R. M. (2014). "Cryptosporidium," in *Microbiology of waterborne diseases*. Eds. S. L. Percival, M. V. Yates, D. W. Williams, R. M. Chalmers and N. F. Gray (Elsevier Ltd), 287–326.

Chartier, C., Mallereau, M. P., and Lenfant, D. (1999). Halofuginone lactate in the control of cryptosporidiosis in neonate kids. *Rev. Medecine Veterinaire* 150 (4), 341–346.

Chartier, C., Mallereau, M. P., and Naciri, M. (1996). Prophylaxis using paromomycin of natural cryptosporidial infection in neonatal kids. *Prev. Veterinary Med.* 25 (3-4), 357–361. doi: 10.1016/0167-5877(95)00511-0

Checkley, W., White, A. C.Jr., Jaganath, D., Arrowood, M. J., Chalmers, R. M., Chen, X. M., et al. (2015). A review of the global burden, novel diagnostics, therapeutics, and vaccine targets for cryptosporidium. *Lancet Infect. Dis.* 15 (1), 85–94. doi: 10.1016/S1473-3099(14)70772-8

Clezy, K., Gold, J., Blaze, J., and Jones, P. (1991). Paromomycin for the treatment of cryptosporidial diarrhoea in AIDS patients. *AIDS* 5 (9), 1146–1147.

Clotet, B., Sirera, G., Cofan, F., Monterola, J. M., Tortosa, F., and Fox, M. (1989). Efficacy of the somatostatin analogue (SMS-201-995), sandostatin, for cryptosporidial diarrhoea in patients with AIDS. *AIDS* 3 (12), 857–858. doi: 10.1097/00002030-198912000-00016

Connolly, G. M., Youle, M., and Gazzard, B. G. (1990). Diclazuril in the treatment of severe cryptosporidial diarrhoea in AIDS patients. *AIDS* 4 (7), 700–701. doi: 10.1097/00002030-199007000-00020

Connor, E. E., Wall, E. H., Bravo, D. M., Evock-Clover, C. M., Elsasser, T. H., Baldwin, R. L. T., et al. (2017). Reducing gut effects from *Cryptosporidium parvum* infection in dairy calves through prophylactic glucagon-like peptide 2 therapy or feeding of an artificial sweetener. *J. Dairy Sci.* 100 (4), 3004–3018. doi: 10.3168/jds.2016-11861

Conti, S., Masocco, M., Pezzotti, P., Toccaceli, V., Vichi, M., Boros, S., et al. (2000). Differential impact of combined antiretroviral therapy on the survival of italian patients with specific AIDS-defining illnesses. *J. Acquir. Immune Defic. Syndr.* 25 (5), 451–458. doi: 10.1097/00042560-200012150-00011

Cook, D. J., Kelton, J. G., Stanisz, A. M., and Collins, S. M. (1988). Somatostatin treatment for cryptosporidial diarrhea in a patient with the acquired immunodeficiency syndrome (AIDS). *Ann. Intern. Med.* 108 (5), 708–709. doi: 10.7326/0003-4819-108-5-708

Corso, P. S., Kramer, M. H., Blair, K. A., Addiss, D. G., Davis, J. P., and Haddix, A. C. (2003). Cost of illness in the 1993 waterborne *Cryptosporidium* outbreak, Milwaukee, Wisconsin. *Emerg. Infect. Dis.* 9 (4), 426–431. doi: 10.3201/eid0904.020417

Current, W. L., and Garcia, L. S. (1991). Cryptosporidiosis. *Clin. Microbiol. Rev.* 4 (3), 325–358. doi: 10.1128/CMR.4.3.325

Current, W. L., and Reese, N. C. (1986). A comparison of endogenous development of three isolates of *Cryptosporidium* in suckling mice. *J. Protozool* 33 (1), 98–108. doi: 10.1111/j.1550-7408.1986.tb05567.x

Current, W. L., Reese, N. C., Ernst, J. V., Bailey, W. S., Heyman, M. B., and Weinstein, W. M. (1983). Human cryptosporidiosis in immunocompetent and immunodeficient persons. studies of an outbreak and experimental transmission. *N Engl. J. Med.* 308 (21), 1252–1257. doi: 10.1056/NEJM198305263082102

D'Antonio, R. G., Winn, R. E., Taylor, J. P., Gustafson, T. L., Current, W. L., Rhodes, M. M., et al. (1985). A waterborne outbreak of cryptosporidiosis in normal hosts. *Ann. Intern. Med.* 103(6 (6 (Pt 1), 886–888. doi: 10.7326/0003-4819-103-6-886

Danziger-Isakov, L. (2014). Gastrointestinal infections after transplantation. *Curr. Opin. Gastroenterol.* 30 (1), 40–46. doi: 10.1097/MOG.0000000000000016

Danziger, L. H., Kanyok, T. P., and Novak, R. M. (1993). Treatment of cryptosporidial diarrhea in an AIDS patient with paromomycin. *Ann. Pharmacother.* 27 (12), 1460–1462. doi: 10.1177/106002809302701209

de Graaf, D. C., Vanopdenbosch, E., Ortega-Mora, L. M., Abbassi, H., and Peeters, J. E. (1999). A review of the importance of cryptosporidiosis in farm animals. *Int. J. Parasitol.* 29 (8), 1269–1287. doi: 10.1016/s0020-7519(99)00076-4

Demonchy, J., Cordier, C., Frealle, E., Demarquette, H., Herbaux, C., Escure, G., et al. (2021). Case report: Two cases of cryptosporidiosis in heavily pretreated patients with myeloma. *Clin. Lymphoma Myeloma Leuk* 21 (6), e545–e547. doi: 10.1016/j.clml.2021.01.019

Denkinger, C. M., Harigopal, P., Ruiz, P., and Dowdy, L. M. (2008). *Cryptosporidium parvum*-associated sclerosing cholangitis in a liver transplant patient. *Transpl Infect. Dis.* 10 (2), 133–136. doi: 10.1111/j.1399-3062.2007.00245.x

de Oliveira-Silva, M. B., de Oliveira, L. R., Resende, J. C., Peghini, B. C., Ramirez, L. E., Lages-Silva, E., et al. (2007). Seasonal profile and level of CD4+ lymphocytes in the occurrence of cryptosporidiosis and cystoisosporidiosis in HIV/AIDS patients in the triangulo mineiro region, Brazil. *Rev. Soc. Bras. Med. Trop.* 40 (5), 512–515. doi: 10.1590/s0037-86822007000500004

De Waele, V., Speybroeck, N., Berkvens, D., Mulcahy, G., and Murphy, T. M. (2010). Control of cryptosporidiosis in neonatal calves: use of halofuginone lactate in two different calf rearing systems. *Prev. Vet. Med.* 96 (3-4), 143–151. doi: 10.1016/j.prevetmed.2010.06.017

Dillingham, R. A., Pinkerton, R., Leger, P., Severe, P., Guerrant, R. L., Pape, J. W., et al. (2009). High early mortality in patients with chronic acquired immunodeficiency syndrome diarrhea initiating antiretroviral therapy in Haiti: a case-control study. *Am. J. Trop. Med. Hyg* 80 (6), 1060–1064. doi: 10.4269/ajtmh.2009.80.1060

Dinler Ay, C., Voyvoda, H., Ulutas, P. A., Karagenc, T., and Ulutas, B. (2021). Prophylactic and therapeutic efficacy of clinoptilolite against *Cryptosporidium parvum* in experimentally challenged neonatal lambs. *Vet. Parasitol.* 299, 109574. doi: 10.1016/j.vetpar.2021.109574

Dionisio, D., Orsi, A., Sterrantino, G., Meli, M., Di Lollo, S., Ibba Manneschi, L., et al. (1998). Chronic cryptosporidiosis in patients with AIDS: stable remission and possible eradication after long-term, low dose azithromycin. *J. Clin. Pathol.* 51 (2), 138–142. doi: 10.1136/jcp.51.2.138

Doumbo, O., Rossignol, J. F., Pichard, E., Traore, H. A., Dembele, T. M., Diakite, M., et al. (1997). Nitazoxanide in the treatment of cryptosporidial diarrhea and other intestinal parasitic infections associated with acquired immunodeficiency syndrome in tropical Africa. *Am. J. Trop. Med. Hyg* 56 (6), 637–639. doi: 10.4269/ajtmh.1997.56.637

Dupuy, F., Valot, S., Dalle, F., Sterin, A., and L'Ollivier, C. (2021). Disseminated *Cryptosporidium* infection in an infant with CD40L deficiency. *IDCases* 24, e01115. doi: 10.1016/j.idcr.2021.e01115

Duru, S. Y., Öcal, N., Yağcİ, B. B., Gazyağcİ, S., Duru, Ö., and Yİldİz, K. (2013). *The therapeutic efficacy of tylosin in calf cryptosporidiosis* Vol. 19 (Kars: Kafkas Üniversitesi Veteriner Fakültesi Dergisi), A175–A180.

Elitok, B., Elitok, O. M., and Pulat, H. (2005). Efficacy of azithromycin dihydrate in treatment of cryptosporidiosis in naturally infected dairy calves. *J. Vet. Intern. Med.* 19 (4), 590–593. doi: 10.1892/0891-6640(2005)19[590:eoadit]2.0.co;2

Eltahan, R., Guo, F., Zhang, H., Xiang, L., and Zhu, G. (2018). Discovery of ebselen as an inhibitor of *Cryptosporidium parvum* glucose-6-phosphate isomerase (CpGPI) by high-throughput screening of existing drugs. *Int. J. Parasitol. Drugs Drug Resist.* 8 (1), 43–49. doi: 10.1016/j.ijpddr.2018.01.003

Eltahan, R., Guo, F., Zhang, H., and Zhu, G. (2019). The action of the hexokinase inhibitor 2-deoxy-d-glucose on *Cryptosporidium parvum* and the discovery of activities against the parasite hexokinase from marketed drugs. *J. Eukaryot Microbiol.* 66 (3), 460–468. doi: 10.1111/jeu.12690

English, E. D., Guerin, A., Tandel, J., and Striepen, B. (2022). Live imaging of the *Cryptosporidium parvum* life cycle reveals direct development of male and female gametes from type I meronts. *PloS Biol.* 20 (4), e3001604. doi: 10.1371/journal.pbio.3001604

Fayer, R. (1992). Activity of sulfadimethoxine against cryptosporidiosis in dairy calves. *J. Parasitol.* 78 (3), 534–537. doi: 10.2307/3283662

Fayer, R., Andrews, C., Ungar, B. L., and Blagburn, B. (1989). Efficacy of hyperimmune bovine colostrum for prophylaxis of cryptosporidiosis in neonatal calves. *J. Parasitol.* 75 (3), 393–397. doi: 10.2307/3282595

Fayer, R., and Ellis, W. (1993). Paromomycin is effective as prophylaxis for cryptosporidiosis in dairy calves. *J. Parasitol.* 79 (5), 771–774. doi: 10.2307/3283619

Fayer, R., and Fetterer, R. (1995). Activity of benzimidazoles against cryptosporidiosis in neonatal BALB/c mice. *J. Parasitol.* 81 (5), 794–795. doi: 10.2307/3283980

Fayer, R., Klesius, P. H., and Andrews, C. (1987). Efficacy of bovine transfer factor to protect neonatal calves against experimentally induced clinical cryptosporidiosis. *J. Parasitol.* 73 (5), 1061–1062. doi: 10.2307/3282539

Fayer, R., Morgan, U., and Upton, S. J. (2000). Epidemiology of *Cryptosporidium*: transmission, detection and identification. *Int. J. Parasitol.* 30 (12-13), 1305–1322. doi: 10.1016/s0020-7519(00)00135-1

Fayer, R., and Santin, M. (2009). *Cryptosporidium xiaoi* n. sp. (Apicomplexa: Cryptosporidiidae) in sheep (*Ovis aries*). *Vet. Parasitol.* 164 (2-4), 192–200. doi: 10.1016/j.vetpar.2009.05.011

Fayer, R., Santin, M., and Macarisin, D. (2010). *Cryptosporidium ubiquitum* n. sp. in animals and humans. *Vet. Parasitol.* 172 (1-2), 23–32. doi: 10.1016/j.vetpar.2010.04.028

Fayer, R., Santin, M., and Trout, J. M. (2008). *Cryptosporidium ryanae* n. sp. (Apicomplexa: Cryptosporidiidae) in cattle (*Bos taurus*). *Vet. Parasitol.* 156 (3-4), 191–198. doi: 10.1016/j.vetpar.2008.05.024

Fayer, R., Santin, M., Trout, J. M., and Greiner, E. (2006). Prevalence of species and genotypes of *Cryptosporidium* found in 1-2-year-old dairy cattle in the eastern united states. *Vet. Parasitol.* 135 (2), 105–112. doi: 10.1016/j.vetpar.2005.08.003

Fayer, R., Santin, M., and Xiao, L. (2005). *Cryptosporidium bovis* n. sp. (Apicomplexa: Cryptosporidiidae) in cattle (*Bos taurus*). *J. Parasitol.* 91 (3), 624–629. doi: 10.1645/GE-3435

Fernandez, S., Fraga, M., Castells, M., Colina, R., and Zunino, P. (2020). Effect of the administration of *Lactobacillus* spp. strains on neonatal diarrhoea, immune parameters and pathogen abundance in pre-weaned calves. *Benef Microbes* 11 (5), 477–488. doi: 10.3920/BM2019.0167

Ferre, I., Benito-Pena, A., Garcia, U., Osoro, K., and Ortega-Mora, L. M. (2005). Effect of different decoquinate treatments on cryptosporidiosis in naturally infected cashmere goat kids. *Vet. Rec* 157 (9), 261–262. doi: 10.1136/vr.157.9.261

Fichtenbaum, C. J., Ritchie, D. J., and Powderly, W. G. (1993). Use of paromomycin for treatment of cryptosporidiosis in patients with AIDS. *Clin. Infect. Dis.* 16 (2), 298–300. doi: 10.1093/clind/16.2.298

Fichtenbaum, C. J., Zackin, R., Feinberg, J., Benson, C., Griffiths, J. K.Team, A.C.T.G.N.W.C.S (2000). Rifabutin but not clarithromycin prevents cryptosporidiosis in persons with advanced HIV infection. *AIDS* 14 (18), 2889–2893. doi: 10.1097/00002030-200012220-00010

Fischer, O. (1983). Attempted therapy and prophylaxis of cryptosporidiosis in calves by administration of sulphadimidine. *Acta Veterinaria Brno* 52 (3-4), 183–190. doi: 10.2754/avb198352030183

Flanigan, T. P., Ramratnam, B., Graeber, C., Hellinger, J., Smith, D., Wheeler, D., et al. (1996). Prospective trial of paromomycin for cryptosporidiosis in AIDS. *Am. J. Med.* 100 (3), 370–372. doi: 10.1016/S0002-9343(97)89499-5

Flanigan, T., Whalen, C., Turner, J., Soave, R., Toerner, J., Havlir, D., et al. (1992). *Cryptosporidium* infection and CD4 counts. *Ann. Intern. Med.* 116 (10), 840–842. doi: 10.7326/0003-4819-116-10-840

Floren, C. H., Chinenye, S., Elfstrand, L., Hagman, C., and Ihse, I. (2006). ColoPlus, a new product based on bovine colostrum, alleviates HIV-associated diarrhoea. *Scand. J. Gastroenterol.* 41 (6), 682–686. doi: 10.1080/00365520500380817

Foudraine, N. A., Weverling, G. J., van Gool, T., Roos, M. T., de Wolf, F., Koopmans, P. P., et al. (1998). Improvement of chronic diarrhoea in patients with advanced HIV-1 infection during potent antiretroviral therapy. *AIDS* 12 (1), 35–41. doi: 10.1097/00002030-199801000-00005

Gathe, J. C.Jr., Mayberry, C., Clemmons, J., and Nemecek, J. (2008). Resolution of severe cryptosporidial diarrhea with rifaximin in patients with AIDS. *J. Acquir. Immune Defic. Syndr.* 48 (3), 363–364. doi: 10.1097/QAI.0b013e31817beb78

Gathe, J., Piot, D., Hawkins, K., Bernal, A., Clemmons, J., and Stool, E. (1990). "Treatment of gastrointestinal cryptosporidiosis with paromomycin (abstract 2121)," in *International Conference on AIDS*(San Francisco, CA).

Geurden, T., Thomas, P., Casaert, S., Vercruysse, J., and Claerebout, E. (2008). Prevalence and molecular characterisation of *Cryptosporidium* and *Giardia* in lambs and goat kids in Belgium. *Vet. Parasitol.* 155 (1-2), 142–145. doi: 10.1016/j.vetpar.2008.05.002

Gharpure, R., Perez, A., Miller, A. D., Wikswo, M. E., Silver, R., and Hlavsa, M. C. (2019). Cryptosporidiosis outbreaks - united state -2017. *MMWR Morb Mortal Wkly Rep.* 68 (25), 568–572. doi: 10.15585/mmwr.mm6825a3

Giadinis, N. D., Papadopoulos, E., Lafi, S. Q., Panousis, N. K., Papazahariadou, M., and Karatzias, H. (2008). Efficacy of halofuginone lactate for the treatment and prevention of cryptosporidiosis in goat kids: An extensive field trial. *Small Ruminant Res.* 76 (3), 195–200. doi: 10.1016/j.smallrumres.2008.01.007

Giadinis, N. D., Papadopoulos, E., Panousis, N., Papazahariadou, M., Lafi, S. Q., and Karatzias, H. (2007). Effect of halofuginone lactate on treatment and prevention of lamb cryptosporidiosis: an extensive field trial. *J. Vet. Pharmacol. Ther.* 30 (6), 578–582. doi: 10.1111/j.1365-2885.2007.00900.x

Girard, P. M., Goldschmidt, E., Vittecoq, D., Massip, P., Gastiaburu, J., Meyohas, M. C., et al. (1992). Vapreotide, a somatostatin analogue, in cryptosporidiosis and other AIDS-related diarrhoeal diseases. *AIDS* 6 (7), 715–718. doi: 10.1097/00002030-199207000-00015

Gobel, E. (1987a). Diagnosis and treatment of acute cryptosporidiosis in the calf. *Tieraerztliche Umschau.* 42, 863–869.

Gobel, E. (1987b). Possibilities of therapy of cryptosporidiosis in calves in problematic farms. zentralblatt für bakteriologie, mikrobiologie und hygiene. *Ser. A: Med. Microbiology Infect. Diseases Virology Parasitol.* 265 (3-4), 490–490.

Goma, F. Y., Geurden, T., Siwila, J., Phiri, I. G. K., Gabriel, S., Claerebout, E., et al. (2007). The prevalence and molecular characterisation of cryptosporidium spp. in small ruminants in Zambia. *Small Ruminant Res.* 72 (1), 77–80. doi: 10.1016/j.smallrumres.2006.08.010

Greenberg, P. D., and Cello, J. P. (1996). Treatment of severe diarrhea caused by *Cryptosporidium parvum* with oral bovine immunoglobulin concentrate in patients with AIDS. *J. Acquir. Immune Defic. Syndr. Hum. Retrovirol* 13 (4), 348–354. doi: 10.1097/00042560-199612010-00008

Grinberg, A., Markovics, A., Galindez, J., Lopez-Villalobos, N., Kosak, A., and Tranquillo, V. M. (2002). Controlling the onset of natural cryptosporidiosis in calves with paromomycin sulphate. *Vet. Rec* 151 (20), 606–608. doi: 10.1136/vr.151.20.606

Grube, H., Ramratnam, B., Ley, C., and Flanigan, T. P. (1997). Resolution of AIDS associated cryptosporidiosis after treatment with indinavir. *Am. J. Gastroenterol.* 92 (4), 726.

Harp, J. A., Jardon, P., Atwill, E. R., Zylstra, M., Checel, S., Goff, J. P., et al. (1996). Field testing of prophylactic measures against *Cryptosporidium parvum* infection in calves in a California dairy herd. *Am. J. Vet. Res.* 57 (11), 1586–1588.

Harris, M., Deutsch, G., MacLean, J. D., and Tsoukas, C. M. (1994). A phase I study of letrazuril in AIDS-related cryptosporidiosis. *AIDS* 8 (8), 1109–1113. doi: 10.1097/00002030-199408000-00011

Hartmann, G., Honikel, K. O., Knusel, F., and Nuesch, J. (1967). The specific inhibition of the DNA-directed RNA synthesis by rifamycin. *Biochim. Biophys. Acta* 145 (3), 843–844. doi: 10.1016/0005-2787(67)90147-5

Hasan, M. M., Stebbins, E. E., Choy, R. K. M., Gillespie, J. R., de Hostos, E. L., Miller, P., et al. (2021). Spontaneous selection of *Cryptosporidium* drug resistance in a calf model of infection. *Antimicrob. Agents Chemother.* 65 (6), e00023–21. doi: 10.1128/AAC.00023-21

Hashmey, R., Smith, N. H., Cron, S., Graviss, E. A., Chappell, C. L., and White, A. C.Jr. (1997). Cryptosporidiosis in Houston, texas. a report of 95 cases. *Med. (Baltimore)* 76 (2), 118–139. doi: 10.1097/00005792-199703000-00004

Hatam-Nahavandi, K., Ahmadpour, E., Carmena, D., Spotin, A., Bangoura, B., and Xiao, L. (2019). *Cryptosporidium* infections in terrestrial ungulates with focus on livestock: a systematic review and meta-analysis. *Parasit Vectors* 12 (1), 453. doi: 10.1186/s13071-019-3704-4

Hayes, E. B., Matte, T. D., O'Brien, T. R., McKinley, T. W., Logsdon, G. S., Rose, J. B., et al. (1989). Large Community outbreak of cryptosporidiosis due to contamination of a filtered public water supply. *N Engl. J. Med.* 320 (21), 1372–1376. doi: 10.1056/NEJM198905253202103

Henry, R. J. (1943). The mode of action of sulfonamides. *Bacteriol Rev.* 7 (4), 175–262. doi: 10.1128/br.7.4.175-262.1943

Hewitt, R. G., Yiannoutsos, C. T., Higgs, E. S., Carey, J. T., Geiseler, P. J., Soave, R., et al. (2000). Paromomycin: no more effective than placebo for treatment of cryptosporidiosis in patients with advanced human immunodeficiency virus infection. AIDS clinical trial group. *Clin. Infect. Dis.* 31 (4), 1084–1092. doi: 10.1086/318155

Hicks, P., Zwiener, R. J., Squires, J., and Savell, V. (1996). Azithromycin therapy for *Cryptosporidium parvum* infection in four children infected with human immunodeficiency virus. *J. Pediatr.* 129 (2), 297–300. doi: 10.1016/s0022-3476(96)70258-5

Hoffman, P. S., Sisson, G., Croxen, M. A., Welch, K., Harman, W. D., Cremades, N., et al. (2007). Antiparasitic drug nitazoxanide inhibits the pyruvate oxidoreductases of *Helicobacter pylori*, selected anaerobic bacteria and parasites, and *Campylobacter jejuni*. *Antimicrob. Agents Chemother.* 51 (3), 868–876. doi: 10.1128/AAC.01159-06

Holmberg, S. D., Moorman, A. C., Von Bargen, J. C., Palella, F. J., Loveless, M. O., Ward, D. J., et al. (1998). Possible effectiveness of clarithromycin and rifabutin for cryptosporidiosis chemoprophylaxis in HIV disease. HIV outpatient study (HOPS) investigators. *JAMA* 279 (5), 384–386. doi: 10.1001/jama.279.5.384

Hong, D. K., Wong, C. J., and Gutierrez, K. (2007). Severe cryptosporidiosis in a seven-year-old renal transplant recipient: case report and review of the literature. *Pediatr. Transplant.* 11 (1), 94–100. doi: 10.1111/j.1399-3046.2006.00593.x

Hoxie, N. J., Davis, J. P., Vergeront, J. M., Nashold, R. D., and Blair, K. A. (1997). Cryptosporidiosis-associated mortality following a massive waterborne outbreak in Milwaukee, Wisconsin. *Am. J. Public Health* 87 (12), 2032–2035. doi: 10.2105/ajph.87.12.2032

Huang, W., Hulverson, M. A., Choi, R., Arnold, S. L. M., Zhang, Z., McCloskey, M. C., et al. (2019). Development of 5-Aminopyrazole-4-carboxamide-based bumped-kinase inhibitors for cryptosporidiosis therapy. *J. Med. Chem.* 62 (6), 3135–3146. doi: 10.1021/acs.jmedchem.9b00069

Huang, M. Z., Li, J., Guan, L., Li, D. Q., Nie, X. M., Gui, R., et al. (2015). Therapeutic effects of acetylspiramycin and garlicin on cryptosporidiosis among drug users. *Int. J. Parasitol. Drugs Drug Resist.* 5 (3), 185–190. doi: 10.1016/j.ijpddr.2015.09.002

Hulverson, M. A., Choi, R., Arnold, S. L. M., Schaefer, D. A., Hemphill, A., McCloskey, M. C., et al. (2017). Advances in bumped kinase inhibitors for human and animal therapy for cryptosporidiosis. *Int. J. Parasitol.* 47 (12), 753–763. doi: 10.1016/j.ijpara.2017.08.006

Hunt, E., Fu, Q., Armstrong, M. U., Rennix, D. K., Webster, D. W., Galanko, J. A., et al. (2002). Oral bovine serum concentrate improves cryptosporidial enteritis in calves. *Pediatr. Res.* 51 (3), 370–376. doi: 10.1203/00006450-200203000-00017

Hussien, S. M., Abdella, O. H., Abu-Hashim, A. H., Aboshiesha, G. A., Taha, M. A., El-Shemy, A. S., et al. (2013). Comparative study between the effect of nitazoxanide and paromomycine in treatment of cryptosporidiosis in hospitalized children. *J. Egypt Soc. Parasitol.* 43 (2), 463–470.

Innes, E. A., Chalmers, R. M., Wells, B., and Pawlowic, M. C. (2020). A one health approach to tackle cryptosporidiosis. *Trends Parasitol.* 36 (3), 290–303. doi: 10.1016/j.pt.2019.12.016

Iroh Tam, P., Arnold, S. L. M., Barrett, L. K., Chen, C. R., Conrad, T. M., Douglas, E., et al. (2021). Clofazimine for treatment of cryptosporidiosis in human immunodeficiency virus infected adults: An experimental medicine, randomized, double-blind, placebo-controlled phase 2a trial. *Clin. Infect. Dis.* 73 (2), 183–191. doi: 10.1093/cid/ciaa421

Ives, N. J., Gazzard, B. G., and Easterbrook, P. J. (2001). The changing pattern of AIDS-defining illnesses with the introduction of highly active antiretroviral therapy (HAART) in a London clinic. *J. Infect.* 42 (2), 134–139. doi: 10.1053/jinf.2001.0810

Jacobson, C., Al-Habsi, K., Ryan, U., Williams, A., Anderson, F., Yang, R., et al. (2018). *Cryptosporidium* infection is associated with reduced growth and diarrhoea in goats beyond weaning. *Vet. Parasitol.* 260, 30–37. doi: 10.1016/j.vetpar.2018.07.005

Jacobson, C., Williams, A., Yang, R., Ryan, U., Carmichael, I., Campbell, A. J., et al. (2016). Greater intensity and frequency of *Cryptosporidium* and *Giardia* oocyst shedding beyond the neonatal period is associated with reductions in growth, carcase weight and dressing efficiency in sheep. *Vet. Parasitol.* 228, 42–51. doi: 10.1016/j.vetpar.2016.08.003

Jain, V., Yogavel, M., Kikuchi, H., Oshima, Y., Hariguchi, N., Matsumoto, M., et al. (2017). Targeting prolyl-tRNA synthetase to accelerate drug discovery against malaria, leishmaniasis, toxoplasmosis, cryptosporidiosis, and coccidiosis. *Structure* 25 (10), 1495–1505 e1496. doi: 10.1016/j.str.2017.07.015

Jarvie, B. D., Trotz-Williams, L. A., McKnight, D. R., Leslie, K. E., Wallace, M. M., Todd, C. G., et al. (2005). Effect of halofuginone lactate on the occurrence of *Cryptosporidium parvum* and growth of neonatal dairy calves. *J. Dairy Sci.* 88 (5), 1801–1806. doi: 10.3168/jds.S0022-0302(05)72854-X

Jasenosky, L. D., Cadena, C., Mire, C. E., Borisevich, V., Haridas, V., Ranjbar, S., et al. (2019). The FDA-approved oral drug nitazoxanide amplifies host antiviral responses and inhibits Ebola virus. *iScience* 19, 1279–1290. doi: 10.1016/j.isci.2019.07.003

Joachim, A., Krull, T., Schwarzkopf, J., and Daugschies, A. (2003). Prevalence and control of bovine cryptosporidiosis in German dairy herds. *Vet. Parasitol.* 112 (4), 277–288. doi: 10.1016/s0304-4017(03)00006-2

Johnson, E. H., Windsor, J. J., Muirhead, D. E., King, G. J., and Al-Busaidy, R. (2000). Confirmation of the prophylactic value of paromomycin in a natural outbreak of caprine cryptosporidiosis. *Vet. Res. Commun.* 24 (1), 63–67. doi: 10.1023/a:1006381522986

Jordan, W. C. (1996). Clarithromycin prophylaxis against *Cryptosporidium* enteritis in patients with AIDS. *J. Natl. Med. Assoc.* 88 (7), 425–427.

Jumani, R. S., Bessoff, K., Love, M. S., Miller, P., Stebbins, E. E., Teixeira, J. E., et al. (2018). A novel piperazine-based drug lead for cryptosporidiosis from the medicines for malaria venture open-access malaria box. *Antimicrob. Agents Chemother.* 62 (4), e01505–e01517. doi: 10.1128/AAC.01505-17

Kacar, Y., Baykal, A. T., Aydin, L., and Batmaz, H. (2022). Evaluation of the efficacy of cow colostrum in the treatment and its effect on serum proteomes in calves with cryptosporidiosis. *Vet. Immunol. Immunopathol.* 248, 110429. doi: 10.1016/j.vetimm.2022.110429

Kadappu, K., Nagaraja, M., Rao, P., and Shastry, B. (2002). Azithromycin as treatment for cryptosporidiosis in human immunodeficiency virus disease. *J. Postgraduate Med.* 48 (3), 179–181.

Karanis, P. (2018). "Cryptosporidium: Waterborne and foodborne transmission and worldwide outbreaks," in *Recent advances in environmental science from the Euro-Mediterranean and surrounding regions* (Cham: Cham: Springer), 41–44.

Katsoulos, P. D., Karatzia, M. A., Dovas, C. I., Filioussis, G., Papadopoulos, E., Kiossis, E., et al. (2017). Evaluation of the in-field efficacy of oregano essential oil administration on the control of neonatal diarrhea syndrome in calves. *Res. Vet. Sci.* 115, 478–483. doi: 10.1016/j.rvsc.2017.07.029

Katz, M. D., Erstad, B. L., and Rose, C. (1988). Treatment of severe cryptosporidium-related diarrhea with octreotide in a patient with AIDS. *Drug Intell. Clin. Pharm.* 22 (2), 134–136. doi: 10.1177/106002808802200206

Keidel, J., and Daugschies, A. (2013). Integration of halofuginone lactate treatment and disinfection with p-chloro-m-cresol to control natural cryptosporidiosis in calves. *Vet. Parasitol.* 196 (3-4), 321–326. doi: 10.1016/j.vetpar.2013.03.003

Kelly, P., Lungu, F., Keane, E., Baggaley, R., Kazembe, F., Pobee, J., et al. (1996). Albendazole chemotherapy for treatment of diarrhoea in patients with AIDS in Zambia: a randomised double blind controlled trial. *BMJ* 312 (7040), 1187–1191. doi: 10.1136/bmj.312.7040.1187

Khalil, I. A., Troeger, C., Rao, P. C., Blacker, B. F., Brown, A., Brewer, T. G., et al. (2018). Morbidity, mortality, and long-term consequences associated with diarrhoea from *Cryptosporidium* infection in children younger than 5 years: a meta-analyses study. *Lancet Global Health* 6 (7), E758–E768. doi: 10.1016/S2214-109x(18)30283-3

Khan, S. M., Debnath, C., Pramanik, A. K., Xiao, L., Nozaki, T., and Ganguly, S. (2010). Molecular characterization and assessment of zoonotic transmission of *Cryptosporidium* from dairy cattle in West Bengal, India. *Vet. Parasitol.* 171 (1-2), 41–47. doi: 10.1016/j.vetpar.2010.03.008

Khan, S. M., Garcia Hernandez, A., Allaie, I. M., Grooms, G. M., Li, K., Witola, W. H., et al. (2022a). Activity of (1-benzyl-4-triazolyl)-indole-2-carboxamides against *Toxoplasma gondii* and *Cryptosporidium parvum*. *Int. J. Parasitol. Drugs Drug Resist.* 19, 6–20. doi: 10.1016/j.ijpddr.2022.04.001

Khan, S. M., Zhang, X., and Witola, W. H. (2022b). *Cryptosporidium parvum* pyruvate kinase inhibitors with *in vivo* anti-cryptosporidial efficacy. *Front. Microbiol.* 12. doi: 10.3389/fmicb.2021.800293

Klein, P. (2008). Preventive and therapeutic efficacy of halofuginone-lactate against *Cryptosporidium parvum* in spontaneously infected calves: a centralised, randomised, double-blind, placebo-controlled study. *Vet. J.* 177 (3), 429–431. doi: 10.1016/j.tvjl.2007.05.007

Kotloff, K. L., Nataro, J. P., Blackwelder, W. C., Nasrin, D., Farag, T. H., Panchalingam, S., et al. (2013). Burden and aetiology of diarrhoeal disease in infants and young children in developing countries (the global enteric multicenter study, GEMS): a prospective, case-control study. *Lancet* 382 (9888), 209–222. doi: 10.1016/S0140-6736(13)60844-2

Koudela, B., and Bokova, A. (1997). The effect of cotrimoxazole on experimental *Cryptosporidium parvum* infection in kids. *Vet. Res.* 28 (4), 405–412.

Krause, I., Amir, J., Cleper, R., Dagan, A., Behor, J., Samra, Z., et al. (2012). Cryptosporidiosis in children following solid organ transplantation. *Pediatr. Infect. Dis. J.* 31 (11), 1135–1138. doi: 10.1097/INF.0b013e31826780f7

Lacey, E. (1988). The role of the cytoskeletal protein, tubulin, in the mode of action and mechanism of drug resistance to benzimidazoles. *Int. J. Parasitol.* 18 (7), 885–936. doi: 10.1016/0020-7519(88)90175-0

Lallemand, M., Villeneuve, A., Belda, J., and Dubreuil, P. (2006). Field study of the efficacy of halofuginone and decoquinate in the treatment of cryptosporidiosis in veal calves. *Vet. Rec* 159 (20), 672–676. doi: 10.1136/vr.159.20.672

Lanternier, F., Amazzough, K., Favennec, L., Mamzer-Bruneel, M. F., Abdoul, H., Tourret, J., et al. (2017). *Cryptosporidium* spp. infection in solid organ transplantation: The nationwide "TRANSCRYPTO" study. *Transplantation* 101 (4), 826–830. doi: 10.1097/TP.0000000000001503

Lee, S., Ginese, M., Beamer, G., Danz, H. R., Girouard, D. J., Chapman-Bonofiglio, S. P., et al. (2018). Therapeutic efficacy of bumped kinase inhibitor 1369 in a pig model of acute diarrhea caused by *Cryptosporidium hominis*. *Antimicrob. Agents Chemother.* 62 (7), e00147–e00118. doi: 10.1128/AAC.00147-18

Lee, S., Ginese, M., Girouard, D., Beamer, G., Huston, C. D., Osbourn, D., et al. (2019). Piperazine-derivative MMV665917: An effective drug in the diarrheic piglet model of *Cryptosporidium hominis*. *J. Infect. Dis.* 220 (2), 285–293. doi: 10.1093/infdis/jiz105

Lee, S., Harwood, M., Girouard, D., Meyers, M. J., Campbell, M. A., Beamer, G., et al. (2017). The therapeutic efficacy of azithromycin and nitazoxanide in the acute pig model of *Cryptosporidium hominis*. *PloS One* 12 (10), e0185906. doi: 10.1371/journal.pone.0185906

Lefay, D., Naciri, M., Poirier, P., and Chermette, R. (2001). Efficacy of halofuginone lactate in the prevention of cryptosporidiosis in suckling calves. *Vet. Rec* 148 (4), 108–112. doi: 10.1136/vr.148.4.108

Legrand, F., Grenouillet, F., Larosa, F., Dalle, F., Saas, P., Millon, L., et al. (2011). Diagnosis and treatment of digestive cryptosporidiosis in allogeneic haematopoietic stem cell transplant recipients: a prospective single centre study. *Bone Marrow Transplant.* 46 (6), 858–862. doi: 10.1038/bmt.2010.200

Le Moing, V., Bissuel, F., Costagliola, D., Eid, Z., Chapuis, F., Molina, J.-M., et al. (1998). Decreased prevalence of intestinal cryptosporidiosis in HIV-infected patients concomitant to the widespread use of protease inhibitors. *AIDS* 12 (11), 1395–1397. doi: 10.1097/00002030-199811000-00026

Lendner, M., Bottcher, D., Delling, C., Ojo, K. K., Van Voorhis, W. C., and Daugschies, A. (2015). A novel CDPK1 inhibitor–a potential treatment for cryptosporidiosis in calves? *Parasitol. Res.* 114 (1), 335–336. doi: 10.1007/s00436-014-4228-7

Liberti, A., Bisogno, A., and Izzo, E. (1992). Octreotide treatment in secretory and cyrptosporidial diarrhea in patients with acquired immunodeficiency syndrome (AIDS): clinical evaluation. *J. Chemother.* 4 (5), 303–305. doi: 10.1080/1120009x.1992.11739182

Li, K., Grooms, G. M., Khan, S. M., Hernandez, A. G., Witola, W. H., and Stec, J. (2020). Novel acyl carbamates and acyl / diacyl ureas show *in vitro* efficacy against *Toxoplasma gondii* and *Cryptosporidium parvum*. *Int. J. Parasitol. Drugs Drug Resist.* 14, 80–90. doi: 10.1016/j.ijpddr.2020.08.006

Li, K., Nader, S. M., Zhang, X., Ray, B. C., Kim, C. Y., Das, A., et al. (2019). Novel lactate dehydrogenase inhibitors with *in vivo* efficacy against *Cryptosporidium parvum*. *PloS Pathog.* 15 (7), e1007953. doi: 10.1371/journal.ppat.1007953

Lindsay, D. S., Upton, S. J., Owens, D. S., Morgan, U. M., Mead, J. R., and Blagburn, B. L. (2000). *Cryptosporidium andersoni* n. sp. (Apicomplexa: Cryptosporiidae) from cattle, *Bos taurus*. *J. Eukaryot Microbiol.* 47 (1), 91–95. doi: 10.1111/j.1550-7408.2000.tb00016.x

Lin, J., Zhou, D., Steitz, T. A., Polikanov, Y. S., and Gagnon, M. G. (2018). Ribosome-targeting antibiotics: Modes of action, mechanisms of resistance, and implications for drug design. *Annu. Rev. Biochem.* 87 (1), 451–478. doi: 10.1146/annurev-biochem-062917-011942

Loeb, M., Walach, C., Phillips, J., Fong, I., Salit, I., Rachlis, A., et al. (1995). Treatment with letrazuril of refractory cryptosporidial diarrhea complicating AIDS. *J. Acquir. Immune Defic. Syndr. Hum. Retrovirol* 10 (1), 48–53. doi: 10.1097/00042560-199509000-00007

Louie, E., Borkowsky, W., Klesius, P. H., Haynes, T. B., Gordon, S., Bonk, S., et al. (1987). Treatment of cryptosporidiosis with oral bovine transfer factor. *Clin. Immunol. Immunopathol.* 44 (3), 329–334. doi: 10.1016/0090-1229(87)90077-8

Love, M. S., Beasley, F. C., Jumani, R. S., Wright, T. M., Chatterjee, A. K., Huston, C. D., et al. (2017). A high-throughput phenotypic screen identifies clofazimine as a potential treatment for cryptosporidiosis. *PloS Negl. Trop. Dis.* 11 (2), e0005373. doi: 10.1371/journal.pntd.0005373

Love, M. S., and Choy, R. K. M. (2021). Emerging treatment options for cryptosporidiosis. *Curr. Opin. Infect. Dis.* 34 (5), 455–462. doi: 10.1097/QCO.0000000000000761

Lunde, C. S., Stebbins, E. E., Jumani, R. S., Hasan, M. M., Miller, P., Barlow, J., et al. (2019). Identification of a potent benzoxaborole drug candidate for treating cryptosporidiosis. *Nat. Commun.* 10 (1), 2816. doi: 10.1038/s41467-019-10687-y

Mac Kenzie, W. R., Hoxie, N. J., Proctor, M. E., Gradus, M. S., Blair, K. A., Peterson, D. E., et al. (1994). A massive outbreak in Milwaukee of cryptosporidium infection transmitted through the public water supply. *N Engl. J. Med.* 331 (3), 161–167. doi: 10.1056/NEJM199407213310304

Maddox-Hyttel, C., Langkjaer, R. B., Enemark, H. L., and Vigre, H. (2006). *Cryptosporidium* and *Giardia* in different age groups of Danish cattle and pigs–occurrence and management associated risk factors. *Vet. Parasitol.* 141 (1-2), 48–59. doi: 10.1016/j.vetpar.2006.04.032

Maggi, P., Larocca, A. M., Quarto, M., Serio, G., Brandonisio, O., Angarano, G., et al. (2000). Effect of antiretroviral therapy on cryptosporidiosis and microsporidiosis in patients infected with human immunodeficiency virus type 1. *Eur. J. Clin. Microbiol. Infect. Dis.* 19 (3), 213–217. doi: 10.1007/s100960050461

Mancassola, R., Reperant, J. M., Naciri, M., and Chartier, C. (1995). Chemoprophylaxis of *Cryptosporidium parvum* infection with paromomycin in kids and immunological study. *Antimicrob. Agents Chemother.* 39 (1), 75–78. doi: 10.1128/AAC.39.1.75

Mancassola, R., Richard, A., and Naciri, M. (1997). Evaluation of decoquinate to treat experimental cryptosporidiosis in kids. *Vet. Parasitol.* 69 (1-2), 31–37. doi: 10.1016/s0304-4017(96)01094-1

Manjunatha, U. H., Vinayak, S., Zambriski, J. A., Chao, A. T., Sy, T., Noble, C. G., et al. (2017). A *Cryptosporidium* PI(4)K inhibitor is a drug candidate for cryptosporidiosis. *Nature* 546 (7658), 376–380. doi: 10.1038/nature22337

Maurya, P. S., Sahu, S., Sudhakar, N. R., Jaiswal, V., Prashant, D. G., Rawat, S., et al. (2016). Cryptosporidiosis in a buffalo calf at meerut, uttar pradesh and its successful therapeutic management. *J. Parasit Dis.* 40 (4), 1583–1585. doi: 10.1007/s12639-015-0734-5

McDonald, V., Korbel, D. S., Barakat, F. M., Choudhry, N., and Petry, F. (2013). Innate immune responses against *Cryptosporidium parvum* infection. *Parasite Immunol.* 35 (2), 55–64. doi: 10.1111/pim.12020

McMeeking, A., Borkowsky, W., Klesius, P. H., Bonk, S., Holzman, R. S., and Lawrence, H. S. (1990). A controlled trial of bovine dialyzable leukocyte extract for cryptosporidiosis in patients with AIDS. *J. Infect. Dis.* 161 (1), 108–112. doi: 10.1093/infdis/161.1.108

Mead, J. R. (2014). Prospects for immunotherapy and vaccines against *Cryptosporidium*. *Hum. Vaccin Immunother.* 10 (6), 1505–1513. doi: 10.4161/hv.28485

Meamar, A. R., Rezaian, M., Rezaie, S., Mohraz, M., Kia, E. B., Houpt, E. R., et al. (2006). *Cryptosporidium parvum* bovine genotype oocysts in the respiratory samples of an AIDS patient: efficacy of treatment with a combination of azithromycin and paromomycin. *Parasitol. Res.* 98 (6), 593–595. doi: 10.1007/s00436-005-0097-4

Meganck, V., Hoflack, G., Piepers, S., and Opsomer, G. (2015). Evaluation of a protocol to reduce the incidence of neonatal calf diarrhoea on dairy herds. *Prev. Vet. Med.* 118 (1), 64–70. doi: 10.1016/j.prevetmed.2014.11.007

Meisel, J. L., Perera, D. R., Meligro, C., and Rubin, C. E. (1976). Overwhelming watery diarrhea associated with a cryptosporidium in an immunosuppressed patient. *Gastroenterology* 70 (6), 1156–1160. doi: 10.1016/S0016-5085(76)80331-9

Mele, R., Morales, M. A. G., Tosini, F., and Pozio, E. (2003). Indinavir reduces *Cryptosporidium parvum* infection in both *in vitro* and *in vivo* models. *Int. J. Parasitol.* 33 (7), 757–764. doi: 10.1016/S0020-7519(03)00093-6

Mendonca, F. L. M., Carvalho, J. G., Silva, R. J., Ferreira, L. C. A., Cerqueira, D. M., Rogge, H. I., et al. (2021). Use of a natural herbal-based feed additive containing isoquinoline alkaloids in newborn calves with cryptosporidiosis. *Vet. Parasitol.* 300, 109615. doi: 10.1016/j.vetpar.2021.109615

Menichetti, F., Moretti, M. V., Marroni, M., Papili, R., and Di Candilo, F. (1991). Diclazuril for cryptosporidiosis in AIDS. *Am. J. Med.* 90 (2), 271–272. doi: 10.1016/0002-9343(91)80174-K

Meuten, D. J., Van Kruiningen, H. J., and Lein, D. H. (1974). Cryptosporidiosis in a calf. *J. Am. Vet. Med. Assoc.* 165 (10), 914–917.

Miao, Y. M., Awad-El-Kariem, F. M., Franzen, C., Ellis, D. S., Muller, A., Counihan, H. M., et al. (2000). Eradication of cryptosporidia and microsporidia following successful antiretroviral therapy. *J. Acquir. Immune Defic. Syndr.* 25 (2), 124–129. doi: 10.1097/00042560-200010010-00006

Miao, Y. M., Awad-El-Kariem, F. M., Gibbons, C. L., and Gazzard, B. G. (1999). Cryptosporidiosis: eradication or suppression with combination antiretroviral therapy? *AIDS* 13 (6), 734–735. doi: 10.1097/00002030-199904160-00019

Missaye, A., Dagnew, M., Alemu, A., and Alemu, A. (2013). Prevalence of intestinal parasites and associated risk factors among HIV/AIDS patients with pre-ART and on-ART attending dessie hospital ART clinic, northeast Ethiopia. *AIDS Res. Ther.* 10 (1), 7. doi: 10.1186/1742-6405-10-7

Moling, O., Avi, A., Rimenti, G., and Mian, P. (2005). Glutamine supplementation for patients with severe cryptosporidiosis. *Clin. Infect. Dis.* 40 (5), 773–774. doi: 10.1086/427948

Moon, H. W., and Bemrick, W. J. (1981). Fecal transmission of calf cryptosporidia between calves and pigs. *Vet. Pathol.* 18 (2), 248–255. doi: 10.1177/030098588101800213

Moon, H. W., Woode, G. N., and Ahrens, F. A. (1982). Attempted chemoprophylaxis of cryptosporidiosis in calves. *Vet. Rec* 110 (8), 181. doi: 10.1136/vr.110.8.181-a

Moore, D. A., Atwill, E. R., Kirk, J. H., Brahmbhatt, D., Herrera Alonso, L., Hou, L., et al. (2003). Prophylactic use of decoquinate for infections with *Cryptosporidium parvum* in experimentally challenged neonatal calves. *J. Am. Vet. Med. Assoc.* 223 (6), 839–845. doi: 10.2460/javma.2003.223.839

Moroni, M., Esposito, R., Cernuschi, M., Franzetti, F., Carosi, G. P., and Fiori, G. P. (1993). Treatment of AIDS-related refractory diarrhoea octreotide. *Digestion* 54 (Suppl. 1), 30–32. doi: 10.1159/000201073

Moskovitz, B. L., Stanton, T. L., and Kusmierek, J. J. (1988). Spiramycin therapy for cryptosporidial diarrhoea in immunocompromised patients. *J. Antimicrob. Chemother.* 22 Suppl B (Supplement_B), 189–191. doi: 10.1093/jac/22.supplement_b.189

Murakoshi, F., Takeuchi, M., Inomata, A., Horimoto, T., Ito, M., Suzuki, Y., et al. (2014). Administration of lasalocid-NA is preventive against cryptosporidiosis of newborn calves. *Vet. Rec* 175 (14), 353. doi: 10.1136/vr.102508

Murdoch, D. A., Bloss, D. E., and Glover, S. C. (1993). Successful treatment of cryptosporidiosis in an AIDS patient with letrazuril. *AIDS* 7 (9), 1279–1280. doi: 10.1097/00002030-199309000-00026

Naciri, M., Mancassola, R., Reperant, J. M., Canivez, O., Quinque, B., and Yvore, P. (1994). Treatment of experimental ovine cryptosporidiosis with ovine or bovine hyperimmune colostrum. *Veterinary Parasitol.* 53 (3-4), 173–190. doi: 10.1016/0304-4017(94)90181-3

Naciri, M., Mancassola, R., Yvore, P., and Peeters, J. E. (1993). The effect of halofuginone lactate on experimental *Cryptosporidium parvum* infections in calves. *Vet. Parasitol.* 45 (3-4), 199–207. doi: 10.1016/0304-4017(93)90075-x

Naciri, M., and Yvore, P. (1989). Efficiency of halofuginone lactate in the treatment of experimental cryptosporidiosis in lambs. *Recueil Medecine Veterinaire* 165 (10), 823–826.

Naciri, M., Yvoré, P., and Levieux, D. (1984). Cryptosporidiose expérimentale du chevreau. influence de la prise du colostrum. essais de traitements. *Les maladies la chèvre. INRA Publications Les colloques l'INRA* 28), 465–471.

Nasir, A., Avais, M., Khan, M. S., Khan, J. A., Hameed, S., and Reichel, M. P. (2013). Treating *Cryptosporidium parvum* infection in calves. *J. Parasitol.* 99 (4), 715–717. doi: 10.1645/12-42.1

Nasrin, D., Blackwelder, W. C., Sommerfelt, H., Wu, Y., Farag, T. H., Panchalingam, S., et al. (2021). Pathogens associated with linear growth faltering in children with diarrhea and impact of antibiotic treatment: The global enteric multicenter study. *J. Infect. Dis.* 224 (12 Suppl 2), S848–S855. doi: 10.1093/infdis/jiab434

Niine, T., Dorbek-Kolin, E., Lassen, B., and Orro, T. (2018). *Cryptosporidium* outbreak in calves on a large dairy farm: Effect of treatment and the association with the inflammatory response and short-term weight gain. *Res. Vet. Sci.* 117, 200–208. doi: 10.1016/j.rvsc.2017.12.015

Nime, F. A., Burek, J. D., Page, D. L., Holscher, M. A., and Yardley, J. H. (1976). Acute enterocolitis in a human being infected with the protozoan *Cryptosporidium*. *Gastroenterology* 70 (4), 592–598. doi: 10.1016/s0016-5085(76)80503-3

Noordeen, F., Faizal, A. C., Rajapakse, R. P., Horadagoda, N. U., and Arulkanthan, A. (2001). Excretion of *Cryptosporidium* oocysts by goats in relation to age and season in the dry zone of Sri Lanka. *Vet. Parasitol.* 99 (1), 79–85. doi: 10.1016/s0304-4017(01)00449-6

Nord, J., Ma, P., DiJohn, D., Tzipori, S., and Tacket, C. O. (1990). Treatment with bovine hyperimmune colostrum of cryptosporidial diarrhea in AIDS patients. *AIDS* 4 (6), 581–584. doi: 10.1097/00002030-199006000-00015

Nsagha, D. S., Njunda, A. L., Assob, N. J. C., Ayima, C. W., Tanue, E. A., Kibu, O. D., et al. (2016). Intestinal parasitic infections in relation to CD4(+) T cell counts and diarrhea in HIV/AIDS patients with or without antiretroviral therapy in Cameroon. *BMC Infect. Dis.* 16, 9. doi: 10.1186/s12879-016-1337-1

O'Connor R, M., Shaffie, R., Kang, G., and Ward, H. D. (2011). Cryptosporidiosis in patients with HIV/AIDS. *AIDS* 25 (5), 549–560. doi: 10.1097/QAD.0b013e3283437e88

Oboh, E., Schubert, T. J., Teixeira, J. E., Stebbins, E. E., Miller, P., Philo, E., et al. (2021). Optimization of the urea linker of triazolopyridazine MMV665917 results in a new anticryptosporidial lead with improved potency and predicted hERG safety margin. *J. Med. Chem.* 64 (15), 11729–11745. doi: 10.1021/acs.jmedchem.1c01136

Okhuysen, P. C., Chappell, C. L., Crabb, J., Valdez, L. M., Douglass, E. T., and DuPont, H. L. (1998). Prophylactic effect of bovine anti-*Cryptosporidium* hyperimmune colostrum immunoglobulin in healthy volunteers challenged with *Cryptosporidium parvum*. *Clin. Infect. Dis.* 26 (6), 1324–1329. doi: 10.1086/516374

Ollivett, T. L., Nydam, D. V., Bowman, D. D., Zambriski, J. A., Bellosa, M. L., Linden, T. C., et al. (2009). Effect of nitazoxanide on cryptosporidiosis in experimentally infected neonatal dairy calves. *J. Dairy Sci.* 92 (4), 1643–1648. doi: 10.3168/jds.2008-1474

Olson, E. J., Epperson, W. B., Zeman, D. H., Fayer, R., and Hildreth, M. B. (1998). Effects of an allicin-based product on cryptosporidiosis in neonatal calves. *J. Am. Vet. Med. Assoc.* 212 (7), 987–990.

Palmieri, F., Cicalini, S., Froio, N., Rizzi, E. B., Goletti, D., Festa, A., et al. (2005). Pulmonary cryptosporidiosis in an AIDS patient: successful treatment with paromomycin plus azithromycin. *Int. J. STD AIDS* 16 (7), 515–517. doi: 10.1258/0956462054308332

Panciera, R. J., Garner, F. M., and Thomassen, R. W. (1971). Cryptosporidial infection in a calf. *Veterinary Pathol.* 8 (5), 479–47+. doi: 10.1177/030098587100800 5-00610

Pantenburg, B., Cabada, M. M., and White, A. C.Jr. (2009). Treatment of cryptosporidiosis. *Expert Rev. Anti Infect. Ther.* 7 (4), 385–391. doi: 10.1586/eri.09.24

Paraud, C., and Chartier, C. (2012). Cryptosporidiosis in small ruminants. *Small Rumin Res.* 103 (1), 93–97. doi: 10.1016/j.smallrumres.2011.10.023

Paraud, C., Pors, I., and Chartier, C. (2010). Evaluation of oral tilmicosin efficacy against severe cryptosporidiosis in neonatal kids under field conditions. *Vet. Parasitol.* 170 (1-2), 149–152. doi: 10.1016/j.vetpar.2010.01.024

Paraud, C., Pors, I., Journal, J. P., Besnier, P., Reisdorffer, L., and Chartier, C. (2011). Control of cryptosporidiosis in neonatal goat kids: efficacy of a product containing activated charcoal and wood vinegar liquid (Obionekk) in field conditions. *Vet. Parasitol.* 180 (3-4), 354–357. doi: 10.1016/j.vetpar.2011.03.022

Pasquali, P., Fayer, R., Zarlenga, D., Canals, A., Marez, T., Gomez Munoz, M. T., et al. (2006). Recombinant bovine interleukin-12 stimulates a gut immune response but does not provide resistance to *Cryptosporidium parvum* infection in neonatal calves. *Vet. Parasitol.* 135 (3-4), 259–268. doi: 10.1016/j.vetpar.2005.05.062

Peeters, J. E., Villacorta, I., Naciri, M., and Vanopdenbosch, E. (1993). Specific serum and local antibody responses against *Cryptosporidium parvum* during medication of calves with halofuginone lactate. *Infect. Immun.* 61 (10), 4440–4445. doi: 10.1128/iai.61.10.4440-4445.1993

Perryman, L. E., Kapil, S. J., Jones, M. L., and Hunt, E. L. (1999). Protection of calves against cryptosporidiosis with immune bovine colostrum induced by a *Cryptosporidium parvum* recombinant protein. *Vaccine* 17 (17), 2142–2149. doi: 10.1016/s0264-410x(98)00477-0

Petermann, J., Paraud, C., Pors, I., and Chartier, C. (2014). Efficacy of halofuginone lactate against experimental cryptosporidiosis in goat neonates. *Vet. Parasitol.* 202 (3-4), 326–329. doi: 10.1016/j.vetpar.2014.02.027

Petersen, H. H., Jianmin, W., Katakam, K. K., Mejer, H., Thamsborg, S. M., Dalsgaard, A., et al. (2015). *Cryptosporidium* and *Giardia* in Danish organic pig farms: Seasonal and age-related variation in prevalence, infection intensity and species/genotypes. *Vet. Parasitol.* 214 (1-2), 29–39. doi: 10.1016/j.vetpar.2015.09.020

Platts-Mills, J. A., Babji, S., Bodhidatta, L., Gratz, J., Haque, R., Havt, A., et al. (2015). Pathogen-specific burdens of community diarrhoea in developing countries: a multisite birth cohort study (MAL-ED). *Lancet Glob Health* 3 (9), e564–e575. doi: 10.1016/S2214-109X(15)00151-5

Plettenberg, A., Stoehr, A., Stellbrink, H. J., Albrecht, H., and Meigel, W. (1993). A preparation from bovine colostrum in the treatment of HIV-positive patients with chronic diarrhea. *Clin. Investig.* 71 (1), 42–45. doi: 10.1007/BF00210962

Raabis, S. M., Ollivett, T. L., Cook, M. E., Sand, J. M., and McGuirk, S. M. (2018). Health benefits of orally administered anti-IL-10 antibody in milk-fed dairy calves. *J. Dairy Sci.* 101 (8), 7375–7382. doi: 10.3168/jds.2017-14270

Redman, D. R., and Fox, J. E. (1993). "The effect of varying levels of DECCOX® on experimental cryptosporidia infections in Holstein bull calves," in *American Association of Bovine Practitioners Proceedings of the Annual Conference*. (Albuquerque, New Mexico: Frontier Printers, Inc.) 157–159.

Robertson, L. J., Björkman, C., Axén, C., and Fayer, R. (2014). "Cryptosporidiosis in farmed animals," in *Cryptosporidium: parasite and disease* (Vienna: Springer), 149–235.

Romeu, J., Miro, J. M., Sirera, G., Mallolas, J., Arnal, J., Valls, M. E., et al. (1991). Efficacy of octreotide in the management of chronic diarrhoea in AIDS. *AIDS* 5 (12), 1495–1499. doi: 10.1097/00002030-199112000-00012

Rossignol, J. F. (2006). Nitazoxanide in the treatment of acquired immune deficiency syndrome-related cryptosporidiosis: results of the united states compassionate use program in 365 patients. *Aliment Pharmacol. Ther.* 24 (5), 887–894. doi: 10.1111/j.1365-2036.2006.03033.x

Rossignol, J. F., Ayoub, A., and Ayers, M. S. (2001). Treatment of diarrhea caused by *Cryptosporidium parvum*: a prospective randomized, double-blind, placebo-controlled study of nitazoxanide. *J. Infect. Dis.* 184 (1), 103–106. doi: 10.1086/321008

Rossignol, J. F., Hidalgo, H., Feregrino, M., Higuera, F., Gomez, W. H., Romero, J. L., et al. (1998). A double-'blind' placebo-controlled study of nitazoxanide in the treatment of cryptosporidial diarrhoea in AIDS patients in Mexico. *Trans. R Soc. Trop. Med. Hyg* 92 (6), 663–666. doi: 10.1016/s0035-9203(98)90804-5

Rossignol, J. F., Kabil, S. M., el-Gohary, Y., and Younis, A. M. (2006). Effect of nitazoxanide in diarrhea and enteritis caused by cryptosporidium species. *Clin. Gastroenterol. Hepatol.* 4 (3), 320–324. doi: 10.1016/j.cgh.2005.12.020

Ross, J., Schatz, C., Beaugrand, K., Zuidhof, S., Ralston, B., Allan, N., et al. (2021). Evaluation of activated charcoal as an alternative to antimicrobials for the treatment of neonatal calf diarrhea. *Vet. Med. (Auckl)* 12, 359–369. doi: 10.2147/VMRR.S337698

Rotte, C., Stejskal, F., Zhu, G., Keithly, J. S., and Martin, W. (2001). Pyruvate : NADP+ oxidoreductase from the mitochondrion of *Euglena gracilis* and from the apicomplexan *Cryptosporidium parvum*: a biochemical relic linking pyruvate metabolism in mitochondriate and amitochondriate protists. *Mol. Biol. Evol.* 18 (5), 710–720. doi: 10.1093/oxfordjournals.molbev.a003853

Rump, J. A., Arndt, R., Arnold, A., Bendick, C., Dichtelmuller, H., Franke, M., et al. (1992). Treatment of diarrhoea in human immunodeficiency virus-infected patients with immunoglobulins from bovine colostrum. *Clin. Investig.* 70 (7), 588–594. doi: 10.1007/BF00184800

Ryan, U. M., Bath, C., Robertson, I., Read, C., Elliot, A., McInnes, L., et al. (2005). Sheep may not be an important zoonotic reservoir for *Cryptosporidium* and *Giardia* parasites. *Appl. Environ. Microbiol.* 71 (9), 4992–4997. doi: 10.1128/AEM.71.9.4992-4997.2005

Ryan, U., Zahedi, A., Feng, Y., and Xiao, L. (2021). An update on zoonotic *Cryptosporidium* species and genotypes in humans. *Anim. (Basel)* 11 (11), 3307. doi: 10.3390/ani11113307

Saez-Llorens, X., Odio, C. M., Umana, M. A., and Morales, M. V. (1989). Spiramycin vs. placebo for treatment of acute diarrhea caused by *Cryptosporidium*. *Pediatr. Infect. Dis. J.* 8 (3), 136–140.

Sahal, M., Karaer, Z., Yasa Duru, S., Cizmeci, S., and Tanyel, B. (2005). Cryptosporidiosis in newborn calves in Ankara region: clinical, haematological findings and treatment with lasalocid-NA. *Dtsch Tierarztl Wochenschr* 112 (6), 203–208, 210.

Sallon, S., Deckelbaum, R. J., Schmid, I. I., Harlap, S., Baras, M., and Spira, D. T. (1988). *Cryptosporidium*, malnutrition, and chronic diarrhea in children. *Am. J. Dis. Child* 142 (3), 312–315. doi: 10.1001/archpedi.1988.02150030086027

Santin, M. (2020). *Cryptosporidium* and *Giardia* in ruminants. *Vet. Clin. North Am. Food Anim. Pract.* 36 (1), 223–238. doi: 10.1016/j.cvfa.2019.11.005

Santín, M., and Trout, J. M. (2007). "Livestock," in *Cryptosporidium and cryptosporidiosis*. Eds. R. Fayer and L. Xiao (Boca Raton, FL: CRC Press), 451–484.

Santin, M., Trout, J. M., and Fayer, R. (2007). Prevalence and molecular characterization of *Cryptosporidium* and *Giardia* species and genotypes in sheep in Maryland. *Vet. Parasitol.* 146 (1-2), 17–24. doi: 10.1016/j.vetpar.2007.01.010

Santin, M., Trout, J. M., and Fayer, R. (2008). A longitudinal study of cryptosporidiosis in dairy cattle from birth to 2 years of age. *Vet. Parasitol.* 155 (1-2), 15–23. doi: 10.1016/j.vetpar.2008.04.018

Santin, M., Trout, J. M., Xiao, L., Zhou, L., Greiner, E., and Fayer, R. (2004). Prevalence and age-related variation of *Cryptosporidium* species and genotypes in dairy calves. *Vet. Parasitol.* 122 (2), 103–117. doi: 10.1016/j.vetpar.2004.03.020

Scaglia, M., Atzori, C., Marchetti, G., Orso, M., Maserati, R., Orani, A., et al. (1994). Effectiveness of aminosidine (paromomycin) sulfate in chronic *Cryptosporidium* diarrhea in AIDS patients: an open, uncontrolled, prospective clinical trial. *J. Infect. Dis.* 170 (5), 1349–1350. doi: 10.1093/infdis/170.5.1349

Schaefer, D. A., Betzer, D. P., Smith, K. D., Millman, Z. G., Michalski, H. C., Menchaca, S. E., et al. (2016). Novel bumped kinase inhibitors are safe and effective therapeutics in the calf clinical model for cryptosporidiosis. *J. Infect. Dis.* 214 (12), 1856–1864. doi: 10.1093/infdis/jiw488

Schmidt, W., Wahnschaffe, U., Schafer, M., Zippel, T., Arvand, M., Meyerhans, A., et al. (2001). Rapid increase of mucosal CD4 T cells followed by clearance of intestinal cryptosporidiosis in an AIDS patient receiving highly active antiretroviral therapy. *Gastroenterology* 120 (4), 984–987. doi: 10.1053/gast.2001.22557

Schnyder, M., Kohler, L., Hemphill, A., and Deplazes, P. (2009). Prophylactic and therapeutic efficacy of nitazoxanide against *Cryptosporidium parvum* in experimentally challenged neonatal calves. *Vet. Parasitol.* 160 (1-2), 149–154. doi: 10.1016/j.vetpar.2008.10.094

Shaw, H. J., Innes, E. A., Morrison, L. J., Katzer, F., and Wells, B. (2020). Long-term production effects of clinical cryptosporidiosis in neonatal calves. *Int. J. Parasitol.* 50 (5), 371–376. doi: 10.1016/j.ijpara.2020.03.002

Shield, J., Melville, C., Novelli, V., Anderson, G., Scheimberg, I., Gibb, D., et al. (1993). Bovine colostrum immunoglobulin concentrate for cryptosporidiosis in AIDS. *Arch. Dis. Child* 69 (4), 451–453. doi: 10.1136/adc.69.4.451

Shirley, D. A., Moonah, S. N., and Kotloff, K. L. (2012). Burden of disease from cryptosporidiosis. *Curr. Opin. Infect. Dis.* 25 (5), 555–563. doi: 10.1097/QCO.0b013e328357e569

Sinkala, E., Katubulushi, M., Sianongo, S., Obwaller, A., and Kelly, P. (2011). In a trial of the use of miltefosine to treat HIV-related cryptosporidiosis in Zambian adults, extreme metabolic disturbances contribute to high mortality. *Ann. Trop. Med. Parasitol.* 105 (2), 129–134. doi: 10.1179/136485911X12899838683160

Slacek, B., Ankenbauer-Perkins, K. L., and Tunnicliffe, A. (1996). Evaluation of colostrum and whey-derived gamma globulins for prevention of cryptosporidiosis in artificially infected neonatal calves. *N Z Vet. J.* 44 (4), 158–160. doi: 10.1080/00480169.1996.35962

Smith, N. H., Cron, S., Valdez, L. M., Chappell, C. L., and White, A. C.Jr. (1998). Combination drug therapy for cryptosporidiosis in AIDS. *J. Infect. Dis.* 178 (3), 900–903. doi: 10.1086/515352

Soave, R., Danner, R. L., Honig, C. L., Ma, P., Hart, C. C., Nash, T., et al. (1984). Cryptosporidiosis in homosexual men. *Ann. Intern. Med.* 100 (4), 504–511. doi: 10.7326/0003-4819-100-4-504

Soave, R., Havlir, D., Lancaster, D., Joseph, P., Leedom, J., Clough, W., et al. (1993). "Azithromycin therapy of AIDS-related cryptosporidial diarrhea: A multi-center, placebo-controlled, double-blind study (abstract 405)," in *33rd Interscience Conference on Antimicrobial Agents and Chemotherapy*(New Orleans, LA).

Sprinz, E., Mallman, R., Barcellos, S., Silbert, S., Schestatsky, G., and Bem David, D. (1998). AIDS-related cryptosporidial diarrhoea: an open study with roxithromycin. *J. Antimicrob. Chemother.* 41 Suppl B (suppl 2), 85–91. doi: 10.1093/jac/41.suppl_2.85

Stebbins, E., Jumani, R. S., Klopfer, C., Barlow, J., Miller, P., Campbell, M. A., et al. (2018). Clinical and microbiologic efficacy of the piperazine-based drug lead MMV665917 in the dairy calf cryptosporidiosis model. *PloS Negl. Trop. Dis.* 12 (1), e0006183. doi: 10.1371/journal.pntd.0006183

Stefańska, B., Sroka, J., Katzer, F., Goliński, P., and Nowak, W. (2021). The effect of probiotics, phytobiotics and their combination as feed additives in the diet of dairy calves on performance, rumen fermentation and blood metabolites during the preweaning period. *Anim. Feed Sci. Technol.* 272, 114738. doi: 10.1016/j.anifeedsci.2020.114738

Swale, C., Bougdour, A., Gnahoui-David, A., Tottey, J., Georgeault, S., Laurent, F., et al. (2019). Metal-captured inhibition of pre-mRNA processing activity by CPSF3 controls *Cryptosporidium* infection. *Sci. Transl. Med.* 11 (517), eaax7161. doi: 10.1126/scitranslmed.aax7161

Swinney, D. C., and Anthony, J. (2011). How were new medicines discovered? *Nat. Rev. Drug Discovery* 10 (7), 507–519. doi: 10.1038/nrd3480

Theodos, C. M., Griffiths, J. K., D'Onfro, J., Fairfield, A., and Tzipori, S. (1998). Efficacy of nitazoxanide against *Cryptosporidium parvum* in cell culture and in animal models. *Antimicrob. Agents Chemother.* 42 (8), 1959–1965. doi: 10.1128/AAC.42.8.1959

Thomson, S., Hamilton, C. A., Hope, J. C., Katzer, F., Mabbott, N. A., Morrison, L. J., et al. (2017). Bovine cryptosporidiosis: impact, host-parasite interaction and control strategies. *Vet. Res.* 48 (1), 42. doi: 10.1186/s13567-017-0447-0

Tomczak, E., McDougal, A. N., and White, A. C.Jr. (2022). Resolution of cryptosporidiosis in transplant recipients: Review of the literature and presentation of a renal transplant patient treated with nitazoxanide, azithromycin, and rifaximin. *Open Forum Infect. Dis.* 9 (1), ofab610. doi: 10.1093/ofid/ofab610

Trad, O., Jumaa, P., Uduman, S., and Nawaz, A. (2003). Eradication of *Cryptosporidium* in four children with acute lymphoblastic leukemia. *J. Trop. Pediatr.* 49 (2), 128–130. doi: 10.1093/tropej/49.2.128

Troeger, C., Blacker, B. F., Khalil, I. A., Rao, P. C., Cao, S. J., Zimsen, S. R. M., et al. (2018). Estimates of the global, regional, and national morbidity, mortality, and aetiologies of diarrhoea in 195 countries: a systematic analysis for the global burden of disease study 2016. *Lancet Infect. Dis.* 18 (11), 1211–1228. doi: 10.1016/S1473-3099(18)30362-1

Trotz-Williams, L. A., Jarvie, B. D., Peregrine, A. S., Duffield, T. F., and Leslie, K. E. (2011). Efficacy of halofuginone lactate in the prevention of cryptosporidiosis in dairy calves. *Vet. Rec* 168 (19), 509. doi: 10.1136/vr.d1492

Trotz-Williams, L. A., Wayne Martin, S., Leslie, K. E., Duffield, T., Nydam, D. V., and Peregrine, A. S. (2007). Calf-level risk factors for neonatal diarrhea and shedding of *Cryptosporidium parvum* in Ontario dairy calves. *Prev. Vet. Med.* 82 (1-2), 12–28. doi: 10.1016/j.prevetmed.2007.05.003

Tuli, L., Gulati, A. K., Sundar, S., and Mohapatra, T. M. (2008). Correlation between CD4 counts of HIV patients and enteric protozoan in different seasons - an experience of a tertiary care hospital in varanasi (India). *BMC Gastroenterol.* 8, 36. doi: 10.1186/1471-230X-8-36

Tyzzer, E. E. (1907). A sporozoan found in the peptic glands of the common mouse. *Exp. Biol. Med.* 5 (1), 12–13. doi: 10.3181/00379727-5-5

Tyzzer, E. E. (1910). An extracellular coccidium, *Cryptosporidium muris* (Gen. et sp. nov.), of the gastric glands of the common mouse. *J. Med. Res.* 23 487-510 (3), 483.

Tyzzer, E. E. (1912). *Cryptosporidium parvum* (sp. nov.), a coccidium found in the small intestine of the common mouse. *Arch. Protistenkd* 26, 394–412.

Tzipori, S., Campbell, I., Sherwood, D., Snodgrass, D. R., and Whitelaw, A. (1980). An outbreak of calf diarrhoea attributed to cryptosporidial infection. *Vet. Rec* 107 (25-26), 579–580.

Tzipori, S., Rand, W., Griffiths, J., Widmer, G., and Crabb, J. (1994). Evaluation of an animal model system for cryptosporidiosis: therapeutic efficacy of paromomycin and hyperimmune bovine colostrum-immunoglobulin. *Clin. Diagn. Lab. Immunol.* 1 (4), 450–463. doi: 10.1128/cdli.1.4.450-463.1994

Tzipori, S., Roberton, D., Cooper, D. A., and White, L. (1987). Chronic cryptosporidial diarrhoea and hyperimmune cow colostrum. *Lancet* 2 (8554), 344–345. doi: 10.1016/s0140-6736(87)90944-5

Tzipori, S., Smith, M., Halpin, C., Angus, K. W., Sherwood, D., and Campbell, I. (1983). Experimental cryptosporidiosis in calves: clinical manifestations and pathological findings. *Vet. Rec* 112 (6), 116–120. doi: 10.1136/vr.112.6.116

Uip, D. E., Lima, A. L., Amato, V. S., Boulos, M., Neto, V. A., and Bem David, D. (1998). Roxithromycin treatment for diarrhoea caused by *Cryptosporidium* spp. in patients with AIDS. *J. Antimicrob. Chemother.* 41 Suppl B (suppl 2), 93–97. doi: 10.1093/jac/41.suppl_2.93

Ungar, B. L., Ward, D. J., Fayer, R., and Quinn, C. A. (1990). Cessation of *Cryptosporidium*-associated diarrhea in an acquired immunodeficiency syndrome patient after treatment with hyperimmune bovine colostrum. *Gastroenterology* 98 (2), 486–489. doi: 10.1016/0016-5085(90)90842-o

Urie, N. J., Lombard, J. E., Shivley, C. B., Adams, A. E., Kopral, C. A., and Santin, M. (2018a). Preweaned heifer management on US dairy operations: Part III. factors associated with *Cryptosporidium* and *Giardia* in preweaned dairy heifer calves. *J. Dairy Sci.* 101 (10), 9199–9213. doi: 10.3168/jds.2017-14060

Urie, N. J., Lombard, J. E., Shivley, C. B., Kopral, C. A., Adams, A. E., Earleywine, T. J., et al. (2018b). Preweaned heifer management on US dairy operations: Part i. descriptive characteristics of preweaned heifer raising practices. *J. Dairy Sci.* 101 (10), 9168–9184. doi: 10.3168/jds.2017-14010

Vandenberg, O., Robberecht, F., Dauby, N., Moens, C., Talabani, H., Dupont, E., et al. (2012). Management of a *Cryptosporidium hominis* outbreak in a day-care center. *Pediatr. Infect. Dis. J.* 31 (1), 10–15. doi: 10.1097/INF.0b013e318235ab64

Van Voorhis, W. C., Hulverson, M. A., Choi, R., Huang, W., Arnold, S. L. M., Schaefer, D. A., et al. (2021). One health therapeutics: Target-based drug development for cryptosporidiosis and other apicomplexa diseases. *Vet. Parasitol.* 289, 109336. doi: 10.1016/j.vetpar.2020.109336

Vargas, S. L., Shenep, J. L., Flynn, P. M., Pui, C. H., Santana, V. M., and Hughes, W. T. (1993). Azithromycin for treatment of severe *Cryptosporidium* diarrhea in two children with cancer. *J. Pediatr.* 123 (1), 154–156. doi: 10.1016/s0022-3476(05)81562-8

Velez, J., Lange, M. K., Zieger, P., Yoon, I., Failing, K., and Bauer, C. (2019). Long-term use of yeast fermentation products in comparison to halofuginone for the control of cryptosporidiosis in neonatal calves. *Vet. Parasitol.* 269, 57–64. doi: 10.1016/j.vetpar.2019.04.008

Velez, J., Velasquez, Z., Silva, L. M. R., Gartner, U., Failing, K., Daugschies, A., et al. (2021). Metabolic signatures of *Cryptosporidium parvum*-infected HCT-8 cells and impact of selected metabolic inhibitors on *C. parvum* infection under physioxia and hyperoxia. *Biol. (Basel)* 10 (1), 1–24. doi: 10.3390/biology10010060

Vermeulen, L. C., Benders, J., Medema, G., and Hofstra, N. (2017). Global *Cryptosporidium* loads from livestock manure. *Environ. Sci. Technol.* 51 (15), 8663–8671. doi: 10.1021/acs.est.7b00452

Viel, H., Rocques, H., Martin, J., and Chartier, C. (2007). Efficacy of nitazoxanide against experimental cryptosporidiosis in goat neonates. *Parasitol. Res.* 102 (1), 163–166. doi: 10.1007/s00436-007-0744-z

Villacorta, I., Peeters, J. E., Vanopdenbosch, E., Ares-Mazas, E., and Theys, H. (1991). Efficacy of halofuginone lactate against *Cryptosporidium parvum* in calves. *Antimicrob. Agents Chemother.* 35 (2), 283–287. doi: 10.1128/AAC.35.2.283

Vinayak, S., Jumani, R. S., Miller, P., Hasan, M. M., McLeod, B. I., Tandel, J., et al. (2020). Bicyclic azetidines kill the diarrheal pathogen *Cryptosporidium* in mice by inhibiting parasite phenylalanyl-tRNA synthetase. *Sci. Transl. Med.* 12 (563), eaba8412–eaba8412. doi: 10.1126/scitranslmed.aba8412

Vinayak, S., Pawlowic, M. C., Sateriale, A., Brooks, C. F., Studstill, C. J., Bar-Peled, Y., et al. (2015). Genetic modification of the diarrhoeal pathogen *Cryptosporidium parvum*. *Nature* 523 (7561), 477–480. doi: 10.1038/nature14651

Viu, M., Quilez, J., Sanchez-Acedo, C., del Cacho, E., and Lopez-Bernad, F. (2000). Field trial on the therapeutic efficacy of paromomycin on natural *Cryptosporidium parvum* infections in lambs. *Vet. Parasitol.* 90 (3), 163–170. doi: 10.1016/s0304-4017(00)00241-7

Volpato, A., Crecencio, R. B., Tomasi, T., Galli, G. M., Griss, L. G., Da Silva, A. D., et al. (2019). Phytogenic as feed additive for suckling dairy calves' has a beneficial effect on animal health and performance. *Anais Da Academia Bras. Cienc.* 91 (4), e20180747. doi: 10.1590/0001-3765201920180747

Wallace, M. R., Nguyen, M. T., and Newton, J. A.Jr. (1993). Use of paromomycin for the treatment of cryptosporidiosis in patients with AIDS. *Clin. Infect. Dis.* 17 (6), 1070–1071. doi: 10.1093/clinids/17.6.1070

Wang, C. C. (1976). Inhibition of the respiration of *Eimeria tenella* by quinolone coccidiostats. *Biochem. Pharmacol.* 25 (3), 343–349. doi: 10.1016/0006-2952(76)90225-2

Wang, R. J., Li, J. Q., Chen, Y. C., Zhang, L. X., and Xiao, L. H. (2018). Widespread occurrence of *Cryptosporidium* infections in patients with HIV/AIDS: Epidemiology, clinical feature, diagnosis, and therapy. *Acta Trop.* 187, 257–263. doi: 10.1016/j.actatropica.2018.08.018

Watanabe, Y., Yang, C. H., and Ooi, H. K. (2005). *Cryptosporidium* infection in livestock and first identification of *Cryptosporidium parvum* genotype in cattle feces in Taiwan. *Parasitol. Res.* 97 (3), 238–241. doi: 10.1007/s00436-005-1428-1

Watarai, S., Tana,, and Koiwa, M. (2008). Feeding activated charcoal from bark containing wood vinegar liquid (Nekka-rich) is effective as treatment for cryptosporidiosis in calves. *J. Dairy Sci.* 91 (4), 1458–1463. doi: 10.3168/jds.2007-0406

Weikel, C., Lazenby, A., Belitsos, P., McDewitt, M., Fleming, H. E.Jr., and Barbacci, M. (1991). Intestinal injury associated with spiramycin therapy of *Cryptosporidium* infection in AIDS. *J. Protozool* 38 (6), 147S.

Weyl-Feinstein, S., Markovics, A., Eitam, H., Orlov, A., Yishay, M., Agmon, R., et al. (2014). Short communication: effect of pomegranate-residue supplement on *Cryptosporidium parvum* oocyst shedding in neonatal calves. *J. Dairy Sci.* 97 (9), 5800–5805. doi: 10.3168/jds.2013-7136

White, A. C.Jr., Chappell, C. L., Hayat, C. S., Kimball, K. T., Flanigan, T. P., and Goodgame, R. W. (1994). Paromomycin for cryptosporidiosis in AIDS: a prospective, double-blind trial. *J. Infect. Dis.* 170 (2), 419–424. doi: 10.1093/infdis/170.2.419

WHO (2009) *Risk assessment of cryptosporidium in drinking water*. Available at: https://www.who.int/publications/i/item/WHO-HSE-WSH-09.04 (Accessed October 26 2022).

Wilke, G., Funkhouser-Jones, L. J., Wang, Y., Ravindran, S., Wang, Q., Beatty, W. L., et al. (2019). A stem-Cell-Derived platform enables complete *Cryptosporidium* development *In vitro* and genetic tractability. *Cell Host Microbe* 26 (1), 123–134 e128. doi: 10.1016/j.chom.2019.05.007

Wilke, G., Wang, Y., Ravindran, S., Stappenbeck, T., Witola, W. H., and Sibley, L. D. (2020). "In vitro culture of cryptosporidium parvum using stem cell-derived intestinal epithelial monolayers," in *Methods in molecular biology* (New York: Springer), 351–372.

Witchel, H. J. (2011). Drug-induced hERG block and long QT syndrome. *Cardiovasc. Ther.* 29 (4), 251–259. doi: 10.1111/j.1755-5922.2010.00154.x

Witola, W. H., Zhang, X., and Kim, C. Y. (2017). Targeted gene knockdown validates the essential role of lactate dehydrogenase in *Cryptosporidium parvum*. *Int. J. Parasitol.* 47 (13), 867–874. doi: 10.1016/j.ijpara.2017.05.002

Wittenberg, D. F., Miller, N. M., and van den Ende, J. (1989). Spiramycin is not effective in treating cryptosporidium diarrhea in infants: results of a double-blind randomized trial. *J. Infect. Dis.* 159 (1), 131–132. doi: 10.1093/infdis/159.1.131

Woolf, G. M., Townsend, M., and Guyatt, G. (1987). Treatment of cryptosporidiosis with spiramycin in AIDS. an "N of 1" trial. *J. Clin. Gastroenterol.* 9 (6), 632–634. doi: 10.1097/00004836-198712000-00005

Wright, S. E., and Coop, R. L. (2007). "Cryptosporidiosis and coccidiosis," in *Diseases of sheep* (Ames, IA, USA: Blackwell Publishing), 179–185.

Xiao, L., Fayer, R., Ryan, U., and Upton, S. J. (2004). *Cryptosporidium* taxonomy: recent advances and implications for public health. *Clin. Microbiol. Rev.* 17 (1), 72–97. doi: 10.1128/CMR.17.1.72-97.2004

Zahedi, A., and Ryan, U. (2020). *Cryptosporidium* - an update with an emphasis on foodborne and waterborne transmission. *Res. Vet. Sci.* 132, 500–512. doi: 10.1016/j.rvsc.2020.08.002

Zhang, X., Kim, C. Y., Worthen, T., and Witola, W. H. (2018). Morpholino-mediated *in vivo* silencing of *Cryptosporidium parvum* lactate dehydrogenase decreases oocyst shedding and infectivity. *Int. J. Parasitol.* 48 (8), 649–656. doi: 10.1016/j.ijpara.2018.01.005

Zulu, I., Kelly, P., Njobvu, L., Sianongo, S., Kaonga, K., McDonald, V., et al. (2005). Nitazoxanide for persistent diarrhoea in Zambian acquired immune deficiency syndrome patients: a randomized-controlled trial. *Aliment Pharmacol. Ther.* 21 (6), 757–763. doi: 10.1111/j.1365-2036.2005.02394.x

Zulu, I., Veitch, A., Sianongo, S., McPhail, G., Feakins, R., Farthing, M. J., et al. (2002). Albendazole chemotherapy for AIDS-related diarrhoea in Zambia–clinical, parasitological and mucosal responses. *Aliment Pharmacol. Ther.* 16 (3), 595–601. doi: 10.1046/j.1365-2036.2002.01182.x

frontiers | Frontiers in Cellular and Infection Microbiology

TYPE Original Research
PUBLISHED 01 March 2023
DOI 10.3389/fcimb.2023.1105126

OPEN ACCESS

EDITED BY
Ivana Klun,
Institute for Medical Research, University of Belgrade, Serbia

REVIEWED BY
Iti Saraav,
Washington University in St. Louis, United States
Awais Ihsan,
COMSATS University Islamabad, Sahiwal Campus, Pakistan

*CORRESPONDENCE
Qingxia Wu
goodwqx@163.com
Kun Li
lk3005@njau.edu.cn

†These authors have contributed equally to this work

SPECIALTY SECTION
This article was submitted to Parasite and Host, a section of the journal Frontiers in Cellular and Infection Microbiology

RECEIVED 22 November 2022
ACCEPTED 16 February 2023
PUBLISHED 01 March 2023

CITATION
Dong H, Chen X, Zhao X, Zhao C, Mehmood K, Kulyar MFA, Bhutta ZA, Zeng J, Nawaz S, Wu Q and Li K (2023) Intestine microbiota and SCFAs response in naturally *Cryptosporidium*-infected plateau yaks.
Front. Cell. Infect. Microbiol. 13:1105126.
doi: 10.3389/fcimb.2023.1105126

Intestine microbiota and SCFAs response in naturally *Cryptosporidium*-infected plateau yaks

Hailong Dong[1†], Xiushuang Chen[2,3†], Xiaoxiao Zhao[2,3], Chenxi Zhao[2,3], Khalid Mehmood[4], Muhammad Fakhar-e-Alam Kulyar[5], Zeeshan Ahmad Bhutta[6], Jiangyong Zeng[7], Shah Nawaz[8], Qingxia Wu[1*] and Kun Li[2,3*]

[1]Key Laboratory of Clinical Veterinary Medicine in Tibet, Tibet Agriculture and Animal Husbandry College, Linzhi, Tibet, China, [2]Institute of Traditional Chinese Veterinary Medicine, College of Veterinary Medicine, Nanjing Agricultural University, Nanjing, China, [3]MOE Joint International Research Laboratory of Animal Health and Food Safety, College of Veterinary Medicine, Nanjing Agricultural University, Nanjing, China, [4]Department of Clinical Medicine and Surgery, Faculty of Veterinary and Animal Sciences, The Islamia University of Bahawalpur, Bahawalpur, Pakistan, [5]College of Veterinary Medicine, Huazhong Agricultural University, Wuhan, China, [6]Laboratory of Biochemistry and Immunology, College of Veterinary Medicine, Chungbuk National University, Cheongju, Chungbuk, Republic of Korea, [7]Institute of Animal Husbandry and Veterinary Medicine, Tibet Academy of Agricultural and Animal Husbandry Sciences, Lhasa, China, [8]Department of Anatomy, Faculty of Veterinary Science, University of Agriculture, Faisalabad, Pakistan

Diarrhea is a severe bovine disease, globally prevalent in farm animals with a decrease in milk production and a low fertility rate. *Cryptosporidium* spp. are important zoonotic agents of bovine diarrhea. However, little is known about microbiota and short-chain fatty acids (SCFAs) changes in yaks infected with *Cryptosporidium* spp. Therefore, we performed 16S rRNA sequencing and detected the concentrations of SCFAs in *Cryptosporidium*-infected yaks. Results showed that over 80,000 raw and 70,000 filtered sequences were prevalent in yak samples. Shannon ($p<0.01$) and Simpson ($p<0.01$) were both significantly higher in *Cryptosporidium*-infected yaks. A total of 1072 amplicon sequence variants were shared in healthy and infected yaks. There were 11 phyla and 58 genera that differ significantly between the two yak groups. A total of 235 enzymes with a significant difference in abundance ($p<0.001$) were found between healthy and infected yaks. KEGG L3 analysis discovered that the abundance of 43 pathways was significantly higher, while 49 pathways were significantly lower in *Cryptosporidium*-infected yaks. The concentration of acetic acid ($p<0.05$), propionic acid ($p<0.05$), isobutyric acid ($p<0.05$), butyric acid ($p<0.05$), and isovaleric acid was noticeably lower in infected yaks, respectively. The findings of the study revealed that *Cryptosporidium* infection causes gut dysbiosis and results in a significant drop in the SCFAs concentrations in yaks with severe diarrhea, which may give new insights regarding the prevention and treatment of diarrhea in livestock.

KEYWORDS

***Cryptosporidium*, yaks, diarrhea, microbiota, SCFAs**

Introduction

The long-haired ruminant yak is a plateau bovine species living in the 3000-5000 m high-altitude regions and is mostly found on the Qinghai Tibet plateau (Li et al., 2022a). Diarrhea is a serious bovine problem detected globally in livestock farms associated with a decrease in fertility rate and milk production, especially neonatal diarrhea is usually found with high morbidity and mortality (Han et al., 2017; Li et al., 2019a; Lan et al., 2021)

Previously, studies revealed that diarrhea contributed to more than 50% of calf mortality in Canada (Smith et al., 2014), and affected 19% of the cattle population in the USA (Smulski et al., 2020), which indeed was the cause of huge economic detriment. Like other bovine animals, diarrhea has been commonly reported in yaks (Diao et al., 2020; Cui et al., 2022; Li et al., 2022a). There have been many biological factors which are associated for diarrhea and leading cause of death in calves (Kim et al., 2021). Many pathogens like bovine viral diarrhea virus, Noroviruses, *Escherichia coli*, *Salmonella* spp., and *Cryptosporidium* spp. have been commonly observed in infected cattle (Meganck et al., 2014; Cui et al., 2022). Among others, *Cryptosporidium* spp. are important zoonotic protozoa infecting various animal species (Li et al., 2019b; Kandeel et al., 2022), and are also generally recognized as the primary agent of cattle diarrhea (Li et al., 2019a; Li et al., 2019b). A previous study reported that the infection of *Cryptosporidium* spp. was an important issue in UK and Scotland (Smith et al., 2014). As yaks and cattle species are economically important for native herdsmen in China (Cheng et al., 2022), infectious diseases like those caused by *Cryptosporidium* spp. may not only affect animal health but are also potential threats leading to public health concerns.

Intestine microbiota is composed of millions of complex and diverse microorganisms, which contribute greatly to host health, nutrition absorption, host metabolism, and immunological development (Zeineldin et al., 2018). Previous studies demonstrated that this bacteria was related to various diseases like Type 2 diabetes (Martinez-Lopez et al., 2022), acute pancreatitis (Mei et al., 2022), obesity (Salazar et al., 2022), and diarrhea (Han et al., 2017; Zeineldin et al., 2018; Li et al., 2022b). Short-chain fatty acids are metabolic products of microbiota, which contribute to the cellular metabolism of the host (Bachem et al., 2019), regulating immune function and suppressing inflammatory reactions (Abdalkareem Jasim et al., 2022). In our previous study, we observed prominent changes in intestinal microbiota in a horse infected with *Cryptosporidium* spp. (Wang et al., 2022). However, scarce information is available about microbiota and SCFAs changes in plateau yaks infected with *Cryptosporidium* spp. Therefore, this study was conducted to explore intestinal microbiota and SCFAs response to natural *Cryptosporidium* infection in plateau yaks.

Materials and methods

Samples

Fecal samples (n=40) were collected from free-ranged yaks in Xining, Qinghai (North latitude 31°36′-39°19′, east longitude 89°35′-103°04′) and examined for *Cryptosporidium* spp. by employing nested PCR (Chen et al., 2022) and positive samples were saved for further analysis. In this study, all the *Cryptosporidium* spp. positive samples (n=4) with equal number of negative samples (n=4) were sequenced and divided into infected (INF) and healthy (H) groups, respectively.

DNA extraction and PCR amplification

The extraction of total genomic DNA was performed by utilizing a commercial TIANamp Stool DNA Kit (Tiangen Biotech (Beijing) Co., Ltd, China) according to the product's specifications. Fecal DNA concentration, purification, and quality examination were performed through NanoDrop 2000 UV-Vis spectrophotometer (Thermo Scientific, USA) and 1.2% agarose gel electrophoresis, respectively. Then the hypervariable regions of bacterial 16S rRNA gene (V3-V4) were amplified using primers 338F and 806R as described in a previous study (Wang et al., 2019). All PCR products were individually subjected to agarose gel electrophoresis, gel extraction, and purification using the PureLink™ PCR Purification kit (Invitrogen™, USA). Finally, the purified DNA products were quantified by piloting QuantiFluor™-ST as guided by the instruction manual (Promega, USA).

Library construction, Illumina miSeq sequencing, and bioinformatics analysis

Library construction was carried out by employing commercial Hieff NGS® OnePot II DNA Library Prep Kit for Illumina® (Yeasen, China) according to the product's instructions, and sequenced through the Illumina NovaSeq platform (Illumina, San Diego, USA). Quality control of sequencing data was performed by employing QIIME2 (https://docs.qiime2.org/2019.1/) to generate amplicon sequence variant (ASV) (Callahan et al., 2016) and taxonomy table (Bokulich et al., 2018). Analysis of variance was performed using ANCOM (Analysis of Composition of Microbiomes), One-way ANOVA, Kruskal Wallis, LEfSe (LDA (Linear Discriminant Analysis) score >2), DEseq2 (p<0.05 and log2 (FoldChange) > 2), clustering heatmap (with Z-score > 0.5 or < -0.5) and evolutionary tree (p<0.05) methods to reveal differences in bacterial abundance among yak samples (Segata et al., 2011; Love et al., 2014; Mandal et al., 2015). Microbial alpha diversities analyses were performed through QIIME2 by calculating indices including observed OTUs, Chao1, Shannon, and Faith's. Microbial beta diversities of principal coordinate analysis (PCoA), nonmetric multidimensional scaling (NMDS) (Vazquez-Baeza et al., 2013), and partial least squares discriminant analysis (PLS-DA) were carried out to explore the structural variation of microbial communities across yak samples. The evolutionary relation tree was constructed by using ggtree in R package.

Function analysis

The potential KEGG Ortholog (KO) functional profiles of yak microbiota was predicted with PICRUSt (Langille et al., 2013) by annotating with MetaCyc and ENZYME database. One-way ANOVA was used to analyze the data, while Duncan test was used as *post-hoc* test to measure the individual differences in microbial function between the yak groups with a $p<0.05$ as statistically significant.

SCFAs detection

The concentrations of SCFAs in fecal samples were detected by employing GC-MS (Hsu et al., 2019; Zhang et al., 2019), and the differences between yak groups were explored *via* t-test.

Statistical analysis

The differences between different yak groups were calculated by the chi-square test piloting IBM SPSS Statistics (SPSS 22.0). *P* values < 0.05 were considered as statistically significant.

Results

Analysis of 16S rDNA sequencing data

In the current study, over 80,000 raw and 70,000 filtered sequences were obtained in yak samples. The non-chimeric sequences ranged from 62,133 to 73,453 in healthy yaks, and 68,173 to 74,350 in infected yaks (Table 1). There were a total of 1072 shared ASVs between the healthy (group H) and infected (group INF) groups. (Figure 1A). Alpha diversity index analysis showed that there was no significant difference in chao1, faith, and observed features between group H and INF, respectively. Shannon ($p<0.01$) and Simpson ($p<0.01$) were both significantly higher in group INF than in group H (Figure 1B).

Grouping of yak microbiota in different taxa

The sequence percentage in different taxa of group H and INF is shown in Figure 2A. At the phylum level, the dominant phyla were *Firmicutes* (69.61%), *Proteobacteria* (8.97%), and *Actinobacteria* (8.72%) in group H, while *Firmicutes* (56.38%) and *Bacteroidetes* (29.83%) were the main phyla in group INF (Figure 2B). At the class level, *Clostridia* (51.13%) and *Bacilli* (17.28%) were the primary classes in healthy yaks, while *Clostridia* (51.13%) and *Bacteroidia* (29.83%) were the major classes in infected yaks (Figure 2C). At the order level, *Clostridiales* (51.13%), *Lactobacillales* (8.20%), and *Bacillales* (8.10%) were the primary orders in healthy yaks, while *Clostridiales* (51.04%) and *Bacteroides* (29.83%) were the main orders in infected yaks (Figure 2D). At the family level, the main families were unclassified, *Ruminococcaceae* and *Lachnospiraceae* in groups H and INF (Figure 2E). At the genus level, unclassified (52.06%), *Pseudomonadaceae Pseudomonas* (6.13%), and *Lactobacillus* (6.00%) were the dominating genera in healthy yaks, while unclassified (69.25%), *Prevotellaceae Prevotella* (5.13%) and *Arthrobacter* (2.45%) were the main genera in infected yaks (Figure 2F). At the species level, the main bacteria in group H were unclassified (87.85%), *Veronii* (6.11%), and *Alactolyticus* (1.66%), while unclassified (95.15%), *Flavefaciens* (1.50%) and *Veronii* (1.12%) were the main bacteria in group INF (Figure 2G).

Shifts of yak microbiota infected by *Cryptosporidium*

To reveal the microbiota difference between healthy and infected yaks, beta diversity analysis was carried out through NMDS, PCoA, Qiime 2β, and PCA analysis. The results showed a huge difference in composition and structure between samples from group H and group INF animals (Figure 3). To explore the microbiota changes caused by *Cryptosporidium* in different taxa, a clustering heatmap (top 20 abundance) and evolutionary tree (top 50 abundance) with heat map analysis were plotted. The results revealed that at the order level, infected yaks showed an abundance of *Bacteroidia* and *Deltaproteobacteria*, while healthy animals

TABLE 1 The sequence data statistic analysis.

Samples	input	filtered	percentage of input passed filter	denoised	merged	percentage of input merged	non-chimeric	percentage of input non-chimeric
H1	93773	86437	92.18	82758	76547	81.63	73453	78.33
H2	88135	81010	91.92	77501	71312	80.91	67743	76.86
H3	91889	85557	93.11	82297	76216	82.94	72913	79.35
H4	80446	74466	92.57	71353	65482	81.4	62133	77.24
INF1	89759	83135	92.62	78940	72488	80.76	68173	75.95
INF2	92942	86291	92.84	82357	75217	80.93	71848	77.3
INF3	89810	83187	92.63	80203	75295	83.84	74350	82.79
INF4	88245	81820	92.72	78721	73786	83.61	71099	80.57

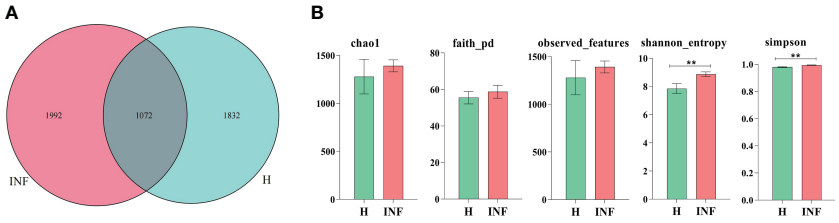

FIGURE 1
ASV venn map and Alpha diversity index analysis. **(A)** Venn map, **(B)** Alpha diversity index. ** refers to significance level, $p<0.05$.

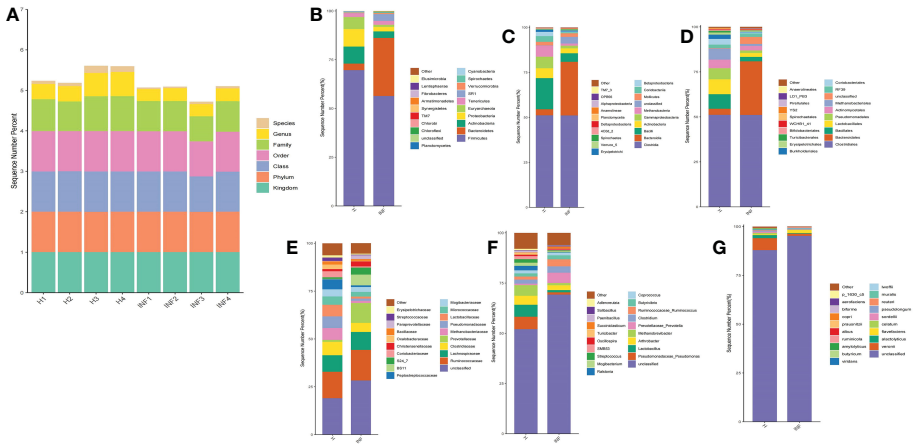

FIGURE 2
Statistical analysis of yak microbiota in different taxa. **(A)** Sequence percentages in different taxa, **(B)** Phylum, **(C)** Class, **(D)** Order, **(E)** Family, **(F)** Genus, **(G)** Species.

showed abundance of *Bacilli*, *Erysipelotrichi*, *Betaproteobacteria*, *Alphaproteobacteria*, and *Nitriliruptoria* as expressed in the clustering heatmap. The evolutionary tree also showed an obvious abundance difference in *Betaproteobacteria*, *Fibrobacteria*, SJA_176, 4C0d_2, *Nitriliruptoria*, *Clostridia*, and *Bacilli* between groups H and INF (Figure 4A). At the order level, the clustering heatmap revealed significant differences in the abundance of *Bacteroidales*, *Lactobacillales*, *Burkholderiales*, *Erysipelotrichales*, YS2, *Turicibacterales* and *Enterobacteriales* between healthy and infected animals. Evolutionary tree detected remarkable differences in the abundance of *Oceanospirillales*, *Burkholderiales*, *Enterobacteriales*, *Fibrobacterales*, *Turicibacterales*, RB046, YS2, *Nitriliruptorales*, *Clostridiales* and *Lactobacillales* between healthy and infected animals (Figure 4B). At the family level, there was a noteworthy difference of *Clostridiaceae*, *Prevotellaceae*, *Lactobacillaceae*, *Peptostreptococcaceae*, BS11, *Christensenellaceae*, *Oxalobacteraceae*, *Paraprevotellaceae*, *Streptococcaceae* and *Erysipelotrichaceae* between groups H and INF as revealed by the clustering heatmap. Evolutionary tree analysis showed a clear difference of *Halomonadaceae*, *Oxalobacteraceae*, *Enterobacteriaceae*, *Streptococcaceae*, *Peptostreptococcaceae*, *Turicibacteraceae*, *Dietziaceae*, *Sanguibacteraceae*, *Nitriliruptoraceae*, *Christensenellaceae*, *Clostridiaceae* and *Lactobacillaceae* between healthy and infected yaks (Figure 4C). At the genus level, interesting difference of *Lactobacillus*, *Prevotellaceae_Prevotella*, *Ralstonia*, *Streptococcus*, SMB53, *Turicibacter*, and *Adlercreutzia* was found between the two yak groups. Evolutionary tree analysis demonstrated that the abundance of *Halomonadaceae*, *Oxalobacteraceae*, *Streptococcaceae*, *Clostridiaceae*, *Turicibacteraceae*, *Planococcaceae*, *Erysipelotrichaceae*, *Sanguibacteraceae*, *Coriobacteriaceae*, *Paraprevotellaceae*, *Ruminococcaceae*, *Lachnospiraceae*, *Clostridiaceae*, *Lactobacillaceae* and *Lachnospiraceae* were significantly different between the two yak groups (Figure 4D). At the species level, the abundance of *alactolyticus*, *celatum*, *reuteri*, *butyricum*, *ruminicola*, *prausnitzii*, *biforme*, p_1630_c5, and *aerofaciens* were noticeably different in groups H and INF. Evolutionary tree analysis uncovered that the abundance of *alactolyticus*, *ruminis*, p_1630_c5, *biforme*, *umbonata*, *aerofaciens*, *prausnitzii*, *butyricum*, *celatum* and *reuteri* were significantly different between healthy and infected animals (Figure 4E).

To further uncover the marker bacteria between healthy and *Cryptosporidium*-infected yaks, we performed one-way ANOVA and Kruskal Wallis tests to determine the significance of the difference and depicted results by DESeq 2 volcano diagram and LEfSe chart, respectively. Results showed that at the phylum level,

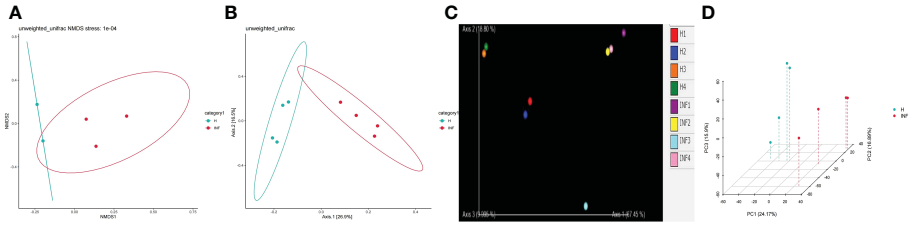

FIGURE 3
Beta diversity analysis between yak groups. **(A)** NMDS, **(B)** PCoA, **(C)** Qiime 2β, **(D)** PCA.

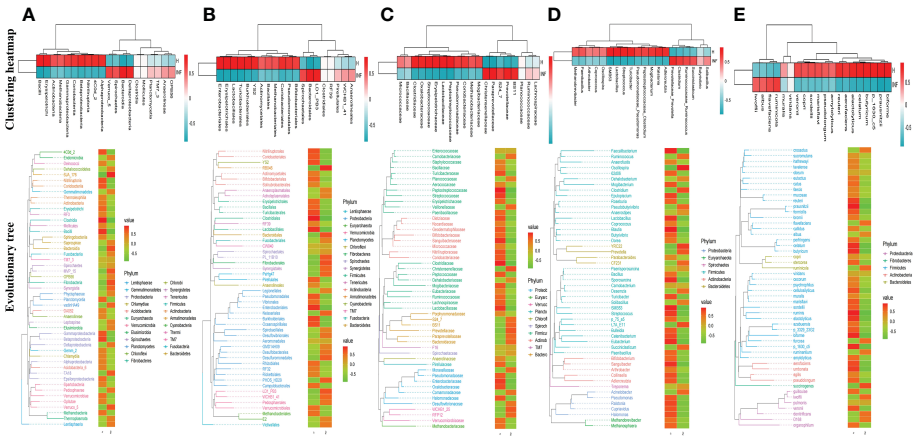

FIGURE 4
Clustering heatmap and evolutionary tree with heat map analysis of yak microbiota in different taxa. **(A)** Class, **(B)** Order, **(C)** Family, **(D)** Genus, **(E)** Species.

the abundance of SR1 ($p<0.0001$), *Bacteroidetes* ($p<0.0001$), *Armatimonadetes* ($p<0.0001$), *Fibrobacteres* ($p<0.01$), and *Synergistetes* ($p<0.01$) were visibly higher in infected yaks, while *Cyanobacteria* ($p<0.0001$), *Proteobacteria* ($p<0.0001$), *Armatimonadetes* ($p<0.0001$), *Euryarchaeota* ($p<0.0001$), *Actinobacteria* ($p<0.01$), *Firmicutes* ($p<0.01$), and *Elusimicrobia* ($p<0.05$) were significantly lower (Figure 5A). At the genus level, the abundance of YRC22 ($p<0.0001$), *Prevotellaceae_Prevotella* ($p<0.0001$), CF231 ($p<0.0001$), L7A_E11 ($p<0.0001$), BF311 ($p<0.0001$), *Desulfovibrio* ($p<0.0001$), *Succiniclasticum* ($p<0.0001$), *Desemzia* ($p<0.0001$), *Anaerovorax* ($p<0.0001$), *Pseudobutyrivibrio* ($p<0.0001$), *Acinetobacter* ($p<0.0001$), *Fibrobacter* ($p<0.0001$), *Ruminococcaceae_Ruminococcus* ($p<0.0001$), *Anaerorhabdus* ($p<0.0001$), *Treponema* ($p<0.0001$), *Selenomonas* ($p<0.001$), *Clostridium* ($p<0.001$), *Shuttleworthia* ($p<0.001$), *Dehalobacterium* ($p<0.001$), TG5 ($p<0.01$), unclassified ($p<0.01$), *Anaerostipes* ($p<0.01$), *Syntrophomonas* ($p<0.01$), *Brachymonas* ($p<0.01$), *Pyramidobacter* ($p<0.01$), SHD_231 ($p<0.05$), *Butyrivibrio* ($p<0.05$), *Desulfobulbus* ($p<0.05$), RFN20 ($p<0.05$), and *Anaerofustis* ($p<0.05$) were significantly higher in infected yaks, while *Turicibacter* ($p<0.0001$), *Lactobacillus* ($p<0.0001$), *Sporosarcina* ($p<0.0001$), *Ralstonia* ($p<0.0001$), *Akkermansia* ($p<0.001$), *Streptococcus* ($p<0.001$), *Methylobacterium* ($p<0.01$), *Adlercreutzia* ($p<0.01$), *Faecalibacterium* ($p<0.01$), *Roseburia* ($p<0.01$), *Paenibacillus* ($p<0.01$), *Methanosphaera* ($p<0.01$), *Pseudomonadaceae_Pseudomonas* ($p<0.01$), *Peptostreptococcaceae_Clostridium* ($p<0.01$), *Slackia* ($p<0.01$), *Cupriavidus* ($p<0.01$), *Halomonas* ($p<0.01$), *Gemmiger* ($p<0.01$), *Dietzia* ($p<0.01$), *Blautia* ($p<0.05$), *Agrobacterium* ($p<0.05$), *Nesterenkonia* ($p<0.05$), *Sanguibacter* ($p<0.05$), *Phascolarctobacterium* ($p<0.05$), *Actinomycetospora* ($p<0.05$), *Bifidobacterium* ($p<0.05$), SMB53 ($p<0.05$), and *Dorea* ($p<0.05$) were significantly lower in infected animals (Figure 5B).

Cryptosporidium infection potentially affected the microbiota function of yaks

The prediction of yaks' microbiota function was carried out by PICRUSt2, and the functional difference between yaks was explored by using one-way ANOVA and Duncan test through R language as previously reported (Zhai et al., 2020). A total of 235 enzymes with a significant difference in abundance ($p<0.001$) were found between healthy and infected yaks, with 119 higher and 116 lower abundance enzymes in INF yaks (Figure 6A). Only one different MetaCys pathway of pentose phosphate pathway (non-oxidative branch) was found between the two yak groups (Figure 6B). KEGG L1 analysis found that the abundance of genetic information

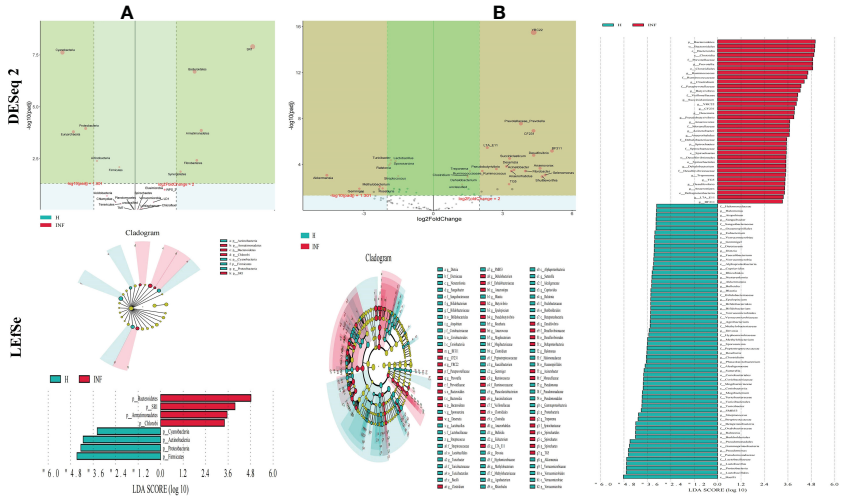

FIGURE 5
Cryptosporidium infection changes microbiota in different taxa through DESeq 2 volcano plot and LEFSe analysis. **(A)** Phylum, **(B)** Genus.

processing was prominently higher in infected yaks, while cellular processes and environmental information processing were significantly lower (Figure 7A). KEGG L2 analysis revealed that the abundance of biosynthesis of other secondary metabolites, glycan biosynthesis, and metabolism, metabolism of cofactors and vitamins, and nucleotide metabolism were remarkably higher in INF yaks, while amino acid metabolism, chemical structure transformation maps, lipid metabolism, metabolism of other amino acids, xenobiotics biodegradation, and metabolism were conspicuously lower (Figure 7B). KEGG L3 analysis discovered that the abundance of 43 pathways was significantly higher in INF yaks, while 49 pathways were significantly lower (Figure 7C).

Cryptosporidium infection decreased the concentration of SCFAs in yaks

The concentration of acetic acid ($p<0.05$), propionic acid ($p<0.05$), isobutyric acid ($p<0.05$), butyric acid ($p<0.05$) and isovaleric acid was significantly lower in infected yaks, respectively, while there was no significant difference of valeric acid and caproic acid between H and INF groups (Figure 8).

Discussion

Cattle diarrhea is still an important worldwide issue on farms, despite observing advanced preventive measures such as herd management, animal facilities and care, feeding and nutrition, and timely medication (Wei et al., 2021). The infectious *Cryptosporidium* was one of the main causative agents of diarrhea with limited available effective treatments (Li et al., 2019a). The harsh climatic conditions with heavy snowfall in the long frigid season (from October to May, with average temperature −15 to −5°C) didn't permit collection of many samples in the Plateau region. Also, very few positive samples (n=4) were observed out of total collected samples (n=40) in the present study. However, a prevalence as low as 1.3% of Cryptosporidium spp. positive samples has been reported in yaks in China region (Li et al., 2020). Moreover, despite the harsh climatic conditions and the low number of positive samples available for

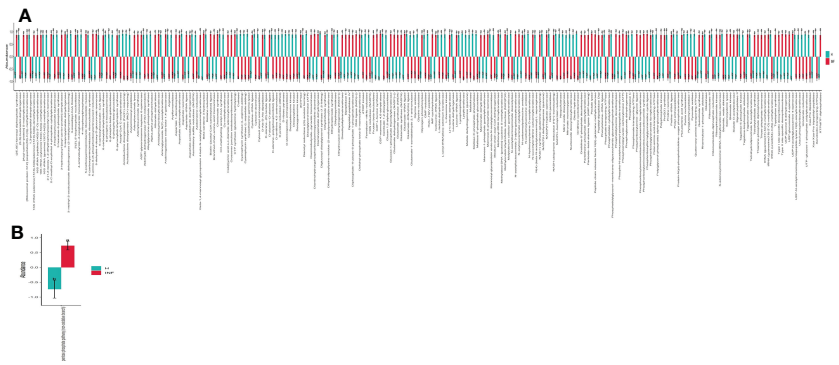

FIGURE 6
Cryptosporidium infection affected enzyme and MetaCys pathway abundance of yaks. **(A)** Enzyme ($p<0.001$), **(B)** MetaCys ($p<0.05$). "a, b" are showing significance relation.

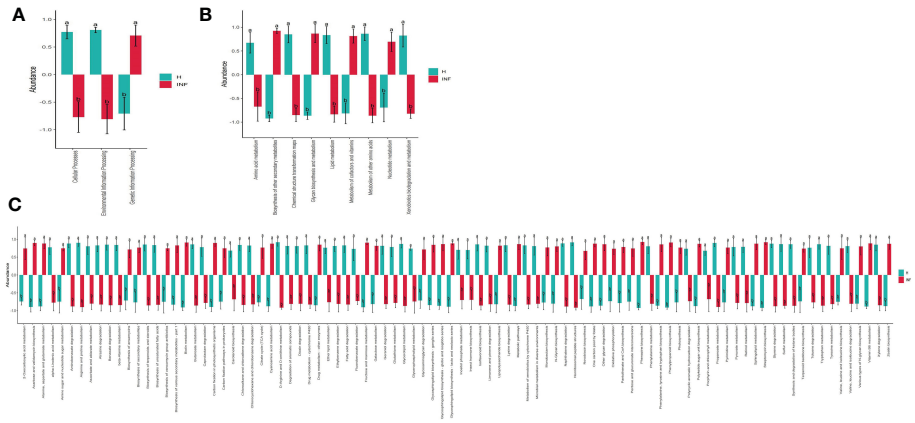

FIGURE 7
Cryptosporidium infection potentially affected the microbiota function of yaks. **(A)** KEGG L1 ($p<0.05$), **(B)** KEGG L2 ($p<0.05$), **(C)** KEGG L3 ($p<0.05$). "a, b" are showing significance relation.

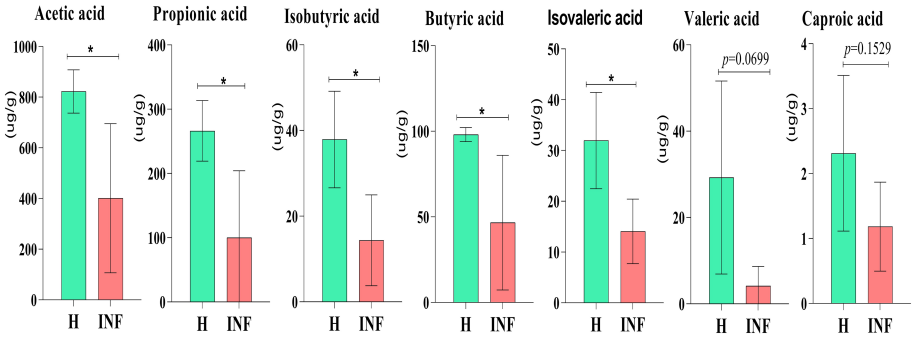

FIGURE 8
Concentration of SCFAs in yaks. Significance is presented as *$p < 0.05$; data are presented as the mean ± SEM (n = 4).

analysis, this number was above the minimum required for high throughput sequencing, and validation of changes of the microbiota (Ray et al., 2019). In the current study, we performed 16S rDNA sequencing of fecal samples collected from healthy and *Cryptosporidium*-infected yaks. Results showed that *Cryptosporidium* infection increased the alpha diversity index of Shannon ($p<0.01$) and Simpson ($p<0.01$) (Figure 1B), which demonstrated the increased microbiota complexity of infected animals. The current results are in line with our previous results found in *Cryptosporidium*-infected horses (Wang et al., 2022). Beta diversity analysis through NMDS, PCoA, Qiime 2β, and PCA analysis revealed microbiota differences between healthy and infected yaks (Figure 3), which were confirmed by comparing the dominating gut microbiota in different taxa (Figures 2, 4). Then we explored the significantly different bacteria between the H and INF groups through DESeq 2 volcano diagram and LEfSe chart analysis. The results showed that a total of 11 phyla and 58 genera were significantly different (Figure 5), which is in accordance with the previously reported results in a study conducted on infected people and horses (Chappell et al., 2016; Wang et al., 2022). The increased genera in yaks were in line with previous studies that found a higher abundance of *Desulfovibrio* and *Butyrivibrio* in colitis patients (Berry and Reinisch, 2013; Gryaznova et al., 2021), *Prevotellaceae_Prevotella* in diarrheic pigs (Yang et al., 2017), *Anaerovorax* in slow growth performers in nursery pigs (Zhai et al., 2020), *Succiniclasticum* in LPS induced dual-flow continuous culture system (Dai et al., 2019), *Pseudobutyrivibrio* in chronic kidney people (Wu et al., 2020), *Anaerorhabdus* in pulmonary fibrosis persons (Tong et al., 2019), *Selenomonas* in gastric cancer patients (Zhang et al., 2021), *Anaerostipes* in diabetic nephropathy patients (Du et al., 2021), *Pyramidobacter* in endoscopic sphincterotomy surgery gallstone patients (Shen et al., 2021), and *Anaerofustis* in Alzheimer people (Hou et al., 2021). The genus of *Acinetobacter* is an underrated food-borne pathogen (Amorim and Nascimento, 2017). A previous study found *Acinetobacter* in acute diarrhea of children (Polanco and Manzi, 2008). The genus of *Treponema* is the main pathogen in bovine dermatitis (Mamuad et al., 2020), *Clostridia* are clinical species and some of them may cause severe infections like colitis (Sanchez Ramos and Rodloff, 2018). Those increased genera may have contributed greatly to diarrhea caused by *Cryptosporidium*. The lower abundance of genera in yaks was in accordance with the results revealing *Turicibacter*

and *Lactobacillus* in *Salmonella*-infected pigs (Garrido et al., 2021), *Akkermansia* and *Roseburiain* in colitis in mouse (Bu et al., 2021; Li et al., 2021), *Adlercreutzia* in influenza virus-infected mouse (Lu et al., 2021), *Faecalibacterium* in pre-eclampsia people (Chen et al., 2020), *Methanosphaera* in sheep without treatment of anthelmintic (Moon et al., 2021), Slackia in Vogt-Koyanagi-Harada patients (Li et al., 2022a; Li et al., 2022b), *Gemmiger* in immune-mediated inflammatory people (Forbes et al., 2018), and *Dorea* in HIV patients (Xu et al., 2021). Those deficient genera in *Cryptosporidium*-infected animals may be the reason for diarrhea in yaks. The genus of *Cupriavidus* was related to mycotoxin biodegradation (AL-Nussairawi et al., 2020), and the dropped *Cupriavidus* in yaks may affect mycotoxin metabolism in yaks. The previous study uncovered probiotics of *Dietzia* as a new therapy for Crohn's disease (Click, 2015), and *Blautia*, *Phascolarctobacterium*, and *Bifidobacterium* are probiotic genera (Papizadeh et al., 2017; Chen et al., 2021; Liu et al., 2021), which demonstrated that *Cryptosporidium* led diarrhea may be due to the decrease of probiotics in the microbiota.

The shifted intestine microflora also changed their functions, as 235 significantly different enzymes were found between healthy and infected yaks ($p<0.001$) (Figure 6A). Only one obvious different MetaCys pathway of pentose phosphate pathway (non-oxidative branch) was found between the two yak groups (Figure 6B). Also, KEGG L3 analysis discovered that the abundance of 92 pathways was significantly different between healthy and infected animals (Figure 7C). Those results may infer that *Cryptosporidium* broke the balance of gut microbiota, which affected the microbiota function and caused diarrhea in yaks.

In the present study, significantly lower concentrations of SCFAs were found in *Cryptosporidium*-infected animals (Figure 8), consistent with yak diarrhea (Li et al., 2022a), LPS-induced piglets (Yang et al., 2021), and dextran sulfate sodium-induced colitis in mouse (Xu et al., 2020). SCFAs play very important roles in host physiology and energy homeostasis (Chambers et al., 2018). Among them, acetate and propionate can provide energy to peripheral tissues (den Besten et al., 2013). A previous study reported that acetate was responsible for maintaining intestine barrier integrity by inhibiting pathogens infection (Skonieczna-Żydecka et al., 2018). In a recent study, it was found that acetate could regulate IgA reactivity (Takeuchi et al., 2021), and propionate contributed to intestinal epithelial turnover and repair (Bilotta et al., 2021). Butyrate is highly related to intestine structure, energy providing to epithelial cells, and regulates immune function (Abdalkareem Jasim et al., 2022). Isobutyric acid and isovaleric acid may be related to mucosal and inflammation responses (Li et al., 2022a). Therefore, the decreased SCFAs in *Cryptosporidium*-infected yaks might have affected the intestinal barrier and immunity of the host (Aho et al., 2021), which potentially caused diarrhea in plateau yaks.

In conclusion, *Cryptosporidium* is an important zoonotic protozoon causing severe diarrhea in young animals; however, limited treatment measures are available. Here we reveal that *Cryptosporidium* infection causes dysbiosis and results in reduced SCFAs in yaks with severe diarrhea, which may give new insights regarding the prevention and treatment of diarrhea in livestock. The low sample size remains the limitation of our study.

Data availability statement

The datasets presented in this study can be found in online repositories. The names of the repository/repositories and accession number(s) can be found below: https://www.ncbi.nlm.nih.gov/, PRJNA880359.

Ethics statement

The animal study was reviewed and approved by ethics committee of Nanjing Agricultural University.

Author contributions

KL and QW, research idea and methodology. HD, XC, XZ, and CZ, reagents, materials, and analysis tools. KL, writing-original draft and preparation. KM, MF-E-A, ZB, QW, JZ, SN, and KL, writing-review and editing. KL, JZ, and QW, visualization and supervision. All authors contributed to the article and approved the submitted version.

Funding

The study was partially supported by the National Natural Science Foundation of China (32102692), the Start-up fund of Nanjing Agricultural University (804131), and the Yak Germplasm innovation and healthy breeding project: Research on the prevention and control of yak infectious diseases for establishing rapid detection methods, prevention and control techniques (XZ202101ZD0002N-05).

Acknowledgments

We thank Bioyi Biotechnology Co., Ltd. (Wuhan, China) for providing sequencing help in our research.

Conflict of interest

The authors declare that the research was conducted in the absence of any commercial or financial relationships that could be construed as a potential conflict of interest.

Publisher's note

References

Abdalkareem Jasim, S., Jade Catalan Opulencia, M., Alexis Ramírez-Coronel, A., Kamal Abdelbasset, W., Hasan Abed, M., Markov, A., et al. (2022). The emerging role of microbiota-derived short-chain fatty acids in immunometabolism. *Int. IMMUNOPHARMACOL* 110, 108983. doi: 10.1016/j.intimp.2022.108983

Aho, V. T. E., Houser, M. C., Pereira, P. A. B., Chang, J., Rudi, K., Paulin, L., et al. (2021). Relationships of gut microbiota, short-chain fatty acids, inflammation, and the gut barrier in parkinson's disease. *Mol. Neurodegener.* 16. doi: 10.1186/s13024-021-00427-6

AL-Nussairawi, M., Risa, A., Garai, E., Varga, E., Szabó, I., Csenki-Bakos, Z., et al. (2020). Mycotoxin biodegradation ability of the cupriavidus genus. *Curr. Microbiol.* 77, 2430–2440. doi: 10.1007/s00284-020-02063-7

Amorim, A. M., and Nascimento, J. D. (2017). Acinetobacter: an underrated foodborne pathogen? *J. Infect. Dev. Ctries* 11, 111–114. doi: 10.3855/jidc.8418

Bachem, A., Makhlouf, C., Binger, K. J., de Souza, D. P., Tull, D., Hochheiser, K., et al. (2019). Microbiota-derived short-chain fatty acids promote the memory potential of antigen-activated CD8+ T cells. *IMMUNITY* 51, 285–297. doi: 10.1016/j.immuni.2019.06.002

Berry, D., and Reinisch, W. (2013). Intestinal microbiota: A source of novel biomarkers in inflammatory bowel diseases? *Best Pract. Res. Clin. Gastroenterol.* 27, 47–58. doi: 10.1016/j.bpg.2013.03.005

Bilotta, A. J., Ma, C., Yang, W., Yu, Y., Yu, Y., Zhao, X., et al. (2021). Propionate enhances cell speed and persistence to promote intestinal epithelial turnover and repair. *Cell Mol. Gastroenterol. Hepatol.* 11, 1023–1044. doi: 10.1016/j.jcmgh.2020.11.011

Bokulich, N. A., Kaehler, B. D., Rideout, J. R., Dillon, M., Bolyen, E., Knight, R., et al. (2018). Optimizing taxonomic classification of marker-gene amplicon sequences with QIIME 2's q2-feature-classifier plugin. *MICROBIOME* 6. doi: 10.1186/s40168-018-0470-z

Bu, F., Ding, Y., Chen, T., Wang, Q., Wang, R., Zhou, J., et al. (2021). Total flavone of abelmoschus manihot improves colitis by promoting the growth of akkermansia in mice. *Sci. REP-UK* 11. doi: 10.1038/s41598-021-00070-7

Callahan, B. J., McMurdie, P. J., Rosen, M. J., Han, A. W., Johnson, A. J. A., and Holmes, S. P. (2016). DADA2: High-resolution sample inference from illumina amplicon data. *Nat. Methods* 13, 581–583. doi: 10.1038/nmeth.3869

Chambers, E. S., Preston, T., Frost, G., and Morrison, D. J. (2018). Role of gut microbiota-generated short-chain fatty acids in metabolic and cardiovascular health. *Curr. Nutr. Rep.* 7, 198–206. doi: 10.1007/s13668-018-0248-8

Chappell, C. L., Darkoh, C., Shimmin, L., Farhana, N., Kim, D., Okhuysen, P. C., et al. (2016). Fecal indole as a biomarker of susceptibility to cryptosporidium infection. *Infect. Immun.* 84, 2299–2306. doi: 10.1128/IAI.00336-16

Chen, G., Hu, P., Xu, Z., Peng, C., Wang, Y., Wan, X., et al. (2021). The beneficial or detrimental fluoride to gut microbiota depends on its dosages. *Ecotoxicol Environ. Saf.* 209, 111732. doi: 10.1016/j.ecoenv.2020.111732

Chen, X., Li, P., Liu, M., Zheng, H., He, Y., Chen, M., et al. (2020). Gut dysbiosis induces the development of pre-eclampsia through bacterial translocation. *GUT* 69, 513–522. doi: 10.1136/gutjnl-2019-319101

Chen, X., Saeed, N. M., Ding, J., Dong, H., Kulyar, M. F., Bhutta, Z. A., et al. (2022). Molecular epidemiological investigation of cryptosporidium sp., giardia duodenalis, enterocytozoon bieneusi and blastocystis sp. *Infection Free-ranged Yaks Tibetan Pigs Plateau. Pak Vet. J.* 2022, 533-539. doi: 10.29261/pakvetj/2022.060

Cheng, H., Ao, S., Yun, L., Weihong, S., Hong, L., Jianbo, L., et al. (2022). RNA-Seq transcriptome analysis to unravel the gene expression profile of ovarian development in xiangxi cattle. *Pak Vet. J.* 42, 222–228. doi: 10.29261/pakvetj/2022.004

Click, R. E. (2015). Crohn's disease therapy with dietzia: the end of anti-inflammatory drugs. *Future Microbiol.* 10, 147–150. doi: 10.2217/fmb.14.133

Cui, Y., Chen, X., Yue, H., and Tang, C. (2022). First detection and genomic characterization of bovine norovirus from yak. *Pathogens* 11, 192. doi: 10.3390/pathogens11020192

Dai, X., Paula, E. M., Lelis, A. L. J., Silva, L. G., Brandao, V. L. N., Monteiro, H. F., et al. (2019). Effects of lipopolysaccharide dosing on bacterial community composition and fermentation in a dual-flow continuous culture system. *J. DAIRY Sci.* 102, 334–350. doi: 10.3168/jds.2018-14807

den Besten, G., van Eunen, K., Groen, A. K., Venema, K., Reijngoud, D., and Bakker, B. M. (2013). The role of short-chain fatty acids in the interplay between diet, gut microbiota, and host energy metabolism. *J. Lipid Res.* 54, 2325–2340. doi: 10.1194/jlr.R036012

Diao, N., Gong, Q., Li, J., Zhao, D., Li, D., Zhao, B., et al. (2020). Prevalence of bovine viral diarrhea virus (BVDV) in yaks between 1987 and 2019 in mainland China: A systematic review and meta-analysis. *Microb. PATHOGENESIS* 144, 104185. doi: 10.1016/j.micpath.2020.104185

Du, X., Liu, J., Xue, Y., Kong, X., Lv, C., Li, Z., et al. (2021). Alteration of gut microbial profile in patients with diabetic nephropathy. *ENDOCRINE* 73, 71–84. doi: 10.1007/s12020-021-02721-1

Forbes, J. D., Chen, C., Knox, N. C., Marrie, R., El-Gabalawy, H., de Kievit, T., et al. (2018). A comparative study of the gut microbiota in immune-mediated inflammatory diseases–does a common dysbiosis exist? *MICROBIOME* 6. doi: 10.1186/s40168-018-0603-4

Garrido, V., Migura-García, L., Gaitán, I., Arrieta-Gisasola, A., Martínez-Ballesteros, I., Fraile, L., et al. (2021). Prevalence of salmonella in free-range pigs: Risk factors and intestinal microbiota composition. *Foods* 10, 1410. doi: 10.3390/foods10061410

Gryaznova, M. V., Solodskikh, S. A., Panevina, A. V., Syromyatnikov, M. Y., Dvoretskaya, Y. D., Sviridova, T. N., et al. (2021). Study of microbiome changes in patients with ulcerative colitis in the central European part of Russia. *Heliyon* 7, e6432. doi: 10.1016/j.heliyon.2021.e06432

Han, Z., Li, K., Shahzad, M., Zhang, H., Luo, H., Qiu, G., et al. (2017). Analysis of the intestinal microbial community in healthy and diarrheal perinatal yaks by high-throughput sequencing. *Microb. PATHOGENESIS* 111, 60–70. doi: 10.1016/j.micpath.2017.08.025

Hou, M., Xu, G., Ran, M., Luo, W., and Wang, H. (2021). APOE-ϵ4 carrier status and gut microbiota dysbiosis in patients with Alzheimer disease. *Front. NEUROSCI-SWITZ* 15. doi: 10.3389/fnins.2021.619051

Hsu, Y., Chen, C., Lin, Y., Wu, W., Chang, L., Lai, C., et al. (2019). Evaluation and optimization of sample handling methods for quantification of short-chain fatty acids in human fecal samples by GC–MS. *J. Proteome Res.* 5, 1948–1957. doi: 10.1021/acs.jproteome.8b00536

Kandeel, M., Akhtar, T., Zaheer, T., Ahmad, S., Ashraf, U., and Omar, M. (2022). Anti-parasitic applications of nanoparticles: A review. *PAK Vet. J.* 42, 135-140. doi: 10.29261/pakvetj/2022.040

Kim, S., Yu, D. H., Jung, S., Kang, J., Park, K., Chae, J. B., et al. (2021). Biological factors associated with infectious diarrhea in calves. *PAK Vet. J.* 41, 531-537. doi: 10.29261/pakvetj/2021.078

Lan, Y., Li, K., and Mehmood, K. (2021). Molecular investigation of important protozoal infections in yaks. *PAK Vet. J.* 41 (4), 557-561. doi: 10.29261/pakvetj/2020.048

Langille, M. G. I., Zaneveld, J., Caporaso, J. G., McDonald, D., Knights, D., Reyes, J. A., et al. (2013). Predictive functional profiling of microbial communities using 16S rRNA marker gene sequences. *Nat. Biotechnol.* 31, 814–821. doi: 10.1038/nbt.2676

Li, B., Du, P., Du, Y., Zhao, D., Cai, Y., Yang, Q., et al. (2021). Luteolin alleviates inflammation and modulates gut microbiota in ulcerative colitis rats. *Life Sci.* 269, 119008. doi: 10.1016/j.lfs.2020.119008

Li, K., Li, Z., Zeng, Z., Li, A., Mehmood, K., Shahzad, M., et al. (2020). Prevalence and molecular characterization of cryptosporidium spp. in yaks (Bos grunniens) in naqu, China. *Microb. Pathog.* 144, 104190. doi: 10.1016/j.micpath.2020.104190

Li, K., Nader, S. M., Zhang, X., Ray, B. C., Kim, C. Y., Das, A., et al. (2019a). Novel lactate dehydrogenase inhibitors with *in vivo* efficacy against cryptosporidium parvum. *PloS Pathog.* 15, e1007953. doi: 10.1371/journal.ppat.1007953

Li, N., Wang, R., Cai, M., Jiang, W., Feng, Y., and Xiao, L. (2019b). Outbreak of cryptosporidiosis due to cryptosporidium parvum subtype IIdA19G1 in neonatal calves on a dairy farm in China. *Int. J. Parasitol.* 49, 569–577. doi: 10.1016/j.ijpara.2019.02.006

Li, M., Yang, L., Cao, J., Liu, T., and Liu, X. (2022b). Enriched and decreased intestinal microbes in active VKH patients. *Invest. Ophthalmol. Vis. Sci.* 63, 21. doi: 10.1167/iovs.63.2.21

Li, K., Zeng, Z., Liu, J., Pei, L., Wang, Y., Li, A., et al. (2022a). Effects of short-chain fatty acid modulation on potentially diarrhea-causing pathogens in yaks through metagenomic sequencing. *Front. Cell Infect. MI* 12. doi: 10.3389/fcimb.2022.805481

Liu, X., Mao, B., Gu, J., Wu, J., Cui, S., Wang, G., et al. (2021). Blautia-a new functional genus with potential probiotic properties? *Gut Microbes* 13, 1–21. doi: 10.1080/19490976.2021.1875796

Love, M. I., Huber, W., and Anders, S. (2014). Moderated estimation of fold change and dispersion for RNA-seq data with DESeq2. *Genome Biol.* 15. doi: 10.1186/s13059-014-0550-8

Lu, W., Fang, Z., Liu, X., Li, L., Zhang, P., Zhao, J., et al. (2021). The potential role of probiotics in protection against influenza a virus infection in mice. *Foods* 10, 902. doi: 10.3390/foods10040902

Mamuad, L. L., Seo, B. J., Faruk, M. S. A., Espiritu, H. M., Jin, S. J., Kim, W., et al. (2020). Treponema spp., the dominant pathogen in the lesion of bovine digital dermatitis and its characterization in dairy cattle. *Vet. Microbiol.* 245, 108696. doi: 10.1016/j.vetmic.2020.108696

Mandal, S., Van Treuren, W., White, R. A., Eggesbø, M., Knight, R., and Peddada, S. D. (2015). Analysis of composition of microbiomes: a novel method for studying microbial composition. *Microbial Ecol. Health Dis.* 26, 27663. doi: 10.3402/mehd.v26.27663

Martinez-Lopez, Y. E., Esquivel-Hernandez, D. A., Sanchez-Castaneda, J. P., Neri-Rosario, D., Guardado-Mendoza, R., and Resendis-Antonio, O. (2022). Type 2 diabetes, gut microbiome, and systems biology: A novel perspective for a new era. *Gut Microbes* 14, 2111952. doi: 10.1080/19490976.2022.2111952

Meganck, V., Hoflack, G., and Opsomer, G. (2014). Advances in prevention and therapy of neonatal dairy calf diarrhoea: a systematical review with emphasis on colostrum management and fluid therapy. *Acta Vet. Scand.* 56, 75. doi: 10.1186/s13028-014-0075-x

Mei, Q., Fu, Y., Huang, Z., Yin, N., Wang, R., Xu, B., et al. (2022). Intestinal TLR4 deletion exacerbates acute pancreatitis through gut microbiota dysbiosis and paneth cells deficiency. *Gut Microbes* 14. doi: 10.1080/19490976.2022.2112882

Moon, C. D., Carvalho, L., Kirk, M. R., McCulloch, A. F., Kittelmann, S., Young, W., et al. (2021). Effects of long-acting, broad spectra anthelmintic treatments on the rumen microbial community compositions of grazing sheep. *Sci. REP-UK* 11. doi: 10.1038/s41598-021-82815-y

Papizadeh, M., Rohani, M., Nahrevanian, H., Javadi, A., and Pourshafie, M. R. (2017). Probiotic characters of bifidobacterium and lactobacillus are a result of the ongoing gene acquisition and genome minimization evolutionary trends. *Microb. PATHOGENESIS* 111, 118–131. doi: 10.1016/j.micpath.2017.08.021

Polanco, N., and Manzi, L. (2008). Oxigenic effect of acinetobacter baumanniiisolated from children with acute diarrhea. *Invest. Clin.* 49, 59–67.

Ray, K. J., Cotter, S. Y., Arzika, A. M., Kim, J., Boubacar, N., Zhou, Z., et al. (2019). High-throughput sequencing of pooled samples to determine community-level microbiome diversity. *Ann. Epidemiol.* 39, 63–68. doi: 10.1016/j.annepidem.2019.09.002

Salazar, N., Ponce-Alonso, M., Garriga, M., Sanchez-Carrillo, S., Hernandez-Barranco, A. M., Redruello, B., et al. (2022). Fecal metabolome and bacterial composition in severe obesity: Impact of diet and bariatric surgery. *Gut Microbes* 14, 2106102. doi: 10.1080/19490976.2022.2106102

Sanchez Ramos, L., and Rodloff, A. C. (2018). Identification of clostridium species using the VITEK® MS. *ANAEROBE* 54, 217–223. doi: 10.1016/j.anaerobe.2018.01.007

Segata, N., Izard, J., Waldron, L., Gevers, D., Miropolsky, L., Garrett, W. S., et al. (2011). Metagenomic biomarker discovery and explanation. *Genome Biol.* 12, R60. doi: 10.1186/gb-2011-12-6-r60

Shen, H., Zhu, J., Ye, F., Xu, D., Fang, L., Yang, J., et al. (2021). Biliary microbial structure of gallstone patients with a history of endoscopic sphincterotomy surgery. *Front. Cell Infect. MI* 10. doi: 10.3389/fcimb.2020.594778

Skonieczna-Żydecka, K., Grochans, E., Maciejewska, D., Szkup, M., Schneider-Matyka, D., Jurczak, A., et al. (2018). Faecal short chain fatty acids profile is changed in polish depressive women. *NUTRIENTS* 10, 1939. doi: 10.3390/nu10121939

Smith, R. P., Clifton-Hadley, F. A., Cheney, T., and Giles, M. (2014). Prevalence and molecular typing of cryptosporidium in dairy cattle in England and Wales and examination of potential on-farm transmission routes. *Vet. Parasitol.* 204, 111–119. doi: 10.1016/j.vetpar.2014.05.022

Smulski, S., Turlewicz-Podbielska, H., Wylandowska, A., and Włodarek, J. (2020). Non-antibiotic possibilities in prevention and treatment of calf diarrhoea. *J. Vet. Res.* 64, 119–126. doi: 10.2478/jvetres-2020-0002

Takeuchi, T., Miyauchi, E., Kanaya, T., Kato, T., Nakanishi, Y., Watanabe, T., et al. (2021). Acetate differentially regulates IgA reactivity to commensal bacteria. *NATURE* 595, 560–564. doi: 10.1038/s41586-021-03727-5

Tong, X., Su, F., Xu, X., Xu, H., Yang, T., Xu, Q., et al. (2019). Alterations to the lung microbiome in idiopathic pulmonary fibrosis patients. *Front. Cell Infect. MI* 9. doi: 10.3389/fcimb.2019.00149

Vazquez-Baeza, Y., Pirrung, M., Gonzalez, A., and Knight, R. (2013). EMPeror: a tool for visualizing high-throughput microbial community data. *GIGASCIENCE* 2, 16. doi: 10.1186/2047-217X-2-16

Wang, Y., Li, X., Chen, X., Kulyar, M. F., Duan, K., Li, H., et al. (2022). Gut fungal microbiome responses to natural cryptosporidium infection in horses. *Front. Microbiol.* 13. doi: 10.3389/fmicb.2022.877280

Wang, W., Zhai, S., Xia, Y., Wang, H., Ruan, D., Zhou, T., et al. (2019). Ochratoxin a induces liver inflammation: involvement of intestinal microbiota. *MICROBIOME* 7. doi: 10.1186/s40168-019-0761-z

Wei, X., Wang, W., Dong, Z., Cheng, F., Zhou, X., Li, B., et al. (2021). Detection of infectious agents causing neonatal calf diarrhea on two Large dairy farms in yangxin county, Shandong province, China. *Front. Veterinary Sci.* 7. doi: 10.3389/fvets.2020.589126

Wu, I., Lin, C., Chang, L., Lee, C., Chiu, C., Hsu, H., et al. (2020). Gut microbiota as diagnostic tools for mirroring disease progression and circulating nephrotoxin levels in chronic kidney disease: Discovery and validation study. *Int. J. Biol. Sci.* 16, 420–434. doi: 10.7150/ijbs.37421

Xu, H., Ou, Z., Zhou, Y., Li, Y., Huang, H., Zhao, H., et al. (2021). Intestinal mucosal microbiota composition of patients with acquired immune deficiency syndrome in guangzhou, China. *Exp. Ther. Med.* 21, 391. doi: 10.3892/etm.2021.9822

Xu, Z., Tang, H., Huang, F., Qiao, Z., Wang, X., Yang, C., et al. (2020). Algal oil rich in n-3 PUFA alleviates DSS-induced colitis *via* regulation of gut microbiota and restoration of intestinal barrier. *Front. Microbiol.* 11, 615404. doi: 10.3389/fmicb.2020.615404

Yang, Q., Huang, X., Zhao, S., Sun, W., Yan, Z., Wang, P., et al. (2017). Structure and function of the fecal microbiota in diarrheic neonatal piglets. *Front. Microbiol.* 8. doi: 10.3389/fmicb.2017.00502

Yang, C., Wang, M., Tang, X., Yang, H., Li, F., Wang, Y., et al. (2021). Effect of dietary Amylose/Amylopectin ratio on intestinal health and cecal microbes' profiles of weaned pigs undergoing feed transition or challenged with escherichia coli lipopolysaccharide. *Front. Microbiol.* 12. doi: 10.3389/fmicb.2021.693839

Zeineldin, M., Aldridge, B., and Lowe, J. (2018). Dysbiosis of the fecal microbiota in feedlot cattle with hemorrhagic diarrhea. *Microb. PATHOGENESIS* 115, 123–130. doi: 10.1016/j.micpath.2017.12.059

Zhai, H., Luo, Y., Ren, W., Schyns, G., and Guggenbuhl, P. (2020). The effects of benzoic acid and essential oils on growth performance, nutrient digestibility, and colonic microbiota in nursery pigs. *Anim. FEED Sci. TECH* 262, 114426. doi: 10.1016/j.anifeedsci.2020.114426

Zhang, X., Li, C., Cao, W., and Zhang, Z. (2021). Alterations of gastric microbiota in gastric cancer and precancerous stages. *Front. Cell Infect. MI* 11. doi: 10.3389/fcimb.2021.559148

Zhang, S., Wang, H., and Zhu, M. (2019). A sensitive GC/MS detection method for analyzing microbial metabolites short chain fatty acids in fecal and serum samples. *TALANTA* 196, 249–254. doi: 10.1016/j.talanta.2018.12.049

frontiers | Frontiers in Cellular and Infection Microbiology

TYPE Original Research
PUBLISHED 14 April 2023
DOI 10.3389/fcimb.2023.1143138

OPEN ACCESS

EDITED BY
Kun Li,
Nanjing Agricultural University, China

REVIEWED BY
De-Hua Lai,
Sun Yat-sen University, China
Ruttayaporn Ngasaman,
Prince of Songkla University, Thailand
Simon Peter Musinguzi,
Kyambogo University, Uganda

*CORRESPONDENCE
Shinuo Cao
shinuo_cao@163.com
Xuenan Xuan
gen@obihiro.ac.jp

†These authors have contributed equally to this work

SPECIALTY SECTION
This article was submitted to Parasite and Host, a section of the journal Frontiers in Cellular and Infection Microbiology

RECEIVED 12 January 2023
ACCEPTED 20 March 2023
PUBLISHED 14 April 2023

CITATION
Zhou M, Xie J, Kawase O, Nishikawa Y, Ji S, Zhu S, Cao S and Xuan X (2023) Characterization of anti-erythrocyte and anti-platelet antibodies in hemolytic anemia and thrombocytopenia induced by *Plasmodium* spp. and *Babesia*spp. infection in mice. *Front. Cell. Infect. Microbiol.* 13:1143138. doi: 10.3389/fcimb.2023.1143138

Characterization of anti-erythrocyte and anti-platelet antibodies in hemolytic anemia and thrombocytopenia induced by *Plasmodium* spp. and *Babesia* spp. infection in mice

Mo Zhou[1,2,3†], Jun Xie[2,3†], Osamu Kawase[4], Yoshifumi Nishikawa[1], Shengwei Ji[1], Shanyuan Zhu[2,3], Shinuo Cao[1,2,3*] and Xuenan Xuan[1*]

[1]National Research Center for Protozoan Diseases, Obihiro University of Agriculture and Veterinary Medicine, Obihiro, Hokkaido, Japan, [2]Jiangsu Key Laboratory for High-tech Research and Development of Veterinary Biopharmaceuticals, Jiangsu Agri-animal Husbandry Vocational College, Taizhou, China, [3]Engineering Technology Research Center for Modern Animal Science and Novel Veterinary Pharmaceutic Development, Jiangsu Agri-animal Husbandry Vocational College, Taizhou, China, [4]Department of Biology, Premedical Sciences, Dokkyo Medical University, Tochigi, Japan

Introduction: Malaria and Babesiosis are acute zoonotic disease that caused by infection with the parasite in the phylum Apicomplexa. Severe anemia and thrombocytopenia are the most common hematological complication of malaria and babesiosis. However, the mechanisms involved have not been elucidated, and only a few researches focus on the possible role of anti-erythrocyte and anti-platelet antibodies.

Methods: In this study, the *Plasmodium yoelii, P. chabaudi, Babesia microti* and *B. rodhaini* infected SCID and ICR mice. The parasitemia, survival rate, platelet count, anti-platelet antibodies, and the level of IFN-γ and interleukin (IL) -10 was tested after infection. Furthermore, the *P. yoelii, P. chabaudi, B. rodhaini* and *B. microti* infected ICR mice were treated with artesunate and diminaze, the development of the anti-erythrocyte and anti-platelet antibodies in chronic stage were examined. At last, the murine red blood cell and platelet membrane proteins probed with auto-antibodies induced by *P. yoelii, P. chabaudi, B. rodhaini*, and *B. microti* infection were characterized by proteomic analysis.

Results and discussion: The high anti-platelet and anti-erythrocyte antibodies were detected in ICR mice after *P. yoelii, P. chabaudi, B. rodhaini, and B. microti infection*. Actin of murine erythrocyte and platelet is a common auto-antigen in *Plasmodium* and *Babesia* spp. infected mice. Our findings indicate that anti-

erythrocyte and anti-platelet autoantibodies contribute to thrombocytopenia and anemia associated with *Plasmodium* spp. and *Babesia* spp. infection. This study will help to understand the mechanisms of malaria and babesiosis-related thrombocytopenia and hemolytic anemia.

KEYWORDS

malaria, Babesiosis, thrombocytopenia, anemia, anti-erythrocyte auto-antibodies, anti-platelet auto-antibodies

Introduction

The intraerythrocytic apicomplexan parasites *Plasmodium* and *Babesia* spp. cause malaria and babesiosis, respectively. Malaria and babesiosis are accountable for significant mortality and morbidity to humans and animals globally (Zoleko Manego et al., 2019; Zottig and Shanks, 2021; Zowonoo et al., 2023). Thrombocytopenia and anemia, are common symptoms of malaria and *Babesia* spp. infection (Yuan-Yuan et al., 2016; Yu et al., 2021; Waked and Krause, 2022). It has been reported that acute malaria infection is associated with autoimmune hemolytic anemia (AIHA), but it has not been well characterized. The symptom of AIHA include shortened red blood cells (RBCs) survival as well as the autoantibodies found in direct antiglobulin tests (DATs). DATs test complement C3d and/or immunoglobulins against autologous RBCs (Santos et al., 2020; Rajapakse and Bakirhan, 2021; Sporn et al., 2021; Ueda, 2022).

Anemia and thrombocytopenia are the most common hematological complications of malaria and babesiosis. Several studies have documented a high rate of thrombocytopenia in malaria patients. Over the past four decades, research has been conducted on the malaria thrombocytopenia, however, the exact mechanism behind this phenomenon remains unclear (Zumla and Hui, 2019; Tao et al., 2020; Tołkacz et al., 2021; Vanheer and Kafsack, 2021; Voisin et al., 2021; Zottig and Shanks, 2021). Thrombocytopenia in malaria is a multifactorial phenomenon likely caused by increased platelet destruction and consumption. The explanation for malaria-induced thrombocytopenia has been proposed by several authors (Coelho et al., 2013). There was some research suggested that the low level of platelet count in malaria might be because of apoptosis and/or activation of platelets. However, immune complexes elicited by malarial antigen may also be able to sequester injured platelets in the spleen and then be phagocytosed by splenic macrophages (Thapa et al., 2009; Lacerda et al., 2011; Zhan et al., 2019). The immune system attacks platelets resulting in immune thrombocytopenia (ITP). There are a few tests available to test antibodies against platelets (Michel et al., 2002). A majority of IgG subclasses are found bound to platelets in ITP. It may be useful to test for platelets-bound IgG in patients with thrombocytopenia.

Plasmodium yoelii and *P. chabaudai* are widely used as murine models to identify parasite induced immune responses. *Babesia rodhaini* and *B. microti* have been served as useful experimental model in mice for the analysis of human babesiosis (Rizk et al., 2020; Ji et al., 2021; Li et al., 2022). Anti-erythrocyte and anti-platelet autoantibodies producing is the crucial step between hematological complication and the host defense mechanisms after *Plasmodium* and *Babesia* spp. infection. To investigate the development of anti-erythrocyte and anti-platelet auto-antibodies and identify the related auto-antigens, in this study, the anti-erythrocyte and anti-platelet auto-antibodies were detected in *Plasmodium* and *Babesia* spp. infected mice, and the mechanism of antibody-mediated hemolytic anemia and thrombocytopenia were investigated.

Materials and methods

Mice ethics statement

From Central Institute for Experimental Animals (CIEA) in Japan, we purchased 6-week-old female ICR mice as well as C.B-17/Icr-scid/scid (SCID) mice. In accordance with the research protocol, the experimental animals were handled under the permit issued by Obihiro's Animal Care and Use in Research Committee Promulgated by Obihiro University of Agriculture and Veterinary Medicine, Japan (Permit Number: 201109–5).

Maintenance of the parasites and mice infections

Plasmodium yoelii, P. chabaudi, B. rodhaini and *B. microti* were maintained in mice by intraperitoneal (i.p.) passage as previously described (Li et al., 2012). SCID mice are severely combined immunodeficient mice. The weight of the thymus, spleen, and lymph nodes was less than 30% of normal, and histologically there were significant lymphocyte defects. To determine the role of B and T lymphocytes in the protection against infection with *P. yoelii, P. chabaudi, B. rodhaini* and *B. microti*, four groups of SCID mice were also infected with *P. yoelii, P. chabaudai, B. rodhaini* and *B. microti* by i.p. inoculation with 10^7 of parasitized erythrocytes (pRBCs). At the same time, four groups of ICR mice were infected with *P. yoelii, P. chabaudai, B. rodhaini* and *B. microti* as mentioned above.

Determination of survival rates and parasitemia

The survival rates and parasitemia of these groups of mice were monitored after *P. yoelii, P. chabaudi, B. rodhaini* and *B. microti* infection. The parasitemia of each mouse was tested by Giemsa-stained thin blood films. The blood samples from the ICR and SCID mice were serially collected every two days post-infection (dpi). The plasma was separated from RBCs by centrifuge (3000 r/min, 3 min), the RBCs and plasma were stored at -70°C until use.

Detection of serum cytokines

The blood samples from the ICR and SCID mice infected with *P. yoelii, P. chabaudi, B. rodhaini* and *B. microti* were serially collected. The plasma was separated and used to detect the serum cytokines. A standard curve was used to determine the concentration of individual cytokines in the samples by using enzyme-linked immunosorbent assay (ELISA) kits. According to the manufacturer's instructions, standard curves were prepared with mouse recombinant IFN-γ and interleukin (IL) -10 (Cusabio Biotech Co., Germany) according to the manufacturer's instructions. Double-antibody one-step sandwich ELISA was used. The samples, standard products, and HRP labeled detection antibodies were added into the coated micropores pre-coated with antibodies, incubated and thoroughly washed. Substrate TMB was added to the micropores for color development. The depth of the color is positively correlated with the concentration of the substance in the sample. The absorbance (OD value) was measured at 450 nm wavelength and the sample concentration was calculated.

Establishment of chronic infection

The mice should survive for more than 60 days to monitor the anti-erythrocyte and anti-platelet autoantibody level during infection. Therefore, we established the chronic infection and tried to extend the survival period of the *Plasmodium* and *Babesia* spp. infected mice. *P. yoelii, P. chabaudi, B. rodhaini* and *B. microti* were infected to 5 ICR mice for each group. The *Plasdodium* spp. infected-mice were treated by Artesunate, and the *Babesia* spp. infected-mice were treated by Diminazen for collecting the chronic stage serum. The parasitemia of each mouse was assessed every 2 days for 60 days. In order to determine the parasitemia percentage, thin blood smears were prepared, fixed in methanol, and stained for 30 minutes with 10% Giemsa solution. The level of parasitemia was estimated according to the matching method. A serial blood sample was collected from the ICR mice every two days. The plasma and RBCs were harvested and stored at -70°C until use.

Platelets and red blood cells (RBCs) membrane isolation

Isolated platelets and RBC membranes were used for ELISA and two-dimensional LC and MS assays. To generate platelet-rich plasma (PRP), whole blood was centrifuged for 10 minutes at 200 x g. Platelets were acidified with citric acid 0.15 M until pH 6.4, then prostaglandin E-1 (PGE-1) was added at 1 mg/mL to prevent aggregation and activation.

After centrifugation, the pellet was resuspended in phosphate buffered saline (PBS). The whole blood was spun to separate packed red cells. To isolate host erythrocyte membrane, packed erythrocytes were extensively washed and lysed. The packed erythrocytes were washed in a ten-fold volume of 1X PBS. For the remaining steps, the washed cells were placed on ice. The washed RBC pellets were lysed with cold lysis buffer; after that, the lysis was spun on a Beckman Coulter ultracentrifuge, and five washes were performed after removing the supernatant. The resulting host membranes were collected and frozen at −70 °C.

Detection of anti-erythrocyte and anti-platelet antibodies

The platelets and RBC membrane were washed two times, 100 ng of platelets and RBC membrane were coated in each well to detect of anti-erythrocyte and anti-platelet antibodies. After blocking, the mice serum collecting at all time points was added (50 μL/well, 100-time diluted) after incubating 1 hour and washing. We add 50 μL/well of a 1:2000 dilution in blocking buffer of HRP-labelled 2nd antibody. ELISA reader was used to read absorbance at 450 nm after incubation with stop solution. The quantity of erythrocyte and platelet-associated immunoglobulin IgM, IgG, IgG1, IgG2a, and IgG2b in plasma were determined by using the ELISA kit.

Two-dimensional electrophoresis (2-DE) and Western blot analysis

The purified platelets and RBC membrane proteins were treated separately with DTT and iodoacetamide, and digested with trypsin. The sample was loaded on IPG strip, rehydration and focusing steps were run with isoelectric focusing carried out simultaneously over 17 hours at a total voltage of 35 kV/h. Second-dimension electrophoresis was performed at 200 volts for 45-50 minutes with Criterion precast gels. In the next step, colloidal Coomassie blue was used to stain the 2DE gels, followed by acetic acid to destain them. At the same time, 2DE gels were detected by Western blot using a mouse serum (diluted 1:100), which was generated in the laboratory by infecting with *Plasmodium* spp. and *Babesia* spp.

Trypsin digestion and two-dimensional LC with MS/MS

In each gel, selected spots were manually removed and dehydrated with acetonitrile for 10 minutes before being dried with a Speed-Vac system. After overnight incubation, each dried protein spot was pipetted with trypsin solution and incubated. A Speed-Vac system was used to dry the supernatants after each step. The peptides were solubilized in 0.5% formic acid using an ultrahigh-performance liquid chromatography system. A reverse phase column Pepmap C18 was used for peptide separation. The most abundant peptides were analyzed by mass spectrometry (MS) using a continuous MS scan followed by 10 times analyses. The Mascot search engine was used to identify proteins in the NCBI Genbank database. The contaminants were excluded during the process.

Statistical analysis

An analysis of one-way Analysis of variance test was used to determine if there were any significant differences between the means of all variables (GraphPad Prism 5; GraphPad Software, Inc.). The significance of P-values was denoted as follows: ns, non-significant; *, $p \leq 0.05$; **, $p \leq 0.01$; ***, $p \leq 0.001$; and ****, $p \leq 0.0001$.

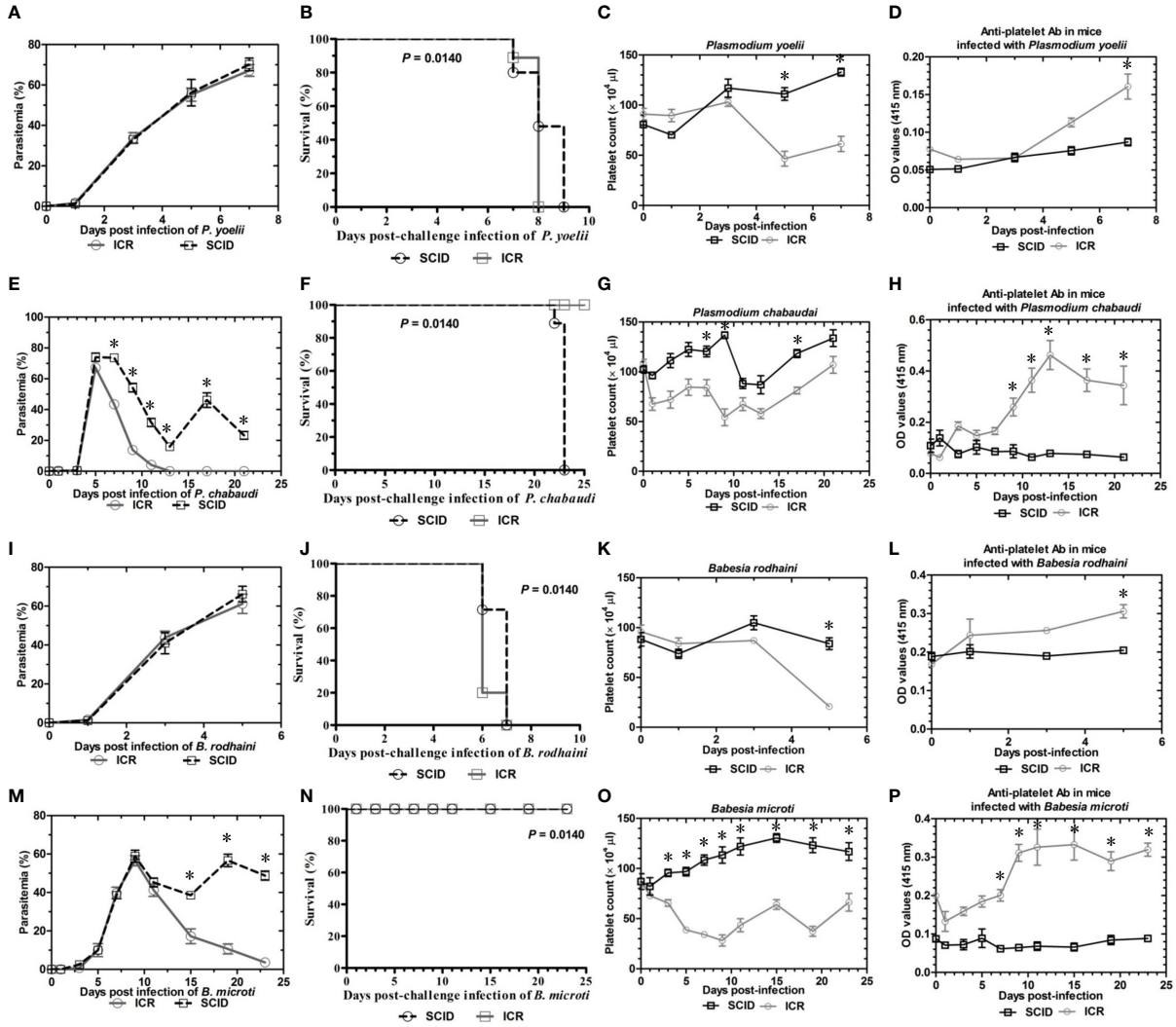

FIGURE 1
Parasitemia and survival rates, platelet counts and anti-platelet antibody of ICR mice and SCID mice after *Plasmodium yoelii, P. chabaudi, Babesia rodhaini* and *B. microti* challenge infection. **(A–D)** Parasitemia profiles of *P. yoelii, P. chabaudi, B. rodhaini* and *B. microti* infected ICR mice and SCID mice. **(B–H)** Survival rates of *P. yoelii, P. chabaudi, B. rodhaini* and *B. microti* infected ICR mice and SCID mice. **(I–L)** Platelet counts of *P. yoelii, P. chabaudi, B. rodhaini* and *B. microti* infected ICR mice and SCID mice. **(M–P)** anti-platelet antibody of *P. yoelii, P. chabaudi, B. rodhaini* and *B. microti* infected ICR mice and SCID mice. I.p. inoculations infected test mice with 10^7 of parasitized erythrocytes (pRBCs). The results are expressed as mean value ± the SD for five mice. The significance of P-values was denoted as follows: ns, non-significant; *, $p \leq 0.05$; **, $p \leq 0.01$; ***, $p \leq 0.001$; and ****, $p \leq 0.0001$.

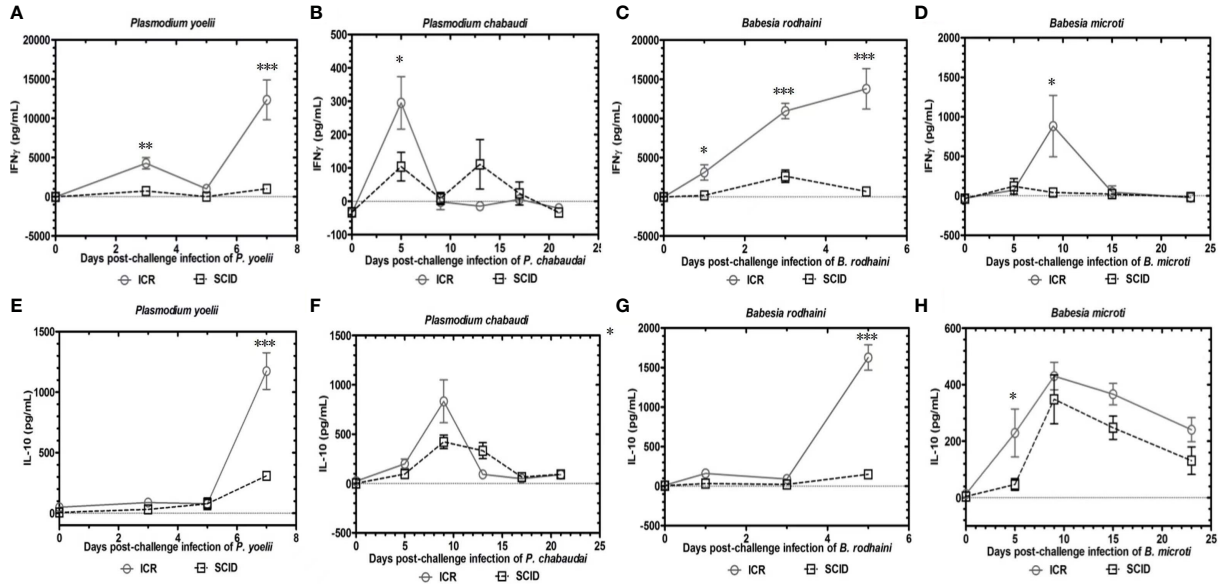

FIGURE 2
Kinetics of serum cytokines of ICR mice and SCID mice after *P. yoelii, P. chabaudi, B. rodhaini* and *B. microti* challenge infection. **(A–D)** Production of IFN-γ. **(E–H)** Production of IL-10 post challenge infection with *P. yoelii, P. chabaudi, B. rodhaini* and *B. microti*. The results are expressed as mean value ± the SD for five mice. The significance of P-values was denoted as follows: ns, non-significant; *, $p \leq 0.05$; **, $p \leq 0.01$; ***, $p \leq 0.001$; and ****, $p \leq 0.0001$.

Results

Thrombocytopenia and parasitemia after *Plasmodium* spp. and *Babesia* spp. infection

To determine the role of B and T lymphocytes during lethal infection with *Plasmodium* spp. and *Babesia* spp, the immune sufficient ICR mice and SCID mice were infected with *P. yoelii*, *P. chabaudi*, *B. microti and B. rodhaini*. The percentage parasitemia, survival rate, platelet count and anti-platelet autoantibodies were tested (Figures 1A–P). In the group that infected with *P. yoelii* and *B. Rodhaini*, all the infected mice died within ten days (Figures 1B, J); parasitemia was similar in ICR and SCID mice (Figures 1A, I). The low survival rate was correlated with the high percentage of parasitemia. In the group that was infected with *P. chabaudi* and *B. microti*, all the mice were alive for more than 20 days (Figures 1F, N); parasitemia was similar in *P. chabaudi*-infected ICR and SCID mice (Figures 1G, O), the parasitemia in *B. microti*-infected ICR and SCID mice was significant different after 20 days infection ($P<0.05$). Both ICR and SCID mice developed rapid increases in parasitemia within one week of infection (Figures 1E, M). Compared with the SCID mice, high anti-platelet autoantibodies were found in *P. yoelii, P. chabaudi, B. microti* and *B. rodhaini* infected ICR mice ($P<0.05$). Furthermore, negative correlation existed between platelet count and anti-platelet in *P. yoelii* (Figures 1C, D), *P. chabaudi* (Figures 1G, H), *B. rodhaini* (Figures 1K, L) and *B. microti* (Figures 1O, P) infected ICR mice. The concentration of individual cytokines in Plasmodium and Babesia spp. infected mice has been tested (Figures 2A–G). Likewise, detectable IFN-γ and IL-10 levels were lower in SCID mice ($P<0.01$) than those detected in ICR mice at days 5 and 7 post challenge with *P. yoelii and B. rodhaini* (Figure 2H). According to these findings, the anti-platelet autoantibodies induced by *Plasmodium* spp. and *Babesia* spp infection might be impaired by B and T lymphocytes.

The *Plasmodium* spp. and *Babesia* spp. infection induces the production of anti-erythrocyte and anti-platelet autoantibodies

To examine the possible contribution of anti-erythrocyte and anti-platelet autoantibodies in thrombocytopenia and hemolytic anemia caused by lethal infection with *Babesia* spp. and *Plasmodium* spp. The chronic *Babesia* spp. and *Plasmodium* spp. infections were established by administering artesunate and diminaze to infected-ICR mice. The trend of parasitemia was similar in *Babesia* spp. and *Plasmodium* spp. infected mice, and hematocrit and parasitemia were negatively correlated (Figures 3A–H). The IgM and IgG reached to the highest level after reaching high parasitemia (Figures 3A–D). These results indicated that

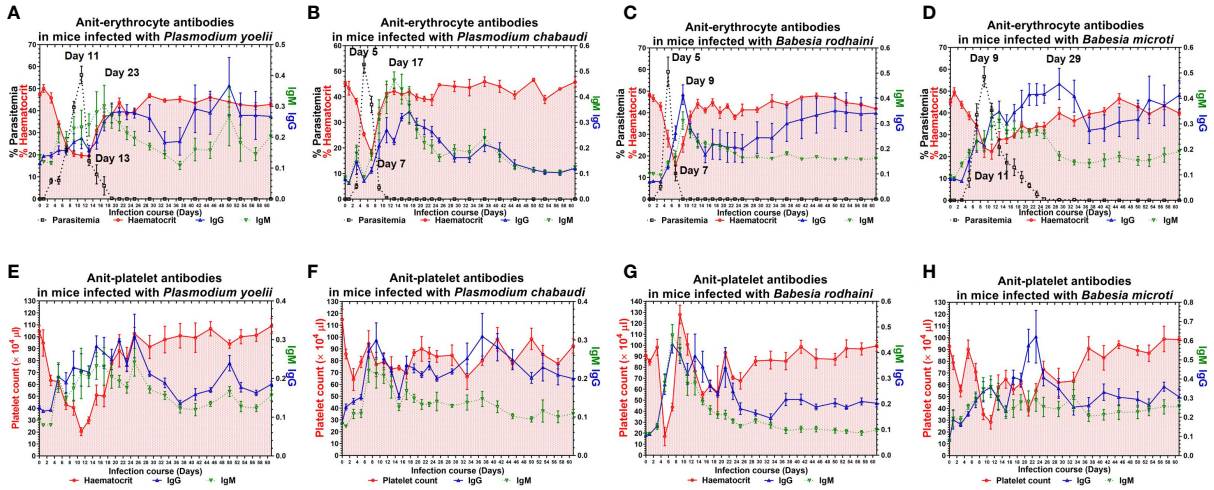

FIGURE 3
The anti-erythrocyte and anti-platelet antibodies of chronically *P. yoelii, P. chabaudi, B. rodhaini* and *B. microti*. infected ICR mice. **(A–D)** The parasitemia, hematocrit, and the production of anti-erythrocyte IgG and IgM in ICR mice challenge infection of *P. yoelii, P. chabaudi, B. rodhaini* and *B. microti*. **(E–H)** The platelet counts and the production of anti-platelet IgG and IgM in ICR mice challenge infection of *P. yoelii, P. chabaudi, B. rodhaini* and *B. microti*. Test mice with chronic *P. yoelii, P. chabaudi, B. rodhaini* and *B. microti* infection, the *Plasmodium* spp. infected mice were treated with artesunate, and the *Babesia* spp. infected mice were treated with diminaze for collecting the chronic stage sera. The parasitemia of each mouse was examined every 2 days for 60 days. The results are expressed as mean value ± the SD for five mice.

Plasmodium spp. and *Babesia* spp. infection lead to the destruction of RBCs and the production of anti-erythrocyte autoantibodies may not be the important reason for anemia. The platelet counts significantly decreased in the mice infected with *Plasmodium* spp. and *Babesia* spp. Moreover, IgM and IgG levels negatively correlated with platelet count (Figures 3E, F). Thus, anti-platelet auto-antibodies may be the cause of thrombocytopenia.

The IgG isotypes of anti-erythrocyte and anti-platelet autoantibodies

The infected mice produced a high amount of anti-platelet and anti-erythrocyte IgG2a and a low amount of IgG1 and IgG2b after *Plasmodium* spp. and *Babesia* spp. infection. The anti-erythrocyte IgG2a was detectable ten days after infection and peaked between 22

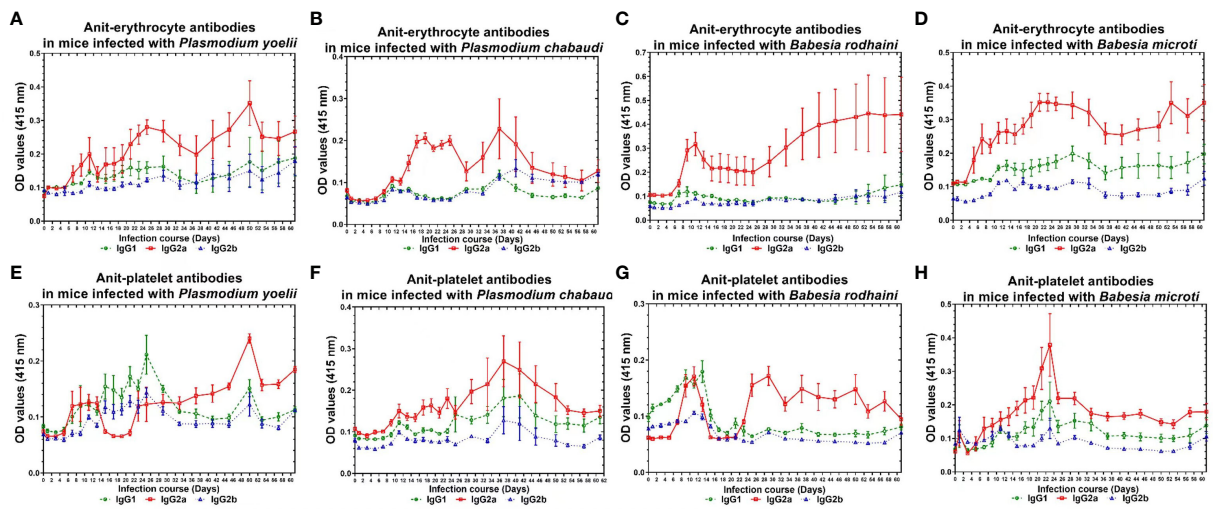

FIGURE 4
The production of anti-erythrocyte and anti-platelet IgG1, IgG2a, IgG2b of of chronically *P. yoelii, P. chabaudi, B. rodhaini* and *B. microti* infected ICR mice. **(A–D)** The production of anti-erythrocyte IgG1, IgG2a, IgG2b in ICR mice challenge infection of *P. yoelii, P. chabauai, B. rodhaini* and *B. microti* **(E–H)**. The anti-platelet IgG1, IgG2a, IgG2b in ICR mice challenge infection of *P. yoelii, P. chabaudi, B. rodhaini* and *B. microti*. Test mice with chronic *P. yoelii, P. chabaudi, B. rodhaini* and *B. microti*. infection, the *Plasmodium* spp. infected mice were treated with artesunate, and the *Babesia rodhaini* infected mice were treated with diminaze for collecting the chronic stage sera. The parasitemia of each mouse was examined every 2 days for 60 days. The results are expressed as mean value ± the SD for five mice.

10.3389/fcimb.2023.1143138

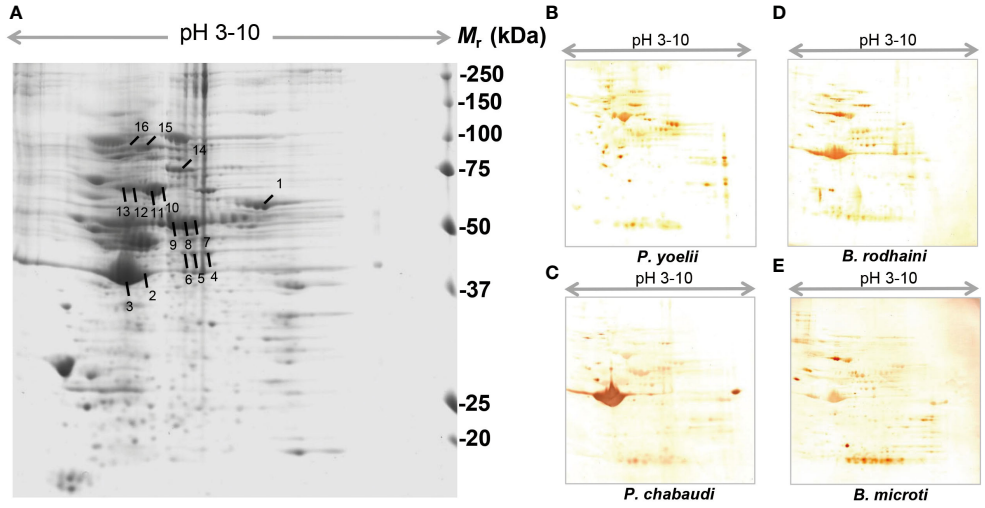

FIGURE 5
Reference image 2DE map of differentially expressed platelet proteins with marked selected spots and Western blot analysis of murine platelet proteins probed with auto-antibodies induced by *P. yoelii, P. chabaudi, B. rodhaini* and *B. microti*. infection. **(A)** Representative 2DE map of murine platelet proteins. **(B)** Western blot analysis of murine platelet proteins probed with auto-antibodies induced by *P. yoelii* infection. **(C)** Western blot analysis of murine platelet proteins probed with auto-antibodies induced by *P. chabaudi* infection. **(D)** Western blot analysis of murine platelet proteins probed with auto-antibodies induced by *B. rodhaini* infection. **(E)** Western blot analysis of murine platelet proteins probed with auto-antibodies induced by *B. microti* infection. A representative 2DE map of murine platelet proteins was obtained by performing the first dimension (IEF) on IPG strips pH 3–10 and the second dimension on 4–12% gradient SDS-PAGE gels. The protein spots were visualized by Coomassie blue staining. The indicated spots were excised from the gel and identified by MS/MS.

and 30 days and 40 and 50 days (Figures 4A–D) in *plasmodium* spp. and *Babesia* spp. infection. The anti-platelet IgG2a was detectable within six days after *Plasmodium* spp. and *Babesia* spp. infection. The anti-platelet IgG2a reached to high level at 24 days and 48 days after illness in *P. yoelii*-infected mice. The *P. chabaudi*-infected mice had elevated levels of anti-platelet antibody at 40 days post-infection. Furthermore, anti-platelet antibody also reached the peak at 22 days post-infection in *B. microti* infected mice. However, the *B. rodhaini*-infected mice developed low moderate levels anti-platelet IgG2a (Figures 4E–H).

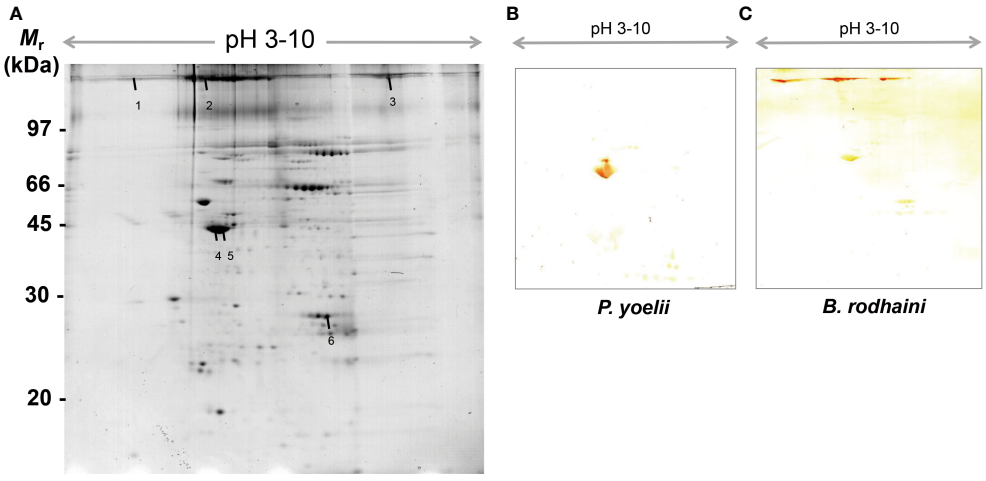

FIGURE 6
Reference image 2DE map of differentially expressed erythrocyte proteins with marked selected spots and Western blot analysis of murine erythrocyte proteins probed with auto-antibodies induced by *P. yoelii* and *B. rodhaini* infection. **(A)** Representative 2DE map of murine erythrocyte proteins. **(B)** Western blot analysis of murine erythrocyte proteins probed with auto-antibodies induced by *P. yoelii* infection. **(C)** Western blot analysis of murine erythrocyte proteins probed with auto-antibodies induced by *B. rodhaini* infection. Representative 2DE map of murine platelet proteins obtained by performing the first dimension (IEF) on IPG strips pH 3–10 and the second dimension on 4–12% gradient SDS-PAGE gels. The protein spots were visualized by Coomassie blue staining. The indicated spots were excised from gel and identified by MS/MS.

10.3389/fcimb.2023.1143138

TABLE 1 Protein identification of murine erythrocyte proteins probed with anti-erythrocyte auto-antibodies.

Spot no.	Accession no.	Protein name	Theoretical M_r (Dr)/*pI*	Sequence coverage (%)	MASCOT value
1	gi|187956529	Spectrin alpha 1	280931/4.94	20%	156
2	gi|187956529	Spectrin alpha 1	280931/4.94	17%	149
3	gi|187956529	Spectrin alpha 1	280931/4.94	18%	141
4	gi|469566230	beta actin	40847/5.56	53%	145
5	gi|512956198	actin	41995/5.29	49%	130
6	gi|156257635	beta-globin	15838/7.86	62%	91

Identification of murine erythrocyte and platelet auto-antigens

In order to further investigate and understand the mechanism of autoimmune antibody-mediated thrombocytopenia and hemolytic anemia, we isolated the platelets and RBC membrane proteins followed by identification of the autoimmune antibody-binding proteins by 2DE and Western blot analysis. 2DE analysis of platelets samples showed differentially expressed spots (Figure 5A). In Figures 5B–E, representative gel images for each group are shown. A total of sixteen spots were selected for mass spectrometry analysis. 2DE image analysis of RBC membrane showed differentially expressed spots (Figure 6A). Each experimental group is represented by a gel image in Figures 6B, C. For mass spectrometry, six spots were chosen. Overall, the results showed that many host polypeptides are bound to autoimmune antibodies specifically ($P<0.05$).

Comparative analysis of the antibody-binding proteins

The selected spots were analyzed by 2D LC-MS/MS after trypsinization to identify the autoimmune antibody-binding proteins. Our study combined Western blot, 2-DE, and proteomic analysis. All of the above proteins have been identified *via* analysis of the antibody-binding proteins. As shown in Tables 1 and 2, the MS/MS spectra have been analyzed. Masses of the peptides identified by LC-MS/MS were compared with sequences from the National Center for Biotechnology Information database (NCBI: http://www.ncbi.nlm.nih.gov/), separately. By using the ion score, we compare the fragment ions to all tryptic peptides calculated from parasites and mice. Actin of murine erythrocyte and platelet is a common auto-antigen in *Plasmodium* spp. and *Babesia* spp. infected mice.

TABLE 2 Protein identification of murine platelet proteins probed with anti-platelet auto-antibodies.

Spot no.	Accession no.	Protein name	Theoretical M_r (Dr)/*pI*	Sequence coverage (%)	MASCOT value
1	gi|148683477	fibrinogen	63570/6.95	26	87
2	gi|49868	beta-actin	39446/5.78	39	104
3	gi|74213524	actin	42066/5.30	73	207
4	gi|568930542	alpha-enolase	47640/6.30	40	139
5	gi|568930542	alpha-enolase	47640/6.30	36	123
6	gi|568930542	alpha-enolase	47640/6.30	46	120
7	gi|33859809	fibrinogen beta chain	55402/6.68	26	100
8	gi|33859809	fibrinogen beta chain	55402/6.68	34	168
9	gi|33859809	fibrinogen beta chain	55402/6.68	25	97
10	gi|26341396	serum albumin precursor	67013/5.49	21	108
11	gi|26341396	serum albumin precursor	67013/5.49	29	166
12	gi|74142813	heat shock cognate 71 kDa protein	50547/6.17	27	87
13	gi|178847300	70kDa heat shock cognate protein	59895/5.91	32	116
14	gi|1430883	zyxin	62063/6.47	20	74
15	gi|148670554	valosin containing protein	91675/5.26	27	127
16	gi|149045716	valosin-containing protein	76799/5.49	43	229

Discussion

Malaria and babesiosis continue to be important diseases in the world. The varied presentations of these diseases and their diversity in terms of hematological manifestations have been well endowed in literature (Zhan et al., 2019; Wang et al., 2020; Varshavsky et al., 2021; Voisin et al., 2021). The most common hematological complications of malaria and babesiosis are thrombocytopenia and anemia. Anemia is caused by a various of pathophysiologic mechanisms, including accelerated RBCs removal by the spleen, obligatory RBCs destruction at parasite schizogony, and ineffective erythropoiesis (Nie et al., 2021; Rizk et al., 2021; Rizk et al., 2022). Recent advancements have shown that a variety of cytokine dysregulations are indeed vital participants in inducing and accelerating the pathogenesis of hemolysis in malaria and babesiosis. They include a significant increase in IFN-γ, IL-6 and IL-1 and a decrease in IL-10 and IL-12 levels. In patients with malaria and babesiosis, autoimmune hemolytic anemia (AIHA) has been described previously (Narurkar et al., 2017; Santos et al., 2020; Rajapakse and Bakirhan, 2021). Several parasite and virus infections have been reported to be associated with AIHA, such as influenza virus, *Leishmania* species, hepatitis virus, and cytomegalovirus. Multiple studies have documented the high frequency of thrombocytopenia in malaria patients (Rodríguez-Morales et al., 2005; Coelho et al., 2013). For more than four decades, researchers have investigated the pathogenesis of malaria thrombocytopenia, but it remains unclear how it occurs (McMorran et al., 2009). According to some studies, malaria may cause low platelet counts due to activation or apoptosis of platelets, which prevents the immune system from removing them. Nevertheless, malarial antigens have also been implicated in sequestering injured platelets in the spleen due to immune complexes formed. In addition, there are some evidences of platelet-associated IgG involvement in malaria thrombocytopenia. Immune-mediated hemolytic anemia and thrombocytopenia in malaria and babesiosis has gathered more attentions in recent years (Lacerda et al., 2011).

We investigated the autoimmune-mediated hemolytic anemia and thrombocytopenia during *Plasmodium* spp. and *Babesia* spp. infection in this study. High levels of anti-platelet auto-antibodies were found in *P. yoelii, P. chabaudi, B. rodhaini and B. microti* infected ICR mice. In contrast, SCID mice displayed lower level of anti-platelet auto-antibodies. There was obvious relation between platelet count and anti-platelet. According to the findings of a previous study, acute malaria and babesiosis infection are associated with AIHA. B and T lymphocytes are the important inducers of the immune effector mechanisms, which are needed for initial control of *Plasmodium* spp. *and Babesia* spp. infection. Therefore, the SCID mice are unable to produce anti-platelet auto-antibodies (Watier et al., 1992; Wheeler et al., 2011; Aschermann et al., 2013). Our data indicate that the absence of B and T lymphocytes impaired the production of anti-platelet auto-antibodies. There are a few possible reasons of the presence of anti-platelet auto-antibodies. Such as the erythrocyte share some similar peptides with platelet, which induced auto-antibodies against both, or the broken erythrocyte induced disrupt of some platelet, which consequently induced anti-platelet auto-antibodies thus lead to more platelet disruption and more antibody. We found that ICR mice infected with *Plasmodium* and *Babesia* species emitted significantly higher levels of IL-10 and IFN-γ. It is a strong support for the idea that the timing and magnitude of specific cytokines influence the severity of malaria and babesiosis. It is necessary to study the cytokine production in *Plasmodium* spp. and *Babesia* spp. infected mice.

In addition, chronic infection with *Plasmodium* spp. and *Babesia* spp. was established after the *Plasdodium* spp. infectedmice were treated by artesunate, and the *Babesia* spp. infectedmice were treated by diminaze. The trend of parasitemia was similar in *Plasmodium* spp. and *Babesia* spp. infected mice, a negative correlation was observed between parasitemia and hematocrit. Moreover, The IgM and IgG reached to the highest level after the day of high parasitemia (Boes et al., 2000). These observations suggest that the production of anti-erythrocyte autoantibody is not the main reason of anemia. Generally, platelet antibodies in ITP are IgG or IgM, but IgA and IgE have also been reported (Klaassen et al., 1989). IgG are responsible for interacting with macrophages in the reticuloendothelial system when antibodies bind to platelets. Complement-mediated lysis can also remove antibodies-sensitized platelets from circulation. Therefore, the platelet-associated IgG and IgM were comparably elevated in the majority of *Plasmodium* spp. and *Babesia* spp. infected mice, and the IgG might be the majority of platelet antibodies in ITP. In this study, the anti-platelet IgG2a and low amounts of IgG1 and IgG2b also was detected after *Plasmodium* spp. and *Babesia* spp. infection.

The autoimmune antibody-binding proteins were identified in the study. The autoimmune antibody-binding proteins identified for platelet and RBC membrane were similar in both subcellular location and function categories. In contrast, membrane-associated cytoskeleton proteins from platelet and RBCs membrane was found (Tables 1, 2). Though we could not rule out that the actual number of platelet and RBC membrane proteins, which were more than that of the membrane-associated cytoskeleton proteins may affect the production of autoimmune antibodies. The membrane associated cytoskeleton proteins triggering the autoimmune response in *Plasmodium* spp. and *Babesia* spp.infected mice require further characterization.

In conclusion, we have demonstrated that the autoimmune response is elicited during *Plasmodium* spp. and *Babesia* spp. infection. The autoimmune antibody may participate in thrombocytopenia and hemolytic anemia and regulate the autoimmune response. As a result of this research, we can develop an effective babesiosis and malaria therapeutic that modulates autoimmune responses for overcoming infection. Understanding of the effector molecules that inhibit autoimmune

responses may provide important clues for future infection control strategies. In addition to antibiotics for the treatment of malaria and babesiosis, ITP treatment should be initiated in severe cases.

Data availability statement

The datasets presented in this study can be found in online repositories. The names of the repository/repositories and accession number(s) can be found in the article/supplementary material.

Ethics statement

The animal study was reviewed and approved by Animal Care and Use in Research Committee Promulgated by Obihiro University of Agriculture and Veterinary Medicine, Japan (Permit Number: 201109–5).

Author contributions

XX, SC, and MZ designed the study. MZ, SC carried out the experiments. OK and YN provide technical support. MZ, SC, JX, SJ, SZ, and XX wrote and read the manuscript, and all authors reviewed the manuscript. All authors contributed to the article and approved the submitted version.

Funding

This work was supported by a grant from the key project of Jiangsu Province's Key Research and Development Plan (modern Agriculture) (BE2020407), the project of Jiangsu Agri-animal Husbandry Vocational College (NSF2022CB04, NSF2022CB25), the Division of Swine Infectious disease prevention and control (NSF2023TC01) and the Qing Lan Project of Jiangsu Province.

Conflict of interest

The authors declare that the research was conducted in the absence of any commercial or financial relationships that could be construed as a potential conflict of interest.

Publisher's note

References

Aschermann, S., Lehmann, C. H., Mihai, S., Schett, G., Dudziak, D., and Nimmerjahn, F. (2013). B cells are critical for autoimmune pathology in scurfy mice. *Proc. Natl. Acad. Sci. U.S.A.* 110, 19042–19047. doi: 10.1073/pnas.1313547110

Boes, M., Schmidt, T., Linkemann, K., Beaudette, B. C., Marshak-Rothstein, A., and Chen, J. (2000). Accelerated development of IgG autoantibodies and autoimmune disease in the absence of secreted IgM. *Proc. Natl. Acad. Sci. U.S.A.* 97, 1184–1189. doi: 10.1073/pnas.97.3.1184

Coelho, H. C., Lopes, S. C., Pimentel, J. P., Nogueira, P. A., Costa, F. T., Siqueira, A. M., et al. (2013). Thrombocytopenia in plasmodium vivax malaria is related to platelets phagocytosis. *PloS One* 8, e63410. doi: 10.1371/journal.pone.0063410

Ji, S., Liu, M., Galon, E. M., Rizk, M. A., Li, J., Li, Y., et al. (2021). *In vitro* screening of novel anti-babesia gibsoni drugs from natural products. *Parasitol. Int.* 85, 102437. doi: 10.1016/j.parint.2021.102437

Klaassen, R. J., van der Lelie, J., Vlekke, A. B., Weigel, H. M., Eeftinck Schattenkerk, J. K., Reiss, P., et al. (1989). The serology and immunochemistry of HIV-induced platelet-bound immunoglobulin. *Blut* 59, 75–81. doi: 10.1007/BF00320253

Lacerda, M. V., Mourão, M. P., Coelho, H. C., and Santos, J. B. (2011). Thrombocytopenia in malaria: Who cares. *Mem. Inst. Oswaldo Cruz* 106 Suppl 1, 52–63. doi: 10.1590/s0074-02762011000900007

Li, Y., Terkawi, M. A., Nishikawa, Y., Aboge, G. O., Luo, Y., Ooka, H., et al. (2012). Macrophages are critical for cross-protective immunity conferred by babesia microti against babesia rodhaini infection in mice. *Infect. Immun.* 80, 311–320. doi: 10.1128/IAI.05900-11

Li, M., Yang, X., Masoudi, A., Xiao, Q., Li, N., Wang, N., et al. (2022). The regulatory strategy of proteins in the mouse kidney during babesia microti infection. *Exp. Parasitol.* 235, 108232. doi: 10.1016/j.exppara.2022.108232

McMorran, B. J., Marshall, V. M., de Graaf, C., Drysdale, K. E., Shabbar, M., Smyth, G. K., et al. (2009). Platelets kill intraerythrocytic malarial parasites and mediate survival to infection. *Science* 323, 797–800. doi: 10.1126/science.1166296

Michel, M., Lee, K., Piette, J. C., Fromont, P., Schaeffer, A., Bierling, P., et al. (2002). Platelet autoantibodies and lupus-associated thrombocytopenia. *Br. J. Haematol.* 119, 354–358. doi: 10.1046/j.1365-2141.2002.03817.x

Narurkar, R., Mamorska-Dyga, A., Nelson, J. C., and Liu, D. (2017). Autoimmune hemolytic anemia associated with babesiosis. *biomark. Res.* 5, 14. doi: 10.1186/s40364-017-0095-6

Nie, Z., Ao, Y., Wang, S., Shu, X., Li, M., Zhan, X., et al. (2021). Erythrocyte adhesion of merozoite surface antigen 2c1 expressed during extracellular stages of babesia orientalis. *Front. Immunol.* 12. doi: 10.3389/fimmu.2021.623492

Rajapakse, P., and Bakirhan, K. (2021). Autoimmune hemolytic anemia associated with human babesiosis. *J. Hematol.* 10, 41–45. doi: 10.14740/jh820

Rizk, M. A., Baghdadi, H. B., El-Sayed, S., Eltaysh, R., and Igarashi, I. (2022). Repurposing of the malaria box for babesia microti in mice identifies novel active scaffolds against piroplasmosis. *Parasit Vectors* 15, 329. doi: 10.1186/s13071-022-05430-4

Rizk, M. A., El-Sayed, S., Alkhoudary, M. S., Alsharif, K. F., Abdel-Daim, M. M., and Igarashi, I. (2021). Compounds from the medicines for malaria venture box inhibit *In vitro* growth of babesia divergens, a blood-borne parasite of veterinary and zoonotic importance. *Molecules* 26, 7118. doi: 10.3390/molecules26237118

Rizk, M. A., El-Sayed, S., Nassif, M., Mosqueda, J., Xuan, X., and Igarashi, I. (2020). Assay methods for *in vitro* and *in vivo* anti-babesia drug efficacy testing: Current progress, outlook, and challenges. *Vet. Parasitol.* 279, 109013. doi: 10.1016/j.vetpar.2019.109013

Rodríguez-Morales, A. J., Sánchez, E., Vargas, M., Piccolo, C., Colina, R., Arria, M., et al. (2005). Occurrence of thrombocytopenia in plasmodium vivax malaria. *Clin. Infect. Dis.* 41, 130–131. doi: 10.1086/430837

Santos, M. A., Tierney, L. M.Jr, and Manesh, R. (2020). Babesiosis-associated warm autoimmune hemolytic anemia. *J. Gen. Intern. Med.* 35, 928–929. doi: 10.1007/s11606-019-05506-5

Sporn, Z. A., Fenves, A. Z., Sykes, D. B., and Al-Samkari, H. (2021). Severe babesiosis with associated splenic infarcts and asplenia. *Proc. IEEE Glob Humanit Technol. Conf* 34, 597–599. doi: 10.1080/08998280.2021.1930632

Tao, Z. Y., Liu, W. P., Dong, J., Feng, X. X., Yao, D. W., Lv, Q. L., et al. (2020). Purification of plasmodium and babesia- infected erythrocytes using a non-woven fabric filter. *Trop. BioMed.* 37, 911–918. doi: 10.47665/tb.37.4.911

Thapa, R., Biswas, B., Mallick, D., Sardar, S., and Modak, S. (2009). Childhood plasmodium vivax malaria with severe thrombocytopenia and bleeding manifestations. *J. Pediatr. Hematol. Oncol.* 31, 758–759. doi: 10.1097/MPH.0b013e3181b7eb12

Tołkacz, K., Rodo, A., Wdowiarska, A., Bajer, A., and Bednarska, M. (2021). Impact of babesia microti infection on the initiation and course of pregnancy in BALB/c mice. *Parasit Vectors* 14, 132. doi: 10.1186/s13071-021-04638-0

Ueda, Y. (2022). [Advances in understanding the pathogenesis and treatment of autoimmune hemolytic anemia]. *Rinsho Ketsueki* 63, 1014–1025. doi: 10.11406/rinketsu.63.1014

Vanheer, L. N., and Kafsack, B. (2021). Activity comparison of epigenetic modulators against the hemoprotozoan parasites babesia divergens and plasmodium falciparum. *ACS Infect. Dis.* 7, 2277–2284. doi: 10.1021/acsinfecdis.0c00853

Varshavsky, T., Cuthbert, D., and Riggs, R. (2021). Babesiosis in the emergency department: A case report. *J. Emerg. Med.* 61, e7–e10. doi: 10.1016/j.jemermed.2021.01.040

Voisin, O., Monpierre, L., Le Lorc'h, E., Pilmis, B., Le Monnier, A., Mourad, J. J., et al. (2021). A typical babesiosis in an immunocompetent patient. *Ann. Biol. Clin. (Paris)* 79, 456–459. doi: 10.1684/abc.2021.1675

Waked, R., and Krause, P. J. (2022). Human babesiosis. *Infect. Dis. Clin. North Am.* 36, 655–670. doi: 10.1016/j.idc.2022.02.009

Wang, F., Jiang, J. F., Tian, J., and Du, C. H. (2020). [Clinical characteristics, diagnosis and treatment of human babesiosis: A review]. *Zhongguo Xue Xi Chong Bing Fang Zhi Za Zhi* 33, 218–224. doi: 10.16250/j.32.1374.2020168

Watier, H., Verwaerde, C., Landau, I., Werner, E., Fontaine, J., Capron, A., et al. (1992). T-Cell-dependent immunity and thrombocytopenia in rats infected with plasmodium chabaudi. *Infect. Immun.* 60, 136–142. doi: 10.1128/iai.60.1.136-142.1992

Wheeler, K., Tardif, S., Rival, C., Luu, B., Bui, E., Del Rio, R., et al. (2011). Regulatory T cells control tolerogenic versus autoimmune response to sperm in vasectomy. *Proc. Natl. Acad. Sci. U.S.A.* 108, 7511–7516. doi: 10.1073/pnas.1017615108

Yu, L., Liu, Q., Luo, W., Zhao, J., Alzan, H. F., and He, L. (2021). The structural basis of babesia orientalis lactate dehydrogenase. *Front. Cell Infect. Microbiol.* 11. doi: 10.3389/fcimb.2021.790101

Yuan-Yuan, L., Heng, P., Huai-Min, Z., Jian, L., and Shao-Li, X. (2016). [Investigation of two blood parasitic protozoa infection in farmed macaca fascicularis in guangxi zhuang autonomous region]. *Zhongguo Xue Xi Chong Bing Fang Zhi Za Zhi* 28, 141–145. doi: 10.16250/j.32.1374.2015241

Zhan, X., He, J., Yu, L., Liu, Q., Sun, Y., Nie, Z., et al. (2019). Identification of a novel thrombospondin-related anonymous protein (BoTRAP2) from babesia orientalis. *Parasit Vectors* 12, 200. doi: 10.1186/s13071-019-3457-0

Zoleko Manego, R., Koehne, E., Kreidenweiss, A., Nzigou Mombo, B., Adegbite, B. R., Dimessa Mbadinga, L. B., et al. (2019). Description of plasmodium falciparum infections in central Gabon demonstrating high parasite densities among symptomatic adolescents and adults. *Malar. J.* 18, 371. doi: 10.1186/s12936-019-3002-9

Zottig, V. E., and Shanks, G. D. (2021). Historical perspective: The evolution of post-exposure prophylaxis for vivax malaria since the Korean war. *MSMR* 28, 8–10.

Zowonoo, F., Iverson, G., Doyle, M., and Richards, S. L. (2023). Retrospective spatiotemporal analysis of malaria cases reported between 2000 and 2020 in north Carolina, USA. *Travel Med. Infect. Dis.* 51, 102505. doi: 10.1016/j.tmaid.2022.102505

Zumla, A., and Hui, D. (2019). Emerging and reemerging infectious diseases: Global overview. *Infect. Dis. Clin. North Am.* 33, xiii–xxix. doi: 10.1016/j.idc.2019.09.001

Frontiers in
Cellular and Infection Microbiology

Investigates how microorganisms interact with their hosts

Explores bacteria, fungi, parasites, viruses, endosymbionts, prions and all microbial pathogens as well as the microbiota and its effect on health and disease in various hosts.

Discover the latest Research Topics

See more →

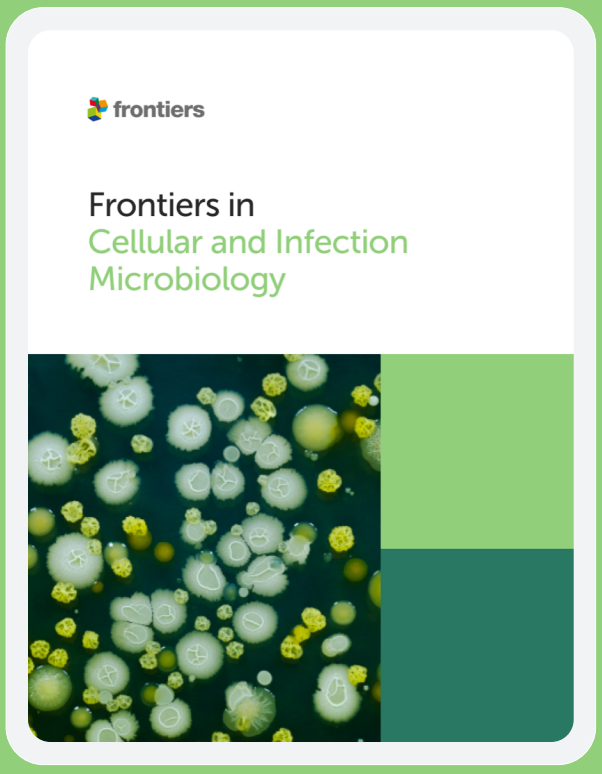

Frontiers

Avenue du Tribunal-Fédéral 34
1005 Lausanne, Switzerland
frontiersin.org

Contact us

+41 (0)21 510 17 00
frontiersin.org/about/contact